IMPACT OF MICROBIOME ON GUT MUCOSAL IMMUNITY IN HEALTH AND DISEASE

EDITED BY: Oscar Gilberto Gomez-Duarte, Pearay Ogra, Tobias R. Kollmann and Cecil Czerkinsky

PUBLISHED IN: Frontiers in Immunology and Frontiers in Microbiology

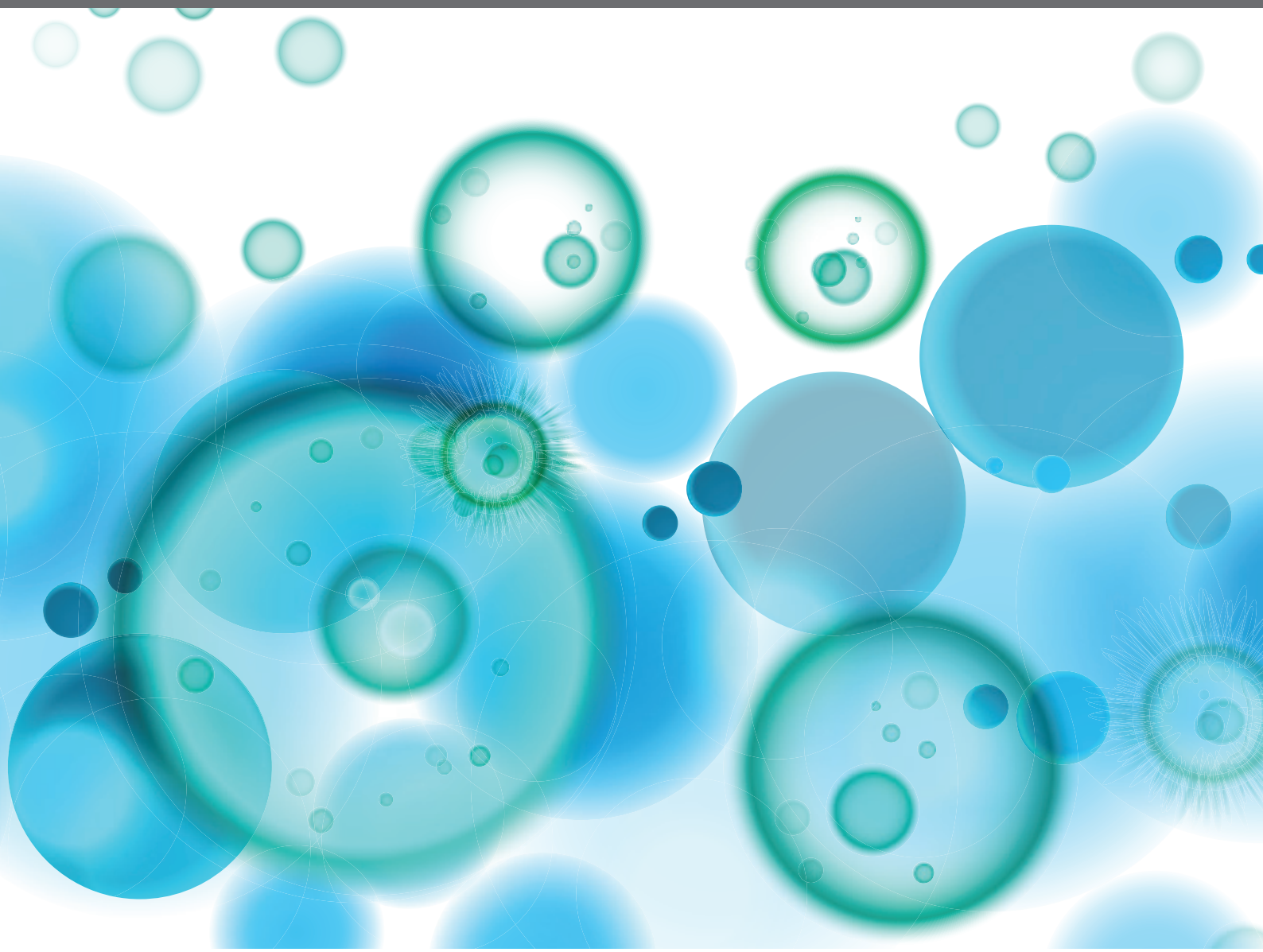

frontiers Research Topics

Frontiers eBook Copyright Statement

The copyright in the text of individual articles in this eBook is the property of their respective authors or their respective institutions or funders. The copyright in graphics and images within each article may be subject to copyright of other parties. In both cases this is subject to a license granted to Frontiers.

The compilation of articles constituting this eBook is the property of Frontiers.

Each article within this eBook, and the eBook itself, are published under the most recent version of the Creative Commons CC-BY licence. The version current at the date of publication of this eBook is CC-BY 4.0. If the CC-BY licence is updated, the licence granted by Frontiers is automatically updated to the new version.

When exercising any right under the CC-BY licence, Frontiers must be attributed as the original publisher of the article or eBook, as applicable.

Authors have the responsibility of ensuring that any graphics or other materials which are the property of others may be included in the CC-BY licence, but this should be checked before relying on the CC-BY licence to reproduce those materials. Any copyright notices relating to those materials must be complied with.

Copyright and source acknowledgement notices may not be removed and must be displayed in any copy, derivative work or partial copy which includes the elements in question.

All copyright, and all rights therein, are protected by national and international copyright laws. The above represents a summary only. For further information please read Frontiers' Conditions for Website Use and Copyright Statement, and the applicable CC-BY licence.

ISSN 1664-8714
ISBN 978-2-83250-402-4
DOI 10.3389/978-2-83250-402-4

About Frontiers

Frontiers is more than just an open-access publisher of scholarly articles: it is a pioneering approach to the world of academia, radically improving the way scholarly research is managed. The grand vision of Frontiers is a world where all people have an equal opportunity to seek, share and generate knowledge. Frontiers provides immediate and permanent online open access to all its publications, but this alone is not enough to realize our grand goals.

Frontiers Journal Series

The Frontiers Journal Series is a multi-tier and interdisciplinary set of open-access, online journals, promising a paradigm shift from the current review, selection and dissemination processes in academic publishing. All Frontiers journals are driven by researchers for researchers; therefore, they constitute a service to the scholarly community. At the same time, the Frontiers Journal Series operates on a revolutionary invention, the tiered publishing system, initially addressing specific communities of scholars, and gradually climbing up to broader public understanding, thus serving the interests of the lay society, too.

Dedication to Quality

Each Frontiers article is a landmark of the highest quality, thanks to genuinely collaborative interactions between authors and review editors, who include some of the world's best academicians. Research must be certified by peers before entering a stream of knowledge that may eventually reach the public - and shape society; therefore, Frontiers only applies the most rigorous and unbiased reviews.
Frontiers revolutionizes research publishing by freely delivering the most outstanding research, evaluated with no bias from both the academic and social point of view. By applying the most advanced information technologies, Frontiers is catapulting scholarly publishing into a new generation.

What are Frontiers Research Topics?

Frontiers Research Topics are very popular trademarks of the Frontiers Journals Series: they are collections of at least ten articles, all centered on a particular subject. With their unique mix of varied contributions from Original Research to Review Articles, Frontiers Research Topics unify the most influential researchers, the latest key findings and historical advances in a hot research area! Find out more on how to host your own Frontiers Research Topic or contribute to one as an author by contacting the Frontiers Editorial Office: frontiersin.org/about/contact

IMPACT OF MICROBIOME ON GUT MUCOSAL IMMUNITY IN HEALTH AND DISEASE

Topic Editors:
Oscar Gilberto Gomez-Duarte, University at Buffalo, United States
Pearay Ogra, University at Buffalo, United States
Tobias R. Kollmann, University of Western Australia, Australia
Cecil Czerkinsky, Institut National de la Santé et de la Recherche Médicale (INSERM), France

Citation: Gomez-Duarte, O. G., Ogra, P., Kollmann, T. R., Czerkinsky, C., eds. (2022). Impact of Microbiome on Gut Mucosal Immunity in Health and Disease. Lausanne: Frontiers Media SA. doi: 10.3389/978-2-83250-402-4

Table of Contents

05 ***Editorial: Impact of Microbiome on Gut Mucosal Immunity in Health and Disease***
Oscar G. Gómez-Duarte and Pearay L. Ogra

08 ***Protective Effects of* Lactobacillus plantarum *16 and Paenibacillus polymyxa 10 Against* Clostridium perfringens *Infection in Broilers***
Li Gong, Baikui Wang, Yuanhao Zhou, Li Tang, Zihan Zeng, Huihua Zhang and Weifen Li

20 ***Bacterial and Fungal Gut Community Dynamics Over the First 5 Years of Life in Predominantly Rural Communities in Ghana***
Nelly Amenyogbe, Dennis Adu-Gyasi, Yeetey Enuameh, Kwaku Poku Asante, Dennis Gyasi Konadu, Seyram Kaali, David Dosoo, Pinaki Panigrahi, Tobias R. Kollmann, William W. Mohn and Seth Owusu-Agyei

32 ***Insight Into Polysaccharides From* Panax ginseng *C. A. Meyer in Improving Intestinal Inflammation: Modulating Intestinal Microbiota and Autophagy***
Dandan Wang, Shuai Shao, Yanqiu Zhang, Daqing Zhao and Mingxing Wang

49 ***Fecal Bacteria Implicated in Biofilm Production Are Enriched and Associate to Gastrointestinal Symptoms in Patients With APECED – A Pilot Study***
Iivo Hetemäki, Ching Jian, Saila Laakso, Outi Mäkitie, Anne-Maria Pajari, Willem M. de Vos, T. Petteri Arstila and Anne Salonen

61 ***Gut Microbial Metabolite Pravastatin Attenuates Intestinal Ischemia/Reperfusion Injury Through Promoting IL-13 Release From Type II Innate Lymphoid Cells* via *IL–33/ST2 Signaling***
Fan Deng, Jing-Juan Hu, Xiao Yang, Qi-Shun Sun, Ze-Bin Lin, Bing-Cheng Zhao, Zhi-Wen Yao, Si-Dan Luo, Ze-Ling Chen, Ying Liu, Zheng-Zheng Yan, Cai Li, Wei-Feng Liu and Ke-Xuan Liu

78 **Lactiplantibacillus plantarum*–Nomad and Ideal Probiotic***
Mario Fidanza, Pinaki Panigrahi and Tobias R. Kollmann

91 ***Profiling Tryptophan Catabolites of Human Gut Microbiota and Acute-Phase Protein Levels in Neonatal Dried Blood Specimens***
Anne-Christine Aust, Eliska Benesova, Veronika Vidova, Katerina Coufalikova, Sona Smetanova, Ivo Borek, Petr Janku, Eva Budinska, Jana Klanova, Vojtech Thon and Zdenek Spacil

107 ***GPR35 in Intestinal Diseases: From Risk Gene to Function***
Berna Kaya, Hassan Melhem and Jan Hendrik Niess

116 ***Prenatal Maternal Stress Exacerbates Experimental Colitis of Offspring in Adulthood***
Yue Sun, Runxiang Xie, Lu Li, Ge Jin, Bingqian Zhou, Huan Huang, Mengfan Li, Yunwei Yang, Xiang Liu, Xiaocang Cao, Bangmao Wang, Wentian Liu, Kui Jiang and Hailong Cao

133 ***Differential Signature of the Microbiome and Neutrophils in the Oral Cavity of HIV-Infected Individuals***
Eliana Perez Rosero, Samantha Heron, Juan Jovel, Conar R. O'Neil, Shannon Lee Turvey, Pallavi Parashar and Shokrollah Elahi

148 ***A New Formulation of Probiotics Attenuates Calcipotriol-Induced Dermatitis by Inducing Regulatory Dendritic Cells***
Beilei Xu, Shiqi Ling, Xiaoqiang Xu, Xiaochun Liu, Ao Wang, Yuan Zhou, Yang Luo, Wei Li and Xu Yao

160 ***Potential Association Between Dietary Fibre and Humoral Response to the Seasonal Influenza Vaccine***
Alissa Cait, Anna Mooney, Hazel Poyntz, Nick Shortt, Angela Jones, Aurélie Gestin, Katie Gell, Alix Grooby, David O'Sullivan, Jeffry S. Tang, Wayne Young, Darmiga Thayabaran, Jenny Sparks, Tess Ostapowicz, Audrey Tay, Sally D. Poppitt, Sarah Elliott, Georgia Wakefield, Amber Parry-Strong, Jacqui Ralston, Richard Beasley, Mark Weatherall, Irene Braithwaite, Elizabeth Forbes-Blom and Olivier Gasser

171 ***"Osteomicrobiology": The Nexus Between Bone and Bugs***
Asha Bhardwaj, Leena Sapra, Abhay Tiwari, Pradyumna K. Mishra, Satyawati Sharma and Rupesh K. Srivastava

193 ***Altered Gut Microbiome and Fecal Immune Phenotype in Early Preterm Infants With Leaky Gut***
Jose M. Lemme-Dumit, Yang Song, Hnin Wai Lwin, Claudia Hernandez-Chavez, Sripriya Sundararajan, Rose M. Viscardi, Jacques Ravel, Marcela F. Pasetti and Bing Ma

207 ***Bruton's Tyrosine Kinase Supports Gut Mucosal Immunity and Commensal Microbiome Recognition in Autoimmune Arthritis***
Rachel H. Bonami, Christina E. Thurman, Sonam Verma, Camille S. Westlake, Lindsay E. Nyhoff, Bridgette B. Barron, Andrea Reboldi and Peggy L. Kendall

222 ***Altered Intestinal Microbiomes and Lipid Metabolism in Patients With Prolonged Disorders of Consciousness***
Jie Yu, Qisheng Cheng, Fangping He, Fanxia Meng, Yamei Yu, Chuan Xu, Xinrui Wen, Lirong Hong, Jian Gao, Jingqi Li, Gang Pan, Ming D. Li and Benyan Luo

238 ***The Gut Bacteria Dysbiosis Contributes to Chronic Graft-Versus-Host Disease Associated With a Treg/Th1 Ratio Imbalance***
Yulian Wang, Lisi Huang, Tian Huang, Suxia Geng, Xiaomei Chen, Xin Huang, Peilong Lai, Xin Du and Jianyu Weng

frontiers | Frontiers in Immunology

TYPE Editorial
PUBLISHED 20 September 2022
DOI 10.3389/fimmu.2022.1005156

Check for updates

OPEN ACCESS

EDITED AND REVIEWED BY
Imtiaz Ahmed Khan,
George Washington University,
United States

*CORRESPONDENCE
Oscar G. Gómez-Duarte
oscargom@buffalo.edu
Pearay L. Ogra
plogra@buffalo.edu

SPECIALTY SECTION
This article was submitted to Microbial Immunology, a section of the journal Frontiers in Immunology

RECEIVED 28 July 2022
ACCEPTED 07 September 2022
PUBLISHED 20 September 2022

CITATION
Gómez-Duarte OG and Ogra PL (2022) Editorial: Impact of microbiome on gut mucosal immunity in health and disease. *Front. Immunol.* 13:1005156. doi: 10.3389/fimmu.2022.1005156

COPYRIGHT
© 2022 Gómez-Duarte and Ogra. This is an open-access article distributed under the terms of the Creative Commons Attribution License (CC BY). The use, distribution or reproduction in other forums is permitted, provided the original author(s) and the copyright owner(s) are credited and that the original publication in this journal is cited, in accordance with accepted academic practice. No use, distribution or reproduction is permitted which does not comply with these terms.

Editorial: Impact of microbiome on gut mucosal immunity in health and disease

Oscar G. Gómez-Duarte* and Pearay L. Ogra*

Division of Pediatric Infectious Diseases, Department of Pediatrics, Jacobs School of Medicine and Biomedical Sciences, University at Buffalo, State University of New York, Buffalo, NY, United States

KEYWORDS

gut, immune response, microbiome, bacteria, inflammation

Editorial on the Research Topic
Impact of microbiome on gut mucosal immunity in health and disease

Early studies on immunoglobulin A, the very first identified marker of adaptive immunity in the gut mucosa, quickly led the way to the constantly expanding research field of mucosal immunology. In parallel, gut microbiome, initially studied using conventional microbiology techniques, has expanded with metagenomics technology and metabolomics to uncover an unprecedented amount of information on multiple factors and regulatory pathways linking and modifying the gut immune system as well as distant organ-systems including the central nervous system. The human gut has an abundant microbial load of bacterial genus, representing >2,000 microbial species (>160 species/individual). It is estimated that for every human cell in the body, there may be as many as 1-10 bacterial cells resident in mucosal surfaces (1). These interactions between the gut's immune system and microbiome are established from early postnatal development to later stages in life to maintain a homeostatic status but also to allow the host confront the challenges imposed by infectious and non-infectious diseases. Bacteria, fungi, and viruses, major components of the gut microbiome heavily influence mucosal immunity in the mammalian host. Gut and respiratory pathogens continue to challenge the human host with mild to lethal infections. The effect of microbiome on the development of a healthy and robust gut immune response is critical for survival as demonstrated by immune response studies conducted on germ-free animal models and other systems (2). Similarly, microbiome's influence on gut immune response contributes directly or indirectly to inflammatory disorders and/or autoimmune conditions in the susceptible host.

In this Research Topic, a collection of studies using cutting-edge technology provides information on how microbiome influences gut mucosal immune responses in the healthy host and in hosts affected by inflammatory conditions. Other studies explore how modifications to the microbiome or its metabolic products have a potential as therapeutic agents in the control of intestinal or even extra-intestinal conditions.

Development of a healthy gut immune response at early age is affected by multiple factors including prematurity. Lemme-Dumit et al. provided evidence of three distinct microbiota types differentially associated with intestinal permeability, maternal breastfeeding, and immunological profiles among less than 33 week gestation early preterm infants. The *Staphylococcus epidermidis*, and *Enterobacteriaceae*-predominant microbiota types were associated with increased intestinal permeability, reduced breastmilk feeding, and less defined fecal cytokine profile. On the other hand, a lower intestinal permeability was associated with increased levels of fecal IL-1alpha/beta and a microbiota type that included a wide array of anaerobes with expanded fermentative capacity. These findings may explain, at least in part, the role of intestinal permeability in the pathogenesis of necrotizing enterocolitis in premature infants. Amenyogbe et al. evaluated bacterial and fungal fecal microbiota in rural Ghanaian children and found that bacterial communities differed systematically across the age spectrum in composition and diversity. Corresponding maternal fecal and breastmilk microbiotas had a dramatic change in the maternal postpartum microbiota, including abundance of *E. coli* and lower proportion of *Prevotella* in the first compared to the fourth week postpartum. The dynamics of mother's bacterial microbiota at the time of birth may have important consequences for children's health. Sun et al. described the possible negative effects of prenatal maternal stress on intestinal development, impaired barrier function, and gut dysbiosis in a murine model. They also considered the possible role of persistent overgrowth of *Desulfovibrio* in the offspring and its associated colitis in adulthood.

Microbial metabolites generated by individual bacterial species, a collection of different species, or as a result of the host-microbiome virtually countless metabolite combinations, have the ability to influence gut structure and function in many different ways. In this Research Topic, Kaya et al., reported on the metabolite-sensing G-protein coupled receptors (GPCRs) ability to bind to metabolites and trigger signals important for cell function. These receptors provide a link between immune system, gut microbiota, and metabolic system and some GPR35 gene variants are even implicated in gut-related diseases such as inflammatory bowel disease. Different effect of metabolites in the intestine was reported by Deng et al., the gut metabolite pravastatin attenuated intestinal ischemia/reperfusion injury by stimulating IL-13 secretion from type II innate lymphoid cells *via* IL-33/ST2 signaling, a novel mechanism that may have a potential as therapeutic use in cases of intestinal ischemia/reperfusion injury.

In addition to the effect of gut microbiome on the gut immune system, it is fascinating the effect it has in homeostasis of distant organs systems. One review by Bhardwaj et al, described how gut microbiome, prebiotics, and probiotics participate in the regulation of host bone homeostasis, and on the contrary, how dysbiosis of the gut microbiota may lead to bone disease, including osteoporosis. Yu et al., reported on how intestinal microbiome among hospitalized patients in vegetative state versus minimally conscious state significantly differs and how small-chain fatty acid's production due to this differential bacterial presence were reduced in vegetative state patients compared to other groups.

Authors also explored the potential therapeutic use of probiotics and other bacterial organisms on gut disease conditions. Fidanza et al. reviewed *Lactoplantibacillus platanarum* and its ecological and metabolic flexibility allowing it to thrive in multiple environments and making it an probiotic with potential applications for treatment or prophylaxis of a variety of disorders. Gong et al. found that *L. plantarum* and *Paenibacillus polymyxa* given to one-day chicks protected them against *Clostridium perfringens* infection through improved composition and metabolic pathways of the intestinal microbiota, intestinal structure, inflammation, and anti-apoptosis. Furthermore, Xu et al. reported on how probiotic mixtures significantly alleviated skin inflammation of chemically-induced atopic dermatitis in mice by increased production of regulatory T cells and regulatory dendritic cells in mesenteric lymph nodes. Finally, Cait et al., provided evidence on how a high fiber diet and the resulting short-chain fatty acid metabolites are associated with enhanced antibody response to seasonal influenza vaccination.

The elegant studies presented in this Research Topic using cutting-edge technology allow us to better understand the mechanisms by which gut microbiota and their metabolites affect gut immune responses as well as systemic immune responses to intrinsic and extrinsic antigenic stimuli during early or late development. It also provides evidence of microbial and metabolic signatures associated with a variety of host states of health or disease conditions. Furthermore, it provided evidence on how gut immune system modifiers, such as microbial organisms, food products and metabolites may have therapeutic potential to a variety of conditions. Regulating gut microbiota and the intrinsic and extrinsic metabolomics it may be possible to control gut immune response locally or distally. Finally, each area of research exploring the relationship between gut microbiome and gut immune system in health and disease keep uncovering more questions than answers that should be the basis for novel and exciting research in the near future.

Author contributions

Both authors made substantial contributions to the conception and design of the editorial. OG-D wrote the first draft of the manuscript and both, OG-D and PO, extensively and critically revised the draft and added important intellectual

content. Once both authors were satisfied with the final draft, they provided approval for publication.

Conflict of interest

The authors declare that the research was conducted in the absence of any commercial or financial relationships that could be construed as a potential conflict of interest.

Publisher's note

All claims expressed in this article are solely those of the authors and do not necessarily represent those of their affiliated organizations, or those of the publisher, the editors and the reviewers. Any product that may be evaluated in this article, or claim that may be made by its manufacturer, is not guaranteed or endorsed by the publisher.

References

1. Gómez-Duarte OG, Ogra PL. Development of mucosal immunity: Functional interactions with mucosal microbiome in health and disease. *CIR* (2019) 15:154–65. doi: 10.2174/1573395515666190225153529

2. Hooper LV, Wong MH, Thelin A, Hansson L, Falk PG, Gordon JI. Molecular analysis of commensal host-microbial relationships in the intestine. *Science* (2001) 291:881–4. doi: 10.1126/science.291.5505.881

frontiers in Immunology

ORIGINAL RESEARCH
published: 18 February 2021
doi: 10.3389/fimmu.2020.628374

Protective Effects of *Lactobacillus plantarum* 16 and Paenibacillus polymyxa 10 Against *Clostridium perfringens* Infection in Broilers

Li Gong[1,2], *Baikui Wang*[1], *Yuanhao Zhou*[1], *Li Tang*[1], *Zihan Zeng*[1], *Huihua Zhang*[2*] *and Weifen Li*[1*]

[1] Key Laboratory of Molecular Animal Nutrition of the Ministry of Education, College of Animal Sciences, Institute of Feed Science, Zhejiang University, Hangzhou, China, [2] School of Life Science and Engineering, Foshan University, Foshan, China

OPEN ACCESS

Edited by:
Oscar Gilberto Gomez-Duarte, University at Buffalo, United States

Reviewed by:
Zhendong Cai, Ningbo University, China
Werner Solbach, University of Lübeck, Germany

***Correspondence:**
Weifen Li
wfli@zju.edu.cn
Huihua Zhang
hhzhang2@163.com

Specialty section:
This article was submitted to Microbial Immunology, a section of the journal Frontiers in Immunology

Received: *11 November 2020*
Accepted: *31 December 2020*
Published: *18 February 2021*

Citation:
Gong L, Wang B, Zhou Y, Tang L, Zeng Z, Zhang H and Li W (2021) Protective Effects of Lactobacillus plantarum 16 and Paenibacillus polymyxa 10 Against Clostridium perfringens Infection in Broilers. Front. Immunol. 11:628374. doi: 10.3389/fimmu.2020.628374

This study aimed to investigate the protective effects of *Lactobacillus plantarum* 16 (Lac16) and *Paenibacillus polymyx*a 10 (BSC10) against *Clostridium perfringens* (Cp) infection in broilers. A total of 720 one-day-old chicks were randomly divided into four groups. The control and Cp group were only fed a basal diet, while the two treatment groups received basal diets supplemented with Lac16 (1×10^8 cfu·kg^{-1}) and BSC10 (1×10^8 cfu·kg^{-1}) for 21 days, respectively. On day 1 and days 14 to 20, birds except those in the control group were challenged with 1×10^8 cfu *C. perfringens* type A strain once a day. The results showed that both Lac16 and BSC10 could ameliorate intestinal structure damage caused by *C. perfringens* infection. *C. perfringens* infection induced apoptosis by increasing the expression of Bax and *p53* and decreasing Bcl-2 expression and inflammation evidence by higher levels of *IFN-γ, IL-6, IL-1β*, *iNOS*, and *IL-10* in the ileum mucosa, and NO production in jejunal mucosa, which was reversed by Lac16 and BSC10 treatment except for *IL-1β* ($P < 0.05$). Besides, the two probiotics restored the intestinal microbiota imbalance induced by *C. perfringens* infection, characterized by the reduced *Firmicutes* and *Proteobacteria* and the increased *Bacteroidetes* at the phyla level and decreased *Bacteroides fragilis* and *Gallibacterium anatis* at the genus level. The two probiotics also reversed metabolic pathways of the microbiota in *C. perfringens*-infected broilers, including B-vitamin biosynthesis, peptidoglycan biosynthesis, and pyruvate fermentation to acetate and lactate II pathway. In conclusion, Lac16 and BSC10 can effectively protect broilers against *C. perfringens* infection through improved composition and metabolic pathways of the intestinal microbiota, intestinal structure, inflammation, and anti-apoptosis.

Keywords: *Clostridium perfringens*, *Lactobacillus plantarum* 16, *Paenibacillus polymyx*a 10, broilers, apoptosis, immunity, microbiota, metabolic pathways

INTRODUCTION

Necrotic enteritis (NE) caused by *Clostridium perfringens* (Cp) is a severe gastrointestinal disease responsible for the annual loss of at least $ 6 billion in the poultry industry worldwide (1, 2). The disease usually occurs in two forms, including clinical and subclinical forms. The clinical form is characterized by a sudden rise in flock mortality with no premonitory signs, while the subclinical form is associated with intestinal damage, impaired absorption of nutrients, and poor overall performance in poultry (3). Moreover, as a common foodborne pathogen that affects humans, *C. perfringens* poses a serious threat to human health *via* contaminated poultry (4). Antibiotics have been used as the most effective measure to control *C. perfringens* infection in livestock (5). However, due to the emergence of antibiotic-resistant bacteria and the effect of antibiotics on the microbiome (6), there is an urgent need to find suitable alternatives to reduce the incidence of necrotic enteritis and maintain animal and human health in the post-antibiotics era.

Probiotics are live microorganisms, which when administered in adequate amounts exert their benefits on the host (7). The use of probiotics is a promising measure for the prevention of intestinal diseases, such as colitis (8), inflammatory bowel disease (9), and diarrhea (10). Besides, probiotics can protect the host against pathogen invasion by manipulating the complex gut ecosystems through competitive exclusion, production of antimicrobial compounds, stimulation of the host immune system development, *etc* (11). Fukata et al. (12) revealed that *Lactobacillus acidophilus* or *Streptococcus faecalis* could reduce *C. perfringens* infection in young chickens. Numerous other studies have also shown that some microorganisms, including *Bacillus* (13), *Lactobacilli* (14), *Enterococci* (15), and *yeast* (16), could alleviate the severity and damage of NE in chicken *via* different mechanisms. *Lactobacillus johnsonii* BS15 was reported to prevent NE by ameliorating lipid metabolism and intestinal microflora (14), while *Lactobacillus fermentum* 1.2029 regulated the expression levels of cytokines and TLR in chicken (17). Our previous studies also found that *Lactobacillus plantarum* Lac16 and *Paenibacillus polymyxa* BSC10 could inhibit the growth and virulence-associated gene expressions of *C. perfringens in vitro* (unpublished data) and regulate the mRNA expression of cytokines and TLR in chicken macrophage (HD11) cell line infected with *C. perfringens* (unpublished data). Therefore, the present study aimed to investigate the protective effects of Lac16 and BSC10 against *C. perfringens* in broilers.

MATERIALS AND METHODS

Bacterial Strain Preparation

The *Lactobacillus plantarum* 16 (Lac16) (CCTCC, NO. M2016259) was isolated by our laboratory and preserved in China Center for Type Culture Collection. *Paenibacillus polymyxa 10* (BSC10) (CGMCC 1.10711) was obtained from the China General Microbiological Culture Collection Center. *Clostridium perfringens* (ATCC13124) was purchased from Guangdong Microbial Culture Collection Center.

Probiotics Lac16 and BSC10 were cultured in MRS or Luria–Bertani (LB) broth overnight at 37°C in an anaerobic system or a shaking incubator, respectively. *Clostridium perfringens* was cultured in Reinforced Clostridium Medium for 24 h under an anaerobic environment. The bacteria were harvested after centrifugation at 4,000 × g for 15 min at 4°C, respectively. After three-time washing with sterile phosphate buffer saline (PBS, pH 7.3), the prepared *Lactobacillus* and *Bacillus* powders (1×10^{10} cfu/g) were diluted with starch and added into the basal diet to a final concentration of 10^8 cfu/kg, respectively. The same amount of starch was added to each group to compensate for the difference in the nutrient composition of the diets.

Chicken Husbandry and Experimental Design

A total of 720 *Cobb* 500 broiler chicks were purchased from ZhengDa Broilers Development Center of Zhejiang University (Hangzhou, China) and reared in XinXin Broiler Farm (Jiaxing, China). These 1-day-old chicks with similar weights were randomly allocated to four groups with six replicates per group and 30 chickens per replicate. The two probiotic treatment groups received the diets consisting of Lac16 and BSC10 (10^8 cfu·kg^{-1} feed) for 21 days, respectively, while the control group and Cp group were only fed the basal diet (**Table 1**) during the whole trial. On day 1 and days 14 to 20, birds of all groups except the control group were orally challenged with 1×10^8 cfu *C. perfringens* type A strain once a day. The chickens were exposed to a 24 h lighting device and kept with ambient temperature gradually decreasing from 32°C to 26°C at the rate of 2°C per week. Broilers were provided freshwater and feed *ad libitum*. The study was carried out according to the guidelines of the Animal Care and Use Committee of Zhejiang University.

TABLE 1 | Ingredients and nutrition composition of basal diet (%).

Item	1–21 d
Ingredients	
Corn	60.00
Soybean meal	28.50
Fish meal	2.00
Wheat middling	4.50
Dicalcium phosphate	1.30
Limestone	2.25
50% choline chloride	0.15
Salt	0.30
Vitamin and mineral premix1	1.00
Total	100.00
Calculated Nutrient Level	
CP	22.39
Total P	0.70
Ca	1.00
Lys	1.17
Met + Cys	0.65
Met	0.48
ME (MJ/kg)	12.22

[1]*Premix compound each kilogram contained: vitamin A, 12,500 IU; vitamin D, 32,500 IU; vitamin E, 18.75 IU; vitamin K, 32.65 mg; vitamin B2, 6 mg; vitamin B12, 0.025 mg; Biotin, 0.0325 mg; Folic acid, 1.25 mg; Nicotinic acid, 50 mg; vitamin B3, 12 mg; Cu, 8 mg; Fe 80 mg; Zn, 75 mg; Mn, 100 mg; Se, 0.15 mg; I, 10.35 mg.*

Sample Collection and Treatment

At the end of the experimental period, two chickens per cage with a weight close to the average of the group were selected and immediately slaughtered by exsanguination. The intestine was collected by simultaneously washing with cold sterile PBS to remove the attached impurity, and the jejunal mucosa and ileum mucosa were gently scraped. Jejunal samples were diluted with nine-time volumes of sterile ice-cold normal saline (0.9%) based on the sample weight and then homogenized using a hand-held glass homogenizer. The tissue supernatants were collected by centrifuging at 3,500×g for 10 min at 4°C, and the concentration of protein was determined by a BCA protein assay kit according to the manufacturer's instruction (Pierce, Rockford, IL) and stored at −80°C for further study.

Ileal Morphology and Immunohistochemistry

Approximately 1 cm of distal ileum was dissected for histomorphology analysis. Ileal tissues were fixed (in 4% paraformaldehyde overnight), dehydrated, and embedded in paraffin according to the standard procedure (18). The paraffin-embedded tissues were cut into 5 μm thick and subsequently subjected to hematoxylin and eosin staining and observed by a light microscope (Nikon Eclipse80i, Tokyo, Japan). The immunohistochemistry staining was carried out as described previously with minor modification (18). Briefly, after dewaxing and rehydration, the tissue sections underwent microwave antigen retrieval in sodium citrate buffer (0.01 M, pH 6.0) for 20 min. Endogenous peroxidase activity was blocked with 3% hydrogen peroxide and then using 10% goat serum (ZSGB-BIO, Beijing, China) as a non-specific binding block for 30 min at room temperature. The sections were incubated overnight at 4°C with polyclonal rabbit antibody Bax (BIOSS, Beijing, China) or BCl-2 (BIOSS, Beijing, China). The tissues were incubated with Biotinylated secondary antibodies (Polink-2 plus polymer HRP anti-rabbit or anti-mouse, ZSGB-BIO, Beijing, China) and further visualized with a diaminobenzidine-tetrachloride (DAB) kit (TIANGEN RA110, Beijing, China). All sections were counterstained with hematoxylin for 3 min.

TUNEL Assay

Apoptosis in ileum tissue was analyzed by the terminal dUTP-nick end labeling kit (Roche, Germany). Briefly, the paraffin-embedded tissue sections of ileum were incubated with proteinase K working solution at 37°C for 25 min and washed three times with PBS, and then incubated with permeabilization solution for 20 min. Following three times with PBS, the samples were incubated with TUNEL reaction mixture for 60 min at 37°C in a humidified chamber and strained with DAPI for 10 min and rinsed with PBS for three times. The cell nuclei were identified using UV light microscopy (Nikon, Japan) and TUNEL-positive cells were identified as brilliant green.

RNA Extraction and RT-qPCR

The RNA was extracted using Takara RNAiso Plus Kit (Japan) following the manufacturer's protocol. The purity and concentration of total RNA were determined using a Nanodrop Spectrophotometer (ND-2000, Thermo Fisher Scientific). The reverse transcription of total RNA was performed by Reverse Transcriptase M-MLV Kit (RNase H-) according to the manufacturer's instruction. The qRT-PCR assay was conducted with the ABI 7500 fluorescence detection system using SYBR green (Takara, SYBR Premix Ex Taq TM II Kit) detection. Each sample was measured in duplicate. Relative quantitation of all gene expression was calculated using the $2^{-\triangle\triangle Ct}$ method, and the β-actin served as the internal reference gene (19). Primers used in the current study were designed using the Primer Express 3.0 software (Applied Biosystems, Foster City, CA), and the specificity of primers was assessed by melting curve analysis. Primers are listed in **Table 2**.

Detection of iNOS Activity and NO Production

The activity of inducible nitric oxide synthase (iNOS) and production of Nitric oxide (NO) in the jejunal mucosa were measured strictly according to the manufacturer's protocols (Jiancheng Bioengineering Institute, Nanjing, China).

DNA Extraction and Library Construction of Cecum Content

The cecal contents of twelve chickens from four groups (Control, Cp, Cp+Lac16, Cp+BSC10) were collected on day 21. The fecal

TABLE 2 | Primers used in the experiment.

Gene	Primer sequence (5′–3′)	Accession number
Bax	GTGATGGCATGGGACATAGCTC TGGCGTAGACCTTGCGGATAA	XM_015274882.1
P53	CCCATCCTCACCATCCTTACA CTTCAGCATCTCATAGCGGC	XM_420232
Occludin	TCATCCTGCTCTGCCTCATCT CATCCGCCACGTTCTTCAC	NM_205128.1
Claudin1	CATACTCCTGGGTCTGGTTGGT GACAGCCATCCGCATCTTCT	NM_001013611.2
MUC-2	TTCATGATGCCTGCTCTTGTG CCTGAGCCTTGGTACATTCTTGT	XM_421035
ZO-1	CTTCAGGTGTTTCTCTTCCTCCTC CTGTGGTTTCATGGCTGGATC	XM_413773
Caspase-9	TCAGACATCGTATCCTCCA AAGTCACAGCAGGGACA	XM_424580.6
Caspase-3	ACTCTGGAAATTCTGCCTGATGAC CATCTGCATCCGTGCCTGA	NM_204725.1
BCL-2	GATGACCGAGTACCTGAACC CAGGAGAAATCGAACAAAGGC	NM_205339.2
IL-1β	CGACATCAACCAGAAGTGCTT GTCCAGGCGGTAGAAGATGA	NM_204524.1
IL-6	CAGGACGAGATGTGCAAGAA TAGCACAGAGACTCGACGTT	NM_204628.1
IL-10	ACCAGTCATCAGCAGAGCAT CCTCCTCATCAGCAGGTACTC	NM_001004414
TGF-β	TCTCGGAGCAGCGGATAGA AATCCAAGGTTCCTGTCTCTGT	JQ423909.1
iNOS	CACGTGTTAAGGATGCCCCT GCCCAATAGCCACCTTCAGT	NM_204961
IFN-γ	ACACTGACAAGTCAAAGCCGC AGTCGTTCATCGGGAGCTTG	NM_205149
β-actin	CAACACAGTGCTGTCTGGTGGTA ATCGTACTCCTGCTTGCTGATCC	NM 205518

DNA was extracted using TIANamp DNA Stool Mini Kit (TianGen, Beijing), and the quality was checked by agarose gel electrophoresis. All of the extracted DNA samples were stored at −80°C for further processing.

DNA library was constructed by TruSeq Nano DNA LT Library Preparation Kit (FC-121-4001). DNA was fragmented using dsDNA Fragmentase (NEB, M0348S) by incubating at 37°C for 30 min. Library construction begins with fragmented cDNA. Blunt-end DNA fragments are generated using a combination of fill-in reactions and exonuclease activity, and size selection is performed with provided sample purification beads. An A-base is then added to the blunt ends of each strand, preparing them for ligation to the indexed adapters. Each adapter contains a T-base overhang for ligating the adapter to the A-tailed fragmented DNA. These adapters contain the full complement of sequencing primer hybridization sites for single, paired-end, and indexed reads. Single- or dual-index adapters are ligated to the fragments and the ligated products are amplified with PCR by the following conditions. The initial denaturation was at 95°C for 3 min, 8 cycles of denaturation at 98°C for 15 sec, annealing at 60°C for 15 s, and extension at 72°C for 30 s, and then final extension at 72°C for 5 min.

Metagenomics Analysis of Taxonomic Profiling and Functional Profiling

Raw sequencing reads were processed to obtain valid reads for further analysis. Assessment of sequence quality was used in fastqc. The host genome sequence was removed using the Best Match Tagger (BMTagger), referred to the genome of gga_ref_Gallus_gallus-5.0. Using fastq_to_fasta, the fq format data was converted to fasta format, which further used the filter_fasta.py command in QIIME to remove the host genome sequence. The remaining sequence was regarded as the intestinal flora DNA sequence for further analysis. The species composition was analyzed using MetaPhlAn2 (20), the cladogram was conducted with GraPhlAn, and the heatmap was drawn with metaphlan_hclust_heatmap.py The functional profiling of microbiota was analyzed using HUMAnN2, referred to the uniref90_ec_filtered_diamond database and the uniref50_ec_filtered_diamond database (21).

Principal component analysis of gene family was performed using prompt R package. Heatmap of metabolic pathway abundance was drawn using the fold-change value (log2 transformed) using the pheatmap R package. The Kyoto Encyclopedia of Genes and Genomes (KEGG) pathway was analyzed using the KEGG online service tools' KEGG mapper.

Statistical Analysis

All data were analyzed by a one-way analysis of variance (ANOVA) followed by Tukey multiple comparisons procedure using SPSS 22.0 software (SPSS Inc., Chicago, IL, USA). Statistical significance was declared at $P < 0.05$ and trend at $P < 0.1$. The data were expressed as mean ± SD, and graphs were generated by GraphPad Prism 7.0 software. Statistical analyses and data visualization for fecal microbiota were conducted using the R program (version 3.6.1).

RESULTS

Lac16 and BSC10 Alleviated Intestinal Mucosal Injury Induced by *C. perfringens* Infection

Hematoxylin–eosin staining showed that the damaged intestinal structure and shorter villus were observed in *C. perfringens*-infected birds, which were recovered by probiotics treatment (**Figure 1A**). Besides, the *C. perfringens* infection significantly increased the expression of intestinal barrier-related genes, such as *claudin1* (*CLDN1*), *occludin*-1 (*ZO-1*), and *mucin*-2 (*MUC2*) in the ileum ($P < 0.05$). However, the expression of *OCLN* in the Cp + Lac16 group was significantly lower compared with the Cp group (**Figure 1B**).

Lac16 and BSC10 Attenuated Apoptosis Induced by *C. perfringens* Infection

The mRNA expression levels of pro-apoptosis genes in the ileum mucosa, including *Bax, p53*, *Caspase-9* were up-regulated in *C. perfringens*-infected birds ($P < 0.05$). However, Lac16 and BSC10 treatment downregulated the expression levels of the pro-apoptosis genes except for *Caspase-9* in the Lac16 group ($P < 0.05$). Moreover, a significant increase in *Bcl-2* mRNA level was observed in the Lac16 group compared to the *C. perfringens*-infected birds ($P < 0.05$) (**Figure 2A**). The result of Bax immunohistochemistry demonstrated that compared with the control group, *C. perfringens* infection increased the number of Bax positive cells, while Lac16 restored them to a normal level. BSC10 also showed a slight decrease in the number of Bax positive cells compared with the Cp group (**Figure 2B**). *C. perfringens* infection significantly decreased the number of Bcl-2-positive cells, while probiotic treatment alleviated the decrease (**Figure 2C**). TUNEL assay results demonstrated that *C. perfringens* infection enhanced the number of positive cells in the ileum, while there was a decline following Lac16 or BSC10 treatment (**Figure 2D**).

Lac16 and BSC10 Down-Regulated *C. perfringens*-Induced Inflammatory Response

C. perfringens infection increased the expression of anti-inflammatory cytokine *IL-10* and pro-inflammatory cytokines, *IFN-γ, IL-6, IL-1β*, and *iNOS* ($P < 0.05$) (**Figure 3A**), while Lac16 or BSC10 treatment significantly decreased the expression levels of *IL-6* ($P < 0.05$), *iNOS* ($P < 0.05$), *IFN-γ* ($P < 0.05$), and *IL-10* ($P < 0.1$ and $P < 0.05$, respectively). Compared with the Cp group, Lac16 supplementation down-regulated *TGF-β* expression ($P < 0.05$). Nitric oxide (NO) and inducible nitric oxide synthase (iNOS) actively participated in the host defense in response to *C. perfringens* infection. As depicted in **Figures 3B, C**, the highest iNOS activity and NO production in the jejunal mucosa was observed in the Cp group but decreased following Lac16 or BSC10 treatment.

Lac16 and BSC10 Re-Shifted the Intestinal Microbiota Composition in Cp-Infected Broilers

As shown in **Supplemental Figure S1**, phylogenetic analysis revealed the most abundant composition of fecal microbiota at

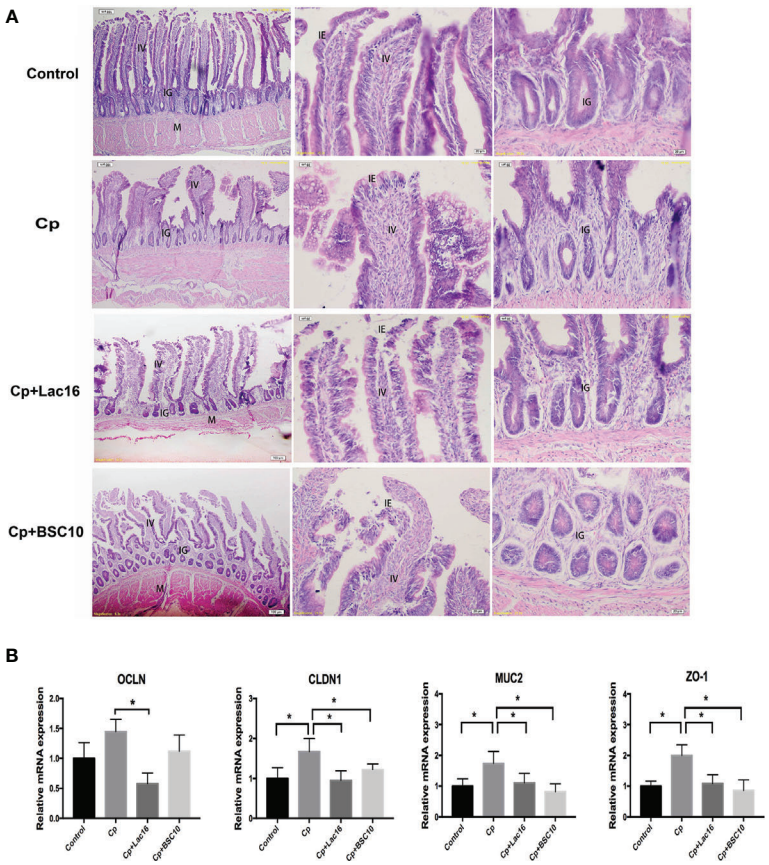

FIGURE 1 | Probiotics *Lactobacillus plantarum* 16 (Lac16) and *Paenibacillus polymyxa* 10 (BSC10) alleviated intestinal mucosal injury induced by *Clostridium perfringens* (Cp) infection. **(A)** From the left to the right column, hematoxylin–eosin (HE) staining showing the integral morphology of the ileum, the villus, and the grand in the Control, Cp, Cp + Lac16, and Cp + BSC10 groups. Magnification, ×100, ×200, and ×200, respectively. IV, intestinal villus; IE, intestinal epithelium; IG, intestinal glands; M, muscularis. n = 6/group. **(B)** The mRNA expression of barrier-related genes assessed by RT-PCR. CLDN, Claudin; OCLN1, Occludin 1; ZO-1, Zonula occludins-1; MUC2, Mucin 2. Data were expressed as mean ± SD (n = 12). *indicates statistically significant difference ($P < 0.05$).

the family, genus, and species levels among all groups. At the family level, *Rikenellaceae, Bacteroidaceae*, and *Oscillospiraceae* were dominant. The composition of gut microbiota at the phylum level is shown in **Figure 4A**. The predominant phyla were *Firmicutes, Bacteroidetes*, and *Proteobacteria*, which were more than 99%. *C. perfringens* infection decreased the relative abundance of *Firmicutes* and *Proteobacteria*, and increased *Bacteroidetes*, while probiotic treatment increased the relative abundance of *Firmicutes* and decreased *Bacteroidetes*. At the genus level, the gut microbiota was dominated by genus *Allistipes*, accounting for 50.41%, followed by *Bacteroides* and *Oscillibacter*, accounting for 16.97 and 13.08%, respectively. Lac16 or BSC10 treatment enhanced the relative abundance of *Oscillibacter* but decreased *Allistipes* and *Bacteroides* (**Figure 4B**). Principal Components Analysis (PCA) showed the different clusters of microbial communities among the four groups, with PC1 accounting for 20.6% of the total variation and PC2 accounting for 15.7% (**Figure 4C**). Four bacterial species that were enriched in all groups included, *Alistipes, Bacteroides, Osciliibacter*, and *Escherichia* (**Figure 4D**). *C. perfringens* infection enriched *Gallibacterium anatis* and those that decreased included *Erysipellotrichaceac, Subdoligranulum, Anaerotruncus, Ruminococcus, Pseudoflavonifractor*, and *Oscillibacter*, which were found to be increased in the probiotic treatment groups. The abundance of *Bacteroides fragilis* was significantly decreased in the Cp + BSC10 group, compared with the Cp and Cp + Lac16 group.

Functional Capacity of the Gut Microbiome Related to Metabolic Pathways

The functional capacity of the gut microbiome was evaluated using metagenomic sequencing data. We classified the predicted genes by aligning and assigning them to pathways using the HUMAnN2 database. PCA analysis of the gene family abundance revealed dramatic changes between the Cp group and other groups (**Supplemental Figure S2**). *C. perfringens* infection changed the microbiota composition and metabolic

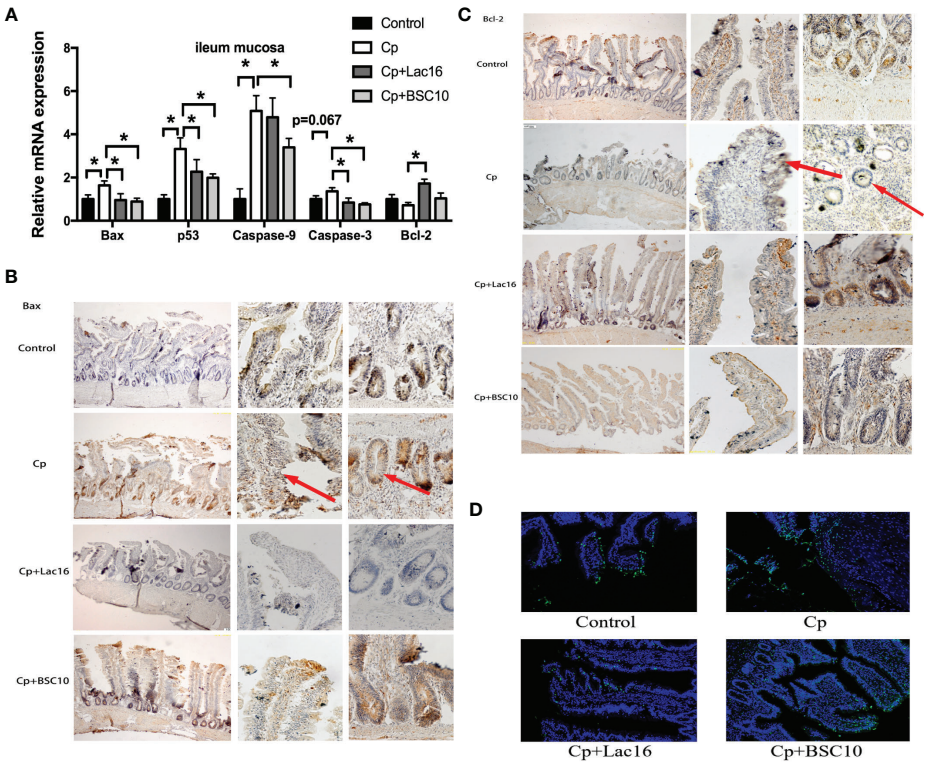

FIGURE 2 | Probiotics treatment attenuated apoptosis induced by *Clostridium perfringens* (Cp) infection. The apoptosis-related gene expression in the ileum mucosa **(A)** (n = 12/group). Representative images of the immunohistochemical staining of Bax **(B)** and Bcl-2 **(C)** in the ileum mucosa (n = 6/group). The positive cells are stained brown. From the left to the right column, the integral morphology of the ileum, the villus, and the grand are seen (magnification ×100, × 400, and × 400, respectively). **(D)** TUNEL immunofluorescence data showing the distribution of apoptosis cells (brilliant green) in the ileum mucosa. Magnification, × 200. n = 6/group. * indicates statistically significant difference ($P < 0.05$).

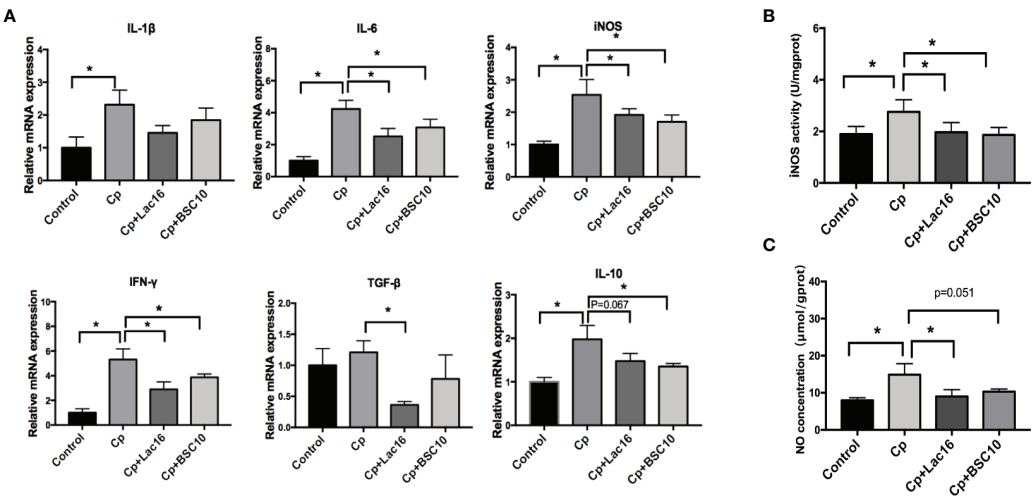

FIGURE 3 | *Lactobacillus plantarum* 16 (Lac16) and *Paenibacillus polymyxa* 10 (BSC10) down-regulated the *C. perfringens*-induced inflammatory response. **(A)** cytokines gene expression profiles in the ileum mucosa determined by RT-qPCR. The iNOS activity **(B)** and NO production **(C)** in jejunal mucosa were measured using commercial kits. Results are presented as mean ± SD (n = 12/group, *represents significant differences ($P < 0.05$).

pathways, including enhancing B-vitamin biosynthesis (for example, folate biosynthesis as shown in **Supplemental Figure S3**), peptidoglycan biosynthesis (**Supplemental Figure S4**), amino acid biosynthesis and ribonucleotide biosynthesis, *etc*, and decreased pyruvate fermentation to acetate and lactate II pathway, which was reversed by probiotic supplementation (**Figure 5**).

DISCUSSION

Numerous studies have demonstrated that probiotics exert antimicrobial activity against *C. perfringens* through different mechanisms. In our previous study, increased intestinal lesion scores and decreased growth performance of broilers were observed after *C. perfringens* challenge, which was ameliorated in broilers pretreated with Lac16 and BSC10 (unpublished data). Therefore, the current study aimed to investigate the protective effects of Lac16 and BSC10 against *C. perfringens* in broilers through the regulation of the intestinal mucosal structure, apoptosis, inflammation, and intestinal microbiota.

Gut integrity is a prerequisite for maintaining the host homeostasis. The intestinal mucosal barrier comprises connecting epithelial cells that are overlaid by host-secreted mucous layer and serve as the first line of defense against pathogens and potentially harmful commensal bacteria (22, 23). Impaired intestinal mucosal barrier caused by intestinal pathogens compromises the immune tolerance of the intestines and causes a systemic inflammatory response, which aggravates systemic immune response and host body damage (24). Consistent with a previous study (25), the present study demonstrated that probiotics Lac16 and BSC10 treatment could improve the intestinal morphology of *C. perfringens* infected broilers. MUC2 is the main component of mucins which binds several pathogens and inhibits external bacterial access to the epithelial cells (26). Previous studies have shown that the expression of MUC2 is suppressed in infected broilers (27, 28). However, Fasina et al. (29) reported that *Salmonella Typhimurium* infection increased the number of goblet cells and mucin level in the jejunum of broilers, indicating that the infected birds can capture and eliminate the pathogens from the epithelial surface by enhancing mucin expression (30).

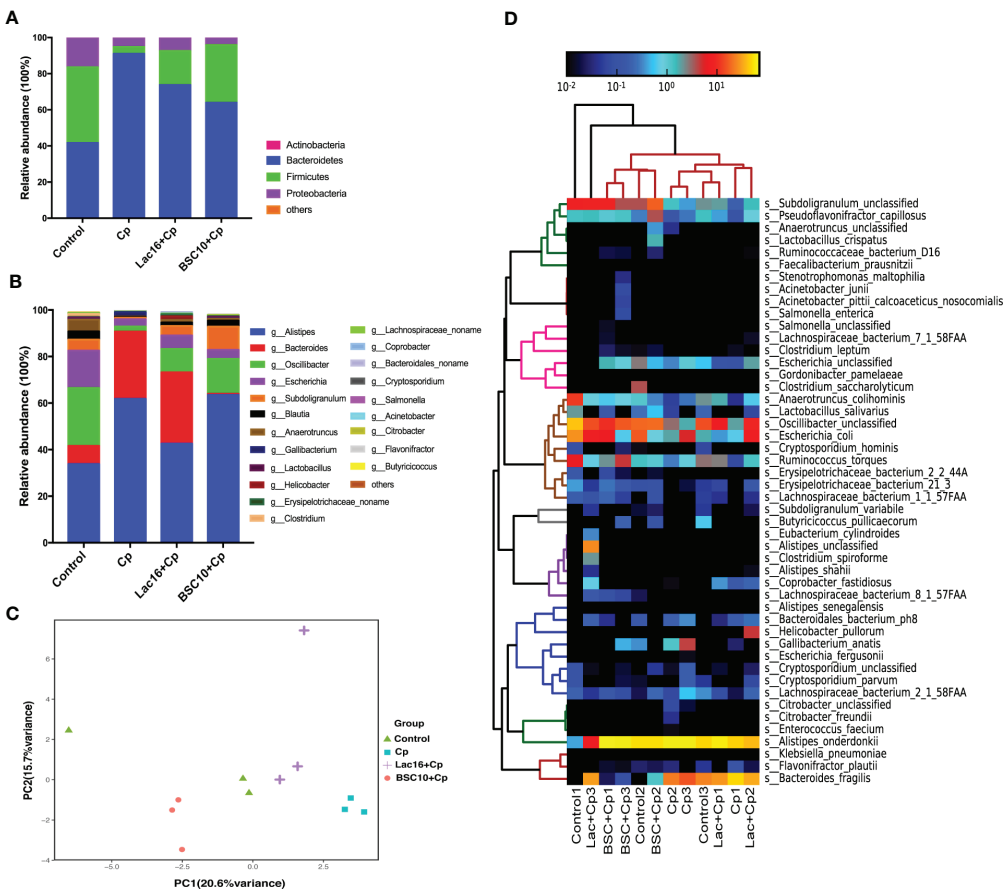

FIGURE 4 | Bacterial taxonomic composition of cecum contents. **(A)** The relative abundance of bacterial phyla (mean of each group); **(B)** The top 15 genus abundance (mean of each group); **(C)** Principal component analysis of the dissimilarity among the microbial samples using prompt R package; **(D)** Heatmap of species abundance by MetaPhlAn2. n = 3/group.

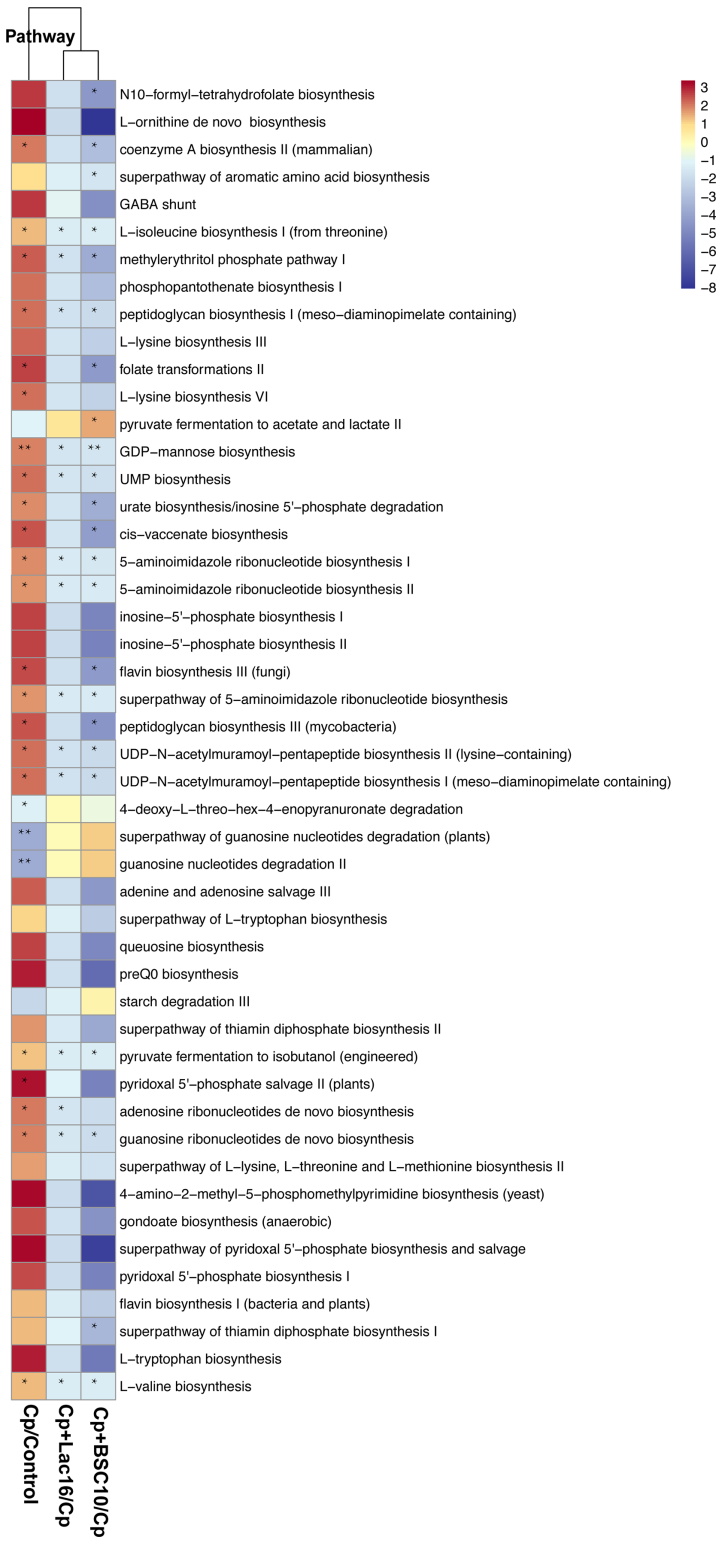

FIGURE 5 | The functional profile of cecum contents. Differences in metabolic pathways expression of the microbiota among different treatment groups evaluated using the HUMAnN2 metabolic analysis network. The representative metabolic pathway is selected by a one-way ANOVA test, and the fold changes of pathway abundance were calculated using the formula Cp/Control, Cp + Lac16/Cp, and Cp + BSC10/Cp. The significant difference is defined as the fold change > 2 or fold change < 0.5. A heatmap is drawn using the fold-change value (log_2 transformed) of the metabolic pathway abundance using the pheatmap R package. * indicates statistically significant difference ($P < 0.05$).

We also found that the MUC2 expression was significantly increased in *C. perfringens* infected broilers but decreased after probiotic supplementation. Our results may unravel novel strategy for improving mucus barrier to inhibit *C. perfringens* infection. Occludin and claudin are two of the most important components of tight junctions, and they exhibit beneficial effects on epithelial barrier function (31). Similar with the result of MUC2 expression, the present study showed that *C. perfringens* infection significantly up-regulated the relative expression levels of ZO-1 and CLDN1, which was contrary to results from previous studies (32, 33). One plausible explanation was that up-regulating the expression levels of barrier-related genes in infected chicken was beneficial for decreasing *C. perfringens* to pass through the epithelial layers and intestinal damage. However, the probiotic supplementation could decrease the number of *C. perfringens* and improve intestinal health status, which resulted in the decreased expression of occludin and claudin.

Apoptosis is regulated by the dynamic balance between the expression of pro-apoptosis proteins, such as Bax, and the anti-apoptosis protein, such as Bcl-2. Once the imbalance occurs, cytochrome c is released from the mitochondria and subsequently activates Apaf1/Caspase 9 and downstream executioner Caspase 3, thereby initiating cell apoptosis (34). p53 is a multiple function protein that induces apoptosis by promoting the expression of pro-apoptosis genes, such as Bax, and inhibits anti-apoptosis genes, such as survivin, thereby activating the caspase-dependent pathway and ultimately triggering apoptosis (35). Wu et al. (36) reported that *Lactobacillus rhamnosus* GG stimulates apoptosis by increasing p53 expression and decreasing Bcl-2 and Bcl-xl protein in the ilea of HRV-infected pigs. In the present study, the results of mRNA expression and immunohistochemistry of apoptosis-related genes showed that the probiotics could ameliorate *C. perfringens*-induced apoptosis in the ileum by up-regulating anti-apoptosis genes and down-regulating pro-apoptosis genes in broilers, and these findings were consistent with previous findings (37). Moreover, p53 mRNA expression in the probiotics groups was down-regulated compared with the Cp group, suggesting that the probiotics inhibited cell apoptosis in the ileum through the p53 signaling pathway during *C. perfringens* infection.

Accumulating evidence demonstrates that iNOS-derived NO and pro-inflammatory cytokines exert multiple modulatory effects on the host immune response against various infections (38, 39). Besides, pro-inflammatory cytokines modulate host immunity against multiple pathogens through differentiation and proliferation of immune cells, apoptosis, and NO production (40). However, excessive inflammatory responses cause tissue injury. The increase in NO production and iNOS activity and increased expression of pro-inflammatory cytokines, such as *IL-1β, IL-6, iNOS*, and *IFN-γ* demonstrate that *C. perfringens* infection induces a strong inflammatory response and causes severe tissue damage (41). However, in the present study, probiotics reduced the inflammatory response, thus inhibiting excessive inflammatory damage in infected broilers. Similar results have also been observed in birds infected with *Salmonella enteritidis* (42) and *Escherichia coli* (43). Interleukin-10 is an anti-inflammatory cytokine that inhibits T cell proliferation and the production and function of many proinflammatory cytokines (44). In the present study, the level of *IL-10* decreased following treatment with the probiotics in *C. perfringens* infected broilers, and this was attributed to a decreased inflammatory response.

The microbiota plays a major role in host growth and health and significantly contributes to the regulation of the host immune system, nutrient synthesis, energy metabolism, and prevention of enteric pathogen infection (45). The gut microbial composition and function are reported to be modulated by dietary probiotic supplementation (46). The increase in *Firmicutes* contributes to energy efficiency, while the *Firmicutes/Bacteroides* ratio is associated with growth performance and host health (47, 48). A high proportion of *Proteobacteria* in the gut is an indicator of metabolic disorders, immune disorders, and an unstable gut microbial community structure in the host (49). In the present study, increased *Firmicutes/Bacteroidetes* ratio and a decline in *Proteobacteria* were associated with improved intestinal health in broilers supplemented with probiotics.

Bacteroides fragilis is generally regarded as a gut commensal and leads to an increased risk of infection and disease when it leaks into the bloodstream or surrounding tissue (50). Even though *Bacteroides fragilis* has an anti-inflammatory property, toxigenic *B. fragilis* induces intestinal inflammation and can cause bowel disease and colon cancer (51). *Gallibacterium* is an indigenous bacterial pathogen in chicken and one of the major pathogens causing reproductive tract disorders in laying hens (52). Butyrate is an important energy source for gut enterocytes, and can reduce the inflammatory response and gastrointestinal pathogens, regulate the gut bacterial ecology, and stimulate villi growth (53, 54). Two probiotics increased some beneficial bacteria and butyrate-producing bacteria, such as *Ruminococcus, Oscillibacter, Pseudoflavonifractor*, and *Erysipellotrichaceac and* decreased *Gallibacterium* in *C. perfringens*-infected birds. In addition, BSC10 decreased *Bacteroides fragilis*. Together with the results of the PCA, we speculated that the two probiotics could restore the intestinal microbiota disturbance induced by *C. perfringens* infection with minor differences.

Alterations in the intestinal microflora composition are closely related to the metabolic alterations in the gut microbiota. In the present study, *C. perfringens* infection changed the microbiota composition and metabolic pathways, including enhancing B-vitamin biosynthesis, peptidoglycan biosynthesis, amino acid biosynthesis, and ribonucleotide biosynthesis, etc., and decreased pyruvate fermentation to acetate and lactate II pathway, which were reversed by probiotic supplementation. Acetate and lactate are known to inhibit the growth of gut pathogens, suggesting that probiotics exert antibacterial properties by increasing the production of acetate and lactate in response to *C. perfringens*. B-vitamins are important in numerous metabolism processes, including fat and carbohydrate metabolism and DNA synthesis. Hosts cannot produce enough B-vitamins and have to be supplemented either from the diet or the gut microbiota (55). An increased risk of colitis correlates with a deficiency of genetic pathways involved in polyamine transport and B vitamin biosynthesis (56, 57). Dubin et al. (58) found that three modules

involved in the biosynthesis of B vitamins (riboflavin (B2), pantothenate (B5), and thiamine (B1)) were more abundant in colitis free patients. Besides, Ford et al. (59) reported that high-dose vitamin-B supplementation reduced oxidative stress and inflammation. Inconsistent with some previous studies, the present study showed that the vitamin-B biosynthetic pathway was enriched in the Cp group but decreased in the probiotics group. We speculated that *C. perfringens* induced a compensatory synthesis of vitamin-B against oxidative damage and inflammation, while *Lactobacillus* and *Bacillus* synthesized vitamin-B in the gut to maintain normal levels in the organism, hence no need to supply exogenous Vitamin-B after probiotic treatment. Peptidoglycan (PGN) is a component of the cell wall in both Gram-positive and Gram-negative bacteria, and it triggers inflammatory responses through multiple pattern-recognition receptors (60). The most well-defined sensors of the peptidoglycan are NOD-like receptors (NLRs), which promote pathogen clearance by inducing the secretion of pro-inflammatory cytokines and chemokines and other host defense pathways, including autophagy (61). Peptidoglycan predominantly induces the Th1 immune response. Besides, bacteria-derived peptidoglycan can activate Paneth cells to produce defensins that protect the host from pathogenic bacteria (62). Therefore, in the present study, downregulation of the peptidoglycan biosynthetic pathway in the probiotic groups indicated that probiotics might protect against *C. perfringens*-infections by inhibiting excessive inflammatory response, and these findings were also consistent with the results of cytokines expression levels in the ileum mucosa.

CONCLUSION

In our study, the two probiotics have similar molecular mechanism against *C. perfringens* infection, including improving the composition and metabolic pathways of the intestinal microbiota, intestinal structure, inflammation, and anti-apoptosis. There are some differences in anti-apoptosis and the composition and metabolic pathways of the intestinal microbiota of these two probiotics.

DATA AVAILABILITY STATEMENT

The datasets presented in this study can be found in online repositories. The names of the repository/repositories and accession number(s) can be found below: https://www.ncbi.nlm.nih.gov/ sra/PRJNA675467.

ETHICS STATEMENT

The animal study was reviewed and approved by the Animal Care and Use Committee of Zhejiang University.

AUTHOR CONTRIBUTIONS

WL, LG, and HZ conceived and designed the experiments. LG and BW performed the experiments. LG and WL analyzed the data. LG, LT, and ZZ made the figures. LG and WL wrote the paper. WL, YZ, and HZ revised the manuscript. All authors contributed to the article and approved the submitted version.

FUNDING

This study is supported by the National Natural Science Foundation of China (No. 31472128 and 31672460), the Natural Science Foundation of Zhejiang Province (No. LZ20C170002), National High-Tech R&D Program (863) of China (No. 2013AA102803D), the Major Science and Technology Project of Zhejiang Province (No. 2006C12086), PRC.

SUPPLEMENTARY MATERIAL

The Supplementary Material for this article can be found online at: https://www.frontiersin.org/articles/10.3389/fimmu.2020.628374/full#supplementary-material

Supplementary Figure 1 | Phylogenetic analysis of the microbiota composition.

Supplementary Figure 2 | Principal component analysis of the gene family using the prompt R package.

Supplementary Figure 3 | KEGG map of the folate biosynthesis (map 00790) pathway. The fold changes of pathway abundance are calculated using the formula Cp/Control, Cp + Lac16/Cp, and Cp + BSC10/Cp. The significant difference is defined as the fold change >2 or fold change <0.5. The up-regulated, fold changes are labeled as green, blue, and purple, respectively, while the down-regulated fold changes are labeled as red, yellow, and pink, respectively. The brown color represents the collection of green, yellow, and pink, while the gray color represents the collection of red, blue, and purple.

Supplementary Figure 4 | KEGG map of the peptidoglycan biosynthetic (map 00550) pathway. The fold changes of pathway abundance are calculated using the formula Cp/Control, Cp + Lac16/Cp, and Cp + BSC10/Cp. The significant difference is defined as the fold change >2 or folds change <0.5. The up-regulated fold changes are labeled as green, blue, and purple, while the downregulated are labeled as red, yellow, and pink. The brown color represents the collection of green, yellow, and pink, while the gray color represents the collection of red, blue, and purple.

REFERENCES

1. Timbermont L, Haesebrouck F, Ducatelle R, Van Immerseel F. Necrotic Enteritis in Broilers: An Updated Review on the Pathogenesis. *Avian Pathol* (2011) 40:341–7. doi: 10.1080/03079457.2011.590967
2. Wade B, Keyburn AL, Seemann T, Rood JII, Moore RJ. Binding of Clostridium Perfringens to Collagen Correlates with the Ability to Cause Necrotic Enteritis in Chickens. *Vet Microbiol* (2015) 180:299–303. doi: 10.1016/j.vetmic.2015.09.019
3. Kaldhusdal M, Schneitz C, Hofshagen M, Skjerve E. Reduced Incidence of Clostridium Perfringens-Associated Lesions and Improved Performance in Broiler Chickens Treated with Normal Intestinal Bacteria from Adult Fowl. *Avian Dis* (2001) 45:149–56.
4. Mora ZV, Macías-Rodríguez ME, Arratia-Quijada J, Gonzalez-Torres YS, Nuño K, Villarruel-López A. Clostridium Perfringens as Foodborne Pathogen in Broiler Production: Pathophysiology and Potential Strategies for Controlling Necrotic Enteritis. *Anim (Basel)* (2020) 10:1718–43. doi: 10.3390/ani10091718

5. Dahiya JP, Wilkie DC, Kessel AGV, Drew MD. Potential Strategies for Controlling Necrotic Enteritis in Broiler Chickens in Post-Antibiotic Era. *Anim Feed Sci Technol* (2006) 129:60–88. doi: 10.1016/j.anifeedsci.2005.12.003
6. Shojadoost B, Vince AR, Prescott JF. The Successful Experimental Induction of Necrotic Enteritis in Chickens by Clostridium Perfringens: A Critical Review. *Vet Res* (2012) 43:74. doi: 10.1186/1297-9716-43-74
7. Hill C, Guarner F, Reid G, Gibson GR, Merenstein DJ, Pot B, et al. The International Scientific Association for Probiotics and Prebiotics Consensus Statement on the Scope and Appropriate Use of the Term Probiotic. *Nat Rev Gastro Hepat* (2014) 11:506–14. doi: 10.1038/nrgastro.2014.66
8. Chen Y, Zhang L, Hong G, Huang C, Qian W, Bai T, et al. Probiotic Mixtures with Aerobic Constituent Promoted the Recovery of Multi-Barriers in Dss-Induced Chronic Colitis. *Life Sci* (2020) 240:117089. doi: 10.1016/j.lfs.2019.117089
9. Jakubczyk D, Leszczyńska K, Górska S. The Effectiveness of Probiotics in the Treatment of Inflammatory Bowel Disease (Ibd)-a Critical Review. *Nutrients* (2020) 12:1973–97. doi: 10.3390/nu12071973
10. Cai J, Zhao C, Du Y, Zhang Y, Zhao M, Zhao Q. Comparative Efficacy and Tolerability of Probiotics for Antibiotic-Associated Diarrhea: Systematic Review with Network Meta-Analysis. *U Eur Gastroent J* (2018) 6:169–80. doi: 10.1177/2050640617736987
11. Geeraerts S, Delezie E, Ducatelle R, Haesebrouck F, Devreese B, Van IF. Vegetative Bacillus Amyloliquefaciens Cells Do Not Confer Protection against Necrotic Enteritis in Broilers Despite High Antibacterial Activity of Its Supernatant against Clostridium Perfringens in Vitro. *Brit Poult Sci* (2016) 57:324–9. doi: 10.1080/00071668.2016.1169246
12. Fukata T, Hadate Y, Baba E, Arakawa A. Influence of Bacteria on Clostridium Perfringens Infections in Young Chickens. *Avian Dis* (1991) 35:224–7.
13. Jayaraman S, Thangavel G, Kurian H, Mani R, Mukkalil R, Chirakkal H. Bacillus Subtilis Pb6 Improves Intestinal Health of Broiler Chickens Challenged with Clostridium Perfringens-Induced Necrotic Enteritis. *Poult Sci* (2013) 92:370–4. doi: 10.3382/ps.2012-02528
14. Qing X, Zeng D, Wang H, Ni X, Liu L, Lai J, et al. Preventing Subclinical Necrotic Enteritis through Lactobacillus Johnsonii Bs15 by Ameliorating Lipid Metabolism and Intestinal Microflora in Broiler Chickens. *Amb Express* (2017) 7:139. doi: 10.1186/s13568-017-0439-5
15. Caly DL, D'Inca R, Auclair E, Drider D. Alternatives to Antibiotics to Prevent Necrotic Enteritis in Broiler Chickens: A Microbiologist's Perspective. *Front Microbiol* (2015) 6:1336. doi: 10.3389/fmicb.2015.01336
16. Layton SL, Hernandez-Velasco X, Chaitanya S, Xavier J, Menconi A, Latorre JD, et al. The Effect of a Lactobacillus-Based Probiotic for the Control of Necrotic Enteritis in Broilers. *Food Sci Nutr* (2013) 4:1–7. doi: 10.4236/fns.2013.411A001
17. Cao L, Yang XJ, Li ZJ, Sun FF, Wu XH, Yao JH. Reduced Lesions in Chickens with Clostridium Perfringens-Induced Necrotic Enteritis by Lactobacillus Fermentum 1.20291. *Poult Sci* (2012) 91:3065–71. doi: 10.3382/ps.2012-02548
18. Liu X, Lin X, Mi Y, Li J, Zhang C. Grape Seed Proanthocyanidin Extract Prevents Ovarian Aging by Inhibiting Oxidative Stress in the Hens. *Oxid Med Cell Longev* (2018) 2018:1–16. doi: 10.1155/2018/9390810
19. Livak KJ, Schmittgen TD. Analysis of Relative Gene Expression Data Using Real-Time Quantitative Pcr and the 2(-Delta Delta C(T)) Method. *Methods* (2001) 25:402–8. doi: 10.1006/meth.2001.1262
20. Truong DT, Franzosa EA, Tickle TL, Scholz M, Weingart G, Pasolli E, et al. Erratum: Metaphlan2 for Enhanced Metagenomic Taxonomic Profiling. *Nat Methods* (2015) 12:902–3. doi: 10.1038/nmeth.3589
21. Abubucker S, Segata N, Goll J, Schubert AM, Izard J, Cantarel BL, et al. Metabolic Reconstruction for Metagenomic Data and Its Application to the Human Microbiome. *PLoS Comput Biol* (2012) 8:e1002358. doi: 10.1371/journal.pcbi.1002358
22. Martens EC, Neumann M, Desai MS. Interactions of Commensal and Pathogenic Microorganisms with the Intestinal Mucosal Barrier. *Nat Rev Microbiol* (2018) 16:457–70. doi: 10.1038/s41579-018-0036-x
23. Citi S. Intestinal Barriers Protect against Disease. *Science* (2018) 359:1097–98. doi: 10.1126/science.aat0835
24. Kelsall BL. Innate and Adaptive Mechanisms to Control [Corrected] Pathological Intestinal Inflammation. *J Pathol* (2010) 214:242–59. doi: 10.1002/path.2373
25. Li Z, Wang W, Lv Z, Liu D, Guo Y. Bacillus Subtilis and Yeast Cell Wall Improve the Intestinal Health of Broilers Challenged by Clostridium Perfringens. *Brit Poult Sci* (2017) 58:635–43. doi: 10.1080/00071668.2017.1370697
26. Mcauley JL, Linden SK, Png CW, King RM, Pennington HL, Gendler SJ, et al. Muc1 Cell Surface Mucin Is a Critical Element of the Mucosal Barrier to Infection. *J Clin Invest* (2007) 117:2313–24. doi: 10.1172/JCI26705
27. Forder RE, Nattrass GS, Geier MS, Hughes RJ, Hynd PII. Quantitative Analyses of Genes Associated with Mucin Synthesis of Broiler Chickens with Induced Necrotic Enteritis. *Poult Sci* (2012) 91:1335–41. doi: 10.3382/ps.2011-02062
28. Lee YS, Lee SH, Gadde UD, Oh ST, Lee SJ, Lillehoj HS. Allium Hookeri Supplementation Improves Intestinal Immune Response against Necrotic Enteritis in Young Broiler Chickens. *Poult Sci* (2018) 97:1899–908. doi: 10.3382/ps/pey031
29. Fasina YO, Hoerr FJ, McKee SR, Conner DE. Influence of Salmonella Enterica Serovar Typhimurium Infection on Intestinal Goblet Cells and Villous Morphology in Broiler Chicks. *Avian Dis* (2010) 54:841–7. doi: 10.1637/9055-090809-Reg.1
30. Lindén SK, Florin THJ, Mcguckin MA. Mucin Dynamics in Intestinal Bacterial Infection. *PLoS One* (2008) 3:e3952. doi: 10.1371/journal.pone.0003952
31. Fanning AS, Jameson BJ, Jesaitis LA, Anderson JM. The Tight Junction Protein Zo-1 Establishes a Link between the Transmembrane Protein Occludin and the Actin Cytoskeleton. *J Biol Chem* (1998) 273:29745–53. doi: 10.1074/jbc.273.45.29745
32. Du E, Wang W, Gan L, Li Z, Guo S, Guo Y. Effects of Thymol and Carvacrol Supplementation on Intestinal Integrity and Immune Responses of Broiler Chickens Challenged with Clostridium Perfringens. *J Anim Sci Biotechnol* (2016) 7:19. doi: 10.1186/s40104-016-0079-7
33. Gadde UD, Oh S, Lee Y, Davis E, Zimmerman N, Rehberger T, et al. Dietary Bacillus Subtilis-Based Direct-Fed Microbials Alleviate Lps-Induced Intestinal Immunological Stress and Improve Intestinal Barrier Gene Expression in Commercial Broiler Chickens. *Res Vet Sci* (2017) 114:236–43. doi: 10.1016/j.rvsc.2017.05.004
34. Li P, Nijhawan D, Budihardjo I, Srinivasula SM, Ahmad M, Alnemri ES, et al. Cytochrome C and Datp-Dependent Formation of Apaf-1/Caspase-9 Complex Initiates an Apoptotic Protease Cascade. *Cell* (1997) 91:479–89. doi: 10.1016/s0092-8674(00)80434-1
35. Hoffman WH, Biade S, Zilfou JT, Chen J, Murphy M. Transcriptional Repression of the Anti-Apoptotic Survivin Gene by Wild Type P53. *J Biol Chem* (2002) 277:3247–57. doi: 10.1074/jbc.M106643200
36. Wu S, Yuan L, Zhang Y, Liu F, Li G, Wen K, et al. Probiotic Lactobacillus Rhamnosus Gg Mono-Association Suppresses Human Rotavirus-Induced Autophagy in the Gnotobiotic Piglet Intestine. *Gut Pathog* (2013) 5:22–2. doi: 10.1186/1757-4749-5-22
37. Wang H, Ni X, Qing X, Liu L, Lai J, Khalique A, et al. Probiotic Enhanced Intestinal Immunity in Broilers against Subclinical Necrotic Enteritis. *Front Immunol* (2017) 8:1592–605. doi: 10.3389/fimmu.2017.01592
38. Crhanova M, Hradecka H, Faldynova M, Matulova M, Havlickova H, Sisak F, et al. Immune Response of Chicken Gut to Natural Colonization by Gut Microflora and to Salmonella Enterica Serovar Enteritidis Infection. *Infect Immun* (2011) 79:2755–63. doi: 10.1128/iai.01375-10
39. García-Ortiz A, Serrador JM. Nitric Oxide Signaling in T Cell-Mediated Immunity. *Trends Mol Med* (2018) 24:412–27. doi: 10.1016/j.molmed.2018.02.002
40. Torchinsky MB, Garaude J, Martin AP, Blander JM. Innate Immune Recognition of Infected Apoptotic Cells Directs T(H)17 Cell Differentiation. *Nature* (2009) 458:78. doi: 10.1038/nature07781
41. Van Immerseel F, De Buck J, Pasmans F, Huyghebaert G, Haesebrouck F, Ducatelle R. Clostridium Perfringens in Poultry: An Emerging Threat for Animal and Public Health. *Avian Pathol* (2004) 33:537–49. doi: 10.1080/03079450400013162
42. Adhikari P, Lee CH, Cosby DE, Cox NA, Kim WK. Effect of Probiotics on Fecal Excretion, Colonization in Internal Organs and Immune Gene Expression in the Ileum of Laying Hens Challenged with Salmonella Enteritidis. *Poult Sci* (2019) 98:1235–42. doi: 10.3382/ps/pey443
43. Wang W, Li Z, Han Q, Guo Y, Zhang B, D'Inca R. Dietary Live Yeast and Mannan-Oligosaccharide Supplementation Attenuate Intestinal Inflammation and Barrier Dysfunction Induced by Escherichia Coli in Broilers. *Br J Nutr* (2016) 116:1878–88. doi: 10.1017/s0007114516004116

44. Taylor A, Verhagen J, Blaser K, Akdis M, Akdis CA. Mechanisms of Immune Suppression by Interleukin-10 and Transforming Growth Factor-Beta: The Role of T Regulatory Cells. *Immunology* (2010) 117:433–42. doi: 10.1111/j.1365-2567.2006.02321.x
45. Clavijo V, Flórez MJV. The Gastrointestinal Microbiome and Its Association with the Control of Pathogens in Broiler Chicken Production: A Review. *Poult Sci* (2018) 97:1006–21. doi: 10.3382/ps/pex359
46. Cisek AA, Binek M. Chicken Intestinal Microbiota Function with a Special Emphasis on the Role of Probiotic Bacteria. *Pol J Vet Sci* (2014) 17:385–94. doi: 10.2478/pjvs-2014-0057
47. Kelder T, Stroeve JHM, Bijlsma S, Radonjic M, Roeselers G. Correlation Network Analysis Reveals Relationships between Diet-Induced Changes in Human Gut Microbiota and Metabolic Health. *Nutr Diabetes* (2014) 4:e122. doi: 10.1038/nutd.2014.18
48. Singh KM, Shah T, Deshpande S, Jakhesara SJ, Koringa PG, Rank DN, et al. High through Put 16s Rrna Gene-Based Pyrosequencing Analysis of the Fecal Microbiota of High Fcr and Low Fcr Broiler Growers. *Mol Biol Rep* (2012) 39:10595–602. doi: 10.1007/s11033-012-1947-7
49. Shin NR, Whon TW, Bae JW. Proteobacteria: Microbial Signature of Dysbiosis in Gut Microbiota. *Trends Biotechnol* (2015) 33:496–503. doi: 10.1016/j.tibtech.2015.06.011
50. Kuwahara T, Yamashita A, Hirakawa H, Nakayama H, Toh H, Okada N, et al. Genomic Analysis of Bacteroides Fragilis Reveals Extensive DNA Inversions Regulating Cell Surface Adaptation. *Proc Natl Acad Sci U S A* (2004) 101:14919. doi: 10.1073/pnas.0404172101
51. Zakharzhevskaya NB, Vanyushkina AA, Altukhov IA, Shavarda AL, Butenko IO, Rakitina DV, et al. Outer Membrane Vesicles Secreted by Pathogenic and Nonpathogenic Bacteroides Fragilis Represent Different Metabolic Activities. *Sci Rep* (2017) 7:5008–23. doi: 10.1038/s41598-017-05264-6
52. Wang C, Pors SE, Olsen RH, Bojesen AM. Transmission and Pathogenicity of Gallibacterium Anatis and Escherichia Coli in Embryonated Eggs. *Vet Microbiol* (2018) 217:76–81. doi: 10.1016/j.vetmic.2018.03.005
53. Zhang Y, Yu K, Chen H, Su Y, Zhu W. Caecal Infusion of the Short-chain Fatty Acid Propionate Affects the Microbiota and Expression of Inflammatory Cytokines in the Colon in a Fistula Pig Model. *Microb Biotechnol* (2018) 11:859–68. doi: 10.1111/1751-7915.13282
54. Leeson S, Namkung H, Antongiovanni M, Lee EH. Effect of Butyric Acid on the Performance and Carcass Yield of Broiler Chickens. *Poult Sci* (2005) 84:1418–22. doi: 10.1093/ps/84.9.1418
55. Dakshinamurti K. *Handbook of Vitamins. 4th ed.* New York: Crc Press (2007).
56. Kuroki F, Iida M, Tominaga M, Matsumoto T, Hirakawa K, Sugiyama S, et al. Multiple Vitamin Status in Crohn's Disease. *Dig Dis Sci* (1993) 38:1614–8. doi: 10.1007/BF01303168
57. Ellestadsayed JJ, Nelson RA, Adson MA, Palmer WM, Soule EH. Pantothenic Acid, Coenzyme a, and Human Chronic Ulcerative and Granulomatous Colitis. *Am J Clin Nutr* (1976) 29:1333–8. doi: 10.1097/00006199-197511000-00014
58. Dubin K, Callahan MK, Ren B, Khanin R, Viale A, Ling L, et al. Intestinal Microbiome Analyses Identify Melanoma Patients at Risk for Checkpoint-Blockade-Induced Colitis. *Nat Commun* (2016) 7:10391. doi: 10.1038/ncomms10391
59. Ford TC, Downey LA, Simpson T, McPhee G, Oliver C, Stough C. The Effect of a High-Dose Vitamin B Multivitamin Supplement on the Relationship between Brain Metabolism and Blood Biomarkers of Oxidative Stress: A Randomized Control Trial. *Nutrients* (2018) 10:1860–72. doi: 10.3390/nu10121860
60. Lebeer S, Vanderleyden J, De Keersmaecker SC. Host Interactions of Probiotic Bacterial Surface Molecules: Comparison with Commensals and Pathogens. *Nat Rev Microbiol* (2010) 8:171–84. doi: 10.1038/nrmicro2297
61. Philpott DJ, Sorbara MT, Robertson SJ, Croitoru K, Girardin SE. Nod Proteins: Regulators of Inflammation in Health and Disease. *Nat Rev Immunol* (2014) 14:9–23. doi: 10.1038/nri3565
62. Wolf AJ, Underhill DM. Peptidoglycan Recognition by the Innate Immune System. *Nat Rev Immunol* (2018) 18:243–54. doi: 10.1038/nri.2017.136

Conflict of Interest: The authors declare that the research was conducted in the absence of any commercial or financial relationships that could be construed as a potential conflict of interest.

Copyright © 2021 Gong, Wang, Zhou, Tang, Zeng, Zhang and Li. This is an open-access article distributed under the terms of the Creative Commons Attribution License (CC BY). The use, distribution or reproduction in other forums is permitted, provided the original author(s) and the copyright owner(s) are credited and that the original publication in this journal is cited, in accordance with accepted academic practice. No use, distribution or reproduction is permitted which does not comply with these terms.

frontiers in Microbiology

ORIGINAL RESEARCH
published: 06 July 2021
doi: 10.3389/fmicb.2021.664407

Bacterial and Fungal Gut Community Dynamics Over the First 5 Years of Life in Predominantly Rural Communities in Ghana

Nelly Amenyogbe[1,2†], Dennis Adu-Gyasi[3†], Yeetey Enuameh[3,4], Kwaku Poku Asante[3], Dennis Gyasi Konadu[3], Seyram Kaali[3], David Dosoo[3], Pinaki Panigrahi[5], Tobias R. Kollmann[2,6], William W. Mohn[7*‡] and Seth Owusu-Agyei[3,8‡]*

[1] Department of Experimental Medicine, University of British Columbia, Vancouver, BC, Canada, [2] Systems Vaccinology, Telethon Kids Institute, Perth, WA, Australia, [3] Research and Development Division, Ghana Health Service, Kintampo Health Research Centre, Kintampo North, Ghana, [4] Department of Epidemiology and Biostatistics, School of Public Health, Kwame Nkrumah University of Science and Technology, Kumasi, Ghana, [5] Pediatrics Academic Department, Georgetown University Medical Centre, Washington, DC, United States, [6] Department of Pediatrics, University of British Columbia, Vancouver, BC, Canada, [7] Department of Microbiology and Immunology, Life Sciences Institute, University of British Columbia, Vancouver, BC, Canada, [8] Institute of Health Research, University of Health and Allied Sciences, Ho, Ghana

Background: Bacterial and fungal microbiotas are increasingly recognized as important in health and disease starting early in life. However, microbiota composition has not yet been investigated in most rural, low-resource settings, and in such settings, bacterial and fungal microbiotas have not been compared. Thus, we applied 16S and ITS2 amplicon sequencing, respectively, to investigate bacterial and fungal fecal microbiotas in rural Ghanaian children cross-sectionally from birth to 5 years of age. Corresponding maternal fecal and breast milk microbiotas were additionally investigated.

Results: While bacterial communities differed systematically across the age spectrum in composition and diversity, the same was not observed for the fungal microbiota. We also identified a novel and dramatic change in the maternal postpartum microbiota. This change included much higher abundance of *Escherichia coli* and much lower abundance of *Prevotella* in the first vs. fourth week postpartum. While infants shared more bacterial taxa with their mother's stool and breast milk than with those of unrelated mothers, there were far fewer shared fungal taxa.

Conclusion: Given the known ability of commensal fungi to influence host health, the distinct pattern of their acquisition likely has important health consequences. Similarly, the dynamics of mothers' bacterial microbiotas around the time of birth may have important consequences for their children's health. Both topics require further study.

Keywords: breast milk, child, fungi, bacteria, post partum microbiome

OPEN ACCESS

Edited by:
Stéphane Ranque, Aix-Marseille Université, France

Reviewed by:
Jianjun Qiao, Zhejiang University, China
Marisa Mariel Fernandez, Institute of Studies on Humoral Immunity (IDEHU), Argentina

****Correspondence:***
Nelly Amenyogbe
n.akuvy@gmail.com
William W. Mohn
wmohn@mail.ubc.ca

† These authors have contributed equally to this work and share first authorship

‡ These authors have contributed equally to this work and share senior authorship

Specialty section:
This article was submitted to Microbial Immunology, a section of the journal Frontiers in Microbiology

Received: *05 February 2021*
Accepted: *26 May 2021*
Published: *06 July 2021*

Citation:
Amenyogbe N, Adu-Gyasi D, Enuameh Y, Asante KP, Konadu DG, Kaali S, Dosoo D, Panigrahi P, Kollmann TR, Mohn WW and Owusu-Agyei S (2021) Bacterial and Fungal Gut Community Dynamics Over the First 5 Years of Life in Predominantly Rural Communities in Ghana. Front. Microbiol. 12:664407. doi: 10.3389/fmicb.2021.664407

INTRODUCTION

The dynamics of the bacterial gut microbiota have been well studied but mostly in resource-rich settings. These surveys have shown microbial diversity to increase with age and reach adult-like profiles by 2–3 years (Palmer et al., 2007; Yatsunenko et al., 2012; Subramanian et al., 2014; Backhed et al., 2015; Bokulich et al., 2016; Stewart et al., 2018). The breast milk bacterial microbiota has also been studied using culture-based (Jimenez et al., 2008; Solis et al., 2010; Jost et al., 2013) and culture-independent (Cabrera-Rubio et al., 2012; Moossavi et al., 2019) approaches, which revealed its potential to seed the infant intestinal microbiota (Martin et al., 2012). These findings together with disease-specific surveys have identified the bacterial microbiota as a key factor shaping health in early life (Arrieta et al., 2014).

In contrast, the fungal gut microbiota has been far less studied, despite emerging evidence that fungi are also key modulators of health and disease (Jiang et al., 2017; Shao et al., 2019). Examples include recent mouse studies demonstrating that fungi effectively calibrate mucosal immune responses with an emphasis on Th17 immunity and neutrophil function (Shao et al., 2019) and that colonization with *Candida albicans* increases survival of systemic viral challenge (Jiang et al., 2017). Sequence-based surveys of infant fungal microbiotas have also revealed that a higher abundance of specific fungal taxa is associated with the development of allergic disease later in childhood (Arrieta et al., 2018). The human fungal microbiota in early life has been surveyed in very few studies and in select populations: Europe (Norway, Florence, and Luxembourg) and America (Puerto Rico and Ecuador) (Strati et al., 2016; Schei et al., 2017; Wampach et al., 2017; Arrieta et al., 2018; Ward et al., 2018). Based on diverse study designs, *Candida*, *Aspergillus*, and *Saccharomyces* feature prominently in newborns and older infants. There is, however, no clear age-dependent trajectory of fungal microbiota taxonomic composition (Strati et al., 2016; Schei et al., 2017; Wampach et al., 2017) or diversity (Strati et al., 2016; Wampach et al., 2017) in the first 2 years of life, aside from lower diversity in 10-day-old newborns vs. 3-month-olds or their mothers (Schei et al., 2017). There were also no clear trajectories identified during the first month of life in a more granular assessment of the newborn fungal microbiota (Ward et al., 2018).

The breast milk fungal microbiota has only recently been profiled using a culture-independent approach (Boix-Amoros et al., 2019), revealing dominance by *Malassezia* spp. also commonly found on skin and compositional differences across diverse populations, which were confirmed in separate studies (Heisel et al., 2019; Moossavi et al., 2020). Beyond this, the fungal composition of human breast milk has not been investigated.

Despite the importance of both the bacterial and fungal gut microbiota in influencing the developmental trajectory toward health or disease, to our knowledge, these two have never been jointly investigated in early life, which is likely the most important period of development. Equally surprising, despite the well-established fact that the maternal stool and breast milk microbiotas shape the newborn's microbiota, no study so far has captured this interaction between mother and infant across the bacterial and fungal domains. We thus conducted a cross-sectional bacterial and fungal microbiota survey encompassing fecal microbiotas of children in the first 5 years of life plus fecal and breast milk microbiotas of mothers of children one month and younger.

MATERIALS AND METHODS

Ethics Approval and Consent to Participate

All work in this study was in accordance with ethical guidelines at the University of British Columbia and done under the approved ethics protocol number H11-01423. Separate ethical approval was obtained from the Kintampo Health Research Centre Institutional Ethics Committee (KHRCIEC_2016-14).

Study Participants

Study participants were recruited in the Kintampo North Municipality, located in the former Brong Ahafo Region (now Bono-East Region) in the middle-belt of Ghana, and serving as part of the Kintampo Health Research Centre (KHRC) study area. Prospective participants were selected from the database of the Kintampo Health and Demographic Surveillance System (KHDSS). Expectant mothers of newborn participants were approached during pregnancy, or mothers of older children, who were recruited into the study were approached to participate in the study. Inclusion criteria for this study were for participants to be (a) living in the study area, (b) healthy with no known congenital defects, (c) under 63 months, and (d) to have provided written informed consent. An exclusion criterion was refusal to provide informed consent. Study participant recruitment was stratified by the age groups outlined: the newborn period [day of life (DOL) 0–5; DOL 13–17; DOL 26–35]; 3 months (DOL 83–115), 6 months (DOL 165–200), 1 year; month of life (MOL) 11–13; 2 years, MOL 22–26; 3 years, MOL 33–39; and 5 years, MOL 57–63.

Stool and Breast Milk Sample Collection

Field workers supplied mothers with sterile containers and scoops to collect stool samples from soiled diapers. Stool samples were collected from the diapers of children with sterile plastic spoons transported to the clinical laboratory at the KHRC. Additionally, mothers of participants who were 0–1 or 4–5 weeks old and were exclusively breastfed were asked to provide stool and breast milk samples in supplied sterile containers. All samples collected in the study were kept in cold boxes with ice packs and sent to the laboratory within 2 h. At the clinical laboratory, stool and breast milk samples were split into multiple 1.0-ml aliquots and stored at −80°C until further analysis. Biospecimens were transported to the University of British Columbia on dry ice with temperature monitoring *via* World Courier Inc.

Stool DNA Extraction for Amplicon Sequencing

DNA was extracted from swabs using the MagAttract PowerSoil DNA KF kit (Qiagen Cat. No. 27000-4-KF) using the manufacturer's protocol for the KingFisher Flex platform with the following modification using approximately 200 mg bulk stool loaded into each 96-well plate with sterile wooden picks.

Breast Milk DNA Extraction for Amplicon Sequencing

Total DNA was extracted from 0.7–1.0 mL breast milk using the Qiagen DNease PowerSoil DNA extraction kit (Qiagen Cat. 12830-50) with the following modifications: frozen breast milk samples were thawed on ice and transferred to 2.0 ml screw-top tubes (VWR Cat. 211-0440) and spun for 10 min at 4°C at 20,000 g to pellet all particles. The lipid portion of the milk remained on top of the aqueous phase after centrifugation. The lipid layer was retained, and the aqueous phase between the pellet and whey layer was carefully removed with a 200-μL micropipette. The contents of one Qiagen 0.1-mm glass bead tube (Qiagen 13118-50) was then added to each sample with 500 μL Bead Solution and 200 μL phenol:chloroform:IAA pH 7–8 (Ambion Cat. AM 9730, pH adjusted with included Tris buffer). Then, 60 μL of C1 was added, and samples were homogenized in a FastPrep bead mill for 30 s at 5.5 m/s for two cycles with a 5-min wait in between. The remainder of the protocol was carried out according to manufacturer's instructions, and samples were eluted in 2 × 30 μL (total of 60 μL).

16S Amplicon Sequencing

Samples were submitted to Microbiome Insights Inc. (Vancouver, BC, Canada) for PCR amplification and DNA sequencing targeting the V4 region of the 16S rRNA gene. Library preparation was done using a previously published protocol (Kozich et al., 2013) with the details and product information outlined below. Here, 10 μL of the final product was used to normalize to 1–2 ng/μL using the SepalPrep Normalization Prep Plate Kit (Thermo Fisher Cat. A1051001), and 5 μL of each normalized sample was pooled into a single library per 96-well plate. Library pools were further concentrated using the DNA Clean and Concentrator kit (Zymo Cat. D4013). A dilution series was performed for each of the pooled libraries for subsequent quality control (QC) steps. Each pool was analyzed using the Agilent Bioanalyzer using the High Sensitivity DS DNA assay (Agilent Cat. 5047-4626) to determine approximate fragment size and to verify library integrity. Library pools with unintended amplicons were purified using the Qiagen QIAquick Gel Extraction Kit (Qiagen Cat. 28706). Pooled library concentrations were determined using the KAPA Library Quantification Kit for Illumina (KAPA Cat. KK4824). The final libraries were loaded at 8 pM, with an additional PhiX spike-in of 20%. The amplicon library was sequenced on the MiSeq using the MiSeq 500 Cycle V2 Reagent Kit (Illumina Cat. MS-102-2003).

Paired-end reads were assembled using MOTHUR version 1.37.2, following the MiSeq SOP (Schloss et al., 2009; accessed Aug 2018)[1]. Operational taxonomic units (OTUs) were clustered at 97% identity and classified using the GreenGenes 13_8_99 database (DeSantis et al., 2006).

ITS2 Amplicon Sequencing

Processing for ITS2 amplicon sequencing was identical to that used for 16S amplicon sequencing, except with the following differences: Primers and PCR conditions were previously described (Gweon et al., 2015). Paired-end reads were trimmed at the non-overlapping ends, and high-quality reads were classified using UNITE (v. 7.1) (Koljalg et al., 2005).

16S and ITS2 Sequencing Quality Control

The potential for contamination was addressed by co-sequencing DNA amplified from specimens and from four template-free PCR controls and extraction kit reagents processed the same way as the specimens (two for breast milk specimens). Two positive controls, consisting of cloned SUP05 DNA, were also included (number of copies = 2*10^6). Breast milk samples were extracted and PCR amplified separately from the stool samples but sequenced on the same lane. Given the different distributions of contaminating OTUs from breast milk blanks compared to stool, QC was done for the breast milk samples separately. Contaminating OTUs can come from two main sources: from PCR and extraction reagents and carryover from neighboring samples during the extraction and amplification process. OTUs were considered reagent contaminants and removed from the dataset if they were present in over 50% of blank samples and their count geometric mean plus one standard deviation was greater than that in the samples. Using this approach, OTUs with high counts in many samples (mainly including taxa commonly known to be highly abundant in these sample types) were not flagged for removal, despite their presence in blanks. For OTUs whose mean counts were high in the samples but also found in over 50% of blanks, the mean count plus standard deviation from the blanks was subtracted from each of the samples. Samples with total counts under 1,000 were also removed. Once filtered, data from breast milk and stool were recombined for further analysis.

Statistical Analysis

Alpha Diversity

We used the *phyloseq* R package (Charlop-Powers and Brady, 2015) to compute alpha and beta diversity. We estimated microbial diversity with abundance-dependent (Shannon) and independent (Observed richness) metrics after subsampling the OTU table to account for unequal sampling depth. To test for relationships between age, we used the Wilcoxon test comparing each age bin to the Mothers of one-month-old (DOL 26–35) infants, as this was considered the adult microbiota group. *p*-values were adjusted using the Bonferroni correction, and adjusted *p*-values under 0.05 were considered significant.

[1]https://www.mothur.org/wiki/MiSeq_SOP

Community Composition

Beta diversity was computed using the Bray–Curtis index. Sample clustering was visualized using non-metric-multidimensional scaling (NMDS). To test whether child age (all age bins except maternal samples) explained community composition, we used the Adonis test from R package *vegan* (Oksanen et al., 2017) using age in days calculated between the time interval between participant's date of birth and visit date. To test if community composition between 5-year-olds (age bin MOL 57–63; 5 years) and younger children differed, we computed the Bray–Curtis distance of individuals in each bin to their distance to all individuals in the MOL 57–63 bin. The Wilcoxon rank-sum test was then used to compare distances between each bin to the median distance among the 5-year-olds to others in the same bin. *p*-values were adjusted using the Bonferroni correction, and adjusted *p*-values under 0.05 were considered significant.

Differential Abundance

To identify OTUs differentially abundant between mothers of 0–5-day-old vs. 26–35-day-old infants, we used the Wald test implemented in the R package *DESeq2* (Love et al., 2014). Differential abundance was considered significant if the Benjamini–Hochberg adjusted *p*-value was less than 0.05. To further visualize select bacterial genera differentially abundant between maternal groups and their abundance across the age spectrum, we aggregated OTU counts by genus-level assignment and confirmed that the genera differed between groups using the Wilcoxon rank-sum test.

Shared Operational Taxonomic Units Between Mother and Infant

For shared OTU analysis, OTUs were considered present if their relative abundance was over 0.01%. For stool and breast milk separately, we calculated the number of shared OTUs between newborns and their mothers and newborns and unrelated mothers. Because the number of unrelated pairs was much greater than related pairs, we randomly subsampled the unrelated pairs, selecting the same number as related pairs in each analysis. The median number of shared OTUs between related and unrelated pairs and 0–5 and 25–36 days postpartum was then compared using the Wilcoxon rank-sum test.

RESULTS

Sample Summary: Amplicon Sequencing

After quality filtering, we retained a total of 2.9 million reads, representing 4,492 bacterial OTUs. These OTUs represented 435 unique taxa classified at the genus level or above. Five samples yielded fewer than 1,000 reads and were excluded from downstream analysis. The remainder yielded between 2,600 and 31,200 reads per sample, with most fecal samples yielding greater than 10,000 (**Supplementary Figure 1A**).

After quality filtering, we retained a total of 2.5 million reads representing 1,772 fungal OTUs, representing 375 unique taxa classified at the genus level or above. Fifty-nine samples contained fewer than 1,000 reads and were excluded from downstream analysis. The remainder contained between 1,200 and 96,500 reads per sample (**Supplementary Figure 1B**). Samples with no detectable fungi over our count threshold were found in both infant and adult stool samples alike (**Supplementary Figure 1C**). The proportion of samples in each age stratification with no detectable fungi was highly variable but usually below 50%.

Bacterial and Fungal Alpha Diversity Across the Age Spectrum

To measure alpha diversity (the microbial diversity in any single sample), we used both observed richness, the number of distinct OTUs present, and the Shannon Diversity Index, which reflects both richness and evenness. We compared diversity of fecal communities in each age bin to that of the 1-month postpartum mothers, representing an adult microbiota. Alpha diversity of fecal bacterial communities increased with age. Observed bacterial richness was lower than that of adults until 3 years and Shannon diversity until 2 years (**Figure 1A**). Fungal fecal microbiota diversity of only a few age bins differed from adult diversity; otherwise, there was no clear trend for fungal diversity vs. age, except that it was lower during the first week of life (**Figure 1B**). Interestingly, the mothers of those newborns also had lower fungal richness than 1-month postpartum mothers. Most samples, especially from after 2 years of age, contained fewer fungal OTUs (less than 60 OTUs in most samples), while between 100 and 300 bacterial OTUs were detected during this time.

Bacterial and Fungal Communities Across the Age Spectrum

Beta diversity (community composition) of fecal bacterial communities differed across the age spectrum and, expectedly, was distinct from breast milk bacterial communities (**Figures 2A,B**). There was no such trend for fungal fecal communities. While child age contributed to 18% of the variance of fecal bacterial communities (PERMANOVA $p = 0.001$), it accounted for only 2% of variance in fecal fungal communities (PERMANOVA $p = 0.015$). We did not identify one NMDS axis that drove an age gradient for either community. To further assess community composition across the age spectrum, we determined the similarity of communities in each age bin to those at 5 years. Fecal bacterial communities from all age bins, except 3 years, differed from those at 5 years (**Figure 2C**). Expectedly, fecal fungal communities did not follow this trend.

Relative abundances of the 25 most abundant genera clearly revealed bacterial taxonomic shifts over the age spectrum (**Figure 3A**). In keeping with the literature on bacteria (Koenig et al., 2011; Stewart et al., 2018), newborns were dominated by *Escherichia coli* in the first week of life, and it remained abundant up to 6 months. Then, *Bifidobacteria* were dominant from 1 month to 1 year. Subsequently, the diversity of genera increased, and *Prevotella* became dominant, similar

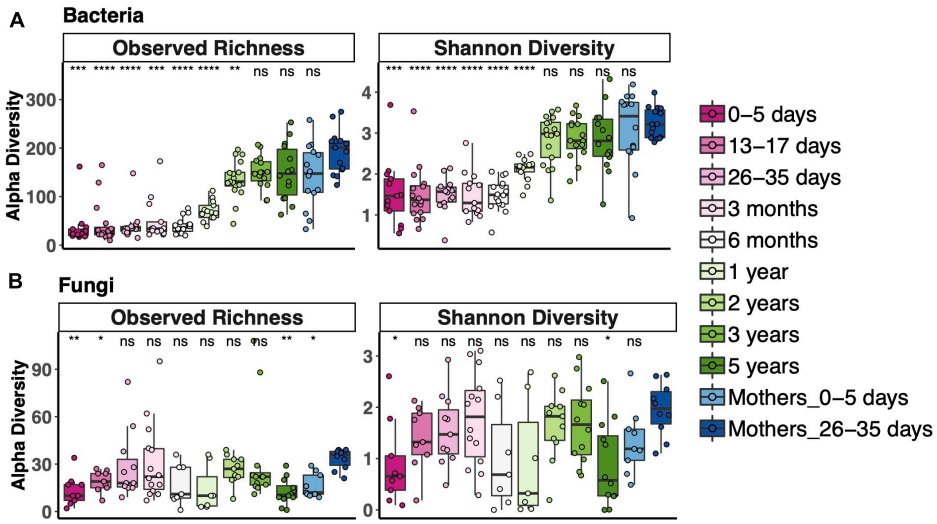

FIGURE 1 | Alpha diversity across the age spectrum for bacterial fecal communities **(A)** and fungal fecal communities **(B)**. Coding indicates values significantly different from those of adult communities (Mothers of 26–35-day-old newborns): $^{****}p < 0.0001$, $^{***}p < 0.001$, $^{**}p < 0.01$, $^{*}p < 0.05$; Wilcoxon rank-sum test adjusted using the Bonferroni correction. Boxplots indicate medians with first and third quartiles (25–75%). Whiskers extend no farther than 1.5*IQR from the hinge.

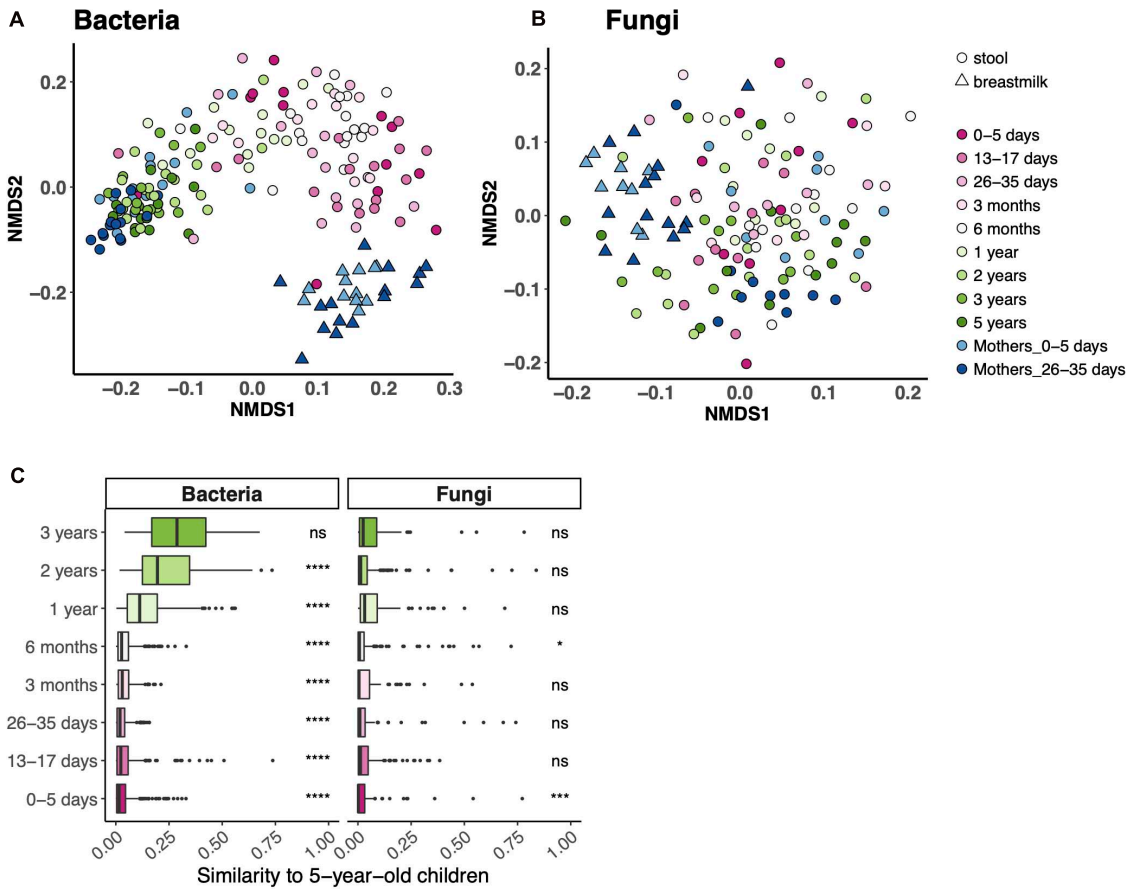

FIGURE 2 | Bacterial and fungal communities across the age spectrum. **(A,B)** Ordinations of community composition based on Bray–Curtis distance for bacterial **(A)** and fungal **(B)** fecal communities. **(C)** Bray–Curtis distance between each age bin and 5 years. $^{****}p < 0.0001$, $^{***}p < 0.001$, $^{*}p < 0.05$, Wilcoxon rank-sum test, adjusted using the Bonferroni correction.

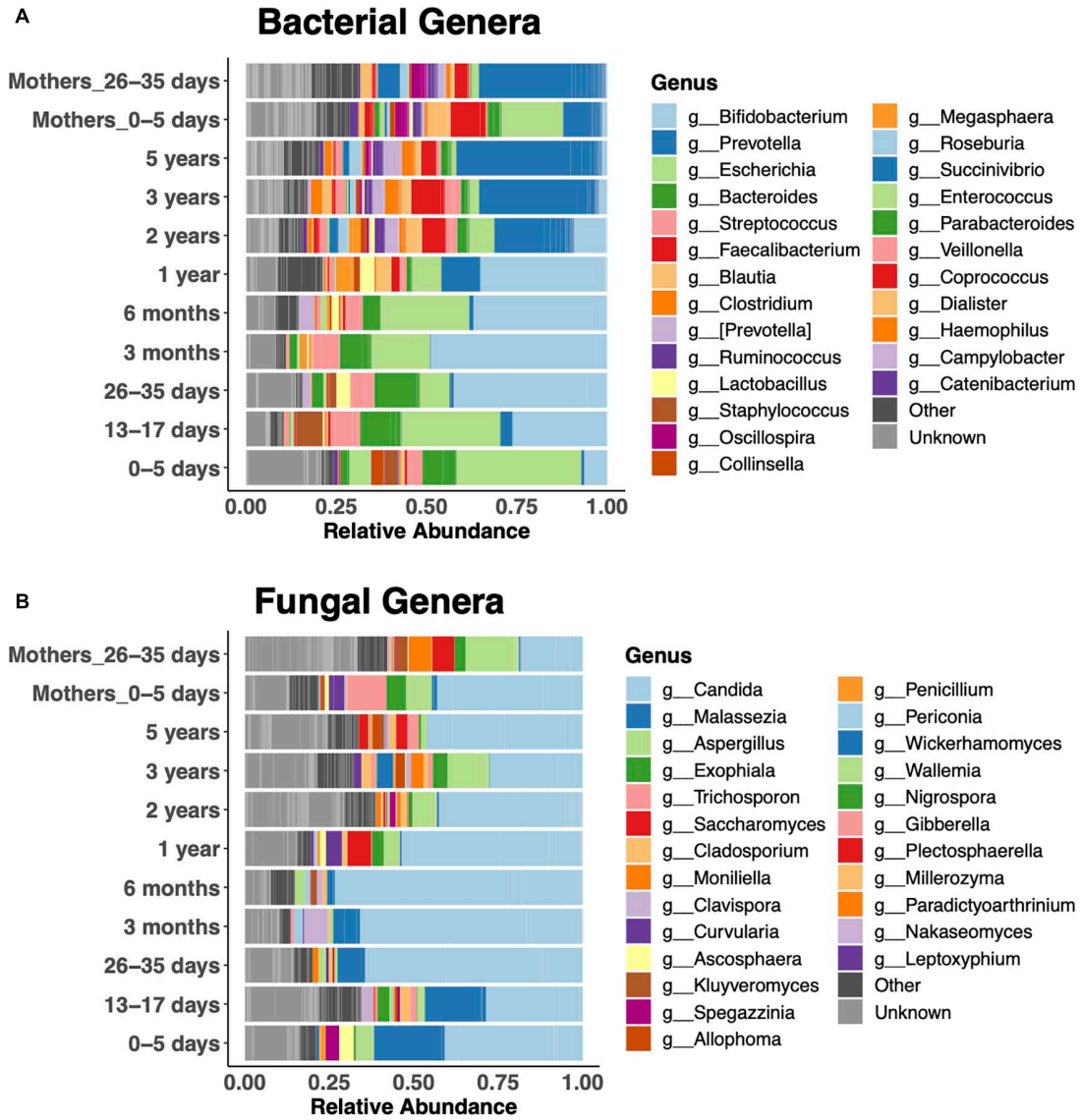

FIGURE 3 | Relative abundance of the 25 most abundant genera. Bacterial **(A)** and fungal **(B)** community composition across the age spectrum.

to the adult microbiota. *Bacteroides* was abundant during the first year, until the increase in *Prevotella*. Children were dominated by either *Bacteroides* or *Prevotella* at any given time (**Supplementary Figure 2**). *Faecalibacterium* was abundant after the first year. The fecal fungal microbiota was dominated by *Candida* (primarily *Candida albicans* and *Candida tropicalis*) in children of all ages (**Figure 3B**). *Malassezia* featured prominently in the first 3 months of life, while *Aspergillus* was prominent after the first year.

Maternal Bacterial Microbiota

Our study revealed dramatic differences in bacterial stool microbiotas of mothers in the first postpartum week vs. 1 month postpartum (**Figure 3A**). We further explored this difference by measuring the Bray–Curtis distance between mothers' microbiotas at both time points to their respective children at 1 week, finding that mothers in the first vs. fourth postpartum week harbored a bacterial microbiota significantly more similar to that of newborns (**Figure 4A**). We identified 68 OTUs differentially abundant between the two mother groups, representing 34 taxa at the genus level or above (**Figure 4B**). Abundances of some taxa obviously contributed to the similarity of microbiotas of mothers 1 week postpartum and their children at 1 week. Thus, in both mothers and infants from 1 to 4 weeks after birth, *Prevotella* had increasing abundance, while *Escherichia* had decreasing abundance (**Figures 4C,D**). Other taxa, such as *Faecalibacterium* and *Blautia*, were more abundant in mothers 1 week vs. 4 weeks postpartum, yet were virtually absent in their infants at 1 week (**Figures 4E,F**). We also found that, at 1 week, newborns shared more bacterial but not fungal

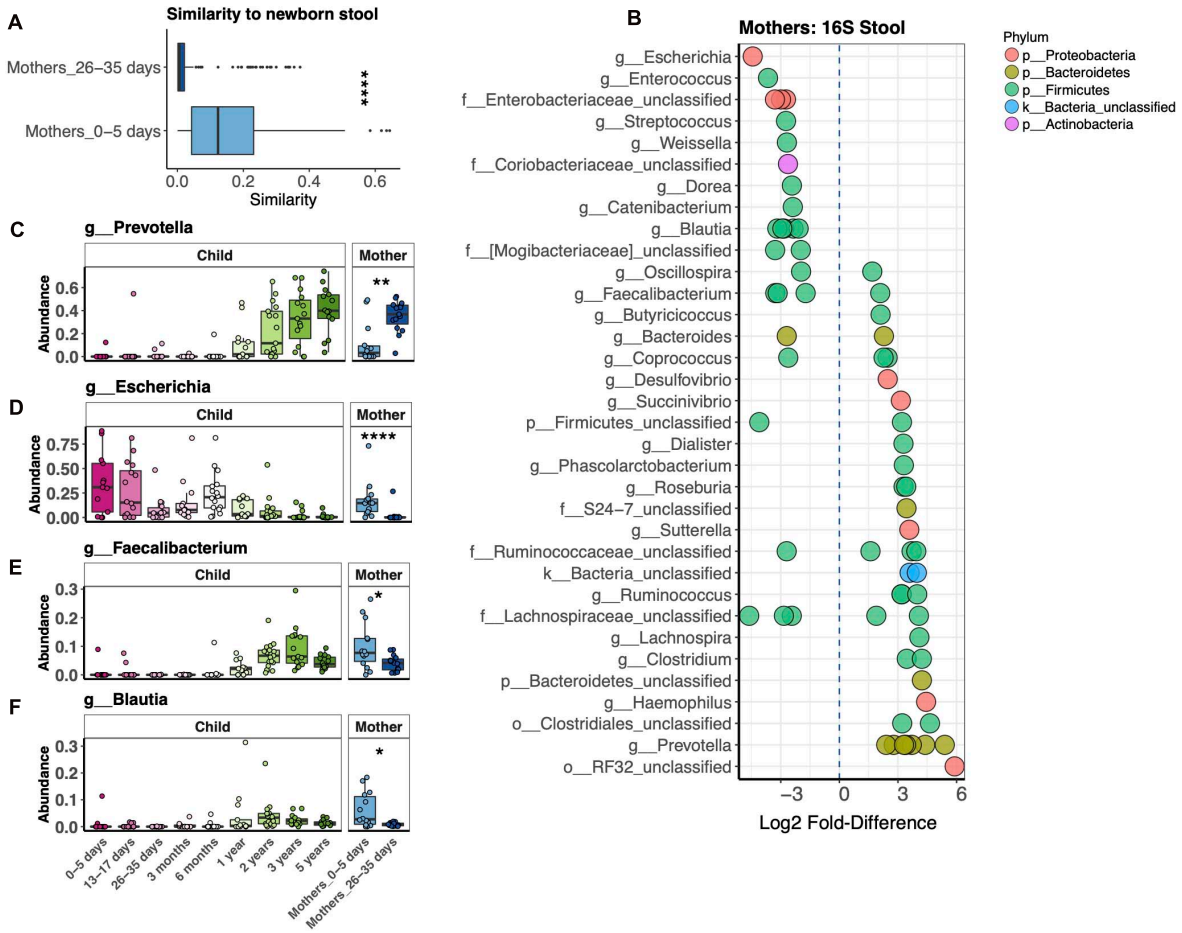

FIGURE 4 | Comparison of fecal bacterial microbiotas of mothers 1 and 4 weeks postpartum and children at 1 week. **(A)** Average pairwise similarity of the microbiotas of mothers vs. those of their children. **(B)** Operational taxonomic units (OTUs) identified by DESeq2 differentially abundant between mothers 1 week vs. 4 weeks postpartum. Negative fold-difference indicates greater abundance 1 week postpartum. **(C–F)** Relative abundance of selected taxa that were differentially abundant between mothers 1 week vs. 4 weeks postpartum. $^{****}p < 0.0001$, $^{**}p < 0.01$, $^{*}p < 0.05$, Wilcoxon rank-sum test, adjusted using the Bonferroni correction.

OTUs with their mother vs. with unrelated mothers, but this was no longer the case at 1 month (**Supplementary Figures 3A,B**). OTUs most commonly shared by mother–infant pairs include members of *Escherichia*, *Enterococcus*, and *Streptococcus*, all of which are of higher relative abundance in newborns than in their mothers (**Supplementary Figure 3C**). Only two fungal OTUs were commonly shared between mother–infant pairs (**Supplementary Figure 3D**).

Bacterial and Fungal Communities in Mother's Breast Milk

Breast Milk is a well-recognized modulator of the infant gut microbiota, serving both as a source of colonizing bacteria and bacterial growth substrates. The relationship of breast milk and the fungal microbiota has not been well described. Thus, we compared the bacterial and fungal community composition of both breast milk and fecal microbiotas. Breast milk microbiotas were typically dominated by skin taxa of both bacteria (*Streptococcus*, *Staphylococcus*, or *Corynebacterium*; **Figure 5A**) and fungi (*Malassezia*, including *Malassezia restricta*, *Malassezia globosa*, *and Malassezia furfur*; **Figure 5B**). Alpha diversity did not differ between breast milk samples collected in the first or fourth postpartum week for either bacteria or fungi. Only minor differences in community composition were found between the first and fourth postpartum week, including only eight differentially abundant bacterial OTUs (**Figure 5C**) and no differentially abundant fungal OTUs. For bacterial communities, mother–infant pairs shared significantly more OTUs than unrelated pairs at both postpartum time points (**Figure 5D**). While fungal data were available for fewer pairs, we found a significant difference between related and unrelated pair sharing 4 weeks postpartum (**Figure 5E**). The most commonly shared bacterial OTUs belonged to typical skin commensal genera, *Streptococcus* and *Staphylococcus*, which had higher relative abundance in the breast milk than in the newborn stool. Shared OTUs between mother and infant pairs also included gut commensals

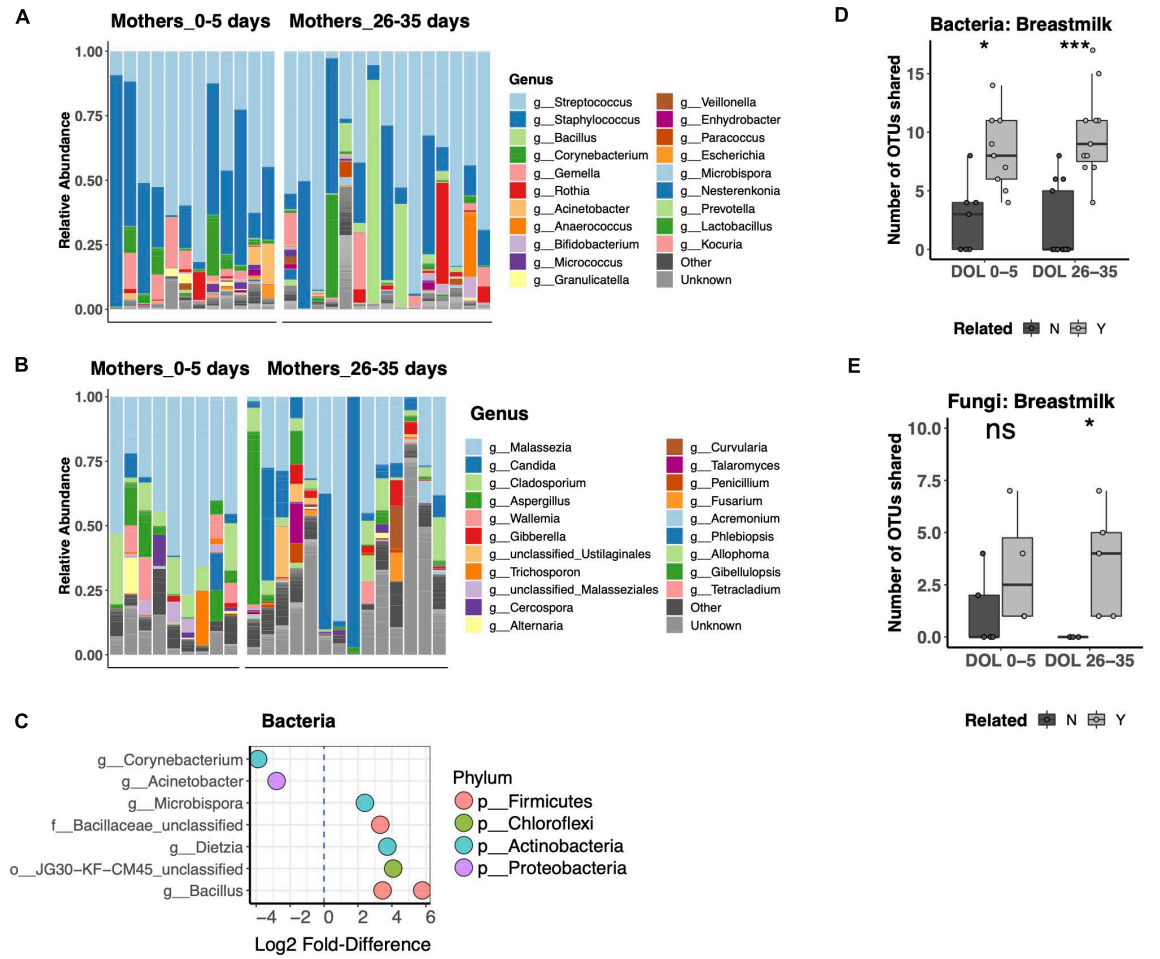

FIGURE 5 | Breast milk bacterial and fungal community composition. **(A,B)** Top 25 most abundant bacterial **(A)** and fungal **(B)** genera across all samples reveal that both communities are dominated by common skin taxa but also contain a diverse repertoire of microbes at lower abundances. **(C)** Differentially abundant taxa between mothers in the first compared to the fourth postpartum week. **(D,E)** Number of shared bacterial **(D)** and fungal **(E)** operational taxonomic units (OTUs) between mother–infant pairs in the first and fourth postpartum weeks. Statistics: $^{***}p < 0.001$, $^{*}p < 0.05$, Wilcoxon rank-sum test, adjusted using the Bonferroni correction.

Bifidobacterium and *Bacteroides*, both of which were of higher relative abundance in the newborn's stool than in his or her mother's milk (**Supplementary Figure 4A**). Shared fungal OTUs were much more limited and did not have a clear pattern of differing abundance between mother and child (**Supplementary Figure 4B**).

DISCUSSION

Here, we report for the first time the bacterial and fungal microbiota dynamics during early childhood in a rural Ghanaian setting. In conducting a direct comparison between bacterial and fungal gut communities, we demonstrated how the two follow very distinct developmental patterns, having contrasting associations with the mother's microbiota. We also found a previously unreported and surprising compositional difference in maternal stool microbiotas during the postpartum period.

We found undetectable levels of fungi in a large subset of stool samples from children and mothers in a rural African setting. This finding is consistent with a previous study in Norway, an urban high-resource setting (Schei et al., 2017). We additionally confirmed that the samples with undetectable fungi, including those from the youngest age groups, contained readily amplifiable bacterial genes, providing further evidence that the lack of detectable fungi in these samples reflected their absence or extremely low abundance, rather than sample processing artifacts. However, extraction protocols optimal for bacteria may have failed to lyse fungal cells. Interestingly, most breast milk samples were positive for fungi, especially those from 4 weeks postpartum, while we did not detect fungi in half of the corresponding breastfeeding infants.

As in our study, increasing bacterial (Bokulich et al., 2016; Stewart et al., 2018) and unchanging fungal (Strati et al., 2016; Wampach et al., 2017) richness and diversity during infancy were previously reported, but never together in the same study.

However, the timing of increases in bacterial richness and diversity in our study differed from those in other studies in both high- and low-resource regions. In our Ghanaian cohort, richness and diversity remained stable over the first year of life and dramatically increased thereafter. In studies of American and European cohorts, alpha diversity steadily increased from birth to 2 years (Bokulich et al., 2016) or 3 months to 5 years (Stewart et al., 2018), respectively. Numbers of observed OTUs increased steadily from birth to 3 years among Amerindian and Malawian infants (Yatsunenko et al., 2012) and from birth to 2 years in an Indian setting (Chandel et al., 2017). The distinct timing in our study may reflect lifestyles, diet, or an environment unique to this study cohort in Ghana.

The bacterial succession we observed, with sequential dominance by *E. coli* in the first 5 days of life, *Bifidobacterium* and *Bacteroides* in early infancy, and *Prevotella* after the first year, was consistent with previous studies of newborn and adult microbiotas (Koenig et al., 2011; Stewart et al., 2018). The Bacteroidetes phylum in older children and adults is typically dominated by either *Bacteroides* or *Prevotella* (De Filippo et al., 2010; Yatsunenko et al., 2012; Lin et al., 2013). *Prevotella* was dominant in adults in rural Ghana, as demonstrated among the 1-month postpartum women in our study. We found that *Bacteroides* was abundant in the Ghanaian infants prior to 1 year, after which *Prevotella* became dominant. The ability of *Bacteroides* species to utilize human milk oligosaccharides (HMOs) (Marcobal et al., 2011) as well as diet-derived polysaccharides (Flint et al., 2015) as an energy source is thought to contribute to their unique ability to persist in both infant and adult guts. However, *Prevotella* appears to outcompete *Bacteroides* in adults with a fiber-rich diet (Wu et al., 2011). This difference occurs early in life in this Ghanaian population, probably associated with differences in children's diets at this time.

We found dominance of the gut fungal microbiota of some children by *Candida* sp., as has been found in some (Wampach et al., 2017; Ward et al., 2018) but not other (Strati et al., 2016; Arrieta et al., 2018) studies. We also detected an early increase in the relative abundance of *Malassezia* that was not seen in other studies of newborns (Schei et al., 2017; Ward et al., 2018). Given the high relative abundance of this taxon in breast milk in our study and another (Boix-Amoros et al., 2019) and evidence of its transmission from mother to newborn (Nagata et al., 2012), absence of this taxon in other studies is puzzling but may reflect regional differences in maternal breast milk fungal microbiotas or methodologies.

We were surprised to find substantial differences between the gut bacterial microbiotas of mothers 1 week vs. 4 weeks postpartum. These dramatic differences were not due to cross-contamination between maternal and infant samples, as mothers in both groups were sampled using the same protocol, and samples from both groups were processed simultaneously. Given the cross-sectional study design, we cannot definitively conclude that the microbiota changed in these women over this time. However, both the 3-month recruitment window and the greater microbiota similarity of mothers and their infants 1 week postpartum imply that such a change is the most likely interpretation of the data. Studies of the stool microbiota during pregnancy have yielded mixed results, with some studies showing no change in community composition during pregnancy (Bisanz et al., 2015; DiGiulio et al., 2015) and others showing substantial shifts (Koren et al., 2012; Ferrocino et al., 2018). The latter two studies showed an increase in Proteobacteria during pregnancy, which is consistent dominance of Proteobacteria that we observed 1 week postpartum. However, our finding of a low relative abundance of *Prevotella* 1 week postpartum is novel and was one of the greatest differences we observed in the postpartum period. We also observed a high relative abundance of *Faecalibacterium* 1 week postpartum, associated with decreased inflammation and protection from inflammatory bowel diseases (Sokol et al., 2008), and *Blautia*, negatively associated with type 1 diabetes (Murri et al., 2013) and gestational diabetes mellitus (GDM) without prescribed dietary intervention (Ferrocino et al., 2018). Together, our findings suggest that differences in maternal microbiota around the time of birth reflect both increases in taxa common to newborns (*Escherichia*) and decreases in taxa absent in newborns (*Prevotella*), as well as increases in abundance of taxa not abundant in infants but with potential health benefits to the mother (*Faecaibacterim* and *Blautia*).

We did not identify fungal taxa that were differentially abundant in the gut microbiota 1 week vs. 4 weeks postpartum. We also did not identify many commonly shared fungal OTUs between pairs. In contrast to the bacterial gut microbiota, the fungal gut microbiota of mothers does not appear to be substantially affected by postpartum time and does not appear to strongly influence colonization of the infant's gut using the methods we applied.

We found that common skin taxa dominated breast milk bacterial (*Streptococcus*, *Staphylococcus*) and fungal (*Malassezia*) communities, as previously shown (Murphy et al., 2017; Williams et al., 2017; Boix-Amoros et al., 2019; Moossavi et al., 2019). When dominant in a mother's breast milk, OTUs of these taxa tended to be present at lower relative abundance in her infant's gut microbiota, consistent with the breast milk being a source for these organisms colonizing the infant gut. However, it is important to note that detection of their DNA in breast milk and feces does not demonstrate that these OTUs colonize, or even survive, these two environments. Further investigation is required to determine if these skin taxa have any function in breast milk or the gut. OTUs of common gut taxa (*Bifidobacterium*, *Bacteroides*, *Lactobacillus*, and *Rothia*) were also frequently shared between a mother's breast milk and her infant's gut microbiota, as previously reported (Murphy et al., 2017). However, the gut commensals tended to have higher relative abundance in the gut than the breast milk, suggesting that the infant's (or mother's) gut was a source for these organisms colonizing the breast milk. Overall, our study identifies strong and novel associations between the microbiotas of breast milk and the infant gut, particularly in the case of bacteria vs. fungi.

There are limitations in the study worth noting. Amplicon Sequence Variants (ASVs) are becoming an increasingly popular approach as an alternative to the OTU clustering performed in our study. However, we submit that ASV analysis would

only have a minor impact on our conclusions based on a recent study demonstrating that both ASV and OTU approaches reveal biologically meaningful and comparable results (Glassman and Martiny, 2018). With this, others have cautioned against abandoning OTU approaches for sequencing applications targeting a single variable region (Johnson et al., 2019). Independent of sequencing approach and given the cross-sectional design, this study cannot definitively prove that differences among age groups represent microbiota changes over time, although such changes are the most compelling interpretation of the results. Sample size and a lack of data on infant and mother health and on mode of delivery limited the analysis to effects of age but did not include other host factors that also may have influenced the microbiotas.

CONCLUSION

The goal of this study was to assess, for the first time, the bacterial and fungal gut microbiota composition of children in Ghana to help identify microbial signatures relevant to the health of women and their children. In doing so, we not only identified bacterial and fungal community dynamics shared with other study cohorts but also identified characteristics not previously reported. Unique to the Ghanaian cohort, alpha diversity was low and stable during the first year of life, and *Prevotella* became the dominant bacterial genus between the first and second year. Also, the mother's bacterial microbiota differed drastically between 1 and 4 weeks postpartum. While mothers are a major source of bacteria colonizing newborns, the sources of colonizing fungi are less apparent.

FUTURE DIRECTIONS

This small cross-sectional study broadly assessed ecology mother–newborn bacterial and fungal microbiotas, together with the microbiota in children over the first 5 years in rural Ghana. Crucial insights from this study inform future approaches to identify microbial signatures relevant to the health of women and their children. Based on our findings, longitudinal studies will address the following questions:

1. What demographic or environmental factors explain differences in maternal microbiotas after childbirth? And are these changes associated with maternal health or disease?
2. Are there host microbiota (bacterial and fungal) signatures associated with increased risk for, or protection from, severe disease, especially in the newborn period?
3. Are commensal fungi identified in mother–infant pairs transient or do they represent a stable community of commensal microbes coinhabiting the gut with bacteria?

These studies will inform novel interventions targeting the microbiota to improve the health of mothers and their children.

DATA AVAILABILITY STATEMENT

The datasets presented in this study can be found in online repositories. The names of the repository/repositories and accession number(s) can be found below: https://www.ncbi.nlm.nih.gov/, bioproject/PRJNA658595. All codes and data used to generate the results presented in this manuscript are publicly accessible on GitHub using the following URL: https://github.com/nelly-amenyogbe/Bacterial_Fungal_Communities_Rural_Ghana.

ETHICS STATEMENT

The studies involving human participants were reviewed and approved by All work in this study was in accordance to ethical guidelines at the University of British Columbia and done under the approved ethics protocol number H11-01423. Separate ethical approval was obtained from the Kintampo Health Research Centre Institutional Ethics Committee (KHRCIEC_2016-14). For participants under the age of 18, Written informed consent to participate in this study was provided by the participants' legal guardian/next of kin.

AUTHOR CONTRIBUTIONS

SO-A, DA-G, NA, TK, KA, YE, and PP contributed to the study design. DA-G, YE, SK, and DD facilitated participant recruitment and sample collection. NA and WM generated the amplicon sequencing data. NA performed the statistical analyses and prepared the manuscript. WM and SO-A substantially edited the manuscript. All authors contributed to editing the manuscript.

FUNDING

This work was supported by the Canadian Institutes of Health Research (PJT-148781) and the Ghana Health Service infrastructure at Kintampo Health Research Centre.

ACKNOWLEDGMENTS

We are grateful to the management and staff of Kintampo Health Research Centre, Research and Development Division, Ghana Health Service, who supported the conduct of this study with very little funding. We thank to the Kintampo community, especially the families that allowed and consented for mothers and their children to participate in this study.

SUPPLEMENTARY MATERIAL

The Supplementary Material for this article can be found online at: https://www.frontiersin.org/articles/10.3389/fmicb.2021.664407/full#supplementary-material

REFERENCES

Arrieta, M. C., Arevalo, A., Stiemsma, L., Dimitriu, P., Chico, M. E., Loor, S., et al. (2018). Associations between infant fungal and bacterial dysbiosis and childhood atopic wheeze in a nonindustrialized setting. *J. Allergy Clin. Immunol.* 142, 424–434.e10.

Arrieta, M. C., Stiemsma, L. T., Amenyogbe, N., Brown, E. M., and Finlay, B. (2014). The intestinal microbiome in early life: health and disease. *Front. Immunol.* 5:427.

Backhed, F., Roswall, J., Peng, Y., Feng, Q., Jia, H., Kovatcheva-Datchary, P., et al. (2015). Dynamics and stabilization of the human gut microbiome during the first year of life. *Cell Host Microbe* 17, 690–703.

Bisanz, J. E., Enos, M. K., PrayGod, G., Seney, S., Macklaim, J. M., Chilton, S., et al. (2015). Microbiota at multiple body sites during pregnancy in a rural tanzanian population and effects of moringa-supplemented probiotic yogurt. *Appl. Environ. Microbiol.* 81, 4965–4975. doi: 10.1128/aem.00780-15

Boix-Amoros, A., Puente-Sanchez, F., du Toit, E., Linderborg, K. M., Zhang, Y., Yang, B., et al. (2019). Mycobiome profiles in breast milk from healthy women depend on mode of delivery, geographic location and interaction with bacteria. *Appl. Environ. Microbiol.* 85, e2994–e2918.

Bokulich, N. A., Chung, J., Battaglia, T., Henderson, N., Jay, M., Li, H., et al. (2016). Antibiotics, birth mode, and diet shape microbiome maturation during early life. *Sci. Transl. Med.* 8:343ra82. doi: 10.1126/scitranslmed.aad7121

Cabrera-Rubio, R., Collado, M. C., Laitinen, K., Salminen, S., Isolauri, E., and Mira, A. (2012). The human milk microbiome changes over lactation and is shaped by maternal weight and mode of delivery. *Am. J. Clin. Nutr.* 96, 544–551. doi: 10.3945/ajcn.112.037382

Chandel, D. S., Perez-Munoz, M. E., Yu, F., Boissy, R., Satpathy, R., Misra, P. R., et al. (2017). Changes in the gut microbiota after early administration of oral synbiotics to young infants in India. *J. Pediatr. Gastroenterol. Nutr.* 65, 218–224. doi: 10.1097/mpg.0000000000001522

Charlop-Powers, Z., and Brady, S. F. (2015). phylogeo: an R package for geographic analysis and visualization of microbiome data. *Bioinformatics* 31, 2909–2911. doi: 10.1093/bioinformatics/btv269

De Filippo, C., Cavalieri, D., Di Paola, M., Ramazzotti, M., Poullet, J. B., Massart, S., et al. (2010). Impact of diet in shaping gut microbiota revealed by a comparative study in children from Europe and rural Africa. *Proc. Natl. Acad. Sci. U.S.A.* 107, 14691–14696. doi: 10.1073/pnas.1005963107

DeSantis, T. Z., Hugenholtz, P., Larsen, N., Rojas, M., Brodie, E. L., Keller, K., et al. (2006). Greengenes, a chimera-checked 16S rRNA gene database and workbench compatible with ARB. *Appl. Environ. Microbiol.* 72, 5069–5072. doi: 10.1128/aem.03006-05

DiGiulio, D. B., Callahan, B. J., McMurdie, P. J., Costello, E. K., Lyell, D. J., Robaczewska, A., et al. (2015). Temporal and spatial variation of the human microbiota during pregnancy. *Proc. Natl. Acad. Sci. U.S.A.* 112, 11060–11065.

Ferrocino, I., Ponzo, V., Gambino, R., Zarovska, A., Leone, F., Monzeglio, C., et al. (2018). Changes in the gut microbiota composition during pregnancy in patients with gestational diabetes mellitus (GDM). *Sci. Rep.* 8:12216.

Flint, H. J., Duncan, S. H., Scott, K. P., and Louis, P. (2015). Links between diet, gut microbiota composition and gut metabolism. *Proc. Nutr. Soc.* 74, 13–22. doi: 10.1017/s0029665114001463

Glassman, S. I., and Martiny, J. B. H. (2018). . Broadscale ecological patterns are robust to use of exact sequence variants versus operational taxonomic units. *mSphere* 3, e148–e118.

Gweon, H. S., Oliver, A., Taylor, J., Booth, T., Gibbs, M., Read, D. S., et al. (2015). PIPITS: an automated pipeline for analyses of fungal internal transcribed spacer sequences from the Illumina sequencing platform. *Methods Ecol. Evol.* 6, 973–980. doi: 10.1111/2041-210x.12399

Heisel, T., Nyaribo, L., Sadowsky, M. J., and Gale, C. A. (2019). Breastmilk and NICU surfaces are potential sources of fungi for infant mycobiomes. *Fungal Genet. Biol.* 128, 29–35. doi: 10.1016/j.fgb.2019.03.008

Jiang, T. T., Shao, T. Y., Ang, W. X. G., Kinder, J. M., Turner, L. H., Pham, G., et al. (2017). Commensal fungi recapitulate the protective benefits of intestinal bacteria. *Cell Host Microbe* 22, 809–816.e4.

Jimenez, E., Delgado, S., Maldonado, A., Arroyo, R., Albujar, M., Garcia, N., et al. (2008). Staphylococcus epidermidis: a differential trait of the fecal microbiota of breast-fed infants. *BMC Microbiol.* 8:143. doi: 10.1186/1471-2180-8-143

Johnson, J. S., Spakowicz, D. J., Hong, B. Y., Petersen, L. M., Demkowicz, P., Chen, L., et al. (2019). Evaluation of 16S rRNA gene sequencing for species and strain-level microbiome analysis. *Nat. Commun.* 10:5029.

Jost, T., Lacroix, C., Braegger, C., and Chassard, C. (2013). Assessment of bacterial diversity in breast milk using culture-dependent and culture-independent approaches. *Br. J. Nutr.* 110, 1253–1262. doi: 10.1017/s0007114513000597

Koenig, J. E., Spor, A., Scalfone, N., Fricker, A. D., Stombaugh, J., Knight, R., et al. (2011). Succession of microbial consortia in the developing infant gut microbiome. *Proc. Natl. Acad. Sci. U.S.A.* 108(Suppl. 1), 4578–4585. doi: 10.1073/pnas.1000081107

Koljalg, U., Larsson, K. H., Abarenkov, K., Nilsson, R. H., Alexander, I. J., Eberhardt, U., et al. (2005). UNITE: a database providing web-based methods for the molecular identification of ectomycorrhizal fungi. *New Phytol.* 166, 1063–1068. doi: 10.1111/j.1469-8137.2005.01376.x

Koren, O., Goodrich, J. K., Cullender, T. C., Spor, A., Laitinen, K., Backhed, H. K., et al. (2012). Host remodeling of the gut microbiome and metabolic changes during pregnancy. *Cell* 150, 470–480. doi: 10.1016/j.cell.2012.07.008

Kozich, J. J., Westcott, S. L., Baxter, N. T., Highlander, S. K., and Schloss, P. D. (2013). Development of a dual-index sequencing strategy and curation pipeline for analyzing amplicon sequence data on the MiSeq Illumina sequencing platform. *Appl. Environ. Microbiol.* 79, 5112–5120. doi: 10.1128/aem.01043-13

Lin, A., Bik, E. M., Costello, E. K., Dethlefsen, L., Haque, R., Relman, D. A., et al. (2013). Distinct distal gut microbiome diversity and composition in healthy children from Bangladesh and the United States. *PLoS One* 8:e53838. doi: 10.1371/journal.pone.0053838

Love, M. I., Huber, W., and Anders, S. (2014). Moderated estimation of fold change and dispersion for RNA-seq data with DESeq2. *Genome Biol.* 15, 550.

Marcobal, A., Barboza, M., Sonnenburg, E. D., Pudlo, N., Martens, E. C., Desai, P., et al. (2011). *Bacteroides* in the infant gut consume milk oligosaccharides via mucus-utilization pathways. *Cell Host Microbe* 10, 507–514. doi: 10.1016/j.chom.2011.10.007

Martin, V., Maldonado-Barragan, A., Moles, L., Rodriguez-Banos, M., Campo, R. D., Fernandez, L., et al. (2012). Sharing of bacterial strains between breast milk and infant feces. *J. Hum. Lact.* 28, 36–44. doi: 10.1177/0890334411424729

Moossavi, S., Fehr, K., Derakhshani, H., Sbihi, H., Robertson, B., Bode, L., et al. (2020). Human milk fungi: environmental determinants and inter-kingdom associations with milk bacteria in the CHILD Cohort Study. *BMC Microbiol.* 20:146. doi: 10.1186/s12866-020-01829-0

Moossavi, S., Sepehri, S., Robertson, B., Bode, L., Goruk, S., Field, C. J., et al. (2019). Composition and variation of the human milk microbiota are influenced by maternal and early-life factors. *Cell Host Microbe* 25, 324.e–335.e.

Murphy, K., Curley, D., O'Callaghan, T. F., O'Shea, C. A., Dempsey, E. M., O'Toole, P. W., et al. (2017). The composition of human milk and infant faecal microbiota over the first three months of life: a pilot study. *Sci. Rep.* 7:40597.

Murri, M., Leiva, I., Gomez-Zumaquero, J. M., Tinahones, F. J., Cardona, F., Soriguer, F., et al. (2013). Gut microbiota in children with type 1 diabetes differs from that in healthy children: a case-control study. *BMC Med.* 11:46. doi: 10.1186/1741-7015-11-46

Nagata, R., Nagano, H., Ogishima, D., Nakamura, Y., Hiruma, M., and Sugita, T. (2012). Transmission of the major skin microbiota, Malassezia, from mother to neonate. *Pediatr. Int.* 54, 350–355. doi: 10.1111/j.1442-200x.2012.03563.x

Oksanen, J., Blanchet, G., Friendly, M., Kindt, R., Legendre, P., McGlinn, D., et al. (2017). *vegan: Community Ecology Package*. Available online at: https://CRAN.R-project.org/package=vegan.

Palmer, C., Bik, E. M., DiGiulio, D. B., Relman, D. A., and Brown, P. O. (2007). Development of the human infant intestinal microbiota. *PLoS Biol.* 5:e177. doi: 10.1371/journal.pbio.0050177

Schei, K., Avershina, E., Oien, T., Rudi, K., Follestad, T., Salamati, S., et al. (2017). Early gut mycobiota and mother-offspring transfer. *Microbiome* 5:107.

Schloss, P. D., Westcott, S. L., Ryabin, T., Hall, J. R., Hartmann, M., Hollister, E. B., et al. (2009). Introducing mothur: open-source, platform-independent, community-supported software for describing and comparing microbial communities. *Appl. Environ. Microbiol.* 75, 7537–7541. doi: 10.1128/aem.01541-09

Shao, T. Y., Ang, W. X. G., Jiang, T. T., Huang, F. S., Andersen, H., Kinder, J. M., et al. (2019). Commensal candida albicans positively calibrates systemic th17 immunological responses. *Cell Host Microbe* 25, 404–417.e6.

Sokol, H., Pigneur, B., Watterlot, L., Lakhdari, O., Bermudez-Humaran, L. G., Gratadoux, J. J., et al. (2008). Faecalibacterium prausnitzii is an anti-inflammatory commensal bacterium identified by gut microbiota analysis of Crohn disease patients. *Proc. Natl. Acad. Sci. U.S.A.* 105, 16731–16736. doi: 10.1073/pnas.0804812105

Solis, G., de Los Reyes-Gavilan, C. G., Fernandez, N., Margolles, A., Gueimonde, M. (2010). Establishment and development of lactic acid bacteria and bifidobacteria microbiota in breast-milk and the infant gut. *Anaerobe* 16, 307–310. doi: 10.1016/j.anaerobe.2010.02.004

Stewart, C. J., Ajami, N. J., O'Brien, J. L., Hutchinson, D. S., Smith, D. P., Wong, M. C., et al. (2018). Temporal development of the gut microbiome in early childhood from the TEDDY study. *Nature* 562, 583–588.

Strati, F., Di Paola, M., Stefanini, I., Albanese, D., Rizzetto, L., Lionetti, P., et al. (2016). Age and gender affect the composition of fungal population of the human gastrointestinal tract. *Front. Microbiol.* 7:1227. doi: 10.3389/fmicb.2016.01227

Subramanian, S., Huq, S., Yatsunenko, T., Haque, R., Mahfuz, M., Alam, M. A., et al. (2014). Persistent gut microbiota immaturity in malnourished Bangladeshi children. *Nature* 510, 417–421. doi: 10.1038/nature13421

Wampach, L., Heintz-Buschart, A., Hogan, A., Muller, E. E. L., Narayanasamy, S., Laczny, C. C., et al. (2017). Colonization and succession within the human gut microbiome by archaea, bacteria, and microeukaryotes during the first year of life. *Front. Microbiol.* 8:738. doi: 10.3389/fmicb.2017.00738

Ward, T. L., Dominguez-Bello, M. G., Heisel, T., Al-Ghalith, G., Knights, D., and Gale, C. A. (2018). Development of the human mycobiome over the first month of life and across body sites. *mSystems* 3, e00140–17.

Williams, J. E., Carrothers, J. M., Lackey, K. A., Beatty, N. F., York, M. A., Brooker, S. L., et al. (2017). Human milk microbial community structure is relatively stable and related to variations in macronutrient and micronutrient intakes in healthy lactating women. *J. Nutr.* 147, 1739–1748.

Wu, G. D., Chen, J., Hoffmann, C., Bittinger, K., Chen, Y. Y., Keilbaugh, S. A., et al. (2011). Linking long-term dietary patterns with gut microbial enterotypes. *Science* 334, 105–108. doi: 10.1126/science.1208344

Yatsunenko, T., Rey, F. E., Manary, M. J., Trehan, I., Dominguez-Bello, M. G., Contreras, M., et al. (2012). Human gut microbiome viewed across age and geography. *Nature* 486, 222–227. doi: 10.1038/nature11053

Conflict of Interest: The authors declare that the research was conducted in the absence of any commercial or financial relationships that could be construed as a potential conflict of interest.

Copyright © 2021 Amenyogbe, Adu-Gyasi, Enuameh, Asante, Konadu, Kaali, Dosoo, Panigrahi, Kollmann, Mohn and Owusu-Agyei. This is an open-access article distributed under the terms of the Creative Commons Attribution License (CC BY). The use, distribution or reproduction in other forums is permitted, provided the original author(s) and the copyright owner(s) are credited and that the original publication in this journal is cited, in accordance with accepted academic practice. No use, distribution or reproduction is permitted which does not comply with these terms.

frontiers in Immunology

ORIGINAL RESEARCH
published: 20 July 2021
doi: 10.3389/fimmu.2021.683911

Insight Into Polysaccharides From *Panax ginseng* C. A. Meyer in Improving Intestinal Inflammation: Modulating Intestinal Microbiota and Autophagy

Dandan Wang[1,2], *Shuai Shao*[3], *Yanqiu Zhang*[1], *Daqing Zhao*[2,4] *and Mingxing Wang*[1,2*]

[1] College of Chinese Medicine, Changchun University of Chinese Medicine, Changchun, China, [2] Jilin Provincial Key Laboratory of BioMacromolecules of Chinese Medicine, Jilin Ginseng Academy, Changchun University of Chinese Medicine, Changchun, China, [3] College of Pharmacy, Changchun University of Chinese Medicine, Changchun, China, [4] Jilin Ginseng Academy, Changchun University of Chinese Medicine, Changchun, China

OPEN ACCESS

Edited by:
Tobias R. Kollmann, University of Western Australia, Australia

Reviewed by:
Sharvan Sehrawat, Indian Institute of Science Education and Research Mohali, India
Fengliang Jin, South China Agricultural University, China

***Correspondence:**
Mingxing Wang
cc_wmx@163.com

Specialty section:
This article was submitted to Microbial Immunology, a section of the journal Frontiers in Immunology

Received: 22 March 2021
Accepted: 02 July 2021
Published: 20 July 2021

Citation:
Wang D, Shao S, Zhang Y, Zhao D and Wang M (2021) Insight Into Polysaccharides From Panax ginseng C. A. Meyer in Improving Intestinal Inflammation: Modulating Intestinal Microbiota and Autophagy. Front. Immunol. 12:683911. doi: 10.3389/fimmu.2021.683911

Polysaccharides from *Panax ginseng* C. A. Meyer (P. ginseng) are the main active component of P. ginseng and exhibit significant intestinal anti-inflammatory activity. However, the therapeutic mechanism of the ginseng polysaccharide is unclear, and this hinders the application for medicine or functional food. In this study, a polysaccharide was isolated from P. ginseng (GP). The primary structure and morphology of the GP were studied by HPLC, FT-IR spectroscopy, and scanning electron microscopy (SEM). Further, its intestinal anti-inflammatory activity and its mechanism of function were evaluated in experimental systems using DSS-induced rats, fecal microbiota transplantation (FMT), and LPS-stimulated HT-29 cells. Results showed that GP modulated the structure of gut microbiota and restored mTOR-dependent autophagic dysfunction. Consequently, active autophagy suppressed inflammation through the inhibition of NF-κB, oxidative stress, and the release of cytokines. Therefore, our research provides a rationale for future investigations into the relationship between microbiota and autophagy and revealed the therapeutic potential of GP for inflammatory bowel disease.

Keywords: ***Panax ginseng*** **C. A. Meyer, polysaccharide, intestinal inflammation, gut microbiota, autophagy**

INTRODUCTION

Inflammatory bowel disease (IBD) consists of a group of disorders including Crohn's disease (CD) and ulcerative colitis (UC) and is a kind of recurrent, refractory gastrointestinal disease (1). At present, the incidence of IBD increases yearly. Inflammatory infiltration, redox imbalance, and gut microbiota dysbiosis are involved in the initiation, development, and exacerbation of intestinal inflammatory diseases. Intestinal epithelium plays an important role in maintaining gut homeostasis and is the main defense against pathogen invasion (2). It has been reported that the regulation of gut microbiota can alleviate the inflammatory response induced by dextran sodium sulphate (DSS) in mice. Lipopolysaccharide (LPS) is the main component of the cell walls of many

Gram-negative bacteria. The inseparable relationship between microbiota dysbiosis, LPS content, and abnormal immune response has been reported previously (3, 4). Toll-like receptor 4 (TLR4), which is abundantly expressed in intestinal epithelial cells, is a gene coding receptor for bacterial LPS (5, 6). An abnormal microbiome, especially with microbes that produce LPS, triggers intestinal inflammation, and TLR4 might be the initial point of microbial interaction. Activated TLR4 recruits the downstream molecule MyD88 to trigger the phosphorylation of MAPKs (7), and it is indispensable in orchestrating the secretion of inflammatory cytokines and oxidative stress response throughout the initiation, development, and exacerbation of IBD (8–10).

Autophagy, a highly conserved process that evolved in eukaryotes, is involved in maintaining organism homeostasis *via* lysosome-mediated self-digestion and recycling of organelles and proteins (11, 12). Cells trigger autophagy under various stress, such as exposure to toxic environments, starvation, and ischemiareperfusion (13). It has been reported that autophagy dysfunction increased susceptibility to inflammatory intestinal diseases (14–17). Repairing hampered autophagy normalized redox imbalance, increased the clearance of intracellular bacteria, and alleviated inflammation in intestinal mucosa (18); thus, it has become a new target of clinical drug development for IBD. Mounting evidence suggests the inseparable association between autophagy impairment and inflammation injury (19–21). mTOR, a highly conserved serine/threonine protein kinase, negatively regulates autophagy upstream, and it has demonstrated great autophagy activating and inflammation attenuating efficacy in silencing mTOR (22). Interestingly, TLR4-MyD88-MAPK is one of the important pathways in mTOR regulation, and recent research clearly revealed the relationship between them (19). Accumulating evidence indicates that autophagy and inflammation are linked by reciprocal regulation through the microflora-TLR4-mTOR axis. Mechanistically, microbiota dysbiosis activates the TLR4-MyD88-MAPK pathway, which is followed by the phosphorylation of mTOR to inhibit autophagy, thereby aggravating inflammatory injury and oxidative stress (19). Although the roles of microflora in modulating inflammation and autophagy have had increased attention in regard to IBD, the development of related drugs is still in its infancy.

Panax ginseng C. A. Meyer (P. ginseng) has been widely used as an herb and functional food in the world (23). It has been reported that the active components of *Panax ginseng* have anti-inflammatory and immunomodulatory effects on IBD (24). The polysaccharide of P. ginseng has obvious beneficial effects, including gut microbiota regulation, intestinal mucosal barrier protection, autophagy promotion, and alleviation of inflammation and oxidative stress (24). However, the exact target and mechanism of the P. ginseng polysaccharide in gut microbiota and autophagy modulation is not well understood. Fecal microbiota transplantation (FMT) is one of the most effective ways to regulate the gut microbiota and can potentially reveal the function of microbiota and establish the causal relationship between flora and disease (25). At present, the use of FMT with P. ginseng polysaccharide to treat diseases through intestinal flora is still unknown. Therefore, the present study aims to purify crude polysaccharides from P. ginseng and to evaluate its gut microbiota and intestinal anti-inflammatory activity in dextran sulfate sodium (DSS)-induced rats with FMT. The mechanism of reciprocal regulation between inflammation and autophagy was estimated by LPS-induced inflammatory intestinal mucosal cells (HT-29 cells). Additionally, the changes in cytokines, reactive oxygen species (ROS), and autophagic proteins were detected in order to investigate the protective mechanism of the microbiota-autophagy relationship. Our study provides a reliable theoretical basis for the application of ginseng polysaccharide as a functional food material in the treatment of intestinal diseases.

MATERIALS AND METHODS

Reagents

P. ginseng was purchased from Wudu County (Gansu Province, China). The roots of P. ginseng were dried in the shade and ground into powder. Standard monosaccharides, including rhamnose, arabinose, xylose, mannose, glucose, galactose, glucuronic acid, and galacturonic acid were all obtained from the National Institute for the Control of Pharmaceutical and Biological Products (Beijing, China). All chemicals used were of analytical grade unless otherwise specified.

Isolation and Purification of Polysaccharide

Briefly, the dry three-year roots of Radix ginseng (2,000 g) were smashed into crude powder (60-80 mesh) and extracted three times with water (20 L) by continuously stirring at 80°C for two hours each time. The combined aqueous extracts were filtered through a cotton cloth bag and centrifuged (1,500 g for 15 min) and were subsequently concentrated in a rotary evaporator at 60°C. Then, the ethanol solution was brought to a final concentration of 80%. The sediment was dissolved in water, continuously stirred at 4°C for 12 hours, and the precipitate was removed by centrifugation (1,500 g for 15 min). The aqueous extract was then filtered and concentrated, followed by the addition of Sevage reagent (butanol and chloroform at a 1:4 ratio) to deproteinate the sample (26). Then, the supernatant was concentrated to a proper volume under reduced pressure and lyophilized to get the ginseng polysaccharide (GP).

Analysis of the Primary Structure and Morphological Properties of GP

Analysis of Chemical and Physical Properties

The total carbohydrate, uronic acid, and protein contents were quantified by the phenol–sulfuric acid method (27), m-hydroxydiphenyl (28), and Bradford method (29) using glucose, glucuronic acid, and bovine serum albumin as standards, respectively.

Monosaccharide Composition Analysis

The monosaccharide components were analyzed by converting the sugars into PMP derivatives (30), which were then detected by HPLC (Shimadzu 2010, Japan) and C18 column (Shimadzu, Japan) and controlled by a Uniport HP N-2000 data station.

FT-IR Analysis

The vibrations of molecules and polar bonds among different atoms were studied by FT-IR spectroscopy (iD1 Transmission Nicolet iS5, Thermo Fisher, USA), with recorded frequencies ranging from 4,000 to 500 cm^{-1} (31). FT-IR measurements were performed for each sample, which were mixed with dried KBr powder and then compressed into salt discs.

Molecular Weight Analysis

The molecular weight of the GP was determined by a gel-permeation chromatography (GPC) system (ELEOS System, Wyatt Technology, USA) equipped with a Waters 515 pump and DRI detector. The columns were a Shodex OHpak SB-806 in sequence with 803 columns, which were eluted with 0.02% $NaNO_3$ at a flow rate of one mL/min. The temperatures of the column and RI detector were maintained at 40°C. Dextran standards (Mw = 180, 2,700, 9,750, 36,800, and 135,350 Da) were used to establish a standard curve. Empower GPC software (ASTRA5.3.4, Wyatt Technology, USA) was used for data processing (32).

Scanning Electron Microscopy (SEM) Analysis of Morphological Properties

The micro-structures and surface morphologies of GP were characterized by scanning electron microscopy (SEM). A proper amount of polysaccharide sample powder was glued to the conductive adhesive of the experimental bench. The floating sample was blown off with a rubber suction bulb and placed in a gold conductive layer of 10 nm thickness in a vacuum. The accelerating voltage of the electron gun was 20 KV, and the sample was observed by the SEM.

Animals

The animal experiment protocol (No. 20200128006) was approved by the Changchun University of Chinese Medicine. SD rats weighing 200-250 g (half of which were male) were purchased from the School of Pharmacy, Jilin University (SCXK 2016-0001). All rats were given standard food and water for seven days prior to experimentation and were randomly divided into the blank group (control), intestinal inflammation group (DSS) (19, 22), low-dose GP treatment group (DSS + GP-L, 50mg/kg), middle-dose GP treatment group (DSS + GP-M, 100mg/kg), and high-dose GP treatment group (DSS + GP-H, 200mg/kg); each group consisted of 10 rats. Experimental procedures used for the animals and administration methods were based on previously reported experimental protocols (33). The rats fasted for 12 hours on the last day, and each rat was anesthetized and euthanized. The blood from each rat was collected from the common carotid artery. Ten grams of fresh feces from the rats in each group were collected and weighed in a sterilized beaker, and 50 ml of 37°C sterile normal saline was added, stirred, and filtered with double-layer sterile gauze. The filtrate was then centrifugated at 6,000 g/min for 15 min (centrifugation radius: 10 cm), and then the sediment was suspended in 100 ml of normal saline to obtain the fecal bacteria solution. FMT (5 ml/kg) was administered by gavage once a day for 14 days. The distal parts of the colon tissues were stored in a -80°C refrigerator for section or Western blot analysis. Feces were collected for further metabolite analysis. Blood was centrifuged, and the supernatant was stored at -20°C for later testing. The relative serum levels of IL-1β, IL-6, and TNF-α were determined using ELISA kits (Beyotime Institute of Biotechnology, Shanghai, China) according to the manufacturer's instructions.

Immunohistochemistry Analysis of Intestinal Tissues

Immunohistochemistry analysis was conducted to evaluate the expression of relative proteins. The paraffin-embedded tissue sections were deparaffinized and treated with hydrogen peroxide (3 m/v) for 15 min to remove endogenous peroxidase. Antigen retrieval was performed by blocking the samples in goat serum for 10 min at 22°C. The following antibodies were added and incubated for 12 hours at 4°C: anti-TLR4 antibody (Servicebio, GB11519, 1:500), anti-LC3B antibody (Abcam, ab86714, 1:500), and anti-NF-κB p65 antibody (Servicebio, GB13025-1, 1:500). Cy3 (Servicebio, GB21303) and FITC (Servicebio, GB22303) secondary antibodies (1:250) were used for visualization. Tissue sections were mounted and analyzed using an inverted fluorescence microscope (Nikon Eclipse TI-SR) and imaging system (Nikon DS-U3).

The Measurement of Endotoxin

Colon contents endotoxins were extracted in with 0.05% Tween-20 in pyrogen-free water (34). Fecal endotoxins were determined using Limulus amaebocyte lysate (LAL) kit (ThermoFisher, USA) as described previously (35).

Gut Microbiota Analysis

Gut microbiota was examined as before by 16S ribosomal RNA analysis on the Illumina MiSeq platform (Illumina, San Diego, USA) according to standard protocols (36). DNA was extracted from the colon using an Omega Biotek Mag-Bind Soil DNA Kit (Omega Bio-Tek, USA). Purified PCR products were prepared using Q5® High-Fidelity DNA Polymerase (NEB, USA); products were then quantified, and each PCR sample was diluted five times to 20 ng/μL. The PCR amplification system consisted of the following: PCR mixed product sample (2 μL), 5× reaction buffer (5 μL), 5× GC buffer (5 μL), dNTP (2.5 mM 2 μL), forward primer (10 μM, 1 μL), reverse primer (10 μM, 1 μL), Q5 DNA Polymerase (0.25 μL), DNA template (2 μL), and 8.75 μL ddH_2O. PCR amplification of the 16S rRNA genes of the V3–V4 region was performed using the forward primer 338F 5'-ACTCCTACGGGAGGCAGCA-3' and the reverse primer 806R 5'-GGACTACHVGGGTWTCTAAT-3'. Sample-specific 7-bp barcodes were incorporated into the primers for multiplex sequencing. The PCR components contained 5 μl of Q5 reaction buffer (5×), 5 μl of Q5 High-Fidelity GC buffer (5×), 0.25 μl of Q5 High-Fidelity DNA Polymerase (5 U/μl), 2 μl

(2.5 mM) of dNTPs, 1 μl (10 uM) of each forward and reverse primer, 2 μl of DNA template, and 8.75 μl of ddH_2O. Thermal cycling consisted of initial denaturation at 98°C for 2 min, followed by 25 cycles of denaturation at 98°C for 15 s, annealing at 55°C for 30 s, and extension at 72°C for 30 s, with a final extension of 5 min at 72°C. The amplicon library was then used for paired-end sequencing (2 × 250 bp) on an Illumina MiSeq platform (Illumina, San Diego, USA) according to standard protocols.

Cell Culture and Treatment

The human epithelial colorectal adenocarcinoma HT-29 cell line was obtained from the Procell Life Science and Technology Company and was maintained in DMEM with 10% FBS, 1% nonessential amino acids, and gentamicin (50 μg/mL) at 37°C and 5% CO_2; the medium was replaced every two days. For parameter measurements, the culture medium was seeded onto 6-well plates at a density of 5×10^5 cells/well (Corning Inc., Corning, NY, USA). The cells were incubated with 1 mM 3-MA or 10 μM rapamycin for 1 hour. To induce inflammatory damage, the cells were exposed to LPS (1 μg/ml) at 37°C for 6 hours. HT-29 cells were transfected with 10 pmol of siRNA for TLR4 using Lipofectamine RNAiMAX according to the manufacturer's instructions. The cellular proteins were obtained for western blot analysis as previously described (37).

Western Blotting

For Western blot analysis, the total proteins from the colon cells were collected in RIPA lysis buffer (Beyotime, Beijing, China). Samples (40 μg each) were separated onto 12% SDS-PAGE gels and transferred to a PVDF membrane (Millipore Corp., Billerica, MA, USA). Membranes were incubated overnight with related primary antibodies at a 1:1000 dilution.

Statistical Analysis

Experiments were performed in triplicate, and results are presented as the mean ± standard deviation (SD). The Student's t-test was utilized for statistical evaluation using the SPSS 16.0 statistical software package (SPSS Inc., USA), and a $P < 0.05$ was considered statistically significant.

RESULTS

Characterization of Polysaccharide

Isolation and Determination of GP

GP were extracted by using the classical method of hot water extraction followed by ethanol precipitation. Then, Sevage reagent was used to deproteinate the aqueous extracts. The crude polysaccharide yield devoid of proteins was found to be 7.5% of the total dry weight. In addition, the polysaccharides were dissolved in water after alcohol precipitation, and the water solubility of the polysaccharides could be greatly increased. The extraction procedure is shown in **Figure 1A**.

Physicochemistry Analysis

The total carbohydrate and uronic acid contents of GP were 82.3% and 10.2%, respectively. After Sevage reagent treatment, the protein content of GP decreased from 23.1 to 7.1%. The sugar components were analyzed by converting the sugars into PMP derivatives. HPLC results showed that GP was composed of galacturonic acid (GalA), glucose (Glc), galactose (Gal), and arabinose (Ara) in a molar ratio of 1.6 to 5.1 to 1.0 to 1.6, respectively (**Figure 1B**).

FT-IR Analysis

The GP was analyzed by FT-IR spectroscopy with recorded frequencies ranging from 4,000 to 500 cm^{-1} (**Figure 1C**). A wide absorption peak at 3,446 cm^{-1} in the region of 3,500-3,200 cm^{-1} showed stretching vibrations of O-H and N-H, indicating intramolecular hydrogen bonds. Two peaks in the 3,000-2,800 cm^{-1} region and the 1,400-1,200 cm^{-1} region were angular vibrations of C-H, which indicated that the GP is a polysaccharide compound. The peak at 1,633 cm^{-1} indicates the stretching vibration of the C = O in the acetyl group. The absorption peak at 789 cm^{-1} is the flat pyranose α-type C-H bond in the sugar units.

Morphology Analysis

Scanning electron microscopy (100x and 3,000x) showed that the surface of the GP is rough and irregular (**Figure 1D**). It is speculated that this phenomenon may be due to cross-linking and aggregation between molecular chains. It is suggested that there is a strong interaction between the molecules of the samples, and all of them are amorphous. In addition, the GP contained a porous honeycomb structure, which may be formed by the sublimation of ice crystals during freeze-drying or may be related to the side chain of the polysaccharide.

Molecular Weight Distribution Analysis

The average weight molecular weight (Mw) of the GP mainly distributed in the range of 10-320 kDa by HPGPC and special GPC software (**Figure 1E**). It was revealed that the polysaccharides have four main peaks with molecular weights of 26, 56, 152, and 275 kDa and distribution percentages of 26.6%, 55%, 13.7%, and 4.8%, respectively. In addition, the average difference in Mw between the peaks was 63 kDa, indicating that the GP is a mixture of a series of hetero-polysaccharides.

GP Alleviates Intestinal Injury in Rats With DSS-Induced Colitis

DSS was used to establish an experimental model of rats with intestinal inflammation as described previously (19, 22). HE stains clearly revealed that GP alleviated severe lesions in colon tissue, such as those that had histopathological characteristics of mucosal damage, necrosis, and inflammatory infiltration in DSS rats (**Figure 2A**). Compared to the control group, the histological observation of the colon of the rats in the DSS model group demonstrated that the inflammatory cell infiltration occurred in the mucosa. The loss of goblet cells and epithelium, distorted crypts, and edema were also found in the DSS model group. After treatment with different doses of GP, the results showed notable histologic improvements in the crypt architecture as well as

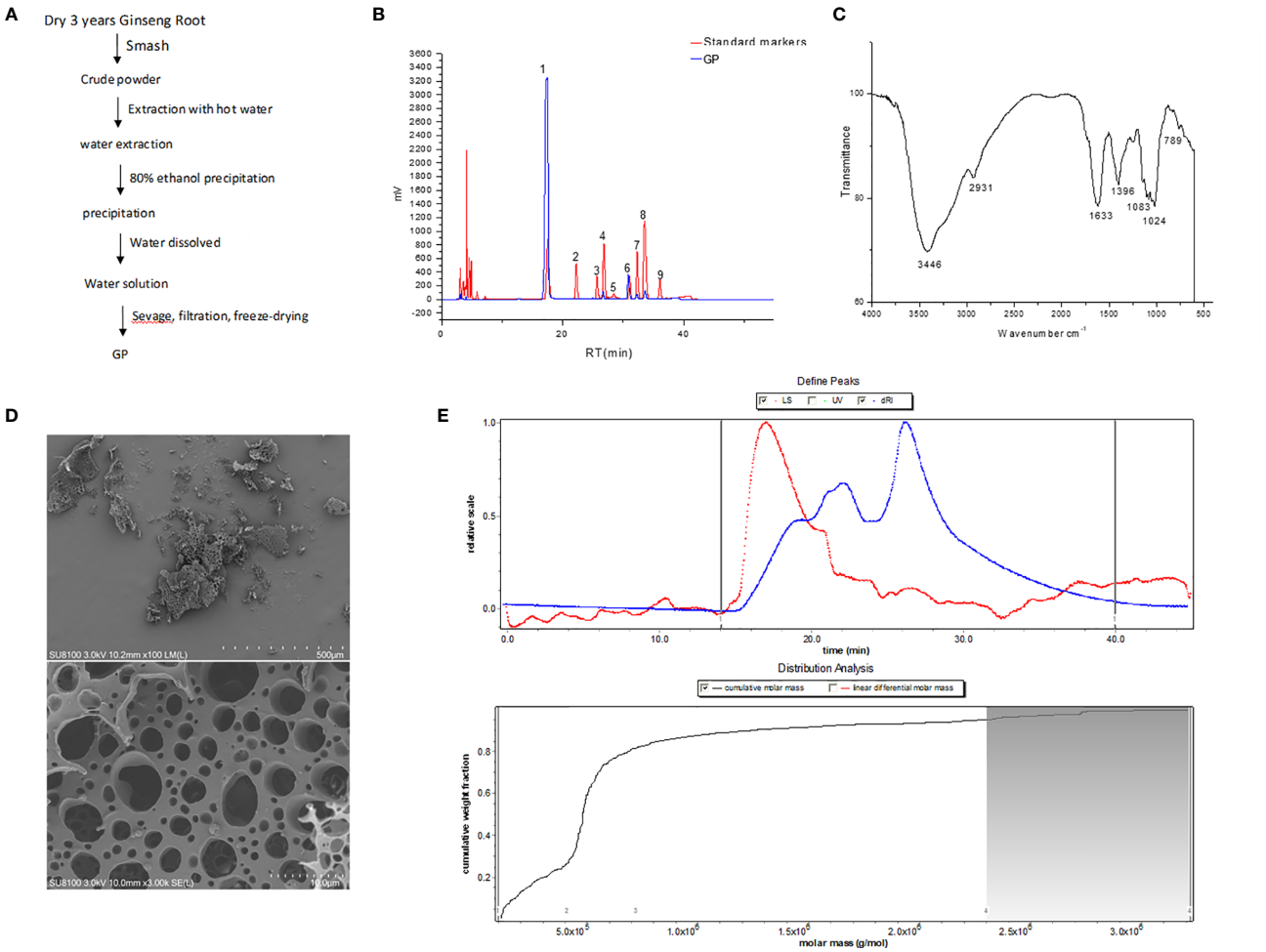

FIGURE 1 | Description and analysis of GP **(A)** Summarized extraction procedure. **(B)** HPLC of monosaccharide PMP derivatization. 1. PMP. 2. Mannose. 3. Rhamnose. 4. Glucuronic acid. 5. Galacturonic acid. 6. Glucose. 7. Galactose. 8. Arabinose. 9. Fucose. **(C)** Infrared spectroscopy. **(D)** Morphology by SEM. **(E)** Molecular weight distribution.

reductions in edema, mucosal injury, and inflammatory infiltration. In the GP-H group, the histopathological properties of the colon of the rats were the most obviously improved, and ulcer healing lines appeared in some tissues (**Figure 2B**). Furthermore, DSS-treated rats showed profound body weight loss; the change in body weight declined 86.96% when compared to the initial weight. Notably, GP treatment significantly attenuated the loss of body weight. Especially in the high-dose GP group (DSS + GP-H), the change in body weight recovered to 151.05% after 14 days of treatment (**Figure 2C**). Rats in the DSS + GP-L and DSS + GP-M groups also exhibited body weight recovery to certain extents. These results demonstrated that DSS can successfully induce inflammatory intestinal injury in rats, and high-dose GP treatment achieved the best curative effect *in vivo*. Therefore, the high-dose GP group can be used for further studies to obtain more biological information. Additionally, GP treatment also reversed the DSS-induced inflammatory response, as evidenced by the spleen weight and the serum levels of IL-1β, IL-8, and TNF-α (**Figures 2D–G**). (From here forward, the DSS + GP group refers to the DSS + GP-H group if not otherwise mentioned).

GP Improved the Structure of Gut Microbiota in DSS-Induced Rats

Effect of GP on the Diversity of Gut Microbiota

The Shannon index is a key index used to evaluate microbial community diversity. Compared with the control group, the Shannon index in the model group decreased significantly ($P < 0.01$). The Shannon index of the GP group was significantly higher than that of the model group ($P < 0.05$; **Figure 3A**). The results showed that the microbiota diversity of the model group was lower than that of the normal rats, but GP could restore the microbiota diversity.

Effect of GP on Bacterial Community Structure

We analyzed the differences in bacterial abundance in rats before and after GP administration at the phylum and genus levels, and the heatmaps are shown in **Figures 3B, C**. Compared with the

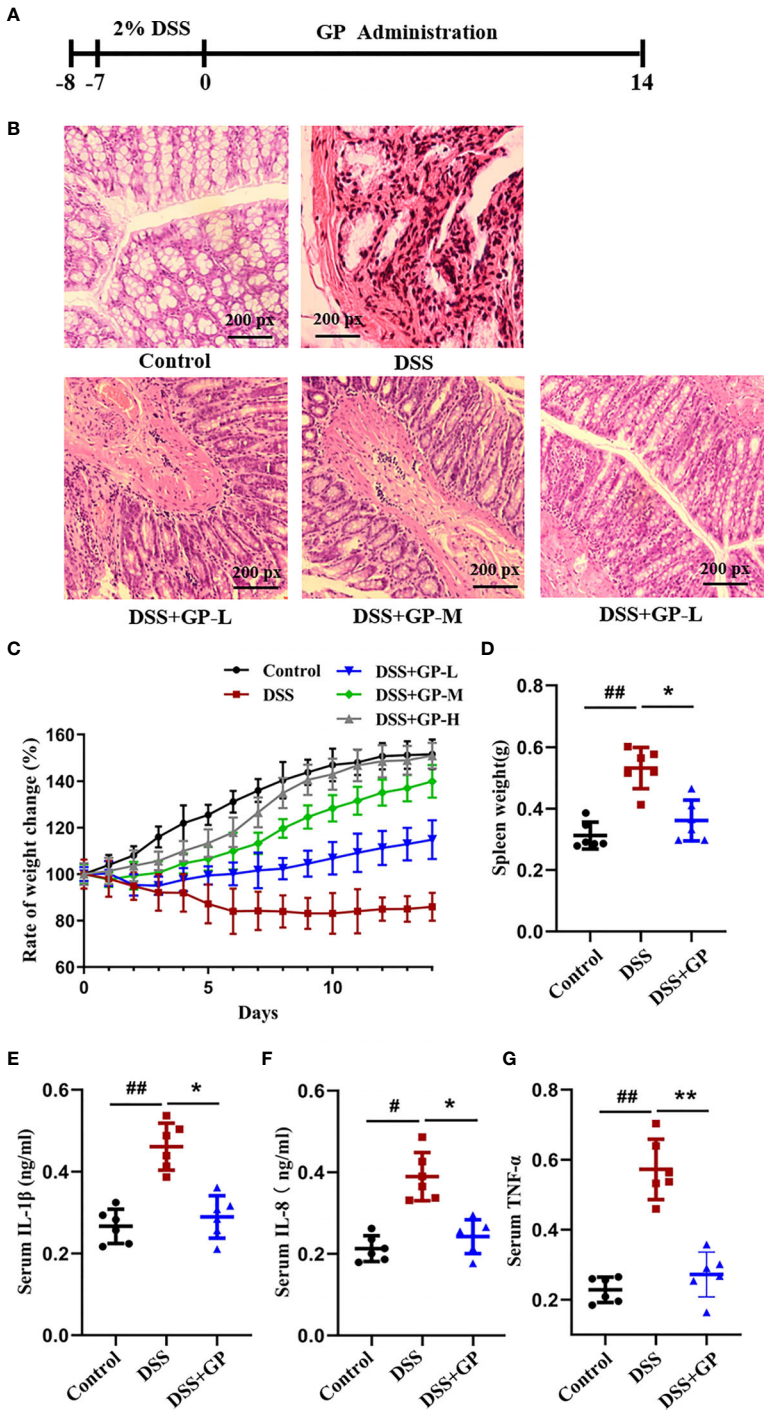

FIGURE 2 | GP alleviated the intestinal inflammation in rats with DSS induced colitis. **(A)** Experimental operation process. **(B)** H&E stained sections of the differently treated rats as described above. **(C, D)** The effects of GP on Rats' basal body weight and Spleen weight. **(E–G)** Changes of cytokines in different groups *in vivo*. All data shown are representative of 3 independent experiments. Bars in graphs represent mean ± SD, $^{\#}P < 0.05$, $^{\#\#}P < 0.01$ VS Control group; $^{*}P < 0.05$, $^{**}P < 0.01$ VS DSS group.

blank group, the abundance of Gram-positive Firmicutes bacteria in the model group decreased significantly, while the abundance of Gram-negative *Bacteroidetes, Verrucomicrobia, Proteobacteria, Tenericutes, Cyanobacteria, and Deferribacteres* increased significantly (38). The abundance of Gram-negative bacteria decreased significantly after GP administration. Next,

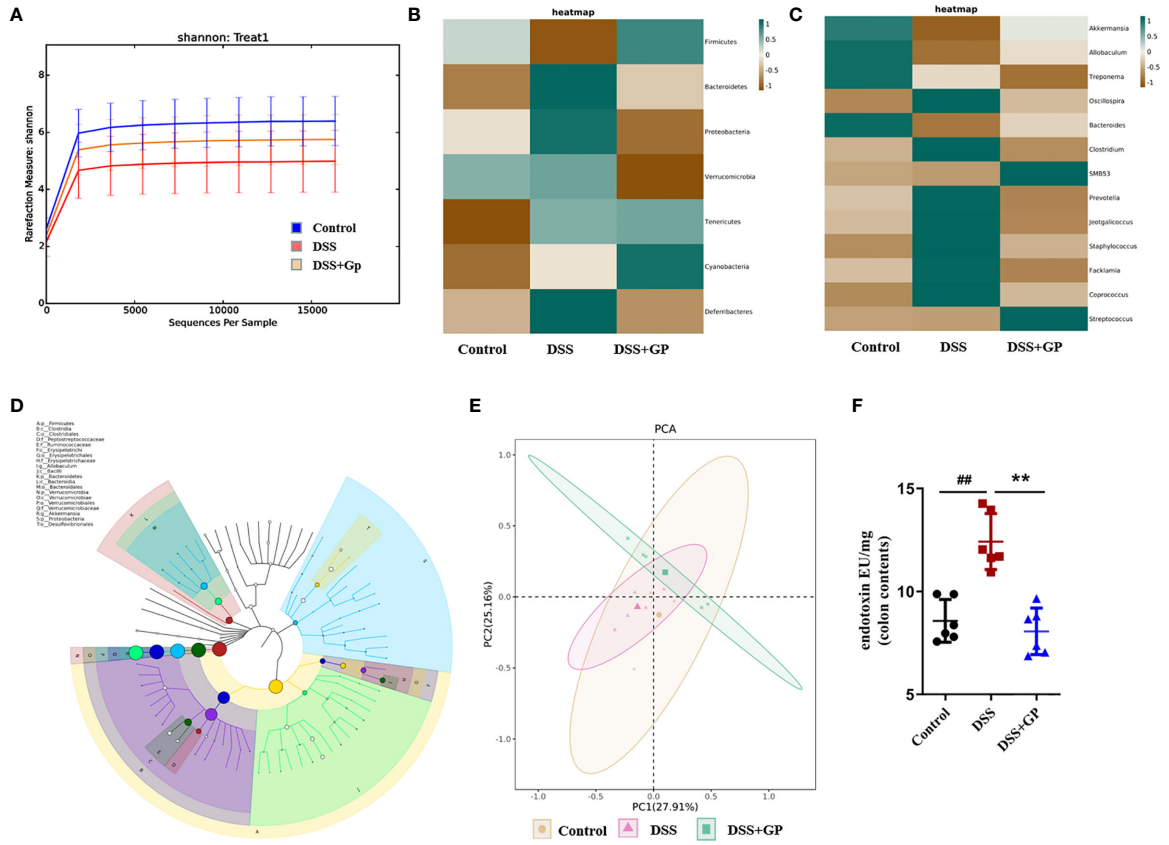

FIGURE 3 | Effects of GP on gut microbiota. **(A)** Rarefaction curves of OTU quantity. **(B)** Heatmap at the level of phylumgenus. **(C)** Heatmap at the level of genus. **(D)** A phylogenetictree of OTUs by GraPhlAn visualization. **(E)** PCA analysis. **(F)** LPS in colon contents. Bars in graphs represent mean ± SD, $^{\#\#}P < 0.01$ VS Control group; $^{**}P < 0.01$ VS DSS group.

Grapeland was used to construct a hierarchical tree of the composition of the sample population at each classification level to explore the dominant microbial groups (**Figure 3D**). The results showed that the dominant species at the phylum level were *Firmicutes, Bacteroidetes, Verrucomicrobia and Proteobacteria*, and the dominant species at the genus level were *Akkermansia, Allobaculum*, and *Oscillospira*. It is suggested that the above bacteria can be used as a characteristic index for future fecal microbiota transplantation. Community composition analyses at the taxonomic levels of phylum and genus have preliminarily proved that the bacterial community structure before and after GP treatment is significantly different. We further used principal component analysis (PCA) to analyze the overall structure of the flora before and after the occurrence of intestinal inflammation and under the intervention of GP, which also proved that there were significant differences between the three groups (**Figure 3E**).

Effect of GP on LPS in Colon Contents

It should be noted that lipopolysaccharide (LPS), one of the components of the cell walls of Gram-negative bacteria in intestinal flora, can cause chronic intestinal inflammation. We determined the endotoxin levels in colon cells (LPS), and they increased 1.45-fold after DSS stimulation. GP treatment reversed the LPS to near the normal level (**Figure 3F**).

Corroborating the above data and the previous reports (32, 39), we demonstrated that the increased levels of LPS were associated with the rising abundance of Gram-negative bacteria in the intestines of the DSS-induced model rats and that GP could regulate the structure of gut microbiota and reduce the abundance of Gram-negative bacteria that produce LPS.

GP Quenched Intestinal Injury and Restored DSS-Decreased Levels of Autophagy in DSS-Induced Rats

When the abundance of Gram-negative bacteria increases, the content of LPS increased consequently and is then recognized by Toll-like receptor 4 (TLR4) on the intestinal cell membrane. This directs a subsequent intracellular reaction and finally leads to an inflammatory response and autophagy inhibition (40). The expression levels of TLR4, IκBα, and NF-κB p65 protein from the rat colon are associated with the inflammatory response and were analyzed by immunofluorescence and Western blot, as shown in **Figure 4**. Compared with the control group, the fluorescence of TLR4 in the model group was significantly enhanced, which indicated that the protein expression level

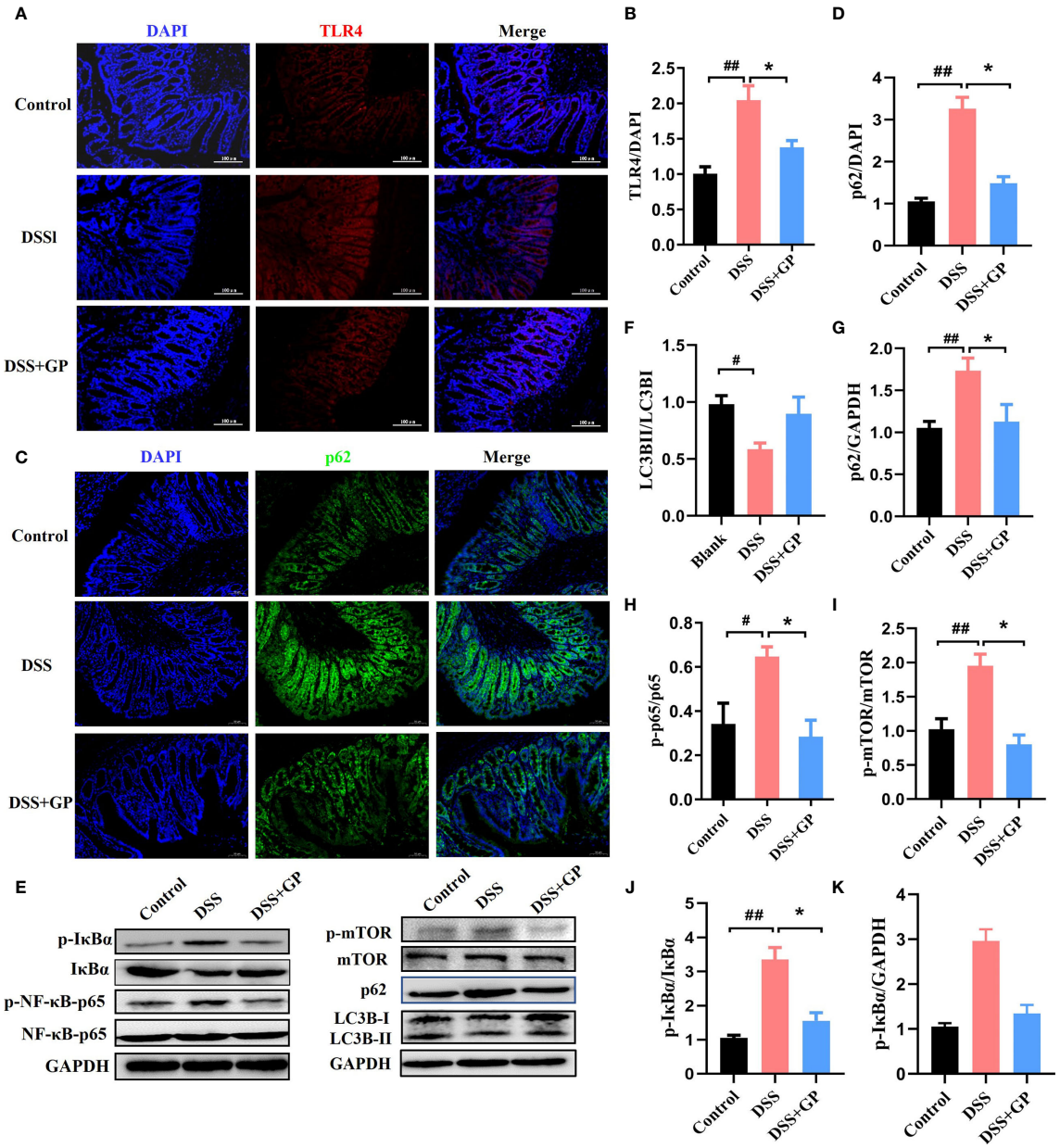

FIGURE 4 | GP inhibits inflammation *via* TLR4 pathway and activates mTOR dependent autophagy in DSS-induced colitis *in vivo*. **(A, C)** Immunofluorescence for TLR4 and p62 was performed on colon sections. **(B, D)** The expressions of TLR4 and p62 were calculated relative to DAPI staining from three independent experiments. **(E)** The expression of autophagy-related and inflammation-related proteins measured by western blot. **(F–K)** The expressions of proteins were quantified by the ratio of phosphorylated protein/total protein and total amount protein/GAPDH. All data shown are representative of 3 independent experiments. Bars in graphs repr Activated TLR4 directly triggers the phosphorylation of mTOR. With the increase of TLR4 in the DSS group, the phosphorylated mTOR was upregulated followed by the dysfunction of autophagy. To investigate whether autophagy was impaired in DSS-induced intestinal inflammation, the expression of autophagy-related proteins (including LC3B, p62, and phosphorylated mTOR) were evaluated by immunofluorescence and Western blot. Compared with the control group, the expression of p62, a cargo protein degraded inside autolysosomes, was upregulated after DSS stimulation, indicating the inhibition of autophagy. Defective autophagy was further confirmed by the decrease in LC3BII/LC3BI when compared with the control group. Autophagy was recovered to a normal level after treatment with GP, indicated by decreased p62 and increased LC3BII/LC3BI levels. These results demonstrated that GP relieved intestinal inflammation by promoting mTOR-dependent autophagy and blocking the inflammatory cascade. Bars in graphs represent mean ± SD, $^{\#}P < 0.05$, $^{\#\#}P < 0.01$ VS Control group; $^{*}P < 0.05$ VS DSS group.

was increased. Notably, GP significantly reversed the DSS-increased expression of TLR4. In addition, the phosphorylation of IκBα was significantly decreased after GP treatment, which suggested that the nuclear translocation of NF-κB was inhibited. As a consequence, GP also reduced the DSS-induced NF-κB activation. In conclusion, GP treatment markedly suppressed

DSS-induced intestinal inflammation through the downregulation of TLR4 and the NF-κB pathway.

Spearman Correlation Analysis of the Bacterial Genera With Highest Abundance and Their Phenotypes

To assess potential association between gut microbiota changes and host autophagy-related phenotypes, we conducted a Spearman correlation analysis of the bacterial genera with the highest abundance and their autophagy-related phenotypes in rats. *p:Akkermansia* from the phylum Verrucomicrobia–*g:Akkermansia* showed significant negative correlation with serum endotoxin, while exhibiting significant positive correlation with LC3BII/LC3BI. On the other hand, there was a highly significant positive correlation between *p_Firmicutes–g_Lactobacillus* and serum endotoxin. *p_Firmicutes–g_Oscillospira, p_*Firmicutes*–g:Lactobacillus, p_Actinobacteria–g_Corynebacterium,and p_Actinobacteria–g_Adlercreutzia* showed significant positive correlation with TLR4 (**Figure 5**). Taken together, these findings indicate that GP treatment inhibited levels of Gram-negative bacteria, inflammation in the intestinal system and enhanced autophagy *via* TLR4.

Fecal Microbiome Transplantation Supplemented With GP Suppressed Intestinal Inflammation and Improved Autophagy

To validate the potential impact of GP on alleviating intestinal inflammation and on microbe-autophagy interactions, we performed FMT experiments by using oral gavage in rats (**Figure 6A**). 20 rats were randomly divided into four groups: DSS (FMT), DSS + GP (FMT), blank (FMT), and blank (normal rats). The body weight changes of rats in the DSS (FMT), DSS + GP (FMT), blank (FMT), and blank groups are shown in **Figure 6B**. Blank (FMT) and blank groups showed similar body weight changes, which indicated that the FMT operation had little effect on the mice. The body weight of the rats transplanted with DSS-treated microbiota decreased significantly, while the rats transplanted with DSS+GP (FMT)-treated microbiota recovery the body weight. HE staining of pathological sections showed that the colon epitheliums of the blank (FMT) and blank group were intact without hyperemia, edema, hemorrhage, or inflammatory cell infiltration. In the DSS (FMT) group, the intestinal epithelial structure was incomplete, and crypt abscesses, a reduction in goblet cells, and large number of neutrophil infiltrations were observed. Compared with the DSS (FMT) group, the colon epithelial cells in the DSS + GP (FMT) group were less damaged, and the crypt abscesses and inflammatory infiltrations were relieved (**Figure 6C**).

The bacterial profiles of the donor mice were measured using 16S rRNA sequencing to investigate the effects of GP on the fecal microbiome of mice. The Simpson Diversity Index of the operational taxonomic unit level in the DSS + GP (FMT) group was significantly higher than that of the DSS (FMT) group, indicating that GP alters the richness and diversity of the microbial community. Significant separations were observed among the four groups during PCA (**Figure 6D**), which is similar to the result of hierarchical clustering. Further PCA showed that the overall structure of the microbiota had significant differences

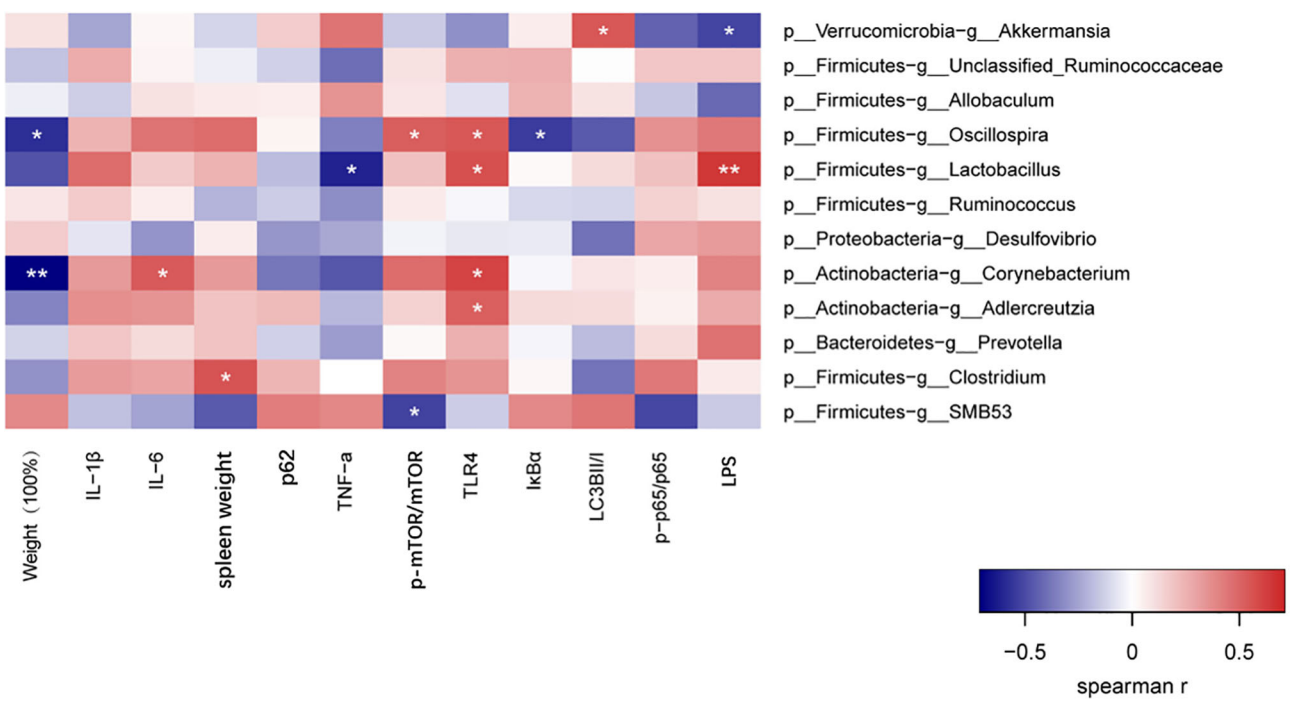

FIGURE 5 | Spearman correlation analysis of the bacterial genera with highest abundance and phenotypes. *P < 0.05, **P < wfi 20.01.

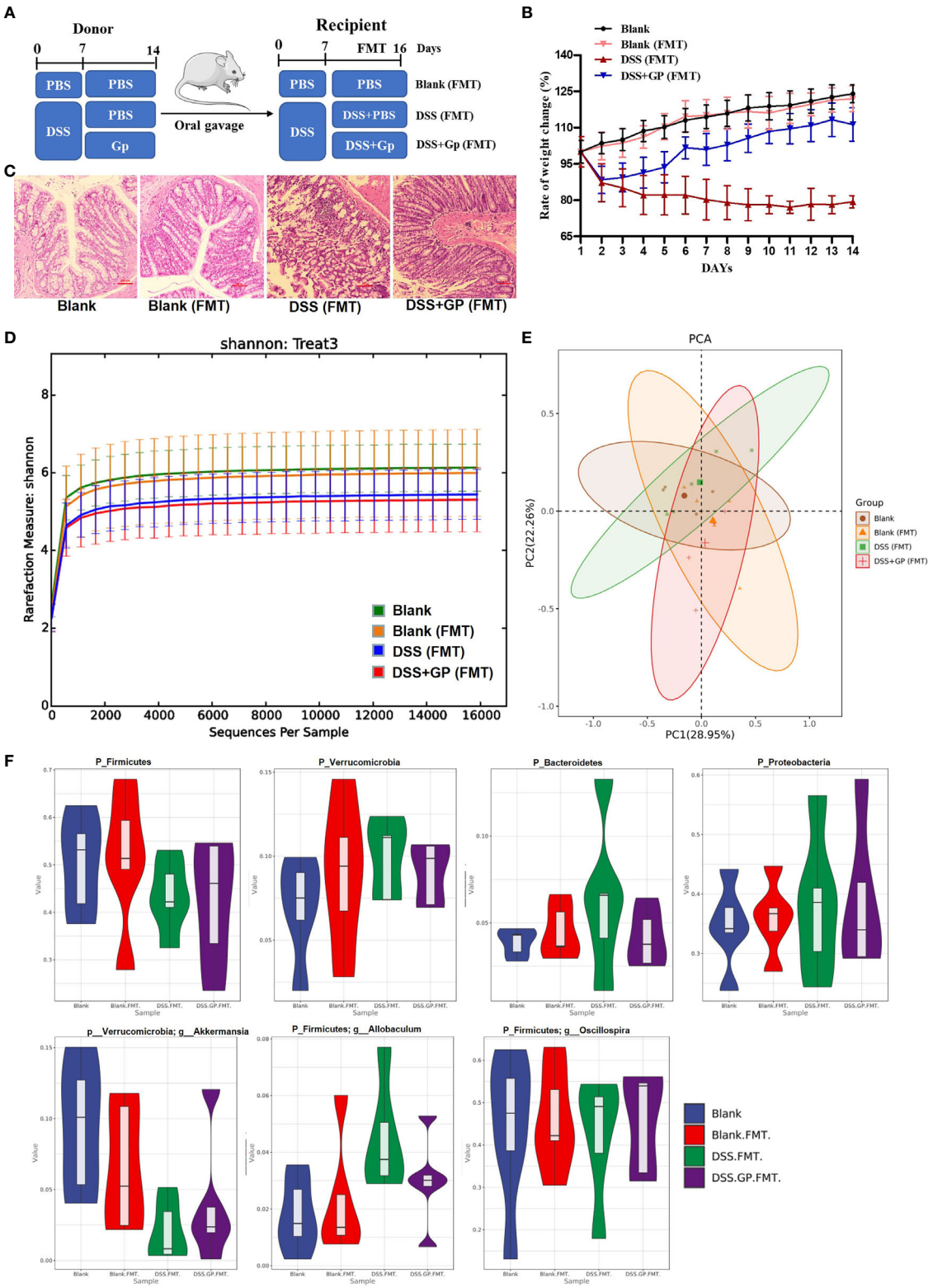

FIGURE 6 | Transplanting of fecal microbiome intervened by GP improves intestinal inflammation. **(A)** The experimental protocol for FMT. **(B)** Changes of body weight (n=10). **(C)** Histopathological changes after HE staining. **(D)** Rarefaction curves of OUT quantity. **(E)** PCA analysis. **(F)** The gut microbiota composition among experimental groups at phylum/genus level.

in the four groups (**Figure 6E**). The comparison of gut microflora with high abundance at the phylum and genus levels in each group is shown in **Figure 6F**. Compared with blank group, there was no significant change in the phylum and genus levels of blank (FMT) bacteria. Compared with blank and blank (FMT) groups, the abundance of *p_ Firmicutes* and *p_Verrucomicrobia-g_Akkermansia* in the DSS (FMT) group was significantly lower, while the abundance of *p_Verrucomicrobia*, *p_Bacteroidetes, p_Proteobacteria*, and p_Firmicutes-g_*Allobaculum* were significantly higher. The abundances of the above bacteria in the DSS + GP (FMT) group and the DSS (FMT) group showed the opposite trend of change except *p_Firmicutes*-g _*Oscillospira*.

To validate the protective effect of GP on intestinal inflammation associated with the microbe-TLR4-autophagy axis, we detected the levels of several key proteins using Western blot analysis. FMT had almost no effects on the TLR4 pathway and mTOR-dependent autophagy, as shown in **Figure 7**. Meanwhile, the rats transplanted with DSS-treated microbiota showed a marked activation of the classic TLR4-p38 MAPK-NF-κB inflammatory pathway (**Figures 7A, B**) as well as the phosphorylation of mTOR. Subsequently, the accumulation of p62 and the decrease of LCBII/LC3BI suggested defective autophagy. Notably, there was significant attenuation of TLR4 and degradation of p62 after FMT with GP-treated microbiota, which achieved similar therapeutic effects compared to GP lavage. In summary, the potential mechanism of GP on ameliorating intestinal inflammation *via* regulation of the gut microbiota and which was associated with TLR4-autophagy.

Blocking TLR4-mTOR Ameliorates Inflammation *via* Promoting Autophagy in LPS-Induced HT-29 Cell

The relationship between intestinal flora disturbance and TLR4-autophagy axis has been widely accepted (41, 42), and gut-derived lipopolysaccharides (LPSs) seem to be the linkage between them. According to the *in vivo* results, related mechanisms of gut microbiota-TLR4-autophagy regulation were subsequently explored in LPS-induced HT-29 cells. To explore whether the release of NF-κB-induced cytokines and oxidative stress were associated with autophagy, we chose 3-MA

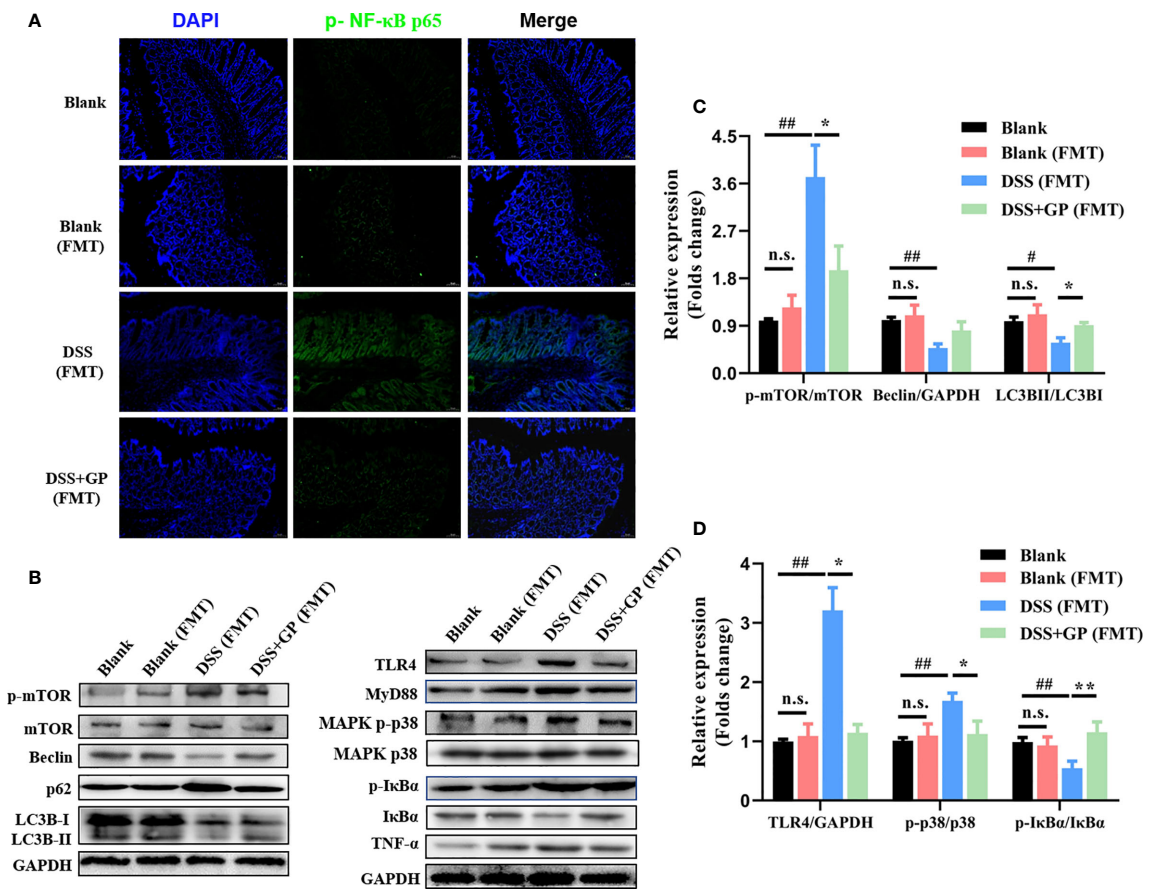

FIGURE 7 | Transplanting of fecal microbiome intervened by GP improves intestinal inflammation. **(A)** Immunofluorescence for p-NF-κB was performed on colon sections. **(B)** The expression of autophagy-related and inflammation-related proteins measured by western blot. **(C, D)** The expressions of proteins were quantified by the ratio of phosphorylated protein/total protein and total amount protein/GAPDH. All data shown are representative of 3 independent experiments. Bars in graphs represent mean ± SD, $^{\#}P < 0.05$, $^{\#\#}P < 0.01$ VS Control group; $^{*}P < 0.05$, $^{**}P < 0.01$ VS DSS group, n.s., no significant differences.

and rapamycin as the inhibitor and activator of autophagy, respectively. Firstly, pro-inflammatory cytokines were determined as shown in **Figure 8A**. When cells were treated with one μg/mL LPS for six hours, IL-8 and IL-1β levels increased by nearly three-fold; these levels ameliorated to a certain extent after rapamycin treatment (an autophagy activator). When autophagy was inhibited by 3-MA, the release of LPS-induced inflammatory cytokines dramatically increased even higher than that of the LPS-induced group. Secondly, the expressions of p62, LC3B, and Beclin-1 were determined by Western blot analysis (**Figure 8B**). In the second lane of **Figure 8**, it can be seen that LPS blocked autophagy *via* the activation of mTOR and activated an inflammatory transcription factor, which is consistent with previous reports (19, 22). While the expression of Beclin-1, degradation of p62, and conversion of LC3B were increased significantly in the rapamycin groups, this was also accompanied with the inhibition of NF-κB p65. As expected, suppression of autophagy by 3-MA significantly inhibited the level of autophagy and dramatically deteriorated the inflammation. The results above indicated that impaired autophagy was involved in LPS-induced inflammation in HT-29 cells.

Recent research has focused on Toll-like receptors (TLRs), which might be involved in orchestrating LPS-induced autophagy inhibition and inflammation aggravation *via* mTOR (19). Thus, we next sought to investigate whether TLR4 is a potential target of governance of the activation of autophagy. As shown in **Figure 8**, LPS significantly upregulated the expression of TLR4 and its downstream signaling molecules MyD88 and p38 MAPK in HT-29 cells, which coincided with high phosphorylation levels of mTOR and inhibition of autophagy. Autophagy-related proteins in TLR4 siRNA transfected cells further confirmed the regulation role of TLR4. TLR4 siRNA attenuated the autophagy impairment and inflammation activation induced by LPS, while 3-MA and rapamycin exhibited almost no effect on TLR4-MyD88. Corroborating the data above, we demonstrated that LPS-decreased autophagy was governed by the upstream TLR4-mTOR pathway. Additionally, autophagy was involved in inhibiting cytokine secretion and protecting cells from oxidative stress.

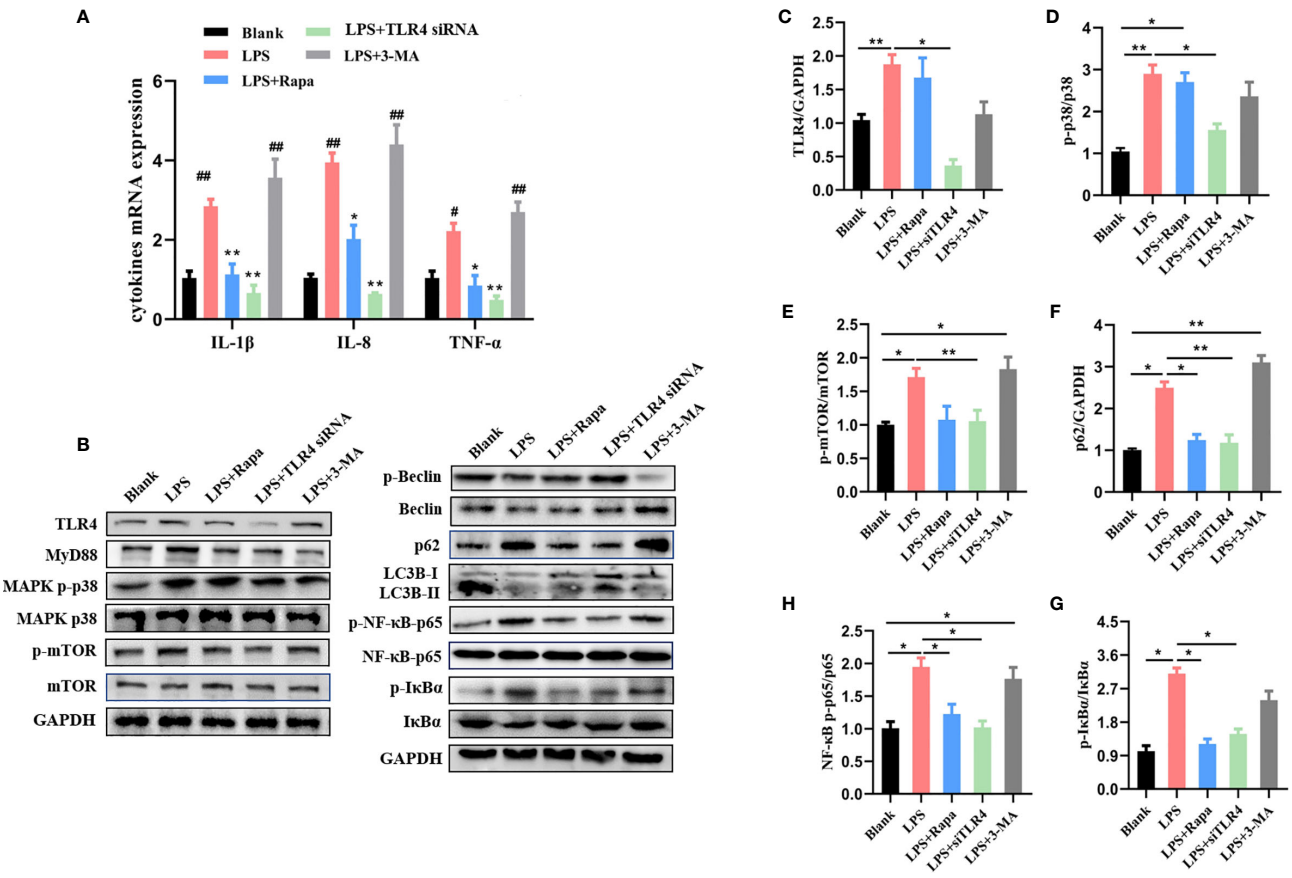

FIGURE 8 | Blocking upstream TLR4-MAPK pathway activated autophagy and quenched inflammation. **(A)** Changes of cytokines contents in different groups in LPS-induced HT-29 cells. **(B)** The changes of autophagy-related and inflammation-related proteins measured by western blot. **(C–H)** The expressions of proteins were quantified by the ratio of phosphorylated protein/total protein and total amount protein/GAPDH. All data shown are representative of 3 independent experiments. Bars in graphs represent mean ± SD, *P < 0.05, **P < 0.01. $^{\#}$P < 0.05, $^{\#\#}$P < 0.01 VS Control group.

DISCUSSION

Inflammatory bowel disease (IBD) is a kind of chronic, nonspecific intestinal inflammation, which includes ulcerative colitis and Crohn's disease. Acetaminophen and non-steroidal anti-inflammatory drugs are the primary clinical treatment, but long-term usage of these can cause kidney and digestive system damage. It is urgent to develop effective treatment strategies, including therapeutics and functional foods.

P. ginseng is a perennial herb. It has been used for thousands of years in China, Japan, and Korea as a traditional medicine. Its chemical properties and pharmacological activities have drawn attention from across the world. Ginseng is available in liquid or solid forms for consumption, and its anti-inflammatory effects have been reported in many studies. Modern pharmacological studies have shown that P. ginseng has therapeutic effects on intestinal system diseases, such as ulcerative colitis, Crohn's bowel disease, and intestinal cancer (43). The polysaccharide is an important active component of P. ginseng in mediating the inflammatory response and immune function and has obvious inhibitory effects on many pathogenic bacteria (44). In this study, polysaccharide from P. ginseng was isolated and simi-purified, and its basic physicochemical properties were studied by HPLC, FT-IR, and GPC. The morphology of the polysaccharide was also characterized by SEM analysis. Further, the activity of GP on intestinal inflammation was evaluated by a model of DSS-induced intestinal inflammation in rats. Our results showed that the weight loss of rats in the GP treatment group was inhibited, and the intestinal mucosa loss as well as the infiltration of inflammatory cells in the lamina propria was reduced in the treatment group after the administration of GP. This indicates that GP has a therapeutic effect on DSS-induced colitis in rats, but the specific mechanism is still unclear.

There are at least 10^{14} microorganisms that reside in human intestines which are involved in the host's immune response, metabolism, and homeostasis maintenance (45). A large number of clinical and experimental studies have shown that many natural plant polysaccharides can play a therapeutic role in intestinal inflammation by regulating the imbalance of gut microbiota (46). Similar results were found in this study: compared with the normal group, the model group of rats had obvious intestinal flora imbalances, while the administration of GP caused a recovery effect on the gut microbiota in model rats. Compared with the model group, the abundance of Gram-negative bacteria decreased significantly after GP administration. It is clear that inflammatory bowel disease is closely related to the regulation of the structure and composition of the intestinal microbiota; however, the pathways involved in the regulation and how to remedy the change in intestinal flora still required elucidation. At present, although there are reports that polysaccharides from P. ginseng can regulate intestinal flora and play a therapeutic role in inflammatory bowel disorders such as IBD and UC, this conclusion overemphasizes the role of intestinal flora and fails to describe the causal mechanism of intestinal flora in the process of disease treatment.

Gut microbiome disorder is closely related to the incidence of a variety of intestinal diseases. In the pathological state of inflammatory bowel disease, the chronic accumulation of activated neutrophils, macrophages, and dendritic cells leads to a change in intestinal flora structure, especially the proliferation of many Gram-negative opportunistic pathogens. Lipopolysaccharide (LPS) is an essential component of the cell wall of Gram-negative bacteria that is involved in triggering the inflammatory cascade (2). Gut microbiota-derived Lipopolysaccharides is closely related to the intestinal flora and abnormally activates the host immune response through TLR4. TLR4 is the receptor for LPS and is of great importance to the self-repair of intestinal epithelial cells (47). Activated TLR4-induced phosphorylation of IκBα *via* the downstream signaling molecule MyD88 eventually leads to the translocation of NF-κB and the release of cytokines including IL-lβ, IL-8 and TNF-α. TNF-α is an important initiator of inflammation, which can cause a microcirculatory disturbance of colonic mucosa and weaken the mucosal barrier, leading to mucosal damage and inflammatory cell infiltration (48). Clinical studies also confirm that the level of TNF-α in serum is positively correlated with the severity of IBD (49). IL-1β increases the cytokines produced by macrophages, such as IL-6, TNF-α, and IL-8, which can promote the aggregation of neutrophils to inflammatory sites and then cause intestinal mucosal tissue damage as well as an intestinal inflammatory response (50). Thus, blocking the TLR4 pathway is an alternative strategy for the development of anti-intestinal inflammation drugs or functional foods (51). In our study, GP markedly suppressed DSS-increased expression of TLR4 and reduced the recruitment of downstream proteins, which was accompanied by decreased cytokines and also the repairment of intestinal mucosa. Our data confirmed that the therapeutic effect of GP on intestinal inflammation is associated with the downregulation of TLR4 expression (**Figure 9**).

Autophagy, a highly conserved process that evolved in eukaryotes, is involved in maintaining organism homeostasis *via* lysosome-mediated self-digestion and recycling of organelles and proteins. Although the pathogenesis of IBD is ambiguous, studies have pointed out that autophagic dysfunction is a key factor in the persistence of intestinal inflammation (19). Pioneer evidence from genome-wide association studies suggested that defective autophagy is associated with an increased risk of IBD (52, 53). Several roles of autophagy in gut inflammation have been summarized: elimination of pathogens, regulation of antigen presentation, governance of the secretion of cytokines, and maintenance of lymphocyte homeostasis. Notably, the accumulation of p62 in DSS-induced rats confirms the dysfunction of autophagy in the pathologicalprocess of intestinal inflammation. After treatment with GP, both groups of rats with intestinal inflammation presented diminished levels of phosphorylated mTOR, LC3B, and Beclin-1, which paralleled with a decrease of p62.

On the basis above, we further discussed the interaction between gut microbiome, TLR4 and autophagy, aiming to reveal the potential mechanism of the impact of GP on intestinal inflammation. In this study, 16S rRNA sequencing was used to evaluate the changes in intestinal flora before and after GP administration. The Spearman correlation coefficient

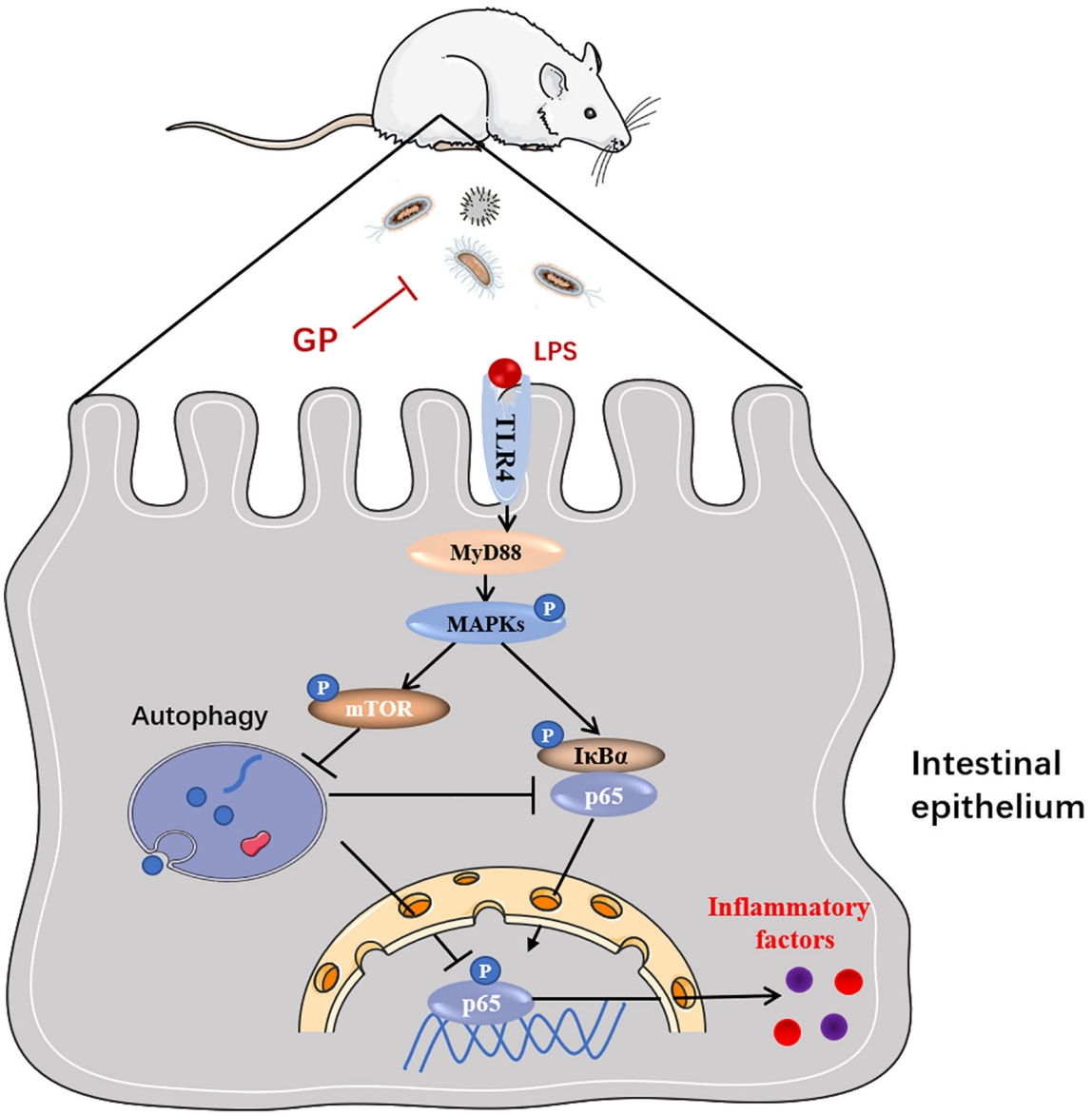

FIGURE 9 | Schematic representation of the proposed mechanism of GP on ameliorating intestinal inflammation.

was used to evaluate the correlation between high abundances of bacteria at the genus level and important characteristics of intestinal inflammation in order to explore the correlation between intestinal flora and autophagy, inflammation and oxidative stress. The results showed that the expression of TLR4 was positively correlated with four of the bacteria with high abundance in intestinal flora. *p:* Verrucomicrobia–*g:Akkermansia* showed significant negative correlation with serum endotoxin, while displaying significant positive correlation with LC3BII/I. It can be seen that changes in intestinal flora, TLR4 pathway activation, and autophagy disorder are connected together in the occurrence and development of intestinal inflammation.

In recent years, the focus of research on intestinal flora has changed from association to modulation (54). The most convincing experimental evidence of the role of intestinal microbiota in human diseases can be obtained from relevant experiments of intestinal flora transplantation (FMT) (55). However, there are few studies on the treatment of inflammatory bowel disease by FMT with the addition of GP. Therefore, indirect experimental animal models are needed to establish causal relationships between altered microbiomes and disease pathogenesis. In this study, FMT-related experiments showed that GP could improve the symptoms of DSS-induced intestinal inflammation by inhibiting the TLR4-NF-κB pathway and activating mTOR-dependent autophagy.

Recently, emerging research has focused on the connection between inflammation and autophagy (21). Accumulating evidence indicates that inflammation and autophagy are linked

by reciprocal regulation, and they are orchestrated by the upstream TLR4-mTOR pathway. It has been reported that inhibiting autophagy is a novel role of the TLR4-MyD88 in intestinal epithelial dysfunction. Subsequently, the release of NF-κB-induced cytokines was orchestrated by autophagy. In addition to previous research, our data also demonstrated that TLR4-MyD88 is involved in the regulation of mTOR phosphorylation, and that mTOR is a newfound intersection between inflammation and autophagy. Blocking the TLR4 pathway not only promotes the repair of autophagy, but also suppresses the disaggregation of IκBα-NF-κB complex through inhibiting the phosphorylation of IκBα. The transcription factor NF-κB is present an inactive state complex with the inhibitory IκB proteins (56). Phosphorylation of IκBα results in the release and nuclear translocation of active NF-κB (57). Consequently, diverse group of extracellular signals are activated including inflammatory cytokines, growth factors, and chemokines. Importantly, autophagy also participates in reducing the degradation of the IκBα-NF-κB complex (58). Treatment with 3-MA deteriorated the LPS-induced inflammatory response in HT-29 cells. Meanwhile, rapamycin, an autophagy activator, ameliorated inflammation to a great extent, which further indicates that autophagy is involved in suppressing NF-κB activation.

Therefore, for the first time, this study elucidated that polysaccharide purified from P. ginseng ameliorates intestinal inflammation through regulating gut microbiota by experiments with FMT and repaired the defective autophagy. Our research revealed the mechanism concerning the intestinal anti-inflammatory effect of GP and provided a promising therapy for IBD.

CONCLUSION

The present results highlighted that the purified polysaccharides from P. ginseng showed intestinal anti-inflammatory effects in DSS-induced rats by regulating gut microbiota and mTOR-dependent autophagy. It was suggested that GP-treated intestinal flora transplantation elevated autophagy and suppressed inflammatory response that was associated with the downregulation of LPS-producing bacteria. Consequently, NF-κB-induced inflammation was attenuated *via* the activation of mTOR-dependent autophagy. The results suggested the view that LPS maybe the potential linker between microbiota and autophagy, and GP may have potential in intestinal inflammation disease therapies, providing a foundation for the potential utilization of polysaccharide from P. ginseng for functional foods and complementary medicines.

DATA AVAILABILITY STATEMENT

The datasets presented in this study can be found in online repositories. The names of the repository/repositories and accession number(s) can be found in the article/supplementary material.

ETHICS STATEMENT

The animal experiment protocol (No. 20200128006) was approved by the Changchun University of Chinese Medicine. Written informed consent was obtained from the owners for the participation of their animals in this study.

AUTHOR CONTRIBUTIONS

DW is the first authors. MW obtained funding. MW, DW, and SS designed the study. YZ and DZ collected the data. MW and DW drafted the manuscript. All authors contributed to the article and approved the submitted version.

FUNDING

This work was supported by the National Key Research and Development Program of China [2017YFC1702100], the National Natural Science Foundation of China [81603276, U19A2013 and 82004099], the Department of Science and Technology of Jilin Province [20190101010JH, 20200201419JC and 202002053JC], and the Science and Technology Projects in Jilin Province Department of Education [JJKH20200903KJ].

REFERENCES

1. Rooks MG, Garrett WS. Gut Microbiota, Metabolites and Host Immunity. *Nat Rev Immunol* (2016) 16(6):341–52. doi: 10.1038/nri.2016.42
2. Barker N. Adult Intestinal Stem Cells: Critical Drivers of Epithelial Homeostasis and Regeneration. *Nat Rev Mol Cell Biol* (2014) 15(1):19–33. doi: 10.1038/nrm3721
3. Miller YI, Choi SH, Wiesner P, Bae YS. The SYK Side of TLR4: Signalling Mechanisms in Response to LPS and Minimally Oxidized LDL. *Br J Pharmacol* (2012) 167(5):990–9. doi: 10.1111/j.1476-5381.2012.02097.x
4. Rogers M, Moore R, Cohen J. The Relationship Between Faecal Endotoxin and Faecal Microflora of the C57BL Mouse. *J Hygiene* (1985) 95(2):397–402. doi: 10.1017/S0022172400062823
5. Di Lorenzo F, Kubik Ł., Oblak A, Lorè NI, Cigana C, Lanzetta R, et al. Activation of Human Toll-Like Receptor 4 (TLR4)·Myeloid Differentiation Factor 2 (MD-2) by Hypoacylated Lipopolysaccharide From a Clinical Isolate of Burkholderia Cenocepacia. *J Biol Chem* (2015) 290(35):21305–19. doi: 10.1074/jbc.M115.649087
6. Medzhitov R, Preston-Hurlburt P, Janeway CAJr. A Human Homologue of the Drosophila Toll Protein Signals Activation of Adaptive Immunity. *Nature* (1997) 388(6640):394–7. doi: 10.1038/41131
7. Wang Q, Dziarski R, Kirschning CJ, Muzio M, Gupta D. Micrococci and Peptidoglycan Activate TLR2–>MyD88–>IRAK–>TRAF–>NIK–>IKK–>NF-kappaB Signal Transduction Pathway That Induces Transcription of Interleukin-8. *Infect Immun* (2001) 69(4):2270–6. doi: 10.1128/IAI.69.4.2270-2276.2001
8. Tan CQ, Gao X, Guo L, Huang H. Exogenous IL-4-Expressing Bone Marrow Mesenchymal Stem Cells for the Treatment of Autoimmune Sensorineural Hearing Loss in a Guinea Pig Model. *BioMed Res Int* (2014) 2014:856019. doi: 10.1155/2014/856019

9. Russell SE, Horan RM, Stefanska AM, Carey A, Leon G, Aguilera M, et al. IL-36α Expression is Elevated in Ulcerative Colitis and Promotes Colonic Inflammation. *Mucosal Immunol* (2016) 9(5):1193–204. doi: 10.1038/mi.2015.134
10. Verkade HJ, Bezerra JA, Davenport M, Schreiber RA, Mieli-Vergani G, Hulscher JB, et al. Biliary Atresia and Other Cholestatic Childhood Diseases: Advances and Future Challenges. *J Hepatol* (2016) 65(3):631–42. doi: 10.1016/j.jhep.2016.04.032
11. Dikic I, Elazar Z. Mechanism and Medical Implications of Mammalian Autophagy. *Nat Rev Mol Cell Biol* (2018) 19(6):349–64. doi: 10.1038/s41580-018-0003-4
12. Mizushima N. A Brief History of Autophagy From Cell Biology to Physiology and Disease. *Nat Cell Biol* (2018) 20(5):521–7. doi: 10.1038/s41556-018-0092-5
13. Netea-Maier RT, Plantinga TS, van de Veerdonk FL, Smit JW, Netea MG. Modulation of inflammation by autophagy: Consequences for human disease. *Autophagy* (2016) 12(2):245–60. doi: 10.1080/15548627.2015.1071759
14. François A, Terro F, Janet T, Rioux Bilan A, Paccalin M, Page G. Involvement of Interleukin-1β in the Autophagic Process of Microglia: Relevance to Alzheimer's Disease. *J Neuroinflamm* (2013) 10:151. doi: 10.1186/1742-2094-10-151
15. Hang TTN, Lapaquette P, Bringer MA, Darfeuille-Michaud A. Autophagy and Crohn's Disease. *J Innate Immun* (2013) 5(5):434–43. doi: 10.1159/000345129
16. Kuenzig ME, Yim J, Coward S, Eksteen B, Seow CH, Barnabe C, et al. The NOD2-Smoking Interaction in Crohn's Disease is Likely Specific to the 1007fs Mutation and may be Explained by Age at Diagnosis: A Meta-Analysis and Case-Only Study. *EBioMedicine* (2017) 21:188–96. doi: 10.1016/j.ebiom.2017.06.012
17. Strisciuglio C, Duijvestein M, Verhaar AP, Vos AC, van den Brink GR, Hommes DW, et al. Impaired Autophagy Leads to Abnormal Dendritic Cell-Epithelial Cell Interactions. *J Crohns Colitis* (2013) 7(7):534–41. doi: 10.1016/j.crohns.2012.08.009
18. Schwerd T, Frivolt K, Clavel T, Lagkouvardos I, Katona G, Mayr D, et al. Exclusive Enteral Nutrition in Active Pediatric Crohn Disease: Effects on Intestinal Microbiota and Immune Regulation. *J Allergy Clin Immunol* (2016) 138(2):592–6. doi: 10.1016/j.jaci.2015.12.1331
19. Zhou M, Xu W, Wang J, Yan J, Shi Y, Zhang C, et al. Boosting mTOR-Dependent Autophagy *via* Upstream TLR4-MyD88-MAPK Signalling and Downstream NF-κb Pathway Quenches Intestinal Inflammation and Oxidative Stress Injury. *EBioMedicine* (2018) 35:345–60. doi: 10.1016/j.ebiom.2018.08.035
20. Santeford A, Wiley LA, Park S, Bamba S, Nakamura R, Gdoura A, et al. Impaired Autophagy in Macrophages Promotes Inflammatory Eye Disease. *Autophagy* (2016) 12(10):1876–85. doi: 10.1080/15548627.2016.1207857
21. Deretic V, Saitoh T, Akira S. Autophagy in Infection, inflammation and immunity. *Nat Rev Immunol* (2013) 13(10):722–37. doi: 10.1038/nri3532
22. Cosin-Roger J, Simmen S, Melhem H, Atrott K, Frey-Wagner I, Hausmann M, et al. Hypoxia Ameliorates Intestinal Inflammation Through NLRP3/mTOR Downregulation and Autophagy Activation. *Nat Commun* (2017) 8(1):98. doi: 10.1038/s41467-017-00213-3
23. Li Z, Ji GE. Ginseng and Obesity. *J Ginseng Res* (2018) 42(1):1–8. doi: 10.1016/j.jgr.2016.12.005
24. Kim EN, Kim TY, Park EK. Panax ginseng Fruit Has Anti-Inflammatory Effect and Induces Osteogenic Differentiation by Regulating Nrf2/HO-1 Signaling Pathway in *In Vitro* and *In Vivo* Models of Periodontitis. *Antioxidants* (2020) 9(12):1121. doi: 10.3390/antiox9121221
25. Khoruts A. Targeting the Microbiome: From Probiotics to Fecal Microbiota Transplantation. *Genome Med* (2018) 10(1):80. doi: 10.1186/s13073-018-0592-8
26. Huang Y, Li N, Wan JB, Zhang D, Yan C. Structural Characterization and Antioxidant Activity of a Novel Heteropolysaccharide From the Submerged Fermentation Mycelia of Ganoderma Capense. *Carbohydr Polym* (2015) 134:752–60. doi: 10.1016/j.carbpol.2015.08.067
27. Dubois M, Gilles KA, Hamilton JK, Rebers PA, Smith F. Colorimetric Method for Determination of Sugars and Related Substances - Analytical Chemistry (ACS Publications). *Springerplus* (1980) 89(5):449–54. doi: 10.1038/168167a0
28. Murado MA, Vázquez JA, Montemayor MI, Cabo ML, del Pilar González M. Two Mathematical Models for the Correction of Carbohydrate and Protein Interference in the Determination of Uronic Acids by the M-Hydroxydiphenyl Method. *Biotechnol Appl Biochem* (2005) 41(Pt 3):209–16. doi: 10.1042/BA20040127
29. Bradford MM. A Rapid and Sensitive Method for the Quantitation of Microgram Quantities of Protein Utilizing the Principle of Protein-Dye Binding. *Anal Biochem* (1976) 72:248–54. doi: 10.1016/0003-2697(76)90527-3
30. Wang J, Li S, Fan Y, Chen Y, Liu D, Cheng H, et al. Anti-Fatigue Activity of the Water-Soluble Polysaccharides Isolated From Panax Ginseng C. *A. Meyer J Ethnopharmacol* (2010) 130(2):421–3. doi: 10.1016/j.jep.2010.05.027
31. Yu C, Irudayaraj J. Spectroscopic Characterization of Microorganisms by Fourier Transform Infrared Microspectroscopy. *Biopolymers* (2005) 77(6):368–77. doi: 10.1002/bip.20247
32. Zhang C, Li Z, Zhang CY, Li M. Extract Methods, Molecular Characteristics, and Bioactivities of Polysaccharide From Alfalfa (Medicago sativa L.). *Nutrients* (2019) 11(5). doi: 10.3390/nu11051181
33. Wang M, Gao Y, Xu D, Gao Q. A Polysaccharide From Cultured Mycelium of Hericium Erinaceus and its Anti-Chronic Atrophic Gastritis Activity. *Int J Biol Macromol* (2015) 81:656–61. doi: 10.1016/j.ijbiomac.2015.08.043
34. Lai KM. Are Cockroaches an Important Source of Indoor Endotoxins? *Int J Environ Res Public Health* (2017) 14(1):91. doi: 10.3390/ijerph14010091
35. Wu TR, Lin CS, Chang CJ, Lin TL, Martel J, Ko YF, et al. Gut Commensal Parabacteroides Goldsteinii Plays a Predominant Role in the Anti-Obesity Effects of Polysaccharides Isolated From Hirsutella Sinensis. *Gut* (2019) 68(2):248–62. doi: 10.1136/gutjnl-2017-315458
36. Shao S, Wang D, Zheng W, Li X, Zhang H, Zhao D, et al. A Unique Polysaccharide From Hericium Erinaceus Mycelium Ameliorates Acetic Acid-Induced Ulcerative Colitis Rats by Modulating the Composition of the Gut Microbiota, short chain fatty acids levels and GPR41/43 respectors. *Int Immunopharmacol* (2019) 71:411–22. doi: 10.1016/j.intimp.2019.02.038
37. Wang M, Kanako N, Zhang Y, Xiao X, Gao Q, Tetsuya K. A Unique Polysaccharide Purified From Hericium Erinaceus Mycelium Prevents Oxidative Stress Induced by H2O2 in Human Gastric Mucosa Epithelium Cell. *PloS One* (2017) 12(7):e0181546. doi: 10.1371/journal.pone.0181546
38. Qin J, Li R, Raes J, Arumugam M, Burgdorf KS, Manichanh C, et al. A Human Gut Microbial Gene Catalogue Established by Metagenomic Sequencing. *Nature* (2010) 464(7285):59–65. doi: 10.1038/nature08821
39. Goris H, de Boer F, van der Waaij D. Kinetics of Endotoxin Release by Gram-Negative Bacteria in the Intestinal Tract of Mice During Oral Administration of Bacitracin and During *In Vitro* Growth. *Scand J Infect Dis* (1988) 20(2):213–9. doi: 10.3109/00365548809032440
40. Chassaing B, Koren O, Carvalho FA, Ley RE, Gewirtz AT. AIEC Pathobiont Instigates Chronic Colitis in Susceptible Hosts by Altering Microbiota Composition. *Gut* (2014) 63(7):1069–80. doi: 10.1136/gutjnl-2013-304909
41. Sacks D, Baxter B, Campbell BCV, Carpenter JS, Cognard C, Dippel D, et al. Multisociety Consensus Quality Improvement Revised Consensus Statement for Endovascular Therapy of Acute Ischemic Stroke. *Int J stroke: Off J Int Stroke Soc* (2018) 13(6):612–32. doi: 10.1177/1747493018778713
42. Han JX, Tao ZH, Qian Y, Yu CY, Li J, Kang ZR, et al. ZFP90 Drives the Initiation of Colitis-Associated Colorectal Cancer *via* a Microbiota-Dependent Strategy. *Gut Microbes* (2021) 13(1):1–20. doi: 10.1080/19490976.2021.1917269
43. Luo Z, Xu W, Zhang Y, Di L, Shan J. A Review of Saponin Intervention in Metabolic Syndrome Suggests Further Study on Intestinal Microbiota. *Pharmacol Res* (2020) 160:105088. doi: 10.1016/j.phrs.2020.105088
44. Guo M, Shao S, Wang D, Zhao D, Wang M. Recent Progress in Polysaccharides From Panax Ginseng C. A. Meyer. *Food Function* (2021) 12(2):494–518. doi: 10.1039/D0FO01896A
45. Michielan A, D'Incà R. Host-Microbiome Interaction in Crohn's Disease: A Familiar or Familial Issue? *World J Gastrointest Pathophysiol* (2015) 6(4):159–68. doi: 10.4291/wjgp.v6.i4.159
46. Sun Q, Cheng L, Zeng X, Zhang X, Wu Z, Weng P. The Modulatory Effect of Plant Polysaccharides on Gut Flora and the Implication for Neurodegenerative Diseases From the Perspective of the Microbiota-Gut-Brain Axis. *Int J Biol Macromol* (2020) 164:1484–92. doi: 10.1016/j.ijbiomac.2020.07.208
47. Jun YK, Kwon SH, Yoon HT, Park H, Soh H, Lee HJ, et al. Toll-Like Receptor 4 Regulates Intestinal Fibrosis *via* Cytokine Expression and Epithelial-Mesenchymal Transition. *Sci Rep* (2020) 10(1):19867. doi: 10.1038/s41598-020-76880-y

48. Sands BE, Kaplan GG. The Role of TNFalpha in Ulcerative Colitis. *J Clin Pharmacol* (2007) 47(8):930–41. doi: 10.1177/0091270007301623
49. Pezelj-Ribarić S, Magasić K, Prpić J, Miletić I, Karlović Z. Tumor Necrosis Factor-Alpha in Peripical Tissue Exudates of Teeth With Apical Periodontitis. *Mediators Inflamm* (2007) 2007:69416. doi: 10.1155/2007/69416
50. Wu P, Guo Y, Jia F, Wang X. The Effects of Armillarisin A on Serum IL-1β and IL-4 and in Treating Ulcerative Colitis. *Cell Biochem Biophys* (2015) 72 (1):103–6. doi: 10.1007/s12013-014-0413-7
51. De Jager PL, Franchimont D, Waliszewska A, Bitton A, Cohen A, Langelier D, et al. The Role of the Toll Receptor Pathway in Susceptibility to Inflammatory Bowel Diseases. *Genes Immun* (2007) 8(5):387–97. doi: 10.1038/sj.gene.6364398
52. Retnakumar SV, Muller S. Pharmacological Autophagy Regulators as Therapeutic Agents for Inflammatory Bowel Diseases. *Trends Mol Med* (2019) 25(6):516–37. doi: 10.1016/j.molmed.2019.03.002
53. Voinchet H, Etienne G, Ghiringelli CB, Pellegrin JL, Viallard JF, Parrens M, et al. [Splenic Marginal Zone Lymphoma and Autoimmunity: Report of Six Cases]. *Rev Med Interne* (2010) 31(1):4–11. doi: 10.1016/j.revmed.2009.05.003
54. Schmidt TSB, Raes J, Bork P. The Human Gut Microbiome: From Association to Modulation. *Cell* (2018) 172(6):1198–215. doi: 10.1016/j.cell.2018.02.044
55. Liu Y, Fan L, Cheng Z, Yu L, Cong S, Hu Y, et al. Fecal Transplantation Alleviates Acute Liver Injury in Mice Through Regulating Treg/Th17 Cytokines Balance. *Sci Rep* (2021) 11(1):1611. doi: 10.1038/s41598-021-81263-y
56. Baeuerle PA, Baltimore D. I Kappa B: A Specific Inhibitor of the NF-Kappa B Transcription Factor. *Sci (New York N.Y.)* (1988) 242(4878):540–6. doi: 10.1126/science.3140380
57. Shi X, Zhu S, Jin H, Fang J, Xing X, Wang Y, et al. The Anti-Inflammatory Effect of KS23, A Novel Peptide Derived From Globular Adiponectin, on Endotoxin-Induced Uveitis in Rats. *Front Pharmacol* (2020) 11:585446. doi: 10.3389/fphar.2020.585446
58. Zhou R, Yazdi AS, Menu P, Tschopp J. A Role for Mitochondria in NLRP3 Inflammasome Activation. *Nature* (2011) 469(7329):221–5. doi: 10.1038/nature09663

Conflict of Interest: The authors declare that the research was conducted in the absence of any commercial or financial relationships that could be construed as a potential conflict of interest.

Copyright © 2021 Wang, Shao, Zhang, Zhao and Wang. This is an open-access article distributed under the terms of the Creative Commons Attribution License (CC BY). The use, distribution or reproduction in other forums is permitted, provided the original author(s) and the copyright owner(s) are credited and that the original publication in this journal is cited, in accordance with accepted academic practice. No use, distribution or reproduction is permitted which does not comply with these terms.

frontiers in Immunology

ORIGINAL RESEARCH
published: 22 July 2021
doi: 10.3389/fimmu.2021.668219

Fecal Bacteria Implicated in Biofilm Production Are Enriched and Associate to Gastrointestinal Symptoms in Patients With APECED – A Pilot Study

Iivo Hetemäki[1], Ching Jian[2], Saila Laakso[3,4,5], Outi Mäkitie[3,4,5,6], Anne-Maria Pajari[7], Willem M. de Vos[2,8], T. Petteri Arstila[1] and Anne Salonen[2]*

[1] Translational Immunology Research Program, University of Helsinki and Helsinki University Hospital, Helsinki, Finland, [2] Human Microbiome Research Program, Faculty of Medicine, University of Helsinki, Helsinki, Finland, [3] Institute of Genetics, Folkhälsan Research Center, Helsinki, Finland, [4] Children's Hospital, University of Helsinki and Helsinki University Hospital, Helsinki, Finland, [5] Clinical and Molecular Metabolism Research Program, Faculty of Medicine, University of Helsinki, Helsinki, Finland, [6] Department of Molecular Medicine, Karolinska Institutet, and Clinical Genetics, Karolinska University Hospital, Stockholm, Sweden, [7] Department of Food and Nutrition, University of Helsinki, Helsinki, Finland, [8] Laboratory of Microbiology, Wageningen University, Wageningen, Netherlands

OPEN ACCESS

Edited by:
Oscar Gilberto Gomez-Duarte, University at Buffalo, United States

Reviewed by:
Gislane Lelis Vilela de Oliveira, São Paulo State University, Brazil
Ping Li, Zhejiang Gongshang University, China

***Correspondence:**
Iivo Hetemäki
iivo.hetemaki@helsinki.fi

Specialty section:
This article was submitted to Microbial Immunology, a section of the journal Frontiers in Immunology

Received: *15 February 2021*
Accepted: *08 July 2021*
Published: *22 July 2021*

Citation:
Hetemäki I, Jian C, Laakso S, Mäkitie O, Pajari A-M, de Vos WM, Arstila TP and Salonen A (2021) Fecal Bacteria Implicated in Biofilm Production Are Enriched and Associate to Gastrointestinal Symptoms in Patients With APECED – A Pilot Study. Front. Immunol. 12:668219. doi: 10.3389/fimmu.2021.668219

Backgrounds and Aims: APECED is a rare autoimmune disease caused by mutations in the Autoimmune Regulator gene. A significant proportion of patients also have gastrointestinal symptoms, including malabsorption, chronic diarrhea, and obstipation. The pathological background of the gastrointestinal symptoms remains incompletely understood and involves multiple factors, with autoimmunity being the most common underlying cause. Patients with APECED have increased immune responses against gut commensals. Our objective was to evaluate whether the intestinal microbiota composition, predicted functions or fungal abundance differ between Finnish patients with APECED and healthy controls, and whether these associate to the patients' clinical phenotype and gastrointestinal symptoms.

Methods: DNA was isolated from fecal samples from 15 patients with APECED (median age 46.4 years) together with 15 samples from body mass index matched healthy controls. DNA samples were subjected to analysis of the gut microbiota using 16S rRNA gene amplicon sequencing, imputed metagenomics using the PICRUSt2 algorithm, and quantitative PCR for fungi. Extensive correlations of the microbiota with patient characteristics were determined.

Results: Analysis of gut microbiota indicated that both alpha- and beta-diversity were altered in patients with APECED compared to healthy controls. The fraction of *Faecalibacterium* was reduced in patients with APECED while that of *Atopobium* spp. and several gram-negative genera previously implicated in biofilm formation, e.g. *Veillonella, Prevotella, Megasphaera* and *Heamophilus*, were increased in parallel to lipopolysaccharide (LPS) synthesis in imputed metagenomics. The differences in gut

microbiota were linked to patient characteristics, especially the presence of anti-*Saccharomyces cerevisiae* antibodies (ASCA) and severity of gastrointestinal symptoms.

Conclusions: Gut microbiota of patients with APECED is altered and enriched with predominantly gram-negative bacterial taxa that may promote biofilm formation and lead to increased exposure to LPS in the patients. The most pronounced alterations in the microbiota were associated with more severe gastrointestinal symptoms.

Keywords: dysbiosis, gut microbiota, immune dysregulation, lps, autoantibodies, atopobium, faecalibacterium, autoimmunity

HIGHLIGHTS

APECED is a rare autoimmune disease caused by mutations in the Autoimmune Regulator gene. A significant proportion of patients have gastrointestinal symptoms, including malabsorption, chronic diarrhea, and obstipation that lead to decrease in the quality of life. The pathological background of the gastrointestinal symptoms remains incompletely understood. We have previously found that patients with APECED have increased immune responses against gut commensals, but previous smaller studies have found only small alterations in the microbiota of the gut of the patients. Our objective was to evaluate whether the intestinal microbiota composition differs between patients with APECED (N=15) and healthy controls, and whether these are associated with the patients' clinical phenotype and gastrointestinal symptoms. We found both alpha- and beta-diversity to be altered in patients with APECED compared to healthy controls. Several gram-negative genera previously implicated in biofilm formation were increased in patients, in parallel with lipopolysaccharide (LPS) synthesis in imputed metagenomics. Interestingly, the most pronounced changes in the microbiota were associated with more severe gastrointestinal symptoms in patients with APECED, suggesting that gut microbiota is a factor to consider when contemplating therapy.

INTRODUCTION

APECED (autoimmune polyendocrinopathy-candidiasis-ectodermal dystrophy, OMIM #240300) is a rare autoimmune disease caused by autosomal recessive mutations in the gene encoding the Autoimmune Regulator (AIRE) (1). AIRE is expressed in medullary thymic epithelial cells where it regulates the expression of tissue-restricted antigens, most likely contributing to thymic negative selection. The lack of a fully functioning AIRE leads to autoimmunity against multiple endocrine organs, resulting in hormonal deficiencies of which hypoparathyroidism and primary adrenal insufficiency are the most common manifestations (1). Practically all patients with APECED have neutralizing anti-cytokine antibodies some of which have been linked susceptibility to *Candida albicans* infections (2).

A significant proportion of patients with APECED present with gastrointestinal (GI) symptoms, such as malabsorption, chronic diarrhea, obstipation, and gastritis (3). The pathological background of the GI symptoms remains incompletely understood, but they have been attributed to multiple factors with autoimmunity being the most common underlying cause. About half of patients with APECED have autoimmunity against gut neuroendocrine cells associated with antibodies against tryptophan hydroxylase (TPH) (4). The loss of neuroendocrine cells leads to decreased serum serotonin levels, which in turn is associated with symptoms of obstipation (5). In addition, around a quarter of the patients exhibit autoimmunity against defensins, culminating in a loss of Paneth cells (6). Anti-defensin antibodies are linked to gut microbiota dysbiosis in Aire -/- mice and diarrhea in humans (6). Autoimmune hepatitis, gastritis, and exocrine pancreatic malfunction also affect patients' GI health.

We have previously detected anti-*Saccharomyces cerevisiae* antibodies (ASCA) and other anti-commensal antibodies in patients with APECED, in a pattern reminiscent of the one seen in Crohn's disease (7). It has been suggested that an overt inflammatory response against normal gut microbiota plays a vital role in the pathogenesis of Crohn's disease, and a deviating gut microbiota, characterized by a decrease of butyrate producers and an increase of pro-inflammatory Proteobacteria, has been observed in a significant number of patients with Crohn's disease (8–11). Previous reports on small numbers of patients (10 and 11 patients) offer some indication that deviations in the gut microbiota might also be a feature of APECED, but the differences between patients and controls have been modest (5, 6). Here we present a characterization of the gut microbiota in, to our knowledge, the largest cohort of APECED patients described so far, showing clear aberrations of the gut microbiota. These changes are similar to the ones observed in Crohn's disease, more pronounced in patients with anti-*Saccharomyces cerevisiae antibodies*, and are associated with chronic diarrhea.

MATERIALS AND METHODS

We invited all patients who have taken part in previous large Finnish clinical studies on APECED (1) to participate in the current study. Additional patients were recruited from all Finnish university hospitals and central hospitals by contacting the respective endocrine units. Out of the 91 Finnish patients enrolled in previous studies (6), 61 were alive at the time of recruitment. Altogether 37 (68%) adult patients consented and

were included in the study during the years of 2015-2016 (12). Fifteen patients (seven females), in the age range of 19 to 70 years (mean, 45.9 years) with a body mass index (BMI) range of 17.7 to 40.7 kg/m^2 (mean, 23.2 kg/m^2) were willing to donate frozen fecal sample and form the study patient group. Fifteen control fecal samples, from healthy individuals (ten females) aged between 20 to 67 years (mean, 34.9 years) with a BMI between 18.1 to 33.0 (mean, 23.9), were selected from an inhouse database to be used as controls. The controls were selected to match patients as closely as possible in relation to age, BMI and sex. Exclusion criteria in the control group were medication for hypercholesterolemia or hypertension, regular or recent (within the past three months) use of antibiotics, extreme sport, smoking, pregnancy, or lactation. Sample processing methodology from sampling to DNA extraction and sequencing was identical between the patient and control samples.

The Ethics committee of the Helsinki University Hospital approved the study protocol, and subjects gave their signed informed consent prior to enrollment. The study was performed according to the principles of the Declaration of Helsinki.

Clinical Data

Clinical details for APECED patients were collected from medical records, through a questionnaire and patient interviews, which included questions on medical history, prior infections, medications, and other relevant parameters. All patients were clinically examined by a medical doctor (S.L.). The grading of the severity of GI symptoms experienced by the patients was done based on discussion and a unanimous decision by two physicians (I.H. and S.L.). The severity of diarrhea was classified according to the degree of symptoms experienced: 1) no symptoms, 2) intermittent diarrhea, episodes of diarrhea separated by obstipation or symptom-free periods, 3) chronic difficult diarrhea.

Sample Collection and Processing of Fecal Samples

Fecal samples for the patients and controls were collected at home and immediately stored at -20°C. They were transported to a study center within 1 week. An uninterrupted frozen cold chain was ensured in the provision and handling of the fecal samples. Bacterial DNA was extracted from ca. 250 mg of fecal matter using the Repeated Bead Beating (RBB) method (13) with the following modifications for automated DNA purification: 340 µl and 145 µl of lysis buffer was added to first and second round of bead beating, respectively. 200 µl of the clarified supernatant collected from the two bead beating rounds was used for DNA extraction with the Ambion Magmax^{TM} -96 DNA Multi-Sample Kit (Thermo Fisher Scientific, USA) using the KingFisherTM Flex automated purification system (Thermo Fisher Scientific, USA). DNA was quantified using Quanti-iT^{TM} Pico Green dsDNA Assay (Invitrogen, San Diego, CA, USA).

Blood samples were collected in the morning between 7 and 10 am after an 8- to 12-hour fast before taking morning medications. Sera were isolated with a standard protocol and stored at -80°C until analyses.

Quantification of Anti-*Saccharomyces cerevisiae* Antibodies

The ASCA were quantified from patient sera with the Anti-*Saccharomyces cerevisiae* Antibodies IgG test kit (Bio-Rad, USA) as instructed by the manufacturer. Values over 15 U/mL were considered positive.

Anti-Tryptophan Hydroxylase Antibodies

Immunoprecipitation of radiolabeled antigens was used to screen sera for autoantibodies against tryptophan hydroxylase-1. Human complementary DNA from the antigen in expression vector was used to perform the assay. *In vitro* transcription and translation were performed in the presence of ^{35}S-methionine, according to the manufacturer's protocol (Promega TNT Systems). Immunoprecipitation was performed in 96-well plates overnight at 4°C at 300 rpm with serum samples (2.5 µl) and 30,000 cpm of radiolabeled protein. A positive control (positive patient serum to each antigen) and a negative control, 4% bovine serum albumin, were included in each plate. All samples were analyzed in duplicates. The immune reaction was transferred to filter plates (Millipore) and immune complexes were captured to Protein A sepharose (nProtein A Sepharose 4 fast flow, GE Healthcare) during a 45 min incubation at 4°C at 300 rpm. After ten washing steps with wash buffer (150mM NaCl, 20 mM TrisHCl pH 8, 0.15% Tween 20, and 0.1% BSA), plates were dried and scintillation fluid (Optiphase, HiSafe 3, PerkinElmer) was added. Radioactivity was then measured in a beta counter (1450 Microbeta Trilux, Wallac). Autoantibody index values were calculated according to the following: (sample value – negative control value)/(positive control value – negative control value) x 100.

Quantitative PCR for Fungi

For qPCR targeting fungal ITS1-region, 5 ng of DNA was mixed with 2 µM of ITS1F and ITS2 primers (14) and 2X Power SYBR green PCR Master Mix (Thermo Fisher, USA) in a total volume of 20 µl. The PCR reaction was performed in the C1000 Touch Thermal Cycler (Bio-Rad, USA) as follows: 95°C for 15 min, followed by 40 cycles of 95°C 15 sec, 55°C 30 sec and 72°C 30 sec and ending in 95°C 1 min and 60°C 1 min. Results were analyzed using the comparative Ct method (15).

Microbiota Analysis

Library preparation and Illumina MiSeq sequencing of the hypervariable V3-V4 regions of the 16S rRNA gene and sequencing data preprocessing for the patient and control samples as well as negative controls were performed as previously described (16).

Sequencing Data Preprocessing Analysis and Statistics

The pre-processing of the sequencing reads, their taxonomic annotation, and statistical analysis were performed using

R package *mare* (Microbiota Analysis in R Easily) (17) as previously described (16, 18). Samples from cases and controls were sequenced in two different MiSeq runs with non-template negative controls. The lowest number of reads per sample was 28175 and the mean number of reads was 72610 for patients and 73661 for controls. The three negative control samples in the run with APECED samples contained 139, 259, and 728 reads assigned to two uncultured lactobacilli. As the reads assigned to *Lactobacillus* in the APECED samples were also mostly assigned to the two uncultured lactobacilli in negative controls, we excluded *Lactobacillus* from all data analyses. To account for the varying sequencing depth, the number of reads per sample was used as an offset in all statistical models. The β-diversity was estimated using Bray-Curtis dissimilarity as the distance measure and the contribution of different variables to microbiota variation was calculated using permutational ANOVA (PERMANOVA) *adonis* function in *vegan* (19) on genus, family and phylum levels. The BMI or gender were not associated with microbiota variation (permutational ANOVA 4% and 3%, respectively, FDR-$P > 0.3$ for both) and were not used as confounding factors. Also, age did not have a statistically significant effect on permutational ANOVA, but it correlated with the relative abundance of some of bacteria of interest in patients (*Faecalibacterium, Megasphaera* and *Prevotella*) so it was used as a confounder in all models. The differences in the microbiota between patients and controls or between patients with different clinical characteristics were analyzed using generalized linear models with negative binomial distribution implemented in the *mare* package for prevalent bacteria i.e. bacterial genera detected in >60% of the samples. P-values were adjusted by the Benjamini-Hochberg method for multiple testing and reported as FDR-*P*. All significant findings from differential abundance testing underwent visual inspection when applicable to eliminate statistically significant findings driven by few extreme values. Only statistically significant and visually validated results are reported. In the univariate data, a statistical difference was evaluated using the Independent-Samples Mann-Whitney U test in SPSS 25 (IBM). For all tests, *P*-values < 0.05 were considered as statistically significant.

Imputed Metagenomic Analysis

Bacterial metagenome content was predicted from the 16S rRNA gene-based microbial compositions. Functional inferences were made from the Kyoto Encyclopedia of Gene and Genomes (KEGG) catalog (20) using PICRUSt2 (21). The "*DESeq*" function in DESeq2 (22) was used to test for differentially abundant KEGG pathways between the groups.

Random Forest Classification

Random forest model was used to evaluate the predictive performance of all identified genera (N = 65) or predicted functions (N = 222) based on leave-one-out cross-validation. The random forest analysis was performed using the default settings of the "randomForest" function implemented in the *randomForest* R package. We then used the receiver operating characteristic (ROC) curve and calculated the area under the ROC curve (AUC), implemented in the *pROC* package, as the measure of performance. The importance of input features was evaluated by mean decrease Gini values.

RESULTS

Wide Spectrum of Intestinal Manifestations in the Patients With APECED

The microbiome samples of altogether 15 patients (7 females) with APECED were investigated. The patients were examined at the median age of 46.4 years (range, 19.3 – 70.1). Characteristics of the patients are presented in **Table 1** in comparison to 22 patients with APECED from whom we were unable to acquire stool samples. The patient characteristics differ little between the two groups suggesting that the sample of patients participating in the study represents well the overall APECED population.

TABLE 1 | Clinical characteristics of the 15 adult patients with APECED included in the present study.

Characteristic N (%) or median (range)	Patient with microbiome analyses N = 15	Patients without microbiome analyses N = 22	*P*-value
Female	7 (47%)	15 (68%)	0.19
Age (year)	46.4 (19.3 – 70.1)	39.5 (21.9 – 62.7)	0.26
Height SDS	-1.5 (-2.9 - +1.3)	-1.2 (-2.6 - +1.4)	0.13
BMI (kg/m^2)	22.7 (17.7 – 40.7)	22.3 (15.0 – 36.6)	0.87
AIRE genotype			
c.769C>T / c.769C>T	12 (80%)	18 (82%)	
c.769C>T / c.967_979del13	2 (13%)	2 (9%)	
c.769C>T / other	1 (7%)	2 (9%)	
Diarrhea (No / episodic / chronic)	6 (40%) / 6 (40%) / 3 (20%)	9 (41 %) / 10 (45%) / 3 (14%)	0.82
Obstipation	4 (27%)	10 (46%)	0.31
Failure of exocrine pancreas	0	4 (18)	0.13
Anti-fungal medication (No / preventive / treatment dose)	11 (73%) / 3 (20%) / 1 (7%)	15 (68%) / 3 (14%) / 4 (18%)	0.65
Probiotics in use	4 (27%)	1 (5%)	0.14

Their clinical and genetic features did not differ from the 22 patients with APECED for whom no data on stool microbiome was available.

All patients harbored at least one copy of the Finnish founder mutation c.769C>T, p.(Arg257Ter) in the *AIRE* gene (NM_000383.4). Altogether 13/15 of patients had primary adrenal insufficiency, and 12/15 had hypoparathyroidism. The patients had median of 7 (range 4-11) disease components of APECED. Additional symptoms, each present in one individual, included high blood pressure, asthma, depression, migraine, APC resistance, hypercholesterolemia and mild hypertrophic cardiomyopathy. All 15 patients had experienced mucocutaneus candidiasis. One patient was using anti-fungal medication with treatment dose and three patients with prophylaxis dose. Either periodic or chronic diarrhea was evident in 60% of the patients. None of the patients had used antibiotics within 1 month prior to the sampling. Four patients were using probiotics at the time of sampling, but these patients did not significantly differ from other patients in their microbial composition (data not shown). None of the controls had used antibiotics within 3 months prior to the sampling and none of them used probiotics.

Microbial Composition of Patients With APECED Is Altered Compared to Healthy Controls

We performed 16S rRNA gene amplicon sequencing to investigate the microbial composition of the stool samples. After processing we had on average 73135 (28175-164233) high quality reads representing overall of 395 operational taxonomic units (OTUs) distributed to 78 bacterial genera, 33 families, 19 orders, 13 classes, and 5 phyla. The microbiota richness ranged from 94 to 220 (mean, 168 *vs.* 152 in patients and controls, respectively; not significant; Mann-Whitney U test). Alpha diversity was significantly higher in patients compared to healthy controls [mean 13.0 (range, 4.2-18.4) *vs.* 6.8 (4.3-10.5); $P < 0.001$; Mann Whitney U test].

We compared the difference between patients and controls in the overall gut microbiota using PERMANOVA based on Bray-Curtis dissimilarity. Patients differed from controls already on the phylum level (14% of variation explained, $P = 0.006$, **Figure 1A**). Bacteroidetes and Proteobacteria were expanded in patients' gut microbiota, while a lower proportion of Firmicutes was found (**Figure 1B**) compared to the controls. On the family level, PERMANOVA indicated a 10% variation in the gut microbiota between the patients and controls ($P = 0.003$). Two patients distinctly differed from others with markedly expanded relative abundance of *Veillonellaceae* and diminished *Ruminococcaceae* (**Figure 1C**). Interestingly, these subjects were two of the three patients reporting the most severe diarrhea.

Beta-diversity between the patients and controls was significantly different also on genus level (10% variation in PERMANOVA, $P = 0.001$). In comparison to healthy controls, the proportion of *Faecalibacterium* was significantly reduced in patients [fold change (fc) = 0.45, FDR-$P = 0.05$, **Table 2**, **Figure 2**]. Multiple genera were significantly overrepresented in the patients. The largest 15-20 fold increase was found in the fraction of *Butyrivibrio*, *Atopobium*, and *Haemophilus* (fc = 15.1, FDR-$P = 7\text{x}10^{-5}$; fc = 18.8, FDR-$P = 7\text{x}10^{-5}$; fc = 17.3, FDR-$P = 0.0003$ respectively, **Table 2** and **Figure 2**). *Atopobium* was almost undetectable in the majority of the controls while it was observed in all patients accounting up to 20.3% of the total microbiota in one patient. The relative abundance of other gram-negative bacteria, *Veillonella* and *Prevotella*, was significantly increased in patients (fc = 5.4, FDR-$P = 0.02$; fc = 2.0, FDR-$P = 0.04$; respectively, **Table 2** and **Figure 2**). Of interest, the reads derived from *Megasphaera* spp. within the *Veillonnellaceae family* accounted for up to 37.1% and 0.8% of reads in two patients, respectively, but was otherwise virtually undetectable in the majority of patients and controls (**Figure 2**). All genera with relative abundances that are significantly different between the patients and controls are summarized in **Table 2**.

Imputed Metagenomic Analysis Reveals Upregulation of Modules Related to Lipopolysaccharide Synthesis

To understand functional implications of the observed taxonomic difference between patients with APECED and controls, we inferred metagenomes using the PICRUSt2 algorithm. This is a computational approach that reconstructs functional composition of a metagenome connecting the sequenced genes to reference genomes. The imputed functions of patients' microbiota differed significantly from those of healthy controls, explaining 9% of the variation in the gut microbiota ($P = 0.02$, **Figure 3A**), which was attributable to the functional modules associated with LPS synthesis that were enriched in patients (**Figure 3B**).

Random forest (RF) classification models were subsequently trained by 5-fold cross-validation using the relative abundances of all genera (N = 65) or imputed functional modules (N = 211). Both RF models including bacterial taxa or predicted functions classified patients with APECED with a comparably robust accuracy, achieving an area under the curve (AUC) of 0.83 and 0.87, respectively (**Figure 3C**). The most important genera selected by the model included *Faecalibacterium* and *Atopobium* (**Supplementary Figure 1A**). The functional modules related to LPS synthesis were among the most important features selected by the random forest model (**Supplementary Figure 1B**).

Dysbiosis in Patients With APECED Is Linked to ASCA Antibodies and Yeast Abundance in the Stool

Having established the differences in the gut microbiota between patients and controls at the level of the entire bacterial community and individual taxa, we next examined whether patient characteristics were linked to gut microbiota deviations. We used the ASCA quantification that was available for all but one of the patients with APECED, and 8/14 (57.1%) were positive, indicating a systemic immune response to fungal products or fungi. Five of the ASCA positive patients had diarrhea including the three patients with most severe symptoms. The ASCA positivity explained 10% of variation in the gut microbiota on the phylum level ($P = 0.05$, **Figure 4A**). As mentioned previously, a lower proportion of Firmicutes was characteristic to patients compared with healthy controls, which

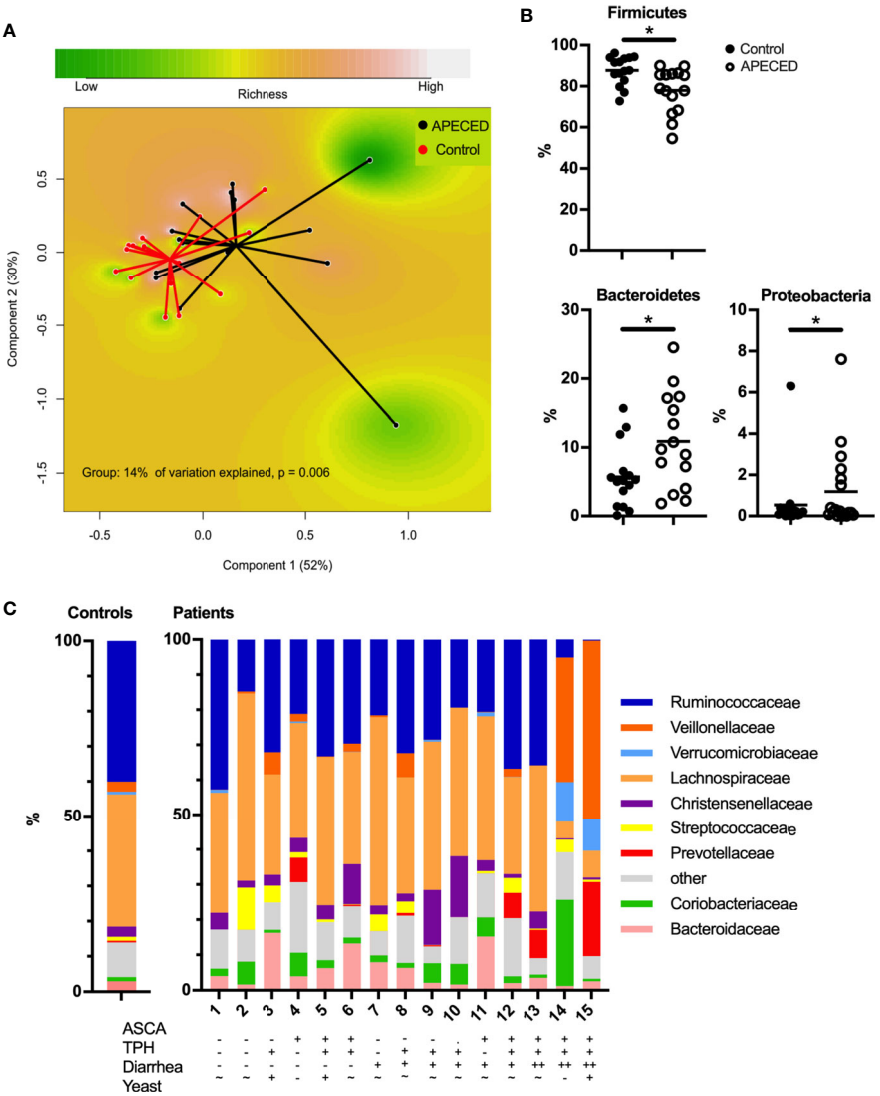

FIGURE 1 | **(A)** Principal coordinate analysis (PCoA) based on Bray–Curtis distances using the phylum-level data showing differences in the gut microbiota compositions between patients with APECED (black) and healthy controls (red). **(B)** The relative abundances of Firmicutes, Bacteroidetes and Proteobacteria in patients with APECED (open circles) compared to healthy controls (black circles). * indicates FDR-*P*-value < 0.05 **(C)** Composition of the gut microbiota at the family level of patients with APECED and healthy controls. For readability, the composition of the controls is shown as mean relative abundance. Anti-*Saccharomyces cerevisiae* antibodies (ASCA), antibodies against tryptophan hydroxylase (TPH), gastrointestinal symptoms and results of stool yeast analysis are shown for each patient. – negative/low, + positive, ++ markedly positive i.e. severe symptoms, ~ average.

was more pronounced in ASCA positive patients (FDR-*P* = $1.1x10^{-6}$ between ASCA+ and ASCA- patients, **Figure 4B**).

Interestingly, the antigen for ASCA antibodies can also be produced by *C. albicans* and infection by this pathogenic yeast has been shown to be able to induce ASCA (23). Patients with APECED are susceptible to chronic candidiasis (1, 2) and all of our patients had suffered from chronic candidiasis at some site of the body with varying severity. We used ITS1 primers to quantify fungi in patient stool microbiota by qPCR. Fungal DNA was amplified in all patient samples and based on the amplification results, the patients were grouped into three categories using a comparative Ct method (median Cq of patients +/- 1 cycles, respectively). Three of the patients had a markedly higher level of fungi in their stool, while two patients had a significantly lower level than other patients. Bacterial composition of these groups differed significantly (21% variation explained in PERMANOVA, *P* = 0.04, **Figure 4C**). Four patients were receiving anti-fungal medication at the time of sampling (one in the low group, the rest in the median group).

Autoimmunity against neuroendocrine cells as measured by TPH antibodies was detected in 60% of the patients (9/15) and was associated with a higher abundance of *Haemophilus*

TABLE 2 | Bacterial genera that differed significantly between patients with APECED and controls.

Phylum	Class	Order	Family	Genus	Mean (%)	Fold Change	Log2 FC	FDR-*P*
Firmicutes	Clostridia	Clostridiales	*Lachnospiraceae*	*Butyrivibrio*	0.30	15.14	3.92	1.1E-05
Actinobacteria	Coriobacteriia	Coriobacteriales	*Coriobacteriaceae*	*Atopobium*	1.38	18.77	4.23	7.2E-05
Proteobacteria	Gammaproteobacteria	Pasteurellales	*Pasteurellaceae*	*Haemophilus*	0.45	17.27	4.11	0.0003
Firmicutes	Clostridia	Clostridiales	*Lachnospiraceae*	*Lachnospira*	0.52	4.41	2.14	0.0003
Firmicutes	Negativicutes	Selenomonadales	*Veillonellaceae*	*Veillonella*	0.78	5.40	2.43	0.02
Firmicutes	Clostridia	Clostridiales	*Christensenellaceae*	*Christensenella*	0.24	7.05	2.82	0.02
Actinobacteria	Actinobacteria	Actinomycetales	*Actinomycetaceae*	*Actinomyces*	0.03	5.08	2.34	0.03
Bacteroidetes	Bacteroidia	Bacteroidales	*Prevotellaceae*	*Prevotella*	2.70	2.00	1.00	0.04
Firmicutes	Clostridia	Clostridiales	*Ruminococcaceae*	*Faecalibacterium*	12.41	0.45	-1.16	0.05
Bacteroidetes	Bacteroidia	Bacteroidales	*Porphyromonadaceae*	*Parabacteroides*	0.36	2.90	1.53	0.07
Actinobacteria	Coriobacteriia	Coriobacteriales	*Coriobacteriaceae*	*Collinsella*	2.24	3.21	1.68	0.07
Bacteroidetes	Bacteroidia	Bacteroidales	*Bacteroidaceae*	*Bacteroides*	5.90	2.08	1.05	0.12

Fold change was estimated with age as a counfounder. P-value was adjusted for multiple testing with Benjamini-Hochber method.

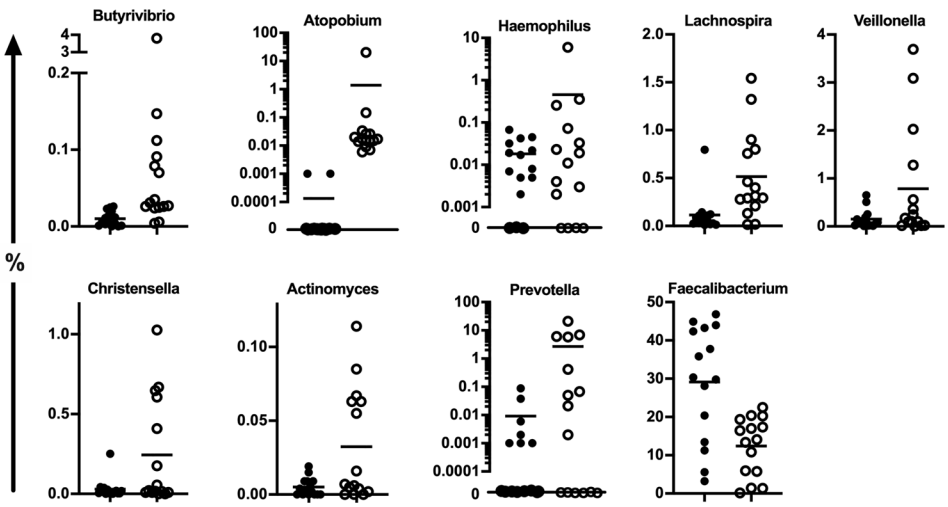

FIGURE 2 | The relative abundance of all the bacterial genera that significantly altered in APECED patients' stool (open circles) compared to healthy controls (black circles) based on the age-adjusted negative binomial models. The results of statistical analysis are summarized in **Table 2**.

(FDR-*P* = 0.001, fc = 65 to patients without anti-TPH antibodies).

Changes in Microbiota Are More Pronounced in Patients With Most Severe Gastrointestinal Symptoms

We examined the associations between the intestinal microbiota and GI symptoms of the patients. Four out of the fifteen patients (26.7%) suffered from intermitting obstipation episodes, but their stool microbiota did not differ from the other patients. The opposite was, however, true for patients reporting symptoms of diarrhea. We divided patients into three groups according to the severity of their symptoms of diarrhea (no symptoms, N = 6; intermittent diarrhea, N = 6; chronic difficult diarrhea, N = 3) and found the fecal microbiota composition to significantly differ among the groups (24% of variation explained in PERMANOVA on the family level, $P = 0.02$; 15% variation explained in PERMANOVA on the genus level, $P = 0.02$, **Figure 4C**). *Atopobium* spp. were overrepresented in patients with intermitted diarrhea and chronic difficult diarrhea (fc = 6.3, FDR-$P = 2x10^{-35}$; fc = 117, FDR-$P = 6x10^{-305}$, respectively, compared to patients without symptoms) while *Faecalibacterium* spp. were less common if a patient had chronic difficult diarrhea (fc = 0.3, FDR-$P = 0.05$ compared to patients without symptoms).

The microbial composition of patients without any GI symptoms (N = 5), also differed from the healthy controls (11% of variation explained in PERMANOVA on the genus level, $P = 0.04$).

DISCUSSION

Our gut microbiota analysis in patients with APECED revealed significant differences in the gut microbiota both at the level of the entire community and individual taxa compared to healthy controls. At the phylum level, we saw a reduction in gram-positive *Firmicutes* and increases in gram-negative *Bacteroidetes*

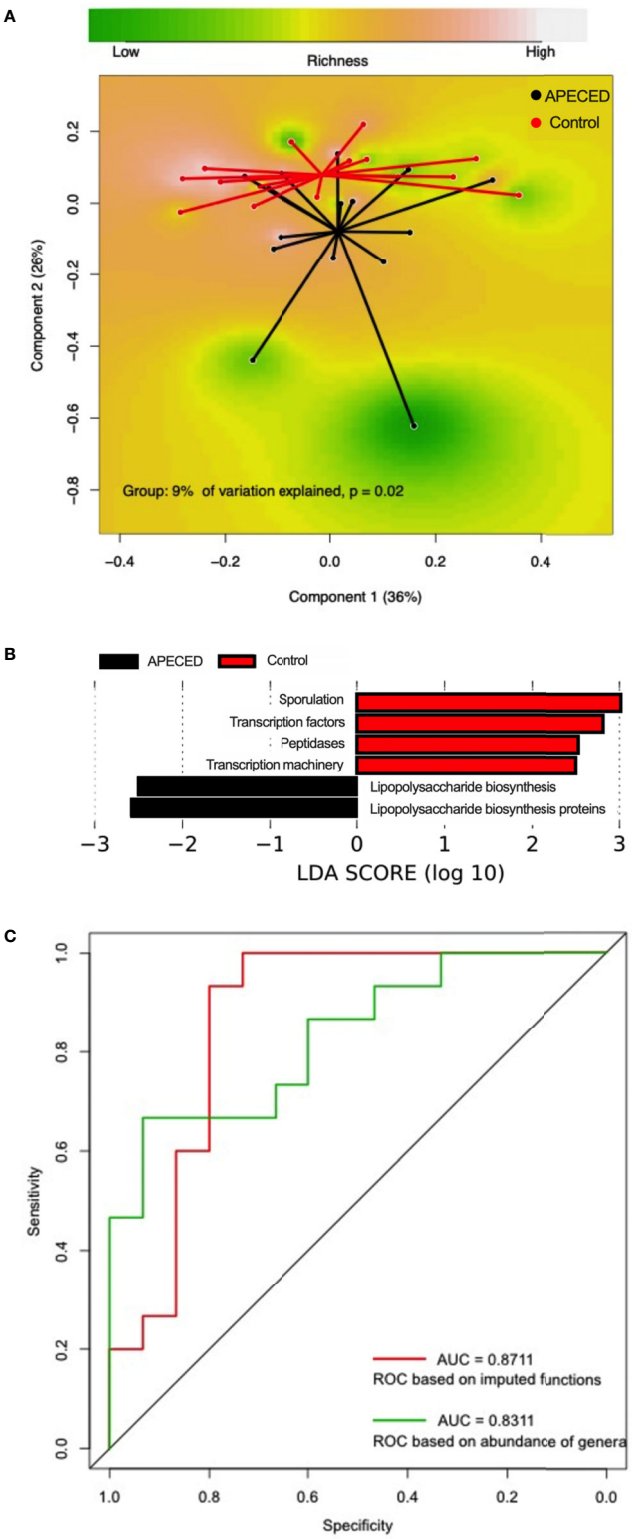

FIGURE 3 | **(A)** Principal coordinate analysis (PCoA) based on Bray–Curtis distances using the predicted functional modules showing differences in the gut microbiota compositions between patients with APECED (black) and healthy controls (red). **(B)** Predicted functional modules significantly overrepresented in patients with APECED (black) and controls (red). **(C)** Receiver operating characteristic (ROC) curves of the cross-validated random forest models constructed using the imputed functions (red) and relative abundances of genera (green).

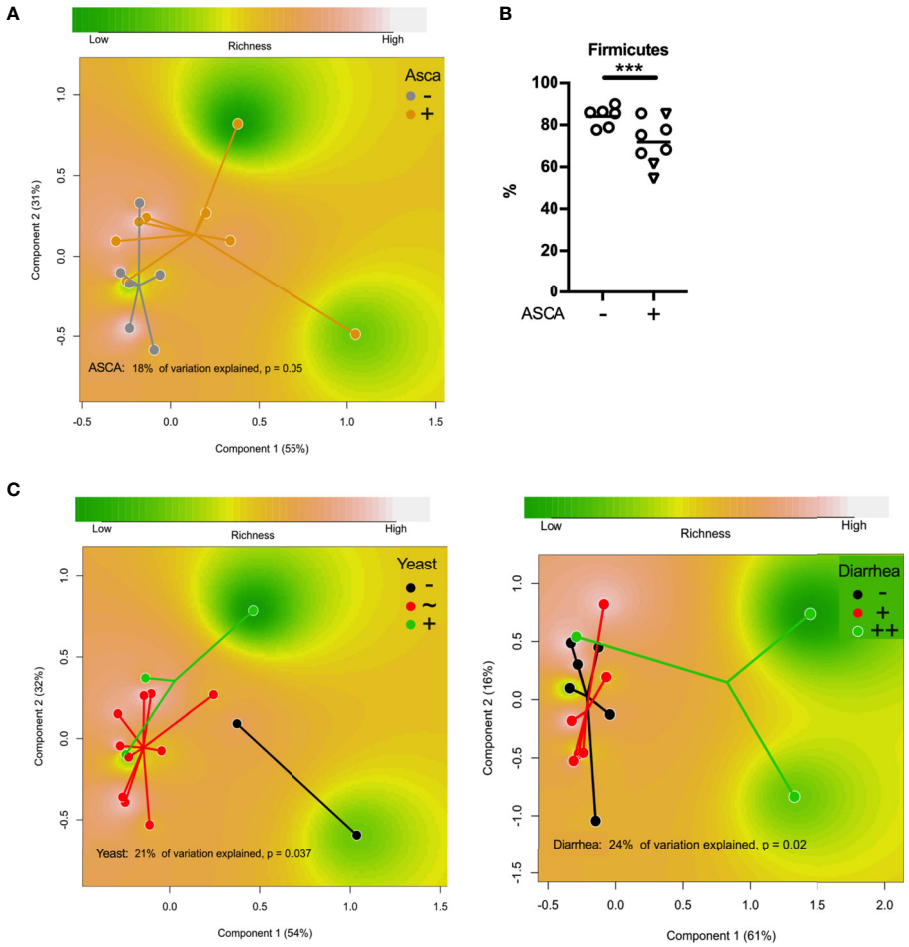

FIGURE 4 | **(A)** Principal coordinate analysis (PCoA) based on Bray–Curtis distances using the phylum-level data showing differences in the gut microbiota compositions between ASCA-positive and ASCA-negative patients with APECED. **(B)** The relative abundance of Firmicutes in patients with or without ASCA. **(C)**Principal coordinate analysis (PCoA) based on Bray–Curtis distances using the genus-level data showing differences in the gut microbiota compositions between patients with APECED ranked according to abundance of yeast in stool and the severity of patient's gastrointestinal symptoms, respectively. *** denotes p-value < 0.001; –, negative/low; +, positive; ++, markedly positive ie. severe symptoms; ~, average.

and *Proteobacteria* in patients with APECED compared to the healthy controls. On the genus level, a reduction in the butyrate producing *Faecalibacterium* represented one of the most apparent features in the gut microbiota of patients with APECED. *Faecalibacterium prausnitzii* is known for its anti-inflammatory properties and it is shown to protect mice from effects of chemically induced colitis (24). Interestingly, a decrease in *Faecalibacterium* spp. has been consistently associated with disrupted gut homeostasis in inflammatory bowel disease (IBD) (9–11).

We detected *Atopobium* spp. in the stool samples from all patients with APECED, and in one patient it accounted up to 20.3% of bacteria. The relative abundance of *Atopobium* ssp. was especially high in patients with severe GI symptoms. *Atopobium* belongs to the Actinobacteria and is capable of producing H2S from sulphur containing amino acids and hence has been implicated in halitosis in the oral cavity (25). *Atopobium* is key to a network of H2S producing bacteria and correlates with the severity of Crohn's disease (10). *Atopobium* has been linked to mitochondrial dysfunction, and the transfer of *Atopobium* triggers colitis in IL10-/- mice (10). Interestingly, *Atopobium* and *Megashaera* spp., enriched in the microbiota of patients with APECED compared to healthy controls, are known to grow in biofilms e.g. in the vaginal (26) and oral (27) ecosystems. Bacterial biofilms, mucosa-associated dense and resistant polymicrobial communities encased in extracellular matrix are very common in IBD patients and typically contain bacteria that can invade intestinal epithelia, potentiate pro-inflammatory signals and communicate *via* quorum sensing (28). It has been proposed that microbial biofilms are virtually absent in the gut of healthy subjects but their presence in patients' intestine could represent an indicator of emerging disease (29). Also *Butyrivibrio* and *Prevotella*, enriched in the patients, may engage in biofilms based on their high genomic content for quorum sensing proteins (30).

In the study showing the pathogenic role of *Atopobium* in Crohn's disease (10), the microbiome analysis was based on samples acquired by mucosal lavage during colonoscopy. It has been shown that samples obtained with endoscopy provide a more sensitive indication of differences between patients with GI disease and controls, whereas much of this difference is lost or blurred in stool samples (8). Thus, the significant increase of biofilm-producing bacteria in the stool samples from patients with APECED likely reflect a marked dysbiosis of the gut. Moreover, we found that the predicted function of LPS biosynthesis in the gut microbiota was significantly elevated in patients with APECED compared to controls, in line with the enrichment of several gram-negative bacterial genera. LPS is a pro-inflammatory molecule of the cell wall of gram-negative bacteria, which can contribute substantially to continued inflammatory response towards commensals, especially in an immunocompromised host and in the presence of disrupted barrier integrity.

A previous study using a smaller cohort of Finnish APECED patients identified an increase in *Haemophilus* genus in ten APECED patients compared to eight controls (5). Our data confirms this feature, but the differences in the gut microbiota between the patients and controls were more substantial and phylogenetically diverse in our study. The increase in strains of *Enterobacteriaceae* family belonging to either *Escherichia* or *Shigella* spp. reported in the previous study was not observed in our data, nor did we observe any differences in other genera belonging to the *Enterobacteriaceae* family. This difference is most likely explained by the fact that our study has a larger sample size, BMI-matched healthy controls from the same age range as the patients, and a fecal DNA extraction method that efficiently captures both gram-positive and gram-negative gut commensals (13). Moreover, two small studies on the salivary microbiota from six and seven APECED patients with age-matched controls found altered bacterial compositions in APECED patients' oral cavity, but their results are mixed and in part discrepant (31, 32).

What, then, triggers the intestinal dysbiosis in APECED patients? Despite its monogenic background, the immunological phenotype of APECED is highly complex, and several factors may be linked to the alterations in intestinal microbiota. We have previously reported that patients with APECED have increased antibody responses against gut commensals (7). In the current study, ASCA antibodies were associated with decreased *Firmicutes* in patients with APECED. ASCA against oligomannose of the yeast were detected in Crohn's disease where it was associated with more severe outcome and could be used as a serological marker of the disease (33, 34), but the clinical significance of these antibodies is unclear. The antibodies likely reflect the pathological process and are not pathogenic *per se*. Patients with APECED also have autoantibodies against Th17-cytokines, such as IL-22 and IL-17 (2). IL-22 contributes to the maintenance of barrier defense and integrity in the gut. Neutralizing antibodies against IL-17 have been linked to defective antifungal defense (2). Interestingly, in a small French study the GI symptoms of patients with APECED were alleviated with antifungal therapy, suggesting possible involvement of intestinal fungi (35). In Crohn's disease, *C. albicans* colonization is more common compared to healthy controls and it is capable of initiating ASCA formation (23, 36). Indeed, *C. albicans* has been suggested to have a causative role in the initial GI inflammation (37). We found the abundance of yeasts in the fecal microbiota to be linked to bacterial alterations, but not to the severity of the GI symptoms experienced by the patients. However, as our samples were taken at the time of established disease, they may not reflect the situation during the initial disruption of gut homeostasis. Anti-cytokine antibodies have also been proposed to account for the bacterial alterations seen in APECED patients' mouth (32).

Another hypothesis explaining the aberrant gut microbiota of patients with APECED is that autoimmunity against neuroendocrine cells or other components of the gut might lead to a disrupted intestinal barrier and subsequent pro-inflammatory intestinal conditions. *Haemophilus*, a well-known Gram-negative genus with members with pathogenic properties was associated with IBD in previous studies (8, 10). Of interest, the relative abundance of members of this genus appears to be very high in patients with anti-TPH antibodies. Finally, the failure of immunoregulatory mechanisms may also have a negative effect on gut homeostasis. Patients with APECED have a defect in regulatory T cells and we have previously shown that at least in some patients, regulatory T cells are decreased in the gut (7). Alterations in the adaptive immunity of patients can thus also contribute to the emergence of disturbances in the gut microbiota.

In summary, our data indicate that several gram-negative bacterial genera were enriched in the gut microbiota of patients with APECED, which may promote dysbiosis and the inflammatory phenotype *via* biofilm production and increased exposure to LPS. This microbiota profile in the patients was associated with more severe GI symptoms. Gastrointestinal manifestations of APECED were initially overlooked amidst severe autoimmune components of the disease, but a significant proportion of patients suffer from various disease manifestations of the GI tract, which can decrease the quality of life (3). Therefore, at least in patients with severe GI symptoms, the gut microbiota is a factor to take into consideration when contemplating therapy.

DATA AVAILABILITY STATEMENT

The datasets presented in this study can be found in online repositories. The names of the repository/repositories and accession number(s) can be found below: European Nucleotide Archive, accession no: PRJEB46143.

ETHICS STATEMENT

The studies involving human participants were reviewed and approved by The Ethics committee of the Helsinki University Hospital. The patients/participants provided their written informed consent to participate in this study.

AUTHOR CONTRIBUTIONS

IH designed and performed experiments, analyzed data with CJ, and wrote the original draft of the manuscript with CJ and AS. SL and OM collected the patient samples and clinical data. A-MP collected the control samples. WV, TA, and AS designed experiments. All authors contributed to the article and approved the submitted version.

FUNDING

This study was funded by the Emil Aaltonen Foundation, University of Helsinki, Academy of Finland (grant 308255), Sigrid Jusélius Foundation, Folkhälsan Research Foundation, Novo Nordisk Foundation, Helsinki University Hospital Research Funds, Pediatric Research Center, Helsinki University Hospital, The Finnish Foundation for Pediatric Research, and The Finnish Medical Foundation.

ACKNOWLEDGMENTS

We would like to thank Olle Kämpe for providing the anti-TPH antibody measurements.

SUPPLEMENTARY MATERIAL

The Supplementary Material for this article can be found online at: https://www.frontiersin.org/articles/10.3389/fimmu.2021.668219/full#supplementary-material

REFERENCES

1. Perheentupa J. Autoimmune Polyendocrinopathy-Candidiasis-Ectodermal Dystrophy. *J Clin Endocrinol Metab* (2006) 91(8):2843–50. doi: 10.1210/jc.2005-2611
2. Kisand K, Boe Wolff AS, Podkrajsek KT, Tserel L, Link M, Kisand KV, et al. Chronic Mucocutaneous Candidiasis in APECED or Thymoma Patients Correlates With Autoimmunity to Th17-Associated Cytokines. *J Exp Med* (2010) 207(2):299–308. doi: 10.1084/jem.20091669
3. Kluger N, Jokinen M, Krohn K, Ranki A. Gastrointestinal Manifestations in APECED Syndrome. *J Clin Gastroenterol* (2013) 47(2):112–20. doi: 10.1097/MCG.0b013e31827356e1
4. Ekwall O, Hedstrand H, Grimelius L, Haavik J, Perheentupa J, Gustafsson J, et al. Identification of Tryptophan Hydroxylase as an Intestinal Autoantigen. *Lancet* (1998) 352(9124):279–83. doi: 10.1016/S0140-6736(97)11050-9
5. Naskali E, Dettmer K, Oefner PJ, Pereira PAB, Krohn K, Auvinen P, et al. Serotonin and Tryptophan Metabolites, Autoantibodies and Gut Microbiome in APECED. *Endocrine Connections* (2019) 8(1):69–77. doi: 10.1530/EC-18-0513
6. Dobes J, Neuwirth A, Dobesova M, Voboril M, Balounova J, Ballek O, et al. Gastrointestinal Autoimmunity Associated With Loss of Central Tolerance to Enteric Alpha-Defensins. *Gastroenterology* (2015) 149(1):139–50. doi: 10.1053/j.gastro.2015.05.009
7. Hetemaki I, Jarva H, Kluger N, Baldauf HM, Laakso S, Bratland E, et al. Anticommensal Responses Are Associated With Regulatory T Cell Defect in Autoimmune Polyendocrinopathy-Candidiasis-Ectodermal Dystrophy Patients. *J Immunol* (2016) 196(7):2955–64. doi: 10.4049/jimmunol.1500301
8. Gevers D, Kugathasan S, Denson LA, Vazquez-Baeza Y, Van Treuren W, Ren B, et al. The Treatment-Naive Microbiome in New-Onset Crohn's Disease. *Cell Host Microbe* (2014) 15(3):382–92. doi: 10.1016/j.chom.2014.02.005
9. Lewis JD, Chen EZ, Baldassano RN, Otley AR, Griffiths AM, Lee D, et al. Inflammation, Antibiotics, and Diet as Environmental Stressors of the Gut Microbiome in Pediatric Crohn's Disease. *Cell Host Microbe* (2015) 18(4):489–500. doi: 10.1016/j.chom.2015.09.008
10. Mottawea W, Chiang CK, Muhlbauer M, Starr AE, Butcher J, Abujamel T, et al. Altered Intestinal Microbiota-Host Mitochondria Crosstalk in New Onset Crohn's Disease. *Nat Commun* (2016) 7:13419. doi: 10.1038/ncomms13419
11. Nagao-Kitamoto H, Kamada N. Host-Microbial Cross-Talk in Inflammatory Bowel Disease. *Immune Netw* (2017) 17(1):1–12. doi: 10.4110/in.2017.17.1.1
12. Laakso S, Borchers J, Toiviainen-Salo S, Pekkinen M, Mäkitie O. Severe Phenotype of APECED (APS1) Increases Risk for Structural Bone Alterations. *Front Endocrinol (Lausanne)* (2020) 11:109. doi: 10.3389/fendo.2020.00109
13. Salonen A, Nikkila J, Jalanka-Tuovinen J, Immonen O, Rajilic-Stojanovic M, Kekkonen RA, et al. Comparative Analysis of Fecal DNA Extraction Methods With Phylogenetic Microarray: Effective Recovery of Bacterial and Archaeal DNA Using Mechanical Cell Lysis. *J Microbiol Methods* (2010) 81(2):127–34. doi: 10.1016/j.mimet.2010.02.007
14. Buee M, Reich M, Murat C, Morin E, Nilsson RH, Uroz S, et al. 454 Pyrosequencing Analyses of Forest Soils Reveal an Unexpectedly High Fungal Diversity. *New Phytol* (2009) 184(2):449–56. doi: 10.1111/j.1469-8137.2009.03003.x
15. Schmittgen TD, Livak KJ. Analyzing Real-Time PCR Data by the Comparative C(T) Method. *Nat Protoc* (2008) 3(6):1101–8. doi: 10.1038/nprot.2008.73
16. Korpela K, Salonen A, Saxen H, Nikkonen A, Peltola V, Jaakkola T, et al. Antibiotics in Early Life Associate With Specific Gut Microbiota Signatures in a Prospective Longitudinal Infant Cohort. *Pediatr Res* (2020) 88(3):438–43. doi: 10.1038/s41390-020-0761-5
17. Korpela K. *Mare: Microbiota Analysis in R Easily*. Github (2016). Online at https://github.com/katrikorpela/mare (Accessed Mar 2021). doi: 10.5281/zenodo.50310
18. Virtanen S, Rantsi T, Virtanen A, Kervinen K, Nieminen P, Kalliala I, et al. Vaginal Microbiota Composition Correlates Between Pap Smear Microscopy and Next Generation Sequencing and Associates to Socioeconomic Status. *Sci Rep* (2019) 9(1):7750. doi: 10.1038/s41598-019-44157-8
19. Oksanen J, Blanchet FG, Friendly M, Kindt R, Legendre P, McGlin D, et al. *Vegan: Community Ecology Package. R Package Version 2.4-3* (2017) (Accessed 2016 Jan 1).
20. Kanehisa M, Goto S, Sato Y, Furumichi M, Tanabe M. KEGG for Integration and Interpretation of Large-Scale Molecular Data Sets. *Nucleic Acids Res* (2012) 40(Database issue):D109–14. doi: 10.1093/nar/gkr988
21. Douglas GM, Maffei VJ, Zaneveld JR, Yurgel SN, Brown JR, Taylor CM, et al. PICRUSt2 for Prediction of Metagenome Functions. *Nat Biotechnol* (2020) 38(6):685–8. doi: 10.1038/s41587-020-0548-6
22. Love MI, Huber W, Anders S. Moderated Estimation of Fold Change and Dispersion for RNA-Seq Data With Deseq2. *Genome Biol* (2014) 15(12):550. doi: 10.1186/s13059-014-0550-8
23. Standaert-Vitse A, Jouault T, Vandewalle P, Mille C, Seddik M, Sendid B, et al. Candida Albicans Is an Immunogen for Anti-Saccharomyces Cerevisiae Antibody Markers of Crohn's Disease. *Gastroenterology* (2006) 130(6):1764–75. doi: 10.1053/j.gastro.2006.02.009
24. Breyner NM, Michon C, de Sousa CS, Vilas Boas PB, Chain F, Azevedo VA, et al. Microbial Anti-Inflammatory Molecule (MAM) From Faecalibacterium Prausnitzii Shows a Protective Effect on DNBS and DSS-Induced Colitis Model in Mice Through Inhibition of NF-κb Pathway. *Front Microbiol* (2017) 8:114. doi: 10.3389/fmicb.2017.00114
25. Blachier F, Beaumont M, Kim E. Cysteine-Derived Hydrogen Sulfide and Gut Health: A Matter of Endogenous or Bacterial Origin. *Curr Opin Clin Nutr Metab Care* (2019) 22(1):68–75. doi: 10.1097/MCO.0000000000000526
26. Mendling W, Palmeira-de-Oliveira A, Biber S, Prasauskas V. An Update on the Role of Atopobium Vaginae in Bacterial Vaginosis: What to Consider When Choosing a Treatment? *A Mini Rev Arch Gynecol Obstet* (2019) 300(1):1–6. doi: 10.1007/s00404-019-05142-8
27. Nallabelli N, Patil PP, Pal VK, Singh N, Jain A, Patil PB, et al. Biochemical and Genome Sequence Analyses of Megasphaera Sp. Strain DISK18 From Dental

Plaque of a Healthy Individual Reveals Commensal Lifestyle. *Sci Rep* (2016) 6:33665. doi: 10.1038/srep33665
28. Srivastava A, Gupta J, Kumar S, Kumar A. Gut Biofilm Forming Bacteria in Inflammatory Bowel Disease. *Microb Pathog* (2017) 112:5–14. doi: 10.1016/j.micpath.2017.09.041
29. Tytgat HLP, Nobrega FL, van der Oost J, de Vos WM. Bowel Biofilms: Tipping Points Between a Healthy and Compromised Gut? *Trends Microbiol* (2019) 27 (1):17–25. doi: 10.1016/j.tim.2018.08.009
30. Won MY, Oyama LB, Courtney SJ, Creevey CJ, Huws SA. Can Rumen Bacteria Communicate to Each Other? *Microbiome* (2020) 8(1):23. doi: 10.1186/s40168-020-00796-y
31. Bruserud Ø, Siddiqui H, Marthinussen MC, Chen T, Jonsson R, Oftedal BE, et al. Oral Microbiota in Autoimmune Polyendocrine Syndrome Type 1. *J Oral Microbiol* (2018) 10(1):1442986. doi: 10.1080/20002297.2018.1442986
32. Kaleviste E, Rühlemann M, Kärner J, Haljasmägi L, Tserel L, Org E, et al. IL-22 Paucity in APECED Is Associated With Mucosal and Microbial Alterations in Oral Cavity. *Front Immunol* (2020) 11:838. doi: 10.3389/fimmu.2020.00838
33. Prideaux L, De Cruz P, Ng SC, Kamm MA. Serological Antibodies in Inflammatory Bowel Disease: A Systematic Review. *Inflamm Bowel Dis* (2012) 18(7):1340–55. doi: 10.1002/ibd.21903
34. Zhang Z, Li C, Zhao X, Lv C, He Q, Lei S, et al. Anti-Saccharomyces Cerevisiae Antibodies Associate With Phenotypes and Higher Risk for Surgery in Crohn's Disease: A Meta-Analysis. *Dig Dis Sci* (2012) 57(11):2944–54. doi: 10.1007/s10620-012-2244-y
35. Proust-Lemoine E, Saugier-Veber P, Lefranc D, Dubucquoi S, Ryndak A, Buob D, et al. Autoimmune Polyendocrine Syndrome Type 1 in North-Western France: AIRE Gene Mutation Specificities and Severe Forms Needing Immunosuppressive Therapies. *Hormone Res Paediatrics* (2010) 74(4):275–84. doi: 10.1159/000297714
36. Standaert-Vitse A, Sendid B, Joossens M, Francois N, Vandewalle-El Khoury P, Branche J, et al. Candida Albicans Colonization and ASCA in Familial Crohn's Disease. *Am J Gastroenterol* (2009) 104(7):1745–53. doi: 10.1038/ajg.2009.225
37. Gerard R, Sendid B, Colombel JF, Poulain D, Jouault T. An Immunological Link Between Candida Albicans Colonization and Crohn's Disease. *Crit Rev Microbiol* (2015) 41(2):135–9. doi: 10.3109/1040841X.2013.810587

Conflict of Interest: The authors declare that the research was conducted in the absence of any commercial or financial relationships that could be construed as a potential conflict of interest.

Copyright © 2021 Hetemäki, Jian, Laakso, Mäkitie, Pajari, de Vos, Arstila and Salonen. This is an open-access article distributed under the terms of the Creative Commons Attribution License (CC BY). The use, distribution or reproduction in other forums is permitted, provided the original author(s) and the copyright owner(s) are credited and that the original publication in this journal is cited, in accordance with accepted academic practice. No use, distribution or reproduction is permitted which does not comply with these terms.

frontiers in Immunology

ORIGINAL RESEARCH
published: 28 September 2021
doi: 10.3389/fimmu.2021.704836

Gut Microbial Metabolite Pravastatin Attenuates Intestinal Ischemia/Reperfusion Injury Through Promoting IL-13 Release From Type II Innate Lymphoid Cells *via* IL–33/ST2 Signaling

Fan Deng[†], *Jing-Juan Hu*[†], *Xiao Yang*, *Qi-Shun Sun*, *Ze-Bin Lin*, *Bing-Cheng Zhao*, *Zhi-Wen Yao*, *Si-Dan Luo*, *Ze-Ling Chen*, *Ying Liu*, *Zheng-Zheng Yan*, *Cai Li*, *Wei-Feng Liu*[*] *and Ke-Xuan Liu*[*]

Department of Anesthesiology, Nanfang Hospital, Southern Medical University, Guangzhou, China

Intestinal ischemia/reperfusion (I/R) injury is a grave condition with high morbidity and mortality. We previously confirmed that intestinal I/R induces intestinal flora disorders and changes in metabolites, but the role of different metabolites in intestinal I/R injury is currently unclear. Based on targeted metabolic sequencing, pravastatin (PA) was determined to be a metabolite of the gut microbiota. Further, intestinal I/R model mice were established through superior mesenteric artery obstruction. In addition, a co-culture model of small intestinal organoids and type II innate lymphoid cells (ILC2s) was subjected to hypoxia/reoxygenation (H/R) to simulate an intestinal I/R model. Moreover, correlation analysis between the PA level in preoperative feces of patients undergoing cardiopulmonary bypass and the indices of postoperative intestinal I/R injury was carried out. IL-33-deficient mice, ILC2-deleted mice, and anti-IL-13 neutralizing antibodies were also used to explore the potential mechanism through which PA attenuates intestinal I/R injury. We demonstrated that PA levels in the preoperative stool of patients undergoing cardiopulmonary bypass were negatively correlated with the indices of postoperative intestinal I/R injury. Furthermore, PA alleviated intestinal I/R injury and improved the survival of mice. We further showed that PA promotes IL-13 release from ILC2s by activating IL-33/ST2 signaling to attenuate intestinal I/R injury. In addition, IL-13 promoted the self-renewal of intestinal stem cells by activating Notch1 and Wnt signals. Overall, results indicated that the gut microbial metabolite PA can attenuate intestinal I/R injury by promoting the release of IL-13 from ILC2s *via* IL-33/ST2 signaling, revealing a novel mechanism of and therapeutic strategy for intestinal I/R injury.

Keywords: intestinal ischemia/reperfusion injury, metabolites, pravastatin, innate lymphoid cells, intestinal stem cells (ISCs), IL-33 and ST2, IL-13

OPEN ACCESS

Edited by:
Oscar Gilberto Gomez-Duarte, University at Buffalo, United States

Reviewed by:
Junmin Zhang, Lanzhou University, China
Jihong Yao, Dalian Medical University, China

****Correspondence:***
Ke-Xuan Liu
liukexuan705@163.com
Wei-Feng Liu
sglwfeng01@21cn.com

[†]*These authors have contributed equally to this work*

Specialty section:
This article was submitted to Microbial Immunology, a section of the journal Frontiers in Immunology

Received: *04 May 2021*
Accepted: *13 September 2021*
Published: *28 September 2021*

Citation:
Deng F, Hu J-J, Yang X, Sun Q-S, Lin Z-B, Zhao B-C, Yao Z-W, Luo S-D, Chen Z-L, Liu Y, Yan Z-Z, Li C, Liu W-F and Liu K-X (2021) Gut Microbial Metabolite Pravastatin Attenuates Intestinal Ischemia/Reperfusion Injury Through Promoting IL-13 Release From Type II Innate Lymphoid Cells via IL–33/ST2 Signaling. Front. Immunol. 12:704836. doi: 10.3389/fimmu.2021.704836

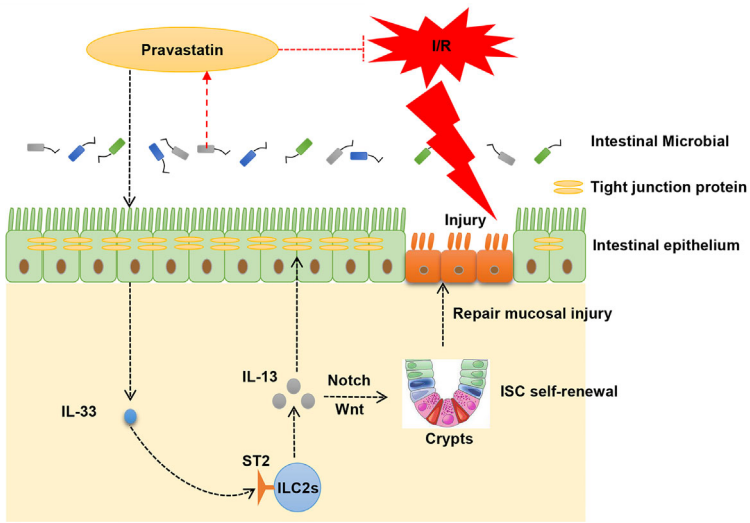

GRAPHICAL ABSTRACT |

INTRODUCTION

Intestinal ischemia/reperfusion (I/R) injury is a severe condition in some critical clinical settings that is commonly associated with serious infection, shock, and some surgical procedures, including cardiopulmonary bypass (CPB), strangulated ileus, and small bowel transplantation, among others (1). Intestinal I/R not only leads to intestinal injury but also causes damage to multiple extraintestinal organs and even death (2, 3). Currently, the potential mechanisms of intestinal I/R injury have not been fully elucidated, and effective therapeutic strategies need to be further explored.

The human intestinal commensal flora and related metabolites have always been considered factors related to the health of the host (4, 5). We previously confirmed that intestinal I/R induces significant intestinal flora disorders and changes in metabolites and showed that intestinal flora metabolites play an important regulatory role in intestinal I/R injury (6). In this study, we found that pravastatin (PA) is a metabolite of intestinal flora through metabolomic analysis. Statins are mainly derived from secondary metabolites of microbial fermentation and chemical synthesis. One study of various microorganisms revealed some fungi and bacteria that can convert compactin to pravastatin, in addition to strain improvement of *Streptomyces xanthochromogenes* RIA 1098 for enhanced pravastatin production (7). Pravastatin is mainly used to reduce cholesterol levels in patients, and it has been confirmed to promote angiogenesis and resistance to oxidative stress (8, 9), but its role in intestinal I/R injury has not been elucidated.

Interleukin-33 is secreted mainly by non-hematopoietic fibroblast, epithelial, and endothelial cells (10). Interleukin-33 released by epithelial cells activates type II innate lymphoid cells (ILC2s) to mount an immune response through the IL-33 receptor ST2 (11). The widely distributed IL–33 receptor ST2 plays a key role in inflammation and homeostasis by mediating IL-33/ST2 signaling (12). Some statins can promote IL-33 release from myocardial tissue (13). However, whether PA facilitates IL-33 release from intestinal tissue and the role of IL-33/ST2 signaling in intestinal I/R injury remains unclear.

ILC2s are required for the regulation of natural immunity and tissue homeostasis (14). ST2 receptors bind IL-33 on the surface of ILC2s, thereby activating these cells to release IL–13 (15–17). However, the role of ILC2s in intestinal I/R injury is unknown. Interleukin-13 plays an important role in regulating the homeostasis of the intestinal barrier (18). When secreted by ILC2s, IL-13 promotes the self-renewal of intestinal stem cells (ISCs) (19). Intestinal barrier homeostasis and ISC self-renewal are essential for repairing the intestinal mucosa after intestinal I/R damage. However, the role of IL-13 secreted by ILC2s during intestinal I/R injury is unclear.

Based on the aforementioned results, we hypothesized that gut microbial metabolite PA could attenuate intestinal I/R injury by promoting IL-13 release from ILC2s *via* IL–33/ST2 signaling. The present study thus aimed to investigate the effect of PA on intestinal I/R injury and elucidate the mechanism *via* which ILC2s are activated to release IL-13 through IL-33/ST2 signaling and through which IL-13 promotes ISC self-renewal. This study will help to elucidate a novel mechanism of intestinal I/R injury and reveal a new therapeutic strategy for clinical practice.

MATERIALS AND METHODS

Animals

Six-to-eight-week-old specific pathogen-free male C57BL/6 mice were purchased from the animal center of Nanfang Hospital of Southern Medical University (Guangzhou, China). IL-33$^{-/-}$ mice

and Rag1$^{-/-}$ mice were purchased from Shanghai Model Organisms Center, Inc, and sterile C57BL/6 mice were purchased from Cyagen Biosciences Company (Suzhou, China). All experimental procedures were carried out in accordance with the National Institutes of Health guidelines and were approved by the local Animal Care and Use Committee of the Nanfang Hospital of Southern Medical University.

Patient Samples

Patients who need cardiopulmonary bypass (CPB) surgery were used as cases for collecting intestinal I/R samples as previously described (20, 21). The enrollment requirements of all patients were carried out in accordance with the standards we established before (6). The study protocol was approved by the Ethical Committee of Nanfang hospital, Southern Medical University (approval number NFEC-202009-k2-01). All individuals gave informed consent to participate. Finally, a total of 20 patients were enrolled. Blood and fecal samples were collected from the 20 patients before surgery.

Blood samples were collected preoperatively (T0) and at 6 h (T1) and 12 h (T2) after surgery for analyses of intestinal fatty-acid binding protein (IFABP) and citrulline, respectively. The level of IFABP in plasma is a confirmed positive marker (22), while citrulline is a reliable negative biomarker for predicting and diagnosing intestinal I/R injury (23). Fecal samples were collected preoperatively, and the levels of PA were quantified by liquid chromatograph-tandem mass spectrometry (LC-MS/MS). IFABP and citrulline in the plasma samples were measured using a human IFABP ELISA Kit (Bio-Swamp, Wuhan, China) and citrulline ELISA Kit (USCN, Wuhan, China), respectively, at multiple time points (T2-T0) to determine concentration differences. The gastrointestinal complication score of the patient on the second day after surgery was performed according to the acute gastrointestinal injury (AGI) standard described previously (24). The detection of PA, IFABP, citrulline and AGI scores were performed by researchers blinded to the group allocation.

Intestinal I/R Mouse Model

The mouse model for intestinal I/R injury was established as in our previous study (1, 6). Briefly, the mice were anesthetized with isoflurane. A non-invasive microvascular artery clip was placed on the superior mesenteric artery for 60 min, and the clip was removed for reperfusion for 2 h.

Extraction and Culture of Organoids and the Establishment of Hypoxia-Reoxygenation (H/R) Models *In Vitro*

The extraction and culture of small intestinal organoids was performed as previously described (6, 25, 26). For the establishment of the organoid H/R model, the organoids were placed in a humid, anaerobic environment at 37°C for 12 h and then placed in an aerobic environment containing 5% CO_2 in a 37°C incubator for 4 h (6).

Experimental Design

To explore the protective effect of PA on intestinal I/R injury *in vivo*, the mice were randomly assigned to a sham group that was manipulated in the same manner as the I/R group but without undergoing I/R surgery, an I/R group, or an I/R + PA group that was injected intraperitoneally (i.p.) with 2 mg/kg PA (MedChemExpress) 1 h before inducing intestinal I/R. Organoids were cultured alone or with ILC2s (H/R co-culture model) (**Supplementary Figure S1A**). To explore the protective effect of PA on the H/R injury *in vitro*, the monocultured organoids and the cocultured organoid and ILC2 group were randomly assigned to a normal control (NC that was manipulated in the same manner as the H/R group but without undergoing H/R surgery, an H/R group, and an H/R + PA group in which the organoids were incubated with 10 μmol/L PA 1 h before H/R (**Supplementary Figure S1G**).

To explore the role of IL-33/ST2 signaling in the protective effect of PA against intestinal I/R injury, wild type (WT) mice were randomly divided into the following groups (**Supplementary Figure S2A**): I/R; (2) I/R + PA; (3) I/R + Anti-IL-33, in which WT mice were injected i.p. with 60 μg/kg Anti-IL-33 neutralizing antibody (R&D Systems, Inc., Minneapolis, USA) 2 h before establishing the intestinal I/R model; (4) I/R + PA + Anti-IL-33, in which WT mice were injected i.p. with 60 μg/kg Anti-IL-33 neutralizing antibody 2 h before intestinal I/R and 2 mg/kg PA 1 h before intestinal I/R in mice; (5) I/R + PA + Anti-ST2, in which WT mice were injected i.p. with 2 mg/kg PA and 1.5 mg/kg Anti-ST2 neutralizing antibody (R&D Systems, Inc.) 1 and 2 h, respectively, before establishing the intestinal I/R model in mice. The IL-33$^{-/-}$ mice (IL-33$^{-/-}$) were randomly assigned to I/R and I/R + PA groups.

To explore the role of the IL-33/ST2 axis in the protective effect of PA against H/R injury, the organoids and ILC2s extracted from WT mice were randomly assigned to H/R, H/R + PA, H/R + Anti-IL-33, H/R + PA + Anti-IL-33, and H/R + PA + Anti-ST2 groups. Each co-culture was incubated with 10 μmol/L PA and 10 mg/mL Anti-ST2 neutralizing antibody 1 and 2 h before H/R, respectively. Meanwhile, co-cultured organoids from IL-33$^{-/-}$ mice and ILC2s from WT mice were randomly assigned to H/R and H/R + PA groups (**Supplementary Figure S3A**).

The role that IL-33 plays in the protective effect of ILC2s against intestinal I/R injury was investigated by randomly dividing Rag1$^{-/-}$ mice into an I/R group (Rag1$^{-/-}$ mice were injected i.p. with control rat IgG2b on days −5 and −2 before I/R), an I/R + rmIL-33 group (Rag1$^{-/-}$ mice were injected i.p. with control rat IgG2b on days −5 and −2 before I/R, and 50 μg/kg rmIL-33 (PeproTech, Minneapolis, MN, USA) 2 h before intestinal I/R), an I/R + ILC2$^{-/-}$ group (Rag1$^{-/-}$ mice were injected i.p. with anti-CD90.2 antibody (30-H12; 250 mg per mouse; Biolegend) on days −5 and −2 before I/R surgery), and an I/R + rmIL-33 + ILC2$^{-/-}$ group (Rag1$^{-/-}$ mice were injected i.p. with anti-CD90.2 antibody on days −5 and −2 before I/R surgery and 50 μg/kg rmIL−33, 2 h before I/R; **Supplementary Figure 4A**). To explore the role of IL-33 in the protective effect of ILC2s against organoid H/R injury, organoids extracted from WT mice without ILC2s were randomly assigned to an H/R group and an H/R + rmIL-33 group, in which the organoids were incubated with 10 ng/mL rmIL-33, 2 h before H/R. Meanwhile, co-culture system of organoids and ILC2s extracted from the WT

mice were divided into two groups, an H/R or H/R + rmIL-33 group (**Supplementary Figure 5A**). To explore the role of IL-13 in the protective effect of PA or IL-33 against intestinal I/R injury, WT mice were randomly divided into six groups as follows (**Supplementary Figure 6A**): (1) I/R group; (2) I/R + PA group; (3) I/R + rmIL-33 group; (4) I/R + anti-IL-13 group (WT mice were injected i.p. with 400 μg/kg anti-IL-13 neutralizing antibody (R&D Systems, Inc.) 2 h before I/R; (5) I/R + PA + anti-IL-13 group; (6) I/R + rmIL-33 + anti-IL-13 group. To explore the role of IL-13 in the protective effect of PA or IL-33 against organoid H/R injury, the co-cultured organoids and ILC2s extracted from the WT mice were randomly assigned to the following groups: H/R, H/R + PA, H/R + rmIL-33, H/R + anti-IL-13 (co-cultures were incubated with 400 μg/kg anti-IL-13 neutralizing antibody 2 h before H/R), H/R + PA + anti-IL-13, and H/R + rmIL-33 + anti-IL-13 (**Supplementary Figure 7A**).

Isolation of Cells From Small Intestine Lamina Propria (LP)

Mouse small intestine LP single cells were harvested as described (27). Small intestines of 6–8-week-old male C57BL/6J mice were gently removed from the peritoneal cavity and placed in ice-cold PBS to remove the mesentery, fat, blood vessels, and the Peyer patches. The intestinal lumen was cut along the longitudinal axis and feces and mucus were removed with PBS until the lumen was clear. The intestinal tissues were chopped into 1–2 mm pieces and transferred to cell dissociation medium to remove IEC and intraepithelial lymphocytes. The remaining tissue was transferred to digestion solution and LP single cell suspension was purified with 40% and 80% Percoll solution (Solarbio).

Flow Cytometric Analysis and Cell Sorting

Mouse small intestine lamina propria (LP) single cells were harvested as described (27). For intracellular cytokine staining, single cell suspensions of LP were stimulated with PMA (25 ng/mL; Sigma-Aldrich, St. Louis, MO, USA) then ionomycin (1 μg/mL; Sigma-Aldrich) for 5 h at 37°C. Brefeldin A (10 μg/mL; Sigma-Aldrich) was added after the first hour of incubation. The cells were sedimented by centrifugation at 600 × g at 4°C, washed with MACS buffer, then nonspecific antibody binding was blocked by incubation with CD16/CD32 antibody (Cat# 14-0161-86, eBioscience, Shanghai, China) for 15 min on ice. The cell surface was stained using APC-Cyanine7-conjugated CD45 Antibody (Cat# A15395, eBioscience), FITC-conjugated mouse Hematopoietic Lineage Antibody Cocktail (Cat# 22-7770-72, eBioscience), and BV421-conjugated Rat Anti-Mouse IL-33R (ST2) antibody (Cat# 566309, BD Biosciences, San Jose, CA, USA). Cells were fixed and permeabilized for intracellular staining using the Foxp3 transcription factor staining buffer set (Cat# 00-5523-00, eBioscience), followed by staining with PE-CF594-conjugated Mouse Anti-GATA3 antibody (Cat# 563510, BD Biosciences), BV786-conjugated Mouse Anti-Mouse RORγt antibody (Cat# 564723, BD Biosciences), and PE-Cyanine7-conjugated IL-13 Monoclonal antibody (Cat# 25-7133-82, eBioscience). Dead cells were excluded by labeling with eFluor 780-conjugated Fixable Viability Dye (Cat# 65-0865-14, eBioscience). Cells were assessed using an LSRFortessa X-20Multidimensional HD Flow Cytometer (BD Biosciences) and the data were analyzed with FlowJo 10 software (BD Biosciences).

We sorted ILC2 in LP single cell suspensions using the MoFlo XDP Ultra-speed flow cell sorting system (Beckman Coulter Inc., Brea, CA, USA). The cell surface was stained using APC-conjugated Rat Anti-Mouse Ly-6A/E (Sca-1; Cat# 17-5981-82, eBioscience), PE-conjugated Anti-Mouse KLRG1 Antibody (Cat# 561621, BD Biosciences), and FITC-conjugated mouse Hematopoietic Lineage Antibody Cocktail (Cat# 22-7770-72, eBioscience). ILC2 were identified as $Lin^{-}Sca\text{-}1^{+}KLRG1^{+}$ (27).

Culture and Expansion of ILC2, Establishment of Co-Cultured Organoids and ILC2 *In Vitro*

We cultured and expanded ILC2 as described (28). Briefly, inoculate 5,000 cells per well in a round bottom 96-well plate, and add 10% (vol/vol) FBS RPMI complete medium containing 10 ng/ml IL-2 to culture and expand. We use 10 ng/ml IL-2 $^{+}$ 10 ng/ml IL-25 in 10% (vol/vol) FBS RPMI complete medium to induce ILC2 cell activation and rapid growth. For cell maintenance, we add 10 ng/ml IL-7 to 10% (vol/vol) FBS RPMI complete medium. Change half of the medium every 2 days. The ILC2 and organoids were co-cultured at a ratio of 25:1 in Matrigel.

Depletion of ILC2s *In Vivo*

For ILC2 depletion, $Rag1^{-/-}$ mice were administered an anti-CD90.2 antibody (30-H12; 250 mg per mouse; Biolegend) or control rat IgG2b on days −5 and −2 before I/R surgery as described (29–32).

Targeted Metabolomics

Targeted metabolomics (PA measurement) was performed by liquid chromatography-tandem mass spectrometry (LC-MS/MS) as described previously (33). Briefly, cecum samples (100 mg) were dissolved in 900 μL of ice-cold water and extracted *via* sonication in water for 10 min. After ethyl acetate was added and the samples were shaken for 3 min, they were centrifuged at 13000 rpm at 4°C for 10 min. The supernatant was collected and dried with nitrogen and then reconstituted with methanol/ammonium acetate pH4.5 (60:40 v/v) for further computer analysis. The chromatographic separation was performed on the Thermo Scientific Prelude SPLC system, and detection was performed using a Thermo TSQ Vantage triple quadrupole mass spectrometer. Data collection and processing were performed with TraceFinderTM software version 3.3 sp1 (Thermo Fisher Scientific Corp., USA).

Detection of Organoid Injury by CCK-8 and Lactate Dehydrogenase (LDH) Assays

The levels of organoid injury were assessed with a CCK-8 kit (Dojindo, Shanghai, China) and LDH kit (Nanjing Jiancheng Bioengineering Institute, Nanjing, China). The detection of CCK-8 and LDH was carried out based on the manufacturers' protocols.

Hematoxylin-Eosin Staining

Hematoxylin-eosin (HE) was used to evaluate local pathological damage of the small intestine, all procedures were carried out as our previous (6). The pathological scores of intestinal mucosal injury were evaluated by blinded technicians, and were grouped according to the Chiu scoring system (34).

Immunofluorescence and Immunohistochemistry

Immunofluorescence and immunohistochemistry were performed as previously described (1). Anti-zona occludens 1 (ZO-1) antibody (ab216880, Abcam, Cambridge, MA, USA), anti-Occludin antibody (ab216327, Abcam), anti-IL-33 antibody (ab187060, Abcam), anti-IL-13 antibody (ab106732, Abcam), and anti-Ki67 antibody (ab16667, Abcam) were used to detect protein expression in the intestinal tissue and organoids. Images were captured at 200× with an Olympus immunofluorescence microscope. Quantification of the relative intensity of protein staining was performed by automated image analysis in five randomly chosen 200× fields for each sample.

RNA Extraction and RT-PCR

RNA was extracted with the TRIzol reagent (Invitrogen, New York, USA). Real-time PCR was performed using the ABI Q5 Real-Time PCR System (Applied Biosystems, Foster City, CA, USA), with the SYBR Green detection protocol (TOYOBO, Tokyo, Japan). The expression of target genes in mice was normalized against that of the housekeeping gene 18S using the $2^{-\Delta\Delta CT}$ method. The target gene primers are shown in **Supplemental Table 1**.

Statistical Analysis

Data were analyzed and performed using GraphPad Prism software (version 7.0) by investigators blinded to the group allocation. The results are expressed as the mean ± SEM. Statistical analyses were performed using two-sided Student's t tests, one-way ANOVA as indicated in the figure legends. *P* values were corrected for Tukey's test (for comparisons between multiple treatment groups). In addition, the Spearman method was used for correlation statistical analysis. A value of $p < 0.05$ was considered significant.

RESULTS

Pravastatin Is a Metabolite of the Intestinal Flora That Is Negatively Correlated With the Degree of Patient Intestinal I/R Injury

Differential metabolites represented by PA were screened using t-tests based on a significance level of $p < 0.05$ and a variable importance in projection > 1. Untargeted metabolomic results showed that intestinal I/R caused a significant decrease in PA content in the mouse cecum (**Figure 1A**), and PA had the potential to reduce intestinal I/R damage. Accordingly, whether the gut microbiota contributed to the PA levels was also determined using targeted metabolomic analysis. PA levels in the ceca of normal or germ-free (GF) mice were determined by the external standard method using LC-MS/MS. Levels of PA were significantly decreased in the ceca of GF mice, compared with those in control mice (**Figure 1B**). Levels of PA were significantly reduced in I/R mice, compared with those in sham mice, but PA injected i.p. significantly reversed this trend (**Figure 1C**). These findings showed that the gut microbiota produce PA.

We then collected stool and plasma samples from patients before (T0) CPB surgery and collected plasma samples from patients at 6 (T1) and 12 h (T2) after CPB surgery, determined acute gastrointestinal injury (AGI) scores at 2 d after surgery, and examined the relationships between PA levels and citrulline, intestinal fatty-acid binding protein (IFABP) concentrations, or AGI scores. Results of correlation analysis did not reveal significant relationships between the PA content in stool and plasma levels of citrulline ($r = 0.216$, $p = 0.358$) or IFABP ($r = 0.048$, $p = 0.837$) at T0 (**Figure 1D**). In contrast, the PA content in the preoperative stool samples was positively correlated with plasma levels of citrulline, which is a negative marker of intestinal I/R injury, at T1 ($r = 0.514$, $p = 0.029$) and T2 ($r = 0.535$, $p = 0.042$) but was negatively correlated with the plasma content of IFABP, a positive marker of intestinal I/R injury, at T1 ($r = -0.540$, $p = 0.026$) and T2 ($r = -0.597$, $p = 0.006$), and the AGI score at 2 d ($r = -0.506$, $p = 0.045$) after surgery (**Figures 1E–G**).

Pravastatin Reduces Mouse Intestinal I/R Injury and Organoid H/R Injury in Co-Cultured Organoids and ILC2s

We found that PA reduced hematoxylin-eosin staining (HE)-based morphological damage and scores (**Figures 2A, B**). Pravastatin also downregulated the mRNA expression of the inflammatory markers *IL-6* and *IL-1β* (**Supplementary Figures 1B, C**), upregulated mRNA and protein levels of the intestinal mucosal barrier markers *ZO-1* and *Occludin* (**Figures 2C, D** and **Supplementary Figures S1D, E**), and upregulated mRNA and protein levels of proliferation marker *Ki67* (**Figures 2C, E** and **Supplementary Figure S1F**) and the mRNA expression of the ISC marker *Lgr5* (**Figure 2F**). Then, we investigated whether PA exerts protective effects in organoids against H/R injury *in vitro*. Intestinal organoids are 3D systems comprising ISCs, Paneth and enteroendocrine cells, and other intestinal cell types (26). However, unlike the protective effect of PA against intestinal I/R injury *in vivo*, PA did not increase organoid viability and did not reduce LDH release after H/R injury in organoids cultured alone (**Figures 2G, H**). These results implied that the protective effect of PA on intestinal I/R injury is mediated by the interaction between IECs and other immune cells rather than by IECs alone. Considering that type 2 immune cells have an important role in PA effects (35) and that ILC2s with various important functions are abundant in small intestine tissues (27), we investigated whether the protective effect of PA on H/R damage to organoids could be restored in

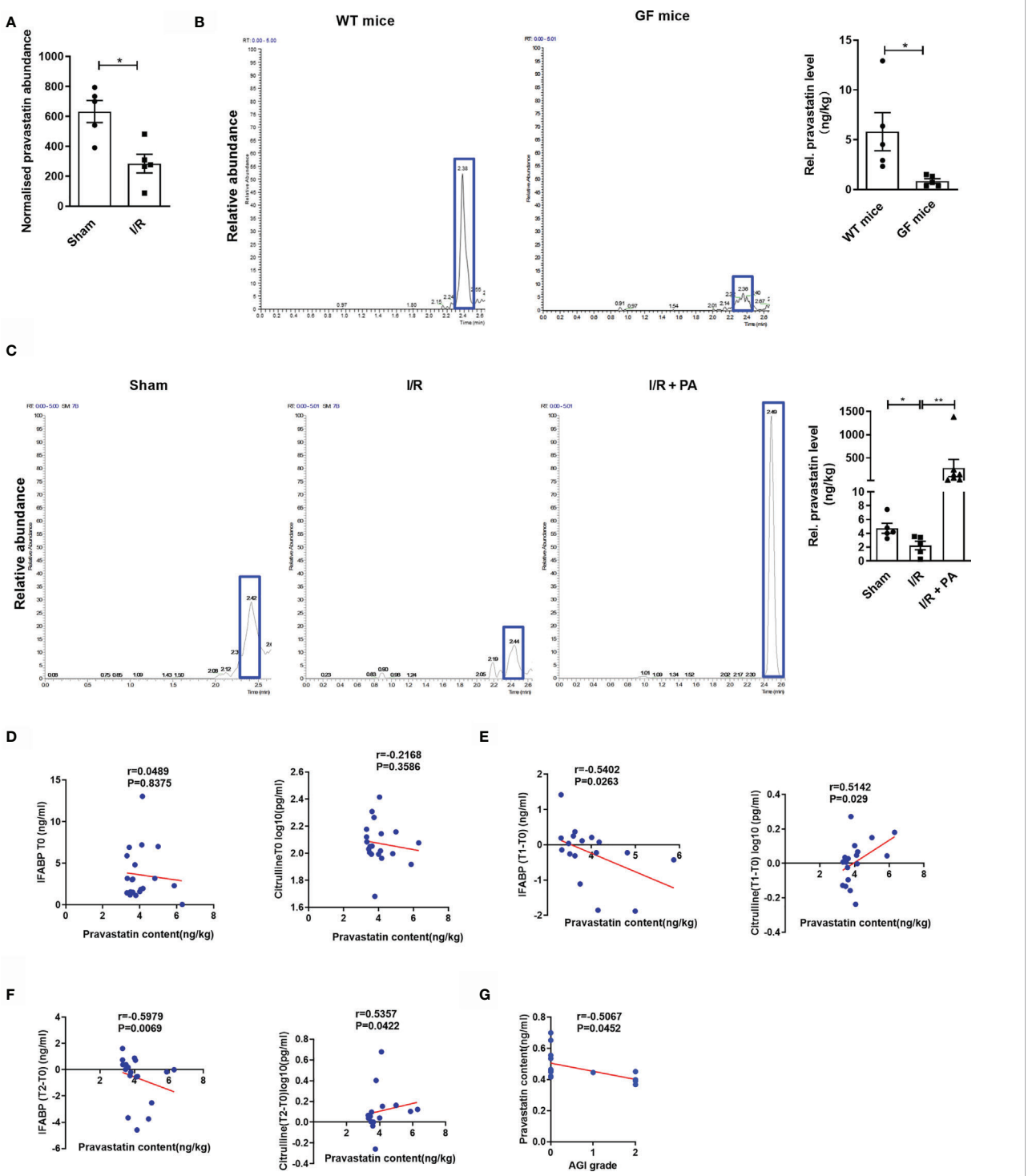

FIGURE 1 | Pravastatin is a metabolite of the intestinal flora and negatively correlated with the degree of patient intestinal I/R injury. **(A)** PA levels in cecum from sham and I/R mice were determined by nontargeted metabolomics (n = 8). **(B)** PA levels in cecum were determined by LC-MS/MS in normal mice and GF mice (n = 6-8). **(C)** PA levels in cecum were determined by LC-MS/MS from sham, I/R and I/R + PA mice (n = 8). **(D–F)** Spearman correlation between the levels of PA in the patients' preoperative stools and the levels of IFABP and citrulline in the plasma at preoperative (T0), 6 h (T1), or 12 h (T2) after surgery. **(G)** Correlation analysis between the levels of PA in the patients' preoperative stools and AGI scores of gastrointestinal complications in patients 2 d after surgery.The results are expressed as the mean ± SEM.*$p < 0.05$, **$p < 0.01$ by two-tailed Student's t test **(A–C)**. PA, pravastatin; I/R, ischemia/reperfusion; LC-MS, liquid chromatograph-mass spectrometer; IFABP, intestinal fatty-acid binding protein; AGI, acute gastrointestinal injury.

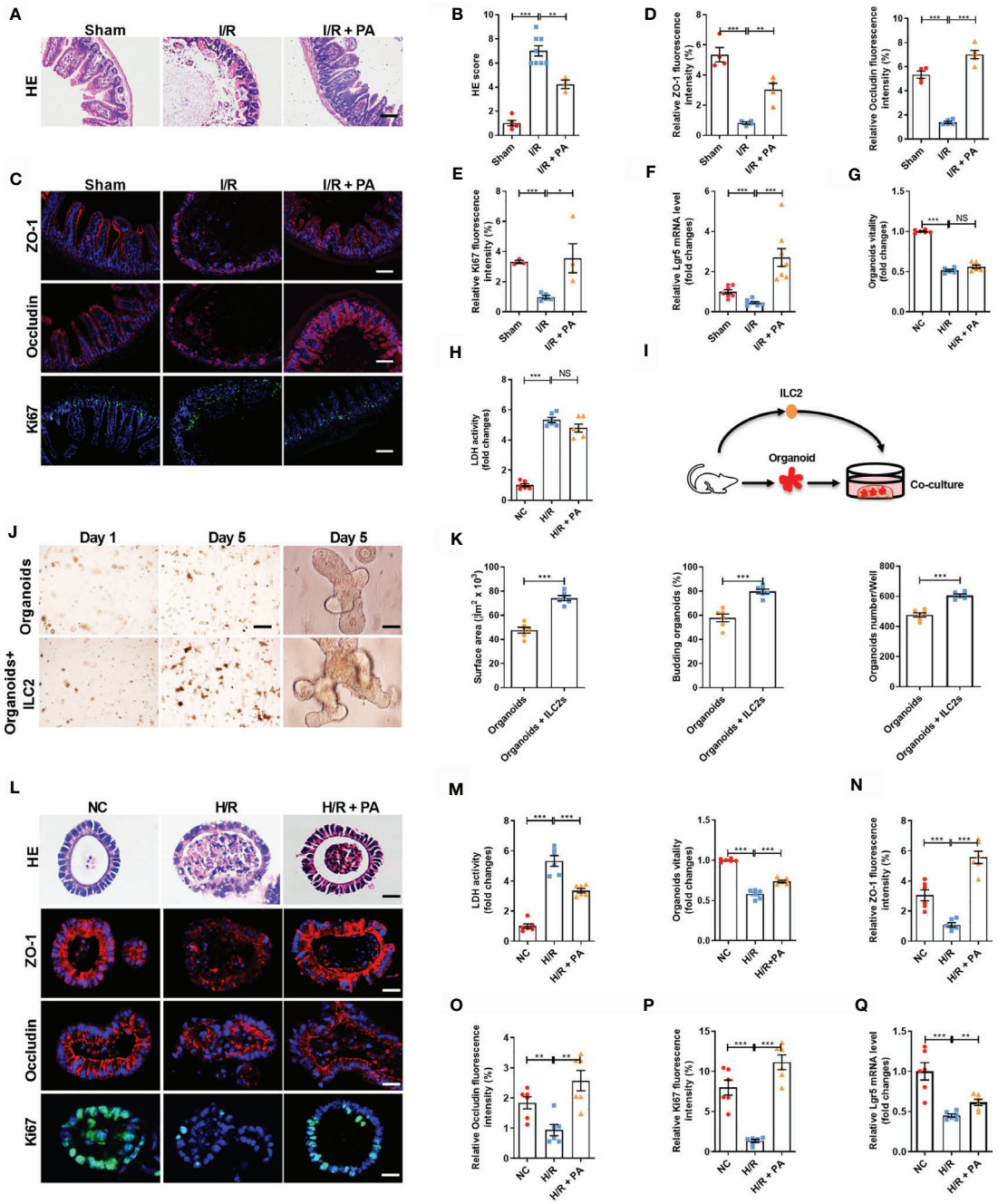

FIGURE 2 | Pravastatin reduced mouse intestinal I/R injury and organoids hypoxia/reoxygenation (H/R) injury in co-cultured organoids and ILC2. **(A, B)** HE staining and pathological damage score of small intestine tissue in sham, I/R and I/R + PA mice, scale bar is 100 μm (n = 8). **(C–E)** The relative protein levels of intestinal tight junction protein ZO-1 and Occludin and cell proliferation marker Ki67 in the ileum were measured by immunofluorescent staining and the relative fluorescence intensity quantification analysis, scale bar is 100 μm (n = 8). **(F)** Relative mRNA level of ISCs self-renewal indicator *Lgr5* was determined by quantitative PCR (n = 8). **(G, H)** Relative organoids viability and LDH levels were detected in organoids cultured alone after H/R (n = 6). **(I)** Schematic representation of co-culture system of organoids and ILC2. **(J)** Brightfield images of organoids without or with group ILC2 at day 1 (scale bar is 400 μm) and day 5 (scale bar is 50 μm), (n = 6). **(K)** Microscopic tracing of organoids to measure surface area, organoids numbers and the percentage of budding organoids at day 5 (n = 6). **(L, M)** HE staining, relative organoids viability and LDH levels were detected in a co-culture system of organoids and ILC2 after H/R, scale bar is 20 μm (n = 6). **(N–P)** The relative fluorescence intensity quantification analysis of ZO-1, Occludin and Ki67 in the organoids, scale bar is 20 μm (n = 6). **(Q)** Relative mRNA level of *Lgr5* in the organoids was measured by quantitative PCR (n = 6). The results are expressed as the mean ± SEM **(B, D, E–H, K, M–Q)**. $^{*}p < 0.05$, $^{**}p < 0.01$, $^{***}p < 0.001$, NS means No statistically significant difference by one-way ANOVA (Tukey's test). PA, pravastatin; I/R, ischemia/reperfusion; ISCs, intestinal stem cells; LDH, lactate dehydrogenase; H/R, hypoxia/reoxygenation; ILC2, type II innate lymphoid cells.

co-cultured ILC2s and organoids (**Figure 2I** and **Supplementary Figure S1G**). The number of co-cultured organoids and the budding ratio were higher and the surface area was larger than those in monocultured organoids (**Figures 2J, K**). Furthermore, PA reduced HE-based morphological damage and levels of LDH released and increased organoid vitality after H/R in the co-culture system (**Figures 2L, M**). Meanwhile, PA upregulated the mRNA and protein levels of *ZO-1* and *Occludin* (**Figures 2L, O** and **Supplementary Figures 1H, I**), the mRNA and protein levels of *Ki67* (**Figures 2L, P** and **Supplementary Figure S1J**), and the mRNA level of *Lgr5* (**Figure 2Q**) in the co-cultures.

Pravastatin Protects Against Intestinal I/R Injury *via* IL-33/ST2 Signaling

Although we confirmed that the protective effect of PA against intestinal I/R injury required the participation of ILC2s, the connection between PA and ILC2s remained unknown. Intestinal I/R damage decreased *IL-33* mRNA and protein levels and *ST2* mRNA levels, effects that were countered by PA (**Figures 3A–C**). These results indicated that IL-33/ST2 signaling might play important role in PA-treated intestinal I/R injury.

Then, neutralizing antibodies against IL-33 (anti-IL-33) or ST2 (anti-ST2) and IL-33$^{-/-}$ mice were used to block IL-33/ST2 signaling (**Supplementary Figure S2A**). The amount of HE-based pathological damage decreased in WT mice administered PA before I/R but not in anti-IL-33- or anti-ST2-treated WT or IL-33$^{-/-}$ mice administered PA (**Figures 3D, E**). The mRNA and protein expression of *ZO-1* and *Occludin* (**Figures 3D, F, G** and **Supplementary Figures S2B, C**), the mRNA and protein expression of *Ki67* (**Figures 3D, H** and **Supplementary Figure S2D**), and the mRNA level of *Lgr5* (**Figure 3I**) were upregulated, whereas the mRNA expression of *IL-6* and *IL-1β* (**Supplementary Figures S2E, F**) was downregulated in PA-treated WT mice but not in anti-IL-33- or anti-ST2-treated WT or IL-33$^{-/-}$ mice administered PA. Meanwhile, the protein expression of IL-33 was upregulated in PA-treated WT mice but not in anti-IL-33-treated WT or IL-33$^{-/-}$ mice administered PA (**Figures 3D, J**). PA also inhibited the reduction in the IL-13^{+}ILC2/ILC2 ratio induced by intestinal I/R, but this did not occur in anti-IL-33- or anti-ST2-treated WT mice administered PA (**Figures 3K, L**). Consistent with the results of flow cytometry, the total protein expression of IL-13 in intestinal tissue was upregulated in PA-treated WT mice but not in anti-IL-33- or Anti-ST2-treated WT or IL-33$^{-/-}$ mice administered PA (**Figures 3M, N**).

Pravastatin Protects Against Organoid H/R Injury *via* IL-33/ST2 Signaling

H/R decreased the expression of IL-33 in the medium in co-cultured organoids and ILC2s, but these changes were counteracted by PA (**Figure 4A**). To further explore the protective mechanism of PA against H/R injury, we added anti-IL-33 or anti-ST2 to the co-cultured ILC2s extracted from WT mice (WT-ILC2s) with organoids from WT mice (WT-organoids) and established co-cultured WT-ILC2 and organoids from IL-33$^{-/-}$ mice (IL-33$^{-/-}$ organoids) to block interactions between IL-33 and ILC2, as well as the subsequent activation of ILC2s (**Supplementary Figure S3A**). Pravastatin inhibited H/R-induced organoid HE-based pathological damage (**Figure 4B**), decreased organoid vitality (**Figure 4C**), and increased LDH release (**Figure 4D**) in co-cultured WT-organoids and WT-ILC2s, but these effects were eliminated by anti-IL-33 or anti-ST2, and no effects were found in co-cultured IL-33$^{-/-}$ organoids and WT-ILC2s. Pravastatin also suppressed the decrease in the mRNA and protein levels of *ZO-1* and *Occludin* (**Figure 4B, E** and **Supplementary Figures S3B, C**), the mRNA and protein levels of *Ki67* (**Figures 4B, F** and **Supplementary Figure S3D**), and the mRNA level of *Lgr5* (**Figure 4G**) caused by H/R in co-cultured WT-organoids and WT-ILC2s, but these effects were eliminated by anti-IL-33 or anti-ST2, and no effects were found in co-cultured IL-33$^{-/-}$ organoids and WT-ILC2s. In addition, PA suppressed the decrease in the protein levels of IL-13 caused by H/R in co-cultured WT-organoids and WT-ILC2s, but these effects were eliminated by anti-IL-33 or anti-ST2, and no effects were found in co-cultured IL-33$^{-/-}$ organoids and WT-ILC2s (**Figure 4H**).

Depletion of ILC2s Abolishes the Protective Effect of IL-33 on Intestinal I/R Injury and Organoid H/R Injury

Interleukin-33 is an important ILC2 activator, but the modulation of ILC2s under intestinal I/R injury and the role of ILC2s in the protective effect of IL-33 on intestinal I/R injury remain unclear. We depleted ILC2s using a previously described antibody depletion method to confirm the role of ILC2s in IL-33-mediated protection against intestinal I/R injury (**Supplementary Figure S4A**) (29–32). Recombinant murine IL-33 (rmIL-33) increased the ratio (%) of ILC2/ILCs and IL-13^{+}ILC2/ILC2 but not in ILC2-deleted mice (**Figures 5A–C**). Compared with that in the I/R group, rmIL-33 decreased the HE-based morphological damage but not in ILC2-deleted mice (**Figures 5D, E**). Furthermore, the mRNA and protein expression of *ZO-1* and *Occludin* was upregulated (**Figures 5D, F** and **Supplementary Figures S4B, C**), the mRNA and protein levels of *Ki67* (**Figures 5D, G** and **Supplementary Figure S4D**) and the mRNA level of *Lgr5* were elevated (**Figure 5H**), and mRNA levels of *IL-6* and *IL-1β* (**Supplementary Figures S4E, F**) were downregulated in mice administered rmIL-33, but the deletion of ILC2s abolished all of these changes.

To explore the role of ILC2 in protection against H/R-induced organoid injury conferred by IL-33, we added rmIL-33 to organoids cultured with and without ILC2s (**Supplementary Figure S5A**). Recombinant murine IL-33 did not affect HE-based pathological damage (**Figure 5I**), organoid vitality (**Figure 5J**), or LDH release (**Figure 5J**) in WT-organoids cultured without ILC2s but increased organoid vitality and decreased HE-based pathological damage and LDH release in WT-organoids co-cultured with ILC2s (**Figures 5I, J**). Recombinant murine IL-33 upregulated the mRNA and

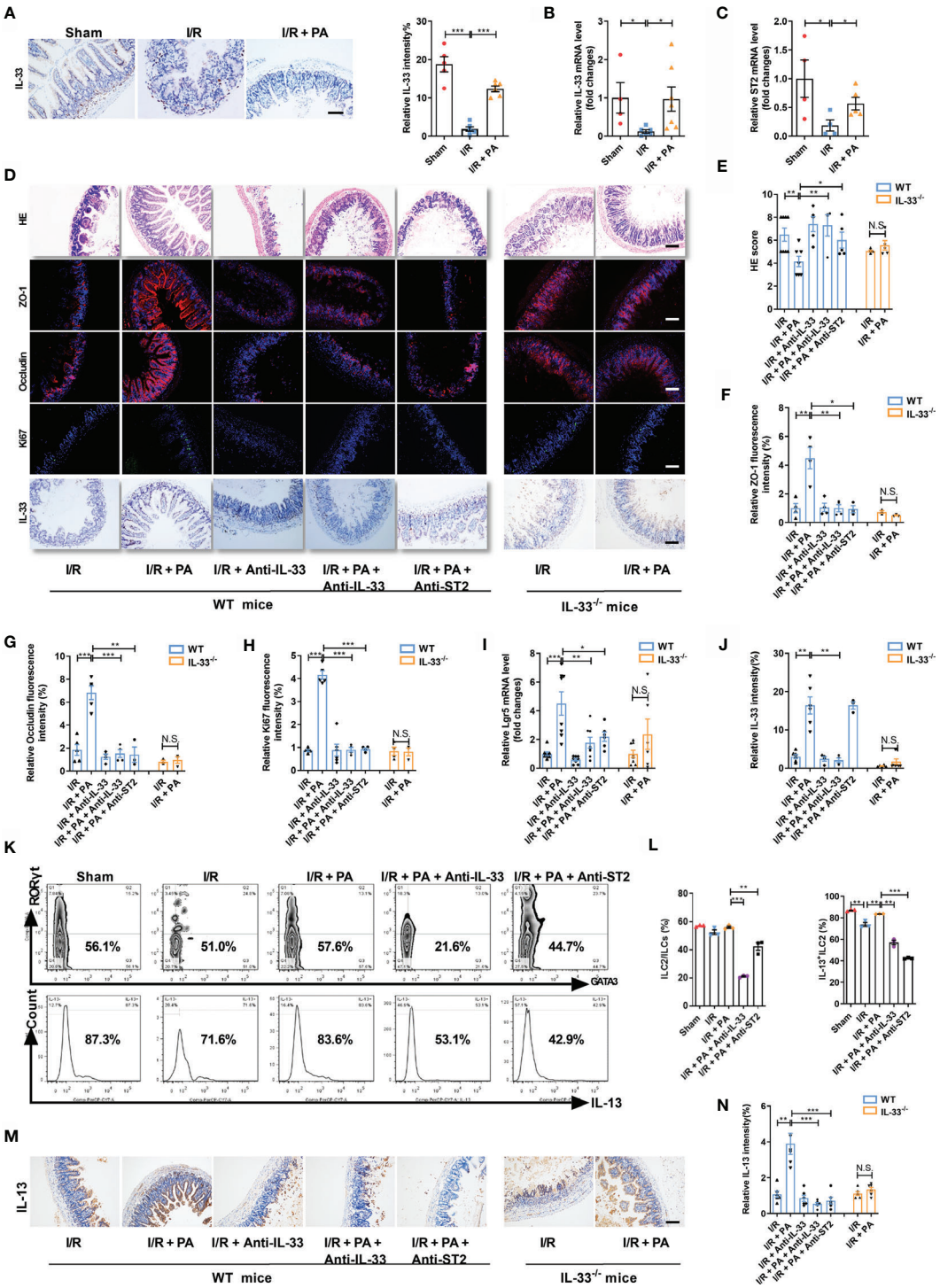

FIGURE 3 | PA protected against intestinal I/R injury *via* an IL-33/ST2 signal. **(A)** IL-33 immunohistochemical staining in the ileum from sham, I/R and I/R + PA mice, scale bar is 100 μm (n = 8). **(B, C)** Relative mRNA levels of IL-33 and IL-33 receptor (ST2) (n = 8). **(D)** HE staining, ZO-1, Occludin and Ki67 immunofluorescent staining and IL-33 immunohistochemical staining in WT mice and IL-33$^{-/-}$ mice, scale bar is 100 μm (n = 8). **(E)** Pathological damage score in the ileum. **(F–H)** The relative fluorescence intensity quantification analysis of ZO-1, Occludin and Ki67 in the ileum. **(I)** The relative mRNA level of *Lgr5* in the ileum was measured by quantitative PCR (n = 8). **(J)** The relative IL-33 intensity quantification analysis in the ileum. **(K, L)** Intestinal lamina propria cells were analyzed by flow cytometry for the ratio of ILC2/ILCs and IL-13^{+}ILC2/ILC2 in WT mice (n = 3-4). **(M, N)** IL-13 immunohistochemical staining and intensity quantification analysis in the ileum, scale bar is 100 μm (n = 8). The results are expressed as the mean ± SEM **(B, C, E–J, N)**. $^{*}p < 0.05$, $^{**}p < 0.01$, $^{***}p < 0.001$, NS means No statistically significant difference by one-way ANOVA (Tukey's test). PA, pravastatin; I/R, ischemia/reperfusion; ILC2, type II innate lymphoid cells.

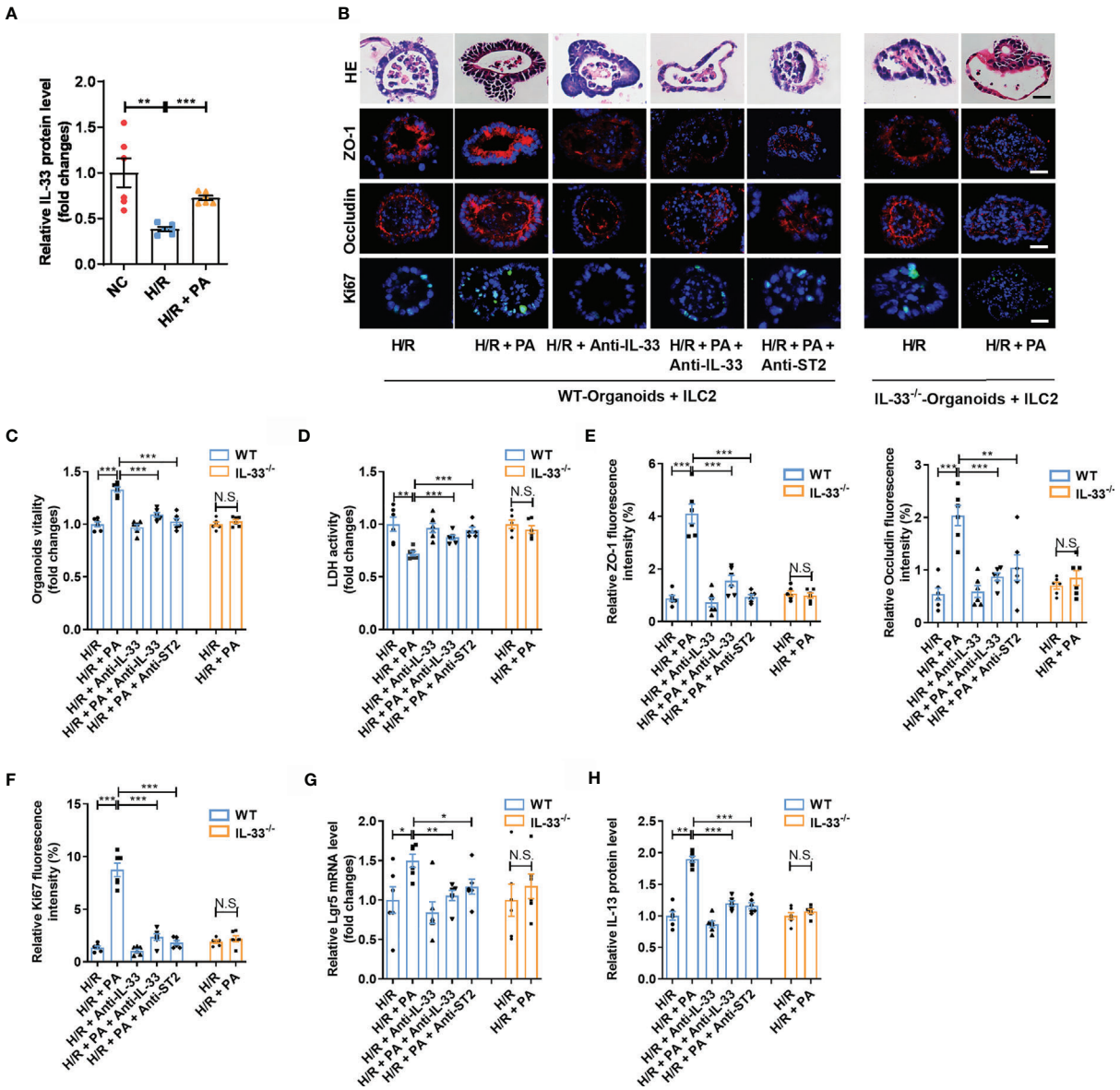

FIGURE 4 | PA protected organoids H/R injury *via* an IL-33/ST2 signal. **(A)** The relative mRNA and protein level of IL-33 in the organoid from WT-Organoids + ILC2. **(B)** HE staining, ZO-1, Occludin and Ki67 immunofluorescent staining in the organoid from WT-Organoids + ILC2, scale bar is 20 μm (n = 6). **(C, D)** Relative organoids viability and LDH levels were detected in a co-culture system of organoids and ILC2 after H/R (n = 6). **(E, F)** The relative fluorescence intensity quantification analysis of ZO-1, Occludin and Ki67 in the organoids (n = 6). **(G)** Relative mRNA level of *Lgr5* in the organoids was measured by quantitative PCR (n = 6). **(H)** The relative protein level of IL-13 in the organoid supernatant determined by ELISA (n = 6). The results are expressed as the mean ± SEM **(A, C–H)**. $^{*}p < 0.05$, $^{**}p < 0.01$, $^{***}p < 0.001$, NS means No statistically significant difference by one-way ANOVA (Tukey's test). PA, pravastatin; H/R, hypoxia/reoxygenation; ILC2, type II innate lymphoid cells; LDH, lactate dehydrogenase; WT-Organoids + ILC2, co-cultured WT-organoids and WT-ILC2; IL-33$^{-/-}$Organoids + ILC2, co-cultured IL-33$^{-/-}$ organoids and WT-ILC2.

protein expression of *ZO-1* and *Occludin* (**Figures 5I, K, L** and **Supplementary Figures S5B, C**), the mRNA and protein expression of *Ki67* (**Figures 5I, M** and **Supplementary Figure S5D**), and the mRNA level of *Lgr5* (**Figure 5N**) in co-cultured WT-organoids and ILC2 systems but not in WT-organoids cultured without ILC2s. These results indicate that the protection of organoids by IL-33 during H/R injury requires ILC2 participation.

The Protective Effect of PA/IL-33 to Alleviate Intestinal I/R Injury Is Mediated by IL-13 Released From ILC2s

Studies have shown that activated ILC2s release large amounts of IL-13 (29, 36). Recombinant murine IL-33 increased the protein levels of IL-13 after I/R but not in ILC2-depleted mice (**Figure 6A**). Recombinant mIL-33 increased the protein levels of IL-13 in the WT-organoids co-cultured with ILC2s after H/R

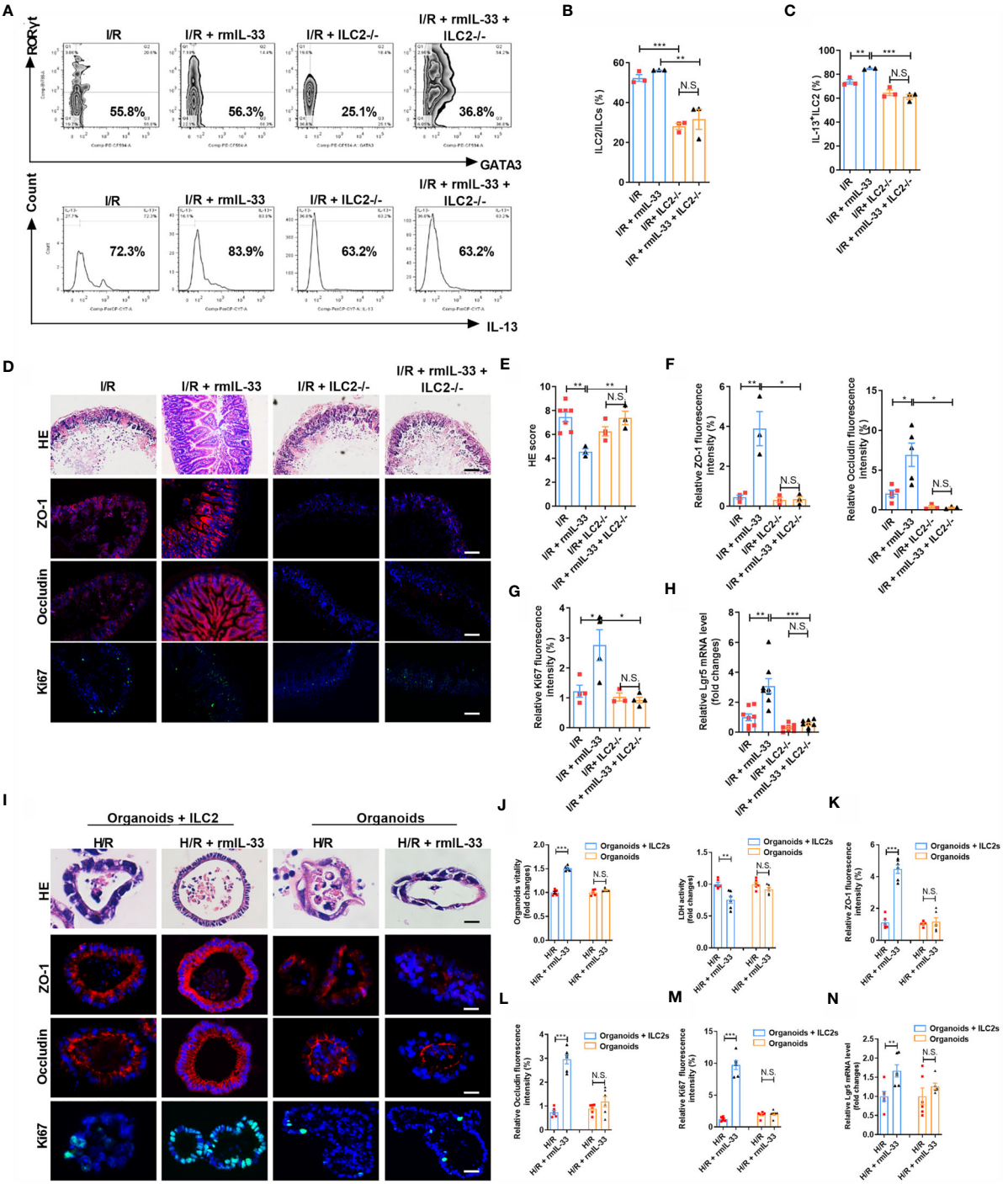

FIGURE 5 | Depletion of ILC2 abolished the protective effect of IL-33 on intestinal I/R injury and organoids H/R injury. **(A–C)** Intestinal lamina propria cells were analyzed by flow cytometry for the ratio of ILC2/ILCs and IL-13^{+}ILC2/ILC2 in Rag1$^{-/-}$ mice (n = 3-4). **(D)** HE staining, ZO-1, Occludin and Ki67 immunofluorescent staining in Rag1$^{-/-}$ mice, scale bar is 100 μm (n = 8). **(E–G)** Pathological damage score and the relative fluorescence intensity quantification analysis of ZO-1, Occludin and Ki67 in the ileum (n = 8). **(H)** The relative mRNA level of *Lgr5* in the ileum was measured by quantitative PCR (n = 8). **(I)** HE staining, ZO-1, Occludin and Ki67 immunofluorescent staining in WT-organoid cultured with and without ILC2, scale bar is 20 μm (n = 6). **(J)** Relative organoids viability and LDH levels were detected in WT-organoid cultured with and without ILC2 after H/R (n = 6). **(K–M)** The relative fluorescence intensity quantification analysis of ZO-1, Occludin and Ki67 in the organoids (n = 6). **(N)** Relative mRNA level of *Lgr5* in the organoids was measured by quantitative PCR (n = 6). The results are expressed as the mean ± SEM **(E–H, J–N)**. *$p < 0.05$, **$p < 0.01$, ***$p < 0.001$ by one-way ANOVA (Tukey's test) **(B–H)**. *$p < 0.05$, **$p < 0.01$, ***$p < 0.001$, NS means No statistically significant difference by two-tailed Student's t test **(J–N)**. PA, Pravastatin; I/R, ischemia/reperfusion; H/R, hypoxia/reoxygenation; ILC2, type II innate lymphoid cells; LDH, lactate dehydrogenase.

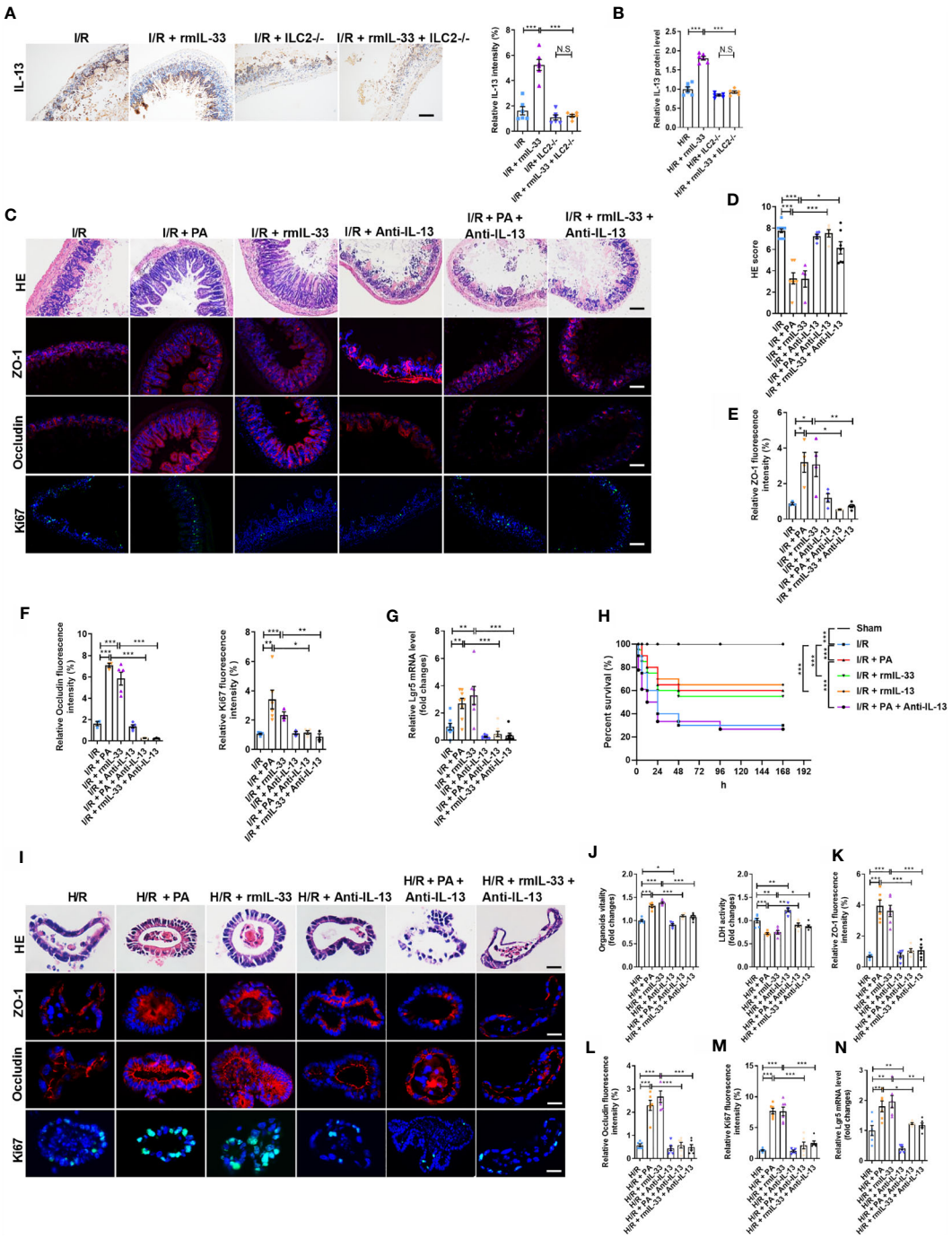

FIGURE 6 | The protection of PA/IL-33 to alleviate intestinal I/R injury was mediated by IL-13 released from ILC2. **(A)** IL-13 immunohistochemical staining and intensity quantification analysis in the ileum, scale bar is 100 μm (n = 8). **(B)** The relative protein level of IL-13 in the organoid supernatant determined by ELISA in WT-organoid cultured with and without ILC2 (n = 6). **(C)** HE staining, ZO-1, Occludin and Ki67 immunofluorescent staining of ileum in WT mice, scale bar is 100 μm (n = 8). **(D–F)** Pathological damage score and the relative fluorescence intensity quantification analysis of ZO-1, Occludin and Ki67 in the ileum (n = 8). **(G)** The relative mRNA level of *Lgr5* in the ileum was measured by quantitative PCR (n = 8). **(H)** Changes in survival rate have been shown. Mice were submitted to ischemia of SMA for 60 min, and survival was monitored on day 7 after reperfusion (n = 20). **(I)** HE staining, ZO-1, Occludin and Ki67 immunofluorescent staining in a co-culture system of organoids and ILC2 after H/R, scale bar is 20 μm (n = 6). **(J)** Relative organoids viability and LDH levels were detected in a co-culture system of organoids and ILC2 after H/R (n = 6). **(K–M)** The relative fluorescence intensity quantification analysis of ZO-1, Occludin and Ki67 in the organoids (n = 6). **(N)** Relative mRNA level of *Lgr5* in the organoids was measured by quantitative PCR (n = 6). The results are expressed as the mean ± SEM **(B, D–G, J–N)**. $^{*}p < 0.05$, $^{**}p < 0.01$, $^{***}p < 0.001$, NS means No statistically significant difference by one-way ANOVA (Tukey's test) and Log-Rank test **(H)**. PA, pravastatin; I/R, ischemia/reperfusion; H/R, hypoxia/reoxygenation; ILC2, type II innate lymphoid cells; SMA, superior mesenteric artery; LDH, lactate dehydrogenase.

but not in WT-organoids cultured without ILC2s (**Figure 6B**). These results indicated that IL-33-activated ILC2s are an important source of IL-13 in the intestine during I/R.

We next investigated the role of IL-13 in the protective effect of PA or IL-33 on intestinal I/R injury using an anti-IL-13 neutralizing antibody (anti-IL-13; **Supplementary Figure S6A**). Pravastatin or rmIL-33 decreased the HE-based pathological damage after I/R, and these effects were abolished by anti-IL-13 (**Figures 6C, D**). The mRNA and protein levels of *ZO-1* and *Occludin* were upregulated (**Figures 6C, E, F** and **Supplementary Figures S6B, C**), the mRNA and protein levels of *Ki67* (**Figure 6C, F** and **Supplementary Figure S6D**) and the mRNA level of *Lgr5* (**Figure 6G**) were elevated, and the mRNA expression of *IL-6* and *IL-1β* was downregulated (**Supplementary Figures S6E, F**) in PA- or rmIL-33-treated mice, but anti-IL-13 abrogated all of these changes induced by PA or rmIL-33. Pravastatin, rmIL-33, and rmIL-13 increased the survival rate of mice after I/R, but the effect of PA was abolished by anti-IL-13 (**Figure 6H**).

To further determine the role of IL-13 released by ILC2 in the protective effects of PA/IL-33 against H/R-induced organoid injury, we added the anti-IL-13 antibody to the co-cultured WT-organoids and WT-ILC2s in the presence of PA or rmIL-33 (**Supplementary Figure S7A**). The organoid vitality was higher and the amount of HE-based pathological damage and levels of released LDH were lower in the PA- or rmIL-33-treated cultures than in the untreated co-cultures during H/R (**Figures 6I, J**). Meanwhile, PA or rmIL-33 upregulated the mRNA and protein levels of *ZO-1* and *Occludin* (**Figures 6I, K, L** and **Supplementary Figures S7B, C**), the mRNA and protein levels of *Ki67* (**Figures 6I, M** and **Supplementary Figure S7D**), and the mRNA level of *Lgr5* in the co-cultures (**Figure 6N**). However, the protective effects of PA or IL-33 against H/R-induced organoid injury in the co-culture systems were abolished by anti-IL-13.

Interleukin-13 Promotes ISC Self-Renewal by Activating the Wnt or Notch Signaling Pathway During Intestinal I/R Injury

The Wnt/β-catenin and Notch signaling pathways are critical for ISC maintenance and self-renewal. We investigated the mechanism through which IL-13 promoted ISC self-renewal using rmIL-13 or anti-IL-13 antibodies. The mRNA expression encoding the Notch ligands *Jagged1*, *Dll1*, and *Hes1*, as well as the mRNA and protein levels of the Notch receptor *Notch1*, was lower in the I/R group than in the sham group (**Figures 7A, C, D**). The mRNA expression of the Notch ligands *Jagged1*, *Dll1*, *Dll4*, and *Hes1* and the mRNA and protein levels of the receptor *Notch1* in the H/R group were lower than those in the NC group (**Figures 7B–D**). These effects were enhanced by an anti-IL-13 antibody and reversed by rmIL-13. The mRNA expression of *Wnt3* (**Figure 7E**), Wnt receptor *Lrp5* (**Figure 7E**), Wnt target genes *C-myc* and *Axin2* (**Figure 7E**) and the protein expression of β-catenin were lower in the I/R group (**Figures 7G, H**), whereas levels of the Wnt antagonist *Dkk1* (**Figure 7E**) were higher than those in the sham group. The mRNA expression of *Wnt3* (**Figure 7F**), Wnt receptors *Lrp5* and *Lrp6* (**Figure 7F**), and the Wnt target genes *C-myc* and *Axin2* (**Figure 7F**) and the protein expression of β-catenin (**Figures 7G, H**) were lower in the H/R group than in the NC group. These changes were strengthened by the anti-IL-13 antibody and reversed by rmIL-13.

DISCUSSION

In the present study, we demonstrated for the first time that PA, identified as a metabolite of intestinal flora, attenuates intestinal I/R injury and improves the survival of animals, accompanied by promoting the self-renewal and proliferation of ISCs. Further, we showed that the protective effects of PA against intestinal I/R injury depends on the activation of ILC2s, mediated by IL-33/ST2 signaling. Interestingly, the current findings also indicated that the protective effects of PA or IL-33 against intestinal I/R injury depend on IL-13 released by activated ILC2s. Moreover, we found that IL-13 promoted ISC self-renewal to maintain the barrier homeostasis during intestinal I/R by activating Notch1 and Wnt signaling. Clinical evidence showed that the levels of PA in preoperative stool of patients undergoing CPB are negatively correlated with the parameters of postoperative intestinal injury, further suggesting that PA can reduce intestinal I/R injury.

Another study by our group confirmed that intestinal I/R leads to significant intestinal flora disorders and changes in metabolites (including capsiate and PA). The gut microbiota metabolite capsiate enhances Gpx4 expression and inhibits ferroptosis by activating TRPV1 in intestinal I/R injury. Based on two independent studies using the same research methods, PA and capsiate were both confirmed to be metabolites of intestinal flora, significantly reduce intestinal and organoid H/R injury, and be related to the level of postoperative intestinal I/R injury in clinical patients. The difference is that capsiate directly reduces intestinal I/R injury, but the PA-mediated reduction in intestinal I/R injury requires the interaction among intestinal epithelial cells, intestinal flora/metabolites, and immune cells. Moreover, as different drugs reduce intestinal I/R injury, their protective mechanisms are also completely different.

Some statins have been reported to reduce organ I/R injury. Simvastatin reduces subsequent intestinal tissue damage by suppressing oxidative stress, inflammatory damage, and apoptosis (37, 38). Atorvastatin has tissue-specific protective activity against intestinal I/R-induced injury (39). However, the role of PA in intestinal I/R injury remained obscure. Here, we confirmed that PA reduced intestinal I/R injury, maintained the intestinal mucosal homeostasis, and promoted ISC self-renewal. We also showed that the protective effects of PA against intestinal I/R injury depend on ILC2 activation *via* IL-33/ST2 signaling. Furthermore, data from patients showed that the levels of PA in preoperative feces of patients undergoing CPB were

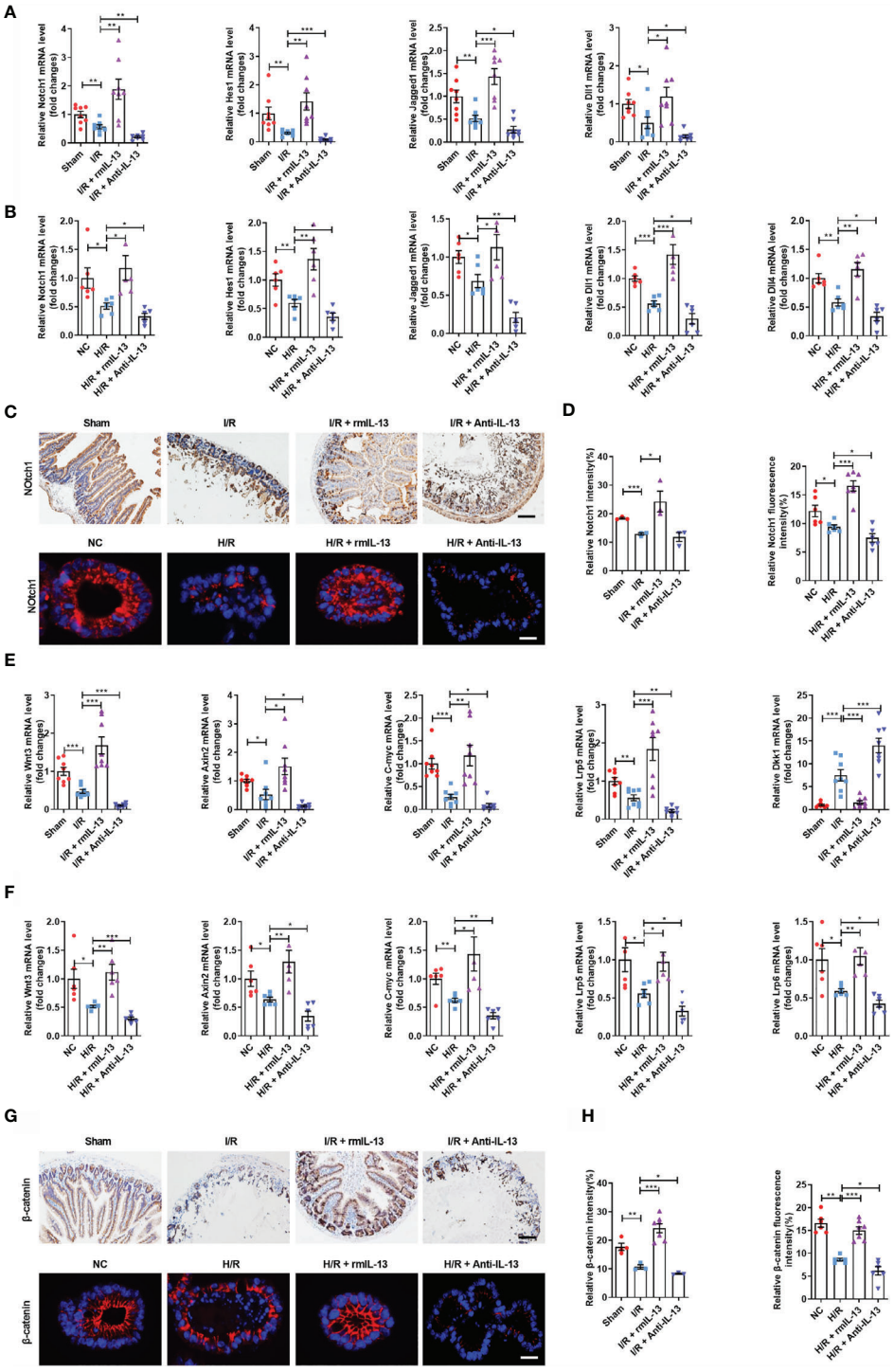

FIGURE 7 | IL-13 promoted the self-renewal of ISCs by activating the Wnt or Notch signaling pathway during intestinal I/R injury *in vivo* and *in vitro*. **(A)** The mRNA levels of *Notch1*, *Hes1*, *Jagged1* and *Dll1* in the ileum were measured by quantitative PCR (n = 8). **(B)** The mRNA levels of *Notch1*, *Hes1*, *Dll1*, *Dll4* and *Jagged1* in the organoids were measured by quantitative PCR (n = 6). **(C, D)** Notch1 protein quantification analysis in the ileum (n = 8, scale bar is 100 μm) and organoids (n = 6, scale bar is 20 μm). **(E)** The mRNA levels of *Wnt3*, *Axin2*, *C-myc*, *Lrp5* and *Dkk1* in the ileum were measured by quantitative PCR (n = 8). **(F)** The mRNA levels of *Wnt3*, *Axin2*, *C-myc*, *Lrp5* and *Lrp6* in the organoids were measured by quantitative PCR (n=6). **(G, H)** Notch1 protein quantification analysis in the ileum (n = 8, scale bar is 100 μm) and organoids (n = 8, scale bar is 20 μm). The results are expressed as the mean ± SEM **(A, B, D, E, F, H)**. $^{*}p < 0.05$, $^{**}p < 0.01$, $^{***}p < 0.001$ by one-way ANOVA (Tukey's test). PA, pravastatin; I/R, ischemia/reperfusion.

negatively correlated with the degree of postoperative intestinal I/R injury. Taken together, PA might be effective for treating intestinal I/R injury.

Interleukin-33 plays an important role in tissue repair and is mainly secreted by non-hematopoietic fibroblasts and epithelial and endothelial cells (12). Fluvastatin, simvastatin, atorvastatin, and lovastatin, but not PA, increase *IL-33* mRNA and intracellular IL-33 protein levels in both human adult cardiac myocytes and fibroblasts (13). In the current study, we showed that PA promoted the release of IL-33 by intestinal epithelial cells. Interleukin-33 might have therapeutic effects on ischemic stroke by promoting macrophage M2 polarization and cytokine production (40). The IL-33-ILC2 axis has a major protective role against renal I/R injury and thus could be a potential therapeutic strategy (29). However, others have also showed a harmful effect of IL-33 by promoting organ I/R injury. Promoting *IL-33* transcription in endothelial cells might contribute to I/R-induced renal injury and fibrosis (41). Interleukin-33 promotes kidney I/R injury *via* iNKT cell recruitment and cytokine production, thus resulting in neutrophil infiltration and activation at injury sites (42). Interleukin-33 promotes the formation of neutrophil extracellular traps, thus exacerbating liver I/R injury (43). The various roles of IL-33 in organ I/R injury might be due to differences in established models that use different organs or because IL-33 acts on different cells, such as ILC2 or neutrophils, to release different cytokines. However, the role of IL-33 in intestinal I/R injury has not been elucidated. ILC2s are innate producers of type 2 cytokines and key regulators of intestinal homeostasis. Depleting ILC2s, but not Tregs, substantially abolishes the protective effect of IL-33 on renal I/R injury (29). Meanwhile, the adoptive transfer of ILC2s reduces kidney I/R injury in mice (36, 44). However, the absence of ILC2s does not change the severity of kidney I/R damage (45). The role of ILC2s in intestinal I/R remained unknown. Here, we showed that the protective effects of PA against intestinal I/R injury depend on IL-33/ST2 signaling to activate ILC2s. Thus, we revealed the key role of IL-33/ST2 signaling and ILC2s in intestinal I/R injury. However, we also found that the absence of ILC2s does not change the severity of intestinal I/R injury. The reason for this phenomenon might be due to redundancy and compensation by other immune cells, such as Treg, AAM, and TH2 cells, as well as the decrease in the abundance of ILC2s during intestinal I/R. Since intestinal I/R is a model of severe acute injury, we measured mouse tissue 2 h after reperfusion. At this time, we found that the endogenous IL-33 level in the intestinal tissue was significantly reduced. Consistent with our results, Maroua Ferhat et al. showed a significant decrease in IL-33 1 h after kidney I/R compared to that in sham-group kidneys (42). Nozomu Sakai et al. found that IL-33 protein expression was decreased at 1 h after liver reperfusion, increased within 4 h after reperfusion, and remained elevated for up to 24 h (46). However, some studies have found that the release of endogenous IL-33 is increased in the early stage of reperfusion. The expression of IL-33 in oligodendrocytes and astrocytes increases rapidly after 60 min of transient middle cerebral artery occlusion (47). Furthermore, acute myocardial infarction leads to a significant increase in the release of IL-33 (48). Therefore, the difference in the level of endogenous IL-33 is not only related to the I/R injury of different organs and tissues but also the time taken for detection after reperfusion.

Interleukin-13 is a multifunctional cytokine secreted by ILC2s (19). It protects against intestinal warm I/R injury and plays a critical role in the regulation of Stat6 and Toll-like receptor-4 signaling (49). Consistent with these findings, we also confirmed that IL-13 reduced intestinal I/R injury. Furthermore, we revealed that PA increased the number of ILC2s and the proportion of IL−13$^+$ ILC2s through the IL-33/ST2 axis, emphasizing the important role of IL-13 released by ILC2s during intestinal I/R injury. Interleukin-13, produced by ILC2s, promotes ISC self-renewal *via* the circular RNA circPan3 (19). However, the effect of IL-13 on ISCs and its underlying mechanism during intestinal I/R remained unclear. Here, we showed that IL-13 promotes ISC self-renewal by activating the Wnt/β-catenin and Notch pathways during intestinal I/R injury.

There are some limitations in this study. Although we demonstrated that PA is a metabolite of the gut microbiota, which can be produced by specific strains, how the PA-producing flora change during intestinal I/R and whether specific strains reduce intestinal I/R injury need further investigation. Although statins have been proven to promote the expression of IL-33 through epigenetic changes and other means (13), this research did not demonstrate how PA regulates IL33 release and whether PA directly regulates IL-33 during intestinal I/R injury. In addition, helminths, allergens, and certain protists induce type 2 immune responses (14). IL-33-mediated ILC2 expansion promotes the rapid activation of mast cells and the intestinal excretion of parasites (50). Products secreted by the mouse parasite *Heligmosomoides polygyrus* suppress type 2 (allergic) immune responses by interfering with the IL-33 pathway (51). PA changed the levels of IL-33, ILC2, and IL-13, but in this study, we did not consider the effect of PA on parasites. In addition, we referred to many references for the dosage of the anti-IL-33 and anti-ST2 neutralizing antibodies to ensure the neutralization efficiency while avoiding the toxic effect as much as possible. However, this research did not directly assess the neutralizing efficiency and toxicity of anti-IL 33 and anti-ST2 *in vivo*.

The present study demonstrated the protective effects of the intestinal flora metabolite PA on intestinal I/R injury, showed that PA promotes IL-13 release from ILC2s through IL-33/ST2 signaling, and confirmed the mechanism through which IL-13 promotes the self-renewal of ISCs. This study sheds light on a novel mechanism of intestinal I/R injury and provides a new therapeutic strategy for preventing intestinal I/R injury in a clinical setting.

DATA AVAILABILITY STATEMENT

The raw data supporting the conclusions of this article will be made available by the authors, without undue reservation.

ETHICS STATEMENT

The studies involving human participants were reviewed and approved by Ethical Committee of Nanfang hospital, Southern Medical University. The patients/participants provided their written informed consent to participate in this study. The animal study was reviewed and approved by Committee of the Nanfang Hospital of Southern Medical University.

AUTHOR CONTRIBUTIONS

FD and K-XL conceived and designed the project. J-JH, B-CZ, and CL performed all clinal experiments. FD, J-JH, and XY performed all animal experiments and analyzed all animal data. Q-SS, Z-BL, Z-LC, YL and Z-ZY performed histology, PCR, intestinal permeability and ELISA experiments. W-FL and CL collected clinical samples and analyzed data. FD, J-JH, and K-XL wrote the paper with the assistance of the other authors. All authors contributed to the article and approved the submitted version.

FUNDING

This work was supported by grants from National Natural Science Foundation, Beijing, China (81671955 to K-XL, 82902010 to J-JH), Key Program of National Natural Science Foundation, Beijing, China (81730058 to K-XL).

ACKNOWLEDGMENTS

The authors thank Peng Chen for technical assistance.

SUPPLEMENTARY MATERIAL

The Supplementary Material for this article can be found online at: https://www.frontiersin.org/articles/10.3389/fimmu.2021.704836/full#supplementary-material

REFERENCES

1. Li Y, Wen S, Yao X, Liu W, Shen J, Deng W, et al. MicroRNA-378 Protects Against Intestinal Ischemia/Reperfusion Injury *via* a Mechanism Involving the Inhibition of Intestinal Mucosal Cell Apoptosis. *Cell Death Dis* (2017) 8 (10):e3127. doi: 10.1038/cddis.2017.508
2. Jia Y, Cui R, Wang C, Feng Y, Li Z, Tong Y, et al. Metformin Protects Against Intestinal Ischemia-Reperfusion Injury and Cell Pyroptosis *via* TXNIP-NLRP3-GSDMD Pathway. *Redox Biol* (2020) 32:101534. doi: 10.1016/j.redox.2020.101534
3. Li Y, Cao Y, Xiao J, Shang J, Tan Q, Ping F, et al. Inhibitor of Apoptosis-Stimulating Protein of P53 Inhibits Ferroptosis and Alleviates Intestinal Ischemia/Reperfusion-Induced Acute Lung Injury. *Cell Death Differ* (2020) 27(9):2635–50. doi: 10.1038/s41418-020-0528-x
4. Lordan C, Thapa D, Ross RP, Cotter PD. Potential for Enriching Next-Generation Health-Promoting Gut Bacteria Through Prebiotics and Other Dietary Components. *Gut Microbes* (2019) 11(1):1–20. doi: 10.1080/19490976.2019.1613124
5. Nogal A, Valdes AM, Menni C. The Role of Short-Chain Fatty Acids in the Interplay Between Gut Microbiota and Diet in Cardio-Metabolic Health. *Gut Microbes* (2021) 13(1):1–24. doi: 10.1080/19490976.2021.1897212
6. Deng F, Zhao BC, Yang X, Lin ZB, Sun QS, Wang YF, et al. The Gut Microbiota Metabolite Capsiate Promotes Gpx4 Expression by Activating TRPV1 to Inhibit Intestinal Ischemia Reperfusion-Induced Ferroptosis. *Gut Microbes* (2021) 13(1):1–21. doi: 10.1080/19490976.2021.1902719
7. Dzhavakhiya VV, Voinova TM, Glagoleva EV, Petukhov DV, Ovchinnikov AI, Kartashov MI, et al. Strain Improvement of Streptomyces Xanthochromogenes RIA 1098 for Enhanced Pravastatin Production at High Compactin Concentrations. *Indian J Microbiol* (2015) 55(4):440–6. doi: 10.1007/s12088-015-0537-5
8. Jayawardana KS, Mundra PA, Giles C, Barlow CK, Nestel PJ, Barnes EH, et al. Changes in Plasma Lipids Predict Pravastatin Efficacy in Secondary Prevention. *JCI Insight* (2019) 4(13):e128438. doi: 10.1172/jci.insight.128438
9. Gu M, Mordwinkin NM, Kooreman NG, Lee J, Wu H, Hu S, et al. Pravastatin Reverses Obesity-Induced Dysfunction of Induced Pluripotent Stem Cell-Derived Endothelial Cells *via* a Nitric Oxide-Dependent Mechanism. *Eur Heart J* (2015) 36(13):806–16. doi: 10.1093/eurheartj/ehu411
10. Eissmann MF, Dijkstra C, Jarnicki A, Phesse T, Brunnberg J, Poh AR, et al. IL-33-Mediated Mast Cell Activation Promotes Gastric Cancer Through Macrophage Mobilization. *Nat Commun* (2019) 10(1):2735. doi: 10.1038/s41467-019-10676-1
11. Faustino LD, Griffith JW, Rahimi RA, Nepal K, Hamilos DL, Cho JL, et al. Interleukin-33 Activates Regulatory T Cells to Suppress Innate Gammadelta T Cell Responses in the Lung. *Nat Immunol* (2020) 21(11):1371–83. doi: 10.1038/s41590-020-0785-3
12. Chen Z, Luo J, Li J, Kim G, Stewart A, Urban JF Jr., et al. Interleukin-33 Promotes Serotonin Release From Enterochromaffin Cells for Intestinal Homeostasis. *Immunity* (2021) 54(1):151–63.e6.. doi: 10.1016/j.immuni.2020.10.014
13. Pentz R, Kaun C, Thaler B, Stojkovic S, Lenz M, Krychtiuk KA, et al. Cardioprotective Cytokine Interleukin-33 Is Up-Regulated by Statins in Human Cardiac Tissue. *J Cell Mol Med* (2018) 22(12):6122–33. doi: 10.1111/jcmm.13891
14. McGinty JW, Ting HA, Billipp TE, Nadjsombati MS, Khan DM, Barrett NA, et al. Tuft-Cell-Derived Leukotrienes Drive Rapid Anti-Helminth Immunity in the Small Intestine But Are Dispensable for Anti-Protist Immunity. *Immunity* (2020) 52(3):528–41.e7. doi: 10.1016/j.immuni.2020.02.005
15. Frisbee AL, Saleh MM, Young MK, Leslie JL, Simpson ME, Abhyankar MM, et al. IL-33 Drives Group 2 Innate Lymphoid Cell-Mediated Protection During Clostridium Difficile Infection. *Nat Commun* (2019) 10(1):2712. doi: 10.1038/s41467-019-10733-9
16. Li S, Bostick JW, Ye J, Qiu J, Zhang B, Urban JFJr., et al. Aryl Hydrocarbon Receptor Signaling Cell Intrinsically Inhibits Intestinal Group 2 Innate Lymphoid Cell Function. *Immunity* (2018) 49(5):915–28 e5. doi: 10.1016/j.immuni.2018.09.015
17. Shimokawa C, Kanaya T, Hachisuka M, Ishiwata K, Hisaeda H, Kurashima Y, et al. Mast Cells Are Crucial for Induction of Group 2 Innate Lymphoid Cells and Clearance of Helminth Infections. *Immunity* (2017) 46(5):863–74 e4. doi: 10.1016/j.immuni.2017.04.017
18. Campbell L, Hepworth MR, Whittingham-Dowd J, Thompson S, Bancroft AJ, Hayes KS, et al. ILC2s Mediate Systemic Innate Protection by Priming Mucus Production at Distal Mucosal Sites. *J Exp Med* (2019) 216(12):2714–23. doi: 10.1084/jem.20180610
19. Zhu P, Zhu X, Wu J, He L, Lu T, Wang Y, et al. IL-13 Secreted by ILC2s Promotes the Self-Renewal of Intestinal Stem Cells Through Circular RNA Circpan3. *Nat Immunol* (2019) 20(2):183–94. doi: 10.1038/s41590-018-0297-6
20. Struck R, Wittmann M, Müller S, Meybohm P, Müller A, Bagci S. Effect of Remote Ischemic Preconditioning on Intestinal Ischemia-Reperfusion Injury in Adults Undergoing On-Pump CABG Surgery: A Randomized Controlled Pilot Trial. *J Cardiothorac Vasc Anesth* (2018) 32(3):1243–7. doi: 10.1053/j.jvca.2017.07.027
21. Adamik B, Kubler A, Gozdzik A, Gozdzik W. Prolonged Cardiopulmonary Bypass Is a Risk Factor for Intestinal Ischaemic Damage and Endotoxaemia. *Heart Lung Circ* (2017) 26(7):717–23. doi: 10.1016/j.hlc.2016.10.012
22. Thuijls G, van Wijck K, Grootjans J, Derikx JP, van Bijnen AA, Heineman E, et al. Early Diagnosis of Intestinal Ischemia Using Urinary and Plasma Fatty

Acid Binding Proteins. *Ann Surg* (2011) 253(2):303–8. doi: 10.1097/SLA.0b013e318207a767
23. Gondolesi G, Ghirardo S, Raymond K, Hoppenhauer L, Surillo D, Rumbo C, et al. The Value of Plasma Citrulline to Predict Mucosal Injury in Intestinal Allografts. *Am J Transplant: Off J Am Soc Transplant Am Soc Transplant Surg* (2006) 6(11):2786–90. doi: 10.1111/j.1600-6143.2006.01513.x
24. Reintam Blaser A, Malbrain MLNG, Starkopf J, Fruhwald S, Jakob SM, De Waele J, et al. Gastrointestinal Function in Intensive Care Patients: Terminology, Definitions and Management. Recommendations of the ESICM Working Group on Abdominal Problems. *Intensive Care Med* (2012) 38(3):384–94. doi: 10.1007/s00134-011-2459-y
25. Zwarycz B, Gracz AD, Rivera KR, Williamson IA, Samsa LA, Starmer J, et al. IL22 Inhibits Epithelial Stem Cell Expansion in an Ileal Organoid Model. *Cell Mol Gastroenterol Hepatol* (2019) 7(1):1–17. doi: 10.1016/j.jcmgh.2018.06.008
26. Deng F, Hu J, Yang X, Wang Y, Lin Z, Sun Q, et al. Interleukin-10 Expands Transit-Amplifying Cells While Depleting Lgr5(+) Stem Cells *via* Inhibition of Wnt and Notch Signaling. *Biochem Biophys Res Commun* (2020) 533 (4):1330–7. doi: 10.1016/j.bbrc.2020.10.014
27. Moro K, Ealey KN, Kabata H, Koyasu S. Isolation and Analysis of Group 2 Innate Lymphoid Cells in Mice. *Nat Protoc* (2015) 10(5):792–806. doi: 10.1038/nprot.2015.047
28. Xu H, Ding J, Porter CBM, Wallrapp A, Tabaka M, Ma S, et al. Transcriptional Atlas of Intestinal Immune Cells Reveals That Neuropeptide Alpha-CGRP Modulates Group 2 Innate Lymphoid Cell Responses. *Immunity* (2019) 51 (4):696–708 e9. doi: 10.1016/j.immuni.2019.09.004
29. Cao Q, Wang Y, Niu Z, Wang C, Wang R, Zhang Z, et al. Potentiating Tissue-Resident Type 2 Innate Lymphoid Cells by IL-33 to Prevent Renal Ischemia-Reperfusion Injury. *J Am Soc Nephrol* (2018) 29(3):961–76. doi: 10.1681/asn.2017070774
30. Engelbertsen D, Foks AC, Alberts-Grill N, Kuperwaser F, Chen T, Lederer JA, et al. Expansion of CD25+ Innate Lymphoid Cells Reduces Atherosclerosis. *Arterioscler Thromb Vasc Biol* (2015) 35(12):2526–35. doi: 10.1161/ATVBAHA.115.306048
31. Hayakawa Y, Ariyama H, Stancikova J, Sakitani K, Asfaha S, Renz BW, et al. Mist1 Expressing Gastric Stem Cells Maintain the Normal and Neoplastic Gastric Epithelium and Are Supported by a Perivascular Stem Cell Niche. *Cancer Cell* (2015) 28(6):800–14. doi: 10.1016/j.ccell.2015.10.003
32. Meyer AR, Engevik AC, Madorsky T, Belmont E, Stier MT, Norlander AE, et al. Group 2 Innate Lymphoid Cells Coordinate Damage Response in the Stomach. *Gastroenterology* (2020) 159(6):2077–91 e8. doi: 10.1053/j.gastro.2020.08.051
33. Zhang X, Vernikovskaya DI, Wang X, Nanovskaya TN, Costantine M, Hankins GDV, et al. Quantitative Determination of Pravastatin and Its Metabolite 3α-Hydroxy Pravastatin in Plasma and Urine of Pregnant Patients by LC-Ms/MS. *Biomed Chromatogr* (2016) 30(4):548–54. doi: 10.1002/bmc.3581
34. Liu WF, Wen SH, Zhan JH, Li YS, Shen JT, Yang WJ, et al. Treatment With Recombinant Trichinella Spiralis Cathepsin B-Like Protein Ameliorates Intestinal Ischemia/Reperfusion Injury in Mice by Promoting a Switch From M1 to M2 Macrophages. *J Immunol* (2015) 195(1):317–28. doi: 10.4049/jimmunol.1401864
35. Zhang X, Xiao S, Li Q. Pravastatin Polarizes the Phenotype of Macrophages Toward M2 and Elevates Serum Cholesterol Levels in Apolipoprotein E Knockout Mice. *J Int Med Res* (2018) 46(8):3365–73. doi: 10.1177/0300060518787671
36. Huang Q, Niu Z, Tan J, Yang J, Liu Y, Ma H, et al. IL-25 Elicits Innate Lymphoid Cells and Multipotent Progenitor Type 2 Cells That Reduce Renal Ischemic/Reperfusion Injury. *J Am Soc Nephrol: JASN* (2015) 26(9):2199–211. doi: 10.1681/ASN.2014050479
37. Yan Y, Lv X, Ma J, Hong G, Li S, Shen J, et al. Simvastatin Alleviates Intestinal Ischemia/Reperfusion Injury by Modulating Omi/HtrA2 Signaling Pathways. *Transplant Proc* (2019) 51(8):2798–807. doi: 10.1016/j.transproceed.2019.04.076
38. Tong F, Dong B, Chai R, Tong K, Wang Y, Chen S, et al. Simvastatin Nanoparticles Attenuated Intestinal Ischemia/Reperfusion Injury by Downregulating BMP4/COX-2 Pathway in Rats. *Int J Nanomed* (2017) 12:2477–88. doi: 10.2147/IJN.S126063
39. Alexandropoulos D, Bazigos GV, Doulamis IP, Tzani A, Konstantopoulos P, Tragotsalou N, et al. Protective Effects of N -Acetylcystein and Atorvastatin Against Renal and Hepatic Injury in a Rat Model of Intestinal Ischemia-Reperfusion. *Biomed Pharmacother* (2017) 89:673–80. doi: 10.1016/j.biopha.2017.02.086
40. Luo Q, Fan Y, Lin L, Wei J, Li Z, Li Y, et al. Interleukin-33 Protects Ischemic Brain Injury by Regulating Specific Microglial Activities. *Neuroscience* (2018) 385:75–89. doi: 10.1016/j.neuroscience.2018.05.047
41. Liu L, Mao L, Wu X, Wu T, Liu W, Yang Y, et al. BRG1 Regulates Endothelial-Derived IL-33 to Promote Ischemia-Reperfusion Induced Renal Injury and Fibrosis in Mice. *Biochim Biophys Acta Mol Basis Dis* (2019) 1865(9):2551–61. doi: 10.1016/j.bbadis.2019.06.015
42. Ferhat M, Robin A, Giraud S, Sena S, Goujon JM, Touchard G, et al. Endogenous IL-33 Contributes to Kidney Ischemia-Reperfusion Injury as an Alarmin. *J Am Soc Nephrol: JASN* (2018) 29(4):1272–88. doi: 10.1681/ASN.2017060650
43. Yazdani HO, Chen H-W, Tohme S, Tai S, Dirk J, van der W, et al. IL-33 Exacerbates Liver Sterile Inflammation by Amplifying Neutrophil Extracellular Trap Formation. *J Hepatol* (2017) 17:S0168–8278. doi: 10.1016/j.jhep.2017.09.010
44. Stremska ME, Jose S, Sabapathy V, Huang L, Bajwa A, Kinsey GR, et al. IL233, A Novel IL-2 and IL-33 Hybrid Cytokine, Ameliorates Renal Injury. *J Am Soc Nephrol* (2017) 28(9):2681–93. doi: 10.1681/asn.2016121272
45. Cameron GJM, Cautivo KM, Loering S, Jiang SH, Deshpande AV, Foster PS, et al. Group 2 Innate Lymphoid Cells Are Redundant in Experimental Renal Ischemia-Reperfusion Injury. *Front Immunol* (2019) 10:826. doi: 10.3389/fimmu.2019.00826
46. Sakai N, Van Sweringen HL, Quillin RC, Schuster R, Blanchard J, Burns JM, et al. Interleukin-33 is Hepatoprotective During Liver Ischemia/Reperfusion in Mice. *Hepatology* (2012) 56(4):1468–78. doi: 10.1002/hep.25768
47. Yang Y, Liu H, Zhang H, Ye Q, Wang J, Yang B, et al. ST2/IL-33-Dependent Microglial Response Limits Acute Ischemic Brain Injury. *J Neurosci* (2017) 37 (18):4692–704. doi: 10.1523/JNEUROSCI.3233-16.2017
48. Yang J, Hu F, Fu X, Jiang Z, Zhang W, Chen K. MiR-128/SOX7 Alleviates Myocardial Ischemia Injury by Regulating IL-33/Sst2 in Acute Myocardial Infarction. *Biol Chem* (2019) 400(4):533–44. doi: 10.1515/hsz-2018-0207
49. Farmer DG, Ke B, Shen XD, Kaldas FM, Gao F, Watson MJ, et al. Interleukin-13 Protects Mouse Intestine From Ischemia and Reperfusion Injury Through Regulation of Innate and Adaptive Immunity. *Transplantation* (2011) 91 (7):737–43. doi: 10.1097/TP.0b013e31820c861a
50. Meiners J, Reitz M, Rudiger N, Turner JE, Heepmann L, Rudolf L, et al. IL-33 Facilitates Rapid Expulsion of the Parasitic Nematode Strongyloides Ratti From the Intestine *via* ILC2- and IL-9-Driven Mast Cell Activation. *PloS Pathog* (2020) 16(12):e1009121. doi: 10.1371/journal.ppat.1009121
51. Osbourn M, Soares DC, Vacca F, Cohen ES, Scott IC, Gregory WF, et al. HpARI Protein Secreted by a Helminth Parasite Suppresses Interleukin-33. *Immunity* (2017) 47(4):739–51 e5. doi: 10.1016/j.immuni.2017.09.015

Conflict of Interest: The authors declare that the research was conducted in the absence of any commercial or financial relationships that could be construed as a potential conflict of interest.

Publisher's Note: All claims expressed in this article are solely those of the authors and do not necessarily represent those of their affiliated organizations, or those of the publisher, the editors and the reviewers. Any product that may be evaluated in this article, or claim that may be made by its manufacturer, is not guaranteed or endorsed by the publisher.

Copyright © 2021 Deng, Hu, Yang, Sun, Lin, Zhao, Yao, Luo, Chen, Liu, Yan, Li, Liu and Liu. This is an open-access article distributed under the terms of the Creative Commons Attribution License (CC BY). The use, distribution or reproduction in other forums is permitted, provided the original author(s) and the copyright owner(s) are credited and that the original publication in this journal is cited, in accordance with accepted academic practice. No use, distribution or reproduction is permitted which does not comply with these terms.

frontiers in Microbiology

REVIEW
published: 06 October 2021
doi: 10.3389/fmicb.2021.712236

Lactiplantibacillus plantarum–Nomad and Ideal Probiotic

Mario Fidanza[1]*, *Pinaki Panigrahi*[2] *and Tobias R. Kollmann*[1]

[1] Telethon Kids Institute, Subiaco, WA, Australia, [2] Georgetown University Medical Center, Department of Pediatrics, Washington, DC, United States

Probiotics are increasingly recognized as capable of positively modulating several aspects of human health. There are numerous attributes that make an ideal probiotic. *Lactiplantibacillus plantarum* (Lp) exhibits an ecological and metabolic flexibility that allows it to thrive in a variety of environments. The present review will highlight the genetic and functional characteristics of Lp that make it an ideal probiotic and summarizes the current knowledge about its potential application as a prophylactic or therapeutic intervention.

Keywords: probiotics, microbiome, *Lactobacillus*, immunology, sepsis, infection, innate immunity

LACTOBACILLUS PLANTARUM–NOMAD AND IDEAL PROBIOTIC

Probiotics are defined as living organisms which, when administered in adequate amounts, confer a health benefit to the host (FAO/WHO 2006). While probiotics have been used in some capacity for centuries, the first report of their proposed health benefits was published more than 100 years ago by Elie Metchnikoff, suggesting that optimizing the composition of intestinal microbes would have a positive effect on health (Metchnikoff, 1907). This has remained precisely what the application of probiotics attempts to accomplish.

Humans are colonized by a diverse and dynamic consortium of microbes that in total outnumber the cells that comprise the human body itself. This consortium is comprised of bacteria viruses, archaea, and other eukaryotic organisms (Cho and Blaser, 2012). The total collection of microbes inhabiting the human body is referred to as the microbiota. The microbiota interacts with the host in a symbiotic relationship and has been shown to play a major role in human immunology, metabolism, and also in multiple disease pathologies (Ogunrinola et al., 2020). Establishment of the microbiota begins before birth, i.e., *in utero* and undergoes rapid sequential compositional changes from the time of birth onward to about 2 years of age when stabilization occurs and the microbiota, compositionally, begins to resemble that of a healthy adult (Greenhalgh et al., 2016; Kapourchali and Cresci, 2020). Thus, early life is the key period during which the microbiota is established (Tamburini et al., 2016; Du Toit, 2017). Of note, this early life period is also characterized by the rapid maturation of immune, metabolic, and neurological pathways (Brook et al., 2017; Harbeson et al., 2018). Given this parallel high-speed development, it should come as no surprise that the microbiota plays a significant role in shaping the maturation and eventual outcomes of many of these developmental pathways (and possibly vice versa). Together, changes across this period exert a profound impact on human health for years, decades - if not life (Zeissig and Blumberg, 2014; Stiemsma and Michels, 2018).

There are several factors that influence early-life microbiota composition and development, such as gestational age at birth, mode of delivery, post-natal feeding practices and environmental factors such as antibiotic exposure (Guo et al., 2021). When the normal patterns of development or the composition of the microbiota are altered in such a way that unfavorable or pathogenic bacteria

OPEN ACCESS

Edited by:
Maryam Dadar, Razi Vaccine and Serum Research Institute, Iran

Reviewed by:
Huaxi Yi, Ocean University of China, China
Robert J. Moore, RMIT University, Australia

***Correspondence:**
Mario Fidanza
mfidanza5@gmail.com

Specialty section:
This article was submitted to Microbial Immunology, a section of the journal Frontiers in Microbiology

Received: *20 May 2021*
Accepted: *09 September 2021*
Published: *06 October 2021*

Citation:
Fidanza M, Panigrahi P and Kollmann TR (2021) Lactiplantibacillus plantarum–Nomad and Ideal Probiotic. Front. Microbiol. 12:712236. doi: 10.3389/fmicb.2021.712236

become more dominant, the microbiota assumes a state of dysbiosis. Dysbiosis has been implicated in a number of disease pathologies including allergy, type-1 diabetes, auto-immune disorders, and metabolic disorders such as obesity (Tilg and Kaser, 2011; Azad et al., 2015; Kostic et al., 2015). The broad overall objective of probiotics is to prevent or ameliorate these extreme states of dysbiosis in order to establish a balanced microbiota that imparts positive benefits to the host (McFarland, 2014; Gagliardi et al., 2018).

Given this complex, interwoven system the successful application of probiotics must take into account several aspects. One such consideration is the timing of administration. As the microbiota from the time of birth to ∼2 years of age is characterized as being highly dynamic, it has been theorized that this period of life represents an intervention window during which probiotic administration can have a meaningful and lasting impact (Du Toit, 2017). Vertical transmission of microbes from mother to infant before and during delivery and subsequently through breastfeeding establishes a situation where interventions could be administered to either the infant and/or the mother in order to achieve positive health benefits (Asnicar et al., 2017; Renelies-Hamilton et al., 2021). There has been several studies assessing the impact of probiotic administration to the pregnant mother, the newborn infant or the nursing mother. Indeed, several recent reviews and meta-analyses of published data indicate probiotic supplementation during this critical window is associated with many positive health benefits (Gritz and Bhandari, 2015; Reid, 2016; Zhang et al., 2016; Baldassarre et al., 2018; Liu et al., 2018; Tsai et al., 2019; Underwood, 2019).

In pregnant mothers, bacterial vaginosis and preeclampsia have been definitively linked to pre-term birth which is associated with numerous short and long-term health complications for the infant. Meta-analyses of published studies suggest that the administration of probiotics to pregnant mothers can reduce the incidence of both bacterial vaginosis and preeclampsia (Lindsay et al., 2013; Huang et al., 2014). A direct link between probiotic supplementation and pre-term birth outcomes has been harder to establish (Othman et al., 2007; Jarde et al., 2018). However, a recent study demonstrated that administration of a probiotic mixture containing *S. faecalis, C. butyricum*, and *B. mesentericus* to high-risk pregnant women was associated with a lower rate of spontaneous pre-term birth, increased gestational age at delivery and decreased intrauterine infections compared to a no probiotic control group (Kirihara et al., 2018). Most studies assessing the impact of probiotic administration to the newborn have been conducted in premature or low birth weight infants. Premature infants are at an increased risk for several adverse outcomes; the impact of probiotic administration on clinically relevant outcomes can therefore be more readily determined. Meta-analyses of these studies have demonstrated that the administration of probiotics significantly reduces the risk of necrotizing enterocolitis, late-onset neonatal sepsis and atopic dermatitis (Zago et al., 2011; Zhao M. et al., 2018; Underwood, 2019).

Another consideration for the successful application of probiotics is the species, strain and composition of the probiotic product that is utilized. There are several functional properties that are required for a bacterial species to be an effective probiotic. Primary characteristics that must be considered are resistance to gastric acid and bile salts, ability to adhere to the intestinal mucosa, and finally sensitivity to antibiotics. Specifically, potential probiotics are evaluated for their ability to persist in the host, favorably alter intestinal microflora, promote intestinal integrity and mobility, modulate host immune responses and finally for their antimicrobial or competitive activity against potentially pathogenic bacteria.

Lactic acid bacteria (LAB) have long been appreciated for their probiotic properties. The health benefits associated with certain fermented foods, which are generally considered rich sources of LAB, have been recognized for millennia. More definitively, even the original Metchnicoff essay identified LAB as potentially being capable of offsetting the effects of harmful bacteria and conferring health benefits on the host. It is therefore not entirely surprising that *Lactobacillus* and *Bifidobacterium* are the most extensively studied bacterial genera in probiotic research. Within these genera, several species and strains with positive health benefits have been identified. Of these, *Lactiplantibacillus plantarum* (formerly *Lactobacillus plantarum)* is an interesting probiotic candidate. It has been demonstrated to possess several fundamental probiotic characteristics, is highly versatile and is capable of successfully colonizing and inhabiting the human gastrointestinal system. This review will cover the characteristics of *L. plantarum* that make it an ideal probiotic candidate as well as highlight the current evidence that administration of *L. plantarum* can confer positive health benefits to humans.

LACTIPLANTIBACILLUS PLANTARUM

Lactiplantibacillus plantarum is a gram-positive lactic acid bacteria species. *L. plantarum* exhibits ecological and metabolic adaptability and is capable of inhabiting a range of ecological niches including fermented foods, meats, plants, and the mammalian gastro-intestinal tract (Filannino et al., 2018). Often, the ability of different bacterial strains to adapt to defined environments is thought to be accomplished by genome specialization that facilitates niche-specific phenotypic fitness. This typically occurs through a process of genome decay in unutilized genes and enrichment of those that impart habitat-specific fitness. This adaptive process generally ensures that individual bacterial strains isolated from the same ecological niche cluster genetically and carry similar niche specific genetic signatures. This has been demonstrated to be the case for *L. gasseri* and *L. jensenii* isolated from human vaginal environments and *L. reuteri* strains isolated from different vertebrate intestinal tracts (Kleerebezem et al., 2003; Mendes-Soares et al., 2014). However, a recent analysis assessing dozens of *L. plantarum* strains for genomic signatures that reflect specific environmental adaptations, demonstrated that this is not the case in *L. plantarum.* Thus, the evolutionary history of this bacterial species does not appear to be directly related to the features of the niches from which they were isolated. This suggests that, unlike most *Lactobacillus* species, *L. plantarum* may acquire and

preserve functional characteristics that are not solely determined by a single habitat (Martino et al., 2016; Filannino et al., 2018). In this manner, *L. plantarum* maintains a diverse functional genome that facilitates a metabolic flexibility that allows it to colonize a variety of environments (Martino et al., 2016; Filannino et al., 2018; Inglin et al., 2018).

RESISTANCE TO THE CONDITIONS OF THE HUMAN GASTROINTESTINAL TRACT

A major hurdle for any probiotic is surviving the harsh conditions of the human gastrointestinal tract. To be effective, a probiotic must first be able to withstand the acidic conditions of the stomach, and then tolerate exposure to bile acids in the small intestine. The stomach is an inhospitable environment. Human gastric juice is primarily composed of pepsin and hydrocholoric acid. This composition results in a cycling pH in the stomach that ranges from about 1.5 during fasting to between 3 and 5 after food intake (Schubert, 1999). Acid resistance is thus considered a primary criterion for the selection of probiotic bacterial strains.

Lactobacillus species employ several strategies to facilitate acid tolerance. These include mechanisms to maintain intracellular pH homeostasis, rapid recycling of damaged proteins and induction of various stress response pathways (Chiang et al., 2014; Wu et al., 2014). Additionally, the acid tolerance of several *Lactobacillus* strains, including *L. plantarum* can be increased by previous exposure to non-lethal acidic conditions in a process known as the acid tolerance response (Foster and Hall, 1991). It is well-established that different strains of the same *Lactobacillus* species have highly variable acid tolerance. While this is also true for *L. plantarum,* numerous studies have demonstrated that the majority of tested *L. plantarum* strains exhibit acid tolerance, albeit to slightly different degrees, through a number of specific and distinct mechanisms (Kaushik et al., 2009; Guidone et al., 2013; Hamon et al., 2014).

Specifically, the acid tolerance mechanisms employed by *L. plantarum* include inducible alterations to the fatty acid composition of the plasma membrane such that the ratio of saturated to unsaturated fatty acids increases upon exposure to low pH conditions causing a significant reduction in membrane fluidity (Huang et al., 2016). Additionally, *L. plantarum* has also been shown to upregulate the expression of phosphofructokinase (*pfk)* and pyruvate-kinase (*pyk)* to facilitate higher rates of sugar metabolism, and in result, greater ATP production which provides energy to drive proton pumps that help maintain intracellular pH homeostasis (Huang et al., 2016). This increase in proton pump function is further facilitated by increased expression of ATP-synthase genes *atpA* and *atpC* (Heunis et al., 2014; Seme et al., 2015; Huang et al., 2016). Finally, *L. plantarum* has also been shown to alter its amino acid metabolism upon exposure to acidic environments. Amino acid metabolism has been shown to play a significant role in maintaining cellular homeostasis and promoting resistance to environmental stresses in multiple lactic acid bacteria species (Reveron et al., 2012; Heunis et al., 2014; Seme et al., 2015). It has been demonstrated that the intracellular concentration of alanine and arginine in particular increase in *L. plantarum* upon exposure to acid stress in a metabolic response that promoted low pH tolerance.

After enduring the low pH of the stomach, a probiotic must also be able to tolerate exposure to bile salts in the small intestine. Bile salts are synthesized in the liver from cholesterol that is conjugated to glycine or taurine residues. These compounds are then released into the small intestine and have a primary role in lipid metabolism. Through detergent disruption of cellular membranes, DNA damage and oxidative stress, bile salts pose a significant challenge for probiotic survival. Bile tolerance is thus another primary criterion for the selection of potential probiotics. While *L. plantarum* employs multiple strategies to withstand the stress of bile salt exposure, there are 4 that are considered critical: (i) induction of bile salt hydrolases (ii) altering membrane composition and fluidity (iii) protecting against oxidative injury and finally (iv) maintaining the proton motive force.

Bile salt hydrolase (*bsh)* is generally considered a major component of bacterial bile tolerance. It is responsible for catalyzing the de-conjugation of glycine and taurine residues from cholesterol. While the exact nature of how bile salt de-conjugation limits the negative impact on cellular homeostasis is unclear, *bsh* expression has been definitively linked to bile tolerance in a number of *Lactobacillus* species (Begley et al., 2006; Pfeiler et al., 2007; Pfeiler and Klaenhammer, 2009). *L. plantarum* carries four *bsh* genes that are upregulated upon exposure to bile salts (Bron et al., 2006; Duary et al., 2012; Gu et al., 2014). The products of these genes represent the first line of bacterial defense against the destructive effects of bile salts in the small intestine.

The commonly characterized *L. plantarum* WCSF1 demonstrates very good tolerance to bile salts in an *in vitro* artificial GI tract environment; this tolerance was accompanied by significant changes in cell morphology (Bron et al., 2004). The morphological change facilitating this tolerance was at least partially attributed to the upregulation of *Cfa2,* a cyclopropane-fatty-acyl-phospholipid synthase that has been shown to alter cell membrane composition and fluidity perhaps imparting resistance to bile salt-induced detergent disruption of cellular membranes (Hamon et al., 2011). To protect against oxidative insult, *L. plantarum* strains have been shown to upregulate the stress-induced glutathione reductase gene and the *metC-cysK* operon upon exposure to bile stress. Finally, by upregulating expression of the F0F1-ATPase, *L. plantarum* facilitates the expulsion of protons from the intracellular environment to help maintain pH homeostasis when exposed to alkaline bile salts (Bron et al., 2004, 2006; Hamon et al., 2011).

ADHERENCE TO INTESTINAL MUCOSA

To impart positive health benefits, a probiotic must be able to colonize and persist in the human gastrointestinal tract. Therefore, an important probiotic selection criterion is the ability to adhere to the human intestinal mucosa. The mucus layer coating the epithelial cells of the gastrointestinal tract serves as a physical barrier to protect against the invasion of pathogenic microbes; on the other hand, it also serves as an important colonization site for commensal bacteria. The intestinal mucus is

comprised primarily of mucins and glycoproteins that assemble into a complex net-like structure that attaches to epithelial cells (Sicard et al., 2017). While the thickness of this mucus layer is variable throughout the digestive tract, in the colon, where microbe concentration is highest, the innermost and densest portion of the mucus layer is typically devoid of bacteria in healthy individuals. Bacterial persistence is therefore largely related to the ability to adhere to mucus or extra-cellular matrix (ECM) components rather than epithelial cells themselves which are typically only in direct contact with invasive pathogenic microbes in the context of certain disease pathologies.

It has been demonstrated that while trypsin treatment significantly reduced the adhesion capacity of *L. plantarum,* it did not eliminate adhesion entirely (Wang G. et al., 2018). This is consistent with other reports on the adhesion properties of *Lactobacillus* species and suggests that non-protein interactions contribute to the adhesion of *L. plantarum* (Deepika and Charalampopoulos, 2010; Jensen et al., 2014). In fact, the initial adhesion interaction is believed to involve non-specific mechanisms. Physical characteristics of the bacterial cell such as surface charge, hydrophobicity and electron donor-acceptor properties can influence bacterial adhesion properties. While the adhesion capacity of *L. plantarum* has been demonstrated to be strain dependent, a positive correlation was found between cell surface hydrophobicity and adhesion capacity (Yadav et al., 2013; Buntin et al., 2017).

In terms of specific interactions, a number of prototypical cell-surface bacterial adhesins contribute to the adhesion capacity of *L. plantarum*. Mannose-specific adhesion (*Msa),* has been identified as a "probiotic gene" and has been definitively linked to mannose-binding and adhesion capacity in *L. plantarum* (Gross et al., 2010; Buntin et al., 2017). As a result, inter-strain variation in the *Msa* gene, particularly in relation to the number of PxxP-repeats in the mucus-binding (MUB) domain, has been associated with inter-strain differences in the adhesive characteristics of *L. plantarum* (Gross et al., 2010). A number of additional adhesin proteins have been implicated in the capacity of *L. plantarum* to adhere to components of the intestinal mucosa. Mucus-binding protein (MucBP) and mucus-adhesion binding protein (MapA) have been shown to be central in the mucin binding capacity of *L. plantarum.* Finally, collagen binding protein (Cbp) and alfa-enolase-1 (EnoA1), a fibronectin binding protein facilitate the binding of *L. plantarum* to epithelial ECM component in *in vitro* models (Ramiah et al., 2007; Castaldo et al., 2009; Gross et al., 2010; Yadav et al., 2013; Buntin et al., 2017).

Recently, a number of unlikely proteins have also been shown to contribute to bacterial adhesion to the intestinal mucosa. These proteins have been termed "moonlighting proteins" in light of their function in several distinct cellular processes. These proteins are generally well-conserved across bacterial species, and often have central roles in key cellular functions such as metabolism and stress responses (Wang et al., 2014). While the mechanisms have not been completely resolved, two moonlighting proteins have been specifically associated with the adhesion capacity of *L. plantarum*. Elongation-factor-Tu (EF-Tu) (Dhanani and Bagchi, 2013) and glyceraldehyde-3-phosphate dehydrogenase (GAPDH) (Wang G. et al., 2018) have been demonstrated to contribute to the adhesion of *L. plantarum.* Antibodies targeting these surface proteins significantly reduced the ability of *L. plantarum* to adhere to both the HT-29 epithelial cell line and porcine mucin. Interestingly, addition of purified EF-Tu or GAPDH significantly increased the adhesion of strains that previously had poor adhesion ability suggesting that these proteins are capable of self-assembly and integration to facilitate bacterial adhesion. Further work will be required to uncover the mechanism underlying how these and other moonlighting proteins contribute to bacterial adhesion.

Most assessments of bacterial adhesion are conducted *in vitro*. These studies generally evaluate the adherence of bacterial strains to immobilized mucin (usually porcine), extra-cellular matrix components or epithelial cell cultures, which generally utilize the HT-29 or Caco-2 lines. Animal models can be used to further validate these *in vitro* findings. Administration of *L. plantarum* has been shown to achieve moderate or long-term colonization of the gastrointestinal tract of both mice and rats (Wang et al., 2009; Daniel et al., 2013). While these studies are informative, they fail to capture the complexities of adherence to the human intestinal mucosa. Human mucosal tissue is obviously more difficult to obtain, therefore probiotic persistence is most commonly evaluated by fecal recovery, that is the duration of time over which the probiotic can be found in fecal samples of subjects who had been administered the probiotic. The number of studies assessing *L. plantarum* persistence in humans is relatively limited. However, Panigrahi and colleagues demonstrated that 7-day administration of *L. plantarum* in combination with a fructooligosaccharide prebiotic to healthy newborns for 7 days resulted in long-term colonization, with a significant number of infants (32%) remaining colonized 6 months after treatment cessation (Panigrahi et al., 2008). These *in vivo* results further validate *in vitro* assessments and suggest that *L. plantarum* is capable of adhering to the human intestinal mucosa and persisting in the mammalian gastrointestinal tract.

PROMOTION OF INTESTINAL INTEGRITY OR MOTILITY

One mechanism by which probiotics may positively influence human health is through the promotion of intestinal integrity or motility. The intestinal epithelial layer is the major barrier that separates the body from the external environment and the consortium of microbes that colonize the gastrointestinal tract. The intestinal epithelial monolayer is comprised of different specialized epithelial cells such as enterocytes, Paneth cells and goblet cells, each of which has distinct functions (Chelakkot et al., 2018). The most abundant of these are enterocytes or intestinal epithelial cells. The primary function of enterocytes is maintenance of barrier integrity, which entails permitting the passage of water and nutrients but preventing the transit of pathogenic microbes or their associated toxins (Chelakkot et al., 2018). Epithelial tight-junction proteins equip the intestinal epithelial cells with this functional capacity by sealing the intercellular space between cells and restricting the transport of molecules across the epithelial barrier. These tight junctions

are composed of several transmembrane and cytosolic proteins that cooperate to efficiently adapt to different environmental demands by sealing or opening to maintain paracellular transport under different physiological conditions. Disruptions to tight junction assembly of function, result in changes in epithelial permeability and can have serious effects on human health. For example, decreased expression of known tight junction proteins such as ZO-1 and occludin, have been shown to be associated with pathologies such as necrotizing enterocolitis (NEC) and inflammatory bowel disease (Hogberg et al., 2013).

L. plantarum has been shown to modulate epithelial barrier function both *in vitro* and *in vivo* through a number of mechanisms. Wang and colleagues demonstrated that administration of *L. plantarum* to piglets significantly counteracted or prevented increases in gut permeability induced by enterotoxigenic *Escherichia coli* (Wang J. et al., 2018). This protective benefit was shown to be conferred through multiple overlapping mechanisms that included maintaining expression of critical tight-function proteins, reducing expression of pro-inflammatory cytokines and modulating gut microbiota composition. This finding is further corroborated by a study in a rat model of NEC in which administration of *L. plantarum* significantly increased the expression of ZO-1 and improved intestinal barrier integrity (Blackwood et al., 2017). However, this beneficial outcome was only observed when *L. plantarum* was administered in combination with the likely pathogenic *Cronobacter sakazakii*. The integrity-protective responses induced by *L. plantarum* may be at least partially mediated through the engagement and activation of TLR-2 in the intestinal epithelium. Specifically, in a trial assessing the effect of *L. plantarum* administration on tight-junction physiology in healthy humans, Karczewski and colleagues demonstrated that *L. plantarum* induced increased expression and trafficking of ZO-1 and occludin tight junction sites through a mechanism that was mediated by TLR-2 signaling (Karczewski et al., 2010).

A recent study also highlighted a role for the *L. plantarum* cell surface protein known as micro integral membrane protein (MIMP) in improving intestinal barrier integrity in a murine DSS induced IBD model (Yin et al., 2018). By modulating lipopolysaccharide (LPS) responses, *L. plantarum* derived MIMP was shown to significantly reduce the production of inflammatory cytokines and in turn significantly reduce gut permeability and the associated IBD pathology (Chelakkot et al., 2018). While more evidence is needed, particularly in *in vivo* models, this evidence suggests that *L. plantarum* is capable of impacting intestinal barrier integrity, particularly when underlying pathologies are present.

Promoting intestinal motility is another possible mechanism through which probiotics can positively influence host health. While specific probiotic strains such as *Bifidobacterium lactis* have been definitively linked to improving intestinal motility, modulating gastrointestinal transit time and alleviating the symptoms associated with constipation, similar studies regarding *L. plantarum* are relatively sparse. Recently however, it has been demonstrated that administration of *L. plantarum* was able to prevent or significantly reduce the symptoms of charcoal induced constipation in mice (Zhao X. et al., 2018). Importantly, a randomized double-blind clinical trial in constipated adults in Malaysia demonstrated that a combination synbiotic preparation of *L. plantarum*, *B. lactis*, and inulin-oligofructose once daily for 12 weeks significantly improved defecation frequency and stool type score (Bristol Stool Form Scale) (Lim et al., 2018). The direct influence of *L. plantarum* in this context is difficult to assess since it was used in combination with *B. lactis* which has previously demonstrated to alleviate symptoms of constipation when administered as a stand-alone probiotic.

ABILITY TO ALTER INTESTINAL FLORA AND INHIBIT THE GROWTH OF POTENTIAL PATHOGENS

The capacity of LAB species to inhibit the growth of pathogenic bacteria has been recognized for centuries, hence the role they have played in preventing food spoilage. The ability to alter the composition of the intestinal flora and inhibit the colonization or growth of pathogenic microbes is a hallmark characteristic of probiotics. There are several mechanisms through which this biological activity can be accomplished, the principal of which include: competition for nutrients and adhesion sites, inducing changes in environmental conditions that are unfavorable to pathogenic bacteria, production of antimicrobial compounds and finally by modulating host immune responses (Corr et al., 2009; Hu et al., 2017).

Unraveling the individual contribution of each of these mechanisms to the overall capacity of specific probiotics to impact the growth of other microbes is remarkably difficult. In reality, these mechanisms likely act concurrently and cooperatively to influence the composition of the host microbiota and prevent the colonization or persistence of pathogenic bacteria. Comparative studies assessing the antimicrobial activity of various probiotic strains have demonstrated that *L. plantarum* frequently exhibits the broadest capacity to inhibit pathogen growth amongst *Lactobacilli* species (Davoodabadi et al., 2015; Ren et al., 2017; Ahn et al., 2018; Arena et al., 2018; Kim A. R. et al., 2019).

Antimicrobial substances produced by probiotics are often naturally occurring bacterial metabolites and can generally be classified into low and high molecular mass compounds (<1,000 and >1,000 Da). The low-molecular mass group, also referred to as the non-bacteriocin group, includes compounds from a wide range of chemical classes such as organic acids, hydrogen peroxide, acetyl-aldehyde, and carbon dioxide. The high-molecular mass group is comprised primarily of proteinaceous compounds referred to as bacteriocins (Arena et al., 2018). Bacteriocins are ribosomally synthesized peptides with antibacterial activity (Cavera et al., 2015; Dicks et al., 2018). Though classification practices are evolving, four classes have been proposed to characterize LAB derived bacteriocins. Class I bacteriocins are referred to as lantibiotics and are characterized primarily based on their post-translational modification. Class II bacteriocins are small, heat-stable non-lanthionine containing bacteriocins that can be sub-divided into 4 distinct subclasses based on their molecular characteristics. Class III bacteriocins

are larger peptides of over 30 kDa that often act in protein-like complexes (Mokoena, 2017). Finally, Class 4 bacteriocins are large complexes that contain lipid or carbohydrate moieties (Wang Y. et al., 2018). The variety of bacteriocins produced by *L. plantarum* generally belong to Class II and are collectively referred to as plantaricins. Plantaricins may be either chromosomally or plasmid encoded and are usually organized within operon clusters that consist of a structural gene(s), an immunity gene, an ABC transporter and an accessory protein that facilitates export (Pal and Srivastava, 2015).

A number of plantaricin compounds have been identified. Broadly, the mechanism of action of these plantaricin compounds is disruption and/or perforation of target cell membranes. In regard to pathogenic bacteria, *L. plantarum* derived plantaricin compounds have shown to be exceptionally effective against gram-positive bacterial pathogens such as *Micrococcus luteum* (Jiang et al., 2018), *Listeria monocytogenes* (Chen et al., 2018), and *Staphylococcus aureus* (Song et al., 2014). Traditionally, plantaricin compounds have been thought to be less effective against gram-negative bacteria, likely due to the outer-membrane of these bacteria providing a protective barrier against plantaricin induced disruption or perforation of the cytoplasmic membrane (Pal and Srivastava, 2014). However, some specific plantaricin compounds such as plantaracin E/F and J/K dipeptides can effectively inhibit gram-negative bacteria like *Escherichia coli* in specific circumstances (Pal and Srivastava, 2014; Song et al., 2014). Interestingly, while also effective on their own, combinations of plantaricin EF and JK potentiated the effect of traditional antibiotics against *Staphylococcus epidermis,* including re-sensitizing the clinically derived antibiotic resistant *S. epidermis 126* strain to gentamicin and tetracycline (Selegard et al., 2019). Select plantaricin species have also shown activity against viruses such as Influenza (Park et al., 2013; Jiang et al., 2017) and fungal species such as *Candida albicans* (Sharma and Srivastava, 2014), *Aspergillus parasiticus* and *Penicillium expansum* (Luz et al., 2018).

In addition to the production and release of antimicrobial compounds, probiotics can inhibit the growth or colonization with potential pathogens by competing for nutrients or adhesion sites. The antagonistic effects of probiotic strains on the adhesion of pathogenic microbes are generally evaluated using human colonic cell lines such as Caco-2 *in vitro* and often also incorporate variables such as low pH and bile-salt exposure in order to better simulate conditions of the human gastrointestinal tract. Lau and Chye demonstrated that *L. plantarum* 0612 was able to competitively inhibit and even displace both *E. coli* and *L. monocytogenes* from Caco-2 monolayers (Chye, 2018). Interestingly, this antagonistic potential was actually increased after *L. plantarum* was exposed to gastrointestinal transit simulation. As the ability to inhibit the adhesion of pathogens is, like many probiotic traits, strain specific, it is also important to note that *L. plantarum* strains derived from humans have been demonstrated to be capable of inhibiting the adhesion of a number of pathogenic microbes to Caco-2 cells by competition and displacement (Jiang et al., 2016).

The ability of *L. plantarum* to inhibit the growth or adhesion of pathogenic microbes has been well-studied *in vitro,* however, because assessing similar characteristics *in vivo* is more complicated, such evidence is substantially more limited. Treatment of C57BL/6J mice with *L. plantarum* has been shown to prevent gastric inflammation and accompanying changes in gastric microbiota composition that are induced by *Helicobacter pylori* infection and DSS treatment (Pan et al., 2016; Zhang et al., 2019). Similarly, mixed *L. plantarum* strains administered to mice prior to or as treatment for *Staphylococcus aureus* infection significantly reduced intestinal inflammation, increased sIgA levels and prevented *S. aureus* induced pathogenic shifts in intestinal microbiota composition (Ren et al., 2017). Finally, in both high-fat diet mouse and rat obesity models, administration of *L. plantarum* alone or in combination with *L. fermentum* not only reduced fat retention but caused a dramatic shift in intestinal microbiota composition via enrichment of *Bifidobacterium* and *Lactobacillus* species relative to controls (Xiuliang Li Xiuyan et al., 2018; Hussain et al., 2020).

In the absence of metabolic disruption or pathogenic challenge, the capacity of *L. plantarum* ZDY2013 to positively influence the composition of the microbiota in healthy mice has been assessed in two independent studies. Using qPCR, Huang and colleagues demonstrated that 2-week administration of *L. plantarum* enhanced the populations of *Bifidobacterium* and *Lactobacillus* species in the colon and cecum and reduced the abundance of potentially enteropathogenic *Enterococcus* and *Clostridium* species (Huang et al., 2015). A separate and more detailed analysis using 16s rDNA sequencing also demonstrated that short and long-term administration of *L. plantarum* significantly altered the microbial composition of the small-intestine of C57BL/6J mice. Although transient, administration of *L. plantarum* led to a significant increase in the richness and diversity of the microbial composition of the small intestine (Xie et al., 2016; Linninge et al., 2019). This change was accompanied by enrichment of numerous *Proteobacteria* species and a corresponding decrease in the abundance of *Bacteriodetes.* While these compositional changes only persisted for the duration of probiotic therapy, they indicate that *L. plantarum* is capable of inducing large scale compositional changes in the intestinal flora.

MODULATE HUMAN IMMUNE FUNCTION

Maintenance of intestinal immune homeostasis is strongly affected by the intestinal microbiota and its interaction with the mucosa. This influence is likely at least partially mediated through the interaction of bacterial cell-wall components or secreted bacterial products with host epithelial or immune effector cells in the intestinal mucosa (de Vos et al., 2017). The nature of these interactions, and their specific immune outcomes are dependent on the species and strain of the participating commensal bacteria, and even though some bacteria have been proven beneficial in certain contexts they may not be beneficial under all clinical circumstances (Gilliland, 1990; Blum and Schiffrin, 2003). Broadly, *L. plantarum* has been demonstrated to have an anti-inflammatory influence on human mucosal immunity. In line with this observation, administration of *L. plantarum* has been shown to reduce immune-mediated

pathology in several experimental models of inflammatory diseases such as atopic dermatitis, colitis, and diabetes (Liu et al., 2011; Han et al., 2012; Jang et al., 2014; Kim I. S. et al., 2019; Toshimitsu et al., 2019).

It is important to note that while the immune-modulatory effect of *L. plantarum* in the context of inflammatory diseases is reasonably well-established, the influence it may have in a sub-clinical inflammatory, or healthy setting may differ significantly. A pair of large-scale *in vitro* screens assessed the capacity of a variety of different *L. plantarum* strains to stimulate cytokine production from either human PBMCs or purified human dendritic cells (Meijerink et al., 2010; van Hemert et al., 2010). Each of these studies assessed the capacity of over 40 different strains of *L. plantarum* to induce IL-12 and IL-10 and compared them to the WCSF-1 reference strain. These studies not only revealed significant inter-strain variability in the capacity to induce either IL-10 or IL-12 but also the ratio at which these cytokines were induced. To identify *L. plantarum* genes with a potential role in modulating human immune responses, inter-strain genetic diversity was correlated with specific capacity to induce cytokines from PBMCs or dendritic cells using comparative genome hybridization. Each of these studies identified a number of candidate genes, however both of them implicated genes involved in the production, transport and regulation of plantaricin compounds as having a significant influence on differential inter-strain cytokine induction capacity. Strains with variations in the plantaricin operon generally induced much higher IL-10/IL-12 ratios and more TNFα than those that did not, potentially making them more desirable probiotics (Meijerink et al., 2010; van Hemert et al., 2010).

On the immune sensory side of the interaction, recognition of *L. plantarum* and other lactic acid probiotics by the mucosal immune system is required for their capacity to confer regulatory benefits to the host. Glycolipids derived from *L. plantarum* have been shown to bind to and signal through the glycolipid pattern recognition receptor Mincle modulating host immune status (Shah et al., 2016). Toll-like receptors (TLRs) have a crucial role in innate defense against invading pathogens and serve as a first-line sensory arm of the immune system. Ren and colleagues demonstrated that TLR engagement and downstream signaling, particularly that of the TLR2/TLR6 heterodimer, is an essential element of the immunomodulatory capacity of *L. plantarum* (Ren et al., 2016) (**Figure 1**). Blocking TLR signaling or inhibiting specific formation of the TLR2/TLR6 heterodimer resulted in significant reduction in *L. plantarum* induced activation of NF-κB/AP-1 signaling, as well as IL-6 and IL-10 production from THP-1 derived macrophages. This is an interesting finding because of the pivotal nature of TLR-2 signaling in maintaining immune homeostasis. This balancing function of TLR-2 is related to its capacity to form heterodimers with both TLR-1 and TLR-6. The TLR1/TLR2 heterodimer has been shown to induce pro-inflammatory cytokines like IL-12 and IL-17, while the TLR2/TLR6 heterodimer has been shown to induce tolerogenic IL-10 based responses (Depaolo et al., 2008; Morita et al., 2017). Fittingly, TLR2/TLR6 signaling agonists have been utilized in the treatment or prevention of many inflammatory diseases such as IBD and mucositis (Depaolo et al., 2008; Sultani et al., 2012). Specifically, TLR2/TLR6 heterodimers promote regulatory T (Treg) cell responses (Ren et al., 2016). Perhaps in further support of the previously described findings, multiple *in vivo* murine studies have demonstrated that administration of *L. plantarum* increased the frequency of both Tregs and regulatory CD103+ dendritic cells. Smelt and colleagues demonstrated administration of *L. plantarum* WCFS1 via intra-gastric gavage every day for 5 days to healthy Balb/c mice induced an increase in the frequency of CD103+ dendritic cells and Tregs in the spleen of treated mice relative to controls (Smelt et al., 2012). In addition, *L. plantarum* administration reduced specific splenic Th2 cell cytokine responses after *ex vivo* re-stimulation.

This result was confirmed and expanded upon in a subsequent study which also observed that administration of *L. plantarum* WCSF1 to healthy mice increased splenic infiltration of regulatory dendritic cells and Tregs and attenuated T helper 2 type responses (Bermudez-Brito et al., 2018). This study expanded upon the previous report by demonstrating that host-microbe interaction at the Peyer's patches was enough to induce

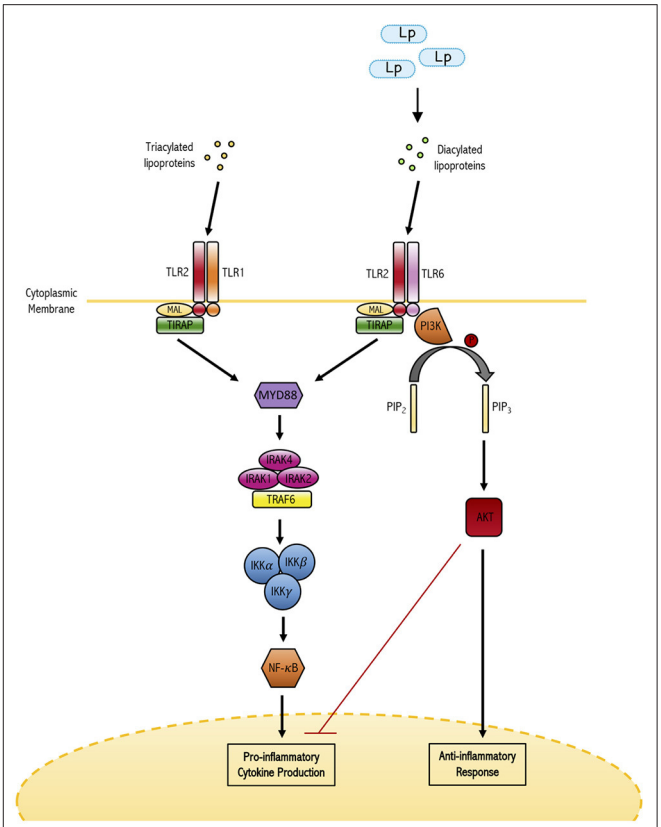

FIGURE 1 | The dual role of TLR-2 in maintaining immune homeostasis. TLR-2 has the capacity to form heterodimers with either TLR-1 or TLR-6. TLRl/2 heterodimers have been shown to bind triacylated lipoproteins frequently derived from gram-negative bacterial species and induce the production of pro-inflammatory cytokines. On the other hand, the TLR2/6 heterodimer binds diacylated lipoproteins derived from gram-positive bacteria (such as *L. plantarum*) and induces anti-inflammatory responses. In this way, TLR-2 signaling plays a major role in differential responses to commensal and potentially pathogenic bacteria.

immunomodulation of host DCs and T cells. This is of interest as probiotics are hypothesized to modulate the immune system through two different pathways: (i) probiotics may be sampled by M cells in the Peyer's patches and passaged to modulate immune effector cells beneath the epithelium or (ii) specific intestinal DCs in the mucosal lamina propria sense probiotics via pattern-recognition receptors. This contact with DCs, via either pathway, influences the maturation of APCs and impacts their interaction with other immune effectors cells, thereby determining the polarization state of the subsequent immune response (Hardy et al., 2013; Bermudez-Brito et al., 2018). Using bioluminescently labeled *L. plantarum,* Bermudez-Brito and colleagues demonstrate that in healthy mice, M-cell sampling of Peyer's patches was a relatively rare occurrence, and that recognition of *L. plantarum* by resident dendritic cells in the Peyer's patches or isolated lymphoid follicles was sufficient to modulate systemic immune responsiveness.

Evidence of *L. plantarum* induced immune modulation in healthy humans remains limited but the existing studies lend further support to *in vitro* and murine model studies that suggest *L. plantarum* can skew toward a regulatory immune phenotype. In a recent study, administration of *L. plantarum* strains was found to prevent non-steroidal anti-inflammatory drug induced reductions in circulating Treg populations (de Vos et al., 2017). This study also assessed the impact of *L. plantarum* on memory responses against tetanus toxoid (TT) antigen and found that by inducing the expression of genes associated with the maintenance of T and B cell function and antigen presentation, *L. plantarum* enhanced responses against TT-antigen in T cell polarization studies. Finally, in the complete absence of any disease or inflammatory stress, a double-blind placebo controlled randomized clinical trial demonstrated that administration of *L. plantarum* significantly altered gene expression profiles in the intestinal mucosa of healthy adults. As determined by biopsies taken from the intestinal duodenal mucosa, living but not heat-killed *L. plantarum* significantly modulated NF-κB dependent pathways (van Baarlen et al., 2009). Strikingly, after consumption of *L. plantarum,* significant induction of genes associated with anti-inflammatory activities such as BCL3, ADM, and IκB was observed, potentially correlating with the establishment of a regulatory or tolerance skewed immune environment (van Baarlen et al., 2009). While administration of *L. plantarum* in different growth phases may have differential effects on the host, collectively, these studies demonstrate the profound capacity of *L. plantarum to* modulate the host immune activity, presumably by skewing toward an anti-inflammatory or regulatory state.

EVIDENCE OF CAPACITY TO TREAT OR IMPROVE HUMAN DISEASE

There is mounting evidence demonstrating that administration of *L. plantarum* can have a beneficial impact on human health, particularly in the context of managing or preventing inflammatory diseases. In a prospective single-arm open trial, Toshimitsu and colleagues assessed the impact of a 12-week treatment with heat-killed *L. plantarum* OLL2712 on glucose metabolism and chronic inflammation in pre-diabetic individuals (Toshimitsu et al., 2019). This study demonstrated that, compared to baseline values, treatment with *L. plantarum* significantly reduced fasting plasma glucose and serum glycoalbumin and resulted in a significant improvement in insulin resistance (HOMA-IR) and insulin sensitivity (QUICKI) indexes. Chronic inflammation is considered to be a primary cause of metabolic disorders and has previously been shown to cause insulin resistance and impair glucose and lipid metabolism (Fantuzzi et al., 2005). In addition to markers of glucose metabolism the above mentioned study also assessed how *L. plantarum* treatment affected the pro-inflammatory cytokine levels in patient serum. Relative to baseline measurement administration of *L. plantarum* significantly reduced serum MCP-1 and IL-6 levels (Toshimitsu et al., 2019). Stratification revealed that the observed reduction in fasting plasma glucose levels was most prominent in the participants that exhibited high baseline pro-inflammatory cytokine expression. In these participants, *L. plantarum* induced a significant reduction in fasting plasma glucose and improvement in insulin resistance indexes that was not observed in individuals with lower baseline pro-inflammatory cytokine expression.

There is also evidence that *L. plantarum* may have cholesterol lowering effects in hypercholesterolaemic adults, potentially lowering the incidence of coronary heart disease (CHD). In a double-blind randomized trial, Costabile and colleagues assessed the impact of twice-daily administered *L. plantarum* ECGC 13110402 for 12 weeks on several measures of blood lipid content (Costabile et al., 2017). This study demonstrated that administration of *L. plantarum* ECGC 13110402, selected primarily for its particularly high bile-salt hydrolase activity, resulted in statistically significant reductions in low density lipoproteins, total cholesterol, and triacylglycerides, while increasing high density lipoprotein levels. Interestingly, in the over 60-year-old population, *L. plantarum* also induced a significant reduction in systolic blood pressure (Costabile et al., 2017). As no significant side-effects or changes to gastrointestinal function were observed, this study suggests that supplementation of existing treatment strategies with administration of *L. plantarum* ECGC 13110402 may be used to reduce the risk of cardiovascular disease, particularly in high-risk subjects with hypercholesterolaemia.

The beneficial effect of *L. plantarum* in animal models of IBS and IBD is well-established (Liu et al., 2011; Jang et al., 2014; Chen et al., 2017). However, evidence of a similar benefit in humans remains relatively limited. In a randomized double-blind placebo-controlled study, the effect of 4-week treatment with *L. plantarum* 299v was assessed in irritable bowel syndrome patients fulfilling the Rome III diagnostic criteria. Ducrotté and his team observed that treatment with *L. plantarum* 299v was associated with significant reduction in patient pain severity and bloating (Ducrotte et al., 2012). In line with many previous IBS trials, a modest placebo response was observed. Despite this however, 78% of the patients on the *L. plantarum* arm scored the treatment efficacy as excellent or good vs. only 8% of patients on the placebo arm. This study supports the findings of a previous randomized double-blind study that also showed significant

pain relief and amelioration of accompanying IBS symptoms in patients receiving 4-week *L. plantarum* 299v treatment in a 20-patient cohort (Niedzielin et al., 2001).

In a landmark study involving more than 4,500 full-term newborns in rural India, Panigrahi and colleagues assessed the efficacy of an orally administered synbiotic containing *L. plantarum* (ATCC-202195) and fructooligosaccharide in preventing infant sepsis. Strain selection and administration protocols for this trial were informed by two pilot studies previously conducted by the same group. The first of these pilot studies demonstrated that *Lactobacillus GG* was a poor colonizer in infants, especially those weighing <1,500 grams (Agarwal et al., 2003). Conversely, the authors subsequently demonstrated that a synbiotic preparation of *L. plantarum* and fructooligosaccharide persisted in infants for months after therapy ended (Panigrahi et al., 2008). In this pilot study, after 7 days of synbiotic treatment, initiated between 1 and 3 days after birth, *L. plantarum* was cultured from 84% of the treated infants after 3 days of treatment and from 95% of the infants on day 28 after birth (Panigrahi et al., 2008). Of the infants colonized at day 28, 100, 94, 88, 56, and 32% remained colonized at months 2, 3, 4, 5, and 6 suggesting that, unlike *Lactobacillus GG, L. plantarum* is capable of efficiently and durably colonizing the newborn gut.

Consequently, Panigrahi and colleagues designed their trial to assess the efficacy of *L. plantarum* and fructooligosaccharide administered to newborns for 7 days beginning on day 2–4 of life in preventing the primary outcome of neonatal sepsis and death (Panigrahi et al., 2017). Community volunteers identified 7,089 cases of suspect sepsis during a population-based screening of women delivering in the study area, of which 4,556 newborns were identified to have sign/symptoms of sepsis by trained pediatricians. They were randomized to receive either the synbiotic preparation ($n = 2,278$) or the placebo ($n = 2,278$), and treated after collection of blood for Bactec culture. A significant (42%) reduction in the primary outcome of neonatal sepsis and death was observed, from 9% in the placebo arm to 5.4% in the treatment arm, indicating that only 27 infants would need to be treated to prevent one primary outcome (Panigrahi 2017). Importantly, a significant reduction was observed in culture positive septicaemia with 27 cases in the control group and only 6 in the treatment group (risk ratio (RR) = 0.22). Synbiotic treatment was also associated with a significant reduction in lower respiratory tract infections (34%) potentially suggesting that probiotic administration not only enhanced gastrointestinal mucosa but also systemic immunity (Panigrahi et al., 2017). Of the evaluated secondary outcomes synbiotic treatment was also associated with a significant reduction in local infections and a greater increase in weight gained since birth at day 60 of life. The observed 42% reduction in sepsis was significantly greater than the anticipated reduction and facilitated early termination of the trial. The results of this trial stand in contrast to two other studies that used probiotics to target sepsis in very preterm infants (Jacobs et al., 2013; Costeloe et al., 2016) and a third, smaller trial, conducted in low birth weight infants in India (Sinha et al., 2015). These differences may be related to probiotic choice, administration schedule or the addition of a prebiotic supplement, but suggest that administration of *L. plantarum* may be capable of reducing the risk of sepsis/pSBI and lower respiratory infections for neonates in developing countries.

FUTURE DIRECTIONS

L. plantarum is capable of inhabiting a wide variety of ecological niches including the human gastrointestinal mucosa. Due to their unique evolutionary history, strains of this species possess a wide range of probiotic characteristics and have shown promise in numerous experimental disease models, as well as human trials. Increasing our understanding of strain specific variation, particularly in relation to probiotic characteristics and imparted health benefits, is now paramount. Characterizing *L. plantarum* strains in such a manner will facilitate standardization of research applications and allow for the more rapid and efficient validation of specific strains for defined health applications. Beyond *L. plantarum*, developing a more comprehensive understanding of the specific genetic and phenotypic characteristics that impart specific probiotic functionalities or health benefits may provide the key for identifying or perhaps engineering more effective probiotic strains. The inherent genetic flexibility that facilitates the nomadic lifestyle of *L. planatrum* may render it particularly amenable to such engineering and may facilitate the production of highly effective probiotic strains.

AUTHOR CONTRIBUTIONS

MF wrote the review with TK. PP provided significant revisions. All authors contributed to the article and approved the submitted version.

REFERENCES

Agarwal, R., Sharma, N., Chaudhry, R., Deorari, A., Paul, V. K., Gewolb, I. H., et al. (2003). Effects of oral *Lactobacillus GG* on enteric microflora in low-birth-weight neonates. *J. Pediatr. Gastroenterol. Nutr.* 36, 397–402. doi: 10.1097/00005176-200303000-00019

Ahn, K. B., Baik, J. E., Park, O. J., Yun, C. H., and Han, S. H. (2018). *Lactobacillus plantarum* lipoteichoic acid inhibits biofilm formation of Streptococcus mutans. *PLoS ONE* 13:e0192694. doi: 10.1371/journal.pone.0192694

Arena, M. P., Capozzi, V., Russo, P., Drider, D., Spano, G., and Fiocco, D. (2018). Immunobiosis and probiosis: antimicrobial activity of lactic acid bacteria with a focus on their antiviral and antifungal properties. *Appl. Microbiol. Biotechnol.* 102, 9949–9958. doi: 10.1007/s00253-018-9403-9

Asnicar, F., Manara, S., Zolfo, M., Truong, D. T., Scholz, M., Armanini, F., et al. (2017). Studying vertical microbiome transmission from mothers to infants by strain-level metagenomic profiling. *mSystems* 2:e00164-16. doi: 10.1128/mSystems.00164-16

Azad, M. B., Konya, T., Guttman, D. S., Field, C. J., Sears, M. R., HayGlass, K. T., et al. (2015). Infant gut microbiota and food sensitization: associations in the first year of life. *Clin. Exp. Allergy* 45, 632–643. doi: 10.1111/cea.12487

Baldassarre, M. E., Palladino, V., Amoruso, A., Pindinelli, S., Mastromarino, P., Fanelli, M., et al. (2018). Rationale of probiotic supplementation during pregnancy and neonatal period. *Nutrients* 10:1693. doi: 10.3390/nu10111693

Begley, M., Hill, C., and Gahan, C. G. (2006). Bile salt hydrolase activity in probiotics. *Appl. Env. Microbiol.* 72, 1729–1738. doi: 10.1128/AEM.72.3.1729-1738.2006

Bermudez-Brito, M., Borghuis, T., Daniel, C., Pot, B., de Haan, B. J., Faas, M. M., et al. (2018). L. plantarum WCFS1 enhances Treg frequencies by activating DCs even in absence of sampling of bacteria in the Peyer Patches. *Sci. Rep*. 8:1785. doi: 10.1038/s41598-018-20243-1

Blackwood, B. P., Yuan, C. Y., Wood, D. R., Nicolas, J. D., Grothaus, J. S., and Hunter, C. J. (2017). Probiotic *Lactobacillus* species strengthen intestinal barrier function and tight junction integrity in experimental necrotizing enterocolitis. *J. Probiotics Heal*. 5:159. doi: 10.4172/2329-8901.1000159

Blum, S., and Schiffrin, E. J. (2003). Intestinal microflora and homeostasis of the mucosal immune response: implications for probiotic bacteria? *Curr. Issues Intest. Microbiol.* 4, 53–60.

Bron, P. A., Marco, M., Hoffer, S. M., Van Mullekom, E., de Vos, W. M., and Kleerebezem, M. (2004). Genetic characterization of the bile salt response in *Lactobacillus plantarum* and analysis of responsive promoters *in vitro* and *in situ* in the gastrointestinal tract. *J. Bacteriol.* 186, 7829–7835. doi: 10.1128/JB.186.23.7829-7835.2004

Bron, P. A., Molenaar, D., de Vos, W. M., and Kleerebezem, M. (2006). DNA micro-array-based identification of bile-responsive genes in *Lactobacillus plantarum*. *J. Appl. Microbiol.* 100, 728–738. doi: 10.1111/j.1365-2672.2006.02891.x

Brook, B., Harbeson, D., Ben-Othman, R., Viemann, D., and Kollmann, T. R. (2017). Newborn susceptibility to infection vs. disease depends on complex *in vivo* interactions of host and pathogen. *Semin. Immunopathol.* 39, 615–625. doi: 10.1007/s00281-017-0651-z

Buntin, N., de Vos, W. M., and Hongpattarakere, T. (2017). Variation of mucin adhesion, cell surface characteristics, and molecular mechanisms among *Lactobacillus plantarum* isolated from different habitats. *Appl. Microbiol. Biotechnol.* 101, 7663–7674. doi: 10.1007/s00253-017-8482-3

Castaldo, C., Vastano, V., Siciliano, R. A., Candela, M., Vici, M., Muscariello, L., et al. (2009). Surface displaced alfa-enolase of *Lactobacillus plantarum* is a fibronectin binding protein. *Microb. Cell Fact*. 8:14. doi: 10.1186/1475-2859-8-14

Cavera, V. L., Arthur, T. D., Kashtanov, D., and Chikindas, M. L. (2015). Bacteriocins and their position in the next wave of conventional antibiotics. *Int. J. Antimicrob. Agents* 46, 494–501. doi: 10.1016/j.ijantimicag.2015.07.011

Chelakkot, C., Ghim, J., and Ryu, S. H. (2018). Mechanisms regulating intestinal barrier integrity and its pathological implications. *Exp. Mol. Med.* 50:103. doi: 10.1038/s12276-018-0126-x

Chen, H., Xia, Y., Zhu, S., Yang, J., Yao, J., Di, J., et al. (2017). *Lactobacillus plantarum* LPOnlly alters the gut flora and attenuates colitis by inducing microbiome alteration in interleukin10 knockout mice. *Mol. Med. Rep.* 16, 5979–5985. doi: 10.3892/mmr.2017.7351

Chen, L., Gu, Q., Li, P., Li, Y., Song, D., and Yang, J. (2018). Purification and characterization of Plantaricin ZJ316, a novel bacteriocin against *Listeria monocytogene*s from *Lactobacillus plantarum* ZJ316. *J. Food Prot.* 81, 1929–1935. doi: 10.4315/0362-028X.JFP-18-306

Chiang, M. L., Chen, H. C., Wu, C., and Chen, M. J. (2014). Effect of acid adaptation on the environmental stress tolerance of three strains of *Vibrio parahaemolyticus*. *Foodborne Pathog. Dis.* 11, 287–294. doi: 10.1089/fpd.2013.1641

Cho, I., and Blaser, M. J. (2012). The human microbiome: at the interface of health and disease. *Nat. Rev. Genet*. 13, 260–270. doi: 10.1038/nrg3182

Chye, L. Y. J. L. F. Y. (2018). Antagonistic effects of *Lactobacillus plantarum* 0612 on the adhesion of selected foodborne enteropathogens in various colonic environments. *Food Control* 91, 237–247. doi: 10.1016/j.foodcont.2018.04.001

Corr, S. C., Hill, C., and Gahan, C. G. (2009). Understanding the mechanisms by which probiotics inhibit gastrointestinal pathogens. *Adv. Food Nutr. Res.* 56, 1–15. doi: 10.1016/S1043-4526(08)00601-3

Costabile, A., Buttarazzi, I., Kolida, S., Quercia, S., Baldini, J., Swann, J. R., et al. (2017). An *in vivo* assessment of the cholesterol-lowering efficacy of *Lactobacillus plantarum* ECGC 13110402 in normal to mildly hypercholesterolaemic adults. *PLoS ONE* 12:e0187964. doi: 10.1371/journal.pone.0187964

Costeloe, K., Bowler, U., Brocklehurst, P., Hardy, P., Heal, P., Juszczak, E., et al. (2016). A randomised controlled trial of the probiotic *Bifidobacterium breve* BBG-001 in preterm babies to prevent sepsis, necrotising enterocolitis and death: the Probiotics in Preterm infantS (PiPS) trial. *Heal Technol Assess* 20, 1–194. doi: 10.3310/hta20660

Daniel, C., Poiret, S., Dennin, V., Boutillier, D., and Pot, B. (2013). Bioluminescence imaging study of spatial and temporal persistence of *Lactobacillus plantarum* and *Lactococcus lactis* in living mice. *Appl. Env. Microbiol*. 79, 1086–1094. doi: 10.1128/AEM.03221-12

Davoodabadi, A., Soltan Dallal, M. M., Rahimi Foroushani, A., Douraghi, M., Sharifi Yazdi, M. K., and Amin Harati, F. (2015). Antibacterial activity of *Lactobacillus* spp. isolated from the feces of healthy infants against enteropathogenic bacteria. *Anaerobe* 34, 53–58. doi: 10.1016/j.anaerobe.2015.04.014

de Vos, P., Mujagic, Z., de Haan, B. J., Siezen, R. J., Bron, P. A., Meijerink, M., et al. (2017). *Lactobacillus plantarum* strains can enhance human mucosal and systemic immunity and prevent non-steroidal anti-inflammatory drug induced reduction in T regulatory cells. *Front. Immunol.* 8:1000. doi: 10.3389/fimmu.2017.01000

Deepika, G., and Charalampopoulos, D. (2010). Surface and adhesion properties of lactobacilli. *Adv. Appl. Microbiol.* 70, 127–152. doi: 10.1016/S0065-2164(10)70004-6

Depaolo, R. W., Tang, F., Kim, I., Han, M., Levin, N., Ciletti, N., et al. (2008). Toll-like receptor 6 drives differentiation of tolerogenic dendritic cells and contributes to LcrV-mediated plague pathogenesis. *Cell Host Microbe* 4, 350–361. doi: 10.1016/j.chom.2008.09.004

Dhanani, A. S., and Bagchi, T. (2013). The expression of adhesin EF-Tu in response to mucin and its role in *Lactobacillus* adhesion and competitive inhibition of enteropathogens to mucin. *J. Appl. Microbiol.* 115, 546–554. doi: 10.1111/jam.12249

Dicks, L. M. T., Dreyer, L., Smith, C., and van Staden, A. D. (2018). A review: the fate of bacteriocins in the human gastro-intestinal tract: do they cross the gut-blood barrier? *Front. Microbiol.* 9:2297. doi: 10.3389/fmicb.2018.02297

Du Toit, A. (2017). Microbiome: getting organized early in life. *Nat. Rev. Microbiol.* 15:135. doi: 10.1038/nrmicro.2017.10

Duary, R. K., Batish, V. K., and Grover, S. (2012). Relative gene expression of bile salt hydrolase and surface proteins in two putative indigenous *Lactobacillus plantarum* strains under *in vitro* gut conditions. *Mol. Biol. Rep.* 39, 2541–2552. doi: 10.1007/s11033-011-1006-9

Ducrotte, P., Sawant, P., and Jayanthi, V. (2012). Clinical trial: *Lactobacillus plantarum* 299v (DSM 9843) improves symptoms of irritable bowel syndrome. *World J. Gastroenterol.* 18, 4012–4018. doi: 10.3748/wjg.v18.i30.4012

Fantuzzi, G., Sennello, J. A., Batra, A., Fedke, I., Lehr, H. A., Zeitz, M., et al. (2005). Defining the role of T cell-derived leptin in the modulation of hepatic or intestinal inflammation in mice. *Clin. Exp. Immunol.* 142, 31–38. doi: 10.1111/j.1365-2249.2005.02898.x

Filannino, P., De Angelis, M., Di Cagno, R., Gozzi, G., Riciputi, Y., and Gobbetti, M. (2018). How *Lactobacillus plantarum* shapes its transcriptome in response to contrasting habitats. *Env. Microbiol.* 20, 3700–3716. doi: 10.1111/1462-2920.14372

Foster, J. W., and Hall, H. K. (1991). Inducible pH homeostasis and the acid tolerance response of *Salmonella typhimurium*. *J. Bacteriol.* 173, 5129–5135. doi: 10.1128/jb.173.16.5129-5135.1991

Gagliardi, A., Totino, V., Cacciotti, F., Iebba, V., Neroni, B., Bonfiglio, G., et al. (2018). Rebuilding the gut microbiota ecosystem. *Int. J. Environ. Res. Public Health* 15:1679. doi: 10.3390/ijerph15081679

Gilliland, S. E. (1990). Health and nutritional benefits from lactic acid bacteria. *FEMS Microbiol. Rev.* 7, 175–188. doi: 10.1111/j.1574-6968.1990.tb04887.x

Greenhalgh, K., Meyer, K. M., Aagaard, K. M., and Wilmes, P. (2016). The human gut microbiome in health: establishment and resilience of microbiota over a lifetime. *Env. Microbiol.* 18, 2103–2116. doi: 10.1111/1462-2920.13318

Gritz, E. C., and Bhandari, V. (2015). The human neonatal gut microbiome: a brief review. *Front. Pediatr*. 3:17. doi: 10.3389/fped.2015.00060

Gross, G., Snel, J., Boekhorst, J., Smits, M. A., and Kleerebezem, M. (2010). Biodiversity of mannose-specific adhesion in *Lactobacillus plantarum* revisited: strain-specific domain composition of the mannose-adhesin. *Benef. Microbes* 1, 61–66. doi: 10.3920/BM2008.1006

Gu, X. C., Luo, X. G., Wang, C. X., Ma, D. Y., Wang, Y., He, Y. Y., et al. (2014). Cloning and analysis of bile salt hydrolase genes from

Lactobacillus plantarum CGMCC No. 8198. *Biotechnol. Lett.* 36, 975–983. doi: 10.1007/s10529-013-1434-9

Guidone, A., Ianniello, R. G., Ricciardi, A., Zotta, T., and Parente, E. (2013). Aerobic metabolism and oxidative stress tolerance in the *Lactobacillus plantarum* group. *World J. Microbiol. Biotechnol.* 29, 1713–1722. doi: 10.1007/s11274-013-1334-0

Guo, J., Han, X., Huang, W., You, Y., and Zhan, J. (2021). Gut dysbiosis during early life: causes, health outcomes, and amelioration via dietary intervention. *Crit. Rev. Food Sci. Nutr.* doi: 10.1080/10408398.2021.1912706. [Epub ahead of print].

Hamon, E., Horvatovich, P., Izquierdo, E., Bringel, F., Marchioni, E., Aoude-Werner, D., et al. (2011). Comparative proteomic analysis of *Lactobacillus plantarum* for the identification of key proteins in bile tolerance. *BMC Microbiol.* 11:63. doi: 10.1186/1471-2180-11-63

Hamon, E., Horvatovich, P., Marchioni, E., Aoude-Werner, D., and Ennahar, S. (2014). Investigation of potential markers of acid resistance in *Lactobacillus plantarum* by comparative proteomics. *J. Appl. Microbiol.* 116, 134–144. doi: 10.1111/jam.12339

Han, Y., Kim, B., Ban, J., Lee, J., Kim, B. J., Choi, B. S., et al. (2012). A randomized trial of *Lactobacillus plantarum* CJLP133 for the treatment of atopic dermatitis. *Pediatr. Allergy Immunol.* 23, 667–673. doi: 10.1111/pai.12010

Harbeson, D., Francis, F., Bao, W., Amenyogbe, N. A., and Kollmann, T. R. (2018). Energy demands of early life drive a disease tolerant phenotype and dictate outcome in neonatal bacterial sepsis. *Front. Immunol.* 9:1918. doi: 10.3389/fimmu.2018.01918

Hardy, H., Harris, J., Lyon, E., Beal, J., and Foey, A. D. (2013). Probiotics, prebiotics and immunomodulation of gut mucosal defences: homeostasis and immunopathology. *Nutrients* 5, 1869–1912. doi: 10.3390/nu5061869

Heunis, T., Deane, S., Smit, S., and Dicks, L. M. (2014). Proteomic profiling of the acid stress response in *Lactobacillus plantarum* 423. *J. Proteome Res.* 13, 4028–4039. doi: 10.1021/pr500353x

Hogberg, N., Stenback, A., Carlsson, P. O., Wanders, A., and Lilja, H. E. (2013). Genes regulating tight junctions and cell adhesion are altered in early experimental necrotizing enterocolitis. *J. Pediatr. Surg.* 48, 2308–2312. doi: 10.1016/j.jpedsurg.2013.06.027

Hu, S., Wang, L., and Jiang, Z. (2017). Dietary additive probiotics modulation of the intestinal microbiota. *Protein Pept. Lett.* 24, 382–387. doi: 10.2174/0929866524666170223143615

Huang, H., Song, L., and Zhao, W. (2014). Effects of probiotics for the treatment of bacterial vaginosis in adult women: a meta-analysis of randomized clinical trials. *Arch. Gynecol. Obs.* 289, 1225–1234. doi: 10.1007/s00404-013-3117-0

Huang, R., Pan, M., Wan, C., Shah, N. P., Tao, X., and Wei, H. (2016). Physiological and transcriptional responses and cross protection of *Lactobacillus plantarum* ZDY2013 under acid stress. *J. Dairy Sci.* 99, 1002–1010. doi: 10.3168/jds.2015-9993

Huang, R., Tao, X., Wan, C., Li, S., Xu, H., Xu, F., et al. (2015). *In vitro* probiotic characteristics of *Lactobacillus plantarum* ZDY 2013 and its modulatory effect on gut microbiota of mice. *J. Dairy Sci.* 98, 5850–5861. doi: 10.3168/jds.2014-9153

Hussain, A., Kwon, M. H., Kim, H. K., Lee, H. S., Cho, J. S., and Lee, Y. I. (2020). Anti-obesity effect of *Lactobacillus plantarum* LB818 is associated with regulation of gut microbiota in high-fat diet-fed obese mice. *J. Med. Food* 23, 750–759. doi: 10.1089/jmf.2019.4627

Inglin, R. C., Meile, L., and Stevens, M. J. A. (2018). Clustering of pan- and core-genome of *Lactobacillus* provides novel evolutionary insights for differentiation. *BMC Genomics* 19:284. doi: 10.1186/s12864-018-4601-5

Jacobs, S. E., Tobin, J. M., Opie, G. F., Donath, S., Tabrizi, S. N., Pirotta, M., et al. (2013). Probiotic effects on late-onset sepsis in very preterm infants: a randomized controlled trial. *Pediatrics* 132, 1055–1062. doi: 10.1542/peds.2013-1339

Jang, S. E., Han, M. J., Kim, S. Y., and Kim, D. H. (2014). *Lactobacillus plantarum* CLP-0611 ameliorates colitis in mice by polarizing M1 to M2-like macrophages. *Int. Immunopharmacol.* 21, 186–192. doi: 10.1016/j.intimp.2014.04.021

Jarde, A., Lewis-Mikhael, A. M., Moayyedi, P., Stearns, J. C., Collins, S. M., Beyene, J., et al. (2018). Pregnancy outcomes in women taking probiotics or prebiotics: a systematic review and meta-analysis. *BMC Pregnancy Childbirth* 18:14. doi: 10.1186/s12884-017-1629-5

Jensen, H., Roos, S., Jonsson, H., Rud, I., Grimmer, S., van Pijkeren, J. P., et al. (2014). Role of *Lactobacillus reuteri* cell and mucus-binding protein A (CmbA) in adhesion to intestinal epithelial cells and mucus *in vitro*. *Microbiology* 160, 671–681. doi: 10.1099/mic.0.073551-0

Jiang, H., Tang, X., Zhou, Q., Zou, J., Li, P., Breukink, E., et al. (2018). Plantaricin NC8 from *Lactobacillus plantarum* causes cell membrane disruption to Micrococcus luteus without targeting lipid II. *Appl. Microbiol. Biotechnol.* 102, 7465–7473. doi: 10.1007/s00253-018-9182-3

Jiang, M., Zhang, F., Wan, C., Xiong, Y., Shah, N. P., Wei, H., et al. (2016). Evaluation of probiotic properties of *Lactobacillus plantarum* WLPL04 isolated from human breast milk. *J. Dairy Sci.* 99, 1736–1746. doi: 10.3168/jds.2015-10434

Jiang, Y., Yang, G., Wang, Q., Wang, Z., Yang, W., Gu, W., et al. (2017). Molecular mechanisms underlying protection against H9N2 influenza virus challenge in mice by recombinant *Lactobacillus plantarum* with surface displayed HA2-LTB. *J. Biotechnol.* 259, 6–14. doi: 10.1016/j.jbiotec.2017.08.011

Kapourchali, F. R., and Cresci, G. A. M. (2020). Early-life gut microbiome-the importance of maternal and infant factors in its establishment. *Nutr. Clin. Pr.* 35, 386–405. doi: 10.1002/ncp.10490

Karczewski, J., Troost, F. J., Konings, I., Dekker, J., Kleerebezem, M., Brummer, R. J., et al. (2010). Regulation of human epithelial tight junction proteins by *Lactobacillus plantarum in vivo* and protective effects on the epithelial barrier. *Am. J. Physiol. Gastrointest. Liver Physiol.* 298, G851–G859. doi: 10.1152/ajpgi.00327.2009

Kaushik, J. K., Kumar, A., Duary, R. K., Mohanty, A. K., Grover, S., and Batish, V. K. (2009). Functional and probiotic attributes of an indigenous isolate of *Lactobacillus plantarum*. *PLoS ONE* 4:e8099. doi: 10.1371/journal.pone.0008099

Kim, A. R., Ahn, K. B., Yun, C. H., Park, O. J., Perinpanayagam, H., Yoo, Y. J., et al. (2019). *Lactobacillus plantarum* lipoteichoic acid inhibits oral multispecies biofilm. *J. Endod.* 45, 310–315. doi: 10.1016/j.joen.2018.12.007

Kim, I. S., Lee, S. H., Kwon, Y. M., Adhikari, B., Kim, J. A., Yu, D. Y., et al. (2019). Oral Administration of beta-Glucan and *Lactobacillus plantarum* alleviates atopic dermatitis-like symptoms. *J. Microbiol. Biotechnol.* 29, 1693–1706. doi: 10.4014/jmb.1907.07011

Kirihara, N., Kamitomo, M., Tabira, T., Hashimoto, T., Taniguchi, H., and Maeda, T. (2018). Effect of probiotics on perinatal outcome in patients at high risk of preterm birth. *J. Obs. Gynaecol. Res.* 44, 241–247. doi: 10.1111/jog.13497

Kleerebezem, M., Boekhorst, J., van Kranenburg, R., Molenaar, D., Kuipers, O. P., Leer, R., et al. (2003). Complete genome sequence of *Lactobacillus plantarum* WCFS1. *Proc. Natl. Acad. Sci. U. S. A.* 100, 1990–1995. doi: 10.1073/pnas.0337704100

Kostic, A. D., Gevers, D., Siljander, H., Vatanen, T., Hyotylainen, T., Hamalainen, A. M., et al. (2015). The dynamics of the human infant gut microbiome in development and in progression toward type 1 diabetes. *Cell Host Microbe* 17, 260–273. doi: 10.1016/j.chom.2015.01.001

Lim, Y. J., Jamaluddin, R., Hazizi, A. S., and Chieng, J. Y. (2018). Effects of synbiotics among constipated adults in serdang, selangor, malaysia-a randomised, double-blind, placebo-controlled trial. *Nutrients* 10:824. doi: 10.3390/nu10070824

Lindsay, K. L., Walsh, C. A., Brennan, L., and McAuliffe, F. M. (2013). Probiotics in pregnancy and maternal outcomes: a systematic review. *J. Matern. Fetal Neonatal Med.* 26, 772–778. doi: 10.3109/14767058.2012.755166

Linninge, C., Xu, J., Bahl, M. I., Ahrne, S., and Molin, G. (2019). *Lactobacillus fermentum* and *Lactobacillus plantarum* increased gut microbiota diversity and functionality, and mitigated Enterobacteriaceae, in a mouse model. *Benef. Microbes* 10, 413–424. doi: 10.3920/BM2018.0074

Liu, Y., Tran, D. Q., and Rhoads, J. M. (2018). Probiotics in disease prevention and treatment. *J. Clin. Pharmacol.* 58, S164–S179. doi: 10.1002/jcph.1121

Liu, Y. W., Su, Y. W., Ong, W. K., Cheng, T. H., and Tsai, Y. C. (2011). Oral administration of *Lactobacillus plantarum* K68 ameliorates DSS-induced ulcerative colitis in BALB/c mice via the anti-inflammatory and immunomodulatory activities. *Int. Immunopharmacol.* 11, 2159–2166. doi: 10.1016/j.intimp.2011.09.013

Luz, C., Izzo, L., Graziani, G., Gaspari, A., Ritieni, A., Manes, J., et al. (2018). Evaluation of biological and antimicrobial properties of freeze-dried whey fermented by different strains of Lactobacillus plantarum. *Food Funct.* 9, 3688–3697. doi: 10.1039/C8FO00535D

Martino, M. E., Bayjanov, J. R., Caffrey, B. E., Wels, M., Joncour, P., Hughes, S., et al. (2016). Nomadic lifestyle of *Lactobacillus plantarum* revealed by comparative genomics of 54 strains isolated from different habitats. *Env. Microbiol.* 18, 4974–4989. doi: 10.1111/1462-2920.13455

McFarland, L. V. (2014). Use of probiotics to correct dysbiosis of normal microbiota following disease or disruptive events: a systematic review. *BMJ Open* 4:5047. doi: 10.1136/bmjopen-2014-005047

Meijerink, M., van Hemert, S., Taverne, N., Wels, M., de Vos, P., Bron, P. A., et al. (2010). Identification of genetic loci in *Lactobacillus plantarum* that modulate the immune response of dendritic cells using comparative genome hybridization. *PLoS ONE* 5:e10632. doi: 10.1371/journal.pone.0010632

Mendes-Soares, H., Suzuki, H., Hickey, R. J., and Forney, L. J. (2014). Comparative functional genomics of *Lactobacillus* spp. reveals possible mechanisms for specialization of vaginal lactobacilli to their environment. *J. Bacteriol.* 196, 1458–1470. doi: 10.1128/JB.01439-13

Metchnikoff, E. (1907). *Immunity in Infective Diseases.* Miami, FL: Univ Press. doi: 10.5962/bhl.title.31465

Mokoena, M. P. (2017). Lactic acid bacteria and their bacteriocins: classification, biosynthesis and applications against uropathogens: a mini-review. *Molecules* 22:1255. doi: 10.3390/molecules22081255

Morita, N., Yamai, I., Takahashi, K., Kusumoto, Y., Shibata, T., Kobayashi, T., et al. (2017). C4b binding protein negatively regulates TLR1/2 response. *Innate Immun.* 23, 11–19. doi: 10.1177/1753425916672312

Niedzielin, K., Kordecki, H., and Birkenfeld, B. (2001). A controlled, double-blind, randomized study on the efficacy of *Lactobacillus plantarum* 299V in patients with irritable bowel syndrome. *Eur. J. Gastroenterol. Hepatol.* 13, 1143–1147. doi: 10.1097/00042737-200110000-00004

Ogunrinola, G. A., Oyewale, J. O., Oshamika, O. O., and Olasehinde, G. I. (2020). The human microbiome and its impacts on health. *Int. J. Microbiol.* 2020:8045646. doi: 10.1155/2020/8045646

Othman, M., Neilson, J. P., and Alfirevic, Z. (2007). Probiotics for preventing preterm labour. *Cochr. Datab. Syst. Rev.* 1:CD005941. doi: 10.1002/14651858.CD005941.pub2

Pal, G., and Srivastava, S. (2014). Inhibitory effect of plantaricin peptides (Pln E/F and J/K) against *Escherichia coli*. *World J. Microbiol. Biotechnol.* 30, 2829–2837. doi: 10.1007/s11274-014-1708-y

Pal, G., and Srivastava, S. (2015). *In vitro* activity of a recombinant ABC transporter protein in the processing of plantaricin E pre-peptide. *Arch. Microbiol.* 197, 843–849. doi: 10.1007/s00203-015-1120-5

Pan, M., Wan, C., Xie, Q., Huang, R., Tao, X., Shah, N. P., et al. (2016). Changes in gastric microbiota induced by *Helicobacter pylori* infection and preventive effects of *Lactobacillus plantarum* ZDY 2013 against such infection. *J. Dairy Sci.* 99, 970–981. doi: 10.3168/jds.2015-10510

Panigrahi, P., Parida, S., Nanda, N. C., Satpathy, R., Pradhan, L., Chandel, D. S., et al. (2017). A randomized synbiotic trial to prevent sepsis among infants in rural India. *Nature* 548, 407–412. doi: 10.1038/nature23480

Panigrahi, P., Parida, S., Pradhan, L., Mohapatra, S. S., Misra, P. R., Johnson, J. A., et al. (2008). Long-term colonization of a *Lactobacillus plantarum* synbiotic preparation in the neonatal gut. *J. Pediatr. Gastroenterol. Nutr.* 47, 45–53. doi: 10.1097/MPG.0b013e31815a5f2c

Park, M. K., Ngo, V., Kwon, Y. M., Lee, Y. T., Yoo, S., Cho, Y. H., et al. (2013). *Lactobacillus plantarum* DK119 as a probiotic confers protection against influenza virus by modulating innate immunity. *PLoS ONE* 8:e75368. doi: 10.1371/journal.pone.0075368

Pfeiler, E. A., Azcarate-Peril, M. A., and Klaenhammer, T. R. (2007). Characterization of a novel bile-inducible operon encoding a two-component regulatory system in *Lactobacillus acidophilus*. *J. Bacteriol.* 189, 4624–4634. doi: 10.1128/JB.00337-07

Pfeiler, E. A., and Klaenhammer, T. R. (2009). Role of transporter proteins in bile tolerance of *Lactobacillus acidophilus*. *Appl. Env. Microbiol.* 75, 6013–6016. doi: 10.1128/AEM.00495-09

Ramiah, K., van Reenen, C. A., and Dicks, L. M. (2007). Expression of the mucus adhesion genes Mub and MapA, adhesion-like factor EF-Tu and bacteriocin gene plaA of *Lactobacillus plantarum* 423, monitored with real-time PCR. *Int. J. Food Microbiol.* 116, 405–409. doi: 10.1016/j.ijfoodmicro.2007.02.011

Reid, G. (2016). Probiotics: definition, scope and mechanisms of action. *Best Pr. Res. Clin. Gastroenterol.* 30, 17–25. doi: 10.1016/j.bpg.2015.12.001

Ren, C., Zhang, Q., de Haan, B. J., Zhang, H., Faas, M. M., and de Vos, P. (2016). Identification of TLR2/TLR6 signalling lactic acid bacteria for supporting immune regulation. *Sci. Rep.* 6:34561. doi: 10.1038/srep34561

Ren, D., Gong, S., Shu, J., Zhu, J., Rong, F., Zhang, Z., et al. (2017). Mixed *Lactobacillus plantarum* strains inhibit *Staphylococcus aureus* induced inflammation and ameliorate intestinal microflora in mice. *Biomed Res. Int.* 2017:7476467. doi: 10.1155/2017/7476467

Renelies-Hamilton, J., Germer, K., Sillam-Dusses, D., Bodawatta, K. H., and Poulsen, M. (2021). Disentangling the relative roles of vertical transmission, subsequent colonizations, and diet on cockroach microbiome assembly. *mSphere* 6:e01023-20. doi: 10.1128/mSphere.01023-20

Reveron, I., de Las Rivas, B., Munoz, R., and Lopez de Felipe, F. (2012). Genome-wide transcriptomic responses of a human isolate of *Lactobacillus plantarum* exposed to p-coumaric acid stress. *Mol. Nutr. Food Res.* 56, 1848–1859. doi: 10.1002/mnfr.201200384

Schubert, M. L. (1999). Regulation of gastric acid secretion. *Curr. Opin. Gastroenterol.* 15, 457–462. doi: 10.1097/00001574-199911000-00002

Selegard, R., Musa, A., Nystrom, P., Aili, D., Bengtsson, T., and Khalaf, H. (2019). Plantaricins markedly enhance the effects of traditional antibiotics against *Staphylococcus epidermidis*. *Futur. Microbiol.* 14, 195–205. doi: 10.2217/fmb-2018-0285

Seme, H., Gjuracic, K., Kos, B., Fujs, S., Stempelj, M., Petkovic, H., et al. (2015). Acid resistance and response to pH-induced stress in two *Lactobacillus plantarum* strains with probiotic potential. *Benef. Microbes* 6, 369–379. doi: 10.3920/BM2014.0069

Shah, S., Nagata, M., Yamasaki, S., and Williams, S. J. (2016). Total synthesis of a cyclopropane-fatty acid alpha-glucosyl diglyceride from *Lactobacillus plantarum* and identification of its ability to signal through Mincle. *Chem. Commun.* 52, 10902–10905. doi: 10.1039/C6CC05631H

Sharma, A., and Srivastava, S. (2014). Anti-Candida activity of two-peptide bacteriocins, plantaricins (Pln E/F and J/K) and their mode of action. *Fungal Biol.* 118, 264–275. doi: 10.1016/j.funbio.2013.12.006

Sicard, J. F., Le Bihan, G., Vogeleer, P., Jacques, M., and Harel, J. (2017). Interactions of intestinal bacteria with components of the intestinal mucus. *Front. Cell. Infect. Microbiol.* 7:387. doi: 10.3389/fcimb.2017.00387

Sinha, A., Gupta, S. S., Chellani, H., Maliye, C., Kumari, V., Arya, S., et al. (2015). Role of probiotics VSL#3 in prevention of suspected sepsis in low birthweight infants in India: a randomised controlled trial. *BMJ Open* 5:e006564. doi: 10.1136/bmjopen-2014-006564

Smelt, M. J., de Haan, B. J., Bron, P. A., van Swam, I., Meijerink, M., Wells, J. M., et al. (2012). L. plantarum, L. salivarius, and L. lactis attenuate Th2 responses and increase Treg frequencies in healthy mice in a strain dependent manner. *PLoS ONE* 7:e47244. doi: 10.1371/journal.pone.0047244

Song, D. F., Zhu, M. Y., and Gu, Q. (2014). Purification and characterization of Plantaricin ZJ5, a new bacteriocin produced by *Lactobacillus plantarum* ZJ5. *PLoS ONE* 9:e105549. doi: 10.1371/journal.pone.0105549

Stiemsma, L. T., and Michels, K. B. (2018). The Role of the microbiome in the developmental origins of health and disease. *Pediatrics* 141:2437. doi: 10.1542/peds.2017-2437

Sultani, M., Stringer, A. M., Bowen, J. M., and Gibson, R. J. (2012). Anti-inflammatory cytokines: important immunoregulatory factors contributing to chemotherapy-induced gastrointestinal mucositis. *Chemother. Res. Pr.* 2012:490804. doi: 10.1155/2012/490804

Tamburini, S., Shen, N., Wu, H. C., and Clemente, J. C. (2016). The microbiome in early life: implications for health outcomes. *Nat. Med.* 22, 713–722. doi: 10.1038/nm.4142

Tilg, H., and Kaser, A. (2011). Gut microbiome, obesity, and metabolic dysfunction. *J. Clin. Invest.* 121, 2126–2132. doi: 10.1172/JCI58109

Toshimitsu, T., Gotou, A., Furuichi, K., Hachimura, S., and Asami, Y. (2019). Effects of 12-wk *Lactobacillus plantarum* OLL2712 treatment on glucose metabolism and chronic inflammation in prediabetic individuals: a single-arm pilot study. *Nutrition* 58, 175–180. doi: 10.1016/j.nut.2018.07.116

Tsai, Y. L., Lin, T. L., Chang, C. J., Wu, T. R., Lai, W. F., Lu, C. C., et al. (2019). Probiotics, prebiotics and amelioration of diseases. *J. Biomed. Sci.* 26:3. doi: 10.1186/s12929-018-0493-6

Underwood, M. A. (2019). Probiotics and the prevention of necrotizing enterocolitis. *J. Pediatr. Surg.* 54, 405–412. doi: 10.1016/j.jpedsurg.2018.08.055

van Baarlen, P., Troost, F. J., van Hemert, S., van der Meer, C., de Vos, W. M., de Groot, P. J., et al. (2009). Differential NF-kappaB pathways induction by *Lactobacillus plantarum* in the duodenum of healthy humans correlating with immune tolerance. *Proc. Natl. Acad. Sci. U. S. A.* 106, 2371–2376. doi: 10.1073/pnas.0809919106

van Hemert, S., Meijerink, M., Molenaar, D., Bron, P. A., de Vos, P., Kleerebezem, M., et al. (2010). Identification of *Lactobacillus plantarum* genes modulating the cytokine response of human peripheral blood mononuclear cells. *BMC Microbiol.* 10:293. doi: 10.1186/1471-2180-10-293

Wang, B., Li, J., Li, Q., Zhang, H., and Li, N. (2009). Isolation of adhesive strains and evaluation of the colonization and immune response by *Lactobacillus plantarum* L2 in the rat gastrointestinal tract. *Int. J. Food Microbiol.* 132, 59–66. doi: 10.1016/j.ijfoodmicro.2009.03.016

Wang, G., Xia, Y., Cui, J., Gu, Z., Song, Y., Chen, Y. Q., et al. (2014). The roles of moonlighting proteins in bacteria. *Curr. Issues Mol. Biol.* 16, 15–22. doi: 10.21775/cimb.016.015

Wang, G., Zhang, M., Zhao, J., Xia, Y., Lai, P. F., and Ai, L. (2018). A surface protein from *Lactobacillus plantarum* increases the adhesion of *Lactobacillus* strains to human epithelial cells. *Front. Microbiol.* 9:2858. doi: 10.3389/fmicb.2018.02858

Wang, J., Ji, H., Wang, S., Liu, H., Zhang, W., Zhang, D., et al. (2018). Probiotic *Lactobacillus plantarum* promotes intestinal barrier function by strengthening the epithelium and modulating gut microbiota. *Front. Microbiol.* 9:1953. doi: 10.3389/fmicb.2018.01953

Wang, Y., Qin, Y., Xie, Q., Zhang, Y., Hu, J., and Li, P. (2018). Purification and characterization of plantaricin LPL-1, a novel class IIa bacteriocin produced by *Lactobacillus plantarum* LPL-1 isolated from fermented fish. *Front. Microbiol.* 9:2276. doi: 10.3389/fmicb.2018.02276

Wu, X., Altman, R., Eiteman, M. A., and Altman, E. (2014). Adaptation of *Escherichia coli* to elevated sodium concentrations increases cation tolerance and enables greater lactic acid production. *Appl. Env. Microbiol.* 80, 2880–2888. doi: 10.1128/AEM.03804-13

Xie, Q., Pan, M., Huang, R., Tian, X., Tao, X., Shah, N. P., et al. (2016). Short communication: modulation of the small intestinal microbial community composition over short-term or long-term administration with *Lactobacillus plantarum* ZDY2013. *J. Dairy Sci.* 99, 6913–6921. doi: 10.3168/jds.2016-11141

Xiuliang Li Xiuyan, M., Yanyan, Z., Xinyang, L., Li, C., Dequan, H., Yue, S., et al. (2018). *Lactobacillus plantarum* and l*actobacillus fermentum* alone or in combination regulate instestinal flora composition and systemic immunity to alleviate obesity syndrome in high-fat diet rat. *Int. J. Food Sci. Technol.* 53, 137–146. doi: 10.1111/ijfs.13567

Yadav, A. K., Tyagi, A., Kaushik, J. K., Saklani, A. C., Grover, S., and Batish, V. K. (2013). Role of surface layer collagen binding protein from indigenous *Lactobacillus plantarum* 91 in adhesion and its anti-adhesion potential against gut pathogen. *Microbiol. Res.* 168, 639–645. doi: 10.1016/j.micres.2013.05.003

Yin, M., Yan, X., Weng, W., Yang, Y., Gao, R., Liu, M., et al. (2018). Micro Integral Membrane Protein (MIMP), a newly discovered anti-inflammatory protein of *Lactobacillus Plantarum*, enhances the gut barrier and modulates microbiota and inflammatory cytokines. *Cell. Physiol. Biochem.* 45, 474–490. doi: 10.1159/000487027

Zago, M., Fornasari, M. E., Carminati, D., Burns, P., Suarez, V., Vinderola, G., et al. (2011). Characterization and probiotic potential of Lactobacillus plantarum strains isolated from cheeses. *Food Microbiol.* 28, 1033–1040. doi: 10.1016/j.fm.2011.02.009

Zeissig, S., and Blumberg, R. S. (2014). Life at the beginning: perturbation of the microbiota by antibiotics in early life and its role in health and disease. *Nat. Immunol.* 15, 307–10. doi: 10.1038/ni.2847

Zhang, F., Li, Y., Wang, X., Wang, S., and Bi, D. (2019). The impact of *Lactobacillus plantarum* on the gut microbiota of mice with DSS-induced colitis. *Biomed Res. Int.* 2019:3921315. doi: 10.1155/2019/3921315

Zhang, G. Q., Hu, H. J., Liu, C. Y., Shakya, S., and Li, Z. Y. (2016). Probiotics for preventing late-onset sepsis in preterm neonates: a PRISMA-compliant systematic review and meta-analysis of randomized controlled trials. *Med* 95:e2581. doi: 10.1097/MD.0000000000002581

Zhao, M., Shen, C., and Ma, L. (2018). Treatment efficacy of probiotics on atopic dermatitis, zooming in on infants: a systematic review and meta-analysis. *Int. J. Dermatol.* 57, 635–641. doi: 10.1111/ijd.13873

Zhao, X., Yi, R., Qian, Y., and Park, K. Y. (2018). Lactobacillus plantarum YS-3 prevents activated carbon-induced constipation in mice. *J. Med. Food* 21, 575–584. doi: 10.1089/jmf.2017.4109

Conflict of Interest: PP isolated and further developed the strain ATCC 202195 that has been licensed to Chr Hansen for commercial production and use in food/supplement.

The remaining authors declare that the research was conducted in the absence of any commercial or financial relationships that could be construed as a potential conflict of interest.

Publisher's Note: All claims expressed in this article are solely those of the authors and do not necessarily represent those of their affiliated organizations, or those of the publisher, the editors and the reviewers. Any product that may be evaluated in this article, or claim that may be made by its manufacturer, is not guaranteed or endorsed by the publisher.

Copyright © 2021 Fidanza, Panigrahi and Kollmann. This is an open-access article distributed under the terms of the Creative Commons Attribution License (CC BY). The use, distribution or reproduction in other forums is permitted, provided the original author(s) and the copyright owner(s) are credited and that the original publication in this journal is cited, in accordance with accepted academic practice. No use, distribution or reproduction is permitted which does not comply with these terms.

frontiers in Microbiology

ORIGINAL RESEARCH
published: 27 October 2021
doi: 10.3389/fmicb.2021.665743

Profiling Tryptophan Catabolites of Human Gut Microbiota and Acute-Phase Protein Levels in Neonatal Dried Blood Specimens

Anne-Christine Aust[1†], Eliska Benesova[1†], Veronika Vidova[1], Katerina Coufalikova[1], Sona Smetanova[1], Ivo Borek[2], Petr Janku[3], Eva Budinska[1], Jana Klanova[1], Vojtech Thon[1] and Zdenek Spacil[1]*

[1]RECETOX, Faculty of Science, Masaryk University, Brno, Czechia, [2]Department of Pediatrics, University Hospital Brno and Masaryk University Medical School, Brno, Czechia, [3]Department of Gynecology and Obstetrics, University Hospital Brno and Masaryk University Medical School, Brno, Czechia

OPEN ACCESS

Edited by:
Tobias R. Kollmann, University of Western Australia, Australia

Reviewed by:
Guillaume Sarrabayrouse, Université de Paris, France
Sridhar Mani, Albert Einstein College of Medicine, United States

***Correspondence:**
Zdenek Spacil
spacil@recetox.muni.cz;
spacil@u.washington.edu

†These authors have contributed equally to this work

Specialty section:
This article was submitted to Microbial Immunology, a section of the journal Frontiers in Microbiology

Received: 08 February 2021
Accepted: 16 September 2021
Published: 27 October 2021

Citation:
Aust A-C, Benesova E, Vidova V, Coufalikova K, Smetanova S, Borek I, Janku P, Budinska E, Klanova J, Thon V and Spacil Z (2021) Profiling Tryptophan Catabolites of Human Gut Microbiota and Acute-Phase Protein Levels in Neonatal Dried Blood Specimens. Front. Microbiol. 12:665743. doi: 10.3389/fmicb.2021.665743

National screening programs use dried blood specimens to detect metabolic disorders or aberrant protein functions that are not clinically evident in the neonatal period. Similarly, gut microbiota metabolites and immunological acute-phase proteins may reveal latent immune aberrations. Microbial metabolites interact with xenobiotic receptors (i.e., aryl hydrocarbon and pregnane-X) to maintain gastrointestinal tissue health, supported by acute-phase proteins, functioning as sensors of microbial immunomodulation and homeostasis. The delivery (vaginal or cesarean section) shapes the microbial colonization, which substantially modulates both the immune system's response and mucosal homeostasis. This study profiled microbial metabolites of the kynurenine and tryptophan pathway and acute-phase proteins in 134 neonatal dried blood specimens. We newly established neonatal blood levels of microbial xenobiotic receptors ligands (i.e., indole-3-aldehyde, indole-3-butyric acid, and indole-3-acetamide) on the second day of life. Furthermore, we observed diverse microbial metabolic profiles in neonates born vaginally and *via* cesarean section, potentially due to microbial immunomodulatory influence. In summary, these findings suggest the supportive role of human gut microbiota in developing and maintaining immune system homeostasis.

Keywords: human gut microbiota, tryptophan and kynurenine metabolism, dried blood specimens, acute-phase proteins, immunomodulation

INTRODUCTION

Dried blood specimens (DBS) are used to quantify circulating levels of drugs (Kloosterboer et al., 2018), metabolites (Sain-van der Velden et al., 2017), and proteins. The advantages over a conventional blood draw include minimally invasive sampling, suitable for neonates and other vulnerable populations, fewer processing and handling steps, and facile storage. Neonatal DBS collected from a heel prick are widely used in nationwide neonatal screening programs for inherited endocrine and metabolic disorders (Mechtler et al., 2012).

The initial exposure to microbiota during and immediately after birth influences the lifelong colonization and modulates the innate and adaptive immune system (Neu and Rushing, 2011), potentially causing a decreased tolerance or an exorbitant antigen representation, inflammatory response, and damage to the mucosal barrier function (Francino, 2018). Natural vaginal delivery (VD) or cesarean delivery (CD) shapes the diversity of commensal, symbiotic, and pathogenic microorganisms colonizing the human body, collectively referred to as the microbiota (Penders et al., 2006; Palmer et al., 2007; Mitsou et al., 2008; Wall et al., 2009). The composition and timing of gut microbiota colonization vary in VD and CD neonates (Bennet and Nord, 1987; Grönlund et al., 1999; Penders et al., 2006; Palmer et al., 2007; Mitsou et al., 2008). Fecal and vaginal microbiota dominate the initial colonization in VD neonates (Mändar and Mikelsaar, 1996; Bezirtzoglou, 1997; Grönlund et al., 1999; Matsumiya et al., 2002; Wall et al., 2009). For instance, microaerophilic *Lactobacillus* species (*ca.* 25% of total microbiota) frequently colonizes VD infants (Matsumiya et al., 2002; Wall et al., 2009). On the other hand, CD neonates are primarily exposed to nosocomial bacteria or topical skin microbiota (Bezirtzoglou, 1997; Grönlund et al., 1999; Mackie et al., 1999; Wall et al., 2009). CD infants' gut microbiota typically contain a smaller share of strict anaerobes such as *Bacteriodetes fragilis* and *Bifidobacteria* (Bennet and Nord, 1987; Grönlund et al., 1999; Torun et al., 2002; Penders et al., 2006; Wall et al., 2009). The initial microbial composition's nuances can modulate the immune system's development and affect the infant's subsequent health (Francino, 2018; Wampach et al., 2018).

The circulating microbial metabolites reflect the diversity of human gut microbiota and endogenous inflammatory markers (i.e., acute-phase proteins—APP) the immune system's reaction. The microbial community builds contact with intestinal epithelial immune cells' receptors and stimulates signaling cascades leading to cell differentiation and inflammatory response control (Romagnani, 2006). Microbial catabolites of aromatic amino acids (e.g., tryptophan) act protectively in the host immune homeostasis, similar to short-chain fatty acids (i.e., acetate, butyrate, and propionate; Jin et al., 2017; Pavlova et al., 2017). Tryptophan catabolites, i.e., indole-3-acetic acid (IAA; Elsden et al., 1976; Smith and Macfarlane, 1996; Finegold et al., 2002; Russell et al., 2013; Roager and Licht, 2018), indole-3-lactic acid (ILA; Aragozzini et al., 1979; Smith and Macfarlane, 1996; Russell et al., 2013; Honoré et al., 2016; Cervantes-Barragan et al., 2017; Dodd et al., 2017; Roager and Licht, 2018), and indole-3-propionic acid (IPA; Elsden et al., 1976; Wikoff et al., 2009; Williams et al., 2014; Dodd et al., 2017; Wlodarska et al., 2017; Roager and Licht, 2018), interact with xenobiotic receptors (i.e., aryl hydrocarbon receptor, AHR, and pregnane X receptor, PXR; Roager and Licht, 2018). The AHR is a ligand-activated transcriptional factor widely expressed in immune cells that attenuates autoimmune responses and ensures gastrointestinal tissue health (**Figure 1A**). The ligand-specific activation of the AHR signaling pathway is immunomodulatory to the host. Microbial tryptophan catabolites regulate the production of pro-inflammatory cytokines (i.e., INF-γ and IL-2) in TH1 cells and anti-inflammatory cytokines (i.e., IL-10) in TH2 cells (Mangge et al., 2014; Alexeev et al., 2016; Lanis et al., 2017; Gao et al., 2018; Krishnan et al., 2018). Microbial AHR ligands modulate intestinal barrier function and the resistance against enteric pathogens (Liu et al., 2018). Indole-3-acetamide (IAM) and indole-3-butyric acid (IBA) are precursors of IAA (**Figure 1B**; Agus et al., 2018). Indole-3-aldehyde (IAld), IAA, IAM, and ILA activate ILC3 through AHR signaling, producing IL-22 to induce resistance against mucosal candidiasis (Zelante et al., 2013; Zhang et al., 2019). IBA, the metabolic product of Clostridia species (Lombard and Dowell, 1983), occurs in human urine (Tonelli et al., 1982) and plasma. IBA cooccurred with the incidence of inflammatory bowel syndrome (IBS) in schizophrenic patients (Cai et al., 2012). A potential mechanism to control inflammation by IBA and IAA is competitive inhibition of phospholipase A_2 (Dileep et al., 2013). ILA reprograms intraepithelial $CD4^+$T cells in immunoregulatory $CD4^+CD8_{\alpha\alpha}^+$ (Cervantes-Barragan et al., 2017). *In vitro* studies in gram-positive and gram-negative bacterial cell cultures (*Bacillus subtilis*, *Pseudomonas aeruginosa*, *Salmonella enterica*, and *Staphylococcus aureus*) demonstrated biofilm formation inhibition by anthranilate (ATA; Li et al., 2017). The interaction between microbial metabolites and the neonates' immune system emphasizes their role in the epithelial barrier function and reveals their importance in the signaling cascade of the immune systems' local and systemic response.

The quantitative profiling of circulating acute-phase proteins (APPs) monitors the systemic inflammatory response (Vidova et al., 2019). APPs are not transportable across the placental barrier and represent a surrogate for the neonate's innate immune system's activation. C-reactive protein (CRP) and serum amyloid A (SAA) are synthesized in hepatocytes (**Figure 1A**) after stimulation by cytokines (i.e., IL-6, IL-1, IL-8, and TNF-α; Heinrich et al., 1990). In healthy individuals,

Abbreviations: A1AT, Alpha-1-antitrypsin; A1AG1, Alpha-1-acid glycoprotein 1; A1AG2, Alpha-1-acid glycoprotein 2; AAT, Aromatic amino acid transferase; acdA, Acyl-CoA dehydrogenase; AFMID, Kynurenine formamidase; AHR, Aryl-hydrocarbon receptor; AO1, Indole acetaldehyde oxidase; APP, Acute-phase protein; ArAT, Aromatic amino acid aminotransferase; ATA, Anthranilate; BCA, Bicinchoninic acid; CD, Cesarean delivery; CELSPAC-TNG, Central European Longitudinal Studies of Parents and Children – The Next Generation; CRP, C-reactive protein; DBS, Dried blood specimens; ECH2, Enoyl-CoA hydratase 2; fldH, Phenyl lactate dehydrogenase; fldBC, Phenyl lactate dehydratase; FoxP3, Forkhead-box-protein 3; HIAA, Hydroxy-indole acetic acid; HMDB, Human Metabolome Database; IAA, Indole-3-acetic acid; IaaH, Indole acetamide hydrolase; IaaO, Indole-3-acetic acid oxidase; IAld, Indole-3-aldehyde; IAM, Indole-3-acetamide; IBA, Indole-3-butyric acid; IBS, Inflammatory bowel syndrome; IDO, Indoleamine-2,3-dioxygenase; ILA, Indole-3-lactic acid; IL-1, Interleukin-1; IL-2, Interleukin-2; IL-6, Interleukin-6; IL-8, Interleukin-8; IL-10, Interleukin 10; IL-22, Interleukin 22; ILC3, Innate lymphoid cells 3; INFγ, Interferon-γ; IPA, Indole-3-propionic acid; KAT, Kynurenine amino transferase; KYN, Kynurenine; KYNU, Kynureninase; LC, Liquid chromatography; MAO, Monoamine oxygenase; MS, Mass spectrometry; NAT, N-acetyl-tryptophan; NAT1, Arylamine N-acetyltransferase 1; PCD, Pyruvate decarboxylase; porB/C, Pyruvate ferredoxin oxidoreductase B and C; PXR, Pregnane X receptor; SAA, Serum amyloid A; SRM, Selected reaction monitoring; TDO, Tryptophan-2,3-dioxygenase; TGF β, Transforming growth factor; TH1, t helper type 1 cells; TH2, t helper type 2 cells; TLR4, Toll like receptor 4; TMO, tryptophan-2-monooxygenase; TNFα, Tumor necrosis factor α; TrD, Tryptophan decarboxylase; TRP, Tryptophan; UHPLC, Ultra-high-performance liquid chromatography; VD, Vaginal delivery; QQQ, Triple quadrupole.

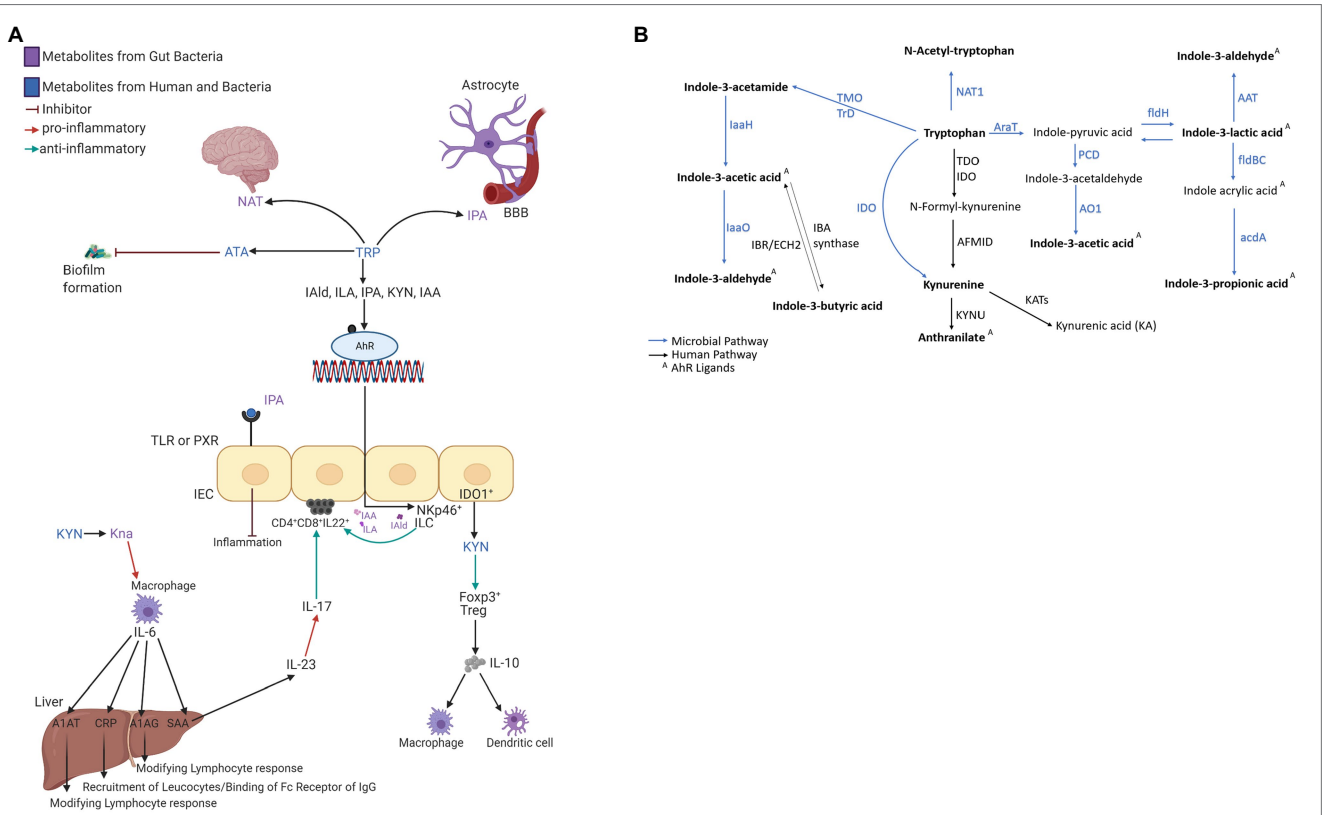

FIGURE 1 | **(A)** The interaction network of microbial tryptophan catabolites and acute-phase proteins mediating the anti-inflammatory and immune-supportive function. **(B)** Microbial and human co-metabolism. Created with BioRender.com.

circulating SAA1, SAA2, and CRP levels are low but increase between 10-fold and 1,000-fold during the acute phase of inflammation (Clyne and Olshaker, 1999; Haran et al., 2013; Buck et al., 2016). SAA1 is arguably a more reliable inflammation marker than CRP as SAA levels rise earlier, more rapidly, and have higher amplitude (Arnon et al., 2007). SAA4 is a constitutive apolipoprotein with a stable blood concentration during the acute phase of inflammation (Yamada et al., 1997; Buck et al., 2016). The initial microbial colonization influenced by the mode of delivery induces measurable perturbations in APPs. Higher concentrations of SAA1 and CRP were reported in VD compared to CD neonates (Marchini et al., 2000). Blood levels of A1AT, A1AG1, and A1AG2 increase by several folds in response to inflammation (Hochepied et al., 2003; Janciauskiene et al., 2011).

In this study, we profiled nine tryptophan catabolites (i.e., ATA, IAA, IAM, IAld, IBA, ILA, IPA, kynurenine—KYN, and N-acetyl tryptophan—NAT) and seven APPs (i.e., A1AT, A1AG1, A1AG2, SAA1, SAA1/2, SAA4, and CRP) in a DBS punch (3 mm or 1/8″, equivalent to 3 µl of blood). We analyzed 134 neonatal DBSs from a birth cohort study: Central European Longitudinal Studies of Parents and Children – The Next Generation (CELSPAC-TNG) to explore early-life immunomodulation attributed to the metabolism of the human gut microbiota. We explored the delivery mode's influence on tryptophan catabolite and acute-phase protein profile.

MATERIALS AND METHODS

Study Design

DBS samples from 134 neonates (20 delivered *via* cesarean section and 114 delivered vaginally) collected under IRB approval were part of the CELSPAC-TNG study at Faculty Hospital Brno (Ethical Committee CELSPAC/EK/4/2016, in 2016–2017). Characteristics of individual neonates, including gestational age, delivery mode, sex, birth weight, birth length, Apgar score, DBS sampling, and anamnesis, are shown in **Supplementary Table S-1**. The study subjects were female ($n = 56$) and male ($n = 78$), with an average birth weight of 3,494 g and an average birth length of 50.5 cm (**Supplementary Tables S-1** and **S-2**). We show the average, minimal, and maximal values for birth length, weight, gestation age, Apgar score, and the delay from the birth to DBS sampling for VD and CD neonates separately in **Supplementary Table S-2**. For DBS sampling, a small amount of capillary blood from the heel prick was soaked into Whatman 903 filter paper and allowed to dry at room temperature for 3 h. DBS punches (1/8″ or 3 mm) were stored in the freezer at −80°C until analysis.

Chemicals and Reagents

Isotopically labeled peptides used as internal standards for protein quantification were from JPT Technologies (Berlin, Germany). Sequences are listed in **Supplementary Table S-3**.

The protein assay protocol was adapted from the previous study (Vidova et al., 2019). Isotopically labelled [$^{13}C_6$] indole-3-acetic acid (cat. #0317333), purity >97%, was from OlChemIm s.r.o. (Olomouc, Czech Republic). Isotopically labeled [$^{13}C_{11}$][$^{15}N_2$] L-tryptophan (cat. #574597), purity ≥98%, was from Sigma-Aldrich (St. Louis, United States). Isotopically labeled [$^{2}D_4$] L-kynurenine (cat. #DLM-7842-PK), purity of 95%, was from Cambridge Isotope Laboratories, Inc. (Tewksbury, Massachusetts, United States). Isotopically labeled [$^{13}C_6$] anthranilic acid (cat. #PR-24225), purity 99%, was from Sigma-Aldrich (St. Louis, Massachusetts, USA). The chemical standard of $_L$-tryptophan (cat. #51145; TraceCERT®), N-acetyl-tryptophan (cat. #PHR1177), indole-3-acetate (cat. #45533), purity 98%, serotonin (cat. #14927), purity ≥ 98%, anthranilic acid (cat. #10680), purity ≥ 99.5%, L-kynurenine (cat. #K8625), purity ≥ 98%, were from Sigma-Aldrich (St. Louis, Massachusetts, USA). The chemical standard indole-3-carboxaldehyde (cat. #A15330), purity 99%, was from Alfa Aesar (Haverhill, Massachusetts, United States). The chemical standard indole-lactic-3- acid (≥97%; cat. #SC-255130), purity ≥ 97%, was from Santa Cruz Biotechnology (Dallas, Texas, USA). Indole-3-butyric acid standard (≥99.0%; cat. #57310) was from Sigma-Aldrich (St. Louis, Massachusetts, United States). Liquid chromatography–mass spectrometry (LC–MS) grade acetonitrile (cat. #0013687802BS) and isopropanol (cat. #0016267802BS) were from Biosolv (Valkenswaard, Netherlands). Formic acid for mass spectrometry (cat. #94318) and ammonium bicarbonate BioUltra ≥99.5% (cat. #09830) were from Sigma-Aldrich (St. Louis, MO). BCA protein assay kit (cat. #23227) was from Thermo Fisher Scientist (Waltham, MA). Deionized water was produced using Millipore Simplicity 185 ultrapure water system (Merck Millipore corp., Billerica, MA).

Metabolite Extraction

The complete DBS sample processing flowchart is shown in **Supplementary Figure S-3**. Based on material availability, one or two 3-mm DBS punches (equivalent to 3 µl and 6 µl of whole blood, respectively) were reconstituted in 150 µl of 50 mM ammonium bicarbonate buffer in an orbital shaker (1,600 rpm, 60 min). We removed a volume of 5 µl for BCA (section Protein Extraction and Processing Protocol, and Mass Spectrometry Assays) and dried the remaining sample in a vacuum concentrator centrifuge (Savant SPD121 P SpeedVac, Thermo Fisher). A volume of 400 µl of 80% isopropanol (*v/v*) was added to a dry sample and vortexed at 200 rpm for 20 min. The sample was briefly centrifuged, supernatant quantitatively transferred into a 96-well plate, and dried in the SpeedVac. Dry extracts were redissolved in 10 µl 5% isopropanol (*v/v*) containing isotopically labeled standards: 200 nM [$^{13}C_6$] indole-3-acetate, 2000 nM [$^{2}H_5$] L-kynurenine, 20,000 nM [$^{13}C_{11}$][$^{15}N_2$] L-tryptophan, 50 nM [$^{2}H_5$][$^{15}N_2$] indole-3-acetamide, 200 nM [$^{13}C_6$] anthranilate (**Supplementary Table S-4**). Several solvents, i.e., 80% isopropanol, 100% isopropanol, 50% isopropanol, 80% acetonitrile, and 100% acetonitrile, were tested for optimal extraction recoveries of metabolites from DBS ($n = 3$). The optimal extraction solvent was 80% isopropanol (data not shown).

Protein Extraction and Processing Protocol, and Mass Spectrometry Assays

DBS proteins were extracted, processed, and analyzed by UHPLC–MS as described previously (Vidova et al., 2019). In brief, the DBS extract's total protein content was determined using BCA (cat. #23227, Thermo Fisher, Waltham, MA) in extracts diluted 100-fold with 50 mM ammonium bicarbonate buffer. A dilution series (31.25–2000 µg/ml) of bovine serum albumin standard in 50 mM ammonium bicarbonate buffer was used to generate a 7-point calibration curve. Spectrophotometric absorbance was measured at 562 nm. Mass spectrometry protein assays were performed in 30 µl of DBS extract mixed with 10 µl of the internal standard solution in 5% of acetonitrile, containing isotopically labeled standard peptides (**Supplementary Table S-3**) and with 3 µl of trypsin (1 µg/µl). Samples were incubated (17 h at 37°C, orbital shaking), and the enzymatic proteolysis was quenched by adding 200 µl of 2% formic acid in water (pH < 3). Tryptic peptides were purified and desalted, applying solid phase extraction (Oasis PRIME HLB 96-well plate, 30 mg, Waters, Milford, MA). The solid-phase extraction protocol: the sample loaded onto the cartridge, washed with 300 µl of 2% formic acid in water (pH < 3), eluted with 50% acetonitrile with 2% formic acid (pH < 3), and the eluate dried in the SpeedVac. Before UHPLC–MS analysis, peptides were reconstituted in 50 µl of 5% acetonitrile with 0.1% formic acid. Processed DBS samples were injected (5 µl) on the UHPLC-QQQ system (Infinity 1,260 and 6495B from Agilent Technologies, United States). We utilized a reversed-phase analytical column (C_{18} Peptide CSH; 1.7 µm, 2.1 mm i.d. × 100 mm; cat. #186006937, Waters, Milford, MA) and the previously described method (Vidova et al., 2019).

Mass Spectrometry Metabolite Profiling

Extracted DBS were analyzed in triplicate. Samples were injected (2 µl) on the UHPLC-QQQ system equipped with a reverse-phase analytical column (Acquity UHPLC CSH™ C_{18} Column; 1.7 µm, 2.1 mm x 100 mm; cat. #186005297, Waters, Milford, MA) thermostated to 40°C. The mobile phase consisted of buffer A (water with 0.1% formic acid) and buffer B (acetonitrile/water; 95:5 with 0.1% formic acid). The gradient elution program (0–14 min) was: 0.0 min 5% B, 5 min 10% B, 10 min 95% B, 11.99 95% B, 12.0 5% B, and 14 min 5% B. The mobile phase flow was 0.3 ml/min. A standard-flow Jet Stream electrospray source operated in positive SRM ion mode with a capillary voltage of 3.5 kV. Additional parameters were: gas flow rate 15 l/min at 160°C, sheath gas pressure 25 PSI at 250°C, and nozzle voltage 500 V. SRM libraries were generated using Optimizer software (Agilent Technologies) on standard solutions of individual metabolites. For the metabolite identification, 2–4 SRM qualifier transitions were monitored per metabolite (**Supplementary Table S-5**), and a best-performing SRM transition was used for the quantification (**Supplementary Figure S-1**). Peak integration and visual inspection were performed in Skyline software (version 20.1.0.155; MacCoss Lab, Univ. of Washington).

Method Validation

Protein assay validation was reported previously (Vidova et al., 2019). Metabolite profiling assays were validated using matrix-matched calibration curves to determine the linearity range, coefficient of determination (R^2), the limit of detection (LOD), and the limit of quantification (LOQ; **Supplementary Figure S-2**). LOD and LOQ were established for isotopically labeled standards [$^2H_5$] [^{15}N] indole-3-acetamide, [$^{13}C_6$] indole-3-acetate, [$^2D_4$] L-kynurenine, [$^{13}C_{11}$] [$^{15}N_2$] L-tryptophan, and [$^{13}C_6$] anthranilic acid in pooled DBS extracts. The dilution series was measured in triplicate. Low concentrations were measured in sextuplicate to determine the standard deviation to establish LOD and LOQ [1] in **Supplementary Table S-4**. The linearity range was from 1 to 1,200 nM for [$^2H_5$] [^{15}N] indole-3-acetamide, from 15 to 40,000 nM for [$^{13}C_6$] indole-3-acetate, from 25 to 7,500 nM for [$^2D_4$] L-kynurenine, from 7.5 to 75,000 nM for [$^{13}C_{11}$] [$^{15}N_2$] L-tryptophan, and from 1 to 880 nM for [$^{13}C_6$] anthranilic acid (**Supplementary Table S-6**).

Metabolite Quantification

Concentrations of indole-3-acetamide, indole-3-acetic acid, L-kynurenine, L-tryptophan, and anthranilic acid were determined in DBS extracts using internal standardization with isotopically labeled standards [$^2H_5$] [^{15}N] indole-3-acetamide, [$^{13}C_6$] indole-3-acetate, [$^2D_4$] L-kynurenine), [$^{13}C_{11}$] [$^{15}N_2$] L-tryptophan, and [$^{13}C_6$] anthranilic acid, at the concentrations of 50, 200, 2000, 20,000, and 200 nM, respectively. The calculation uses the concentration of the isotopically labeled standard in the DBS sample and integrated peak areas of the isotopically labeled standard and corresponding metabolite (Equation 1). The concentration of indole-3-aldehyde, indole-3-propionic acid, indole-3-butyric acid, indole-3-lactic acid, and N-acetyl tryptophan was corrected with the response factor (Equation 2), determined in a conventional manner (Vidova and Spacil, 2017; Equation 3).

$$cmet = \left(\frac{CIS}{AIS} x Amet\right) \quad (1)$$

$$\text{cmet} = \left(\frac{CIS}{AIS} x Amet\right) : RF \quad (2)$$

$$RF = \left(\frac{Amet}{AIS} x \frac{CIS}{Cmet}\right) \quad (3)$$

Statistical Analysis

For metabolites, the median concentration ($n = 3$) was used. Metabolite and protein concentrations were log-transformed before statistical analysis, and values below LOQ and LOD were substituted with $\sqrt{2/2} * LOQ$ and $\sqrt{2/2} * LOD$, respectively. Only analytes with <25% substitution were used for the overall statistical analysis as continuous quantitative variables (Antweiler, 2015; Hazra and Gogtay, 2017) Due to a high percentage of values below LOQ, IAM (>68%), IPA (>73%), SAA1(>76%), and CRP (>98%) were used only as additional categorical variables with two categories - "*below LOD*" and "*above LOD*"; the latter further divided into "*below LOD*," "*below LOQ*," "*above LOQ*" for visualization purposes.

The Chi-square test was used to test the normality of distributions of logarithmically transformed values. Unpaired one-sided *t* test with Welch correction was used to test significant differences between various groups of samples. The resulting values of *p* were adjusted for multiple hypotheses testing using the Benjamini–Hochberg procedure. Results were considered significant at $FDR \leq 0.05$. Pearson correlation coefficients (with values of *p* adjusted by Benjamini–Hochberg procedure) were used to describe correlation among metabolites and proteins. Hierarchical clustering with complete-linkage method on Euclidean distance was applied to hierarchically cluster samples (neonates) and distance derived from Pearson correlation to cluster the analytes. Categorical anamnestic data for neonates and their mothers and additional categorical variables (IAM, IPA, SAA1, and CRP) were used to test differences in metabolite and protein levels and correlations between various groups. All statistical analyses were performed in R version 4.0.0 (R core team, 2020) using additional R packages *ggplot2* (Wickham, 2009), *nortest* (Tests for Normality [R package nortest version 1.0-4], 2021; normality testing), *gplots* (Various R Programming Tools for Plotting Data [R package gplots version 3.0.4], 2021), *heatmap3* (Zhao et al., 2014; hierarchal clustering and heat map), *corrplot* (Visualization of a Correlation Matrix [R package corrplot version 0.84], 2021; correlation matrix plot), and *beeswarm* (CRAN, 2021 – Package beeswarm, 9 AD; boxplots).

RESULTS

Tryptophan and Kynurenine Catabolites and Acute-Phase Proteins in Neonatal Dried Blood Specimens

We profiled TRP, ATA, IAA, IAM, IAld, IBA, ILA, IPA, KYN, and NAT levels in 134 neonatal DBS collected on the second day of life (**Table 1** and **Figure 2A**). ATA, IAA, ILA, IPA, KYN, and TRP blood levels were consistent with previous reports in the Human Metabolome Database (2021; HMDB); IAld, IAM, and IBA neonatal levels were newly established (**Table 1**). IPA, IAM, and SAA1 levels were frequently <LOQ, CRP levels <LOD (see **Supplementary Figures S-4, S-5**). The median SAA1/2, A1AT, A1AG1, A1AG2, and SAA4 blood levels are in **Figure 3A** and **Table 2**. SAA1 blood levels quantified in 33 neonates were elevated (>10 mg/l) in 13 VD neonates.

No significant differences were observed in metabolite (**Figure 2B**) and APP levels (**Figure 3B**) between CD ($n = 20$) and VD ($n = 114$) groups and respective to clinical conditions in mothers and neonates (**Supplementary Figures S-4, S-5**). SAA1/2, SAA4, and A1AG1 showed statistically significantly higher levels ($p < 0.0001$) in sample groups with CRP > LOD compared to samples with CRP < LOD. The same difference was observed in the sample groups with SAA1 above and below LOD (**Supplementary Figure S-6**). The heatmap of protein and metabolite concentrations with rows and columns ordered based on unsupervised clustering of the analytes (Pearson correlation-based distance, main clusters A, B, C) and the DBS samples (Euclidean distance, main clusters D, E) is shown in **Supplementary Figure S-4**. Cluster A represents APPs (however, A1AT shows a weak correlation

TABLE 1 | The lowest, the highest, and median concentrations of tryptophan and kynurenine catabolites in DBS.

Metabolite	Acronym	PubChem CID	# samples >LOQ	Median concentration (mg/L of blood)	The lowest concentration (mg/L of blood)	The highest concentration (mg/L of blood)	HMDB entries (mg/L)	References
Anthranilate	ATA	5,459,842	134	0.0189	0.0086	0.0470	0.0041 +/− 0.0014 [adults (>18 years)]	Duranton et al., 2012
Indole-3-acetic acid	IAA	802	134	0.6739	0.2121	3.8892	0.4992 +/− 0.2996 [adults (>18 years)]	Duranton et al., 2012
Indole-3-aldehyde	IAld	10,256	134	0.5527	0.2138	2.5499	Expected but not quantified	-
Indole-3-acetamide	IAM	397	42	0.0057	0.0010	0.0341	Expected but not quantified	-
Indole-3-butyric acid	IBA	8,617	96	0.0703	0.0170	0.4377	Detected but not quantified	Cai et al., 2012
Indole-3-lactic acid	ILA	92,904	127	0.3641	0.1262	2.7153	0.57 (0.10–1.03) [adults (>18 years)]	Magos, 1987
Indole-3-propionic acid	IPA	3,744	35	0.0072	0.0012	0.0676	0.091 (0.055–0.21) [adults (>18 years)]	Danaceau et al., 2003
Kynurenine	KYN	846	134	17.0882	7.3402	30.5551	1.23 (1.02–1.47) [neonates (0–30 days)]	Herberth et al., 2015
N-Acetyltryptophan	NAT	700,653	108	0.0173	0.0030	0.1382	Not quantified in blood	-
Tryptophan	TRP	6,305	134	2.1699	0.7715	5.7512	3.676–11.23 [neonates (0–30 days)]	Human Metabolome Database, 2021

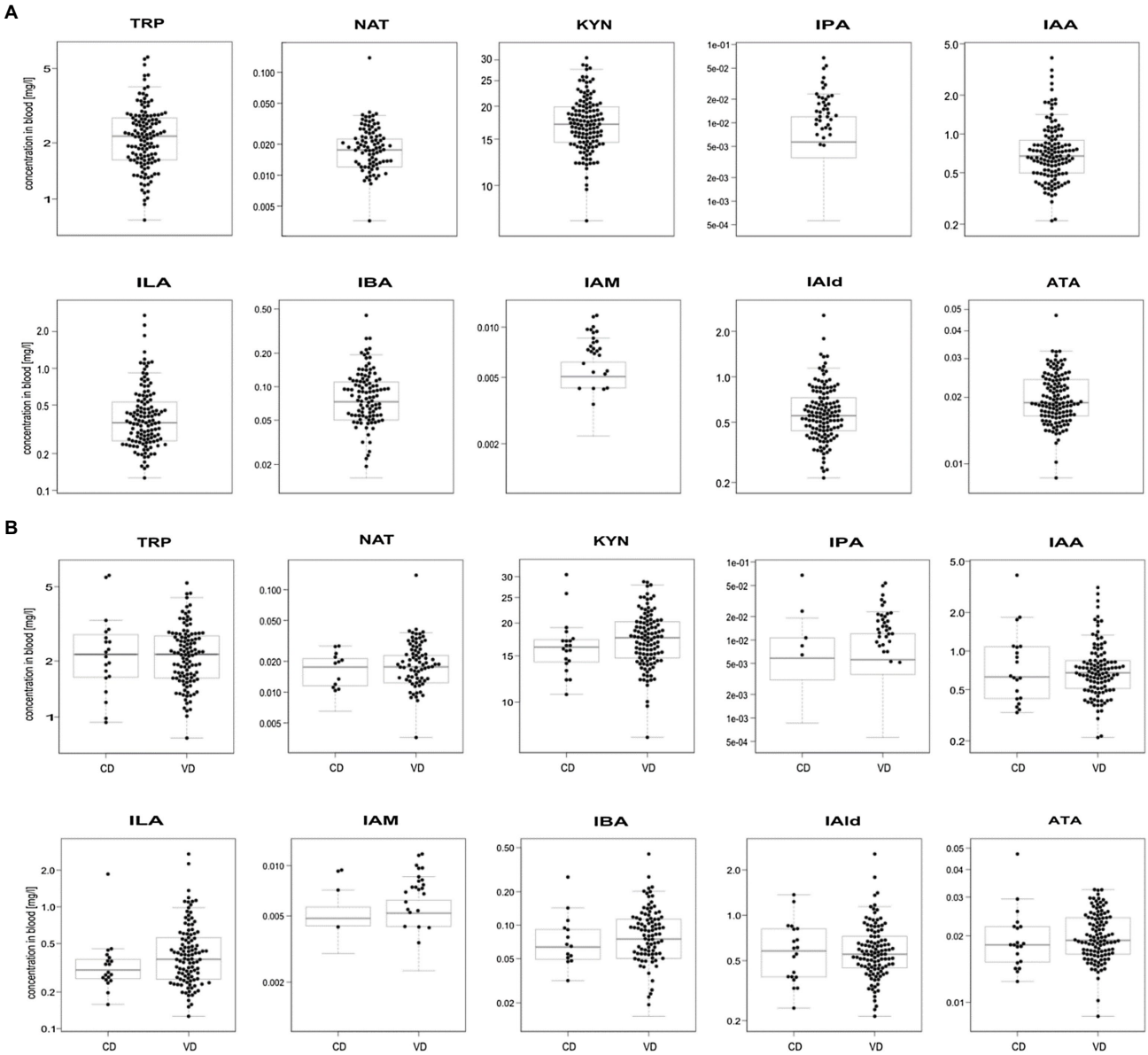

FIGURE 2 | Boxplots of metabolite levels were determined in 134 neonatal DBS **(A)** and grouped according to the delivery mode (VD, vaginal delivery, CD, cesarean delivery; **B**). Sample concentrations >LOQ marked with black dots. Y-axis is in log-scale.

with other APPs), IBA, IAA, and IAld fall into cluster B, and cluster C consists of KYN, ATA, TRP, NAT, and ILA. Clusters D and E split DBS samples into two different groups – cluster E is characterized primarily with higher APP (except A1AT) and metabolites levels. Mothers' and neonates' anamnestic data added into the picture show no parameter related to clusters D or E. Additional categorical variables CRP, SAA1, IPA, and IAM showed in the figure indicate that cluster E is connected with higher CRP and SAA1 levels. Similar and even more apparent trends in neonates' clustering are visible in cluster analysis based on proteins only (**Supplementary Figure S-5**). The APPs SAA1/2, SAA1, CRP, A1AG1, and A1AG2 are elevated in the blood (cluster D in **Supplementary Figure S-5**). High A1AT levels are observed both in cluster D and cluster E (**Supplementary Figure S-5**). In cluster E, there are low levels of other APPs. Elevated A1AT levels are caused by infection and also contraception, pregnancy, thyroid infection, or stress. In neonates, increased A1AT levels in cluster E can be associated with stress factors acting during delivery. However, neonates' anamnestic data did not show any relation to the clusters.

The Correlation Between Metabolite and Acute-Phase Protein Blood Levels

The overall metabolites and proteins correlation matrix plot is shown in **Figure 4**. A negative Pearson's correlation ($p < 0.05$)

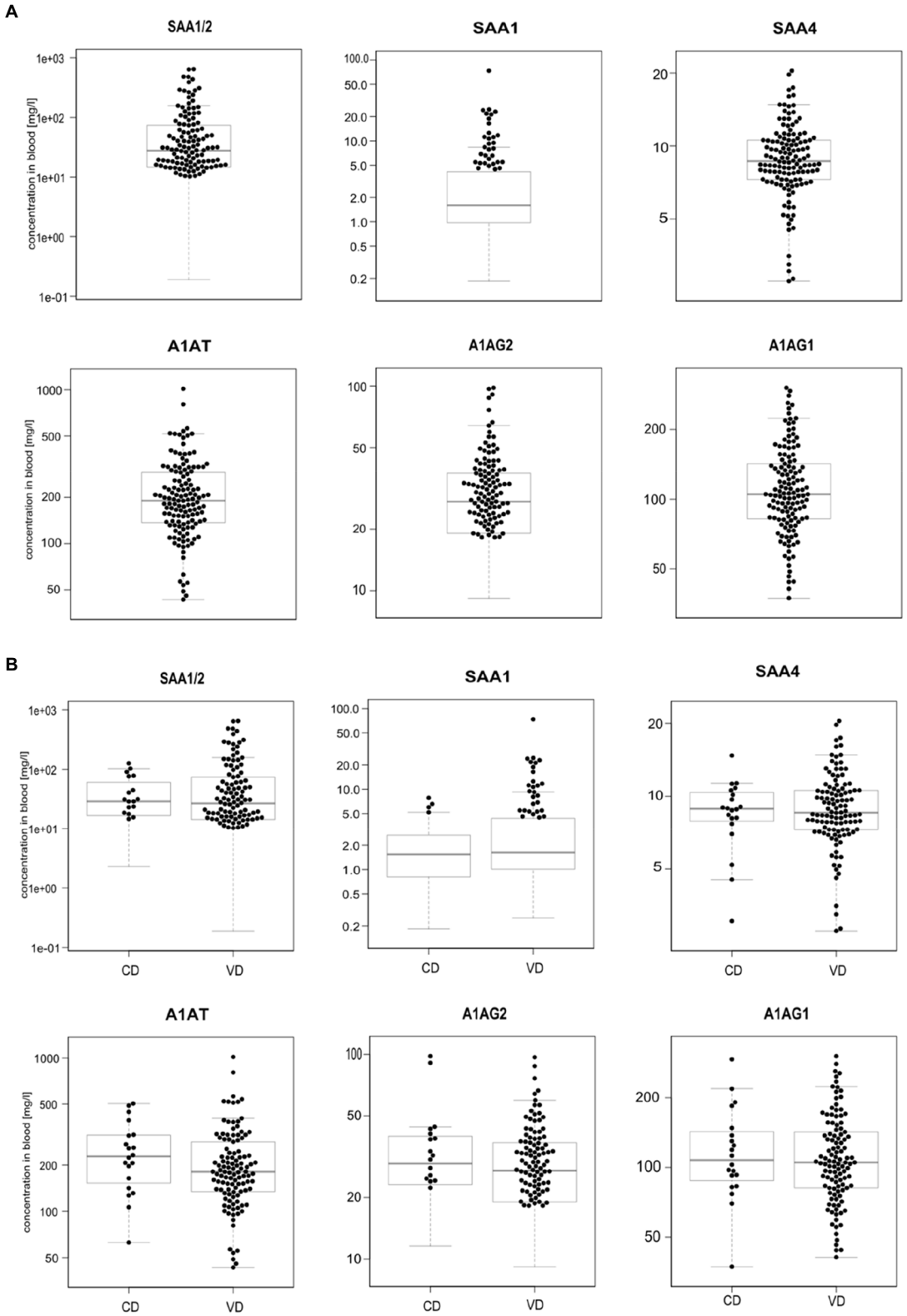

FIGURE 3 | Boxplots of acute-phase protein levels were determined in 134 neonatal DBS **(A)** and grouped according to the delivery mode (VD, vaginal delivery, CD, cesarean delivery; **B**). Sample concentrations >LOQ marked with black dots. Y-axis is in log-scale.

TABLE 2 | The lowest, the highest, and median levels of acute-phase proteins in DBS.

Protein	UniProt entry	Surrogate peptide	# samples >LOQ	Median concentration (mg/L of blood)	The lowest concentration (mg/L of blood)	The highest concentration (mg/L of blood)
SAA1	PODJI8	FFGHGAEDSLADQAANEWGR	33	8.1	<LOQ	73.6
SAA1/2	PODJI8/PODJI9	SFFSFLGEAFDGAR	120	30.9	<LOQ	644.9
SAA4	P35542	FRPDGLPK	134	8.7	2.8	20.4
CRP	P02741	ESDTSYVSLK	2	N/A	<LOQ	7.2
A1AT-1	P01009-1	AVLTIDEK	134	189.8	43.2	1016.1
A1AG1	P02763	NWGLSVYADKPETTK	134	105.0	37.3	302.7
A1AG2	P19652	SDVMYTDWK	107	32.0	<LOQ	98.0

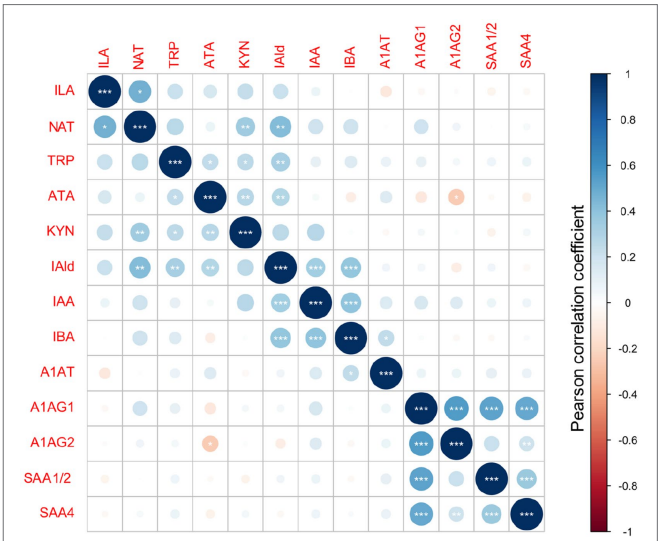

FIGURE 4 | Metabolites and acute-phase proteins correlation in DBS. Values of Pearson correlation coefficients are color-coded. The statistical significance is marked with *** for $p < 0.001$, ** for $p < 0.01$ and * for $p < 0.05$.

was observed for ATA/A1AG2 pair, and a positive Pearson correlation ($p < 0.05$) was between the A1AT/IBA pair. Metabolite precursor and product pairs were correlated ($p < 0.001$) – for instance, IAld/IAA, IAld/IBA, and IBA/IAA (**Figures 1B, 4, 5**). Significant correlations ($p < 0.01$ and $p < 0.001$) for metabolite pairs were observed for VD neonates (**Supplementary Figure S-7**) and all 134 neonates (**Figure 4**).

The VD subgroup (**Supplementary Figure S-7**) showed positive statistically significant correlations between metabolites and nonsignificant correlations between metabolites and proteins. The correlation pattern between metabolites and proteins in the CD subgroup differed from VD neonates (**Supplementary Figure S-7**). Positively correlated were A1AG1/SAA4 proteins ($p < 0.01$) and the A1AG1/A1AG2 isoforms ($p < 0.001$). In contrast with the VD subgroup, putative negative correlations were noted in the CD subgroup for IAA/NAT, IAA/ATA, TRP/IAA, IBA/ATA, ATA/(A1AG1 and A1AG2), IAld/SAA4, and ILA/A1AT pairs (**Supplementary Figure S-7**). Several metabolite/metabolite and metabolite/protein pairs showed a reversed correlation (positive/negative) comparing VD and CD groups. For instance, the ILA/IAA pair positively correlated in VD but negatively in CD neonates (**Supplementary Figure S-8**).

Different enzymes and, therefore, pathways are enriched depending on the delivery mode. The most significant correlations indicate metabolites converted from TRP *via* microbial TMO/TrD in VD neonates (**Figures 4, 5A**). For CD neonates, the enriched enzymes are TMO/TrD and AAT, fldH, and AO1, producing ILA, IAld, and IAA (**Figure 5B**).

DISCUSSION

This study aimed to investigate immunomodulatory microbial tryptophan and kynurenine ligands to AHR and PXR along

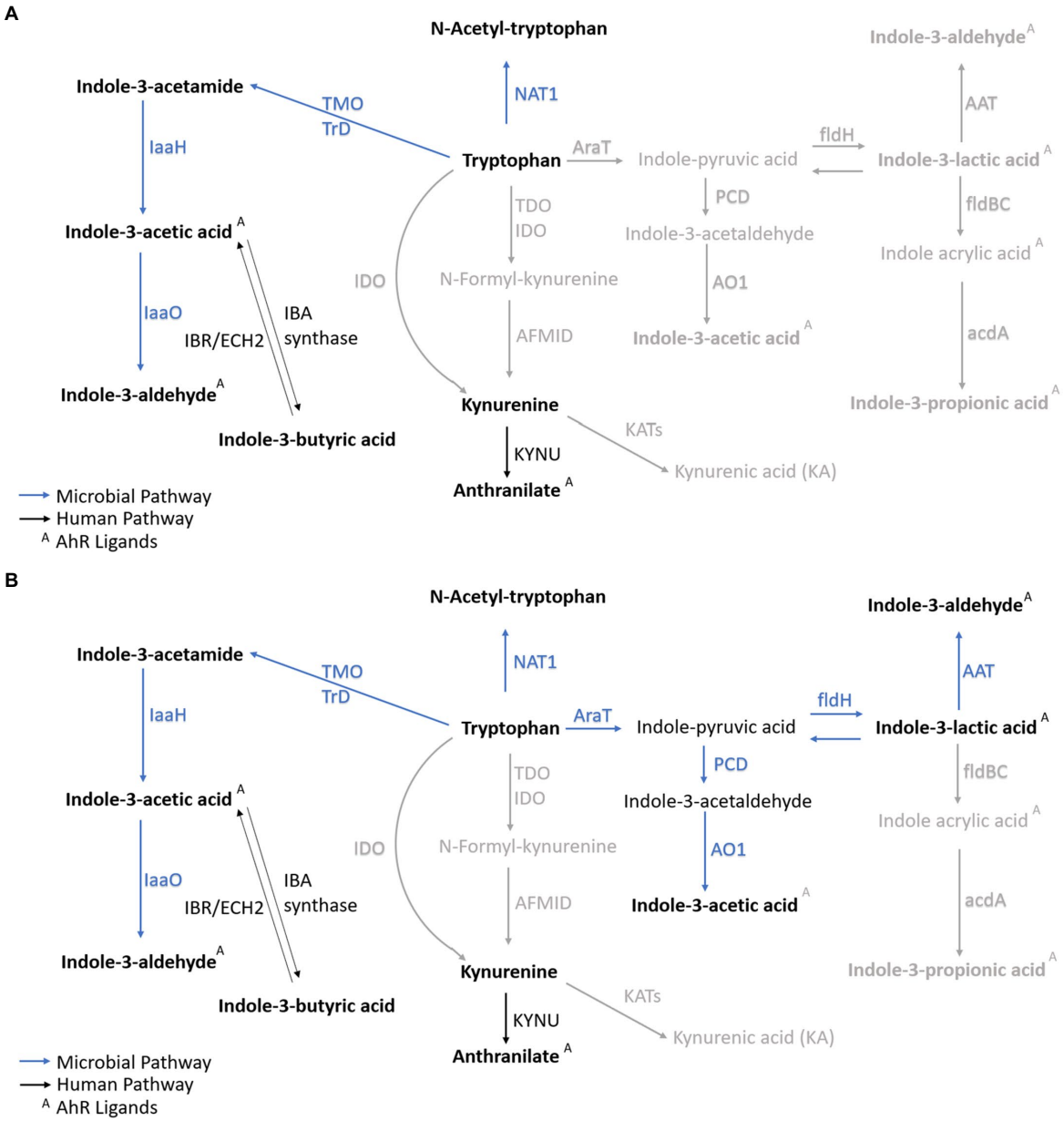

FIGURE 5 | Metabolic profile of VD and CD neonates. Correlated metabolites ($p < 0.01$ and/or $p < 0.001$) in VD neonates **(A)** and CD neonates **(B)** are marked in bold. Nonsignificant correlations are marked in gray. The microbial catabolites with significant correlations are highlighted in dark blue. The host metabolism products are marked in black. ArAT, aromatic amino acid aminotransferase, AAT, aromatic amino acid transferase, acdA, acyl-CoA dehydrogenase, AFMID, kynurenine formamidase, AO1, indole acetaldehyde oxidase, ECH2, enoyl-CoA hydratase-2, fldH, phenyl lactate dehydrogenase, fldBC, phenyl lactate dehydratase, IDO, indoleamine-2,3-dioxygenase, IaaH, indole acetamide hydrolase, IaaO, indole-3-acetic acid oxidase, KYNU, kynureninase, KAT, kynurenine amino transferase, MAO, monoamine oxygenase, NAT1, arylamine N-acetyltransferase 1, porB,C, pyruvate ferredoxin oxidoreductase B and C, PCD, pyruvate decarboxylase, TDO, tryptophan-2,3-dioxygenase, TMO, tryptophan-2-monooxygenase, TrD, tryptophan decarboxylase.

with APP levels in neonatal DBS to explore potential correlations or patterns specific to the delivery mode (CS and VD). We developed a protocol for simultaneous APP quantification and microbial catabolites profiling in neonatal DBS. IAA levels profiled in DBS were reported previously (Dénes et al., 2012; Freeman et al., 2018). However, we are the first to report neonatal IAld, IBA, and IAM levels.

The Mode of Delivery, Circulating Metabolite Profile, and Protein Levels

The circulating profile of tryptophan and kynurenine catabolites and APPs was compared in CD ($n = 20$) and VD ($n = 114$) neonates. Microbial enzymes (i.e., TMO/TrD, NAT1, IaaH, and IaaO) characterize VD neonates' metabolic profiles. On the other hand, AraT, fldH, AAT, and AO1 primarily determined

the CD neonates' metabolite profile. High SAA1 levels (>10 mg/l) were observed in 13 VD neonates. However, the overall difference between VD and CD groups was not statistically significant. The microbial colonization and immune system response develop rapidly on the second day of life (Martin et al., 2010). Shao et al. compared the microbial diversity in CD and VD neonates and found substantial differences between the first and the fourth day of life (Shao et al., 2019).

Supportive Role of Acute-Phase Proteins to the Immune System

We attempted to link metabolite and protein profiles in DBS to clinical anamnestic data. Each APP has a unique role in shaping an infant's immune system, and there is a cross-talk between quantified metabolites and APPs. Once the inflammation signal passes through IL-6 and IL-1 to APP production in hepatocytes, these proteins trigger a systemic response to modulate the immune system (Ackermann, 2017; Zachary, 2017). A1AT inhibits the production of TNF-α and the metalloprotease in macrophages and regulates CD14 and TLR4 expression to reduce pro-inflammatory stimuli (i.e., IL-1 and IL-6) and upregulate anti-inflammatory cytokines (i.e., IL-10, TGF-ß; Breit et al., 1985; Bergin et al., 2012; Baraldo et al., 2015; Cosio et al., 2016). In murine and human studies, A1AT modulates dendritic cells and increases $FoxP3^+$ T-regulatory cells (Marcondes et al., 2014; Berger et al., 2018). Inflammatory cytokines (i.e., IL-6, IL-1, and TNF) primarily regulate APPs production in hepatocytes (Ackermann, 2017; Zachary, 2017). Pro-inflammatory cytokines stimulate an essential IDO1 pathway in macrophages (Alberati-Giani et al., 1996; Prendergast et al., 2011). TRP and KYN are the rate-limiting substrates for the IDO1 enzyme (Zhang et al., 2019).

KYN pathway is one of the main degradation routes for dietary tryptophan (**Figure 1B**). IDO converts TRP to KYN, a crucial metabolite in maintaining immune homeostasis (Ding et al., 2020; Wyatt and Greathouse, 2021). In humans is encoded by the IDO1 gene expressed in immune cells (i.e., monocytes, macrophages, and dendritic cells), necessary in antigen presentation (Nikolaus et al., 2017). As investigated in this study, IDO expression regulates T-cell differentiation to avoid tissue damage and oxidative stress (Le Floc'h et al., 2011). KYN metabolites can cross the blood–brain barrier further and act as neuroprotectants (Roth et al., 2021; Wyatt and Greathouse, 2021). KYN enters the brain from the blood circulation *via* the amino acid transporter, taken up by astrocytes and microglial cells (Atilla and Basak, 2015).

The Interaction Between Catabolites of Tryptophan and Acute-Phase Proteins

TRP, an essential amino acid in human nutrition, cannot be produced in mammalian cells (Atilla and Basak, 2015). The indole catabolites of TRP mediate the immune system development and homeostasis *via* various mechanisms of action. Our results suggest a cross-talk between metabolites and APPs observed as diverse correlations between metabolites and APPs relative to the mode of delivery. For instance, a stronger negative correlation between A1AG2/ATA was observed in CD compared to VD neonates. The APP and metabolite pair, A1AG2 and ATA, both carry out supportive functions essential for developing the neonatal immune system. The metabolites such as ATA and KYN have an epigenetic effect in the methylation and glycosylation of hypothalamic neuronal peptide coding genes and neuronal differentiation-related loci (increase in H3K4 methylation and H2AS40 O-GlcNAcylation). By increasing methylation and histone modification, gene expression is stabilized, and DNA mutation is avoided (Hayakawa et al., 2019).

TRP catabolites are AhR and/or PXR ligands assuring in their function the healthy development of the neonate (Li et al., 2021). The paramount importance is establishing the gut barrier and blood–brain barrier (BBB) function in early life development. The aryl hydrocarbon receptor is a ligand-receptor transcription factor (TF) activated by TRP and its metabolites. The TF is expressed by many immune system cells such as macrophages, dendritic cells, NK cells, B lymphocytes, and subtypes of T cells as Th17 and Treg cells (Ambrosio et al., 2019). PXR is also expressed in many cells, most widely in the liver, intestines, kidneys, and intestinal epithelial cells. The ligand-activated TF is activated by naturally occurring steroids and synthetic glucocorticoids. Furthermore, the PXR receptor controls various physiological processes and the metabolism of lipids, glucose, and bile acids (Illés et al., 2020).

IPA was shown to fortify the intestinal barrier by engaging the PXR. IPA is produced by gut microbiota from dietary TRP, which accumulates the host serum (Danaceau et al., 2003; Dodd et al., 2017). IPA activates PXR and induces downregulation of the toll-like receptors, mainly TLR4, and its downstream signaling pathway. In the murine intestine, IPA downregulated enterocytes-mediated inflammatory cytokine TNFα and upregulated junctional protein markers (Venkatesh et al., 2014). The essential gene for IPA, synthesized by aromatic amino acid metabolism in the gut by the bacterium *Clostridium sporogenes*, is *fldC* with a broad impact on human immune cells (Dodd et al., 2017). The authors observed a different spectrum of adaptive immune response in Δ*fldC* mutant. The *fldC* mutant showed higher circulating myeloid cells, including neutrophils and $Ly6C^+$ monocytes and increased antigen-experienced effector/memory T cells. In addition, secretory IgA levels were increased in *fldC* mutant mice (Dodd et al., 2017). IPA plays an essential role in intestinal barrier regulation, also crucial in the physiological development of neonates after delivery.

IPA has further also radical scavenging activity and has neuronal properties (Kaufmann, 2018). It inhibits β-amyloid fibril formation and can act as a neuroprotectant against various oxidants (Bendheim et al., 2002). IPA also has chemical chaperone activity and suppresses endoplasmic reticulum stress-induced neuronal cell death (Mimori et al., 2019). Further PXR agonists are IAM and IAA. This interaction through the PXR leads to the inhibition of NF-κB signaling pathway (Illés et al., 2020). Therefore, PXR has anti-inflammatory properties (Zhou et al., 2006; Okamura et al., 2020).

We observed significant correlations indicating metabolites conversion from TRP to NAT, IAld, KYN, and ATA *via* microbial TMO/TrD and NAT in VD neonates. The profiled metabolites show the importance of a gut–brain axis in the systemic response and intestinal homeostasis regulation. For example, NAT is a substance P-receptor antagonist (Fernandes et al., 2018) and a neuroprotective agent (Sirianni et al., 2015). IAld, as an AHR agonist, stimulates the production of IL-22 (Zelante et al., 2013). The cytokine IL-22, produced in the liver, kidneys, pancreas, skin, and intestine, induces tissue regeneration and supports antimicrobial molecules' production, helping develop a defense line against tissue damage and microbial infection (Dudakov et al., 2015). The mucosal immune homeostasis was recently investigated in a murine model of autoimmune inflammation. IAld administered in the gut alleviated hepatic inflammation and fibrosis by modulating the intestinal microbiota by activating the AhR-IL-22-axis to restore mucosal integrity (D'Onofrio et al., 2021). It agrees with the finding that microbial-produced IAld further provides mucosal protection from inflammation in the host innate immune system, where the cytokine IL-22 *via* AhR receptor promoted IL-18 expression. Both the innate and the adaptive immune system are involved (Borghi et al., 2019). Furthermore, IAld attenuates the increase in epithelial permeability caused by stimulation with a pro-inflammatory cytokine TNFα in a dose-dependent manner (Scott et al., 2020). IAld regulates gut barrier integrity through tight junctions (e.g., zonulin and occludin) and adherens junctions, which are essential for regulating intestinal permeability (Zihni et al., 2016; Scott et al., 2020).

For CD neonates, the enriched enzymes are TMO/TrD and AAT, fldH, and AO1, producing KYN, ILA, IAld, and IAA. The different enriched enzymes and pathways show that other routes are taken on the second day of life in CD and VD neonates, visible and emphasized in the correlation matrix plots for VD and CD neonates, showing markedly different patterns. The function of ILA was investigated in the gnotobiotic mice model, and it was found that ILA reprograms intraepithelial lymphocytes (IELs, $CD4^+$T cells) into double-positive IELs ($CD8aa^+CD4^+$) with immunoregulatory function (Cervantes-Barragan et al., 2017). Moreover, ILA from breastmilk was identified as an anti-inflammatory metabolite. ILA requires the interaction with TLR4 and the AHR receptor to interfere with its transcription of the inflammatory cytokine IL-8 that causes excessive inflammation in the premature intestine (Meng et al., 2020). *In vivo* and *in vitro* results showed pleiotropic protective effects on immature enterocytes, including anti-inflammatory, antiviral, and developmental regulatory potential in a region-dependent and age-dependent manner. The further transcriptomic analysis showed that ILA has a regulatory effect on the STAT1 pathway. The STAT1 pathway plays an essential role in IL-1β-induced inflammation (Huang et al., 2021).

ATA is a product of dietary tryptophan and has anti-inflammatory properties on Na^+/dicarboxylate cotransporters, NaDC1, and NaCT (Pajor and Sun, 2013). IAA levels positively correlate with intestinal IL-22 levels, through which antimicrobial proteins are targeted, and mucosal inflammation is downregulated (Laurans et al., 2018; Natividad et al., 2018). In addition, IAA has a protective effect against lipopolysaccharide (LPS)-induced inflammatory response and free radical generation in macrophages. IAA significantly ameliorated LPS-induced expression of interleukin-1β (IL-1β), interleukin-6 (IL-6), and monocyte chemoattractant protein-1 (MCP-1) as well as generation of reactive oxidative species (ROS) and nitric oxide (NO). LPS-triggered nuclear translocation of nuclear factor kappa B (NF-κB) p65 was mitigated by IAA treatment (Ji et al., 2020). In a previous study, Ji et al. showed in mice that IAA mitigates high-fat diet-induced evaluation in fasting blood glucose and total plasma cholesterol, low-density lipoprotein cholesterol, and glutamic pyruvic transaminase activity. IAA supports the liver function linked with mitigated total triglycerides and cholesterol concentration and upregulation of genes involved in lipogenesis. Furthermore, IAA was shown to protect against reactive oxygen species and attenuate the inflammatory response in the liver of mice exposed to a high-fat diet (Ji et al., 2019).

Overall, we profiled microbial metabolites of the kynurenine and tryptophan pathway and acute-phase proteins in 3 μl of dried blood, and we first reported neonatal IAld, IBA, and IAM levels. We observed divergent metabolic profiles in VD and CD neonates. The different colonization of the initial microbial metabolites could be caused by distinct microbial tryptophan degradation routes in VD and CD. In VD, the enriched pathways could lead to higher NAT, KYN, and ATA metabolite levels. In CD neonates, the enriched bacterial enzymes could lead to higher KYN, IAld, ILA, and IAA levels. Despite the diverse TRP catabolism, our results point to indole catabolites' distinct profile on the second day of life in VD and CD neonates, demonstrated through different TRP metabolites, independently of unique postnatal microbial colonization at VD and CD (Sanidad and Zeng, 2020).

We quantified in our study indole catabolites in both delivery modalities (vaginal and cesarean delivery) but found no significant differences in both groups. However, this study's limitations are the small number of CD neonates relative to VD and a single-point sampling. Correlations between metabolites and proteins in CD neonates require validation in a more extensive follow-up cohort study. In summary, we attempted to elucidate the mechanism of the immunomodulatory function of microbial metabolites. A further potential distinction will develop in the infant's microbiome composition and metabolite profile over time. Our findings suggest the supportive role of human gut microbiota in developing and maintaining immune system homeostasis.

DATA AVAILABILITY STATEMENT

The datasets presented in this study can be found in online repositories at https://panoramaweb.org/Aust_et_al_SI.url and the ProteomeXchange ID: PXD027606.

ETHICS STATEMENT

The studies involving human participants were reviewed and approved by the Committee for Ethics of CELSPAC: TNG (CELSPAC/EK/4/2016) at University Hospital Brno, Czechia. Written informed consent to participate in this study was provided by the participants' legal guardian/next of kin.

AUTHOR CONTRIBUTIONS

A-CA, EBe, KC, VV, and ZS designed the experiments. A-CA, KC, and EBe carried out the experiments and analyzed the data. IB and PJ recruited the study subjects and collected the biological samples. SS and EBu performed the statistical analysis. A-CA, EBe, VT, and ZS wrote the manuscript with input from all authors. JK, VT, and ZS conceived the study and supervised the project. All authors contributed to the article and approved the submitted version.

FUNDING

The study was supported by the Grant Agency of the Czech Republic (17-24592Y), the RECETOX research infrastructure (LM2018121) financed by the Ministry of Education, Youth and Sports, and Operational Programme Research, Development, and Innovation - project CETOCOEN EXCELLENCE (CZ.02.1.01/0.0/0.0/17_043/0009632) and project CETOCOEN PLUS (CZ.02.1.01/0.0/0.0/15_003/0000469) and the Ministry of Health, the Czech Republic – FNBr (65269705).

SUPPLEMENTARY MATERIAL

The Supplementary Material for this article can be found online at: https://www.frontiersin.org/articles/10.3389/fmicb.2021.665743/full#supplementary-material

REFERENCES

Ackermann, M. R. (2017). "Chapter 3: Inflammation and healing," in *Pathologic Basis of Veterinary Disease. 6th Edn.* ed. J. F. Zachary (Amsterdam, Netherlands: Mosby), 73.e2–131.e2.

Agus, A., Planchais, J., and Sokol, H. (2018). Gut microbiota regulation of tryptophan metabolism in health and disease. *Cell Host Microbe* 23, 716–724. doi: 10.1016/j.chom.2018.05.003

Alberati-Giani, D., Ricciardi-Castagnoli, P., Köhler, C., and Cesura, A. M. (1996). Regulation of the kynurenine metabolic pathway by interferon-gamma in murine cloned macrophages and microglial cells. *J. Neurochem.* 66, 996–1004. doi: 10.1046/j.1471-4159.1996.66030996.x

Alexeev, E. E., Lanis, J. M., Schwisow, K. D., Kominsky, D. J., and Colgan, S. P. (2016). Microbiota-derived tryptophan metabolites activate aryl hydrocarbon receptor and induce IL-10 receptor expression in intestinal epithelia. *FASEB J.* 30:57.2. doi: 10.1096/fasebj.30.1_supplement.57.2

Ambrosio, L. F., Insfran, C., Volpini, X., Rodriguez, E. A., Serra, H. M., Quintana, F. J., et al. (2019). Role of aryl hydrocarbon receptor (AhR) in the regulation of immunity and immunopathology during trypanosoma cruzi infection. *Front. Immunol.* 10:631. doi: 10.3389/fimmu.2019.00631

Antweiler, R. C. (2015). Evaluation of statistical treatments of left-censored environmental data using coincident uncensored data sets. II. Group comparisons. *Environ. Sci. Technol.* 49, 13439–13446. doi: 10.1021/acs.est.5b02385

Aragozzini, F., Ferrari, A., Pacini, N., and Gualandris, R. (1979). Indole-3-lactic acid as a tryptophan metabolite produced by *Bifidobacterium* spp. *Appl. Environ. Microbiol.* 38, 544–546. doi: 10.1128/aem.38.3.544-546.1979

Arnon, S., Litmanovitz, I., Regev, R. H., Bauer, S., Shainkin-Kestenbaum, R., and Dolfin, T. (2007). Serum amyloid A: an early and accurate marker of neonatal early-onset sepsis. *J. Perinatol.* 27, 297–302. doi: 10.1038/sj.jp.7211682

Atilla, E., and Basak, E. A. (2015). *Tryptophan Metabolism: Implications for Biological Processes, Health and Disease. 1st Edn.* eds. A. Engin and A. B. Engin (Totowa, New Jersey, United States: Humana Press).

Baraldo, S., Turato, G., Lunardi, F., Bazzan, E., Schiavon, M., Ferrarotti, I., et al. (2015). Immune activation in α1-antitrypsin-deficiency emphysema. Beyond the protease-antiprotease paradigm. *Am. J. Respir. Crit. Care Med.* 191, 402–409. doi: 10.1164/rccm.201403-0529OC

Bendheim, P. E., Poeggeler, B., Neria, E., Ziv, V., Pappolla, M. A., and Chain, D. G. (2002). Development of indole-3-propionic acid (OXIGON™) for Alzheimer's disease. *J. Mol. Neurosci.* 19, 213–217. doi: 10.1007/s12031-002-0036-0

Bennet, R., and Nord, C. E. (1987). Development of the faecal anaerobic microflora after caesarean section and treatment with antibiotics in newborn infants. *Infection* 15, 332–336. doi: 10.1007/BF01647733

Berger, M., Liu, M., Uknis, M. E., and Koulmanda, M. (2018). Alpha-1-antitrypsin in cell and organ transplantation. *Am. J. Transplant.* 18, 1589–1595. doi: 10.1111/ajt.14756

Bergin, D. A., Hurley, K., McElvaney, N. G., and Reeves, E. P. (2012). Alpha-1 antitrypsin: a potent anti-inflammatory and potential novel therapeutic agent. *Arch. Immunol. Ther. Exp.* 60, 81–97. doi: 10.1007/s00005-012-0162-5

Bezirtzoglou, E. (1997). The intestinal microflora during the first weeks of life. *Anaerobe* 3, 173–177. doi: 10.1006/anae.1997.0102

Borghi, M., Pariano, M., Solito, V., Puccetti, M., Bellet, M. M., Stincardini, C., et al. (2019). Targeting the aryl hydrocarbon receptor with indole-3-aldehyde protects from vulvovaginal candidiasis via the IL-22-IL-18 cross-talk. *Front. Immunol.* 10:2364. doi: 10.3389/fimmu.2019.02364

Breit, S. N., Wakefield, D., Robinson, J. P., Luckhurst, E., Clark, P., and Penny, R. (1985). The role of alpha 1-antitrypsin deficiency in the pathogenesis of immune disorders. *Clin. Immunol. Immunopathol.* 35, 363–380. doi: 10.1016/0090-1229(85)90097-2

Buck, M., Gouwy, M., Wang, J., Snick, J., Opdenakker, G., Struyf, S., et al. (2016). Structure and expression of different serum amyloid A (SAA) variants and their concentration-dependent functions during host insults. *Curr. Med. Chem.* 23, 1725–1755. doi: 10.2174/0929867323666160418114600

Cai, H.-L., Li, H.-D., Yan, X.-Z., Sun, B., Zhang, Q., Yan, M., et al. (2012). Metabolomic analysis of biochemical changes in the plasma and urine of first-episode neuroleptic-naïve schizophrenia patients after treatment with risperidone. *J. Proteome Res.* 11, 4338–4350. doi: 10.1021/pr300459d

Cervantes-Barragan, L., Chai, J. N., Tianero, M. D., Di Luccia, B., Ahern, P. P., Merriman, J., et al. (2017). *Lactobacillus reuteri* induces gut intraepithelial CD4+CD8αα+ T cells. *Science* 357, 806–810. doi: 10.1126/science.aah5825

Clyne, B., and Olshaker, J. S. (1999). The C-reactive protein. *J. Emerg. Med.* 17, 1019–1025. doi: 10.1016/S0736-4679(99)00135-3

Cosio, M. G., Bazzan, E., Rigobello, C., Tinè, M., Turato, G., Baraldo, S., et al. (2016). Alpha-1 antitrypsin deficiency: beyond the protease/antiprotease paradigm. *Ann. Am. Thorac. Soc.* 13(Suppl. 4), S305–S310. doi: 10.1513/AnnalsATS.201510-671KV

CRAN (2021). Package beeswarm (9AD). Available at: https://cran.r-project.org/web/packages/beeswarm/index.html (Accessed August 6, 2021).

Danaceau, J. P., Anderson, G. M., McMahon, W. M., and Crouch, D. J. (2003). A liquid chromatographic-tandem mass spectrometric method for the analysis of serotonin and related indoles in human whole blood. *J. Anal. Toxicol.* 27, 440–444. doi: 10.1093/jat/27.7.440

Dénes, J., Szabó, E., Robinette, S. L., Szatmári, I., Szőnyi, L., Kreuder, J. G., et al. (2012). Metabonomics of newborn screening dried blood spot samples: a novel approach in the screening and diagnostics of inborn errors of metabolism. *Anal. Chem.* 84, 10113–10120. doi: 10.1021/ac302527m

Dileep, K. V., Remya, C., Tintu, I., Haridas, M., and Sadasivan, C. (2013). Interactions of selected indole derivatives with phospholipase A_2: *in silico* and *in vitro* analysis. *J. Mol. Model.* 19, 1811–1817. doi: 10.1007/s00894-012-1741-4

Ding, X., Bin, P., Wu, W., Chang, Y., and Zhu, G. (2020). Tryptophan metabolism, regulatory T cells, and inflammatory bowel disease: a mini review. *Mediat. Inflamm.* 2020:9706140. doi: 10.1155/2020/9706140

Dodd, D., Spitzer, M. H., Van Treuren, W., Merrill, B. D., Hryckowian, A. J., Higginbottom, S. K., et al. (2017). A gut bacterial pathway metabolizes aromatic amino acids into nine circulating metabolites. *Nature* 551, 648–652. doi: 10.1038/nature24661

D'Onofrio, F., Renga, G., Puccetti, M., Pariano, M., Bellet, M. M., Santarelli, I., et al. (2021). Indole-3-carboxaldehyde restores gut mucosal integrity and protects from liver fibrosis in murine sclerosing cholangitis. *Cell* 10:1622. doi: 10.3390/cells10071622

Dudakov, J. A., Hanash, A. M., and van den Brink, M. R. M. (2015). Interleukin-22: immunobiology and pathology. *Annu. Rev. Immunol.* 33, 747–785. doi: 10.1146/annurev-immunol-032414-112123

Duranton, F., Cohen, G., Smet, R., Rodriguez, M., Jankowski, J., Vanholder, R., et al. (2012). Normal and pathologic concentrations of uremic toxins. *J. Am. Soc. Nephrol.* 23, 1258–1270. doi: 10.1681/ASN.2011121175

Elsden, S. R., Hilton, M. G., and Waller, J. M. (1976). The end products of the metabolism of aromatic amino acids by *Clostridia*. *Arch. Microbiol.* 107, 283–288. doi: 10.1007/BF00425340

Fernandes, J., Mudgal, J., Rao, C. M., Arora, D., Basu Mallik, S., Pai, K. S. R., et al. (2018). N-acetyl-L-tryptophan, a substance-P receptor antagonist attenuates aluminum-induced spatial memory deficit in rats. *Toxicol. Mech. Methods* 28, 328–334. doi: 10.1080/15376516.2017.1411412

Finegold, S. M., Molitoris, D., Song, Y., Liu, C., Vaisanen, M.-L., Bolte, E., et al. (2002). Gastrointestinal microflora studies in late-onset autism. *Clin. Infect. Dis.* 35, S6–S16. doi: 10.1086/341914

Francino, M. P. (2018). Birth mode-related differences in gut microbiota colonization and immune system development. *Ann. Nutr. Metab.* 73(Suppl. 3), 12–16. doi: 10.1159/000490842

Freeman, J. D., Rosman, L. M., Ratcliff, J. D., Strickland, P. T., Graham, D. R., and Silbergeld, E. K. (2018). State of the science in dried blood spots. *Clin. Chem.* 64, 656–679. doi: 10.1373/clinchem.2017.275966

Gao, J., Xu, K., Liu, H., Liu, G., Bai, M., Peng, C., et al. (2018). Impact of the gut microbiota on intestinal immunity mediated by tryptophan metabolism. *Front. Cell. Infect. Microbiol.* 8:13. doi: 10.3389/fcimb.2018.00013

Grönlund, M. M., Lehtonen, O. P., Eerola, E., and Kero, P. (1999). Fecal microflora in healthy infants born by different methods of delivery: permanent changes in intestinal flora after cesarean delivery. *J. Pediatr. Gastroenterol. Nutr.* 28, 19–25. doi: 10.1097/00005176-199901000-00007

Haran, J. P., Beaudoin, F. L., Suner, S., and Lu, S. (2013). C-reactive protein as predictor of bacterial infection among patients with an influenza-like illness. *Am. J. Emerg. Med.* 31, 137–144. doi: 10.1016/j.ajem.2012.06.026

Hayakawa, K., Nishitani, K., and Tanaka, S. (2019). Kynurenine, 3-OH-kynurenine, and anthranilate are nutrient metabolites that alter H3K4 trimethylation and H2AS40 O-GlcNAcylation at hypothalamus-related loci. *Sci. Rep.* 9:19768. doi: 10.1038/s41598-019-56341-x

Hazra, A., and Gogtay, N. (2017). Biostatistics series module 9: survival analysis. *Indian J. Dermatol.* 62, 251–257. doi: 10.4103/ijd.IJD_201_17

Heinrich, P. C., Castell, J. V., and Andus, T. (1990). Interleukin-6 and the acute phase response. *Biochem. J.* 265, 621–636. doi: 10.1042/bj2650621

Herberth, G., Offenberg, K., Rolle-Kampczyk, U., Bauer, M., Otto, W., Röder, S., et al. (2015). Endogenous metabolites and inflammasome activity in early childhood and links to respiratory diseases. *J. Allergy Clin. Immunol.* 136, 495–497. doi: 10.1016/j.jaci.2015.01.022

Hochepied, T., Berger, F. G., Baumann, H., and Libert, C. (2003). α1-acid glycoprotein: an acute phase protein with inflammatory and immunomodulating properties. *Cytokine Growth Factor Rev.* 14, 25–34. doi: 10.1016/S1359-6101(02)00054-0

Honoré, A. H., Aunsbjerg, S. D., Ebrahimi, P., Thorsen, M., Benfeldt, C., Knøchel, S., et al. (2016). Metabolic footprinting for investigation of antifungal properties of *Lactobacillus paracasei*. *Anal. Bioanal. Chem.* 408, 83–96. doi: 10.1007/s00216-015-9103-6

Huang, W., Cho, K. Y., Meng, D., and Walker, W. A. (2021). The impact of indole-3-lactic acid on immature intestinal innate immunity and development: a transcriptomic analysis. *Sci. Rep.* 11, 1–17. doi: 10.1038/s41598-021-87353-1

Human Metabolome Database (2021). Showing metabocard for L-Tryptophan (HMDB0000929) (2AD). Available at: https://hmdb.ca/metabolites/HMDB0000929 (Accessed August 6, 2021).

Illés, P., Krasulová, K., Vyhlídalová, B., Poulíková, K., Marcalíková, A., Pečinková, P., et al. (2020). Indole microbial intestinal metabolites expand the repertoire of ligands and agonists of the human pregnane X receptor. *Toxicol. Lett.* 334, 87–93. doi: 10.1016/j.toxlet.2020.09.015

Janciauskiene, S. M., Bals, R., Koczulla, R., Vogelmeier, C., Köhnlein, T., and Welte, T. (2011). The discovery of α1-antitrypsin and its role in health and disease. *Respir. Med.* 105, 1129–1139. doi: 10.1016/j.rmed.2011.02.002

Ji, Y., Gao, Y., Chen, H., Yin, Y., and Zhang, W. (2019). Indole-3-acetic acid alleviates nonalcoholic fatty liver disease in mice via attenuation of hepatic lipogenesis, and oxidative and inflammatory stress. *Nutrients* 11:2062. doi: 10.3390/nu11092062

Ji, Y., Yin, W., Liang, Y., Sun, L., Yin, Y., and Zhang, W. (2020). Anti-inflammatory and anti-oxidative activity of indole-3-acetic acid involves induction of HO-1 and neutralization of free radicals in RAW264.7 cells. *Int. J. Mol. Sci.* 21:1579. doi: 10.3390/ijms21051579

Jin, U.-H., Cheng, Y., Park, H., Davidson, L. A., Callaway, E. S., Chapkin, R. S., et al. (2017). Short chain fatty acids enhance aryl hydrocarbon (Ah) responsiveness in mouse colonocytes and Caco-2 human colon cancer cells. *Sci. Rep.* 7:10163. doi: 10.1038/s41598-017-10824-x

Kaufmann, S. H. E. (2018). Indole propionic acid: a small molecule links between gut microbiota and tuberculosis. *Antimicrob. Agents Chemother.* 62, e00389–e003818. doi: 10.1128/AAC.00389-18

Kloosterboer, S. M., Winter, B. C. M., Bahmany, S., Al-Hassany, L., Dekker, A., Dieleman, G. C., et al. (2018). Dried blood spot analysis for therapeutic drug monitoring of antipsychotics: drawbacks of its clinical application. *Ther. Drug Monit.* 40, 344–350. doi: 10.1097/FTD.0000000000000502

Krishnan, S., Ding, Y., Saedi, N., Choi, M., Sridharan, G. V., Sherr, D. H., et al. (2018). Gut microbiota-derived tryptophan metabolites modulate inflammatory response in hepatocytes and macrophages. *Cell Rep.* 23, 1099–1111. doi: 10.1016/j.celrep.2018.03.109

Lanis, J. M., Alexeev, E. E., Curtis, V. F., Kitzenberg, D. A., Kao, D. J., Battista, K. D., et al. (2017). Tryptophan metabolite activation of the aryl hydrocarbon receptor regulates IL-10 receptor expression on intestinal epithelia. *Mucosal Immunol.* 10, 1133–1144. doi: 10.1038/mi.2016.133

Laurans, L., Venteclef, N., Haddad, Y., Chajadine, M., Alzaid, F., Metghalchi, S., et al. (2018). Genetic deficiency of indoleamine 2,3-dioxygenase promotes gut microbiota-mediated metabolic health. *Nat. Med.* 24, 1113–1120. doi: 10.1038/s41591-018-0060-4

Le Floc'h, N., Otten, W., and Merlot, E. (2011). Tryptophan metabolism, from nutrition to potential therapeutic applications. *Amino Acids* 41, 1195–1205. doi: 10.1007/s00726-010-0752-7

Li, H., Illés, P., Karunaratne, C. V., Nordstrøm, L. U., Luo, X., Yang, A., et al. (2021). Deciphering structural bases of intestinal and hepatic selectivity in targeting pregnane X receptor with indole-based microbial mimics. *Bioorg. Chem.* 109:104661. doi: 10.1016/j.bioorg.2021.104661

Li, X.-H., Kim, S.-K., and Lee, J.-H. (2017). Anti-biofilm effects of anthranilate on a broad range of bacteria. *Sci. Rep.* 7:8604. doi: 10.1038/s41598-017-06540-1

Liu, Z., Li, L., Chen, W., Wang, Q., Xiao, W., Ma, Y., et al. (2018). Aryl hydrocarbon receptor activation maintained the intestinal epithelial barrier function through Notch1 dependent signaling pathway. *Int. J. Mol. Med.* 41, 1560–1572. doi: 10.3892/ijmm.2017.3341

Lombard, G. L., and Dowell, V. R. (1983). Comparison of three reagents for detecting indole production by anaerobic bacteria in microtest systems. *J. Clin. Microbiol.* 18, 609–613. doi: 10.1128/jcm.18.3.609-613.1983

Mackie, R. I., Sghir, A., and Gaskins, H. R. (1999). Developmental microbial ecology of the neonatal gastrointestinal tract. *Am. J. Clin. Nutr.* 69, 1035S–1045S. doi: 10.1093/ajcn/69.5.1035s

Magos, L. (1987). C. Lentner (ed.). Geigy scientific tables, 8th Edn. Vol. 1. Units of measurement. Body fluids. Composition of the body. Nutrition. 1981, 298 pp. Vol. 2. Introduction to statistics. Statistical tables. Mathematical formulae. 1982, 241 pp. Vol. 3. Physical chemistry. Composition of the blood. Haematology. Human somatometric data. 1984, 359 pp. Vol. 4. Biochemistry. Metabolism of xenobiotics. Inborn error of metabolism.

Pharmacogenetics and ecogenetics. 1986, 330 pp. Ciba-geigy, basel, £12.50 each volume. Distributed in U.K. by Farrand Press. *J. Appl. Toxicol.* 7:413. doi: 10.1002/jat.2550070617

Mändar, R., and Mikelsaar, M. (1996). Transmission of mother's microflora to the newborn at birth. *Biol. Neonate* 69, 30–35. doi: 10.1159/000244275

Mangge, H., Stelzer, I., Reininghaus, E., Weghuber, D., Postolache, T. T., and Fuchs, D. (2014). Disturbed tryptophan metabolism in cardiovascular disease. *Curr. Med. Chem.* 21, 1931–1937. doi: 10.2174/09298673216614030410552 6

Marchini, G., Berggren, V., Djilali-Merzoug, R., and Hansson, L.-O. (2000). The birth process initiates an acute phase reaction in the fetus-newborn infant. *Acta Paediatr.* 89, 1082–1086. doi: 10.1111/j.1651-2227.2000.tb03355.x

Marcondes, A. M., Karoopongse, E., Lesnikova, M., Margineantu, D., Welte, T., Dinarello, C. A., et al. (2014). α-1-antitrypsin (AAT)-modified donor cells suppress GVHD but enhance the GVL effect: a role for mitochondrial bioenergetics. *Blood* 124, 2881–2891. doi: 10.1182/blood-2014-04-570440

Martin, R., Nauta, A. J., Ben Amor, K., Knippels, L. M. J., Knol, J., and Garssen, J. (2010). Early life: gut microbiota and immune development in infancy. *Benef. Microbes* 1, 367–382. doi: 10.3920/BM2010.0027

Matsumiya, Y., Kato, N., Watanabe, K., and Kato, H. (2002). Molecular epidemiological study of vertical transmission of vaginal *Lactobacillus* species from mothers to newborn infants in Japanese, by arbitrarily primed polymerase chain reaction. *J. Infect. Chemother.* 8, 43–49. doi: 10.1007/s101560200005

Mechtler, T. P., Stary, S., Metz, T. F., Jesús, V. R., Greber-Platzer, S., Pollak, A., et al. (2012). Neonatal screening for lysosomal storage disorders: feasibility and incidence from a nationwide study in Austria. *Lancet* 379, 335–341. doi: 10.1016/S0140-6736(11)61266-X

Meng, D., Sommella, E., Salviati, E., Campiglia, P., Ganguli, K., Djebali, K., et al. (2020). Indole-3-lactic acid, a metabolite of tryptophan, secreted by *Bifidobacterium longum* subspecies infantis is anti-inflammatory in the immature intestine. *Pediatr. Res.* 88, 209–217. doi: 10.1038/s41390-019-0740-x

Mimori, S., Kawada, K., Saito, R., Takahashi, M., Mizoi, K., Okuma, Y., et al. (2019). Indole-3-propionic acid has chemical chaperone activity and suppresses endoplasmic reticulum stress-induced neuronal cell death. *Biochem. Biophys. Res. Commun.* 517, 623–628. doi: 10.1016/j.bbrc.2019.07.074

Mitsou, E. K., Kirtzalidou, E., Oikonomou, I., Liosis, G., and Kyriacou, A. (2008). Fecal microflora of Greek healthy neonates. *Anaerobe* 14, 94–101. doi: 10.1016/j.anaerobe.2007.11.002

Natividad, J. M., Agus, A., Planchais, J., Lamas, B., Jarry, A. C., Martin, R., et al. (2018). Impaired aryl hydrocarbon receptor ligand production by the gut microbiota is a key factor in metabolic syndrome. *Cell Metab.* 28, 737–749. doi: 10.1016/j.cmet.2018.07.001

Neu, J., and Rushing, J. (2011). Cesarean versus vaginal delivery: long-term infant outcomes and the hygiene hypothesis. *Clin. Perinatol.* 38, 321–331. doi: 10.1016/j.clp.2011.03.008

Nikolaus, S., Schulte, B., Al-Massad, N., Thieme, F., Schulte, D. M., Bethge, J., et al. (2017). Increased tryptophan metabolism is associated with activity of inflammatory bowel diseases. *Gastroenterology* 153, 1504.e2–1516.e2. doi: 10.1053/j.gastro.2017.08.028

Okamura, M., Shizu, R., Abe, T., Kodama, S., Hosaka, T., Sasaki, T., et al. (2020). PXR functionally interacts with NF-κB and AP-1 to downregulate the inflammation-induced expression of chemokine CXCL2 in mice. *Cell* 9:2296. doi: 10.3390/cells9102296

Pajor, A. M., and Sun, N. N. (2013). Nonsteroidal anti-inflammatory drugs and other anthranilic acids inhibit the Na+/dicarboxylate symporter from *Staphylococcus aureus*. *Biochemistry* 52, 2924–2932. doi: 10.1021/bi301611u

Palmer, C., Bik, E. M., DiGiulio, D. B., Relman, D. A., and Brown, P. O. (2007). Development of the human infant intestinal microbiota. *PLoS Biol.* 5:e177. doi: 10.1371/journal.pbio.0050177

Pavlova, T., Vidova, V., Bienertova-Vasku, J., Janku, P., Almasi, M., Klanova, J., et al. (2017). Urinary intermediates of tryptophan as indicators of the gut microbial metabolism. *Anal. Chim. Acta* 987, 72–80. doi: 10.1016/j.aca.2017.08.022

Penders, J., Thijs, C., Vink, C., Stelma, F. F., Snijders, B., Kummeling, I., et al. (2006). Factors influencing the composition of the intestinal microbiota in early infancy. *Pediatrics* 118, 511–521. doi: 10.1542/peds.2005-2824

Prendergast, G. C., Chang, M. Y., Mandik-Nayak, L., Metz, R., and Muller, A. J. (2011). Indoleamine 2,3-dioxygenase as a modifier of pathogenic inflammation in cancer and other inflammation-associated diseases. *Curr. Med. Chem.* 18, 2257–2262. doi: 10.2174/092986711795656072

Roager, H. M., and Licht, T. R. (2018). Microbial tryptophan catabolites in health and disease. *Nat. Commun.* 9:3294. doi: 10.1038/s41467-018-05470-4

Romagnani, S. (2006). Regulation of the T cell response. *Clin. Exp. Allergy* 36, 1357–1366. doi: 10.1111/j.1365-2222.2006.02606.x

Roth, W., Zadeh, K., Vekariya, R., Ge, Y., and Mohamadzadeh, M. (2021). Tryptophan metabolism and gut-brain homeostasis. *Int. J. Mol. Sci.* 22, 1–23. doi: 10.3390/ijms22062973

Russell, W. R., Duncan, S. H., Scobbie, L., Duncan, G., Cantlay, L., Calder, A. G., et al. (2013). Major phenylpropanoid-derived metabolites in the human gut can arise from microbial fermentation of protein. *Mol. Nutr. Food Res.* 57, 523–535. doi: 10.1002/mnfr.201200594

Sain-van der Velden, M. G. M., van der Ham, M., Gerrits, J., Prinsen, H. C. M. T., Willemsen, M., Pras-Raves, M. L., et al. (2017). Quantification of metabolites in dried blood spots by direct infusion high resolution mass spectrometry. *Anal. Chim. Acta* 979, 45–50. doi: 10.1016/j.aca.2017.04.038

Sanidad, K. Z., and Zeng, M. Y. (2020). Neonatal gut microbiome and immunity. *Curr. Opin. Microbiol.* 56, 30–37. doi: 10.1016/j.mib.2020.05.011

Scott, S. A., Fu, J., and Chang, P. V. (2020). Microbial tryptophan metabolites regulate gut barrier function via the aryl hydrocarbon receptor. *Proc. Natl. Acad. Sci. U. S. A.* 117, 19376–19387. doi: 10.1073/pnas.2000047117

Shao, Y., Forster, S. C., Tsaliki, E., Vervier, K., Strang, A., Simpson, N., et al. (2019). Stunted microbiota and opportunistic pathogen colonization in caesarean-section birth. *Nature* 574, 117–121. doi: 10.1038/s41586-019-1560-1

Sirianni, A. C., Jiang, J., Zeng, J., Mao, L. L., Zhou, S., Sugarbaker, P., et al. (2015). N-acetyl-l-tryptophan, but not N-acetyl-d-tryptophan, rescues neuronal cell death in models of amyotrophic lateral sclerosis. *J. Neurochem.* 134, 956–968. doi: 10.1111/jnc.13190

Smith, E. A., and Macfarlane, G. T. (1996). Enumeration of human colonie bacteria producing phenolic and indolic compounds: effects of pH, carbohydrate availability and retention time on dissimilatory aromatic amino acid metabolism. *J. Appl. Bacteriol.* 81, 288–302. doi: 10.1111/j.1365-2672.1996.tb04331.x

Tests for Normality [R package nortest version 1.0-4] (2021). Comprehensive R Archive Network (CRAN)UR. Available at: https://cran.r-project.org/web/packages/nortest/index.html (Accessed August 6, 2021).

Tonelli, D., Gattavecchia, E., and Gandolfi, M. (1982). Thin-layer chromatographic determination of indolic tryptophan metabolites in human urine using Sep-Pak C18 extraction. *J. Chromatogr.* 231, 283–289. doi: 10.1016/s0378-4347(00)81853-8

Torun, M. M., Bahar, H., Gür, E., Taştan, Y., Alikaşifoğlu, M., and Arvas, A. (2002). Anaerobic fecal flora in healthy breast-fed Turkish babies born by different methods. *Anaerobe* 8, 63–67. doi: 10.1006/anae.2002.0415

Various R Programming Tools for Plotting Data [R package gplots version 3.0.4] (2021). Comprehensive R Archive Network (CRAN)UR. Available at: https://cran.r-project.org/web/packages/gplots/index.html (Accessed August 6, 2021).

Venkatesh, M., Mukherjee, S., Wang, H., Li, H., Sun, K., Benechet, A. P., et al. (2014). Symbiotic bacterial metabolites regulate gastrointestinal barrier function via the xenobiotic sensor PXR and toll-like receptor 4. *Immunity* 41, 296–310. doi: 10.1016/j.immuni.2014.06.014

Vidova, V., and Spacil, Z. (2017). A review on mass spectrometry-based quantitative proteomics: targeted and data independent acquisition. *Anal. Chim. Acta* 964, 7–23. doi: 10.1016/j.aca.2017.01.059

Vidova, V., Stuchlikova, E., Vrbova, M., Almasi, M., Klanova, J., Thon, V., et al. (2019). Multiplex assay for quantification of acute phase proteins and immunoglobulin A in dried blood spots. *J. Proteome Res.* 18, 380–391. doi: 10.1021/acs.jproteome.8b00657

Visualization of a Correlation Matrix [R package corrplot version 0.84] (2021). Comprehensive R Archive Network (CRAN)UR. Available at: https://cran.r-project.org/web/packages/corrplot/index.html (Accessed August 6, 2021).

Wall, R., Ross, R. P., Ryan, C. A., Hussey, S., Murphy, B., Fitzgerald, G. F., et al. (2009). Role of gut microbiota in early infant development. *Clin. Med. Pediatr.* 3, 45–54. doi: 10.4137/cmped.s2008

Wampach, L., Heintz-Buschart, A., Fritz, J. V., Ramiro-Garcia, J., Habier, J., Herold, M., et al. (2018). Birth mode is associated with earliest strain-conferred gut microbiome functions and immunostimulatory potential. *Nat. Commun.* 9:5091. doi: 10.1038/s41467-018-07631-x

Wickham, H. (2009). *ggplot2*. New York, NY: Springer-Verlag.

Wikoff, W. R., Anfora, A. T., Liu, J., Schultz, P. G., Lesley, S. A., Peters, E. C., et al. (2009). Metabolomics analysis reveals large effects of gut microflora

on mammalian blood metabolites. *Proc. Natl. Acad. Sci. U. S. A.* 106, 3698–3703. doi: 10.1073/pnas.0812874106

Williams, B. B., van Benschoten, A. H., Cimermancic, P., Donia, M. S., Zimmermann, M., Taketani, M., et al. (2014). Discovery and characterization of gut microbiota decarboxylases that can produce the neurotransmitter tryptamine. *Cell Host Microbe* 16, 495–503. doi: 10.1016/j.chom.2014.09.001

Wlodarska, M., Luo, C., Kolde, R., d'Hennezel, E., Annand, J. W., Heim, C. E., et al. (2017). Indoleacrylic acid produced by commensal peptostreptococcus species suppresses inflammation. *Cell Host Microbe* 22, 25.e6–37.e6. doi: 10.1016/j.chom.2017.06.007

Wyatt, M., and Greathouse, K. L. (2021). Targeting dietary and microbial tryptophan-indole metabolism as therapeutic approaches to colon cancer. *Nutrients* 13:1189. doi: 10.3390/nu13041189

Yamada, T., Wada, A., Yamaguchi, T., Itoh, Y., and Kawai, T. (1997). Automated measurement of a constitutive isotype of serum amyloid A/SAA4 and comparison with other apolipoproteins. *J. Clin. Lab. Anal.* 11, 363–368. doi: 10.1002/(SICI)1098-2825(1997)11:6<363::AID-JCLA10>3.0.CO;2-U

Zachary, J. F. (2017). *Pathologic Basis of Veterinary Disease. 6th Edn*. eds. J. F. Zachary and M. D. McGavin (Mosby).

Zelante, T., Iannitti, R. G., Cunha, C., Luca, A., Giovannini, G., Pieraccini, G., et al. (2013). Tryptophan catabolites from microbiota engage aryl hydrocarbon receptor and balance mucosal reactivity via interleukin-22. *Immunity* 39, 372–385. doi: 10.1016/j.immuni.2013.08.003

Zhang, Z., Tang, H., Chen, P., Xie, H., and Tao, Y. (2019). Demystifying the manipulation of host immunity, metabolism, and extraintestinal tumors by the gut microbiome. *Signal Transduct. Target. Ther.* 4:41. doi: 10.1038/s41392-019-0074-5

Zhao, S., Guo, Y., Sheng, Q., and Shyr, Y. (2014). Heatmap3: an improved heatmap package with more powerful and convenient features. *BMC Bioinformatics* 15(Suppl. 10):P16. doi: 10.1186/1471-2105-15-S10-P16

Zhou, C., Tabb, M., Nelson, E., Grün, F., Verma, S., Sandatrafiei, A., et al. (2006). Mutual repression between steroid and xenobiotic receptor and NF-kappaB signaling pathways links xenobiotic metabolism and inflammation. *J. Clin. Invest.* 116, 2280–2289. doi: 10.1172/JCI26283

Zihni, C., Mills, C., Matter, K., and Balda, M. S. (2016). Tight junctions: from simple barriers to multifunctional molecular gates. *Nat. Rev. Mol. Cell Biol.* 17, 564–580. doi: 10.1038/nrm.2016.80

Conflict of Interest: The authors declare that the research was conducted in the absence of any commercial or financial relationships that could be construed as a potential conflict of interest.

Publisher's Note: All claims expressed in this article are solely those of the authors and do not necessarily represent those of their affiliated organizations, or those of the publisher, the editors and the reviewers. Any product that may be evaluated in this article, or claim that may be made by its manufacturer, is not guaranteed or endorsed by the publisher.

Copyright © 2021 Aust, Benesova, Vidova, Coufalikova, Smetanova, Borek, Janku, Budinska, Klanova, Thon and Spacil. This is an open-access article distributed under the terms of the Creative Commons Attribution License (CC BY). The use, distribution or reproduction in other forums is permitted, provided the original author(s) and the copyright owner(s) are credited and that the original publication in this journal is cited, in accordance with accepted academic practice. No use, distribution or reproduction is permitted which does not comply with these terms.

frontiers in Immunology

MINI REVIEW
published: 01 November 2021
doi: 10.3389/fimmu.2021.717392

GPR35 in Intestinal Diseases: From Risk Gene to Function

Berna Kaya[1], *Hassan Melhem*[1] *and Jan Hendrik Niess*[1,2]*

[1] Department of Biomedicine, University of Basel, Basel, Switzerland, [2] Department of Gastroenterology/Hepatology, Clarunis - University Center for Gastrointestinal and Liver Diseases, Basel, Switzerland

Diet and gut microbial metabolites mediate host immune responses and are central to the maintenance of intestinal health. The metabolite-sensing G-protein coupled receptors (GPCRs) bind metabolites and trigger signals that are important for the host cell function, survival, proliferation and expansion. On the contrary, inadequate signaling of these metabolite-sensing GPCRs most likely participate to the development of diseases including inflammatory bowel diseases (IBD). In the intestine, metabolite-sensing GPCRs are highly expressed by epithelial cells and by specific subsets of immune cells. Such receptors provide an important link between immune system, gut microbiota and metabolic system. Member of these receptors, GPR35, a class A rhodopsin-like GPCR, has been shown to be activated by the metabolites tryptophan-derived kynurenic acid (KYNA), the chemokine CXCL17 and phospholipid derivate lysophosphatidic acid (LPA) species. There have been studies on GPR35 in the context of intestinal diseases since its identification as a risk gene for IBD. In this review, we discuss the pharmacology of GPR35 including its proposed endogenous and synthetic ligands as well as its antagonists. We elaborate on the risk variants of GPR35 implicated in gut-related diseases and the mechanisms by which GPR35 contribute to intestinal homeostasis.

Keywords: GPR35, microbiota, metabolites, ligand-receptor interactions, risk variants, inflammatory bowel diseases

OPEN ACCESS

Edited by:
Oscar Gilberto Gomez-Duarte, University at Buffalo, United States

Reviewed by:
Jochen Mattner, University Hospital Erlangen, Germany
Stefano Fiorucci, University of Perugia, Italy

***Correspondence:**
Jan Hendrik Niess
janhendrik.niess@unibas.ch

Specialty section:
This article was submitted to Microbial Immunology, a section of the journal Frontiers in Immunology

Received: *30 May 2021*
Accepted: *18 October 2021*
Published: *01 November 2021*

Citation:
Kaya B, Melhem H and Niess JH (2021) GPR35 in Intestinal Diseases: From Risk Gene to Function. Front. Immunol. 12:717392. doi: 10.3389/fimmu.2021.717392

INTRODUCTION

The gastrointestinal tract is home to the vast majority of microbiota in the body most of which are colonized in the distal intestine (1). The gut microbiota consists of microorganisms including bacteria, viruses, parasites, and fungi. These microorganisms co-evolved with the host to form a symbiotic relationship. Intestinal microbiota is crucial for the regulation of the host metabolism and immunity. In turn, the intestinal immune system is tasked to establish tolerance towards the microbial community and to prevent pathogen invasion. The intestine is covered by an epithelial cell layer which forms a physical and biochemical barrier between the microbiota and the host (2). A compromised barrier integrity and/or dysregulated immune responses causes loss of tolerance to microbials and/or food antigens. This loss of tolerance is central to the pathogenesis of chronic intestinal disorders such as celiac disease, food allergies, and inflammatory bowel diseases (IBD) including Crohn's disease (CD) and ulcerative colitis (UC) in genetically susceptible individuals (3).

Since the incidence of IBD patients has rapidly increased in developing countries, it is unlikely that genetic factors alone are the main cause of rising rates of IBD (4). Thus, doubtlessly, environmental

exposure significantly contributes to the development of IBD. Among environmental factors, dietary nutrients are increasingly recognized for their contribution to the pathogenesis of IBD (5, 6). Specifically, a fiber-rich diet lowers risk of Crohn's disease whereas a "western" diet containing poly-unsaturated fatty acids, and trans-fats is associated with IBD (7, 8). In this context, there is increasing evidence that host and/or microbiota-derived metabolites shape the host intestinal immune system by activating signaling cascades in epithelial and immune cells. These metabolites can evoke an immunological response through distinct pathways. Certain metabolites such butyrate and propionate can act as histone deacetylase inhibitors or transcriptional coactivators and thereby control gene expression intracellularly. In addition, dietary metabolites can signal *via* G protein-coupled receptors (GPCRs) (9). GPCRs can recognize host-derived metabolites such as medium- and long-chain fatty acids or secondary metabolites that undergo fermentation by the gut microbiota including fiber-derived short-chain fatty acids. Short-chain fatty acids such as butyrate, acetate, propionate, and nicotinic acid activate anti-inflammatory responses and bind to GPCRs including GPR41, GPR43 and GPR109A on epithelial and immune cells such as dendritic cells and regulatory T cells (10–12). Beside influencing host immunity and mucosal barrier integrity, dietary metabolites may affect the composition of the intestinal microbiota. This review focuses on the metabolites-sensing GPR35, which is a newly characterized receptor that profoundly affects the functions of immune and nonimmune cells in the intestine. we summarize and discuss the experimental findings emphasizing the importance of GPR35 in intestinal health and disease.

G PROTEIN-COUPLED RECEPTOR (GPR) 35

GPR35 is a rhodopsin-like, 7-transmembrane class A GPCR that was discovered in 1998 (13). The *GPR35* is located on chromosome 2q37.3 in humans that can be alternatively spliced into variants resulting in GPR35a or GPR35b. GPR35a encodes for 309 amino acids whereas GPR35b results in a longer N-terminal domain by 31 amino acids (14). Although GPR35b is rather associated with carcinogenesis due to its expression in gastric and colon cancer cells, GPR35a and GPR35b are localized at similar cellular compartments as well as have similar pharmacology. Hence, the functional differences between the two isoforms are not clear and yet to be studied (14–17). There are orthologues of GPR35 in mouse and rat that share 73 and 72% homology with human GPR35a (hGPR35a) and, in less extensively studied non-mammalian species such as *Xenopus tropicalis* (amphibian) with 33% similarity to the hGPCR35a (18, 19). Recently, *Danio rerio* (zebrafish) homolog of hGPR35 has been cloned which led to identification of two paralogs, *gpr35a* and *gpr35b*, that show ~26% and 24% sequence similarity to human *GPR35* (20).

GPR35 is closely related to cannabinoid receptor GPR55, the nicotinic acid receptor HM74 and LPA receptors LPAR4, LPAR5 and LPAR6 (21, 22). However, GPR35 remains an orphan receptor to date, although several potential ligand candidates have been proposed (reviewed extensively below). In this context, kynurenic acid, a tryptophan metabolite, has been suggested as a putative ligand candidate for GPR35 (23). In addition to kynurenic acid, phospholipid derivates LPA species were explored for their potency to activate GPR35 due to the structural similarity of GPR35 to the LPA receptors (24). Furthermore, CXCL17, a mucosal chemokine, was shown activate GPR35 which led to the suggestion to rename GPR35 as chemokine (C-X-C motif) receptor 8 (CXCR8) (25). In the study where GPR35 was first reported, O'Dowd et al. have shown that the expression of the newly identified GPR35 is abundant in the small intestine in rats (13). Other studies reported similar expression pattern in the small intestine and colon of mice and humans. These studies also indicated significant GPR35 expression in the spleen as well as immune cells including monocytes, macrophages, and dendritic cells. On the other hand, lower levels of GPR35 were evident in the stomach, liver, and kidney. Furthermore, *gpr35a* expression was restricted to the zebrafish intestine at larvae stage (20).

In addition to the expression pattern of GPR35, the polymorphisms in the human gene has been investigated by genome wide association studies (26). Importantly, two SNP variants of GPR35 have been associated with IBD that led to the definition of GPR35 as an IBD risk gene (27, 28). Subsequently, this prompted researchers to understand the functions of GPR35 in the intestine under different physiological conditions.

PHARMACOLOGY OF GPR35

Potential Endogenous Ligands

Kynurenic Acid

To understand the function of GPR35, it is crucial to delineate upstream and downstream signaling events of its activation. To this end, Wang and colleagues tested kynurenic acid's ability to activate GPR35 signaling (23). Kynurenic acid is a tryptophan-derived metabolite that is mostly recognized for its roles in the central nervous system as well as anti-inflammatory properties (23, 29, 30). Of note, higher levels of kynurenic acid is evident in serum of inflammatory bowel disease patients (31). In micromolar concentrations, kynurenic acid induces Ca^{2+} influx in the presence of chimeric G proteins *via* human, mouse and rat GPR35 in Chinese hamster ovary cells (23). Furthermore, kynurenic acid led to GPR35 internalization in HeLa cells. Other studies demonstrated that GPR35 deficiency hinders the kynurenic acid-induced adhesion of human peripheral monocytes as well as ant-inflammatory gene expression in adipocytes in mice (32, 33). Nonetheless, although the potency of kynurenic acid for activating the GPR35 is relatively high in mice and rats, the concentrations of kynurenic acid required are 40- to 100- fold higher in humans (32). In addition, in other studies, kynurenic acid failed to activate human GPR35 even at high concentrations (20, 24). This species selectivity of kynurenic acid/GPR35 axis has led to the discussion whether the interaction is physiological, particularly in humans, which causes kynurenic acid to retain a potential endogenous ligand for GPR35 (34).

Lysophosphatidic Acid

GPR35 has also been explored as a receptor for LPA due to its homology to other LPA receptors. Oka et al. have shown that LPA led to Ca^{2+} response, activation of RhoA and ERK phosphorylation in GPR35-transfected cells as well as internalization of GPR35 (24). LPA also induced a transient RhoA activation in vector-transfected control cells which was attributed to the other LPA receptors. LPA is a bioactive phospholipid derivate that is present in cell membrane but also can be produced extracellularly and activate six known GPCRs, LPAR1-6 (35). In a more recent study by Schneditz and colleagues, GPR35 deficiency prevented the LPA-induced Ca^{2+} signaling in bone marrow-derived macrophages (BMDMs). However, the authors hypothesized that the GPR35 deficiency might impair LPA signaling *via* the other LPA receptors (36). GPR35 had not been confirmed as a potential LPA receptor until our group have tested LPA in cells transfected with human GPR35 naturally coupled to an inhibitory G-protein (Gi). In this ligand identification assay, LPA lowered the cAMP signaling suggesting that LPA might induce Gi-mediated signaling (20). The ligand-GPCR interaction studies are challenged by interspecies variances especially including that of GPR35. Despite this complexity, LPA/GPR35 axis have been evident across the species, mouse and zebrafish, where LPA led to GPR35-dependent migration of macrophages as well as TNF cytokine induction marked with activation of NF-kB and ERK pathways. However, it is still not known whether GPR35 directly binds to LPA or regulates LPA signaling by interacting with and modulating the activity of its receptors.

CXCL17

CXCL17, whose expression is associated with mucosal sites, has also been proposed as an endogenous agonist of GPR35 (25, 37, 38). Maravillas-Montero et al. determined that GPR35-transfected cells migrate towards CXCL17 (25, 37, 38). Since CXCL17 acted on GPR35 in nanomolar concentrations that are in a physiological range as opposed to kynurenic acid, the authors suggested to change the nomenclature of GPR35 into CXCR8. However, subsequent studies reported that CXCL17 failed to induce migratory or signaling responses in GPR35-expressing cells (39, 40). In addition, kynurenic acid and zaprinast reduced the effects of CXCL17 in neuropathic pain model in mice further supporting the existence of CXCL17 receptor(s) other than GPR35 (41).

In addition to kynurenic acid, LPA and CXCL17, there have been studies describing potency of other endogenously available molecules for GPR35 including 5,6-dihydroxyindole-2-carboxylic acid (DHICA), 3,3,5-triiodothyronine (reverse T3), and guanosine 3',5'-cyclic monophosphate (cGMP) (**Table 1**) (44, 46). However, these have not been pursued experimentally as GPR35 ligand candidates following their initial identification. In addition to attempts in deorphanizing the GPR35, it is important to mention that Schneditz et al. reported a ligand-independent basal activity of GPR35 *via* its interaction with the Na/K-ATPase (36).

Synthetic Agonists

Zaprinast

Although there has been significant progress in identifying the putative endogenous activators of GPR35, usage of synthetic agonists also proved useful in revealing the molecular pathways involved in GPR35 activation. Of these synthetic agonist, Zaprinast a cyclic guanosine monophosphate-specific phosphodiesterase inhibitor, is one of the most widely known agonists of GPR35 (19). In contrast to the other compounds activating GPR35, zaprinast shows similar potency for human, rat, and mouse GPR35, and therefore serves as an optimal reference in studies (34).

Lodoxamide

Lodoxamide, an anti-inflammatory mast cell stabilizer, is another synthetic agonist for GPR35. However, although

TABLE 1 | Proposed agonists and antagonists of GPR35.

Potential Endogenous Ligands	Source in the intestine	EC50 (human)	EC50 (mouse)	EC50 (rat)	References
Kynurenic acid	Host, Microbiota	217 μM	Not available	66 μM	(23, 42, 43)
LPA	Host, Microbiota	Not available	Not available	Not available	(20, 24)
CXCL17	Host	Not available	Not available	Not available	(25)
DHICA	Host	22 μM	Not available	Not available	(44)
Reverse T3	Host, Microbiota	100 μM	Not available	Not available	(44, 45)
cGMP	Host	131 μM	Not available	Not available	(46)
Synthetic Agonists		**EC50 (human)**	**EC50 (mouse)**	**EC50 (rat)**	**References**
Zaprinast		2-8 μM	1 μM	100 nM	(19, 42)
Lodoxamide		4 nM	Not available	13 nM	(47)
Pamoic acid		30-50 nM	No response	>100 μM	(17, 42)
Amlexanox		Not available	Not assessed	Not available	(48, 49)
Bufrolin		13 nM	Not available	10 nM	(47)
Compound 1		26 nM	17 μM	8 μM	(50)
Cromolyn disodium		Not available	Not available	Not available	(42, 49)
6-bromo-8-(4-methoxybenzamido)-4-oxo-4H-chromene-2-carboxylic acid		Not available	Not assessed	Not available	(51)
Antagonists		**IC50 (human)**	**IC50 (mouse)**	**IC50 (rat)**	**References**
ML-145		~25 nM	No response	No response	(42)
CID2745687		~200 nM	No response	No response	(17, 42)
ML-194		~200 nM	Not assessed	Not assessed	(52)

potency of lodoxamide is high for human and rat GPR35, it is 100-fold lower for the mouse orthologue (47, 53). Nevertheless, lodoxamide has shown to be protective in hepatic fibrosis model in mice which was reversed by a GPR35 antagonist (53). However, due to the concerns over lodoxamide's low potency for mouse GPR35, it remains controversial whether this effect is caused by direct activity of GPR35 or whether there are other molecular pathways involved.

Other synthetic agonists of GPR35 include amlexanox, bufrolin, compound 1, pamoic acid, cromolyn disodium and, 6-bromo-8-(4-methoxybenzamido)-4-oxo-4H-chromene-2-carboxylic acid (**Table 1**). However, most of these compounds either were only tested on human GPR35 expressing cells but not rodent orthologues or have low potencies in the latter species, limiting their usage in rodent studies (18, 48–51).

Antagonists

Receptor antagonists, by definition, are ligands that lead to inhibition of the activity of a receptor. They are crucial for functional studies as well as for investigating protein-protein interactions of receptors. ML-145 is one of the described GPR35 antagonists. It has a higher binding capacity for human GPR35 than mouse and rat orthologues and therefore have been rather used for *in vitro* settings rather than rodent models (42). Similar results were obtained for CID2745687 where both antagonists led to effective inhibition of agonist activities of zaprinast and cromolyn disodium for human GPR35. On the other hand, in this study, neither ML-145 nor CID2745687 have shown antagonism for rodent orthologues of GPR35. Interestingly, Zhao et al. found that CID2745687 is able to inhibit pamoic acid induced GPR35 activation (17). In addition, CID2745687 antagonized kynurenic acid in mouse astrocytes and interfered with pamoic acid-mediated wound repair in young adult mouse colon epithelium cells (54, 55). Lastly, ML-194 has also been introduced as a GPR35 antagonist which remains to be confirmed (52).

RISK VARIANTS OF GPR35

Genome-wide association studies (GWAS) identified 70 SNPs in the coding region of GPR35 gene and the intergenic regions surrounding it. Six of these SNPs have been associated with increased risk of immune-related diseases (**Table 2**) (26, 69). These diseases include IBD, both ulcerative colitis and Crohn's disease, as well as primary sclerosing cholangitis (PSC) (27, 28). Among the IBD-associated SNPs, the rs3749171 variant that causes a threonine to methionine transition in the transmembrane III, T108M, is the most extensively studied. Schneditz and colleagues showed that this variant is hypermorphic leading to hyperactivation of GPR35 (36). In this study, GPR35 T108M resulted in increased proliferation and metabolism in BMDMs and intestinal epithelial cells. In addition, another study from the same group demonstrated that macrophages carrying the T108M have enhanced VEGF and CXCL-8 production as opposed to the reduced levels in GPR35-deficient cells further reinforcing the hyperactivity caused by the variant (70). In addition to these studies, we reported that T108M variant correlated with better clinical outcome in response to TNF blockers IBD patients (20). Notably, in our study, GPR35 signaling facilitated macrophage TNF responses. It is possible that the aberrant TNF resulting from the hypermorphic T108M variant contributes to IBD pathogenesis and therefore leads to a better response to anti-TNF treatment. However, this potential mechanism remains a speculation and need to be studied more extensively. The T108M variant did not affect the agonist potencies for GPR35 profoundly, therefore, the mechanism by which the GPR35 T108M drives the hyperactivation remains unknown (47). The second IBD-associated SNP in GPR35 is rs4676410 which is an upstream intron variant causing a cytosine to thymine substitution. Although rs4676410 has a higher prevalence than T108M (**Table 3**), its function remains to be studied to date. Nevertheless, it is known that it does not cause a change in GPR35 tissue expression in IBD patients (27).

GPR35 IN INTESTINAL HEALTH AND DISEASE

IBD is a collective term to define chronic inflammatory conditions in the gastrointestinal tract including CD and UC. Patients with IBD experience a severely compromised quality of life with symptoms diarrhea, weight loss, abdominal pain, and are more susceptible to colorectal cancer (71). Current IBD treatment options pose a significant burden on the health system due to high costs and resource exhaustion. There is an increasing prevalence for IBD globally particularly in western countries due to the urbanization of life style (72).

The abundant expression of GPR35 in the intestine and its IBD-associated variants give hints towards an important physiological function for GPR35 in the gut. To explore this possibility,

TABLE 2 | Risk variants of GPR35 associated with diseases.

Variant ID	Variant type	Position (ch2):	Substitution	MAF	Linked Diseases	References
rs4676410	Intron	240624322	G>A	0.272	Ankylosing spondylitis, IBD, PSC, systemic lupus erythematosus	(27, 28, 56–59)
rs3749171	Missense	240630275	C>T (T108M)	0.151	CD, UC	(59–62)
rs3749172	Missense	240630832	C>A (S294R)	0.484	CD, coronary artery calcification	(63, 64) (65)
rs4676408	Intergenic	240634984	A>G	0.4	UC, CD	(66)
rs4676406	Intergenic	240639691	T>G	0.374	Ankylosing spondylitis, psoriasis, PSC	(60, 67)
rs34236350	5' UTR	240628909	C>T	0.261	Ankylosing spondylitis, psoriasis	(68)

MAF, Minor Allele Frequency; UTR, Untranslated region.

TABLE 3 | Haplotype frequencies of IBD-associated GPR35 variants across all populations analyzed by LDHap (ldlink.nci.nih.gov/?tab=ldhap).

RS Number	Position (GRCh37)	Allele Frequencies	Haplotypes		
rs4676410	chr2:241563739	G=0.728, A=0.272	G	A	A
rs3749171	chr2:241569692	C=0.849, T=0.151	C	T	C
		Haplotype Count	**3636**	**744**	**617**
		Haplotype Frequency	**0.726**	**0.1486**	**0.1232**

researchers adopted several experimental approaches including *in vitro* culture systems and disease models using rodents. For instance, in a wound healing model, GPR35 agonists, YE120, zaprinast and pamoic acid, promoted wound repair in young adult mouse colon epithelium cells *via* increased migration by fibronectin expression and ERK phosphorylation (55). Furthermore, several lines of evidence from multiple studies have shown that GPR35 is protective in dextran sodium sulfate (DSS) induced colitis mouse model (20, 55, 73). In this model, DSS causes cell death epithelial cells causing a breach in the barrier integrity and therefore dissemination of microbial products which leads to acute inflammation (74). Similar to the wound healing model, GPR35 agonists stimulated fibronectin and ERK activation in the colonic epithelium and therefore facilitated mucosal repair in the DSS model (**Figure 1**) (55). In subsequent studies, including ours, GPR35-deficiency led to exacerbated DSS colitis in mice as measured by clinical signs such as weight loss (20, 73). Nonetheless, these studies lack the genetic models required to dissect the cell specific effects of GPR35.

Our studies described the GPR35 expression across cell types in the intestine where the expression was prominent in epithelial cells as well as macrophages and dendritic cells. The macrophages in the intestine are continuously generated from the extravasating Ly6C^{high} blood monocytes through their

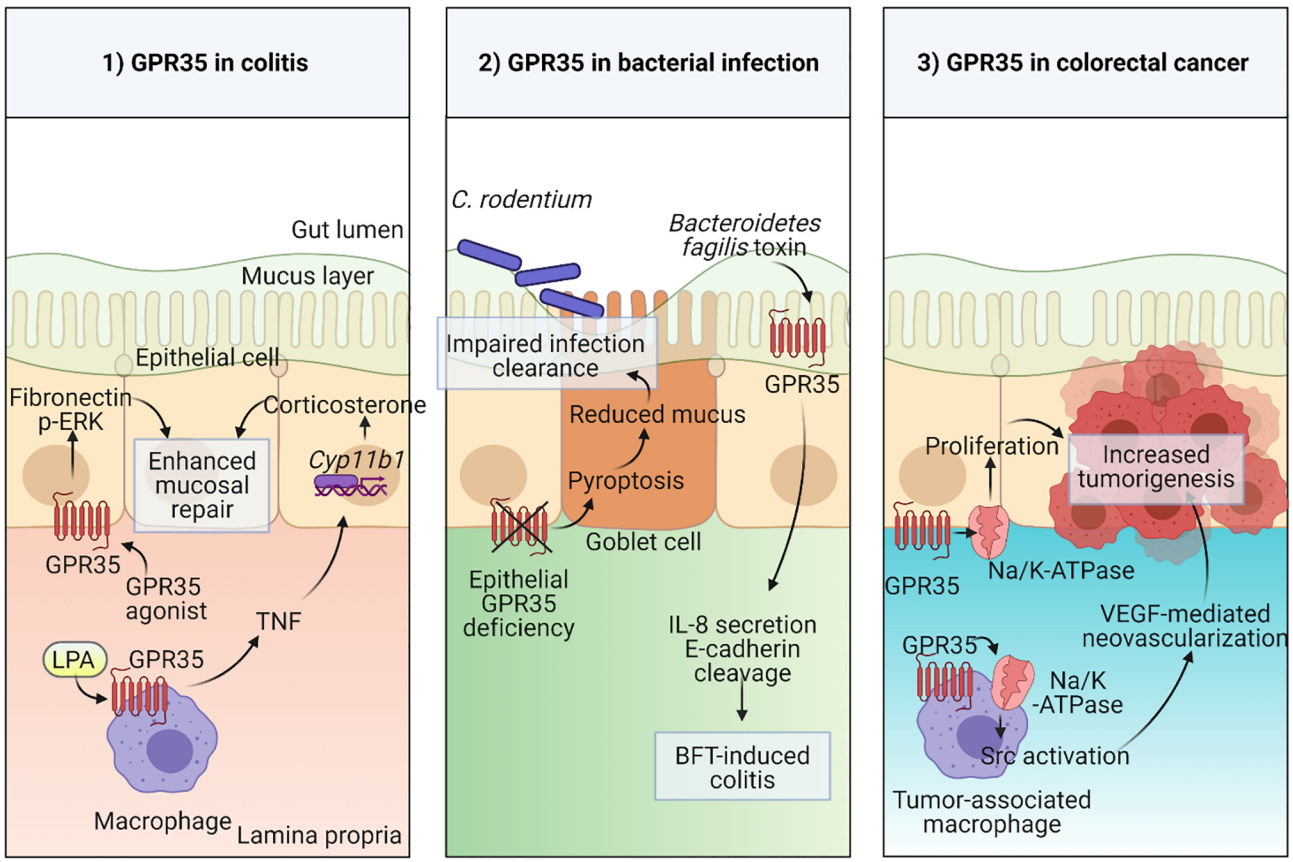

FIGURE 1 | Physiological functions of GPR35 in the intestine 1) Macrophage expressed GPR35 induces TNF accompanied by transcription of *Cyp11b1* encoding for steroidogenic enzyme 11β –hydroxylase in epithelial cells during colitis. In a second mechanism, epithelial GPR35 promotes mucosal repair through ERK and fibronectin-mediated proliferation. 2) Disruption of GPR35 signaling in epithelial cells leads to pyroptosis in goblet cells resulting in reduced mucus production and therefore an impaired mucosal barrier integrity which leads to increased susceptibility to *C. rodentium* infection. GPR35 serves as a sensor in *Bacteroidetes fragilis* toxin (BFT)-induced colitis. 3) GPR35 interaction with Na/K-ATPase pump induces Src activation in both epithelial cells and tumor-associated macrophages (TAMs) in colorectal cancer model *via* increased proliferation in epithelial cells and neovascularization in response to TAM-derived VEGF. Created with BioRender.com.

intermediates (75). They are vital for the maintenance of tolerance at the steady state and search the lumen for antigens by extending their dendrites between epithelial cells (76–78). On the other hand, they can also contribute to inflammatory conditions by producing pro-inflammatory cytokines including TNF (79). Interestingly, in the DSS colitis model, macrophage-specific GPR35 deletion led to elevated inflammation which was accompanied by reduced TNF responses in macrophages as well as intestinal corticosterone production (**Figure 1**) (20). TNF is widely known for its pro-inflammatory effects and its clinically routine use as a target in IBD treatment strategies (80, 81). Nevertheless, it can also play an anti-inflammatory role through corticosterone production in intestinal epithelial cells which is in line with our experimental findings (82, 83). In a more recent study, Pagano et al. revealed that macrophage-expressed GPR35 promotes neoangiogenesis *via* VEGF production and therefore tumor growth in colitis associated and spontaneous models of colon cancer in mice (70). Since neovascularization is not only involved in cancer but also in IBD, this study potentially highlights yet another mechanism by which the GPR35 signaling in macrophages plays a role in IBD pathogenesis (84).

The physiological relevance of epithelial GPR35 in the gut has also been the focus of several studies, since GPR35 is strongly expressed in intestinal epithelial cells (20). As an example, a study from our group explored the role for GPR35 in goblet cell function at the steady state and during *Citrobacter rodentium* infection (85). Deficiency of GPR35 in epithelial cells leads to a decrease in goblet cell numbers and Muc2 expression due to enhanced pyroptosis of goblet cells. Pyroptosis a cell death mechanism where the active caspase-1 and caspase-11 cleave gasdermin D causing pore formation in the cell membrane (86). By inducing pyroptosis, epithelial GPR35 deficiency led to compromised epithelial barrier and therefore susceptibility to *Citrobacter rodentium* infection (**Figure 1**). On the other hand, a recent study has shown that epithelial GPR35 is crucial in sensing the enterotoxigenic *Bacteroides fragilis* toxin (BFT) and initiates an immune response against it (**Figure 1**) (87). Therefore, as opposed to the *Citrobacter rodentium* infection model, epithelial GPR35 deficiency led to protection from BFT-induced colitis. Together, these two studies emphasize that the role of GPR35 signaling in epithelial cells is context-dependent in bacterial infections. Lastly, Schneditz and colleagues examined the physiological relevance of epithelial GPR35 signaling in spontaneous colon cancer model in mice (**Figure 1**) (36). Deletion of epithelial GPR35 led to reduced proliferation and tumor burden in this model, showing that in GPR35 contributes to cell turn over in epithelial cells during tumorigenesis.

CONCLUSION

GPR35 is an emerging GPCR in the intestinal health field with potential implications in IBD as well as colorectal cancer. GPR35 might prove useful as an intermediate player and a messenger between the microbiota and host *via* metabolite-sensing. However, despite the experimental evidence pointing towards potential endogenous ligand candidates for GPR35, the biochemistry of GPR35 is not fully understood. The challenges in the context of GPR35 pharmacology include orthologue selectivity, off-target effects, and lack of knowledge on interactions that are based on direct binding. To overcome these, better pharmacological assays need to be carried out to get a broader overview of the GPR35 signaling.

In this review, we summarized the recent advances in understanding the physiological functions of GPR35 and its IBD-associated risk variant T108M particularly in intestinal macrophages and epithelial cells. However, before GPR35 can be considered as a pharmaceutical target for the treatment of intestinal diseases, more studies are needed to elucidate the mechanisms governed by GPR35 signaling.

AUTHOR CONTRIBUTIONS

JN and BK conceived the content and structure of the manuscript. BK drafted the figures and JN, BK, and HM wrote the text. All authors contributed to the article and revised the final version.

FUNDING

The SNSF grant 310030_175548 to JN supported this manuscript's writing.

REFERENCES

1. Kamada N, Seo SU, Chen GY, Nunez G. Role of the Gut Microbiota in Immunity and Inflammatory Disease. *Nat Rev Immunol* (2013) 13:321–35. doi: 10.1038/nri3430
2. Thoo L, Noti M, Krebs P. Keep Calm: The Intestinal Barrier at the Interface of Peace and War. *Cell Death Dis* (2019) 10:849. doi: 10.1038/s41419-019-2086-z
3. Kim D, Zeng MY, Nunez G. The Interplay Between Host Immune Cells and Gut Microbiota in Chronic Inflammatory Diseases. *Exp Mol Med* (2017) 49: e339. doi: 10.1038/emm.2017.24
4. Molodecky NA, Soon IS, Rabi DM, Ghali WA, Ferris M, Chernoff G, et al. Increasing Incidence and Prevalence of the Inflammatory Bowel Diseases With Time, Based on Systematic Review. *Gastroenterology* (2012) 142:46–54. doi: 10.1053/j.gastro.2011.10.001
5. Lee D, Albenberg L, Compher C, Baldassano R, Piccoli D, Lewis JD, et al. Diet in the Pathogenesis and Treatment of Inflammatory Bowel Diseases. *Gastroenterology* (2015) 148:1087–106. doi: 10.1053/j.gastro.2015.01.007
6. Spooren CE, Pierik MJ, Zeegers MP, Feskens EJ, Masclee AA, Jonkers DM. Review Article: The Association of Diet With Onset and Relapse in Patients With Inflammatory Bowel Disease. *Aliment Pharmacol Ther* (2013) 38:1172–87. doi: 10.1111/apt.12501
7. Ananthakrishnan AN, Khalili H, Konijeti GG, Higuchi LM, de Silva P, Korzenik JR, et al. A Prospective Study of Long-Term Intake of Dietary Fiber and Risk of Crohn's Disease and Ulcerative Colitis. *Gastroenterology* (2013) 145:970–7. doi: 10.1053/j.gastro.2013.07.050

8. Ananthakrishnan AN, Khalili H, Konijeti GG, Higuchi LM, de Silva P, Fuchs CS, et al. Long-Term Intake of Dietary Fat and Risk of Ulcerative Colitis and Crohn's Disease. *Gut* (2014) 63:776–84. doi: 10.1136/gutjnl-2013-305304
9. Melhem H, Kaya B, Ayata CK, Hruz P, Niess JH. Metabolite-Sensing G Protein-Coupled Receptors Connect the Diet-Microbiota-Metabolites Axis to Inflammatory Bowel Disease. *Cells* (2019) 8:450. doi: 10.3390/cells8050450
10. Correa-Oliveira R, Fachi JL, Vieira A, Sato FT, Vinolo MA. Regulation of Immune Cell Function by Short-Chain Fatty Acids. *Clin Transl Immunol* (2016) 5:e73. doi: 10.1038/cti.2016.17
11. Singh N, Gurav A, Sivaprakasam S, Brady E, Padia R, Shi H, et al. Activation of Gpr109a, Receptor for Niacin and the Commensal Metabolite Butyrate, Suppresses Colonic Inflammation and Carcinogenesis. *Immunity* (2014) 40:128–39. doi: 10.1016/j.immuni.2013.12.007
12. Smith PM, Howitt MR, Panikov N, Michaud M, Gallini CA, Bohlooly YM, et al. The Microbial Metabolites, Short-Chain Fatty Acids, Regulate Colonic Treg Cell Homeostasis. *Science* (2013) 341:569–73. doi: 10.1126/science.1241165
13. O'Dowd BF, Nguyen T, Marchese A, Cheng R, Lynch KR, Heng HH, et al. Discovery of Three Novel G-Protein-Coupled Receptor Genes. *Genomics* (1998) 47:310–3. doi: 10.1006/geno.1998.5095
14. Okumura S, Baba H, Kumada T, Nanmoku K, Nakajima H, Nakane Y, et al. Cloning of a G-Protein-Coupled Receptor That Shows an Activity to Transform NIH3T3 Cells and is Expressed in Gastric Cancer Cells. *Cancer Sci* (2004) 95:131–5. doi: 10.1111/j.1349-7006.2004.tb03193.x
15. Guo J, Williams DJ, Puhl HL3rd, Ikeda SR. Inhibition of N-Type Calcium Channels by Activation of GPR35, an Orphan Receptor, Heterologously Expressed in Rat Sympathetic Neurons. *J Pharmacol Exp Ther* (2008) 324:342–51. doi: 10.1124/jpet.107.127266
16. Ali H, AbdelMageed M, Olsson L, Israelsson A, Lindmark G, Hammarstrom ML, et al. Utility of G Protein-Coupled Receptor 35 Expression for Predicting Outcome in Colon Cancer. *Tumour Biol* (2019) 41:1010428319858885. doi: 10.1177/1010428319858885
17. Zhao P, Sharir H, Kapur A, Cowan A, Geller EB, Adler MW, et al. Targeting of the Orphan Receptor GPR35 by Pamoic Acid: A Potent Activator of Extracellular Signal-Regulated Kinase and Beta-Arrestin2 With Antinociceptive Activity. *Mol Pharmacol* (2010) 78:560–8. doi: 10.1124/mol.110.066746
18. Quon T, Lin LC, Ganguly A, Tobin AB, Milligan G. Therapeutic Opportunities and Challenges in Targeting the Orphan G Protein-Coupled Receptor Gpr35. *ACS Pharmacol Transl Sci* (2020) 3:801–12. doi: 10.1021/acsptsci.0c00079
19. Taniguchi Y, Tonai-Kachi H, Shinjo K. Zaprinast, a Well-Known Cyclic Guanosine Monophosphate-Specific Phosphodiesterase Inhibitor, is an Agonist for GPR35. *FEBS Lett* (2006) 580:5003–8. doi: 10.1016/j.febslet.2006.08.015
20. Kaya B, Donas C, Wuggenig P, Diaz OE, Morales RA, Melhem H, et al. Lysophosphatidic Acid-Mediated GPR35 Signaling in CX3CR1(+) Macrophages Regulates Intestinal Homeostasis. *Cell Rep* (2020) 32:107979. doi: 10.1016/j.celrep.2020.107979
21. Fredriksson R, Lagerstrom MC, Lundin LG, Schioth HB. The G-Protein-Coupled Receptors in the Human Genome Form Five Main Families. Phylogenetic Analysis, Paralogon Groups, and Fingerprints. *Mol Pharmacol* (2003) 63:1256–72. doi: 10.1124/mol.63.6.1256
22. Vassilatis DK, Hohmann JG, Zeng H, Li F, Ranchalis JE, Mortrud MT, et al. The G Protein-Coupled Receptor Repertoires of Human and Mouse. *Proc Natl Acad Sci USA* (2003) 100:4903–8. doi: 10.1073/pnas.0230374100
23. Wang J, Simonavicius N, Wu X, Swaminath G, Reagan J, Tian H, et al. Kynurenic Acid as a Ligand for Orphan G Protein-Coupled Receptor GPR35. *J Biol Chem* (2006) 281:22021–8. doi: 10.1074/jbc.M603503200
24. Oka S, Ota R, Shima M, Yamashita A, Sugiura T. GPR35 Is a Novel Lysophosphatidic Acid Receptor. *Biochem Biophys Res Commun* (2010) 395:232–7. doi: 10.1016/j.bbrc.2010.03.169
25. Maravillas-Montero JL, Burkhardt AM, Hevezi PA, Carnevale CD, Smit MJ, Zlotnik A. Cutting Edge: GPR35/CXCR8 Is the Receptor of the Mucosal Chemokine CXCL17. *J Immunol* (2015) 194:29–33. doi: 10.4049/jimmunol.1401704
26. Mackenzie AE, Lappin JE, Taylor DL, Nicklin SA, Milligan G. GPR35 as a Novel Therapeutic Target. *Front Endocrinol (Lausanne)* (2011) 2:68. doi: 10.3389/fendo.2011.00068
27. Imielinski M, Baldassano RN, Griffiths A, Russell RK, Annese V, Dubinsky M, et al. Common Variants at Five New Loci Associated With Early-Onset Inflammatory Bowel Disease. *Nat Genet* (2009) 41:1335–40. doi: 10.1038/ng.489
28. Ellinghaus D, Folseraas T, Holm K, Ellinghaus E, Melum E, Balschun T, et al. Genome-Wide Association Analysis in Primary Sclerosing Cholangitis and Ulcerative Colitis Identifies Risk Loci at GPR35 and TCF4. *Hepatology* (2013) 58:1074–83. doi: 10.1002/hep.25977
29. Vecsei L, Szalardy L, Fulop F, Toldi J. Kynurenines in the CNS: Recent Advances and New Questions. *Nat Rev Drug Discov* (2013) 12:64–82. doi: 10.1038/nrd3793
30. Fallarini S, Magliulo L, Paoletti T, de Lalla C, Lombardi G. Expression of Functional GPR35 in Human iNKT Cells. *Biochem Biophys Res Commun* (2010) 398:420–5. doi: 10.1016/j.bbrc.2010.06.091
31. Forrest CM, Youd P, Kennedy A, Gould SR, Darlington LG, Stone TW. Purine, Kynurenine, Neopterin and Lipid Peroxidation Levels in Inflammatory Bowel Disease. *J BioMed Sci* (2002) 9:436–42. doi: 10.1007/BF02256538
32. Barth MC, Ahluwalia N, Anderson TJ, Hardy GJ, Sinha S, Alvarez-Cardona JA, et al. Kynurenic Acid Triggers Firm Arrest of Leukocytes to Vascular Endothelium Under Flow Conditions. *J Biol Chem* (2009) 284:19189–95. doi: 10.1074/jbc.M109.024042
33. Agudelo LZ, Ferreira DMS, Cervenka I, Bryzgalova G, Dadvar S, Jannig PR, et al. Kynurenic Acid and Gpr35 Regulate Adipose Tissue Energy Homeostasis and Inflammation. *Cell Metab* (2018) 27:378–92.e5. doi: 10.1016/j.cmet.2018.01.004
34. Milligan G. Orthologue Selectivity and Ligand Bias: Translating the Pharmacology of GPR35. *Trends Pharmacol Sci* (2011) 32:317–25. doi: 10.1016/j.tips.2011.02.002
35. Ye X, Chun J. Lysophosphatidic Acid (LPA) Signaling in Vertebrate Reproduction. *Trends Endocrinol Metab* (2010) 21:17–24. doi: 10.1016/j.tem.2009.08.003
36. Schneditz G, Elias JE, Pagano E, Zaeem Cader M, Saveljeva S, Long K, et al. GPR35 Promotes Glycolysis, Proliferation, and Oncogenic Signaling by Engaging With the Sodium Potassium Pump. *Sci Signal* (2019) 12:eaau9048. doi: 10.1126/scisignal.aau9048
37. Lee WY, Wang CJ, Lin TY, Hsiao CL, Luo CW. CXCL17, an Orphan Chemokine, Acts as a Novel Angiogenic and Anti-Inflammatory Factor. *Am J Physiol Endocrinol Metab* (2013) 304:E32–40. doi: 10.1152/ajpendo.00083.2012
38. Burkhardt AM, Tai KP, Flores-Guiterrez JP, Vilches-Cisneros N, Kamdar K, Barbosa-Quintana O, et al. CXCL17 is a Mucosal Chemokine Elevated in Idiopathic Pulmonary Fibrosis That Exhibits Broad Antimicrobial Activity. *J Immunol* (2012) 188:6399–406. doi: 10.4049/jimmunol.1102903
39. Binti Mohd Amir NAS, Mackenzie AE, Jenkins L, Boustani K, Hillier MC, Tsuchiya T, et al. Evidence for the Existence of a CXCL17 Receptor Distinct From GPR35. *J Immunol* (2018) 201:714–24. doi: 10.4049/jimmunol.1700884
40. Park SJ, Lee SJ, Nam SY, Im DS. GPR35 Mediates Lodoxamide-Induced Migration Inhibitory Response But Not CXCL17-Induced Migration Stimulatory Response in THP-1 Cells; Is GPR35 a Receptor for CXCL17? *Br J Pharmacol* (2018) 175:154–61. doi: 10.1111/bph.14082
41. Rojewska E, Ciapala K, Mika J. Kynurenic Acid and Zaprinast Diminished CXCL17-Evoked Pain-Related Behaviour and Enhanced Morphine Analgesia in a Mouse Neuropathic Pain Model. *Pharmacol Rep* (2019) 71:139–48. doi: 10.1016/j.pharep.2018.10.002
42. Jenkins L, Harries N, Lappin JE, MacKenzie AE, Neetoo-Isseljee Z, Southern C, et al. Antagonists of GPR35 Display High Species Ortholog Selectivity and Varying Modes of Action. *J Pharmacol Exp Ther* (2012) 343:683–95. doi: 10.1124/jpet.112.198945
43. Gao J, Xu K, Liu H, Liu G, Bai M, Peng C, et al. Impact of the Gut Microbiota on Intestinal Immunity Mediated by Tryptophan Metabolism. *Front Cell Infect Microbiol* (2018) 8:13. doi: 10.3389/fcimb.2018.00013
44. Deng H, Hu H, Fang Y. Multiple Tyrosine Metabolites are GPR35 Agonists. *Sci Rep* (2012) 2:373. doi: 10.1038/srep00373
45. Frohlich E, Wahl R. Microbiota and Thyroid Interaction in Health and Disease. *Trends Endocrinol Metab* (2019) 30:479–90. doi: 10.1016/j.tem.2019.05.008

46. Southern C, Cook JM, Neetoo-Isseljee Z, Taylor DL, Kettleborough CA, Merritt A, et al. Screening Beta-Arrestin Recruitment for the Identification of Natural Ligands for Orphan G-Protein-Coupled Receptors. *J Biomol Screen* (2013) 18:599–609. doi: 10.1177/1087057113475480
47. MacKenzie AE, Caltabiano G, Kent TC, Jenkins L, McCallum JE, Hudson BD, et al. The Antiallergic Mast Cell Stabilizers Lodoxamide and Bufrolin as the First High and Equipotent Agonists of Human and Rat GPR35. *Mol Pharmacol* (2014) 85:91–104. doi: 10.1124/mol.113.089482
48. Alkondon M, Pereira EF, Todd SW, Randall WR, Lane MV, Albuquerque EX. Functional G-Protein-Coupled Receptor 35 Is Expressed by Neurons in the CA1 Field of the Hippocampus. *Biochem Pharmacol* (2015) 93:506–18. doi: 10.1016/j.bcp.2014.12.009
49. Mackenzie AE. *An Investigation of the Molecular Pharmacology of G Protein-Coupled Receptor 35*. Scotland: Univeristy of Glasgow (2015).
50. Neetoo-Isseljee Z, MacKenzie AE, Southern C, Jerman J, McIver EG, Harries N, et al. High-Throughput Identification and Characterization of Novel, Species-Selective GPR35 Agonists. *J Pharmacol Exp Ther* (2013) 344:568–78. doi: 10.1124/jpet.112.201798
51. Funke M, Thimm D, Schiedel AC, Muller CE. 8-Benzamidochromen-4-One-2-Carboxylic Acids: Potent and Selective Agonists for the Orphan G Protein-Coupled Receptor GPR35. *J Med Chem* (2013) 56:5182–97. doi: 10.1021/jm400587g
52. Heynen-Genel S, Dahl R, Shi S, Sauer M, Hariharan S, Sergienko E, et al. *Selective GPR35 Antagonists - Probe 3, Probe Reports From the NIH Molecular Libraries Program*. Bethesda (MD National Center for Biotechnology Information (US)) (2011).
53. Kim MJ, Park SJ, Nam SY, Im DS. Lodoxamide Attenuates Hepatic Fibrosis in Mice: Involvement of GPR35. *Biomol Ther (Seoul)* (2019) 28:92–7. doi: 10.4062/biomolther.2018.227
54. Berlinguer-Palmini R, Masi A, Narducci R, Cavone L, Maratea D, Cozzi A, et al. GPR35 Activation Reduces Ca2+ Transients and Contributes to the Kynurenic Acid-Dependent Reduction of Synaptic Activity at CA3-CA1 Synapses. *PloS One* (2013) 8:e82180. doi: 10.1371/journal.pone.0082180
55. Tsukahara T, Hamouda N, Utsumi D, Matsumoto K, Amagase K, Kato S. G Protein-Coupled Receptor 35 Contributes to Mucosal Repair in Mice *via* Migration of Colonic Epithelial Cells. *Pharmacol Res* (2017) 123:27–39. doi: 10.1016/j.phrs.2017.06.009
56. C. International Genetics of Ankylosing Spondylitis, Cortes A, Hadler J, Pointon JP, Robinson PC, Karaderi T, et al. Identification of Multiple Risk Variants for Ankylosing Spondylitis Through High-Density Genotyping of Immune-Related Loci. *Nat Genet* (2013) 45:730–8. doi: 10.1038/ng.2667
57. Kichaev G, Bhatia G, Loh PR, Gazal S, Burch K, Freund MK, et al. Leveraging Polygenic Functional Enrichment to Improve GWAS Power. *Am J Hum Genet* (2019) 104:65–75. doi: 10.1016/j.ajhg.2018.11.008
58. Li YR, Li J, Zhao SD, Bradfield JP, Mentch FD, Maggadottir SM, et al. Meta-Analysis of Shared Genetic Architecture Across Ten Pediatric Autoimmune Diseases. *Nat Med* (2015) 21:1018–27. doi: 10.1038/nm.3933
59. Liu JZ, van Sommeren S, Huang H, Ng SC, Alberts R, Takahashi A, et al. Association Analyses Identify 38 Susceptibility Loci for Inflammatory Bowel Disease and Highlight Shared Genetic Risk Across Populations. *Nat Genet* (2015) 47:979–86. doi: 10.1038/ng.3359
60. Ellinghaus D, Jostins L, Spain SL, Cortes A, Bethune J, Han B, et al. Analysis of Five Chronic Inflammatory Diseases Identifies 27 New Associations and Highlights Disease-Specific Patterns at Shared Loci. *Nat Genet* (2016) 48:510–8. doi: 10.1038/ng.3528
61. Jostins L, Ripke S, Weersma RK, Duerr RH, McGovern DP, Hui KY, et al. Host-Microbe Interactions Have Shaped the Genetic Architecture of Inflammatory Bowel Disease. *Nature* (2012) 491:119–24. doi: 10.1038/nature11582
62. Venkateswaran S, Prince J, Cutler DJ, Marigorta UM, Okou DT, Prahalad S, et al. Enhanced Contribution of HLA in Pediatric Onset Ulcerative Colitis. *Inflamm Bowel Dis* (2018) 24:829–38. doi: 10.1093/ibd/izx084
63. Sun YV, Bielak LF, Peyser PA, Turner ST, Sheedy PF2nd, Boerwinkle E, et al. Application of Machine Learning Algorithms to Predict Coronary Artery Calcification With a Sibship-Based Design. *Genet Epidemiol* (2008) 32:350–60. doi: 10.1002/gepi.20309
64. Jung S, Liu W, Baek J, Moon JW, Ye BD, Lee HS, et al. Expression Quantitative Trait Loci (eQTL) Mapping in Korean Patients With Crohn's Disease and Identification of Potential Causal Genes Through Integration With Disease Associations. *Front Genet* (2020) 11:486. doi: 10.3389/fgene.2020.00486
65. Yang SK, Hong M, Oh H, Low HQ, Jung S, Ahn S, et al. Identification of Loci at 1q21 and 16q23 That Affect Susceptibility to Inflammatory Bowel Disease in Koreans. *Gastroenterology* (2016) 151:1096–99.e4. doi: 10.1053/j.gastro.2016.08.025
66. de Lange KM, Moutsianas L, Lee JC, Lamb CA, Luo Y, Kennedy NA, et al. Genome-Wide Association Study Implicates Immune Activation of Multiple Integrin Genes in Inflammatory Bowel Disease. *Nat Genet* (2017) 49:256–61. doi: 10.1038/ng.3760
67. Anderson G, Maes M, Berk M. Inflammation-Related Disorders in the Tryptophan Catabolite Pathway in Depression and Somatization. *Adv Protein Chem Struct Biol* (2012) 88:27–48. doi: 10.1016/B978-0-12-398314-5.00002-7
68. Astle WJ, Elding H, Jiang T, Allen D, Ruklisa D, Mann AL, et al. The Allelic Landscape of Human Blood Cell Trait Variation and Links to Common Complex Disease. *Cell* (2016) 167:1415–29.e19. doi: 10.1016/j.cell.2016.10.042
69. Horikawa Y, Oda N, Cox NJ, Li X, Orho-Melander M, Hara M, et al. Genetic Variation in the Gene Encoding Calpain-10 is Associated With Type 2 Diabetes Mellitus. *Nat Genet* (2000) 26:163–75. doi: 10.1038/79876
70. Pagano E, Elias JE, Schneditz G, Saveljeva S, Holland LM, Borrelli F, et al. Activation of the GPR35 Pathway Drives Angiogenesis in the Tumour Microenvironment. *Gut* (2021) gutjnl-2020-323363. doi: 10.1136/gutjnl-2020-323363
71. Kim ER, Chang DK. Colorectal Cancer in Inflammatory Bowel Disease: The Risk, Pathogenesis, Prevention and Diagnosis. *World J Gastroenterol* (2014) 20:9872–81. doi: 10.3748/wjg.v20.i29.9872
72. Kaplan GG, Windsor JW. The Four Epidemiological Stages in the Global Evolution of Inflammatory Bowel Disease. *Nat Rev Gastroenterol Hepatol* (2021) 18:56–66. doi: 10.1038/s41575-020-00360-x
73. Farooq SM, Hou Y, Li H, O'Meara M, Wang Y, Li C, et al. Disruption of GPR35 Exacerbates Dextran Sulfate Sodium-Induced Colitis in Mice. *Dig Dis Sci* (2018) 63:2910–22. doi: 10.1007/s10620-018-5216-z
74. Laroui H, Ingersoll SA, Liu HC, Baker MT, Ayyadurai S, Charania MA, et al. Dextran Sodium Sulfate (DSS) Induces Colitis in Mice by Forming Nano-Lipocomplexes With Medium-Chain-Length Fatty Acids in the Colon. *PloS One* (2012) 7:e32084. doi: 10.1371/journal.pone.0032084
75. Bain CC, Bravo-Blas A, Scott CL, Perdiguero EG, Geissmann F, Henri S, et al. Constant Replenishment From Circulating Monocytes Maintains the Macrophage Pool in the Intestine of Adult Mice. *Nat Immunol* (2014) 15:929–37. doi: 10.1038/ni.2967
76. Hadis U, Wahl B, Schulz O, Hardtke-Wolenski M, Schippers A, Wagner N, et al. Intestinal Tolerance Requires Gut Homing and Expansion of FoxP3+ Regulatory T Cells in the Lamina Propria. *Immunity* (2011) 34:237–46. doi: 10.1016/j.immuni.2011.01.016
77. Maheshwari A, Kelly DR, Nicola T, Ambalavanan N, Jain SK, Murphy-Ullrich J, et al. TGF-Beta2 Suppresses Macrophage Cytokine Production and Mucosal Inflammatory Responses in the Developing Intestine. *Gastroenterology* (2011) 140:242–53. doi: 10.1053/j.gastro.2010.09.043
78. Niess JH, Brand S, Gu X, Landsman L, Jung S, McCormick BA, et al. CX3CR1-Mediated Dendritic Cell Access to the Intestinal Lumen and Bacterial Clearance. *Science* (2005) 307:254–8. doi: 10.1126/science.1102901
79. Bain CC, Mowat AM. The Monocyte-Macrophage Axis in the Intestine. *Cell Immunol* (2014) 291:41–8. doi: 10.1016/j.cellimm.2014.03.012
80. Hanauer SB, Feagan BG, Lichtenstein GR, Mayer LF, Schreiber S, Colombel JF, et al. Maintenance Infliximab for Crohn's Disease: The ACCENT I Randomised Trial. *Lancet* (2002) 359:1541–9. doi: 10.1016/S0140-6736(02)08512-4
81. Targan SR, Hanauer SB, van Deventer SJ, Mayer L, Present DH, Braakman T, et al. A Short-Term Study of Chimeric Monoclonal Antibody Ca2 to Tumor Necrosis Factor Alpha for Crohn's Disease. Crohn's Disease Ca2 Study Group. *N Engl J Med* (1997) 337:1029–35. doi: 10.1056/NEJM199710093371502
82. Noti M, Corazza N, Mueller C, Berger B, Brunner T. TNF Suppresses Acute Intestinal Inflammation by Inducing Local Glucocorticoid Synthesis. *J Exp Med* (2010) 207:1057–66. doi: 10.1084/jem.20090849
83. Naito Y, Takagi T, Handa O, Ishikawa T, Nakagawa S, Yamaguchi T, et al. Enhanced Intestinal Inflammation Induced by Dextran Sulfate Sodium in

Tumor Necrosis Factor-Alpha Deficient Mice. *J Gastroenterol Hepatol* (2003) 18:560–9. doi: 10.1046/j.1440-1746.2003.03034.x

84. Scaldaferri F, Vetrano S, Sans M, Arena V, Straface G, Stigliano E, et al. VEGF-A Links Angiogenesis and Inflammation in Inflammatory Bowel Disease Pathogenesis. *Gastroenterology* (2009) 136:585–95.e5. doi: 10.1053/j.gastro.2008.09.064
85. Melhem H, Kaya B, Kaymak T, Wuggenig P, Flint E, Roux J, et al. Epithelial GPR35 Protects From Citrobacter Rodentium Infection by Preserving Goblet Cells and Mucosal Barrier Integrity. *bioRxiv* (2021) 2021.03.27.437264. doi: 10.1101/2021.03.27.437264
86. Zhu S, Ding S, Wang P, Wei Z, Pan W, Palm NW, et al. Nlrp9b Inflammasome Restricts Rotavirus Infection in Intestinal Epithelial Cells. *Nature* (2017) 546:667–70. doi: 10.1038/nature22967
87. Boleij A, Fathi P, Dalton W, Park B, Wu X, Huso D, et al. G-Protein Coupled Receptor 35 (GPR35) Regulates the Colonic Epithelial Cell Response to Enterotoxigenic Bacteroides Fragilis. *Commun Biol* (2021) 4:585. doi: 10.1038/s42003-021-02014-3

Conflict of Interest: The authors declare that the research was conducted in the absence of any commercial or financial relationships that could be construed as a potential conflict of interest.

Publisher's Note: All claims expressed in this article are solely those of the authors and do not necessarily represent those of their affiliated organizations, or those of the publisher, the editors and the reviewers. Any product that may be evaluated in this article, or claim that may be made by its manufacturer, is not guaranteed or endorsed by the publisher.

Copyright © 2021 Kaya, Melhem and Niess. This is an open-access article distributed under the terms of the Creative Commons Attribution License (CC BY). The use, distribution or reproduction in other forums is permitted, provided the original author(s) and the copyright owner(s) are credited and that the original publication in this journal is cited, in accordance with accepted academic practice. No use, distribution or reproduction is permitted which does not comply with these terms.

frontiers in Immunology

ORIGINAL RESEARCH
published: 03 November 2021
doi: 10.3389/fimmu.2021.700995

Prenatal Maternal Stress Exacerbates Experimental Colitis of Offspring in Adulthood

Yue Sun[1,2†], Runxiang Xie[1,2†], Lu Li[1,2], Ge Jin[1,2], Bingqian Zhou[1,2], Huan Huang[1,2], Mengfan Li[1,2], Yunwei Yang[1,2], Xiang Liu[1,2], Xiaocang Cao[1,2], Bangmao Wang[1,2], Wentian Liu[1,2], Kui Jiang[1,2] and Hailong Cao[1,2]*

[1] Department of Gastroenterology and Hepatology, General Hospital, Tianjin Medical University, Tianjin, China, [2] Institute of Digestive Diseases, Tianjin Key Laboratory of Digestive Diseases, Tianjin, China

OPEN ACCESS

Edited by:
Oscar Gilberto Gomez-Duarte, University at Buffalo, United States

Reviewed by:
Guillaume Sarrabayrouse, Université de Paris, France
Jian Huang, Coriell Institute for Medical Research, United States

***Correspondence:**
Hailong Cao
caohailong@tmu.edu.cn

[†]These authors have contributed equally to this work

Specialty section:
This article was submitted to Microbial Immunology, a section of the journal Frontiers in Immunology

Received: 27 April 2021
Accepted: 13 October 2021
Published: 03 November 2021

Citation:
Sun Y, Xie R, Li L, Jin G, Zhou B, Huang H, Li M, Yang Y, Liu X, Cao X, Wang B, Liu W, Jiang K and Cao H (2021) Prenatal Maternal Stress Exacerbates Experimental Colitis of Offspring in Adulthood. Front. Immunol. 12:700995. doi: 10.3389/fimmu.2021.700995

The prevalence of inflammatory bowel disease (IBD) is increasing worldwide and correlates with dysregulated immune response because of gut microbiota dysbiosis. Some adverse early life events influence the establishment of the gut microbiota and act as risk factors for IBD. Prenatal maternal stress (PNMS) induces gut dysbiosis and perturbs the neuroimmune network of offspring. In this study, we aimed to investigate whether PNMS increases the susceptibility of offspring to colitis in adulthood. The related index was assessed during the weaning period and adulthood. We found that PNMS impaired the intestinal epithelial cell proliferation, goblet cell and Paneth cell differentiation, and mucosal barrier function in 3-week-old offspring. PNMS induced low-grade intestinal inflammation, but no signs of microscopic inflammatory changes were observed. Although there was no pronounced difference between the PNMS and control offspring in terms of their overall measures of alpha diversity for the gut microbiota, distinct microbial community changes characterized by increases in *Desulfovibrio*, *Streptococcus*, and *Enterococcus* and decreases in *Bifidobacterium* and *Blautia* were induced in the 3-week-old PNMS offspring. Notably, the overgrowth of *Desulfovibrio* persisted from the weaning period to adulthood, consistent with the results observed using fluorescence *in situ* hybridization in the colon mucosa. Mechanistically, the fecal microbiota transplantation experiment showed that the gut microbiota from the PNMS group impaired the intestinal barrier function and induced low-grade inflammation. The fecal bacterial solution from the PNMS group was more potent than that from the control group in inducing inflammation and gut barrier disruption in CaCo-2 cells. After treatment with a TNF-α inhibitor (adalimumab), no statistical difference in the indicators of inflammation and intestinal barrier function was observed between the two groups. Finally, exposure to PNMS remarkably increased the values of the histopathological parameters and the inflammatory

cytokine production in a mouse model of experimental colitis in adulthood. These findings suggest that PNMS can inhibit intestinal development, impair the barrier function, and cause gut dysbiosis characterized by the persistent overgrowth of *Desulfovibrio* in the offspring, resulting in exacerbated experimental colitis in adulthood.

Keywords: early life, prenatal maternal stress, microbiota, mucosal barrier, colitis

INTRODUCTION

Inflammatory bowel disease (IBD), comprising ulcerative colitis and Crohn's disease, involves a group of chronic, recurrent, and destructive intestinal inflammatory conditions (1). The etiology and pathogenesis of IBD have not been entirely expounded yet. IBD is becoming highly prevalent worldwide, showing pronounced growth in newly industrialized countries (2) and posing a challenge to health services. Potential factors that contribute to these transitions of incidence and prevalence include the urbanization, industrialization, and westernization of society (3). Stress has become a sizeable component of modern lifestyle and greatly contributes to the increased prevalence of IBD. The importance of stress on IBD has long been recognized in the literature (4, 5). Stress triggers the flares of patients with IBD (6–11), and the underlying mechanisms include the dysregulation of the gut–brain–microbiome axis and the neuroendocrine system (12, 13).

The early life stage is a pivotal period of developmental plasticity. Recent studies have emphasized maternal influences on fetuses and indicated that early life events (such as the delivery mode, breastfeeding, and antibiotic exposure) can affect the potential risk of IBD (14–17). According to available data, initial intestinal microbial colonization appears immediately after birth (18, 19). Establishment of the intestinal microflora, which occurs in early life, known as the window of opportunity, is of paramount importance to the maturation of the immune system. One hypothesis is that the disruption of the microbiome during the crucial window can aggravate a disease later in life in a manner that influences childhood development and causes long-lasting detrimental consequences of immunopathology (20–22). Neonatal colonizers are mainly derived from maternal microbiota, such as the gut microbiota, vaginal microbiota, and breast milk (23). Perinatal factors, such as nutrition, antibiotic use, and maternal stress, alter the maternal gut microbiota during pregnancy and shape the establishment of the early microbiome in neonates (24, 25).

Growing evidence has suggested that early life adversities, including prenatal and postnatal events, can alter the gut microbiota and make it potentially prone to certain diseases (26–29). Prenatal maternal stress (PNMS) induces gut microbiota dysbiosis, perturbs the neuroimmune network, and upregulates the levels of placental inflammatory factors, and may raise susceptibility to asthma, visceral hypersensitivity, and neurological disorders in offspring through vertical transmission (30–34). In fact, some clinical studies demonstrated that maternal prenatal stress is associated with the composition of infant fecal microbiota (35, 36). Repeated restraint stress from the 14th to the 20th day of embryo development can decrease the density of distal colonic innervation and change the gut microbiota of offspring rats (37). Prenatal stress in early pregnancy leads to changes in the gut niche, transcriptome, and immune cells in the offspring. Furthermore, these changes are linked to alterations in the adult intestinal permeability and microbiota following additional stress in adulthood (38). However, whether or not PNMS increases the susceptibility to IBD in the next generation and what mechanisms are involved are unclear.

Here, we investigated the effects of PNMS on the susceptibility of offspring to colitis in adulthood. We show that PNMS impaired the intestinal development and barrier function in the offspring. We further provide evidence that PNMS can disturb the establishment of the intestinal microflora, induce the persistent overgrowth of *Desulfovibrio*, and engender low-grade colonic inflammation in the offspring. Interestingly, dysbiosis persisted into adulthood, where experimental colitis worsened. Our findings demonstrated that PNMS, one of the common adverse early life events, has negative effects on the intestinal development and microbiota establishment of offspring, thus raising the risk of colitis. The study is of pivotal importance to the study of the pathogenesis of IBD.

MATERIALS AND METHODS

Animals and Prenatal Maternal Stress

Experiments were performed on C57BL/6 mice (provided by Peking Union Medical College). The animals were kept in specific pathogen-free conditions and allowed to acclimatize for 1 week before experimentation. They were fed with an AIN-93M rodent diet and sterile filtered water in a controlled environment under a 12-h light/12-h dark schedule. Mice were mated overnight; a positive vaginal plug was denoted as embryonic day 0 of pregnancy.

A brief description of the experimental flow is shown in **Figure 1A**. Pregnant dams were randomly assigned to either the control (n = 6) or the PNMS (n = 6) group and housed individually. Beginning on E10, pregnant dams assigned to the PNMS group were subjected to variable stress, and the paradigm was modified from the previous study (39). Mice randomly experienced two of the following stressors daily to prevent habituation to stress: constrained inside a 50-ml tube for 60 min, wet bedding with saturated water overnight, lights on during the dark phase, 1 h white noise generated by a speaker (2–20 kHz, 90 dB), and 60 min water avoidance stress. Mice were not subjected to the same stressor for two consecutive days. The morning on which the litter was found was considered postnatal

day (PND) 0. On PND 1, litter size was standardized to four per litter. In the 21 days between birth and weaning, the mice were housed with their mother and littermates. On PND 22, one mouse from each litter was randomly selected and sacrificed. The remaining pups were weaned in the same-sex housing until the end of the assay (three or four in each cage). Offspring was weighed weekly after birth. The Ethics Committee of Tianjin Medical University (Tianjin, China) approved all the animal procedures.

Tissue Collection

Offspring mice 3 and 8 weeks old were euthanized. Small intestine and colon tissues were immediately removed and washed with pre-cooled phosphate-buffered saline (PBS). The small bowel was separated into three segments. For the preparation of paraffin slices, distal tissues were Swiss rolled and fixed with 4% paraformaldehyde. The sections were subsequently used in multiple staining experiments. The proximal tissues of four intestinal segments were collected and placed in a −80°C refrigerator after snap freezing in liquid nitrogen.

Histology and Immunohistochemistry

Paraffin-embedded specimens were sectioned at a thickness of 4 μm and stained with hematoxylin and eosin (HE). For the histological assessment of intestinal development, the villus height and crypt depth of each intestinal section were measured under a light microscope (DM5000 B; Leica, Wetzlar, Germany), and 100 well-oriented, intact villus/crypt of each mouse were randomly selected for evaluation.

For immunohistochemistry, tissue microarray sections were deparaffinized with xylene, rehydrated with gradient concentrations of ethanol, and soaked in 3% hydrogen solution. Then, the sample was exposed to antigen hot retrieval with citrate buffer and further incubated with a blocking serum. After blocking, the tissue slices were incubated overnight with a monoclonal anti-Ki67 (ab16667; Abcam, Cambridge, UK), anti-Muc2 (Santa Cruz Biotechnology, Inc., Santa Cruz, CA, USA), or an anti-lysozyme (ab108508; Abcam) antibody. After incubation, the sections were washed with PBS, incubated with labeled polymer–horseradish peroxidase, and counterstained with 3,3′-diaminobenzidine. The sections were observed under a Leica microscope (DM5000 B; Wetzlar, Germany). Positive cells were counted by observing 100 villi or crypts per mouse from at least five randomly selected fields in a blinded manner. The original magnification of the HE and immunohistochemical staining was ×200.

Immunofluorescent Staining

Small intestine and colon sections (4 μm thick) were deparaffinized and hydrated and then subjected to heat-induced antigen retrieval. PBS with 5% bovine serum albumin (BSA) (Solarbio, Beijing, China) was used as the blocking agent for nonspecific binding. Thereafter, the slides were incubated with an anti-immunoglobulin A (IgA) antibody (ab223410; Abcam) overnight. Then, secondary antibody conjugates, DyLight 488 anti-goat immunoglobulin G (IgG) secondary antibody (Abbkine, Wuhan, China) or anti-rabbit IgG (H&L) secondary antibody, Alexa Fluor® 488 conjugate (Invitrogen, Carlsbad, CA, USA), were added to the sections for 60 min (avoiding light). Finally, 4,6-diamidino-2-phenylindole (DAPI; Solarbio, Beijing, China) marked nuclei blue. Immunofluorescence pictures were obtained under a Pannoramic MIDI II slide scanner (3DHISTECH, Budapest, Hungary) at ×200 magnification. As described previously, the average quantity of positive cells in 100 villi was recorded per mouse. For zonula occludens-1 (ZO-1) immunofluorescence staining, the cells were fixed with 4% (*w*/*v*) paraformaldehyde solution for 15 min and permeabilized with 0.2% (*w*/*v*) Triton X-100 for 10 min. Then, the cells were blocked for 1 h in 10% donkey serum and incubated with anti-ZO-1 (61-7300; Thermo Fisher Scientific, Waltham, MA, USA) overnight at 4°C. Alexa 488-conjugated donkey anti-rabbit IgG and DAPI were incubated with cells separately. Images were obtained at a magnification of ×400.

Intestinal Permeability Measurement

To assess intestinal permeability, the absorption of fluorescein isothiocyanate–dextran (FITC-D) (MW: 4,000 Da; Sigma-Aldrich, St. Louis, MO, USA) from the gut lumen into the plasma was monitored. Mice received FITC-D (6 mg/10 g body weight, 50 mg/ml) through oral gavage for 4 h prior to blood collection. The blood was drawn from the ophthalmic vein and collected with heparinized microcentrifuge tubes. Serum samples were separated through centrifugation at 2,000 rpm for 10 min. The fluorescence intensity of each sample was measured (excitation = 485 nm, emission = 530 nm). The FITC-D concentration was derived from an FITC-D standard curve produced through serial dilution in mouse plasma.

Periodic Acid–Schiff Staining

Colon sections were incubated in 1% periodic acid solution for 10 min, washed, incubated in Schiff's reagent for 40 min, washed again, and counterstained with hematoxylin solution for 5 min. Between each step, the samples were rigorously washed with 1× PBS buffer. Positive cells were calculated by observing 100 villi or crypts per mouse from at least five randomly selected fields in a blinded manner. Images were taken with a Leica microscope (DM5000 B; Wetzlar, Germany) at ×200 magnification.

Real-Time PCR Analysis

The extraction of total RNA from the tissues was performed using an RNeasy Mini Kit (Qiagen, Carlsbad, CA, USA), and then reverse transcription was conducted with a TIANScript Reverse Transcription Kit (TIANGEN Inc. Beijing, China). Quantitative PCR analyses in real time were carried out using a StepOnePlus Real-Time PCR apparatus (Applied Biosystems, Carlsbad, CA, USA) according to the manufacturer's directions. The PCR procedure was performed as follows: incubation (95°C, 10 min), 40 cycles of denaturation (95°C, 15 s), and annealing and extension (60°C, 1 min). Quantification of amplicons was accomplished with SYBR Green fluorescence. The oligonucleotide primer pairs included ZO-1, claudin 3, occludin, Muc2, cryptdin, regenerating islet-derived protein (Reg3γ), interleukin 1 beta (IL-1β), tumor necrosis factor alpha (TNF-α), interferon gamma (IFN-γ), transforming growth factor beta (TGF-β), IL-6, and IL-10, which

were synthesized by GENEWIZ, Inc. (Beijing, China). The sequences are summarized in **Supplementary Table S1**. Relative messenger RNA (mRNA) quantification was calculated using the $2^{-\Delta\Delta CT}$ method.

Western Blotting

Total protein extracts of the colon tissues were harvested with RIPA buffer (Solarbio, Beijing, China). A bicinchoninic acid protein assay kit (Thermo Fisher Scientific) was used in evaluating the protein concentration and homogenizing proteins. Protein samples were loaded onto an SDS-PAGE system for separation and subsequently electrotransferred onto PVDF membranes (Invitrogen). After blocking with BSA, the membranes were incubated with appropriate primary antibodies against β-actin (anti-mouse) and anti-CLDN3 (anti-mouse) and then with horseradish peroxidase (HRP)-conjugated secondary antibodies (all from Cell Signaling Technology, Danvers, MA, USA). An enhanced chemiluminescence (ECL) chromogenic substrate was used in visualizing bands. Proteins were quantified using the ImageJ plot profile tool.

16S rDNA Amplicon Sequencing

Offspring stool specimens were detected at 3 and 8 weeks after birth. Bacterial DNA extraction, 16S ribosomal DNA (rDNA) amplicon sequencing, and 16S rDNA gene analysis were conducted by the Realbio Genomics Institute (Shanghai, China). The QIAamp® Fast DNA Stool Mini Kit (QIAGEN, Hilden, Germany) was used in isolating total genomic bacterial DNA. Bacterial 16S ribosomal RNA (rRNA) genes (V3–V4 regions) were amplified using genomic DNA as the template on a thermal cycler, and specific primers were used (forward: 5′-TCGTCGGC AGCGTCAGA TGTGTATAAGAGACAGCCTACGGGNGGC WGCAG-3′; reverse: 5′-GTCTCGTGGGCTCGGAG ATG TGTATAAGAGACAGGACTACHVGGGTATCTAATCC-3′). PCR was conducted using the high-fidelity enzyme of a KAPA HiFi Hotstart PCR kit to maintain the accuracy and efficiency of amplification. After amplification, purification, and quantification of the fragments, the DNA sample was produced using the Illumina HiSeq™ 2000 platform. The chimeras and singletons were removed, and the operational taxonomic units (OTUs) were obtained at 97% sequence similarity by clustering with USEARCH (v7.0.1090) in the QIIME pipeline. A comparison of the RDP database with the Basic Local Alignment Search Tool (BLAST) program was performed for the analysis of classification. Diversity measure and rank abundance curve analyses were conducted using the abundance data in QIIME. The resulting matrix of distances was obtained through principal coordinate analysis (PCoA) between groups. Differences between and within groups were compared through analysis of similarities (ANOSIM). Abundance and diversity were estimated using the Shannon and Simpson indexes. Linear discriminant analysis (LDA) score histogram and cladogram were created through linear discriminant analysis effect size (LEfSe) analysis. Spearman's correlations were then calculated for the differential bacterial and environmental predictors. The raw sequencing data were uploaded to NCBI (SRA accession: NCBIPRJNA728691).

Fluorescence *In Situ* Hybridization

Fluorescence *in situ* hybridization (FISH) was performed as described previously (40). 16S rRNA-targeted oligonucleotide probes were obtained from probeBase (http://www.microbial-ecology.net/probebase/). *Desulfovibrio* Cy5-conjugated specific probe (ATGTTATCCATGTGTATAGGGC) was labeled with Spectrum-Red (Thermo Fisher Scientific). An FITC-conjugated EUB338 universal bacterial probe (GCTGCCTCCCGTAGG AGT), as the positive control, was labeled with Spectrum-Green (Thermo Fisher Scientific). In brief, 5-μm-thick colon paraffin sections were pretreated and hybridized with the *Desulfovibrio* and EUB338 probes for 5 h. Then, DAPI (Thermo Fisher Scientific) was added after incubation, and the nucleus was stained and observed under a fluorescence microscope (magnification, ×400).

Fecal Microbiota Transplantation

Fresh stool samples (600 mg) were collected from the control and 3-week-old PNMS offspring. In an anaerobic environment, fecal pellets from each group were pooled, homogenized, and suspended in 15 ml of old sterile PBS solution with 0.05% cysteine hydrochloride. After standing for 2 min, the supernatant was collected, transferred to sterile Hungate anaerobic tubes, and stored at −80°C. Eight-week-old mice were divided into two groups [fecal microbiota transplantation (FMT)-Control and FMT-PNMS groups] containing five mice each. The FMT-Control group received fecal transplantation from the control offspring, and the FMT-PNMS group received fecal transplantation from the PNMS offspring. For the ablation of commensal microbiota, the mice received an antibiotic cocktail of ampicillin (200 mg/L), metronidazole (200 mg/L), neomycin (200 mg/L), and vancomycin (200 mg/L) *via* drinking water as described in the literature (41). After 5 days of the mice receiving the antibiotic cocktails, a 200-μl bacterial solution was gavaged to each mouse three times a week for 4 weeks (**Figure 5A**).

Cell Culture and Treatment

Human colonic epithelial Caco-2 cells were cultured in Minimum Essential Medium (MEM; Gibco, Carlsbad, CA, USA) supplemented with 20% FBS (Gibco) and 1.0% non-essential amino acid. This test starved the Caco-2 cells with 0.5% serum medium for 12 h when they had grown to 70%–80% confluence. After starvation, the Caco-2 cells were incubated with fecal bacterial solution (1:200) from the control and 3-week-old PNMS offspring separately for 3 h. Then, the medium was changed to a medium with 0.5% serum and 1% penicillin–streptomycin, and the cells were harvested for experiments 12 h after co-culture with bacterial solution. For the antagonist studies, the cells were incubated with adalimumab (10 μg/ml; Abbott, Chicago, IL, USA) after the addition of fecal bacterial fluid at the end of the experiment. All the cells in each group were collected for the extraction of total protein and RNA.

Experimental Colitis Model

Eight-week-old adult mice were stochastically assigned through feeding with 2% (*w*/*v*) dextran sulfate sodium (DSS, 36–50 kDa;

MP California, USA) solution or water for 5 days to build a colitis model. During the modeling process, the DSS solutions were refreshed daily. We used the disease activity index (DAI), colonic length, spleen weight, and histological change in assessing the severity of colitis. The DAI scoring system was based on weight loss, rectal bleeding, and stool consistency, as described previously (42). The entire colon (from the cecum to the anus) was removed, and the length was measured and recorded. The histological score of the degree of colitis injury was measured with an orderly categorical measurement ranging from 0 to 40 (43). Scoring was performed by multiplying three histological features, namely, extent of inflammatory cell infiltration (0–3), depth of lesions (0–3), and damage of the crypt (0–4), by the corresponding percentage of the affected region (1–4). Histopathological assessment of the colon samples was performed in a blinded manner by a pathologist.

Statistical Analysis

Statistical calculations were conducted with GraphPad Prism (version 8.0). The measurement data were described as the mean ± standard error of the mean (SEM). A *t*-test or the Mann–Whitney *U* test was used between two groups, whereas ANOVA was used among four groups. Statistical significance was set at $p < 0.05$.

RESULTS

PNMS Inhibited Intestinal Development of the 3-Week-Old Offspring

The offspring from the PNMS and control groups followed a similar weight curve during the first 8 weeks of life (**Figure 1C**). Before weaning, the growth of the offspring is mainly supported by breastfeeding and parental care provided by mammalian mothers. Moreover, the gastrointestinal tracts of rodents mature in the third postnatal week. Therefore, the weaning period was used as a key node for the evaluation of maternal influence on the development of offspring in this study. To test whether or not PNMS affects intestinal growth, the villus length in the jejunum and ileum and the crypt depth in the colon were observed through HE staining. Morphometric quantification showed a significant decrease in the average villus length/crypt depth in PNMS mice relative to the control group (**Figures 1B, D**). Similar differences in the intestinal villus structure were not observed in adulthood (data not shown).

The intestinal epithelium continuously self-renews throughout the cell proliferation and differentiation cycles. Differentiated enterocytes arise from intestinal stem cells residing in the crypt region. Here, we evaluated the impact of PNMS on intestinal epithelial cell proliferation and differentiation in 3-week-old mice. The average count of Ki67-positive cells decreased in PNMS pups (**Figure 2A**) compared with that in the control group. Lysozyme immunohistochemical staining suggested a lower count of Paneth cells in PNMS mice (**Figure 2B**). As a critical component of intestinal resistance to infection by enteropathogenic bacteria, Paneth cells secrete antimicrobial peptides, such as cryptdin, defensin, and Reg3γ. Real-time PCR data showed that the mRNA expressions of cryptdin and defensin decreased in PNMS pups (**Figure 2C**). In addition, in comparison with the control pups, PNMS pups showed an obvious decreasing trend with regard to the number of MUC2-positive cells and periodic acid–Schiff (PAS)-positive cells, indicating cell differentiation (**Figures 2D, E**). Meanwhile, Muc2 gene expression in PNMS pups was lower than that in the control pups (**Figure 2C**). These results showed that PNMS has an adverse effect on the intestinal development of offspring.

PNMS Disrupted the Gut Barrier Function of Offspring

The gut barrier is crucial to the maintenance of homeostasis in the gut mucosa. Barrier destruction underlies mucosal inflammation in IBD. Here, the intestinal barrier was evaluated at 3 weeks of age. The concentration of FITC-D in the serum was significantly attenuated in PNMS mice, indicating elevated intestinal epithelial permeability and disrupted intestinal integrity (**Figure 3A**). Tight junctions represent an essential feature of the first defense barrier of the intestine. To further investigate changes in the gut barrier, we evaluated the expressions of the tight junction proteins. The expression levels of ZO-1, claudin 3, occludin, and ZO-1 mRNA were reduced in PNMS mice (**Figure 3B**) compared with those in the control mice. Western blot results showed lower claudin 3 protein levels detected in PNMS mice (**Figure 3C**).

Intestinal secretory immunoglobulin A (sIgA) is a main component of the defense line, preventing pathogenic mucosal adhesion and colonization. We measured the expression of intestinal IgA in the small intestine at the IgA enrichment intestinal tract in 3-week-old pups. Immunofluorescence staining demonstrated that the number of sIgA-positive cells (emphasized by a white arrow in the figure) decreased in the lamina propria of the offspring exposed to PNMS (**Figures 3D, E**). Collectively, PNMS can impair not only the mechanical barrier but also the chemical and immune barriers.

PNMS Induced Low-Grade Intestinal Inflammation in 3-Week-Old Offspring

No microscopic inflammation was observed in the HE-stained sections of the intestinal tissues of 3-week-old pups. Then, we examined the relative expressions of colonic pro-inflammatory cytokines through real-time PCR. The data showed that the mRNA expression levels of IL-1β, IFN-γ, and TNF-α were upregulated in PNMS mice, whereas that of TGF-β did not reach statistical difference (**Figure 3F**). These observations indicated that PNMS in early life induces low-grade inflammation in offspring.

PNMS Induced Overgrowth of *Desulfovibrio* in 3-Week-Old Offspring

To determine whether or not exposure to PNMS results in alterations of the composition of the microbiota, we collected the feces of 3-week-old pups for 16S rDNA sequencing. The overlap and difference of OTUs in the fecal microbiota between

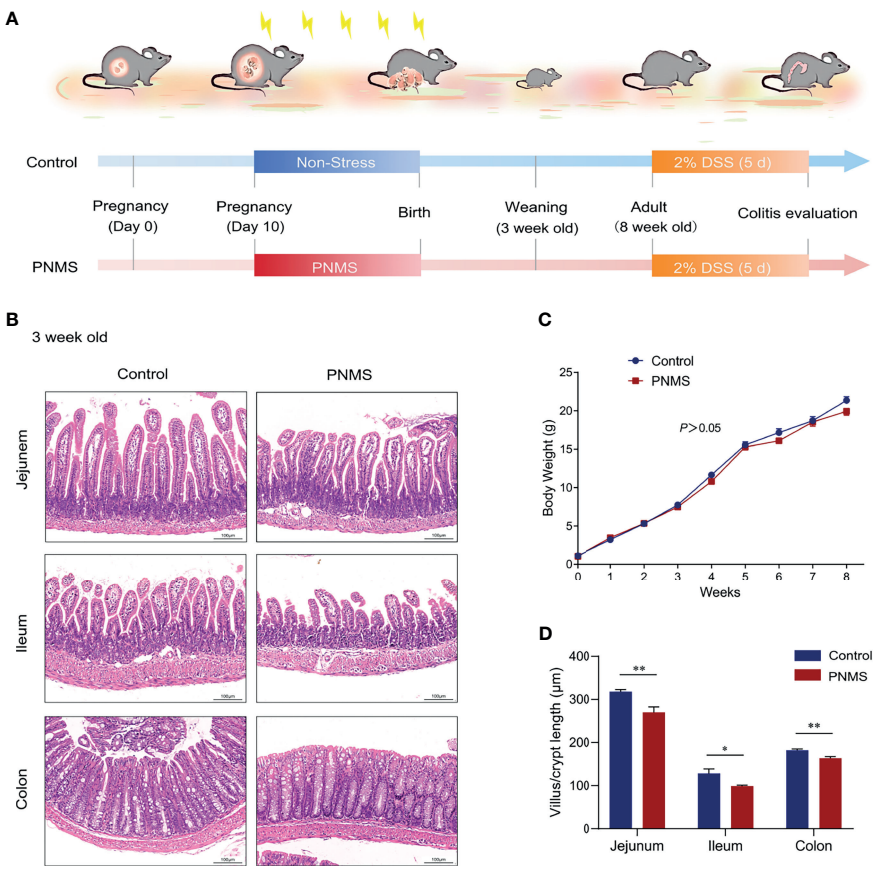

FIGURE 1 | Prenatal maternal stress impaired the intestinal development of 3-week-old offspring. **(A)** Flow diagram of the experimental procedure. **(B)** Microscopic observation of the intestinal and colonic development of 3-week-old pups with hematoxylin and eosin (HE) staining. **(C)** Changes in the body weight of offspring mice from week 0 to week 8. **(D)** Measurement of the villus lengths in the jejunum and ileum and the crypt depths of the colon. *PNMS*, prenatal maternal stress; *DSS*, dextran sulfate sodium. *Scale bar*, 100 μm. Magnification, ×200. $^{*}p < 0.05$, $^{**}p < 0.01$. PNMS ($n = 6$) *vs*. control ($n = 6$).

the two groups were displayed in a Venn diagram (**Figure 4A**). A total of 391 OTUs were obtained from PNMS mice, and 422 OTUs were obtained from control mice, sharing 370 OTUs.

Next, we characterized the bacterial communities to compare the community structure and diversity at different levels. Bacterial composition was assessed at different taxonomic levels (**Figure 4B** and **Supplementary Figures S1A, B**). The relative abundance of the bacterial phyla between the two groups was similar, and no statistical difference was found (**Figure 4B**). The composition of the gut microbiota at the level of bacterial phylum in each specimen is shown in **Supplementary Figure S1C**. No significant difference in the alpha diversity was observed (**Supplementary Figure S1D**). Bacteria with significant differential abundance between the control and PNMS groups were detected (**Figures 4C, D** and **Supplementary Figures S1E, F**). Notably, Desulfovibrionales, Desulfovibrionaceae, and *Desulfovibrio*, which are pro-inflammatory bacteria, increased in the PNMS group. In addition, other potential Gram-positive coccus pathogens, such as *Streptococcus* and *Enterococcus*, increased in the PNMS group. In contrast, Bifidobacteriales, Bifidobacteriaceae, and *Bifidobacterium*, which are growth-promoting and anti-inflammatory probiotics, dramatically decreased in the PNMS group. In parallel, short-chain fatty acid (SCFA)-producing bacteria, such as *Blautia* and *Robinsoniella*, showed significantly reduced abundance in mice exposed to PNMS. Two-color FISH further showed that *Desulfovibrio* was enriched in the colon of PNMS (**Figure 4E**). In-depth analysis revealed a correlation between intestinal microbiota and inflammation. Some specific genera of bacteria (especially *Desulfovibrio*) were positively correlated with intestinal inflammatory factors (**Figure 8B**).

In summary, these findings indicated that exposure to PNMS alters the composition of the intestinal microbiota and, thus, influences the establishment and development of commensal microflora in early life.

Gut Microbiota From the PNMS Group Impaired Intestinal Barrier Function and Induced Low-Grade Inflammation

Through the FMT experiment, we found that the gut microbiota from the PNMS group impaired the intestinal barrier function and induced low-grade inflammation. The fecal bacterial solution from the PNMS offspring significantly reduced the

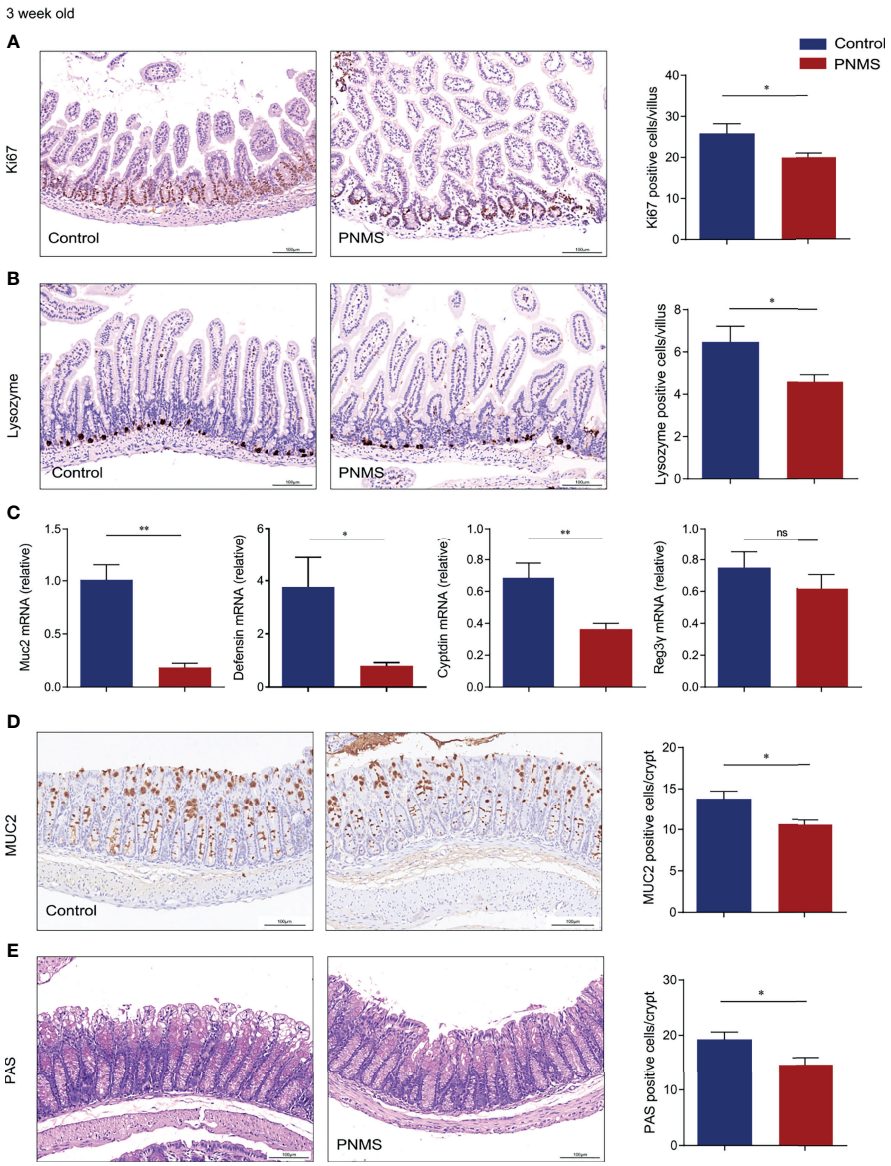

FIGURE 2 | Prenatal maternal stress inhibited the proliferation and differentiation of the intestinal tract in 3-week-old offspring mice. **(A)** Cell proliferation in the small intestine was assessed through Ki-67 immunohistochemical staining. **(B)** Paneth cells in the small intestine were evaluated by lysozyme immunohistochemical staining and the quantification of positively stained cells. **(C)** Relative mRNA expression levels of Muc2 in the colon and defensin, cryptdin, and Reg3γ in the small intestine. **(D)** Immunohistochemical staining for MUC2 mucin (*brown*) in colon tissue section. **(E)** Periodic acid–Schiff (PAS) staining for goblet cells in colon tissue. Quantification of positive cells per villus as shown by the histogram. At least 100 villi were randomly selected for each sample for calculation. *PNMS*, prenatal maternal stress. *Scale bar*, 100 μm. Magnification, ×200. $^{*}p < 0.05$, $^{**}p < 0.01$, $^{ns}p > 0.05$. PNMS ($n = 6$) *vs*. control ($n = 6$).

protein expression of claudin 3 and the relative mRNA levels of claudin 3, occludin, and Muc2 in the colon tissues more potently than did the fecal bacterial solution from the control offspring (**Figures 5B, C**). Furthermore, a subsequent increase in the expressions of the inflammatory factors IL-1β, TNF-α, and IL-6 was observed in the colon of FMT-PNMS mice (**Figure 5D**). These results suggested that the gut microbiota plays important roles in PNMS activities that affect the intestinal health of offspring. In this *in vitro* assay, the fecal bacterial solution was added to the Caco-2 culture. The results showed that the fecal bacterial solution from the PNMS group was more potent than that from the control group in inducing inflammatory cytokine expression and gut barrier disruption in Caco-2 cells (**Figures 5E–I**). The relative mRNA levels of TNF-α and IL-1β were upregulated, and the relative mRNA and protein levels of claudin 3 were downregulated (**Figures 5E–H**). The fluorescence intensity of ZO-1 in the PNMS group was lower than that in the control group (**Figure 5I**). We then determined whether or not

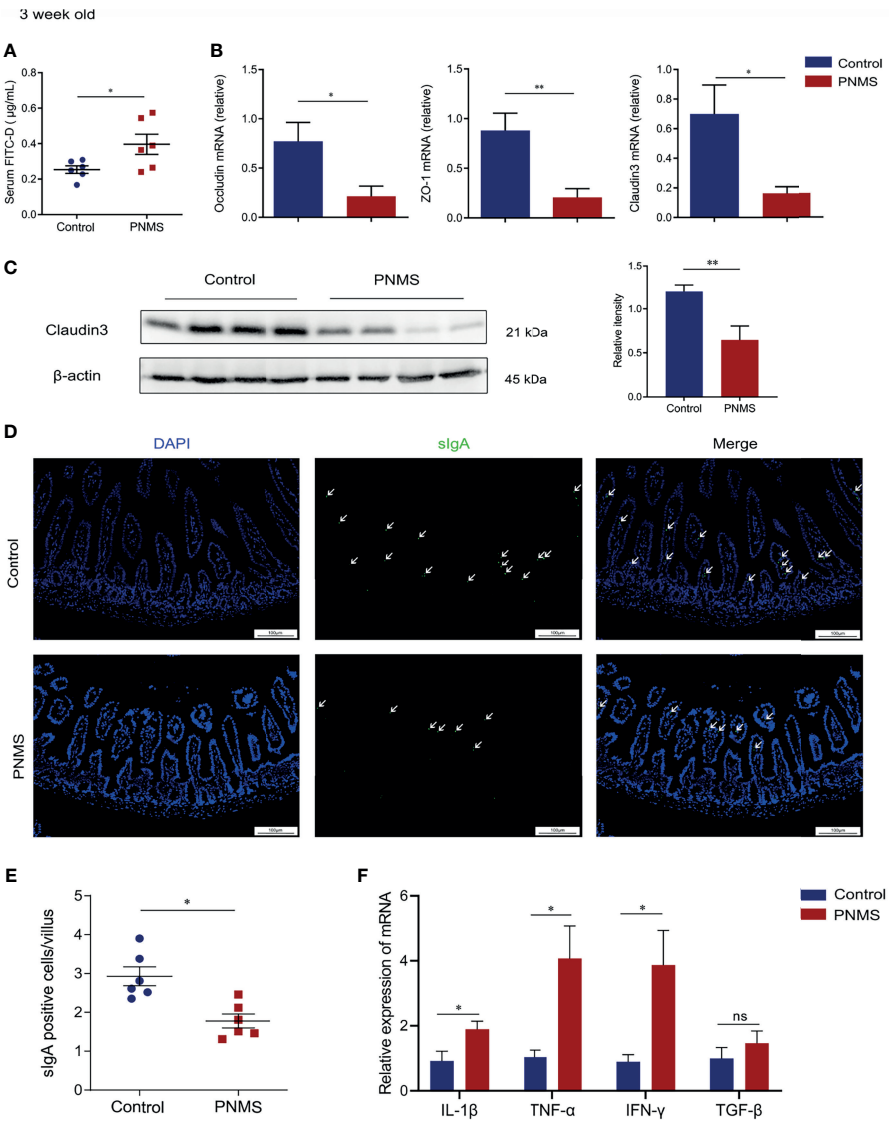

FIGURE 3 | Prenatal maternal stress impaired the intestinal barrier and induced colonic mucosal low-grade inflammation in 3-week-old offspring. **(A)** Intestinal permeability was measured through fluorescein isothiocyanate–dextran (FITC-D) assay. **(B)** Quantification of the relative mRNA expression levels of ZO-1, occludin, and claudin 3. **(C)** Western blot bands and relative quantification of claudin 3 in the colon. **(D)** Immunofluorescence staining of sIgA (*green*) and nuclear staining with DAPI (*blue*) were visualized *via* a fluorescent microscope. **(E)** Number of sIgA-positive cells per intestinal villus. **(F)** mRNA levels of the inflammatory cytokines in the colon. *PNMS*, prenatal maternal stress; *sIgA*, secretory immunoglobulin **(A)** *Scale bar*, 100 μm. Magnification, ×200. $^{*}p < 0.05$, $^{**}p < 0.01$, $^{ns}p > 0.05$. PNMS ($n = 6$) *vs*. control ($n = 6$).

adalimumab can reverse this interaction. The results showed that adalimumab can partially rescue the inflammatory and barrier disruption phenotype (**Figures 5E–I**). No statistical difference in the relative mRNA levels of TNF-α and IL-1β and the relative mRNA and protein levels of claudin 3 was found between the two groups of adalimumab.

Overgrowth of *Desulfovibrio* Induced by PNMS Continued in 8-Week-Old Offspring

To describe the long-term effects of PNMS on the gut microbiota, high-throughput sequencing was performed on the feces of 8-week-old offspring. The results showed that gut dysbiosis characterized by overgrowth of *Desulfovibrio* induced by PNMS continued in the 8-week-old offspring. The Venn diagram showed 370 OTU types in common, 52 OTU types that were exclusive to the control group, and 21 OTU types that were exclusive to the PNMS group (**Figure 6A**). The relative abundance of the bacterial phyla across the two groups showed no statistical difference (**Figure 6B**). Desulfovibrionales, Desulfovibrionaceae, and *Desulfovibrio*, which are associated with inflammation, persisted from 3 to 8 weeks and may play a key role in the susceptibility to colitis in adulthood (**Figures 6C, D**). PCoA at 3 and 8 weeks of age showed that the two

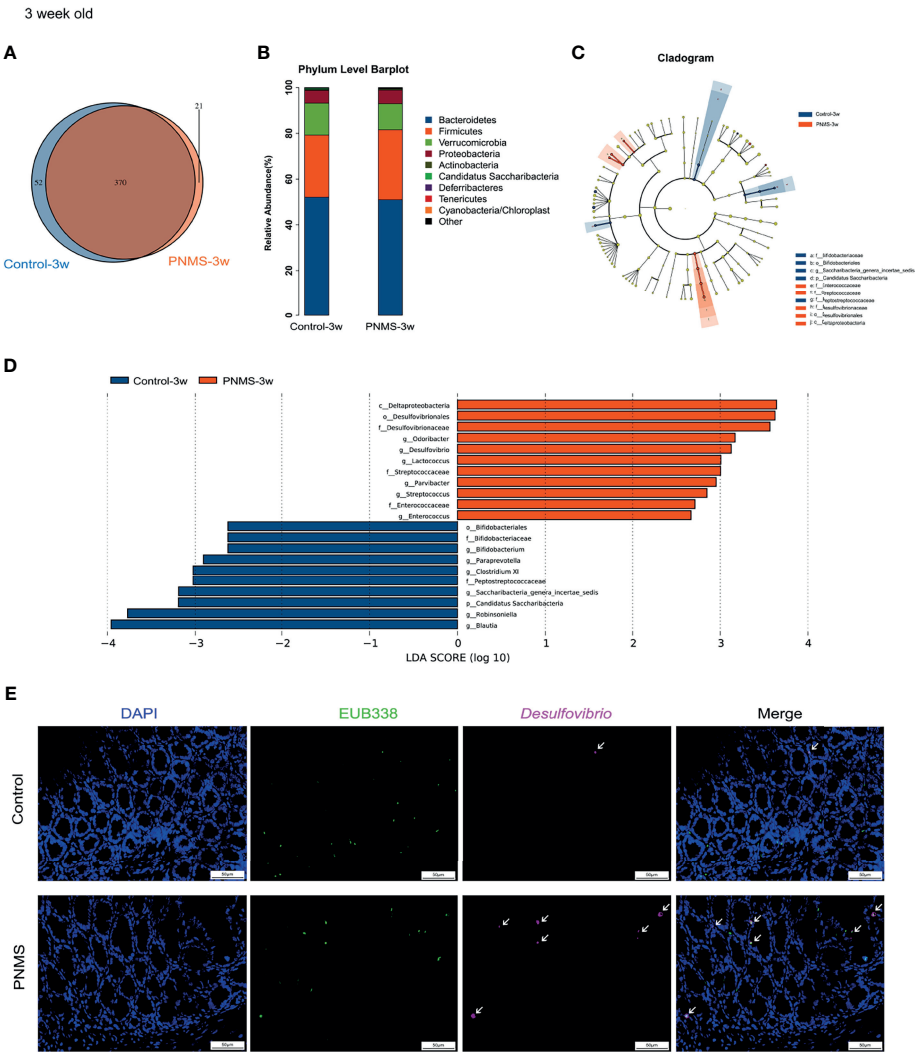

FIGURE 4 | Prenatal maternal stress induced dysbiosis of the gut microbiota in 3-week-old offspring. **(A)** Venn diagram of the operational taxonomic units (OTUs). **(B)** Microbial composition at the level of bacterial phylum. **(C, D)** Cladogram and the linear discriminant analysis (LDA) scores showed significant bacterial differences between the two groups by linear discriminant analysis effect size (LEfSe). **(E)** Fluorescence *in situ* hybridization (FISH) detection of *Desulfovibrio* in colon tissues of the control and PNMS offspring using a fluorescein isothiocyanate (FITC)-conjugated universal bacterial 16S rDNA-directed oligonucleotide probe (EUB338, *green*) and Cy5-conjugated *Desulfovibrio* specific probe (*red*). *PNMS*, prenatal maternal stress. *Scale bar*, 50 μm. Magnification, ×400. Control-3w (n = 15) *vs*. PNMS-3w (n = 15).

groups of mice on a free diet after weaning tended to separate on the microbiota of the offspring (**Figure 6E**). Weighted Unifrac ANOSIM revealed that the differences among the four groups were significant (**Figure 6F**). In addition, the abundance of the pro-inflammatory genus *Prevotalla* increased in PNMS mice compared with that in the control mice at 8 weeks of age.

PNMS Aggravated the Severity of Experimental Colitis in Adult Mice

The establishment of the gut microflora in early life and intestinal mucosal chronic inflammation have far-reaching impacts on intestinal health. In our study, we determined whether or not PNMS in early life increases the susceptibility to colitis in adult mice. Eight-week-old offspring were randomized to one cycle (5 days) of DSS treatment (2% in drinking water) or water treatment. The body weight and defecation of the offspring were recorded daily during the modeling process. Compared with the DAI scores in the normal control, the DAI scores in PNMS mice were significantly higher on the third, fourth, and the fifth day following modeling (**Figure 7A**). In mice without DSS treatment, no difference in the serum concentration of the marker FITC-D was found regardless of PNMS exposure (**Figure 7G**). Interestingly, in the colitis model groups, the mice exposed to PNMS showed higher FITC-D concentrations than did the control mice, suggesting higher intestinal permeability and more severe intestinal barrier destruction. The spleen/body weight ratio and the colon length of the PNMS and control mice were measured as indicators of immune/inflammation response. The colon lengths of the colitis

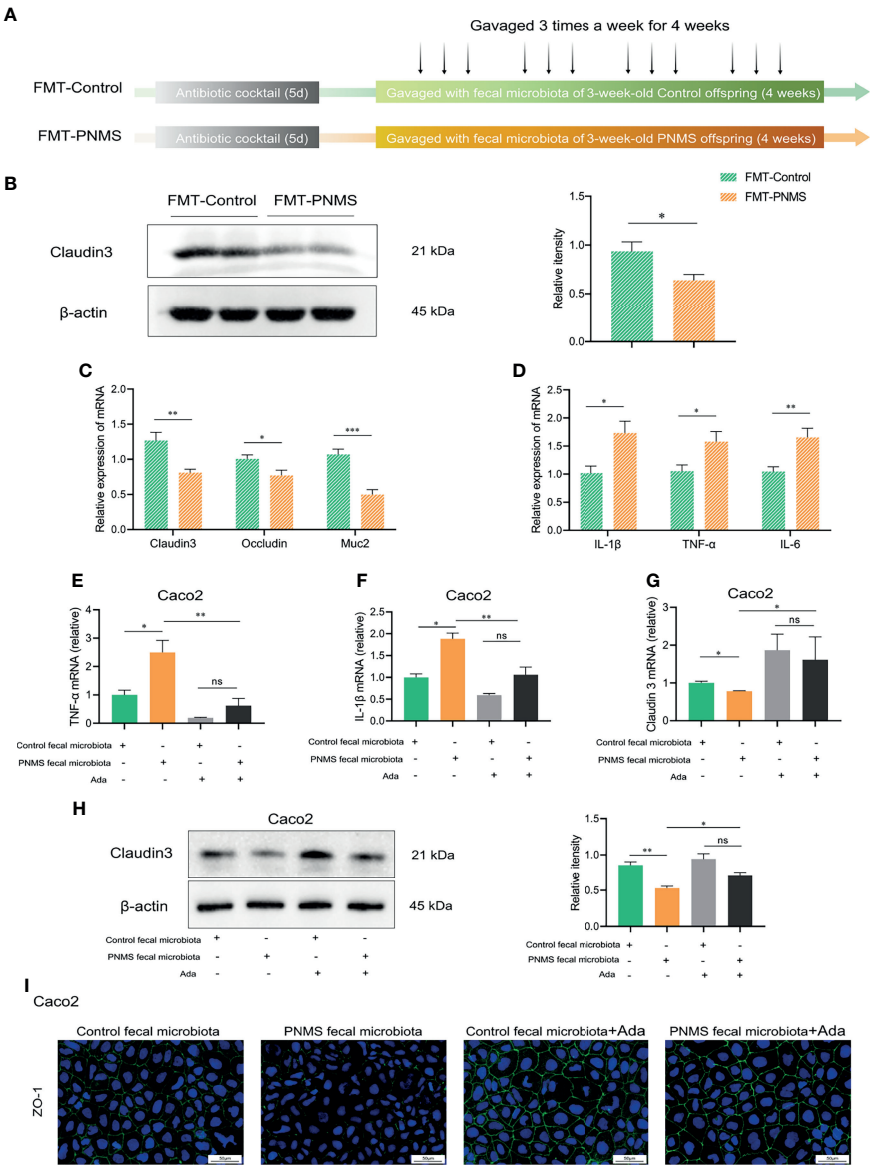

FIGURE 5 | Fecal microbiota from PNMS offspring impaired the gut barrier function and induced low-grade inflammation. **(A)** Experimental workflow. **(B)** Detection of claudin 3 protein by Western blotting. **(C)** Quantification of the relative mRNA expression levels of claudin 3, occludin, and Muc2. **(D)** mRNA levels of the inflammatory cytokines in the colon. **(E–I)** Treatment of Caco-2 cells with the fecal bacterial solution from the control and 3-week-old PNMS offspring mice alone or in combination with adalimumab. **(E, F)** Expressions of TNF-α and IL-1β assessed by quantitative PCR (qPCR). **(G, H)** Expression of claudin 3 assessed by Western blot and qPCR. **(I)** Fluorescence images for ZO-1. *FMT*, fecal microbiota transplantation; *PNMS*, prenatal maternal stress; *Ada*, adalimumab. *Scale bar*, 50 μm. Magnification, ×400. *$p < 0.05$, **$p < 0.01$, ***$p < 0.001$. FMT-control ($n = 5$) *vs*. FMT-PNMS ($n = 5$). ns, $P < 0.05$.

model mice in both groups were shorter than those of the non-model mice (**Figures 7B, C**). Moreover, the colon lengths of the model mice exposed to PNMS were significantly shorter than those of the mice that were not, and the difference was statistically significant (**Figures 7B, C**). In addition, the spleen/body weight ratio showed changes similar to the colon length. In the colitis model groups, PNMS mice had a higher spleen weight-to-body weight ratio than did the control mice, suggesting higher levels of systemic inflammation (**Figure 7F**). Moreover, the histological sections of the colon in the PNMS group showed marked neutrophil and lymphocyte infiltration, crypt damage, and injury of the epithelial structures and had higher histopathological scores (**Figures 7D, E**). Subsequently, we detected the relative expression levels of the pro-inflammatory cytokines in the colitis model mice. Higher mRNA expression levels of IL-1β, IL-6, and TNF-α were observed in mice with PNMS (**Figure 7H**), whereas no statistical difference was found in the expression of IL-10. As expected, the highest proportion of positive *Desulfovibrio* probe was found in the

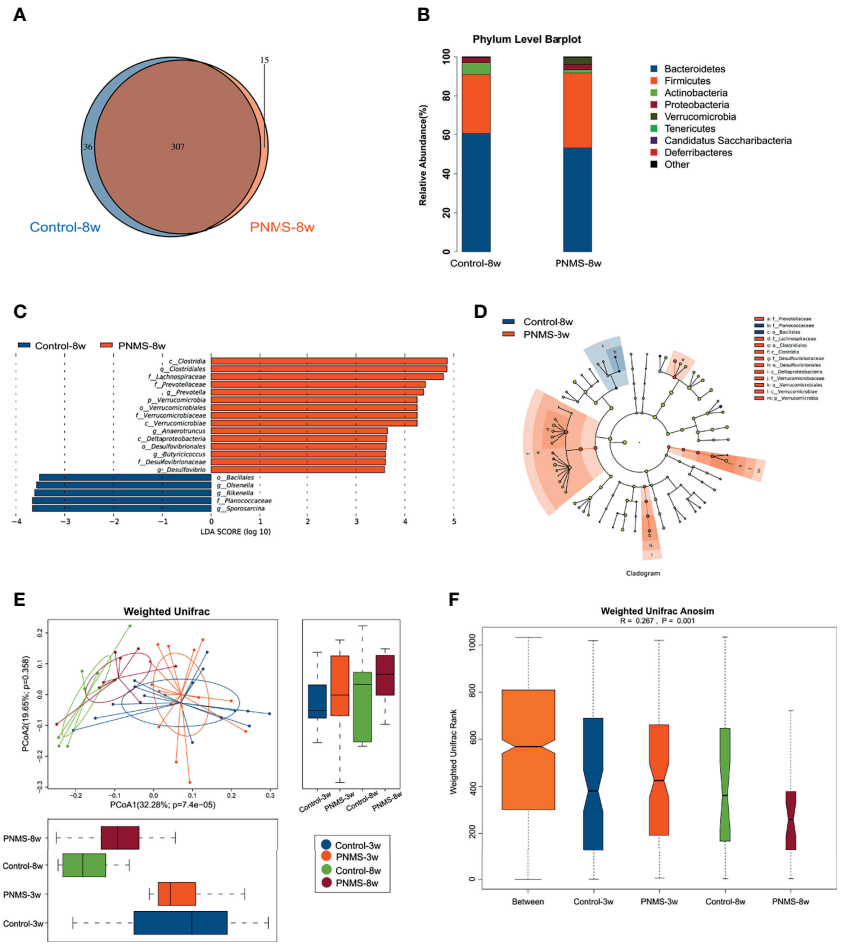

FIGURE 6 | Prenatal maternal stress has a long-term impact on the gut microbiota in the offspring. **(A)** Venn diagram of the operational taxonomic units (OTUs). **(B)** Gut microbiota composition at the phylum level. **(C, D)** Linear discriminant analysis (LDA) scores and the cladogram showed significant bacterial differences between the two groups by linear discriminant analysis effect size (LEfSe). **(E, F)** The gut microbiota of the 3- and 8-week-old offspring were put together for weighted Unifrac principal coordinate analysis (PCoA) and weighted Unifrac analysis of similarities (ANOSIM). *PNMS*, prenatal maternal stress. Control-3w (n = 15) *vs*. PNMS-3w (n = 15) *vs*. Control-8w (n = 8) *vs*. PNMS-8w (n = 8).

colitis model mice exposed to PNMS (**Figure 8A**). Notably, a positive correlation was observed between the abundance of *Desulfovibrio* and the indicators associated with DSS-induced colitis (**Figure 8C**). In general, these findings suggested that PNMS can exacerbate the risk of colitis in adult offspring mice.

DISCUSSION

IBD incidence has been growing at an alarming rate. IBD is increasingly recognized as a serious public health concern worldwide. However, the pathogenesis of IBD is not thoroughly elucidated. Environmental factors, especially early life adversities, have profound and lifelong influences on gut health and contribute to the development of IBD. PNMS can induce far-reaching alterations in the composition of the gut microbiota and correlates with major physiological system outcomes (37, 44). To date, the role of PNMS in IBD susceptibility remains unclear. Our research focused on the influence of PNMS on intestinal growth and development, gut microbiota, gut barrier, and intestinal inflammation in offspring. We found that exposure to PNMS can impair normal intestinal development, disrupt the intestinal barrier function, induce microbiota dysbiosis characterized by persistent overgrowth of *Desulfovibrio*, and exacerbate experimental colitis of offspring in adulthood (**Figure 9**). These findings might refine the understanding of the potential relationship between early life stress and IBD.

Maternal stress is considered one of the important factors in the pathogeny of offspring stress dysregulation and is a prevalent symptom of neuropsychiatric diseases (45–47). Stress is closely related to IBD. The gut and brain possess a bidirectional communication *via* the microbiota–gut–brain axis, involving neural, endocrine, and inflammatory mechanisms. Stress exerts negative effects on the intestine structure, permeability, gut

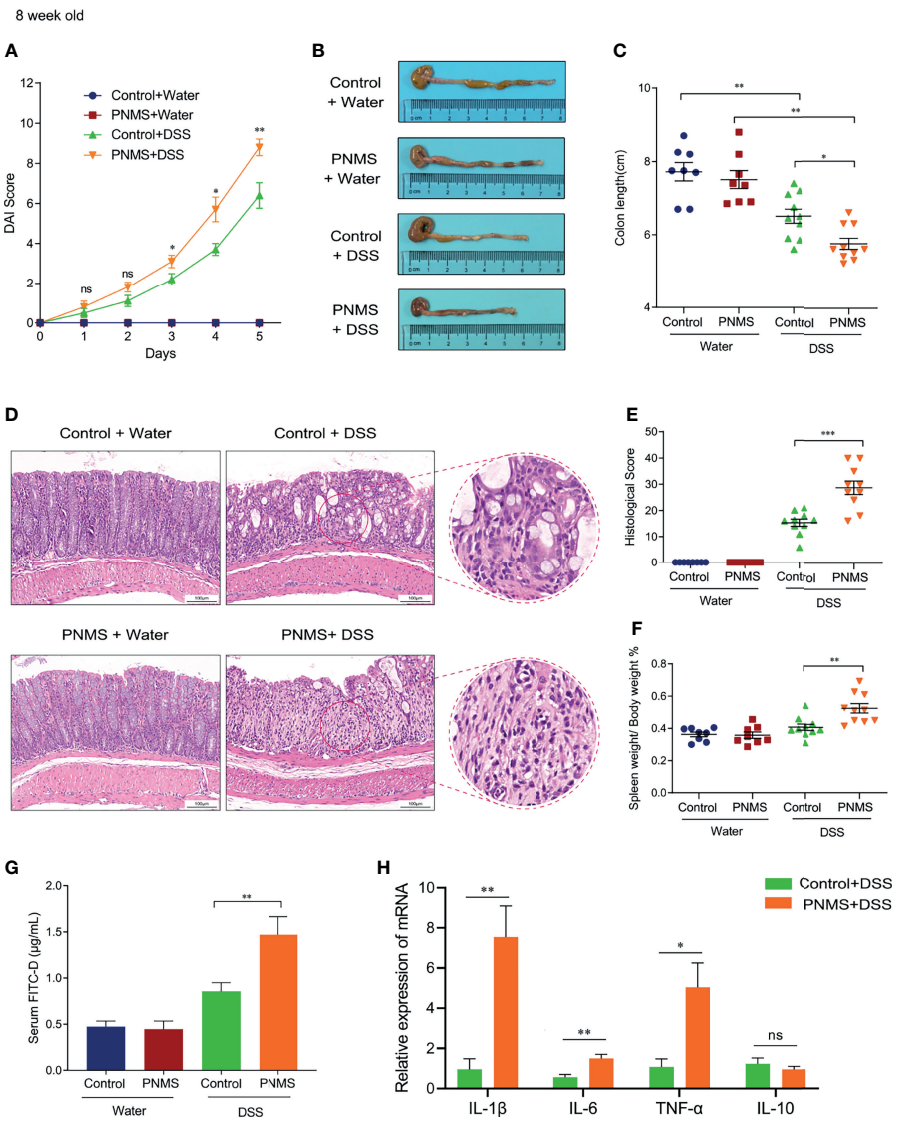

FIGURE 7 | Prenatal maternal stress aggravated the severity of experimental colitis in adult mice. **(A)** Disease activity index (DAI) scores during the process. **(B)** Colon appearance after treatment. **(C)** Colon lengths. **(D)** Histopathological changes of the colon section detected by hematoxylin and eosin (HE) staining. **(E)** Histological scores of colonic inflammation. **(F)** Ratio of spleen weight to body weight. **(G)** Fluorescein isothiocyanate–dextran (FITC-D) intestinal permeability assay. **(H)** Relative mRNA expressions of the inflammation factors in the colon. *PNMS*, prenatal maternal stress; *DSS*, dextran sulfate sodium. *Scale bar*, 100 μm. Magnification, ×200. *$p < 0.05$, **$p < 0.01$, ***$p < 0.001$. Control+Water ($n = 8$), PNMS+Water ($n = 8$), Control+DSS ($n = 10$), PNMS+DSS ($n = 10$). ns, $P < 0.05$.

microbiota, and the mucosal immune system (12, 48). In the present study, we found a "heritable" stress-induced intestinal barrier damage phenotype characterized by an increased intestinal permeability and a decreased intestinal mucin production in the early stage of the next generation. The vertical transmission of the gut bacteria and the subsequent establishment of the microbiota in neonates overlap with the pivotal period of neurodevelopment and the establishment of intestinal immunity (49, 50). Therefore, an altered intestinal flora colonization caused by maternal stress may ultimately have negative downstream effects on the growth and development of the intestinal tract and the immunologic function in neonates. This imprinting may persist and mediate excessive immune activation and raise susceptibility to inflammatory diseases in adulthood. Jašarević et al. conducted RNA sequencing analyses of fetal intestines on day 18.5 of pregnancy between early prenatal stress (EPS)-exposed and control fetuses. EPS-induced alterations in the expressions of transcripts are related to normal gastrointestinal development, energy balance, and immune function in male fetuses (38). Our study found that PNMS has adverse effects on the gut development of mice in the early stage, but the difference was not observed in the adult stage. In addition, EPS caused progeny phenotypes with reduced weight gain, increased acute stress-induced corticosterone levels, and

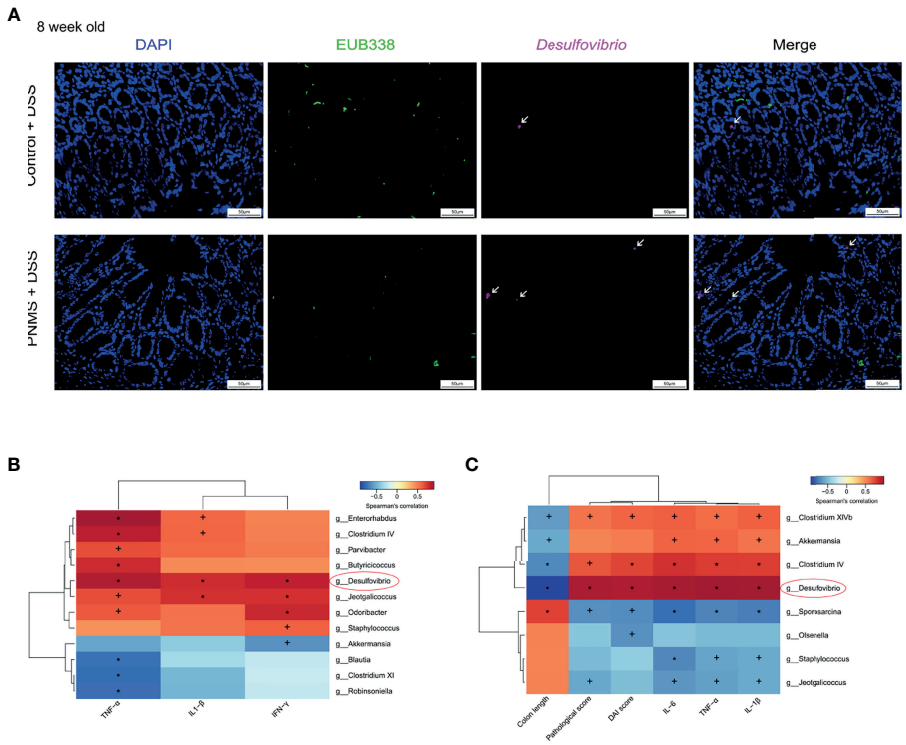

FIGURE 8 | The relative abundance of *Desulfovibrio* increased in PNMS offspring mice and was associated with intestinal inflammation. **(A)** Fluorescence *in situ* hybridization (FISH) detection of *Desulfovibrio* in colon tissues in 8-week-old colitis model offspring. A fluorescein isothiocyanate (FITC)-conjugated universal bacterial 16S rDNA-directed oligonucleotide probe (EUB338, *green*) and a Cy5-conjugated *Desulfovibrio* specific probe (*red*) were applied. **(B, C)** Heatmap of Spearman's correlations between the differential bacteria and markers of intestinal inflammation in 3- and 8-week-old offspring. *DSS*, dextran sulfate sodium; *PNMS*, prenatal maternal stress. *Scale bar*, 50 μm. Magnification, ×400. $^{+}p < 0.05$, $^{*}p < 0.01$ (Spearman's test).

altered hypothalamic gene expression in male offspring. However, no obvious sexual differences with regard to weight changes and stress phenotype were observed in the pups exposed to mid-to-late maternal stress. The different results may be related to periods of the stress paradigm.

In terms of mucosal immunity, we observed that the sIgA production of PNMS pups significantly declined. These results supported evidence from clinical observations of a recent study that used a Canadian infant cohort and investigated the fecal sIgA concentrations of 1,043 infants and the maternal depression and stress symptom trajectories of their mothers. The data showed that infants born to mothers with antepartum depressive symptoms had lower levels of sIgA in their feces (51). Increases in corticosteroids induced by repeated restraint stress can reduce the sIgA secretion into the gut lumen (52). Glucocorticoids can be transferred to fetuses during pregnancy *via* the placenta, especially under stress (33), and this process may explain the lower intestinal IgA concentrations in the pups. The reduction of sIgA in an infant can negatively affect immune maturation and the crosstalk between microbes and sIgA (53), resulting in an upgrowth in the risks of *Clostridiodes difficile* colonization (54) and allergic conditions (55).

The early life stage represents a critical window of growth and development. The assembly of gut microbial communities during early life contributes to immune, endocrine, and other major developmental pathways (56). Many studies found that PNMS can alter the gut microflora in the next generations of human and animal models (36, 37, 44, 57). A cohort study of 56 Dutch healthy infants born vaginally showed that the infants of mothers with high cumulative stress (i.e., high reported stress and high cortisol concentrations) during pregnancy had significantly higher relative abundance rates of Proteobacteria groups known to contain pathogens (related to *Escherichia*, *Serratia*, and *Enterobacter*) and lower relative abundance rates of lactic acid bacteria (i.e., *Lactobacillus*, *Lactococcus*, and *Aerococcus*) and *Bifidobacterium*. Altogether, these characteristics indicate increased levels of inflammation (11, 36). Repeated restraint stress from embryonic day 14 to day 20 significantly reduced the abundance of *Lactobacillus* and increased the abundance of the *Oscillibacter*, *Anaerotruncus*, and *Peptococcus* genera in prenatal stress animals (37). Furthermore, maternal stress can alter the proteins related to vaginal immunity and the abundance of *Lactobacillus*, the prominent taxon in the maternal vagina. Loss of maternal vaginal *Lactobacillus* results in the decreased transmission of this bacterium to the offspring (44).

The period before weaning acts as a unique window of opportunity because pathological consequences appear later in life once the normal development of the immune system is

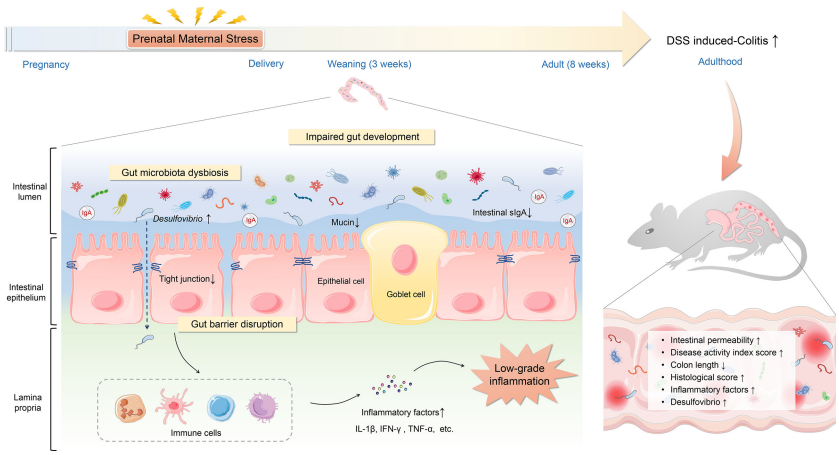

FIGURE 9 | Schematic overview of how prenatal maternal stress increases the susceptibility to colitis in adult offspring. Prenatal maternal stress can impair the intestinal development, disturb the mucosal barrier function, induce low-grade inflammation, alter the composition of the microbiota in offspring, and increase the susceptibility to colitis in adulthood.

perturbed (58, 59). Our study examined the intestinal microbiota of the offspring at 3 weeks of weaning and 8 weeks of adulthood. The results showed that PNMS induced a long-term gut microbiota dysbiosis characterized by the excessive growth of *Desulfovibrio*. Notably, Desulfovibrionales, Desulfovibrionaceae, and *Desulfovibrio* increased in 3- and 8-week-old PNMS mice. *Desulfovibrio*, one of the sulfate-reducing bacteria (SRB), may colonize the intestinal mucosa easily because of its ability to degrade the sulfated mucin of the mucus layer (60). SRB, which can metabolize genotoxic hydrogen sulfide (H_2S), induces colitis in animal models and increases in abundance in patients with IBD (61, 62). A recent study has suggested that an increased intestinal permeability, inflammatory factors, and the intestinal H_2S during weaning are responsible for the long-term pathological imprinting induced by excess calorie intake in early life and gut dysbiosis, leading to an increased risk of colitis in adulthood. The results of the verification experiment revealed that pathological imprinting can be prevented by the neutralization of IFN-γ and TNF-α, the production of hydrogen sulfide, or the normalization of intestinal permeability during weaning (17). In the present study, other pro-inflammatory bacteria, such as *Streptococcus* and *Enterococcus*, increased in 3-week-old PNMS offspring. However, Bifidobacteriales, Bifidobacteriaceae, and *Bifidobacterium* dramatically decreased in the 3-week-old pups with PNMS. Bifidobacteria are reliable indicators of a healthy microbiota in infants (63). Bifidobacteria in the infant gut can be directly acquired from the mother through vertical transmission (64). As a representative of the pioneer infant microbiome in the gut tract, *Bifidobacterium* species have a pivotal role in maintaining gut and immunity homeostasis, promoting intestinal development, and inhibiting the growth of pathogens (65, 66). In parallel, SCFA-producing bacteria, such as *Blautia* and *Robinsoniella*, showed significantly reduced abundance in 3-week-old offspring exposed to PNMS. SCFAs from the microbiome play a critical role in the crosstalk of the microbiota–gut–brain axis (67). The disruption of the brain–gut axis involves changes in neurotransmitters and is perhaps related to intestinal permeability, movement, and sensitivity. To clarify the role of the gut microbiota, we carried out FMT experiments. Interestingly, the feces of PNMS offspring induced low-grade intestinal inflammation and damaged the intestinal barrier function in the *in vivo* and *in vitro* experiments. Moreover, this phenotype can be partially reversed by the TNF-α inhibitor adalimumab. After treatment with adalimumab, no statistical difference in the indicators of inflammation and intestinal barrier function was observed between the two groups. This result suggested that blocking the inflammatory cytokines with neutralizing antibodies abolishes the effect of PNMS. We also found that the gut microbiota of the two groups of mice separated from their mothers during weaning did not tend to remain similar after receiving the same diet for 5 weeks. The intestinal microbiota dysbiosis induced by PNMS continued in the 8-week-old offspring, suggesting that the effect of PNMS on the progeny gut microbiota is persistent, profound, and tremendous. An increasing trend of *Desulfovibrio* and *Prevotella* was observed in 8-week-old adult mice. This trend was associated with chronic inflammatory disease. The pro-inflammatory intestinal microenvironment may persist and cause an indelible immunopathological imprint. Notably, the correlation analysis results showed that the relative abundance of *Desulfovibrio* was highly correlated with the level of inflammation in offspring mice, suggesting that the overgrowth of *Desulfovibrio* in early life is probably responsible for the development of inflammatory diseases later on. Overall, our data suggested that PNMS can induce low-grade intestinal inflammation and gut dysbiosis, is characterized by the increase of pro-inflammatory bacteria, especially *Desulfovibrio*, and the decrease of beneficial bacteria, and may produce long-term pathological imprint on the immune system and ultimately increase the susceptibility to colitis in adult offspring. The administration of antibiotics

targeting *Desulfovibrio* or neutralizing antibodies in early life may provide a new perspective for the prevention of immune-inflammatory diseases.

Our study revealed that PNMS-exposed offspring were more prone to develop experimental colitis. The results have important implications for understanding how early life adversity influences intestinal health. However, potential limitations are present. This exploratory study did not involve experiments in which some perturbations were used to rescue the phenotypes. Future experiments can further define the precise mechanisms. Although no changes in intestinal permeability were detected in the two groups of mice in adulthood before the modeling, they showed disparities after colitis modeling. This result suggested that the gut microbiota is involved in this process. Our exploration of this hypothesis is in progress.

Overall, this study is the first to reveal that PNMS can impair gut development, disturb mucosal barrier function, and induce low-grade inflammation and overgrowth of *Desulfovibrio* in offspring, which contribute to the increased risk of IBD in adulthood. These results reveal a novel perspective on the long-term adverse impacts of maternal stress. Taken together, emotion-focused stress management strategies for mothers should be emphasized to prevent potential risk of IBD.

DATA AVAILABILITY STATEMENT

The raw data of 16S rDNA amplicon sequencing for this experiment has been uploaded to NCBI (SRA accession: PRJNA728691).

ETHICS STATEMENT

The animal study was reviewed and approved by the Ethics Committee of Tianjin Medical University (Tianjin, China).

AUTHOR CONTRIBUTIONS

YS, RX, WL, KJ, and HC designed the research study. YS, RX, LL, GJ, HH, ML, YY, and BZ performed the experiments. YS, RX, LL, XL, and HC analyzed the data. YS, RX, and HC wrote the manuscript. BW, KJ, WL, XC, and HC made critical revisions. All authors who contributed to the design and writing of the paper agreed with the final version of the content of the manuscript.

FUNDING

This research was supported by grants (82070545 and 81970477) from the National Natural Science Foundation of China and the Key Project of Science and Technology Pillar Program of Tianjin (20YFZCSY00020).

ACKNOWLEDGMENTS

We thank the National Natural Science Foundation of China and the Key Project of Science and Technology Pillar Program of Tianjin for their financial support. The funders had no role in the study design, data collection, data analysis, interpretation, and writing and revision of the manuscript.

SUPPLEMENTARY MATERIAL

The Supplementary Material for this article can be found online at: https://www.frontiersin.org/articles/10.3389/fimmu.2021.700995/full#supplementary-material

REFERENCES

1. Park SC, Jeen YT. Genetic Studies of Inflammatory Bowel Disease-Focusing on Asian Patients. *Cells* (2019) 8(5):404. doi: 10.3390/cells8050404
2. Kaplan GG, Windsor JW. The Four Epidemiological Stages in the Global Evolution of Inflammatory Bowel Disease. *Nat Rev Gastroenterol Hepatol* (2021) 18(1):56–66. doi: 10.1038/s41575-020-00360-x
3. Kaplan GG, Ng SC. Understanding and Preventing the Global Increase of Inflammatory Bowel Disease. *Gastroenterology* (2017) 152(2):313–21.e2. doi: 10.1053/j.gastro.2016.10.020
4. Brzozowski B, Mazur-Bialy A, Pajdo R, Kwiecien S, Bilski J, Zwolinska-Wcislo M, et al. Mechanisms by Which Stress Affects the Experimental and Clinical Inflammatory Bowel Disease (IBD): Role of Brain-Gut Axis. *Curr Neuropharmacol* (2016) 14(8):892–900. doi: 10.2174/1570159x14666160404124127
5. Wang SL, Shao BZ, Zhao SB, Chang X, Wang P, Miao CY, et al. Intestinal Autophagy Links Psychosocial Stress With Gut Microbiota to Promote Inflammatory Bowel Disease. *Cell Death Dis* (2019) 10(6):391. doi: 10.1038/s41419-019-1634-x
6. Bitton A, Sewitch MJ, Peppercorn MA, deB Edwardes MD, Shah S, Ransil B, et al. Psychosocial Determinants of Relapse in Ulcerative Colitis: A Longitudinal Study. *Am J Gastroenterol* (2003) 98(10):2203–8. doi: 10.1111/j.1572-0241.2003.07717.x
7. Bitton A, Dobkin PL, Edwardes MD, Sewitch MJ, Meddings JB, Rawal S, et al. Predicting Relapse in Crohn's Disease: A Biopsychosocial Model. *Gut* (2008) 57(10):1386–92. doi: 10.1136/gut.2007.134817
8. Bernstein CN, Singh S, Graff LA, Walker JR, Miller N, Cheang M. A Prospective Population-Based Study of Triggers of Symptomatic Flares in IBD. *Am J Gastroenterol* (2010) 105(9):1994–2002. doi: 10.1038/ajg.2010.140
9. Sexton KA, Walker JR, Graff LA, Bernstein MT, Beatie B, Miller N, et al. Evidence of Bidirectional Associations Between Perceived Stress and Symptom Activity: A Prospective Longitudinal Investigation in Inflammatory Bowel Disease. *Inflamm Bowel Dis* (2017) 23(3):473–83. doi: 10.1097/MIB.0000000000001040
10. Wintjens D, de Jong MJ, van der Meulen-de Jong AE, Romberg-Camps MJ, Becx MC, Maljaars JP, et al. Novel Perceived Stress and Life Events Precede Flares of Inflammatory Bowel Disease: A Prospective 12-Month Follow-Up Study. *J Crohns Colitis* (2019) 13(4):410–6. doi: 10.1093/ecco-jcc/jjy177
11. Araki M, Shinzaki S, Yamada T, Arimitsu S, Komori M, Shibukawa N, et al. Psychologic Stress and Disease Activity in Patients With Inflammatory Bowel Disease: A Multicenter Cross-Sectional Study. *PLoS One* (2020) 15(5):e0233365. doi: 10.1371/journal.pone.0233365
12. Gao X, Cao Q, Cheng Y, Zhao D, Wang Z, Yang H, et al. Chronic Stress Promotes Colitis by Disturbing the Gut Microbiota and Triggering Immune System Response. *Proc Natl Acad Sci USA* (2018) 115(13):E2960–2960E2969. doi: 10.1073/pnas.1720696115

13. Sun Y, Zhang M, Chen CC, Gillilland M3rd, Sun X, El-Zaatari M, et al. Stress-Induced Corticotropin-Releasing Hormone-Mediated NLRP6 Inflammasome Inhibition and Transmissible Enteritis in Mice. *Gastroenterology* (2013) 144 (7):1478–87, 1487.e1-8. doi: 10.1053/j.gastro.2013.02.038
14. Ananthakrishnan AN, Bernstein CN, Iliopoulos D, Macpherson A, Neurath MF, Ali R, et al. Environmental Triggers in IBD: A Review of Progress and Evidence. *Nat Rev Gastroenterol Hepatol* (2018) 15(1):39–49. doi: 10.1038/nrgastro.2017.136
15. Örtqvist AK, Lundholm C, Halfvarson J, Ludvigsson JF, Almqvist C. Fetal and Early Life Antibiotics Exposure and Very Early Onset Inflammatory Bowel Disease: A Population-Based Study. *Gut* (2019) 68(2):218–25. doi: 10.1136/gutjnl-2017-314352
16. Ozkul C, Ruiz VE, Battaglia T, Xu J, Roubaud-Baudron C, Cadwell K, et al. A Single Early-in-Life Antibiotic Course Increases Susceptibility to DSS-Induced Colitis. *Genome Med* (2020) 12(1):65. doi: 10.1186/s13073-020-00764-z
17. Al Nabhani Z, Dulauroy S, Lécuyer E, Polomack B, Campagne P, Berard M, et al. Excess Calorie Intake Early in Life Increases Susceptibility to Colitis in Adulthood. *Nat Metab* (2019) 1(11):1101–9. doi: 10.1038/s42255-019-0129-5
18. Milani C, Duranti S, Bottacini F, Casey E, Turroni F, Mahony J, et al. The First Microbial Colonizers of the Human Gut: Composition, Activities, and Health Implications of the Infant Gut Microbiota. *Microbiol Mol Biol Rev* (2017) 81 (4):e00036–17. doi: 10.1128/MMBR.00036-17
19. Turroni F, Milani C, Duranti S, Lugli GA, Bernasconi S, Margolles A, et al. The Infant Gut Microbiome as a Microbial Organ Influencing Host Well-Being. *Ital J Pediatr* (2020) 46(1):16. doi: 10.1186/s13052-020-0781-0
20. Arrieta MC, Stiemsma LT, Amenyogbe N, Brown EM, Finlay B. The Intestinal Microbiome in Early Life: Health and Disease. *Front Immunol* (2014) 5:427. doi: 10.3389/fimmu.2014.00427
21. Tamburini S, Shen N, Wu HC, Clemente JC. The Microbiome in Early Life: Implications for Health Outcomes. *Nat Med* (2016) 22(7):713–22. doi: 10.1038/nm.4142
22. Ronan V, Yeasin R, Claud EC. Childhood Development and the Microbiome-The Intestinal Microbiota in Maintenance of Health and Development of Disease During Childhood Development. *Gastroenterology* (2021) 160 (2):495–506. doi: 10.1053/j.gastro.2020.08.065
23. Duranti S, Lugli GA, Mancabelli L, Armanini F, Turroni F, James K, et al. Maternal Inheritance of Bifidobacterial Communities and Bifidophages in Infants Through Vertical Transmission. *Microbiome* (2017) 5(1):66. doi: 10.1186/s40168-017-0282-6
24. Bäckhed F, Roswall J, Peng Y, Feng Q, Jia H, Kovatcheva-Datchary P, et al. Dynamics and Stabilization of the Human Gut Microbiome During the First Year of Life. *Cell Host Microbe* (2015) 17(5):690–703. doi: 10.1016/j.chom.2015.04.004
25. Wang S, Egan M, Ryan CA, Boyaval P, Dempsey EM, Ross RP, et al. A Good Start in Life Is Important-Perinatal Factors Dictate Early Microbiota Development and Longer Term Maturation. *FEMS Microbiol Rev* (2020) 44 (6):763–81. doi: 10.1093/femsre/fuaa030
26. Dong TS, Gupta A. Influence of Early Life, Diet, and the Environment on the Microbiome. *Clin Gastroenterol Hepatol* (2019) 17(2):231–42. doi: 10.1016/j.cgh.2018.08.067
27. Dai X, Guo Z, Chen D, Li L, Song X, Liu T, et al. Maternal Sucralose Intake Alters Gut Microbiota of Offspring and Exacerbates Hepatic Steatosis in Adulthood. *Gut Microbes* (2020) 11(4):1046–63. doi: 10.1080/19490976.2020.1738187
28. Xie R, Sun Y, Wu J, Huang S, Jin G, Guo Z, et al. Maternal High Fat Diet Alters Gut Microbiota of Offspring and Exacerbates DSS-Induced Colitis in Adulthood. *Front Immunol* (2018) 9:2608. doi: 10.3389/fimmu.2018.02608
29. Lehtimäki J, Thorsen J, Rasmussen MA, Hjelmsø M, Shah S, Mortensen MS, et al. Urbanized Microbiota in Infants, Immune Constitution, and Later Risk of Atopic Diseases. *J Allergy Clin Immunol* (2020) 148(1):234–43. doi: 10.1016/j.jaci.2020.12.621
30. Wang HJ, Xu X, Xie RH, Rui YY, Zhang PA, Zhu XJ, et al. Prenatal Maternal Stress Induces Visceral Hypersensitivity of Adult Rat Offspring Through Activation of Cystathionine-β-Synthase Signaling in Primary Sensory Neurons. *Mol Pain* (2018) 14:1744806918777406. doi: 10.1177/1744806918777406
31. Gur TL, Shay L, Palkar AV, Fisher S, Varaljay VA, Dowd S, et al. Prenatal Stress Affects Placental Cytokines and Neurotrophins, Commensal Microbes, and Anxiety-Like Behavior in Adult Female Offspring. *Brain Behav Immun* (2017) 64:50–8. doi: 10.1016/j.bbi.2016.12.021
32. Walsh K, McCormack CA, Webster R, Pinto A, Lee S, Feng T, et al. Maternal Prenatal Stress Phenotypes Associate With Fetal Neurodevelopment and Birth Outcomes. *Proc Natl Acad Sci USA* (2019) 116(48):23996–4005. doi: 10.1073/pnas.1905890116
33. McGowan PO, Matthews SG. Prenatal Stress, Glucocorticoids, and Developmental Programming of the Stress Response. *Endocrinology* (2018) 159(1):69–82. doi: 10.1210/en.2017-00896
34. Magnus MC, Wright RJ, Røysamb E, Parr CL, Karlstad Ø, Page CM, et al. Association of Maternal Psychosocial Stress With Increased Risk of Asthma Development in Offspring. *Am J Epidemiol* (2018) 187(6):1199–209. doi: 10.1093/aje/kwx366
35. Aatsinki AK, Keskitalo A, Laitinen V, Munukka E, Uusitupa HM, Lahti L, et al. Maternal Prenatal Psychological Distress and Hair Cortisol Levels Associate With Infant Fecal Microbiota Composition at 2.5 Months of Age. *Psychoneuroendocrinology* (2020) 119:104754. doi: 10.1016/j.psyneuen.2020.104754
36. Zijlmans MA, Korpela K, Riksen-Walraven JM, de Vos WM, de Weerth C. Maternal Prenatal Stress Is Associated With the Infant Intestinal Microbiota. *Psychoneuroendocrinology* (2015) 53:233–45. doi: 10.1016/j.psyneuen.2015.01.006
37. Golubeva AV, Crampton S, Desbonnet L, Edge D, O'Sullivan O, Lomasney KW, et al. Prenatal Stress-Induced Alterations in Major Physiological Systems Correlate With Gut Microbiota Composition in Adulthood. *Psychoneuroendocrinology* (2015) 60:58–74. doi: 10.1016/j.psyneuen.2015.06.002
38. Jašarević E, Howard CD, Morrison K, Misic A, Weinkopff T, Scott P, et al. The Maternal Vaginal Microbiome Partially Mediates the Effects of Prenatal Stress on Offspring Gut and Hypothalamus. *Nat Neurosci* (2018) 21(8):1061–71. doi: 10.1038/s41593-018-0182-5
39. Howerton CL, Morgan CP, Fischer DB, Bale TL. O-GlcNAc Transferase (OGT) as a Placental Biomarker of Maternal Stress and Reprogramming of CNS Gene Transcription in Development. *Proc Natl Acad Sci USA* (2013) 110 (13):5169–74. doi: 10.1073/pnas.1300065110
40. Long X, Wong CC, Tong L, Chu E, Ho Szeto C, Go M, et al. Peptostreptococcus Anaerobius Promotes Colorectal Carcinogenesis and Modulates Tumour Immunity. *Nat Microbiol* (2019) 4(12):2319–30. doi: 10.1038/s41564-019-0541-3
41. Li L, Li X, Zhong W, Yang M, Xu M, Sun Y, et al. Gut Microbiota From Colorectal Cancer Patients Enhances the Progression of Intestinal Adenoma in Apcmin/+ Mice. *EBioMedicine* (2019) 48:301–15. doi: 10.1016/j.ebiom.2019.09.021
42. Adolph TE, Tomczak MF, Niederreiter L, Ko HJ, Böck J, Martinez-Naves E, et al. Paneth Cells as a Site of Origin for Intestinal Inflammation. *Nature* (2013) 503(7475):272–6. doi: 10.1038/nature12599
43. Chidlow JHJr, Langston W, Greer JJ, Ostanin D, Abdelbaqi M, Houghton J, et al. Differential Angiogenic Regulation of Experimental Colitis. *Am J Pathol* (2006) 169(6):2014–30. doi: 10.2353/ajpath.2006.051021
44. Jašarević E, Howerton CL, Howard CD, Bale TL. Alterations in the Vaginal Microbiome by Maternal Stress Are Associated With Metabolic Reprogramming of the Offspring Gut and Brain. *Endocrinology* (2015) 156 (9):3265–76. doi: 10.1210/en.2015-1177
45. Schepanski S, Buss C, Hanganu-Opatz IL, Arck PC. Prenatal Immune and Endocrine Modulators of Offspring's Brain Development and Cognitive Functions Later in Life. *Front Immunol* (2018) 9:2186. doi: 10.3389/fimmu.2018.02186
46. Wadhwa PD. Psychoneuroendocrine Processes in Human Pregnancy Influence Fetal Development and Health. *Psychoneuroendocrinology* (2005) 30(8):724–43. doi: 10.1016/j.psyneuen.2005.02.004
47. Bale TL, Baram TZ, Brown AS, Goldstein JM, Insel TR, McCarthy MM, et al. Early Life Programming and Neurodevelopmental Disorders. *Biol Psychiatry* (2010) 68(4):314–9. doi: 10.1016/j.biopsych.2010.05.028
48. Sun Y, Li L, Xie R, Wang B, Jiang K, Cao H. Stress Triggers Flare of Inflammatory Bowel Disease in Children and Adults. *Front Pediatr* (2019) 7:432. doi: 10.3389/fped.2019.00432
49. Al Nabhani Z, Eberl G. Imprinting of the Immune System by the Microbiota Early in Life. *Mucosal Immunol* (2020) 13(2):183–9. doi: 10.1038/s41385-020-0257-y

50. Macpherson AJ, de Agüero MG, Ganal-Vonarburg SC. How Nutrition and the Maternal Microbiota Shape the Neonatal Immune System. *Nat Rev Immunol* (2017) 17(8):508–17. doi: 10.1038/nri.2017.58
51. Kang LJ, Vu KN, Koleva PT, Field CJ, Chow A, Azad MB, et al. Maternal Psychological Distress Before Birth Influences Gut Immunity in Mid-Infancy. *Clin Exp Allergy* (2020) 50(2):178–88. doi: 10.1111/cea.13551
52. Jarillo-Luna A, Rivera-Aguilar V, Garfias HR, Lara-Padilla E, Kormanovsky A, Campos-Rodríguez R. Effect of Repeated Restraint Stress on the Levels of Intestinal IgA in Mice. *Psychoneuroendocrinology* (2007) 32(6):681–92. doi: 10.1016/j.psyneuen.2007.04.009
53. Dzidic M, Abrahamsson TR, Artacho A, Björkstén B, Collado MC, Mira A, et al. Aberrant IgA Responses to the Gut Microbiota During Infancy Precede Asthma and Allergy Development. *J Allergy Clin Immunol* (2017) 139 (3):1017–25.e14. doi: 10.1016/j.jaci.2016.06.047
54. Bridgman SL, Konya T, Azad MB, Guttman DS, Sears MR, Becker AB, et al. High Fecal IgA is Associated With Reduced Clostridium Difficile Colonization in Infants. *Microbes Infect* (2016) 18(9):543–9. doi: 10.1016/j.micinf.2016.05.001
55. Kukkonen K, Kuitunen M, Haahtela T, Korpela R, Poussa T, Savilahti E. High Intestinal IgA Associates With Reduced Risk of IgE-Associated Allergic Diseases. *Pediatr Allergy Immunol* (2010) 21(1 Pt 1):67–73. doi: 10.1111/j.1399-3038.2009.00907.x
56. Robertson RC, Manges AR, Finlay BB, Prendergast AJ. The Human Microbiome and Child Growth - First 1000 Days and Beyond. *Trends Microbiol* (2019) 27(2):131–47. doi: 10.1016/j.tim.2018.09.008
57. Bailey MT, Lubach GR, Coe CL. Prenatal Stress Alters Bacterial Colonization of the Gut in Infant Monkeys. *J Pediatr Gastroenterol Nutr* (2004) 38(4):414–21. doi: 10.1097/00005176-200404000-00009
58. Olszak T, An D, Zeissig S, Vera MP, Richter J, Franke A, et al. Microbial Exposure During Early Life Has Persistent Effects on Natural Killer T Cell Function. *Science* (2012) 336(6080):489–93. doi: 10.1126/science.1219328
59. Knoop KA, Gustafsson JK, McDonald KG, Kulkarni DH, Coughlin PE, McCrate S, et al. Microbial Antigen Encounter During a Preweaning Interval Is Critical for Tolerance to Gut Bacteria. *Sci Immunol* (2017) 2(18): eaao1314. doi: 10.1126/sciimmunol.aao1314
60. Lennon G, Balfe Á, Bambury N, Lavelle A, Maguire A, Docherty NG, et al. Correlations Between Colonic Crypt Mucin Chemotype, Inflammatory Grade and Desulfovibrio Species in Ulcerative Colitis. *Colorectal Dis* (2014) 16(5): O161–9. doi: 10.1111/codi.12503
61. Figliuolo VR, Dos Santos LM, Abalo A, Nanini H, Santos A, Brittes NM, et al. Sulfate-Reducing Bacteria Stimulate Gut Immune Responses and Contribute to Inflammation in Experimental Colitis. *Life Sci* (2017) 189:29–38. doi: 10.1016/j.lfs.2017.09.014
62. Nguyen LH, Ma W, Wang DD, Cao Y, Mallick H, Gerbaba TK, et al. Association Between Sulfur-Metabolizing Bacterial Communities in Stool and Risk of Distal Colorectal Cancer in Men. *Gastroenterology* (2020) 158 (5):1313–25. doi: 10.1053/j.gastro.2019.12.029
63. Turroni F, Duranti S, Milani C, Lugli GA, van Sinderen D, Ventura M. Bifidobacterium Bifidum: A Key Member of the Early Human Gut Microbiota. *Microorganisms* (2019) 7(11):544. doi: 10.3390/microorganisms 7110544
64. Turroni F, Milani C, Duranti S, Ferrario C, Lugli GA, Mancabelli L, et al. Bifidobacteria and the Infant Gut: An Example of Co-Evolution and Natural Selection. *Cell Mol Life Sci* (2018) 75(1):103–18. doi: 10.1007/s00018-017-2672-0
65. Taft DH, Liu J, Maldonado-Gomez MX, Akre S, Huda MN, Ahmad SM, et al. Bifidobacterial Dominance of the Gut in Early Life and Acquisition of Antimicrobial Resistance. *mSphere* (2018) 3(5):e00441–18. doi: 10.1128/mSphere.00441-18
66. Cukrowska B, Bierła JB, Zakrzewska M, Klukowski M, Maciorkowska E. The Relationship Between the Infant Gut Microbiota and Allergy. The Role of Bifidobacterium Breve and Prebiotic Oligosaccharides in the Activation of Anti-Allergic Mechanisms in Early Life. *Nutrients* (2020) 12(4):946. doi: 10.3390/nu12040946
67. Dalile B, Van Oudenhove L, Vervliet B, Verbeke K. The Role of Short-Chain Fatty Acids in Microbiota-Gut-Brain Communication. *Nat Rev Gastroenterol Hepatol* (2019) 16(8):461–78. doi: 10.1038/s41575-019-0157-3

Conflict of Interest: The authors declare that the research was conducted in the absence of any commercial or financial relationships that could be construed as a potential conflict of interest.

Publisher's Note: All claims expressed in this article are solely those of the authors and do not necessarily represent those of their affiliated organizations, or those of the publisher, the editors and the reviewers. Any product that may be evaluated in this article, or claim that may be made by its manufacturer, is not guaranteed or endorsed by the publisher.

Copyright © 2021 Sun, Xie, Li, Jin, Zhou, Huang, Li, Yang, Liu, Cao, Wang, Liu, Jiang and Cao. This is an open-access article distributed under the terms of the Creative Commons Attribution License (CC BY). The use, distribution or reproduction in other forums is permitted, provided the original author(s) and the copyright owner(s) are credited and that the original publication in this journal is cited, in accordance with accepted academic practice. No use, distribution or reproduction is permitted which does not comply with these terms.

frontiers in Immunology

ORIGINAL RESEARCH
published: 09 November 2021
doi: 10.3389/fimmu.2021.780910

Differential Signature of the Microbiome and Neutrophils in the Oral Cavity of HIV-Infected Individuals

*Eliana Perez Rosero[1], Samantha Heron[1], Juan Jovel[1], Conar R. O'Neil[2], Shannon Lee Turvey[2], Pallavi Parashar[1] and Shokrollah Elahi[1,3,4,5]**

[1] Department of Dentistry, University of Alberta, Edmonton, AB, Canada, [2] Department of Medicine, Division of Infectious Disease, University of Alberta, Edmonton, AB, Canada, [3] Department of Medical Microbiology and Immunology, University of Alberta, Edmonton, AB, Canada, [4] Department of Oncology, University of Alberta, Edmonton, AB, Canada, [5] Li Ka Shing Institute of Virology, Faculty of Medicine and Dentistry, University of Alberta, Edmonton, AB, Canada

OPEN ACCESS

Edited by:
Tobias R Kollmann,
University of Western Australia,
Australia

Reviewed by:
Trim Lajqi,
Heidelberg University Hospital,
Germany
Tiffany Hensley-Mcbain,
McLaughlin Research Institute,
United States

***Correspondence:**
Shokrollah Elahi
elahi@ualberta.ca
orcid.org/0000-0002-7215-2009

Specialty section:
This article was submitted to Viral Immunology, a section of the journal Frontiers in Immunology

Received: 22 September 2021
Accepted: 22 October 2021
Published: 09 November 2021

Citation:
Perez Rosero E, Heron S, Jovel J, O'Neil CR, Turvey SL, Parashar P and Elahi S (2021) Differential Signature of the Microbiome and Neutrophils in the Oral Cavity of HIV-Infected Individuals. Front. Immunol. 12:780910. doi: 10.3389/fimmu.2021.780910

HIV infection is associated with a wide range of changes in microbial communities and immune cell components of the oral cavity. The purpose of this study was to evaluate the oral microbiome in relationship to oral neutrophils in HIV-infected compared to healthy individuals. We evaluated oral washes and saliva samples from HIV-infected individuals (n=52) and healthy controls (n=43). Using 16S-rRNA gene sequencing, we found differential β-diversity using Principal Coordinate Analysis (PCoA) with Bray-Curtis distances. The α-diversity analysis by Faith's, Shannon, and observed OTUs indexes indicated that the saliva samples from HIV-infected individuals harbored significantly richer bacterial communities compared to the saliva samples from healthy individuals. Notably, we observed that five species of Spirochaeta including *Spirochaetaceae*, *Spirochaeta*, *Treponema*, *Treponema amylovorum*, and *Treponema azotonutricum* were significantly abundant. In contrast, *Helicobacter* species were significantly reduced in the saliva of HIV-infected individuals. Moreover, we found a significant reduction in the frequency of oral neutrophils in the oral cavity of HIV-infected individuals, which was positively related to their $CD4^+$ T cell count. In particular, we noted a significant decline in CD44 expressing neutrophils and the intensity of CD44 expression on oral neutrophils of HIV-infected individuals. This observation was supported by the elevation of soluble CD44 in the saliva of HIV-infected individuals. Overall, the core oral microbiome was distinguishable between HIV-infected individuals on antiretroviral therapy compared to the HIV-negative group. The observed reduction in oral neutrophils might likely be related to the low surface expression of CD44, resulting in a higher bacterial diversity and richness in HIV-infected individuals.

Keywords: neutrophils, oral microbiome, HIV infection, galectin-9, CD44

INTRODUCTION

The oral cavity is a unique environment that comprises immune cells, soluble immune mediators, microbial communities, food antigens/foreign materials, soft and hard tissues (1, 2). Although most of the research has been focused on bacterial communities, the oral cavity harbors a large collection of viruses, fungi, and bacteriophages (3). Saliva flow, soluble salivary components such as antimicrobial peptides (4), immune cells, and mucosal epithelial cells in cross-talk with oral microbiome work together to sustain an immune homeostatic state under normal physiological conditions (5, 6). For example, SLPI (salivary secretory leukocyte protease inhibitor), defensins, sIgA, lactoferrin, and lysosome in the saliva play a protective role against viral infections (e.g. HIV) (7). However, upon the acquisition of HIV infection and disease progression due to the elimination/reduction of HIV-target cells ($CD4^+$ and Th17 cells) (7–9), patients become prone to opportunistic infections such as candidiasis and other oral manifestations (e.g. Kaposi's sarcoma) (10, 11). Notably, elimination of Th17 cells and reduction in IL-17 result in decreased recruitment of innate immune cells especially neutrophils into the oral cavity (12). Besides, HIV-infected individuals with lower $CD4^+$ T cell count even when on antiretroviral therapy (ART) exhibit decreased neutrophil frequency in their blood circulation (13).

Neutrophils are the most abundant leukocytes in the blood circulation and also in the oral cavity (14). The interaction of neutrophils with symbiotic microbial communities plays a crucial role in immune homeostasis at the mucosal surfaces such as the oral cavity (15). However, dysbiotic microbiota at the mucosal surfaces (e.g. gingival crevice) activate neutrophils which results in an exacerbated inflammatory response (16). The oral cavity is an important peripheral microenvironment for neutrophils given its richness with bacterial communities (17). Additionally, bacterial communities can directly or indirectly (e.g. activation of macrophage, dendritic cells, and lymphocytes) influence neutrophil recruitment and activation in oral tissues (15, 18). For example, germ-free mice have decreased neutrophils and their progenitors in the oral cavity compared to wild-type mice (19). It has also been reported that bacterial communities enhance neutrophils aging (20). As such, aged neutrophils exhibit an inflammatory phenotype by increased production of reactive oxygen species (ROS) (21). Moreover, chronic conditions can influence microbial communities at the mucosal surfaces including the oral cavity. For example, diabetes can modify the oral microbiome to exacerbate periodontal disease (22).On the other hand, the dysbiotic oral microbiome has been reported to be associated with colorectal and pancreatic cancers (23–25). Nevertheless, the impact of HIV infection on the oral microbiome is controversial. Some studies support microbiome modifications, and some do not. These discrepancies could be related to various factors such as the study design, detection methods, and sampling (e.g., saliva, oral wash, or subgingival). For example, it was reported that HIV infection modulates oral fungi population and cigarette smoking in HIV-infected individuals was associated with greater microbial diversity (26). It appears that HIV infection shifts oral microbial communities towards a dysbiotic state (27). In particular, higher levels of cultivable microbes were isolated from the saliva of HIV-infected individuals compared to the HIV-uninfected group (28, 29). Other clinical variables are associated with alterations in the composition of oral microbial communities in HIV-infected individuals on ART (29). Although the potential influence of ART on the oral microbiome is debatable, it is reported that ART partially reverses HIV-induced oral microbiota alteration (29). ART treatment appeared to be associated with significantly greater bacterial richness and diversity (30). These studies demonstrate that HIV infection and/or ART adds another layer of complexity to the tight interplay between the immune system and microbial communities in the oral cavity. However, the impact of HIV infection and/or microbial communities on oral neutrophils and vice versa have remained unexplored.

Neutrophils are crucial players in immune homeostasis in the oral cavity (31). However, in inflammatory conditions such as periodontitis, the accumulation of activated neutrophils can result in tissue damage and bone loss (32). The activation of circulatory neutrophils results in cellular polarization, which facilitates tissue extravasation (33). CD44, a type I transmembrane glycoprotein, is one of the extracellular adhesion molecules that impacts neutrophil rolling and tissue migration (34). As such, lack of CD44 was associated with decreased neutrophil migration to inflamed tissue in CD44 KO mice (35). Besides, the interaction of CD44 with hyaluronate enhances neutrophil phagocytosis *in vitro* (36). Recently, we reported that CD44 interacts with Galectin-9 (Gal-9) on blood neutrophils (37). Gal-9 as a beta-galactosidase binding protein has a wide range of immunomodulatory properties depending on interaction with its corresponding receptors (38). We found that CD44 depalmitoylate during neutrophil activation and facilitates the movement of CD44 out of the lipid raft, and subsequently Gal-9 shedding from neutrophils in HIV-infected individuals (37). This process results in increased soluble plasma Gal-9 in HIV-infected individuals which subsequently enhances T cell activation *via* interaction with CD44 on T cells (37). Therefore, Gal-9 shedding from neutrophils might explain a potential source for the elevated plasma Gal-9 in HIV-infected individuals (39).

In the present study, we show that HIV-infected individuals have a different and richer bacterial composition in their saliva than healthy controls. Besides, we observed a significant reduction in the proportion of oral neutrophils in HIV-infected individuals, in particular, in those with lower $CD4^+$ T cell count. Additionally, we observed downregulation of CD44 surface expression on oral neutrophils in HIV-infected individuals, which potentially explains their decreased frequency in the oral cavity of HIV infected-individuals.

MATERIALS AND METHODS

Study Population

For this study, we recruited sixty-one HIV-infected individuals including: a) on ART with low $CD4^+$ T cell count (< 200 cells/mm^3, n=11); b) on ART with high $CD4^+$ count (>200 cells/mm^3, n=40); c) Long-term non-progressors (40) (LTNPs, n=9) and

d) ART-native, n=2) through the Northern Alberta HIV Program in Edmonton, Canada (**Supplementary Tables 1, 2**). All the work presented in this manuscript was conducted on HIV-infected individuals receiving ART except **Figures 2C, D**, which compares the frequency of neutrophils in different HIV-infected groups. Also, a total of 43 healthy controls (HCs) defined as HIV, Hepatitis B virus, and Hepatitis C virus seronegative individuals without active oral disease were recruited at the University of Alberta for comparison. The institutional ethics review boards at the University of Alberta approved the study with the protocols (Pro00070528 and Pro000064046). All study participants gave written informed consent to participate in the study.

Sample Collection

Participants avoided eating or drinking for at least 30 minutes before the sample collection. Saliva samples were obtained followed by oral washes from the study participants. Saliva samples were aliquoted and stored at -80°C until use.

Oral wash was performed 5 times using 15 ml of phosphate-buffered saline solution (PBS) for 30 seconds with 3 minutes' intermission between rinses. Samples were centrifuged at 2000 rpm for 10 min, supernatants were discarded, and cell pellets were resuspended in culture media (RPMI-1640) supplemented with 10% fetal bovine serum (FBS) (Sigma) and 1% penicillin-streptomycin (Sigma). Cell suspensions were filtered through 100, 70, and 50 µm sterile strainers (Fischer Scientific), centrifuged and resuspended in culture media for further analysis. Blood samples of 16 HCs and 15 HIV-infected individuals on ART were subjected to gradient separation using Ficoll-Paque Premium (GE). The peripheral blood mononuclear cell (PBMC) fraction was removed, and the remaining red blood cell pellet was lysed using red blood cell lysis buffer for 10 minutes (0.155M NH_4Cl, 10mM $KHCO_3$, and 0.1mM EDTA) to isolate polymorphonuclear cells according to our previous methods (37, 41).

Flow Cytometry Analysis

Fluorophore antibodies with specificity to antigens of human cells were purchased from BD Biosciences, Thermo Fisher Scientific, and/or R&D. We used anti-CD15 (clone W6D3, Cat#555402), anti-Gal-9 (clone 9M1-3, Cat#50-9116-42), anti-CD44 (clone 515, Cat#562890), anti-CD16 (clone 3G8, Cat#557744) and anti-CD32 (clone FLI8.26, Cat#744259). Cell viability was evaluated by LIVE/DEAD Kit (ThermoFisher Scientific Cat#L34966). Apoptosis assay was performed using the PE Annexin V Apoptosis Detection Kit I (BD Biosciences Cat#55963) according to the manufacturer's protocol. Stained cells were fixed in 4% paraformaldehyde before acquiring on an LSRFortessa-SORP or LSRFortessa X-20 flow cytometers (BD Biosciences), and data were analyzed using the FlowJo (version 10).

Cytokine, CD44, and Gal-9 Measurement

The liquid fraction of the saliva was 2-fold diluted for cytokine quantification. We specifically measured TNF-α, IL-8, IL-6, IL-10, IL-13, IL-1B, IFN-γ using V-plex Plus pro-inflammatory kit from Meso Scale Discovery (MSD Cat#K15054D-1), according to the manufacturer's instruction and our previous reports (41, 42). Similarly, CD44 (R&D Systems; DY7045-05) and Gal-9 (R&D; DY 2045) concentrations were quantified by ELISA.

Neutrophil Migration Assay

Chemotaxis was evaluated by the Cell Invasion Assay (Millipore Sigma, Cat. ECM 555). Blood neutrophils (n=10) and oral neutrophils (n=6) from HCs (n=10) were isolated and 0.5 million cells were used per well. Cells were pre-incubated in a 96 well plate with the anti-CD44 antibody (TermoFisher, Cat. 16-0441-85) at 37°C, for 30 min. Then cells were transported to the upper chamber of the migration assay and incubated in the presence or absence of soluble Galectin-9 (1.5 ng/ml) for 3 hours at 37°C. N-Formylmethionyl-leucyl-phenylalanine fMLP (50 µm, Sigma Aldrich, Cat. F3506-10MG) was used as a chemoattractant in the lower chamber. Culture media was used as the negative control. The migrated cells were lyzed and quantified by measuring the relative fluorescence units per manufacturing protocol using the plate reader a5 480/520 nm.

Bacterial DNA Isolation

Saliva aliquots from sex and age paired participants were centrifuged and pellets were used for DNA isolation using the QIAamp DNA Mini Kit (Cat# 51304). Pellets were mixed with 20 µl of Proteinase K and 200 µl of in-house lysis buffer (100 mL of 0.5 M sodium chloride, 0.005 M tris aminomethane-pH8, 0.05M ethylenediaminetetraacetic acid with pH 8, and 4% sodium dodecyl sulfate), briefly vortexed, and incubated at 56°C water bath for 60 min, followed by 15 min incubation at 70°C. Then 200 µl of buffer AL (from the kit) was added for a final 10-minute incubation at 70°C, accompanied by DNA column extraction according to the manufacturer's instructions.

16SrRNA Illumina MiSeq Sequencing

V3-V4 variable regions of 16S rRNA were amplified from genomic DNA samples. Amplicons were generated using the following primers: Forward Primer = 5' CGTCGGCAGC GTCAGATGTGTATAAGAGACAGCCTACGGGNGG CWGCAG and Reverse Primer = 5' TCTCGTGGGCTCGG AGATGTGTATAAGAGACAGGACTAC HVGGGTATCT AATCC (IDT). Thus, generated PCR products were indexed using Illumina's Nextera XT kit. Sequencing was performed on Illumina's MiSeq platform using a 250-bp paired-end sequencing kit at The Applied Genomic Core (TAGC), University of Alberta.

Sequencing data were demultiplexed and binned into individual samples according to their barcodes and further bioinformatic analysis was performed using the QIIME2 pipeline (2021.4). The first step of this analysis was to join the paired-end reads (1 and 2) with a minimum of 100 bp overlap and 0 mismatches. Reads were then quality filtered by removing sequences having more than 10 sites with a Phred quality score less than 20. Next, reads were denoised into amplicon sequence variants (ASVs) using the DADA method. Taxonomy classification at the phylum, family, and genus levels was done by comparing ASVs to the Green genes bacterial reference database (v. 13.5). Diversity indices (Evenness, Observed OTUs, Shannon's diversity, and Faith's phylogenetic index)

and distances between samples (Bray-Curtis, weighted- and unweighted-Unifrac) were all calculated in QIIME2 to profile oral microbiota. Before taxonomy classification and generating alpha and beta diversity metrics, data were rarefied across samples for normalization such that all samples have the same number of total reads.

Statistical Analysis

This was performed in GraphPad Prism 9 (GraphPad Software, Inc.). D'Agostino & Pearson test was used for normality check, being samples non-parametrical Mann-Whitney U tests for unpaired data or Wilcoxon signed-rank tests for paired data were used. When comparing more than two groups, the Kruskal Wallis test was used. Means and standard deviations (mean ± SD) are used to present the data. Correlation analysis was performed by nonparametric Spearman correlation.

RESULTS

Differential Bacterial Communities in the Oral Cavity of HIV-Infected Individuals Compared to HCs

We first compared the two groups in terms of β-diversity using Principal Coordinate Analysis (PCoA) with Bray-Curtis distances. The results indicated a differential clustering of bacterial communities in the saliva of HIV-infected compared to healthy individuals (**Figure 1A**). Distances within groups versus distances across groups were determined by ANOSIM, which was significant (P=0.001). ADONIS or differences between the group's centroid was also significant (P=0.003). The Alpha diversity analysis by Faith's, Shannon, and observed OTUs indexes showed that the saliva samples from HIV-infected individuals harbored significantly richer bacterial communities compared to the saliva samples from HCs (**Figure 1B**)

To further determine which bacterial communities were different between the groups, we compared them at different levels. At the phylum level, we found Spirochaetes' phylum was significantly enriched in the saliva samples of HIV-infected individuals compared to HCs (**Figures 1C, D**). When bacterial communities were compared at the species level (**Figure 1E**), we observed that five species of Spirochaeta including *Spirochaetaceae*, *Spirochaeta*, *Treponema*, Treponema *amylovorum*, and *Treponema azotonutricum* were significantly abundant in the saliva of HIV-infected individuals compared to HCs (**Figure 1F**). The volcano plot shows further differences in bacterial species among the groups. Species that were enriched in the saliva of HIV-infected individuals are shown in the right upper quadrant, and bacterial species that were less prevalent in the saliva of HIV-infected individuals are shown in the upper left quadrant of the volcano plot (**Figure 1G**). Bacterial species with mean counts less than 1 were not accounted for. We found that bacterial communities belonging to *Spirochaetes*, *Bacteroidetes*, *Firmicutes*, and *TM7* species were significantly enriched in the saliva samples from HIV-infected individuals, respectively (**Figures 1H–J**). In contrast, we noted a significantly lower abundance of Proteobacteria phylum (in particular *Helicobacter*) in the saliva of HIV-infected individuals compared to HCs (**Figure 1K**). We used 97% sequence identity for binning analysis. Overall, our results show a significant difference in bacterial communities in the oral cavity of HIV-infected compared to uninfected individuals. To exclude potential effects of sex/age, saliva specimens were age-sex-matched for the microbiome studies.

A Lower Proportion of Neutrophils in the Oral Cavity Is Related to the Clinical Status of HIV-Infected Individuals

To better understand the possible role of immune components of the oral cavity in HIV-infected individuals on the bacterial composition, we focused on neutrophils as the most abundant immune cells in the oral cavity (43). In agreement with previous reports, we found that neutrophils were the most abundant cells in the oral cavity. However, HIV-infected individuals had significantly lower percentages of neutrophils in their oral cavity compared to HCs (**Figures 2A, B**). Both oral and blood neutrophils co-express CD15 and CD16 (**Supplementary Figures 1A, B**). Notably, we observed significantly lower percentages of neutrophils in the oral cavity of ART-naive and patients on ART compared to HCs (**Figures 2C, D**). In contrast, we found a similar proportion of oral neutrophils in the oral cavity of HIV-infected LTNPs compared to HCs (**Figures 2C, D**). These observations suggest that the disease status may impact the frequency of neutrophils at the mucosal surfaces. Moreover, we did not find any significant difference in the frequency of other immune cells (e.g., dendritic cells, monocytes, and B cells) in the oral cavity of HIV-infected versus HCs except $CD4^+$ T cells. Although, in general, the percentage of T cells was very low (a few %), we found significantly lower percentages of $CD4^+$ T cells but not $CD8^+$ T cells in the oral cavity of HIV-infected individuals compared to HCs (**Supplementary Figures 1C–G**).

Gal-9 Is Downregulated on the Surface of Blood but Not Oral Neutrophils in HIV-Infected Individuals

Recently, we showed that Gal-9 is downregulated from the surface of blood neutrophils in HIV-infected individuals compared to HCs (37). Therefore, we decided to investigate whether this was the case for oral neutrophils. Our observations reconfirmed that the frequency of Gal-9 expressing blood neutrophils was significantly lower in HIV-infected individuals compared to HCs (**Figures 2E, F**). However, we found a smaller portion of Gal-9 expressing oral neutrophils compared to their siblings in the blood, without any significant difference between the HIV-infected individuals on ART and HCs (**Figures 2E, F**). Moreover, we measured the intensity of Gal-9 and found that the Mean fluorescence intensity (MFI) of Gal-9 was significantly

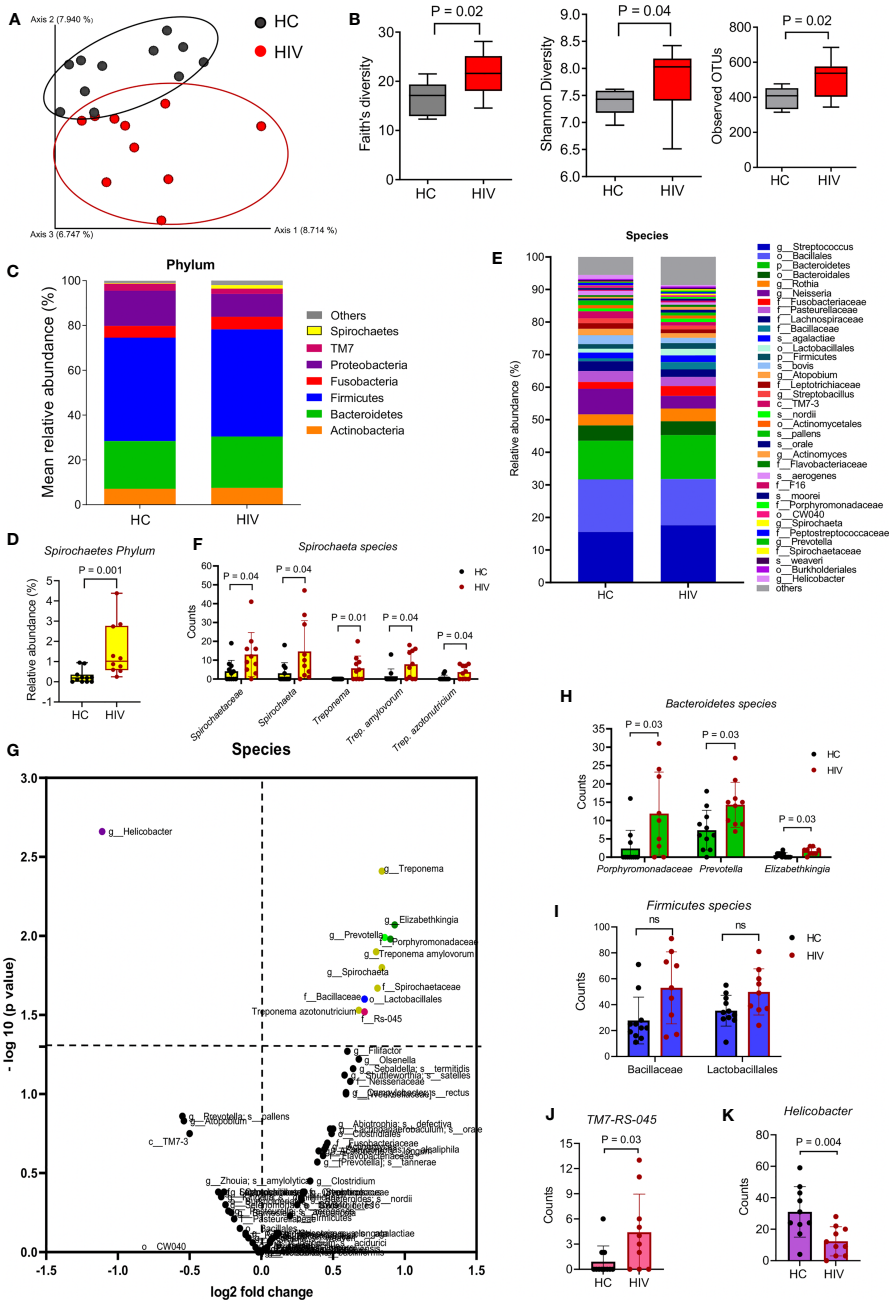

FIGURE 1 | Differential oral microbiome in the saliva of HIV-infected compared to healthy individuals. **(A)** Beta diversity in bacterial communities is shown by Principal coordinates analysis (PCOA) of Bray-Curtis Distances, in gray HCs (n = 11), in red HIV-infected individuals (n = 10), and each symbol represents an individual. **(B)** Alpha diversity in bacterial communities determine by Faith's, Shannon's, and observed OTUs indexes. **(C)** Comparison of the saliva microbiota at phylum level in HCs versus HIV-infected group. **(D)** Comparison of *Spirochaete's* phylum in the saliva of HCs versus HIV-infected individuals. **(E)** Comparison of the saliva microbiota at the species level in HCs versus HIV-infected group. Approximately, 32% of all taxa resolved could be classified at the species level. All other taxa are also included in the barplot at the lowest level they could be resolved (see legend: s_: species, g_: genus, f_: family, o_: order, c_ class, p_: phylum). **(F)** Comparison of unclassified *Spirochaetaceae, Spirochaeta, Treponema, Trep. amylovorum*, and *Trep. Azotonutricum* from *Spirochaete's* phylum in the saliva of HCs versus HIV-infected individuals. **(G)** The volcano plot comparing bacterial Genus in the saliva samples from HCs versus HIV-infected individuals. All genus that exceeded the dotted line marked at 1.3 were considered significant. **(H)** Comparison of *Bacteroidetes* genus members *Prophyromonadaceae, Prevotella, and Elizabethkingia* in saliva samples of HCs versus HIV-infected individuals. **(I)** Comparison of *Firmicutes* genus members *Bacillaceae and Lactobacillales* in saliva samples of HCs versus HIV-infected individuals. **(J)** Comparison of *Sebaldella* genus from *Fusobacteria* phyla (TM7-RS=045) in saliva samples of HCs versus HIV-infected individuals. **(K)** Comparison of *Helicobacter* genus in saliva samples of HCs versus HIV-infected individuals. ns, no significant.

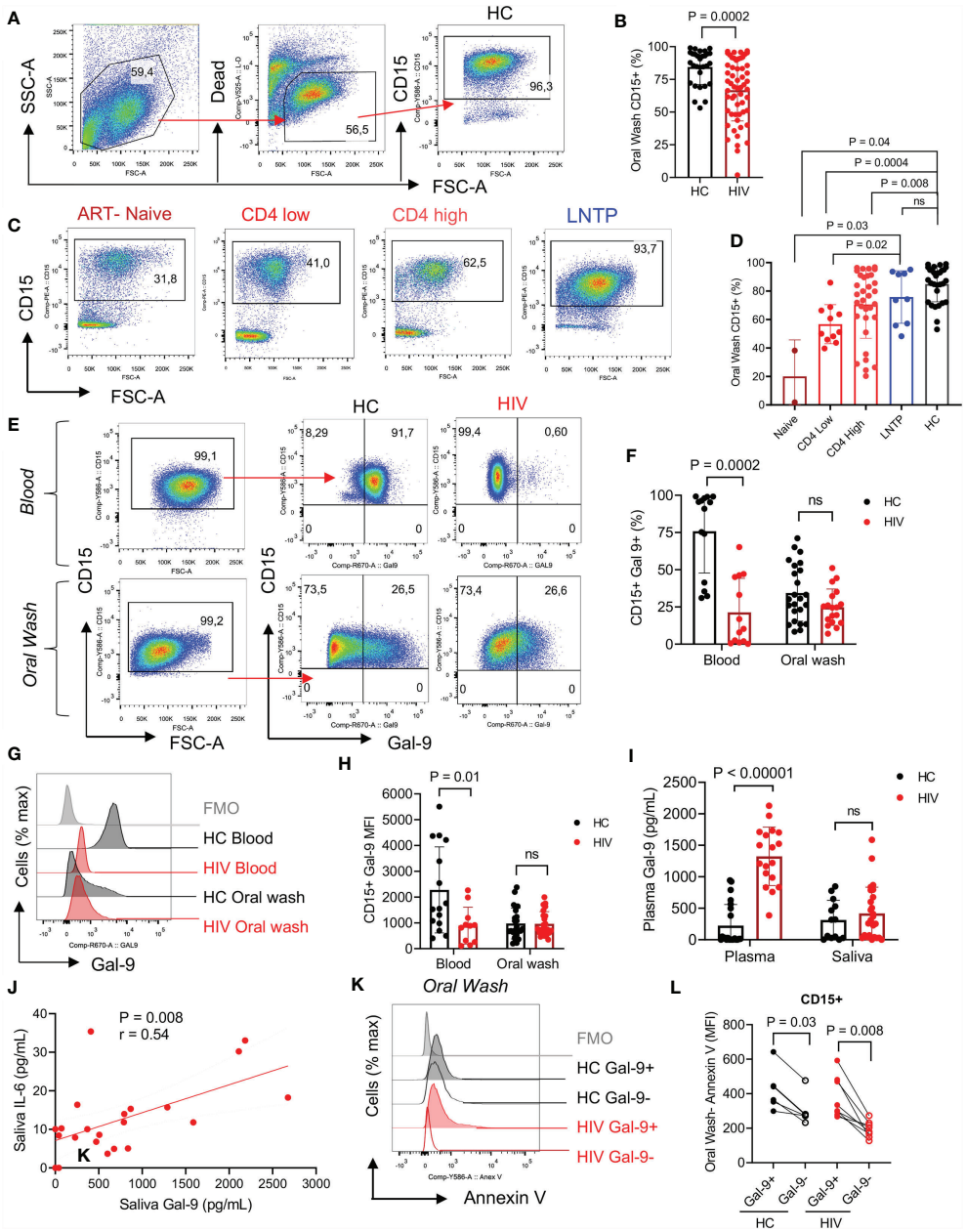

FIGURE 2 | Neutrophils in the oral cavity are decreased in HIV-infected individuals and have low surface Gal-9. **(A)** Representative flow cytometry plots for CD15$^+$ neutrophil identification in the oral wash. **(B)** Cumulative data of percentages of CD15$^+$ cells in the oral washes of HCs compared to HIV-infected individuals. **(C)** Representative flow cytometry plots, and **(D)** cumulative data of neutrophils in oral washes of different HIV-infected individuals (ART-naïve, on ART with low CD4$^+$ T cell count (< 200 cells/ul) or high CD4$^+$ T cell count (> 200 cells/ul), and long-term non-progressor (LTNP) compared to HCs. **(E)** Representative flow cytometry plots, and **(F)** cumulative data of Gal-9 surface expression in neutrophils from the blood and oral washes of HIV and healthy individuals. **(G)** Representative histogram plots, and **(H)** cumulative data of Gal-9 expression measured by the Mean Fluorescence Intensity (MFI) on blood and oral neutrophils of HIV-infected and healthy individuals. **(I)** Cumulative data of soluble Gal-9 in the plasma and saliva of HIV-infected and healthy individuals as measured by ELISA. **(J)** Cumulative data of a positive correlation between the saliva Gal-9 with the saliva IL-6 (Spearman correlation, r = 0.54, P = 0.008). **(K)** Representative histogram plots, and **(L)** cumulative data of apoptosis in oral neutrophils in regard to Gal-9 expression measured by Annexin V assay. ns, no significant.

lower on the surface of blood neutrophils from HIV-infected individuals (**Figures 2G, H**). However, this was not the case for the oral neutrophils (**Figures 2G, H**). We also quantified the concentration of soluble Gal-9 in the plasma and saliva samples. Although soluble Gal-9 was significantly elevated in the plasma of HIV-infected individuals as we have reported elsewhere (39), we did not find any difference in the soluble Gal-9 levels in the saliva between the groups (**Figure 2I**).

Soluble Gal-9 Is Positively Correlated With IL-6 in the Saliva of HIV-Infected Individuals

Since Gal-9 has been reported as a contributing factor to the cytokine storm in COVID-19 patients (41), we reasoned to evaluate the correlation of saliva Gal-9 levels with pro-inflammatory cytokines. We found that Gal-9 levels were positively correlated with IL-6 in the saliva (**Figure 2J**). This may suggest the potential role of soluble Gal-9 in the activation status of neutrophils in the oral cavity of HIV-infected individuals. However, this was not the case for other quantified pro-inflammatory cytokines (e.g., IL-1β, IL-8, TNF-α and IFN-γ) in the saliva.

Downregulation of Surface Gal-9 Makes Oral Neutrophils Less Apoptotic

IL-6 has been related to increased neutrophil survival (44) and an activated status can prolong the lifespan of neutrophils (45). Thus, we decided to investigate differences in Gal-9+ versus Gal-9- oral neutrophils. Recently, we have reported that stimulation of blood neutrophils with LPS results in the downregulation of Gal-9 at the gene and protein levels (37). Thus, we proposed that activated neutrophils lose their surface Gal-9, which in turn increases their lifespan. Indeed, we found that in HCs and HIV-infected individuals, neutrophils that did have surface Gal-9 were less apoptotic compared to their Gal-9 expressing counterparts (**Figures 2K, L**). These observations suggest that the downregulation of Gal-9 may act as a mechanism of enhanced neutrophil survival.

CD44 Is Downregulated From the Surface of Oral Neutrophils in HIV-Infected Individuals

Unstimulated blood neutrophils express high levels of surface Gal-9 which is bound to CD44 (37). Therefore, we decided to determine whether the same pattern exists for oral neutrophils. Similar to our previous finding, we found all blood neutrophils expressed CD44, however, this was about 50% for oral neutrophils (**Figure 3A**). Interestingly, we observed that the percentage of CD44 expressing neutrophils was significantly lower in the oral cavity of HIV-infected individuals (**Figures 3A, B**). Moreover, we found a significant reduction in the intensity of CD44 expression on oral neutrophils from HIV-infected individuals versus HCs (**Figures 3C, D**). When the expression of CD44 in the blood and oral neutrophils was analyzed, we found a lower frequency of CD44 expressing neutrophils and even CD44 expression level on oral neutrophils compared to their counterparts in the blood in both HCs and HIV-infected individuals (**Figures 3E–G**). These observations led us to measure the soluble CD44 concentration in the saliva, which showed a significant elevation of CD44 levels in the saliva of HIV-infected compared to healthy individuals (**Figure 3H**). This might explain that oral neutrophils in HIV-infected individuals shed CD44 that can be detected in their saliva. Moreover, we found that the soluble Gal-9 promotes the migration of blood neutrophils *in vitro* (**Figure 3I**). In particular, we observed that this effect was CD44 dependent as the pre-incubation of neutrophils with the anti-CD44 antibody abrogated this effect (**Figure 3I**). Although a similar trend was observed for Gal-9 on neutrophils from the oral cavity, this effect did not reach a significant level (**Supplementary Figure 1H**). Therefore, these findings may suggest that CD44 in the blood is upregulated to facilitate neutrophil migration into peripheral tissues, but once they reach their action site it is downregulated to keep neutrophils in their destination.

Soluble CD44 Is Associated With Inflammatory Cytokines and Bacterial Diversity

To further understand the possible role of soluble CD44 in the oral cavity, we found that it was positively correlated with saliva pro-inflammatory cytokines IL-6 and IL-8 in HIV-infected individuals (**Figures 3J, K**). Remarkably, we noted a positive correlation between the soluble CD44 with Faith's bacterial diversity index in HIV-infected individuals (**Figure 3L**). To further delineate the correlation between neutrophils and the oral microbiome, we measured the frequency of CD44 expressing neutrophils and the intensity of CD44 expression on oral neutrophils from HIV-infected versus HCs that were subjected to the microbiome analysis. We found that oral neutrophils had a significantly lower proportion and expression level of CD44 compared to their counterparts in HCs (**Figures 3M, N**). These observations suggest that microbial-derived molecules and/or other factors in the oral cavity may influence the expression of CD44 in HIV-infected individuals.

CD32 Is Highly Expressed in Oral Neutrophils From HIV-Infected Individuals and in $CD44^+$ Neutrophils

To further determine the activation status of neutrophils, we measured the expression of CD32. We found that CD32 was significantly upregulated in oral neutrophils of HIV-infected compared to healthy individuals (**Figures 4A–C**). CD32 has been described to participate in the interaction of neutrophils and uptake of IgG-opsonized viral particles (46). Thus, we decided to investigate whether aged oral neutrophils expressing CD44 had different CD32 expressions compared to CD44-negative counterparts. We found that $CD44^+$ oral neutrophils had significantly a higher expression of CD32 compared to their $CD44^-$ counterparts in both HIV-infected and healthy individuals (**Figure 4D**). In addition, we noted that although $CD44^+$ neutrophils were more activated, both $CD44^+$ and $CD44^-$ neutrophils in HIV-infected individuals had significantly higher expression of CD32 compared to their counterparts in HCs (**Figures 4E–G**). These results suggest that neutrophils in the oral cavity of HIV-infected individuals have an activated phenotype compared to their counterparts in HCs.

Patients' Demographics and Oral Health Associated Factors

To better understand whether observed changes were associated with other variables in both groups, we examined their sex, age, medications, oral health (brushing, flossing, using mouthwash),

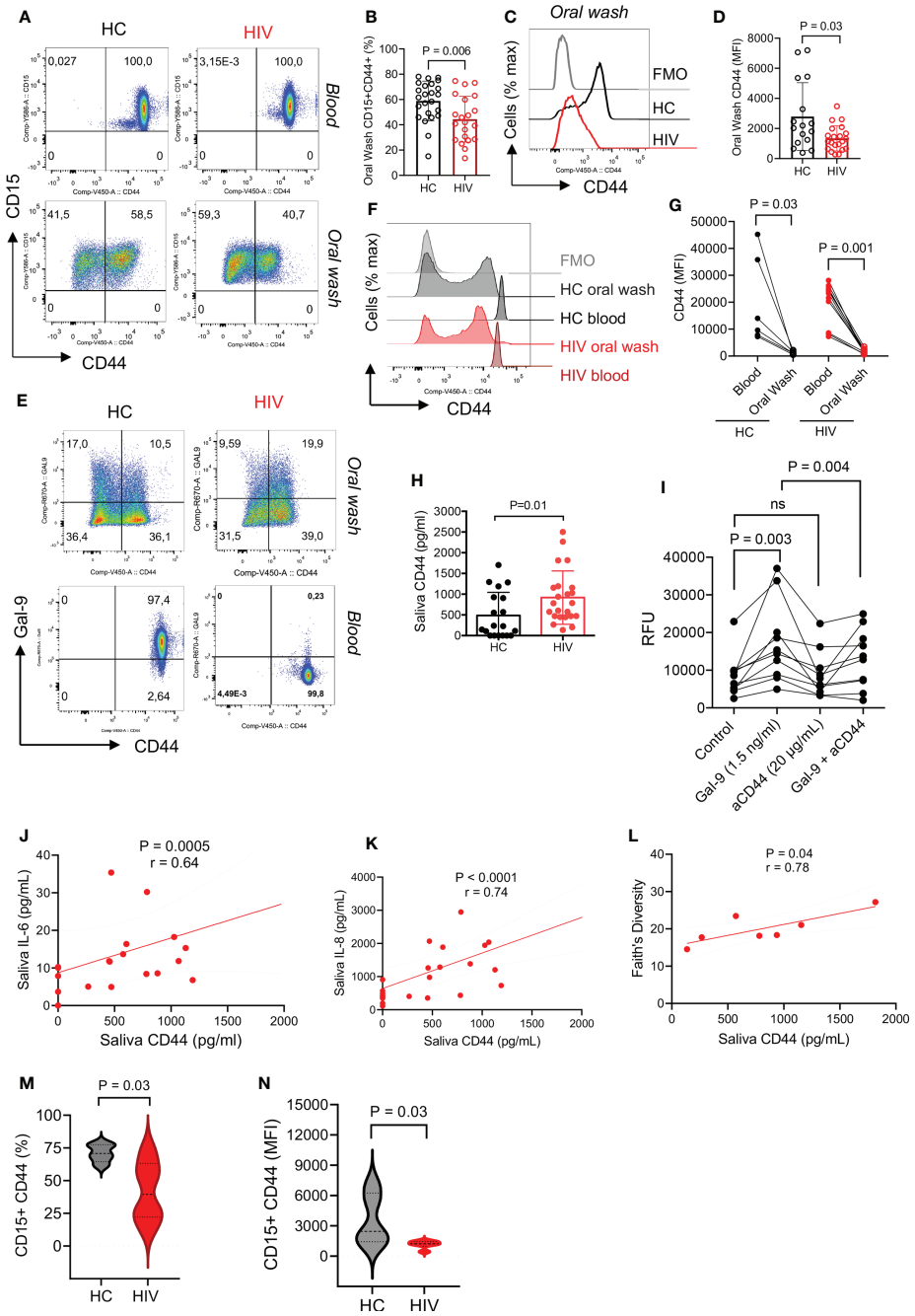

FIGURE 3 | CD44 is downregulated from the surface of oral neutrophils in HIV-infected individuals. **(A)** Representative flow cytometry plots of CD45 expression on blood and oral neutrophils. **(B)** Cumulative data of CD45 expression on oral neutrophils of HIV-infected versus healthy individuals. **(C)** Representative histogram plots, and **(D)** cumulative data of CD44 expression (MFI) in oral neutrophils of HV-infected individuals vs. HCs. **(E)** Representative flow cytometry plots of co-expression of CD44 and Gal-9 in oral and blood neutrophils in HIV-infected vs. healthy individuals. **(F)** Representative histogram plots, and **(G)** cumulative data of CD44 expression (MFI) in the blood and oral neutrophils of HIV-infected vs. healthy individuals. **(H)** Concentrations of soluble CD44 in the saliva of HIV-infected vs. healthy individuals as measured by ELISA. **(I)** Cumulative data showing blood neutrophil migration in the presence of soluble Gal-9 (1.5 ng/ml), anti-CD44 antibody (20 µg/ml), or soluble Gal-9 (1.5 ng/ml) plus anti-CD44 antibody while all wells were treated with fMLP (50 µm). **(J)** Cumulative results showing a positive correlation between the soluble CD44 with IL-6 in the saliva of HIV-infected individuals, calculated by Spearman correlation **(K)** Cumulative results showing a positive correlation between the soluble CD44 with IL-8 in the saliva of HIV-infected individuals, calculated by Spearman correlation. **(L)** Cumulative data showing a positive correlation between the soluble CD44 with bacterial Faith's diversity, measured by Spearman correlation. **(M)** Cumulative data of percentages of neutrophils expression CD44 in the oral cavity of HCs versus HIV-infected individuals that were subjected to 16S gene sequencing. **(N)** Cumulative data of the intensity of CD44 expression on neutrophils from the oral cavity of HCs versus HIV-infected individuals that were subjected to 16S gene sequencing. ns, no significant.

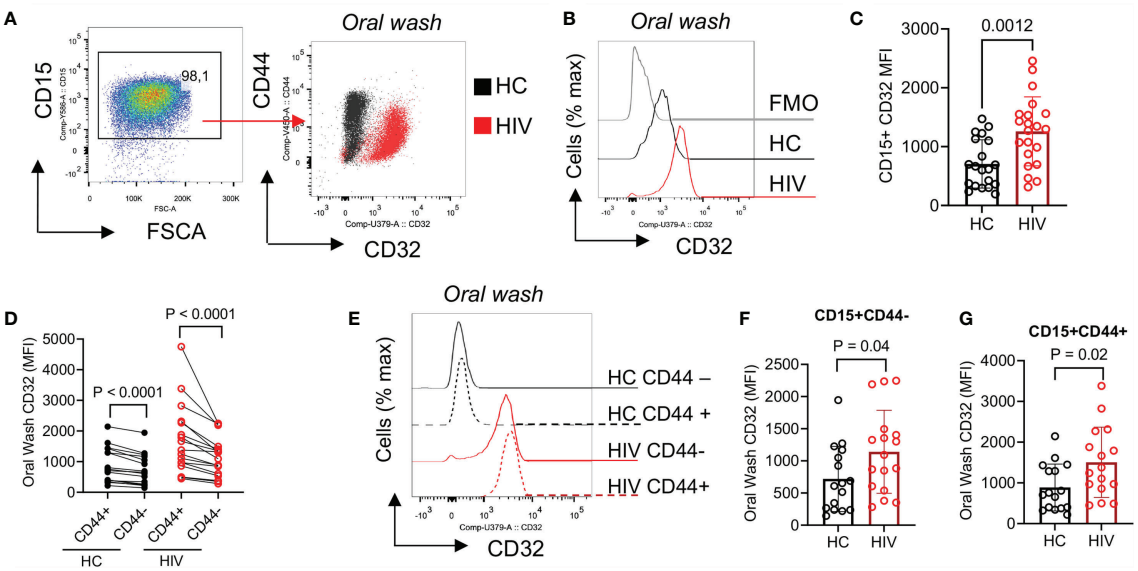

FIGURE 4 | Differential expression of CD32 on neutrophils from HIV-infected individuals versus healthy individuals. **(A)** Representative flow cytometry plots of CD32 expression on neutrophils of an HIV-infected vs. a healthy individual. **(B)** Representative histogram plots, and **(C)** cumulative data of CD32 expression (MFI) in oral neutrophils from HIV-infected vs. healthy individuals. **(D)** Cumulative data of CD32 expression in regards to CD44 on neutrophils of HCs vs. HIV-infected individuals. flow cytometry plot of neutrophils from oral washes and their coexpression of CD44 and CD32 in HIV patients shown in red and HCs in black. Note the higher expression of CD32 in neutrophils of HIV patients. **(E)** Representative histogram plots, and **(F)** cumulative data of CD32 expression (MFI) in $CD44^-$, and **(G)** $CD44^+$ populations of oral neutrophils from HCs and HIV-infected individuals. Significance was calculated by the Kruskal Wallis test.

and other habits (smoking, alcohol, and recreational drug use) into our analysis (**Supplementary Table 3**). We found that groups were differently distributed based on their sex (P=0.028) (**Figure 5A**). While HCs consisted of 16 Males and 27 females, the HIV cohort was composed of 37 males and 24 females. In terms of age, for statistical analysis the Fischer exact test was applied that showed age was also different between groups (P= 0.027). HCs had more participants <50 years compared to HIV-infected individuals who were 50 < years old (**Figure 5B**). Excluding LTNPs and naïve patients, the rest of HIV-infected individuals were receiving ART. Also, some HIV-infected individuals (n=33) had other comorbidities (mainly diabetes, high cholesterol, and blood pressure, rheumatoid arthritis, anxiety-depression, and chronic pain). In contrast, a small portion of HIV-uninfected participants (n=13) had underlying conditions and were receiving related medications at the time of examination.

Also, the participant's had differences in their habits as was analyzed by Fischer's exact test. The HIV-infected group had a significantly higher number of smokers compared to HCs (P < 0.0001). The same pattern was true for recreational drug/cannabis in HIV-infected individuals compared to HCs (P=0.002) (**Figure 5C**). However, alcohol consumption was similar between the groups (**Figure 5C**). Regarding oral health, HIV-infected individuals flossed less often compared to HCs (P= 0.0001) (**Figure 5C**). In terms of brushing, mouthwash use, and the self-reported evaluation for bleeding on brushing (a tool for periodontitis risk prediction), we did not find any difference between the groups (**Figure 5C**). Finally, we correlated the proportion of neutrophils in oral washes ($CD15^+$ cells) with habit practices in HIV-infected versus HCs. We found that HCs tend to have more neutrophils in their oral wash compared to HIV-infected individuals regardless of their habits (**Figure 5D**). Also, we noted that alcohol consumption, daily brushing, mouthwash use, and flossing significantly impacted neutrophil % in HCs vs HIV-infected individuals. Of note, the self-report for bleeding on brushing did not impact neutrophil percentages in the oral wash.

DISCUSSION

In this study, we investigated microbial communities in the saliva of HIV-infected and age-sex-matched HCs. We found differential bacterial compositions in the saliva of HIV-infected compared to healthy individuals. Our results are in agreement with another report that demonstrated differential bacterial clusters in the oral washes of a larger cohort of HIV-infected individuals versus HCs regardless of other contributing factors (e.g. smoking, missing teeth, gingivitis, candida infection, etc.) (29). We observed differences in bacterial α-diversity (e.g., Shannon and Faith's indexes) and bacterial richness, which supports HIV-associated salivary dysbiosis. Although previous work investigated dysbiosis of the tongue (47) and periodontal tissues in HIV-infected individuals (48), our results support that saliva expectoration provides a non-invasive, less expensive, and informative approach for oral cavity microbiome-related studies. In addition to microbiome studies, our study bridges the

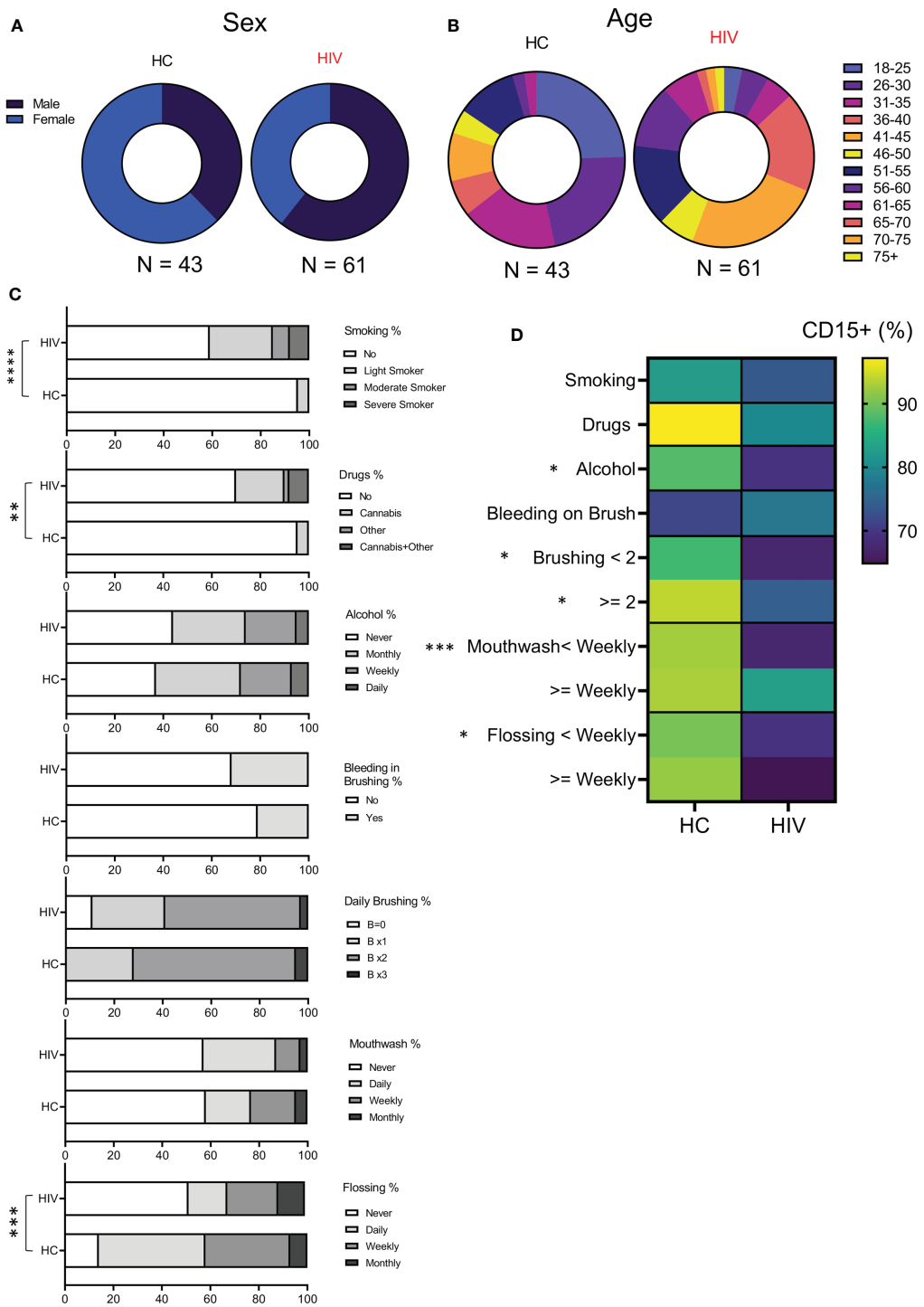

FIGURE 5 | Demographics and habits assessment of participants. **(A)** Showing the sex distribution with 37% and 63% females and males, respectively in HCs, 61% and 39% for males and females in HIV-infected group. **(B)** Showing the age distribution among participants. HC group was enriched with younger population according to Fischer's exact test analysis (P = 0.02). **(C)** Cumulative data illustrating participant's habits such as smoking, drug use, alcohol consumption, daily oral health. **(D)** Cumulative data showing the correlation of neutrophils' percentages with study participants' habits. (****P < 0.0001, ***P = 0.0001, **P < 0.001, *P < 0.05).

correlation between HIV-immune status, oral soluble mediators, and oral neutrophils. In a previous work, major difference in the phyla of *Bacteroidetes*, *Firmicutes*, *Proteobacteria* and *TM7* in the saliva of HIV-infected individuals versus HCs has been documented (49). Our results were somewhat similar in identifying increases in oral *Spirochaetes, Bacteroidetes, Firmicutes*, and *TM7* in HIV-infected individuals. Such differential oral microbiome composition may be related to systemic inflammation and impaired pulmonary function in HIV-infected individuals as a contributing factor to chronic obstructive pulmonary disease (COPD) (50). Since all of our study subjects for the oral microbiome-related studies were on ART, we were unable to investigate the potential effects of ART on the oral microbiome. However, it was reported that the dysbiotic oral microbiome was not fully restored after effective ART, although some microbiota were restored (51). Furthermore, ART, viral load, and $CD4^+$ T cell count differentially contribute to salivary dysbiosis resulting in reduced or increased different bacterial species (27).

It is difficult to differentiate between various factors without longitudinal studies pre-infection, pre-ART, the type of ART regimens, and well-matched HIV-infected untreated controls sampling. In general, oral health, habits such as smoking, and drinking may influence the oral microbial communities. Although in our cohort we did not observe any difference between the HIV-infected vs. the control group in terms of periodontitis, higher bacterial diversity and richness have been reported in HIV-infected individuals with severe periodontitis (52). Therefore, oral health can have direct effects on the microbial communities as increased bacterial diversity and richness have been associated with periodontal disease (53). Prior work also reported gingival bleeding, decayed teeth, periodontal pockets, and smoking habits as important contributing factor to oral dysbiosis (54). In our study, we observed that the HIV-infected group was more enriched with smokers, people who use recreational drug, and individuals who had poor adherence to oral health. These factors may influence the general oral health and subsequently the microbial composition of the oral cavity. For example, smoking has been associated with alteration in the oral microbiome. In particular, it has been reported that smoking enhances bacterial colonization in the upper respiratory tract in HCs, and even more pronounced in HIV-infected individuals (50, 55).

Although a greater abundance of *streptococcus* mutants, *lactobacillus*, and *candida* species has been in the saliva of HIV-infected individuals (47), we did not find such differences. Instead, we discovered significantly higher abundance of *Spirochaetes* (*Spirochaetacea*, *Spirochaeta, and Treponema), Porphyromonadaceae, Prevotella, Elizabethkingia, TM7* in the saliva of HIV-infected individuals. These observations are in agreement with a report showing an increased abundance of *Prevotella* in HIV-infected individuals (27). Similarly, an increase in *Porphyromonadaceae* in the saliva of HIV-infected individuals was reported at the start of ART when compared to 24 weeks later (30). Interestingly, the *Porphyromonadaceae family* harbors the well know periodontal pathogens *Phorphyromona gingivalis* and *Tannerella Forsythia* (56, 57). It is reported that *Phorphyromona gingivalis* partners with HIV-virus to co-infect mucosal epithelial cells, *in vitro* (58). Based on this observation, the abundance of *Phorphyormonas* in the oral cavity may facilitate HIV acquisition at the mucosal sites. However, further studies are required to support this hypothesis. *TM7-RS-045* or *Saccharibacteria* is a recently discovered commensal oral bacteria that abides at the expense of *Actynomices* bacteria, however, its role in the oral cavity is not well defined (59). In our cohort, we observed an increase of *TM7*, although we did not observe any difference in the abundance of *Actinomyces species*. A previous study, in support of our results, reported a higher abundance of *TM7, Treponema, and Prevotella* in the oral washes of HIV-infected individuals (29). Particularly, *Treponema denticola* associated with *Porphyromonas gingivalis, and Tanerella forsythia* form the "red complex", which are the main pathogenic bacteria involved in periodontitis (60, 61) (53). Therefore, consistently our data suggest that HIV-infected individuals have increased bacterial communities associated with periodontal conditions. Besides, *Prevotella* is reported to be more abundant in the gastrointestinal tract (GI) of men who have sex with men (62). The GI microbiome can be altered by different types of sexual practices. For example, men who have sex with men present a distinct GI microbiome composition when compared to men who have sex with women (63, 64). Therefore, the type of sexual practice may influence the GI and oral microbiome composition. Although we did not obtain such information from our study subjects, we had a mixed population of males/females for the microbiome analysis. Furthermore, a higher abundance of *Prevotella* is related to a lower abundance of Th17 cells and IFN-I genes expression in the GI of HIV-infected individuals (65). Moreover, the presence of *Prevotella* is associated with increased HIV acquisition in the genital tract (66). We found *Elizabethkingia* was another abundant bacteria in the saliva of HIV-infected individuals. *Elizabethkingia* is a multidrug-resistant bacteria associated with life-threatening infections in immunocompromised individuals (67). Thus, the presence of bacterial species like *Porphyromonadacea* and *Elizabethkingia* in the saliva of HIV-infected individuals may predispose them to such bacterial infections.

On the other hand, we found that *Helicobacter* was significantly decreased in the saliva of HIV-infected individuals. The presence of *Helicobacter pillory* in the dental plaque of HIV-infected individuals with *H. pillory*-induced gastritis has been reported (68, 69). However, its correlation with the stomach infection has been challenged (70) despite reports that the oral cavity should be considered as the secondary site for its colonization (71). However, our results are in agreement with another report that indicated the reduced frequency of *H. papillary*-induced gastric infection in HIV-infected individuals (72).

Our further analysis in understanding the immune components of the oral cavity in HIV-infected individuals demonstrated a significant decrease in the proportion of oral neutrophils which was associated with disease progression (e.g., $CD4^+$ T cell count). Notably, LTNPs exhibited the same frequency of neutrophils in their oral cavity compared to HCs. This observation provides another novel insight into the uniqueness of this rare group of HIV-infected individuals as we have reported elsewhere (73–75). Therefore, considering the crucial role of oral neutrophils in

immune homeostasis in the oral cavity, their lower frequency may predispose HIV-infected individuals to opportunistic infections. As such, it is possible to speculate that decreased frequency of oral neutrophils in individuals with lower $CD4^+$ T cell count may reflect the depletion of Th17 cells at their mucosal sites (76). Subsequently, a lower Th17 cell population reduces neutrophils' recruitment to the oral cavity. On the other hand, lower Th17 cells at the mucosal sites of the oral cavity may predispose HIV-infected individuals to oral candidiasis, considering the protective role of IL-17 against *Candida albicans* (77). Although we were unable to investigate the cross-talk between neutrophils and the oral microbiome, the salivary increase of *Treponema* species may potentially be related to neutrophil dysfunction in HIV-infected individuals (78). Deficiency in neutrophils chemotaxis and polarization in HIV-infected individuals (79) might explain another reason for reduced neutrophil frequency in HIV-infected individuals. On a supporting note, we observed significantly reduced expression and frequency of $CD44^+$ neutrophils in the oral cavity of HIV-infected individuals. CD44 is expressed on neutrophils and contributes to neutrophil crawling and extravasation (35). Therefore, lower CD44 expression on neutrophils from HIV-infected individuals may provide another underlying mechanism for their impairment. Subsequently, we found elevated levels of soluble CD44 in the saliva of HIV-infected individuals compared to HCs. The role of soluble CD44 in the saliva of HIV-infected individuals is still unknown and required further investigation. However, the salivary CD44 appears to be a surrogate marker in detection of head and neck squamous cell carcinoma (HNSCC) (80). Of note, we found a positive correlation between soluble CD44 and IL-6 in the saliva of HIV-infected individuals.

IL-6 has been reported as exhibiting both pro-and anti-inflammatory functions. Certain protective aspects of IL-6 influence leukocyte migration such as prevention of neutrophil accumulation at the site of inflammation/infection (81, 82). As such, exposure of IL-6 deficient mice to respiratory endotoxin resulted in a higher number of neutrophil accumulation in their lungs compared to wild-type mice (81).

Therefore, it is possible to suggest that the saliva level of IL-6 may influence neutrophil recruitment to the oral cavity as it enhances neutrophil egress (83). On the other hand, we found that Gal-9 interaction with CD44 enhances neutrophil migration *in vitro*. However, Gal-9 appears to exhibit different effects on neutrophil chemotaxis. For example, Gal-9 deficient mice experienced reduced neutrophil response to respiratory infection (84). In contrast, increased neutrophil infiltration following ischemic injury in Gal-9 deficient mice has been reported (85). Although Gal-9 may regulate neutrophil infiltration at the site of inflammation by modulating regulatory T cells and Th17 cells (86), our observations support that Gal-9 *via* interaction with CD44 enhances neutrophil migration. Finally, the association between the saliva CD44 levels and the microbial Faith's diversity suggests a cross-talk between neutrophils and the composition/abundance of microbial communities in the oral cavity.

We are aware of many study limitations that may have influenced our results. Although we attempted to have age-sex-matched study subjects, due to the COVID-19 pandemic we had limited options in terms of access to study cohorts. We also noted a higher prevalence of cigarette smoking, people with substance use disorder, and individual with poor oral health in the HIV-infected group, which might have influenced our results. Moreover, we were unable to analyze the impact of ART on neutrophils and/or microbiome in our cohort because all of our study subjects were on ART. Also, HIV-infected individuals had more underlying conditions compared to the HCs. However, for the microbiome studies we selected subjects without major underlying health conditions apart from HIV infection. Finally, due to a very low cell yield in the oral washes, we were unable to perform functional studies to better characterize oral neutrophil functions compared to their counterparts in the blood.

In summary, our data provide a novel insight into the impact of HIV infection on oral neutrophils. In particular, we discovered that oral neutrophils in HIV-infected individuals have significantly higher expression of CD32 but lower expression of CD44. The influence of Gal-9:CD44 on neutrophil migration highlights an important role for Gal-9 in neutrophil movement. Thus, the lower frequency of neutrophils in the oral cavity of HIV-infected individuals could be explained by the downregulation of CD44 expression. More importantly, we found elevated levels of soluble salivary CD44 which was positively correlated with Faith's diversity of the microbiome.

Overall, our results support the differential oral microbiome diversity and richness in HIV-infected individuals. Although further studies in larger cohorts are required, our results provide a novel insight into the immune-microbiota relationship in the oral cavity.

DATA AVAILABILITY STATEMENT

The original contributions presented in the study are publiclyavailable. This data can be found here: https://www.ncbi.nlm.nih.gov/, PRJNA766045.

ETHICS STATEMENT

The studies involving human participants were reviewed and approved by the human ethics board at the University of Alberta. The patients/participants provided their written informed consent to participate in this study.

AUTHOR CONTRIBUTIONS

ER performed most of the immunological and microbiome related experiments, analyzed the data and wrote the first draft. SH performed some of the experiments. JJ assisted with 16S rRNA data analysis. CO'N and ST recruited HIV-infected individuals for the study. PP provided resources and scientific advice. SE conceived the original idea, designed and supervised all of the research, assisted in data analysis and re-wrote the manuscript. All authors contributed to the article and approved the submitted version.

FUNDING

This study was supported by a Foundation Grant from the Canadian Institutes of Health Research (CIHR) and a CIHR New Investigator Salary Award (both to SE).

ACKNOWLEDGMENTS

The authors would like to thank the University of Alberta Faculty of Medicine and Dentistry's Flow cytometry facility, which has received financial support from the faculty of Medicine and Dentistry and the Canadian Foundation for Innovation (CFI) awards to contributing investigators. We also thank HIV-infected individuals from the Northern Alberta HIV program, and healthy individuals for their invaluable contribution to this study.

SUPPLEMENTARY MATERIAL

The Supplementary Material for this article can be found online at: https://www.frontiersin.org/articles/10.3389/fimmu.2021.780910/full#supplementary-material

REFERENCES

1. Moutsopoulos NM, Moutsopoulos HM. The Oral Mucosa: A Barrier Site Participating in Tissue-Specific and Systemic Immunity. *Oral Dis* (2018) 24:22–5. doi: 10.1111/odi.12729
2. Dewhirst FE, Chen T, Izard J, Paster BJ, Tanner ACR, Yu WH, et al. The Human Oral Microbiome. *J Bacteriol* (2010) 192:5002–17. doi: 10.1128/JB.00542-10
3. Baker JL, Bor B, Agnello M, Shi W, He X. Ecology of the Oral Microbiome: Beyond Bacteria. *Trends Microbiol* (2017) 25:362–74. doi: 10.1016/j.tim.2016.12.012
4. Elahi S, Buchanan RM, Attah-Poku S, Townsend HG, Babiuk LA, Gerdts V. The Host Defense Peptide Beta-Defensin 1 Confers Protection Against Bordetella Pertussis in Newborn Piglets. *Infect Immun* (2006) 74:2338–52. doi: 10.1128/IAI.74.4.2338-2352.2006
5. Lü FX, Jacobson RS. Oral Mucosal Immunity and HIV/SIV Infection. *J Dent Res* (2007) 86:216–26. doi: 10.1177/154405910708600305
6. Feller L, Altini M, Khammissa RAG, Chandran R, Bouckaert M, Lemmer J. Oral Mucosal Immunity. *Oral Surg Oral Med Oral Pathol Oral Radiol* (2013) 116:576–83. doi: 10.1016/j.oooo.2013.07.013
7. Heron SE, Elahi S. HIV Infection and Compromised Mucosal Immunity: Oral Manifestations and Systemic Inflammation. *Front Immunol* (2017) 8:241. doi: 10.3389/fimmu.2017.00241
8. Zicari S, Sessa L, Cotugno N, Ruggiero A, Morrocchi E, Concato C, et al. Immune Activation, Inflammation, and Non-AIDS Co-Morbidities in HIV-Infected Patients Under Long-Term ART. *Viruses* (2019) 11(3):200. doi: 10.3390/v11030200
9. Pandiyan P, Younes S-A, Ribeiro SP, Talla A, McDonald D, Bhaskaran N, et al. Mucosal Regulatory T Cells and T Helper 17 Cells in HIV-Associated Immune Activation. *Front Immunol* (2016) 7:228. doi: 10.3389/FIMMU.2016.00228
10. Indrastiti RK, Wardhany II, Soegyanto AI. Oral Manifestations of HIV: Can They be an Indicator of Disease Severity? (A Systematic Review). *Oral Dis* (2020) 26:133–6. doi: 10.1111/odi.13394
11. Nittayananta W, Tao R, Jiang L, Peng Y, Huang Y. Oral Innate Immunity in HIV Infection in HAART Era. *J Oral Pathol Med* (2016) 45:3–8. doi: 10.1111/jop.12304
12. Abusleme L, Moutsopoulos NM. IL-17: Overview and Role in Oral Immunity and Microbiome. *Oral Dis* (2017) 23:854–65. doi: 10.1111/odi.12598
13. Levine AM, Karim R, Mack W, Gravink DJ, Anastos K, Young M, et al. Neutropenia in Human Immunodeficiency Virus Infection: Data From the Women's Interagency HIV Study. *Arch Intern Med* (2006) 166:405–10. doi: 10.1001/ARCHINTE.166.4.405
14. Moonen CGJ, Hirschfeld J, Cheng L, Chapple ILC, Loos BG, Nicu EA. Oral Neutrophils Characterized: Chemotactic, Phagocytic, and Neutrophil Extracellular Trap (NET) Formation Properties. *Front Immunol* (2019) 10:635. doi: 10.3389/fimmu.2019.00635
15. Zhang D, Frenette PS. Cross Talk Between Neutrophils and the Microbiota. *Blood* (2019) 133:2168. doi: 10.1182/BLOOD-2018-11-844555
16. Hajishengallis G. Immunomicrobial Pathogenesis of Periodontitis: Keystones, Pathobionts, and Host Response. *Trends Immunol* (2014) 35:3–11. doi: 10.1016/J.IT.2013.09.001
17. Fine N, Tasevski N, McCulloch CA, Tenenbaum HC, Glogauer M. The Neutrophil: Constant Defender and First Responder. *Front Immunol* (2020) 11:571085. doi: 10.3389/fimmu.2020.571085
18. Uriarte SM, Edmisson JS, Jimenez-Flores E. Human Neutrophils and Oral Microbiota: A Constant Tug-of-War Between a Harmonious and a Discordant Coexistence. *Immunol Rev* (2016) 273:282–98. doi: 10.1111/imr.12451
19. Deshmukh HS, Liu Y, Menkiti OR, Mei J, Dai N, O'Leary CE, et al. The Microbiota Regulates Neutrophil Homeostasis and Host Resistance to Escherichia Coli K1 Sepsis in Neonatal Mice. *Nat Med* (2014) 20:524–30. doi: 10.1038/nm.3542
20. Zhang D, Chen G, Manwani D, Mortha A, Xu C, Faith JJ, et al. Neutrophil Ageing Is Regulated by the Microbiome. *Nat* (2015) 525:528–32. doi: 10.1038/NATURE15367
21. Adrover JM, Nicolás-Ávila JA, Hidalgo A. Aging: A Temporal Dimension for Neutrophils. *Trends Immunol* (2016) 37:334–45. doi: 10.1016/j.it.2016.03.005
22. Xiao E, Mattos M, Vieira GHA, Chen S, Corrêa JD, Wu Y, et al. Diabetes Enhances IL-17 Expression and Alters the Oral Microbiome to Increase Its Pathogenicity. *Cell Host Microbe* (2017) 22:120–128.e4. doi: 10.1016/j.chom.2017.06.014
23. Flynn KJ, Baxter NT, Schloss PD. Metabolic and Community Synergy of Oral Bacteria in Colorectal Cancer. *mSphere* (2016) 1(3):e00102–16. doi: 10.1128/MSPHERE.00102-16
24. Öğrendik M. Medical Hypothesis Oral Bacteria in Pancreatic Cancer: Mutagenesis of the P53 Tumour Suppressor Gene. *Int J Clin Exp Pathol* (2015) 8:11835–6.
25. Whitmore SE, Lamont RJ. Oral Bacteria and Cancer. *PloS Pathog* (2014) 10:e1003933. doi: 10.1371/JOURNAL.PPAT.1003933
26. Mukherjee PK, Chandra J, Retuerto M, Tatsuoka C, Ghannoum MA, McComsey GA. Dysbiosis in the Oral Bacterial and Fungal Microbiome of HIV-Infected Subjects Is Associated With Clinical and Immunologic Variables of HIV Infection. *PloS One* (2018) 13:e0200285. doi: 10.1371/JOURNAL.PONE.0200285
27. Lewy T, Hong BY, Weiser B, Burger H, Tremain A, Weinstock G, et al. Oral Microbiome in HIV-Infected Women: Shifts in the Abundance of Pathogenic and Beneficial Bacteria Are Associated With Aging, HIV Load, CD4 Count, and Antiretroviral Therapy. *AIDS Res Hum Retroviruses* (2019) 35:276–86. doi: 10.1089/aid.2017.0200
28. Li Y, Saxena D, Chen Z, Liu G, Abrams WR, Phelan JA, et al. HIV Infection and Microbial Diversity in Saliva. *J Clin Microbiol* (2014) 52:1400–11. doi: 10.1128/JCM.02954-13
29. Griffen AL, Thompson ZA, Beall CJ, Lilly EA, Granada C, Treas KD, et al. Significant Effect of HIV/HAART on Oral Microbiota Using Multivariate Analysis. *Sci Rep* (2019) 9:19946. doi: 10.1038/s41598-019-55703-9
30. Presti RM, Handley SA, Droit L, Ghannoum M, Jacobson M, Shiboski CH, et al. Alterations in the Oral Microbiome in HIV-Infected Participants After Antiretroviral Therapy Administration Are Influenced by Immune Status. *Aids* (2018) 32:1279–87. doi: 10.1097/QAD.0000000000001811
31. Scott DA, Krauss JL. Neutrophils in Periodontal Inflammation. *Periodontal Dis* (2011) 15:56–83. doi: 10.1159/000329672
32. Berezow AB, Darveau RP. Microbial Shift and Periodontitis. *Periodontol 2000* (2011) 55:36–47. doi: 10.1111/j.1600-0757.2010.00350.x

33. Lokuta MA, Nuzzi PA, Huttenlocher A. Analysis of Neutrophil Polarization and Chemotaxis. *Methods Mol Biol* (2007) 412:211–29. doi: 10.1007/978-1-59745-467-4_14
34. McDonald B, Kubes P. Interactions Between CD44 and Hyaluronan in Leukocyte Trafficking. *Front Immunol* (2015) 6:68. doi: 10.3389/fimmu.2015.00068
35. Khan AI, Kerfoot SM, Heit B, Liu L, Andonegui G, Ruffell B, et al. Role of CD44 and Hyaluronan in Neutrophil Recruitment. *J Immunol* (2004) 173:7594–601. doi: 10.4049/jimmunol.173.12.7594
36. Lu CH, Lin CH, Li KJ, Shen CY, Wu CH, Kuo YM, et al. Intermediate Molecular Mass Hyaluronan and CD44 Receptor Interactions Enhance Neutrophil Phagocytosis and IL-8 Production *via* P38- and ERK1/2-MAPK Signalling Pathways. *Inflammation* (2017) 40:1782–93. doi: 10.1007/s10753-017-0622-5
37. Dunsmore G, Rosero EP, Shahbaz S, Santer DM, Jovel J, Lacy P, et al. Neutrophils Promote T-Cell Activation Through the Regulated Release of CD44-Bound Galectin-9 From the Cell Surface During HIV Infection. *PloS Biol* (2021) 19:e3001387. doi: 10.1371/JOURNAL.PBIO.3001387
38. Merani S, Chen W, Elahi S. The Bitter Side of Sweet: The Role of Galectin-9 in Immunopathogenesis of Viral Infections. *Rev Med Virol* (2015) 25:175–86. doi: 10.1002/rmv.1832
39. Elahi S, Niki T, Hirashima M, Horton H. Galectin-9 Binding to Tim-3 Renders Activated Human CD4+ T Cells Less Susceptible to HIV-1 Infection. *Blood* (2012) 119:4192–204. doi: 10.1182/blood-2011-11-389585
40. Shahbaz S, Dunsmore G, Koleva P, Xu L, Houston S, Elahi S. Galectin-9 and VISTA Expression Define Terminally Exhausted T Cells in HIV-1 Infection. *J Immunol* (2020) 204(9):2474–91. doi: 10.4049/jimmunol.1901481
41. Bozorgmehr N, Mashhouri S, Rosero EP, Xu L, Shahbaz S, Sligl W, et al. Galectin-9, a Player in Cytokine Release Syndrome and a Surrogate Diagnostic Biomarker in SARS-CoV-2 Infection. *MBio* (2021) 12(3):e00384–21. doi: 10.1128/MBIO.00384-21
42. Bozorgmehr N, Okoye I, Oyegbami O, Xu L, Fontaine A, Cox-Kennett N, et al. Expanded Antigen-Experienced CD160+CD8+effector T Cells Exhibit Impaired Effector Functions in Chronic Lymphocytic Leukemia. *J Immunother Cancer* (2021) 9:e002189. doi: 10.1136/jitc-2020-002189
43. Rijkschroeff P, Jansen IDC, van der Weijden FA, Keijser BJF, Loos BG, Nicu EA. Oral Polymorphonuclear Neutrophil Characteristics in Relation to Oral Health: A Cross-Sectional, Observational Clinical Study. *Int J Oral Sci* (2016) 8:191–8. doi: 10.1038/ijos.2016.23
44. Asensi V, Valle E, Meana A, Fierer J, Celada A, Alvarez V, et al. *In Vivo* Interleukin-6 Protects Neutrophils From Apoptosis in Osteomyelitis. *Infect Immun* (2004) 72:3823. doi: 10.1128/IAI.72.7.3823-3828.2004
45. Prince LR, Whyte MK, Sabroe I, Parker LC. The Role of TLRs in Neutrophil Activation. *Curr Opin Pharmacol* (2011) 11:397–403. doi: 10.1016/j.coph.2011.06.007
46. Cotter MJ, Zaiss AK, Muruve DA. Neutrophils Interact With Adenovirus Vectors *via* Fc Receptors and Complement Receptor 1. *J Virol* (2005) 79:14622–31. doi: 10.1128/JVI.79.23.14622-14631.2005
47. Dang AT, Cotton S, Sankaran-Walters S, Li CS, Lee CYM, Dandekar S, et al. Evidence of an Increased Pathogenic Footprint in the Lingual Microbiome of Untreated HIV Infected Patients. *BMC Microbiol* (2012) 12:153. doi: 10.1186/1471-2180-12-153
48. Aas JA, Barbuto SM, Alpagot T, Olsen I, Dewhirst FE, Paster BJ. Subgingival Plaque Microbiota in HIV Positive Patients. *J Clin Periodontol* (2007) 34:189–95. doi: 10.1111/j.1600-051X.2006.01034.x
49. Saxena D, Li Y, Devota A, Pushalkar S, Abrams W, Barber C, et al. Modulation of the Orodigestive Tract Microbiome in HIV-Infected Patients. *Oral Dis* (2016) 22:73–8. doi: 10.1111/ODI.12392
50. Yang L, Dunlap DG, Qin S, Fitch A, Li K, Koch CD, et al. Alterations in Oral Microbiota in HIV Are Related to Decreased Pulmonary Function. *Am J Respir Crit Care Med* (2020) 201:445–57. doi: 10.1164/rccm.201905-1016OC
51. Li J, Chang S, Guo H, Ji Y, Jiang H, Ruan L, et al. Altered Salivary Microbiome in the Early Stage of Hiv Infections Among Young Chinese Men Who Have Sex With Men (Msm). *Pathogens* (2020) 9:1–19. doi: 10.3390/pathogens9110960
52. Noguera-Julian M, Guillén Y, Peterson J, Reznik D, Harris EV, Joseph SJ, et al. Oral Microbiome in HIV-Associated Periodontitis. *Med (United States)* (2017) 96 96(12):e5821. doi: 10.1097/MD.0000000000005821
53. Lamont RJ, Koo H, Hajishengallis G. The Oral Microbiota: Dynamic Communities and Host Interactions. *Nat Rev Microbiol* (2018) 16:745–59. doi: 10.1038/s41579-018-0089-x
54. Takeshita T, Kageyama S, Furuta M, Tsuboi H, Takeuchi K, Shibata Y, et al. Bacterial Diversity in Saliva and Oral Health-Related Conditions: The Hisayama Study. *Sci Rep 2016 61* (2016) 6:1–11. doi: 10.1038/srep22164
55. Lawani MB, Morris A. The Respiratory Microbiome of HIV-Infected Individuals. *Expert Rev Anti Infect Ther* (2016) 14:719–29. doi: 10.1080/14787210.2016.1206469
56. Khor B, Snow M, Herrman E, Ray N, Mansukhani K, Patel KA, et al. Interconnections Between the Oral and Gut Microbiomes: Reversal of Microbial Dysbiosis and the Balance Between Systemic Health and Disease. *Microorganisms* (2021) 9:1–22. doi: 10.3390/microorganisms9030496
57. Saxena D, Li Y, Yang L, Pei Z, Poles M, Abrams WR, et al. Human Microbiome and HIV/AIDS. *Curr HIV/AIDS Rep* (2012) 9:44–51. doi: 10.1007/s11904-011-0103-7
58. Mantri CK, Chen C, Dong X, Goodwin JS, Xie H. Porphyromonas Gingivalis–Mediated Epithelial Cell Entry of HIV-1. *J Dent Res* (2014) 93:794. doi: 10.1177/0022034514537647
59. Bor B, Bedree JK, Shi W, McLean JS, He X. Saccharibacteria (TM7) in the Human Oral Microbiome. *J Dent Res* (2019) 98:500–9. doi: 10.1177/0022034519831671
60. Curtis MA, Diaz PI, Van Dyke TE. The Role of the Microbiota in Periodontal Disease. *Periodontology* (2000) 83:14–25. doi: 10.1111/prd.12296
61. Darveau RP. Periodontitis: A Polymicrobial Disruption of Host Homeostasis. *Nat Publ Gr* (2010) 8(7):481–90. doi: 10.1038/nrmicro2337
62. Vujkovic-Cvijin I, Sortino O, Verheij E, Sklar J, Wit FW, Kootstra NA, et al. HIV-Associated Gut Dysbiosis is Independent of Sexual Practice and Correlates With Noncommunicable Diseases. *Nat Commun* (2020) 11:1–15. doi: 10.1038/s41467-020-16222-8
63. Armstrong AJS, Shaffer M, Nusbacher NM, Griesmer C, Fiorillo S, Schneider JM, et al. An Exploration of Prevotella-Rich Microbiomes in HIV and Men Who Have Sex With Men. *Microbiome 2018 61* (2018) 6:1–16. doi: 10.1186/S40168-018-0580-7
64. Noguera-Julian M, Rocafort M, Guillén Y, Rivera J, Casadellà M, Nowak P, et al. Gut Microbiota Linked to Sexual Preference and HIV Infection. *EBioMedicine* (2016) 5:135–46. doi: 10.1016/J.EBIOM.2016.01.032
65. Pinacchio C, Scagnolari C, Iebba V, Santinelli L, Innocenti GP, Frasca F, et al. High Abundance of Genus Prevotella Is Associated With Dysregulation of IFN-I and T Cell Response in HIV-1-Infected Patients. *AIDS* (2020) 34:1467–73. doi: 10.1097/QAD.0000000000002574
66. Buvé A, Jespers V, Crucitti T, Fichorova RN. The Vaginal Microbiota and Susceptibility to HIV. *Aids* (2014) 28:2333–44. doi: 10.1097/QAD.0000000000000432
67. Lin JN, Lai CH, Yang CH, Huang YH. Elizabethkingia Infections in Humans: From Genomics to Clinics. *Microorganisms* (2019) 7(9):295. doi: 10.3390/microorganisms7090295
68. Bıcak DA, Akyuz S, Kıratlı B, Usta M, Urganci N, Alev B, et al. The Investigation of Helicobacter Pylori in the Dental Biofilm and Saliva Samples of Children With Dyspeptic Complaints. *BMC Oral Heal 2017 171* (2017) 17:1–12. doi: 10.1186/S12903-017-0361-X
69. Al Asqah BDSM, Al Hamoudi BDSN, Anil BDSS, Al jebreen FRCPC A, Khalid Al-hamoudi W. Is the Presence of Helicobacter Pylori in the Dental Plaque of Patients With Chronic Periodontitis a Risk Factor for Gastric Infection? *Can J Gastroenterol* (2009) 23(3):177–9. doi: 10.1155/2009/950527
70. Ji Y, Liang X, Lu H. Analysis of by High-Throughput Sequencing: Helicobacter Pylori Infection and Salivary Microbiome. *BMC Oral Health* (2020) 20(1):84. doi: 10.1186/s12903-020-01070-1
71. Yee JKC. Helicobacter Pylori Colonization of the Oral Cavity: A Milestone Discovery. *World J Gastroenterol* (2016) 22:641–8. doi: 10.3748/wjg.v22.i2.641
72. Nevin DT, Morgan CJ, Graham DY, Genta RM. Helicobacter Pylori Gastritis in HIV-Infected Patients: A Review. *Helicobacter* (2014) 19:323–9. doi: 10.1111/hel.12131
73. Elahi S, Dinges WL, Lejarcegui N, Laing KJ, Collier AC, Koelle DM, et al. Protective HIV-Specific CD8+ T Cells Evade T Reg Cell Suppression. *Nat Med* (2011) 17:989–95. doi: 10.1038/nm.2422

74. Elahi S, Horton H. Association of HLA-Alleles With the Immune Regulation of Chronic Viral Infections. *Int J Biochem Cell Biol* (2012) 44:1361–5. doi: 10.1016/j.biocel.2012.05.003
75. Elahi S, Shahbaz S, Houston S. Selective Upregulation of CTLA-4 on CD8+ T Cells Restricted by HLA-B*35Px Renders Them to an Exhausted Phenotype in HIV-1 Infection. *PloS Pathog* (2020) 16:e1008696. doi: 10.1371/JOURNAL.PPAT.1008696
76. Elhed A, Unutmaz D. Th17 Cells and HIV Infection. *Curr Opin HIV AIDS* (2010) 5:146–50. doi: 10.1097/COH.0b013e32833647a8
77. Gaffen SL, Hernandez-Santos N, Peterson AC. IL-17 Signaling in Host Defense Against Candida Albicans. *Immunol Res* (2011) 50:181. doi: 10.1007/S12026-011-8226-X
78. Jones MM, Vanyo ST, Visser MB. The Msp Protein of Treponema Denticola Interrupts Activity of Phosphoinositide Processing in Neutrophils. *Infect Immun* (2019) 87(11):e00553–19. doi: 10.1128/IAI.00553-19
79. Mócsai A, Walzog B, Lowell CA. Intracellular Signalling During Neutrophil Recruitment. *Cardiovasc Res* (2015) 107:373–85. doi: 10.1093/cvr/cvv159
80. Franzmann EJ, Reategui EP, Carraway KL, Hamilton KL, Weed DT, Goodwin WJ. Salivary Soluble CD44: A Potential Molecular Marker for Head and Neck Cancer. *Cancer Epidemiol Biomarkers Prev* (2005) 14:735–9. doi: 10.1158/1055-9965.EPI-04-0546
81. Xing Z, Gauldie J, Cox G, Baumann H, Jordana M, Lei XF, et al. IL-6 is an Antiinflammatory Cytokine Required for Controlling Local or Systemic Acute Inflammatory Responses. *J Clin Invest* (1998) 101:311–20. doi: 10.1172/JCI1368
82. Barton BE, Jackson JV. Protective Role of Interleukin 6 in the Lipopolysaccharide-Galactosamine Septic Shock Model. *Infect Immun* (1993) 61:1496–9. doi: 10.1128/IAI.61.4.1496-1499.1993
83. Florentin J, Zhao J, Tai YY, Vasamsetti SB, O'Neil SP, Kumar R, et al. Interleukin-6 Mediates Neutrophil Mobilization From Bone Marrow in Pulmonary Hypertension. *Cell Mol Immunol* (2021) 18:374–84. doi: 10.1038/s41423-020-00608-1
84. Steichen AL, Simonson TJ, Salmon SL, Metzger DW, Mishra BB, Sharma J. Alarmin Function of Galectin-9 in Murine Respiratory Tularemia. *PloS One* (2015) 10(4):e0123573. doi: 10.1371/journal.pone.0123573
85. Hirao H, Uchida Y, Kadono K, Tanaka H, Niki T, Yamauchi A, et al. The Protective Function of Galectin-9 in Liver Ischemia and Reperfusion Injury in Mice. *Liver Transplant* (2015) 21:969–81. doi: 10.1002/lt.24159
86. Robinson BS, Arthur CM, Evavold B, Roback E, Kamili NA, Stowell CS, et al. The Sweet-Side of Leukocytes: Galectins as Master Regulators of Neutrophil Function. *Front Immunol* (2019) 10:1762. doi: 10.3389/fimmu.2019.01762

Conflict of Interest: The authors declare that the research was conducted in the absence of any commercial or financial relationships that could be construed as a potential conflict of interest.

Publisher's Note: All claims expressed in this article are solely those of the authors and do not necessarily represent those of their affiliated organizations, or those of the publisher, the editors and the reviewers. Any product that may be evaluated in this article, or claim that may be made by its manufacturer, is not guaranteed or endorsed by the publisher.

Copyright © 2021 Perez Rosero, Heron, Jovel, O'Neil, Turvey, Parashar and Elahi. This is an open-access article distributed under the terms of the Creative Commons Attribution License (CC BY). The use, distribution or reproduction in other forums is permitted, provided the original author(s) and the copyright owner(s) are credited and that the original publication in this journal is cited, in accordance with accepted academic practice. No use, distribution or reproduction is permitted which does not comply with these terms.

frontiers in Immunology

ORIGINAL RESEARCH
published: 16 November 2021
doi: 10.3389/fimmu.2021.775018

A New Formulation of Probiotics Attenuates Calcipotriol-Induced Dermatitis by Inducing Regulatory Dendritic Cells

Beilei Xu[1], Shiqi Ling[1], Xiaoqiang Xu[2], Xiaochun Liu[1], Ao Wang[1], Yuan Zhou[1], Yang Luo[1], Wei Li[3] and Xu Yao[1]**

[1] Department of Allergy and Rheumatology, Jiangsu Key Laboratory of Molecular Biology for Skin Diseases and STIs, Hospital for Skin Diseases, Institute of Dermatology, Chinese Academy of Medical Sciences and Peking Union Medical College, Nanjing, China, [2] Department of Bioinformatics, 01life Institute, Shenzhen, China, [3] Department of Dermatology, Huashan Hospital, Fudan University, Shanghai, China

OPEN ACCESS

Edited by:
Tobias R. Kollmann, University of Western Australia, Australia

Reviewed by:
David Martino, University of Western Australia, Australia
Alissa Cait, Victoria University of Wellington, New Zealand

***Correspondence:**
Xu Yao
dryao_xu@126.com
Wei Li
liweiderma@163.com

Specialty section:
This article was submitted to Microbial Immunology, a section of the journal Frontiers in Immunology

Received: *13 September 2021*
Accepted: *25 October 2021*
Published: *16 November 2021*

Citation:
Xu B, Ling S, Xu X, Liu X, Wang A, Zhou Y, Luo Y, Li W and Yao X (2021) A New Formulation of Probiotics Attenuates Calcipotriol-Induced Dermatitis by Inducing Regulatory Dendritic Cells. Front. Immunol. 12:775018. doi: 10.3389/fimmu.2021.775018

Atopic dermatitis (AD) is a recurrent chronic inflammatory skin disease affecting up to 30% of the children population, and immuno-regulatory therapy that could modify the course of disease is urgently needed. Probiotics have demonstrated therapeutic effects on AD and could potentially regulate the disease process. However, the efficacy of probiotics for AD is inconsistent among different studies, which is mainly due to the elusive mechanism and different species and (or) strains used. In this study, we designed a mixture of five strains of probiotics (named IW5) and analyzed the effect and mechanism of IW5 on calcipotriol (MC903)-induced AD-like dermatitis. We found that IW5 significantly alleviated skin inflammation of the MC903-induced AD in mice. Administration with IW5 induced increased production of regulatory T cells and regulatory dendritic cells (DCregs) in the mesenteric lymph nodes. We also found that the diversity of the gut microbiota in the mice with MC903-induced dermatitis was increased after IW5 administration, and the level of butyrate in the gut was elevated. In cell culture, butyrate induced the production of DCregs. Our study revealed the therapeutic effects of a newly designed probiotics mixture and uncovered a possible mechanism, providing a foundation for future clinical studies.

Keywords: probiotics, atopic dermatitis, regulatory T cells, regulatory dendritic cells, gut microbiota, short-chain fatty acids, butyrate

INTRODUCTION

Atopic dermatitis (AD) is a common chronic inflammatory skin disease characterized by intensive itch, dry skin, and eczematous dermatitis (1). Barrier dysfunction, type 2-dominant skin inflammation, and skin/gut dysbiosis play important roles in the pathogenesis of AD. There has been great progress in the treatment of AD in recent years, for example, the biologics and Janus kinase inhibitors have demonstrated excellent efficacy in moderate to severe AD; however, AD is still refractory and often relapses when the treatment of biologics or JAK inhibitors is stopped. Thus, immuno-regulatory therapy that could modify the course of disease is urgently needed. Probiotics

have potent immuno-regulatory effects and have shown preventive and therapeutic effects in inflammatory disorders by inducing the differentiation of regulatory T cells (Tregs) and balancing Th1/Th2 immune responses (2, 3). Many clinical studies have explored the efficacy of probiotics for the treatment of AD, and majority of the studies have demonstrated significant therapeutic effects on AD (4–11). However, meta-analyses on the clinical trials exploring the efficacy of probiotics in AD reveal that there is no significant difference between the group of probiotics and the control when the data are combined (12, 13). Whereas stratified analyses do show therapeutic effects of the probiotics, for example, Asian population, 1-18 years-old children and adolescents, and moderate to severe AD patients have significantly improved efficacy (14). The inconsistent results for probiotics might be because that the mechanism of the probiotics is not clear, and each probiotics species and (or) strain has different effect.

Several studies have explored the mechanism of probiotics for the treatment of allergic diseases. Administration with *Bifidobacterium* strain to mice results in increased expression of IL-10, TGF-β, IDO, and PD-1 within the mucosal $CD103^+$ DCs, which, in turn, induce the development of Tregs (15). *Lactobacillus paracasei* L9 prevents food allergy in mice by inducing the production of regulatory dendritic cells (DCregs) and $Foxp3^+$ Tregs (16). It has been reported that gut microbiota regulates immune responses through the production of short-chain fatty acids (SCFAs) such as acetate, propionate, and butyrate by fermentation of dietary fiber (17, 18). Microbiota-derived SCFAs promote $CD103^+$ DCs to induce the differentiation of Tregs and increase the production of IL-10, suppressing colonic inflammation and carcinogenesis (19). It has been reported that the levels of SCFAs are decreased in the gut of AD patients (20). However, whether probiotics exert their function through the production of SCFAs is not clear.

In this study, we designed a mixture of probiotics by combining 5 strains of bacteria (named IW5) according to previous reports (21–26) and investigated the immuno-modulatory properties of IW5 in the calcipotril (MC903)-induced AD mouse model. We found that IW5 had significant therapeutic effects on the mouse model of AD, and administration with IW5 induced increased production of Tregs and DCregs in the mesenteric lymph nodes (MLNs). Our study revealed the effect and uncovered a possible mechanism of a newly designed formulation of probiotics, providing a foundation for future clinical studies.

MATERIALS AND METHODS

Animals

Six to eight weeks-old female BALB/c mice were purchased from the Laboratory Animal Center of the Nanjing Medical University (Nanjing, Jiangsu, China). All the mice were maintained with a 12-h light/dark cycle at 22–24°C under specific pathogen-free condition. A standard extruded pellet diet and water were supplied unlimited. Animal experimental procedures were ethically reviewed and approved by the Animal Welfare Ethics Review Committee of the Institute of Dermatology, Chinese Academy of Medical Sciences.

Probiotics Preparation

The probiotics mixture, Indiv Wellness (IW5), was composed of five strains of probiotics: *Bifidobacterium lactis* UABLa-12, *Lactobacillus acidophilus* La-14, *Lactobacillus helveticus* R0052, *Lactobacillus salivarius* LS97, and *Lactobacillus casei* LC89. Probiotics were provided by 01life Institute (Shenzhen, Guangdong, China) as a lyophilized powder form, containing 5×10^{10} CFU active probiotics per gram.

Mice Experiment

AD-like dermatitis was produced by topical application with 2 nmol of MC903 (calcipotriol; Leo Pharma, Ballerup, Denmark) in ethanol on each ear of mice once daily for 12 consecutive days as previously described (27). Once the dermatitis was fully induced, 1 nmol of MC903 was applied daily for 27 days to maintain the skin inflammation. At the same time, mice were intragastrically administered with 200 μl IW5-L (2×10^8 CFU IW5) or IW5-H (1×10^9 CFU IW5) daily for 27 days (**Figure 1A**), and intragastrical phosphate-buffered saline (PBS; Gibco, Carlsbad, CA, USA) was used as control. For prevention experiment, mice were first intragastrically treated with IW5-H or PBS daily for 23 days, then were topically treated with PBS or MC903 for 12 days (**Figure S1A**). At the time points indicated, full thickness of the ears was measured with a micrometer. At the end of the treatment, mice were euthanized using CO_2. Skin tissue was either fixed in formalin for histopathological analysis or stored at -80°C for mRNA expression detection. Blood samples were collected for ELISA. The cervical lymph nodes (CLNs), MLNs, and spleens were harvested for further Fluorescence-activated cell sorting (FACS) analysis and cell culture.

Histopathological Analysis

The ear of mice was cut into pieces, fixed in 4% formalin, and six micrometer sections were prepared and stained with hematoxylin and eosin (H&E) for evaluation of the epidermal thickness and inflammation. Sections were also stained with toluidine blue for analysis of mast cell infiltration.

Ex Vivo Cell Culture and Treatment

CLNs, MLNs, and spleens were harvested and grinded with syringe pistons, and then were filtered through a 200-mesh strainer to get single-cell suspension for cell culture and flow cytometry. For isolation of splenocytes, red blood cells were removed by RBC lysis buffer (Miltenyi Biotec, Bergisch Gladbach, Germany). Single-cell suspensions of CLNs were resuspended in RPMI 1640 culture medium (Gibco) supplemented with 10% heat-inactivated fetal calf serum (FBS; Gibco), 100 U/ml penicillin, and 100 μg/ml streptomycin at a concentration of 10^6 cells per milliliter and placed in a plate precoated with 2 μg/ml anti-CD3 and anti-CD28 monoclonal antibodies (mAbs; eBioscience, San Diego, CA, USA). Following 5 days of culture, the supernatants were harvested and stored at −80°C for IL-4, IFN-γ, IL-10, and TGF-β1 measurement using ELISA.

For experiments of $CD4^+$ T Cells and $CD11c^+$ DCs co-culture, $CD4^+$ T cells were sorted from splenocytes of wild-

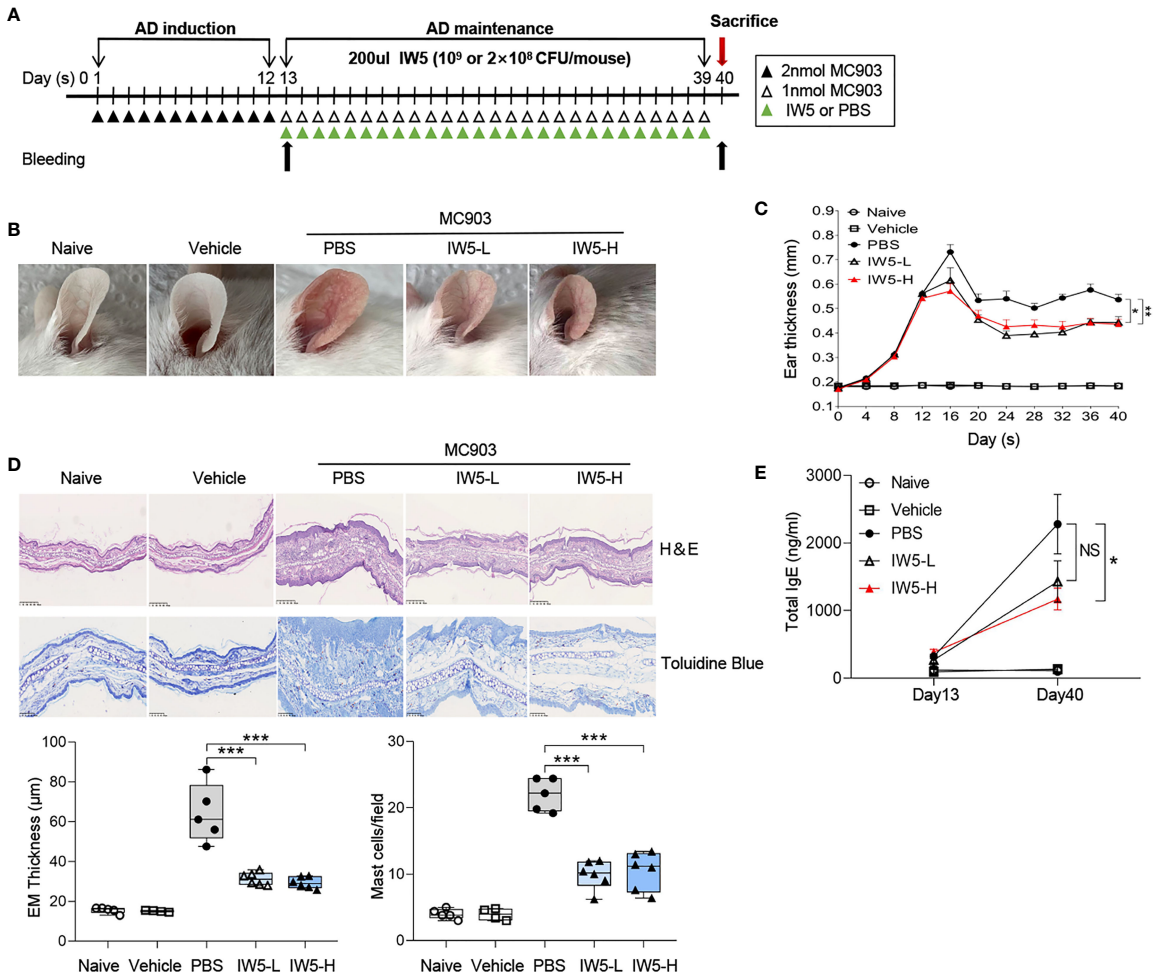

FIGURE 1 | IW5 ameliorates MC903-induced AD symptoms in mice. **(A)** Experimental design. Mice were topically treated with MC903 for 12 days and then gavaged with IW5-L (2×10^8 CFU IW5), or IW5-H (10^9 CFU IW5) daily for 27 days. Oral feeding of PBS to the MC903-treated mice was used as control for probiotics, and mice with EtOH painted on the ears were used as vehicle control for the MC903-induced AD model. **(B)** Gross appearance of the ears on day 40. **(C)** Dynamic changes of ear thickness at the indicated time points. **(D)** Histology of skin lesion. Hematoxylin and eosin (H&E) staining shows the thickness of the epidermis (EM) (original magnification ×100, Scale bar = 250 μm), and toluidine blue staining shows the infiltration of mast cells (original magnification ×200, Scale bar = 100 μm). **(E)** Levels of serum total IgE at day 13 and day 40 as measured by ELISA. Data are shown as means ± SEMs, and representative of data from three independent experiments. Student's t-test (unpaired; n = 5~6); *P < 0.05, **P < 0.01, ***P < 0.001 *vs.* PBS group. NS, not significant.

type BALB/c mice by CD4 MicroBeads UltraPure kit (Miltenyi Biotec), and $CD11c^+$ cells were sorted from the MLNs of mice that were intragastrically given 200 μl IW5-H (10^9 CFU) daily for 20 days by CD11c-PE antibody (eBioscience) and PE MicroBeads UltraPure kit (Miltenyi Biotec). $CD11c^+$ DCs (10^5 cells/ml) were co-cultured with $CD4^+$ naïve T cells (10^6 cells/ml) for 5 days, in the presence of TGF-β1 (0.5 ng/ml; Peprotech, Rocky Hill, NJ, USA) and IL-2 (10 ng/ml; Peprotech) in RPMI 1640 culture medium supplemented with 10% heat-inactivated FBS, 100 U/ml penicillin and 100 μg/ml streptomycin. Then cells were subjected to $CD4^+$ $CD25^+$ $Foxp3^+$ Tregs analysis by flow cytometry.

For the experiment of $CD11c^+$ DC culture, $CD11c^+$ DC cells were isolated from splenocytes of wild-type BALB/c mice as previously described. $CD11c^+$ DCs (10^6 cells/ml) were co-cultured with live IW5 (10^7 CFU/ml), or SCFAs (Butyric, Acetic or Propionic; 1mmol/L; Sigma-Aldrich, St. Louis, MO, USA) for 24 h, in the presence of LPS (0.5ug/ml; Sigma-Aldrich) in RPMI 1640 culture medium supplemented with 10% heat-inactivated FBS. After incubation, the supernatants were harvested and examined for IL-6, IL-12p70, and IL-10 using ELISA, and the cells were analyzed for proliferation and expression of CD80, MHCII, and PD-L1 by flow cytometry.

ELISA

For analysis of serum total IgE, 96-well microplate was pre-coated with 100 μl/well of purified rat anti-mouse IgE (1 μg/mL) overnight at 4°C, then blocked with 200 μl/well of 10% FBS at room temperature for 30 minutes, followed by incubation with diluted sera at room temperature for 2 hours. Biotin rat anti-

mouse IgE (2 μg/mL) was added afterward. Then, after washing the plate was incubated with 100 μl/well of streptavidin-HRP. After 30 mins at room temperature, tetramethylbenzidine (TMB, Beyotime, Shanghai, China) was added and the reaction was stopped by adding 50 μl/well of 2M H_2SO_4. The absorbance was measured at wavelength 450 nm. The levels of IFN-γ, IL-4, IL-10, and TGF-β1 in the supernatants were measured using the ELISA kits (all from Fcmacs, FMS-ELM027, FMS-ELM004, FMS-ELM009, FMS-ELM029, Nanjing, Jiangsu, China); the levels of IL-6 and IL-12p70 in the supernatants were measured using the ELISA kits (all from NOVUS Biologicals, Littleton, Colorado, USA) according to the manufacturer's instructions.

Quantitative RealTime PCR (RT-qPCR)

Total RNA was extracted from the ear skin using TRIzol reagent (Invitrogen, Carlsbad, CA, USA), according to the manufacturer's instructions. Complementary DNA (cDNA) was synthesized and the following mRNA expression of each gene was measured using AceQ qPCR SYBR Green Master Mix (Vazyme Biotech Co., Ltd, Nanjing, Jiangsu, China). Cycling condition was 95°C for 15s and 60°C for 30s for 40 cycles. Results were normalized to β-actin and was determined using $2^{-\Delta\Delta CT}$ calculation method. Primer sequences were shown in **Supplementary Table 1**.

Flow Cytometry

Single-cell suspension (10^6 cells/tube) was incubated with anti-CD16/32 antibody to block Fc receptors for 15min at 4°C. For surface staining, the cells were stained with antibodies or matched isotype control for 20 min at 4°C in the dark. The antibodies included anti-mouse CD3-PECY7, CD4-FITC, CD8-Percpcy5.5, CD25-APC, CD11c-PE, CD86-APC, CD80-PerCP-eFlour710, PD-L1-PECY7, MHCII-Alexa Flour 700, MHCII-APC, and CD103-FITC antibodies (all from Biolegend, San Diego, CA, USA). For intracellular staining, cells were cultured in the presence of 2μl/ml cell stimulation cocktail (eBioscience) for 6 h. The cells were fixed and permeabilized using fixation and permeabilization solutions, then stained with anti-mouse Foxp3-PE, IL4-PE, IFN-γ-APC, IL10-PE antibodies (all from eBioscience), or isotype control for 30 min at 4°C in the dark. The cells were detected using BD FACSVerse (BD Biosciences, Franklin Lakes, NJ, USA) or Aurora (Cytek, Fremont, CA, USA), and data were analyzed using the FlowJo 10.0.7 software (Tree Star, Ashland, OR, USA).

Microbiome Analysis

Fresh feces of mice were collected sterilely and stored at −80°C. Fecal DNA was extracted using a previously described method (28) and sequenced the V3 to V4 region of bacterial 16S rRNA genes in 2 × 250 bp paired-end (PE) mode on the NovaSeq platform (Illumina, USA) according to the manufacturer's instructions. The V3–V4 region of bacterial 16S rRNA gene was amplified with a pair of region-specific primers (Forward: CCTACGGGNGGCWGCAG; Reverse: GACTACHVGGGTATCTAATCC). Sequencing libraries were generated using the TruSeq® DNA PCR-Free Sample Preparation Kit (Illumina) following the manufacturer's recommendations and index codes were added. The library quality was assessed on the Qubit@ 2.0 Fluorometer (Thermo Scientific) and Agilent Bioanalyzer 2100 system. Raw reads were joined using FLASH (v1.2.11) with default parameters and trimmed with Trimmomatic (v0.39) using specified settings ("ILLUMINACLIP:/share/app/Trimmomatic-0.39/adapters/TruSeq3-PE.fa:2:30:10 LEADING:3 TRAILING:3 SLIDINGWINDOW:4:20 MINLEN:200"). Processed data were then analyzed using QIIME-2020.2 software (https://docs.qiime2.org/2020.2/), and ASVs were analyzed using deblur method. Alpha diversity was evaluated using the Observed ASVs counts, Shannon index and Faith Phylogenetic Diversity (Faith PD), and Wilcoxon rank-sum test was conducted to identify statistical significance between two groups. Bray-Curtis distance measured at the ASV level was used to determine the dissimilarity of the microbial community, and intergroup comparison was conducted using PERMANOVA with 9999 permutations in the R package vegan. Generated ASVs were then further classified into taxonomy with q2-classify using the SILVA database (release 132). Kruskal-Wallis test was used to identify differential genus or ASVs between groups. A minimum occurrence frequency cutoff of 30% for each feature in either group was applied to filter genus or ASVs before differential analysis. P-values of less than 0.05 were considered to indicate significant results.

SCFAs Quantitative Analysis

GC-MS analysis of SCFAs in the feces and serum of mice was performed on an Agilent HP-INNOWAX (Agilent Technologies Inc., Palo Alto, CA, USA) with capillary columns. Feces and serum was homogenized with 15% phosphoric acid, internal standard solution (Isocaproic acid), and diethyl ether, then centrifuged at 12,000 × g for 10 min at 4°C. The supernatants were then collected for GC-MS analysis.

Statistical Analysis

The difference between individual pairs was calculated using Student's t-test in the case of parameters. For nonparametric data, the Mann–Whitney test was used to determine statistical significance. All data were analyzed with GraphPad Prism V 8.0.1 and R 3.5.1 (GraphPad Software, La Jolla, CA, USA). Differences were considered statistically significant when P-value was <0.05.

RESULTS

IW5 Alleviated Skin Inflammation in Mouse Model of AD

To investigate the effects of IW5 on AD, a mouse model of AD was produced by topical application with MC903; then two doses of IW5 were intragastrically administrated to the AD mice after 12 days of MC903 application (**Figure 1A**). The AD model induced by MC903 exhibited obvious skin inflammation manifesting as erythema, edema, crust, and scale, accompanied by increased levels of total serum IgE (**Figures 1B–E**). However, the AD mice receiving two doses of IW5 (IW5-L or IW5-H) showed significantly improved dermatitis, as evidenced by milder morphological appearance, decreased ear thickness, and less inflammatory cell infiltration (**Figures 1B–D**). The IW5-H group, but not the IW5-L group, also showed a decreased level of serum total IgE that was

markedly elevated in the AD model mice (**Figure 1E**). Preventive effects of IW5 were further investigated, and the result showed that the mice receiving intragastrical IW5 first and topical MC903 later also demonstrated significantly decreased skin inflammation (**Figure S1**). Collectively, these data suggested that oral administration with the probiotics mixture IW5 alleviated MC903-induced AD-like dermatitis, in a dose-dependent manner.

IW5 Inhibited Th2 Immune Responses in AD Model and Induced Tregs Production

Next, the differentiation and polarization of T cells in the AD mice after IW5 treatment were assessed. The proportions of Th1 ($CD4^+$ IFN-γ^+) and Th2 ($CD4^+$ IL-4^+) cells were increased in the CLNs of the AD mouse model; whereas in the AD mice receiving oral IW5, the percentage of Th1 cells (IW5-H *vs.* PBS; mean diff=-0.578%, P<0.001) and Th2 cells (IW5-H *vs.* PBS; mean diff=-0.68%, P<0.01) in the CLNs was significantly decreased (**Figures 2A**, **S2A, D**). The percentages of Th1 and Th2 cells in the MLNs (IW5-H *vs.* PBS; Th1 cells; mean diff=-0.094%, P>0.05; Th2 cells; mean diff=-0.254%, P>0.05) and spleens (IW5-H *vs.* PBS; Th1 cells; mean diff=-0.01% P>0.05; Th2 cells; mean diff=–0.156%, P>0.05) of the AD mice treated with IW5 were also lower than those of the AD model control, but the difference was not statistically significant (**Figures S2B, C**). The expression of TSLP, IL-4, IL-13, and IL-6 in skin lesions of the AD mice after IW5 treatment were markedly decreased

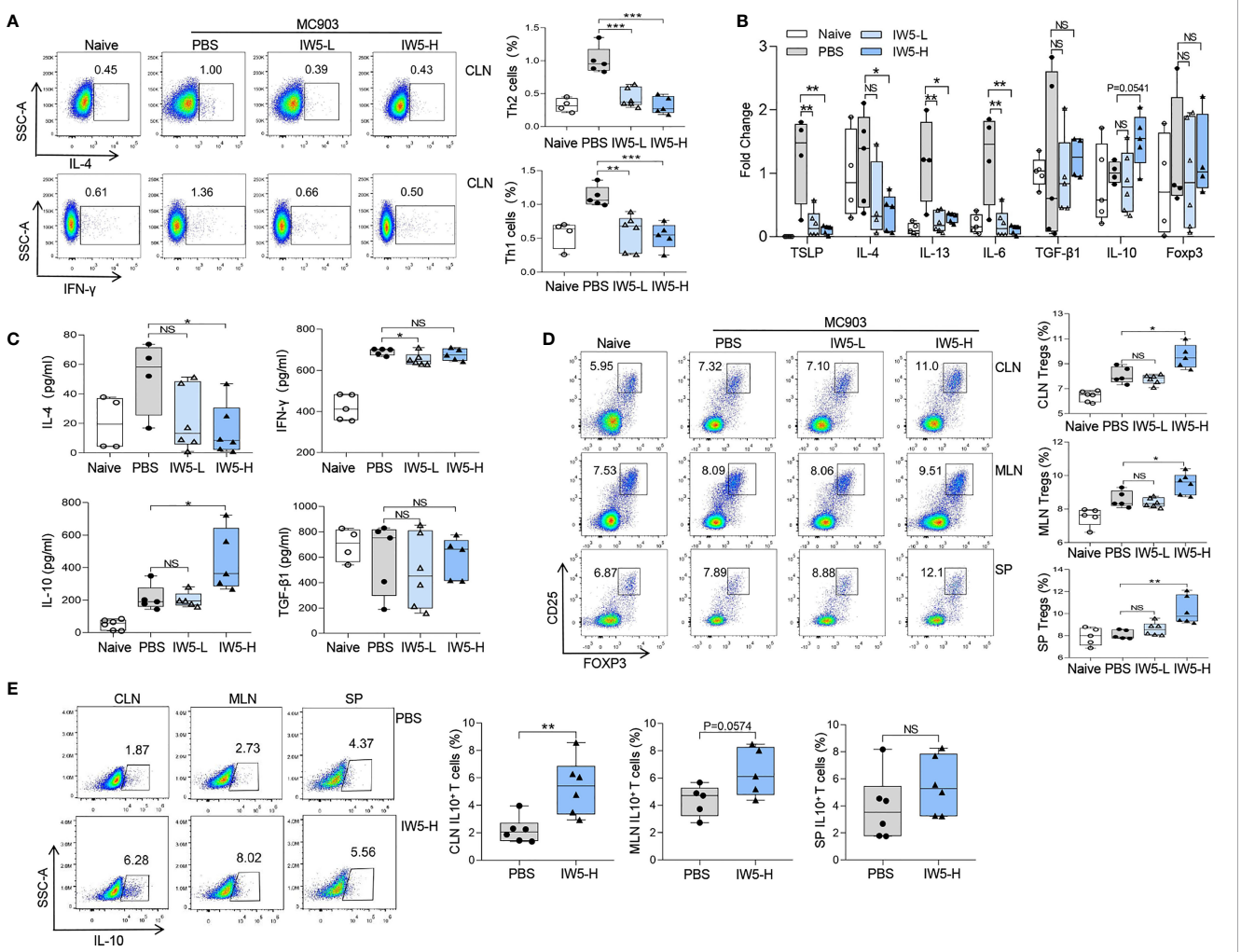

FIGURE 2 | IW5 inhibits Th1 and Th2 polarization and promotes Tregs differentiation. **(A–D)** AD mice were orally administrated with IW5-L or IW5-H for 27 days, and the cervical lymph nodes (CLNs), mesenteric lymph nodes (MLNs), and spleens were collected on day 40 for further analysis. Th1 ($CD4^+$ IFNγ^+) and Th2 ($CD4^+$ IL-4^+) cells from the CLNs **(A)**, and Tregs ($CD4^+$ $CD25^+$ $Foxp3^+$) from the CLNs, MLNs, and spleens **(D)** were analyzed by flow cytometry. RT-qPCR shows mRNA expression of various cytokines from the ear lesional skin **(B)**, and ELISA shows concentrations of IL-4, IFN-γ, IL-10, and TGF-β1 in supernatants of cells from the CLNs **(C)**. **(E)** BALB/c mice were administrated with IW5-H (10^9 CFU IW5) or PBS daily for 20 days. Percentages of $CD4^+$ IL-10^+ T cells from the CLNs, MLNs, and spleens were measured by flow cytometry. Data are shown as means ± SEMs, and representative of data from three independent experiments. Student's t-test (unpaired; n = 4~6); *P < 0.05, **P < 0.01, ***P < 0.001 *vs.* PBS group. NS, not significant.

(**Figures 2B**, **S2E**). Single cells from the CLNs of IW5-treated AD mice were then cocultured with anti-CD3 and anti-CD28 mAbs, and the levels of IL-4 and IFN-γ in the supernatant of culture were much lower than those of cells from the AD model control (**Figure 2C**). These data indicated that IW5 attenuated the polarization of Th1 and Th2 in AD mice.

The proportion of Tregs ($CD4^+$ $CD25^+$ $Foxp3^+$) in the AD mice upon IW5 treatment was also analyzed. The result showed that the proportion of Tregs was significantly higher in the CLNs (mean diff=1.496%, P=0.0208), MLNs (mean diff=0.939%, P=0.0240), and spleens (mean diff=2.191%, P<0.01) of the AD mice receiving IW5-H compared to the AD mice receiving PBS (**Figures 2D** and **S2F**). The proportion of Tregs was also increased in the AD mice receiving IW5-L, but without statistical significance, indicating a dose-dependent effect of IW5. The concentration of IL-10 in the supernatants of CLN cell culture was increased in the IW5-H-treated AD mice compared with the AD model control, and the expression of IL-10 in the skin lesions of the IW5-H-treated AD mice was also elevated. However, there was no significant difference in the level of TGF-β1 between the IW5-treated AD mice and the AD model control (**Figures 2B, C**). These data indicated that the increased production of Tregs was induced through IL-10, but not TGF-β1.

We further analyzed $CD4^+$ $IL\text{-}10^+$ T cells in the naïve mice receiving oral IW5 and found that the percentages of $CD4^+$ $IL\text{-}10^+$ T cells in MLNs (mean diff=2.09%, P=0.0574) and CLNs (mean diff=3.153%, P<0.01) were higher in the IW5-treated mice compared to the PBS-treated mice (**Figures 2E**, **S2A**). The percentages of $CD4^+$ $IL\text{-}10^+$ T cells in the spleens (mean diff=1.615%, P>0.05) of the IW5-treated mice were also higher than those from the PBS-treated control mice, but the difference was not statistically significant (**Figure 2E**). Collectively, these results demonstrated that IW5 induced the differentiation of Tregs, and inhibited Th1 and Th2 immune responses in the mouse model of AD.

IW5 Induced the Production of DCregs

$CD103^+$ DCs are considered as the iconic mucosal DCregs, which induce the production of $Foxp3^+$ Tregs (29). We then analyzed the number of DCregs in naïve mice after IW5 administration. The result of FACS showed that the percentage of $CD103^+$ DCs ($CD11c^+$ $MHCII^+$ $CD103^+$) was increased in the MLNs (IW5-H *vs.* PBS; mean diff=3.26%, P=0.0164; IW5-L *vs.* PBS; mean diff=3.04%, P=0.0149), CLNs (IW5-H *vs.* PBS; mean diff=11.019%, P<0.01; IW5-L *vs.* PBS; mean diff=10.385%, P<0.001) of the mice treated with IW5-H or IW5-L (**Figures 3A**, **S3A**). Whereas in the spleens, the percentage of $CD103^+$ DCs (IW5-H *vs.* PBS; mean diff=6.894%, P=0.0449) was increased only in the IW5-H-treated mice (**Figure 3A**). The expression of CD80, CD86, and MHCII on $CD11c^+$ DCs from the mice treated with IW5-H was lower than those of the cells from the mice treated with PBS (**Figure 3B**). $CD11c^+$ DCs were next isolated from the spleens of naïve mice and cultured in the presence of IW5 for 24 h, and the number of $CD103^+$ DCs and the concentration of IL-10 in the supernatant were increased significantly (**Figures S3B, C**). $CD11c^+$ DCs isolated from the MLNs of IW5-H treated mice were cocultured with naïve $CD4^+$ T cells isolated from naïve mice spleens for 5 days, and the number of Tregs (IW5-H *vs.* PBS; mean diff=0.878%, P=0.0289) was higher compared with those cocultured with $CD11c^+$ DCs from the PBS-treated mice (**Figure 3C**). Collectively, these results demonstrated that IW5 induced the expansion of DCregs *in vivo* and *in vitro*, which promoted the differentiation of Tregs.

IW5 Increased Gut Microbiota Diversity and SCFAs Production in AD Mouse Model

Next, we explored the effects of IW5 on the gut microbiota and their metabolites, SCFAs, in the mouse model with AD (30–33). Mice feces were collected before and after IW5 treatment in the MC903-induced AD model, and 16s rRNA was amplified and sequenced for analysis of the community structure and specific microbes of the gut microbiota. The result showed that the alpha diversity of the AD model mice was increased after oral administration with IW5, as indicated by the observed ASVs, chao1 index, and faith pd index (**Figure 4A**). Principal coordination (PCoA) analysis based on the ASV levels further demonstrated the changes in the microbial composition (**Figure S4A**). At the genus level, the abundance of *Bacteroides* was decreased and that of *Bifidobacterium* was increased in the AD model mice after oral IW5 administration (**Figure 4B**). Furthermore, the levels of acetate, propionate, and butyrate in the feces of the IW5-H-treated AD mice were significantly higher than those from the feces of the control AD mice. The levels of isobutyrate, valerate, isovalerate, and caproate had the same trend of increase but did not show statistical differences (**Figures 4C**, **S4B**), and there was no difference in serum level of SCFAs between IW5-treated mice and MC903 control mice (**Figure S4C**). These data demonstrated that IW5 restored the decreased diversity of the gut microbiota in the AD mice induced by MC903 application and increased the production of SCFAs.

Butyrate Induced the Production of DCregs *In Vitro*

The effects of butyrate on DCregs and Tregs were also explored. $CD11c^+$ DCs were isolated from the spleens of naive mice and were treated with 1mmol/L SCFA (acetate, propionate, or butyrate respectively) in culture for 24 h. The proportion of DCregs was significantly increased after butyrate treatment as shown by the result of flow cytometry analysis (**Figure 5A**). The proportion of $CD103^+$ DCs (Butyrate *vs.* PBS; mean diff=6.297%, P<0.001) and expression level of PD-L1 on $CD11c^+$ DCs in the presence of butyrate were higher than those of cells cultured in control medium, and the concentration of IL-10 in culture supernatant was also increased (**Figures 5B, C**). Whereas acetate and propionate didn't show any effects on $CD103^+$ DCs. These results indicated that butyrate was the key immuno-modulatory metabolite during IW5 treatment.

DISCUSSION

Extensive studies have proven that probiotics have potent immuno-modulatory effects and have been used in the

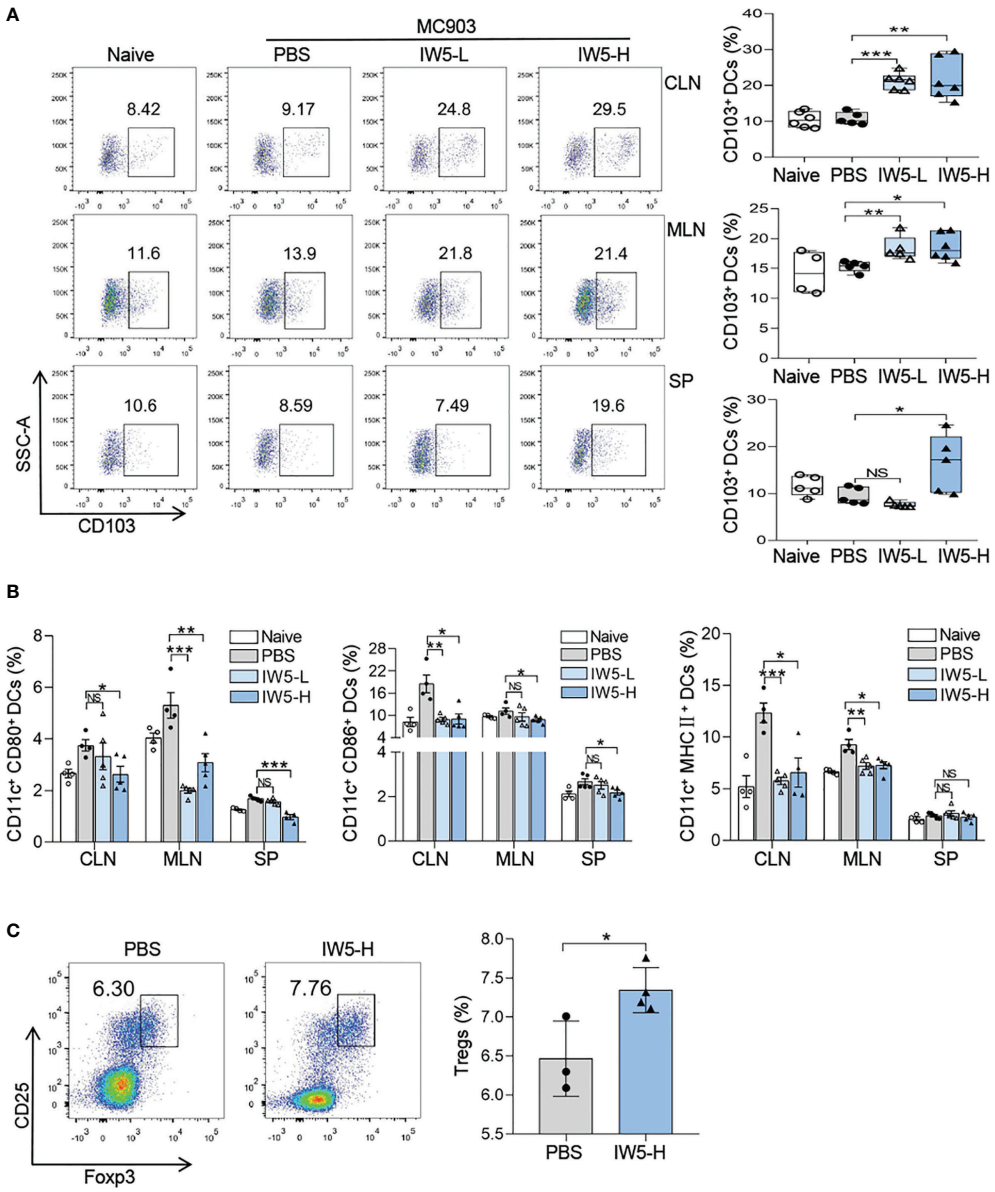

FIGURE 3 | IW5 promotes DCregs expansion and Tregs differentiation. **(A, B)** AD mice were orally administrated with IW5-L or IW5-H daily for 27 days, and the CLNs, MLNs, and spleens were collected on day 40 for further analysis. $CD103^+$ DCs ($CD11c^+$ $MHCII^+$ $CD103^+$) were examined by flow cytometry **(A)**. Expression levels of CD80, CD86, and MHCII on $CD11c^+$ DCs were examined by flow cytometry **(B)**. **(C)** BALB/c mice were orally administrated with IW5-H daily for 20 days. $CD11c^+$ DCs from the MLNs were co-cultured with $CD4^+$ T cells from naive mice spleens for 5 days. The proportion of $CD4^+$ $CD25^+$ $Foxp3^+$ Tregs was measured by flow cytometry. Data are shown as means ± SEMs, and representative of data from three independent experiments. Student's t-test (unpaired; n = 3~6); $^*P < 0.05$, $^{**}P < 0.01$, $^{***}P < 0.001$ *vs.* PBS group. NS, not significant.

prevention and treatment of many diseases (34); however, the role of probiotics in allergic diseases, such as AD, remains poorly understood. In the present study, we demonstrated that the probiotics mixture IW5 had significant therapeutic and preventive effects on a mouse model of AD-like dermatitis, by inducing DCregs and Tregs. We also found that oral IW5 administration increased the diversity of the gut microbiota in the AD model and induced the production of butyrate that promoted the differentiation of DCregs (**Figure 6**). Our study revealed the therapeutic effects of a newly designed probiotics mixture that play a regulatory role in skin inflammation.

We first assessed the effects of IW5, an innovative combination of probiotics, on the MC903-induced AD mouse model. We compared the effects of two concentrations of IW5 and found that the high-dose probiotics exerted more pronounced effects on skin inflammation (**Figures 1A, E**),

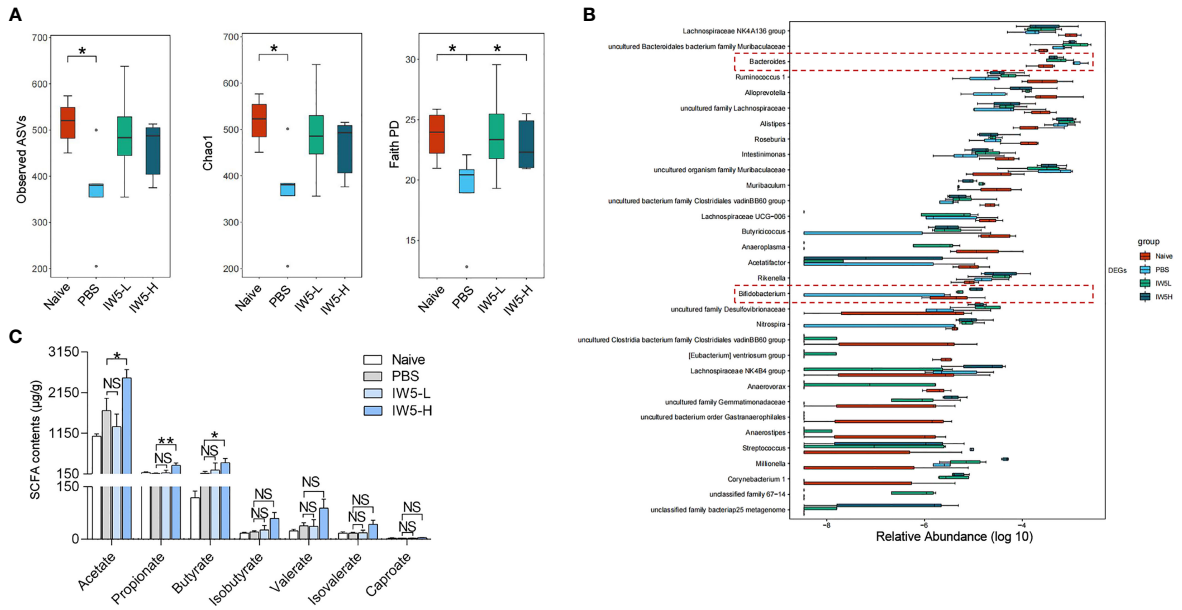

FIGURE 4 | IW5 modulates fecal microbiota composition and SCFAs production. Mice feces were collected from the MC903-induced AD model before and after IW5 treatment. **(A)** Alpha-diversity of the gut microbiota as indicated by the observed ASVs, chao1 index, and faith pd index. **(B)** Relative abundance of the gut microbiota at the genus level. **(C)** Contents of acetate, propionate, butyrate, isobutyrate, valerate, isovalerate, and caproate in fecal samples. Data are shown as means ± SEMs, and representative of data from three independent experiments. Student's t-test for parameters, and Mann-Whitney test for nonparametric data. (unpaired; n = 4~6); *P < 0.05, **P < 0.01 *vs.* PBS group. NS, not significant.

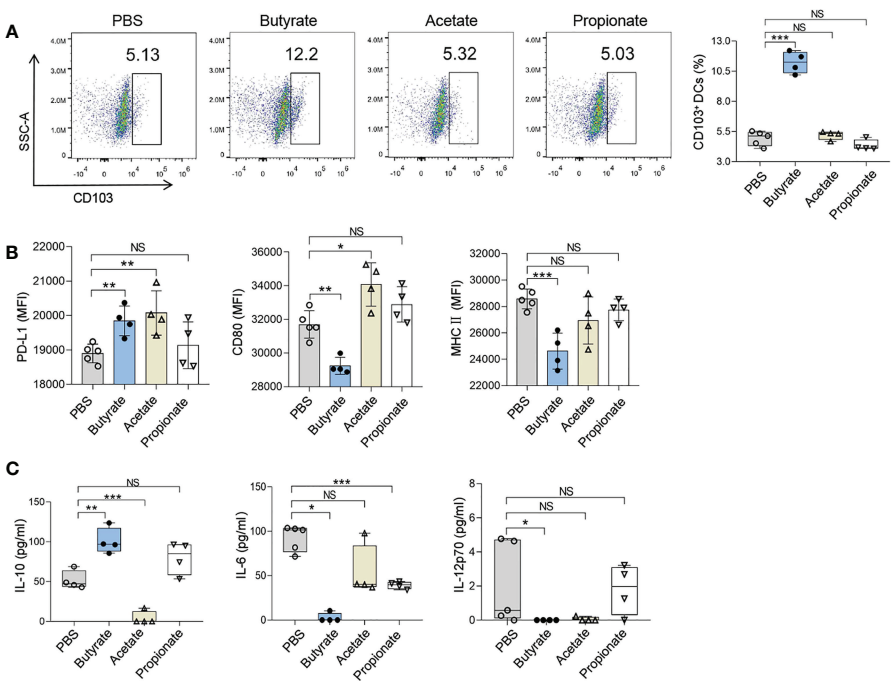

FIGURE 5 | Butyrate promotes the *ex vivo* induction of DCregs. $CD11c^+$ DCs from the spleen of naive mice were incubated with SCFAs for 24 h. **(A)** Numbers of $CD103^+$ DCs ($CD11c^+$ $MHCII^+$ $CD103^+$) were measured by flow cytometry. **(B)** MFIs of CD80, MHCII, or PD-L1 on $CD11c^+$ DCs were measured by flow cytometry. **(C)** Levels of IL-6, IL-10, and IL-12p70 in the supernatants of $CD11c^+$ DCs were measured by ELISA. Data are shown as means ± SEMs, and representative of data from three independent experiments. Student's t-test (unpaired; n = 4~5); *P < 0.05, **P < 0.01, ***P < 0.001 *vs.* PBS group. NS, not significant.

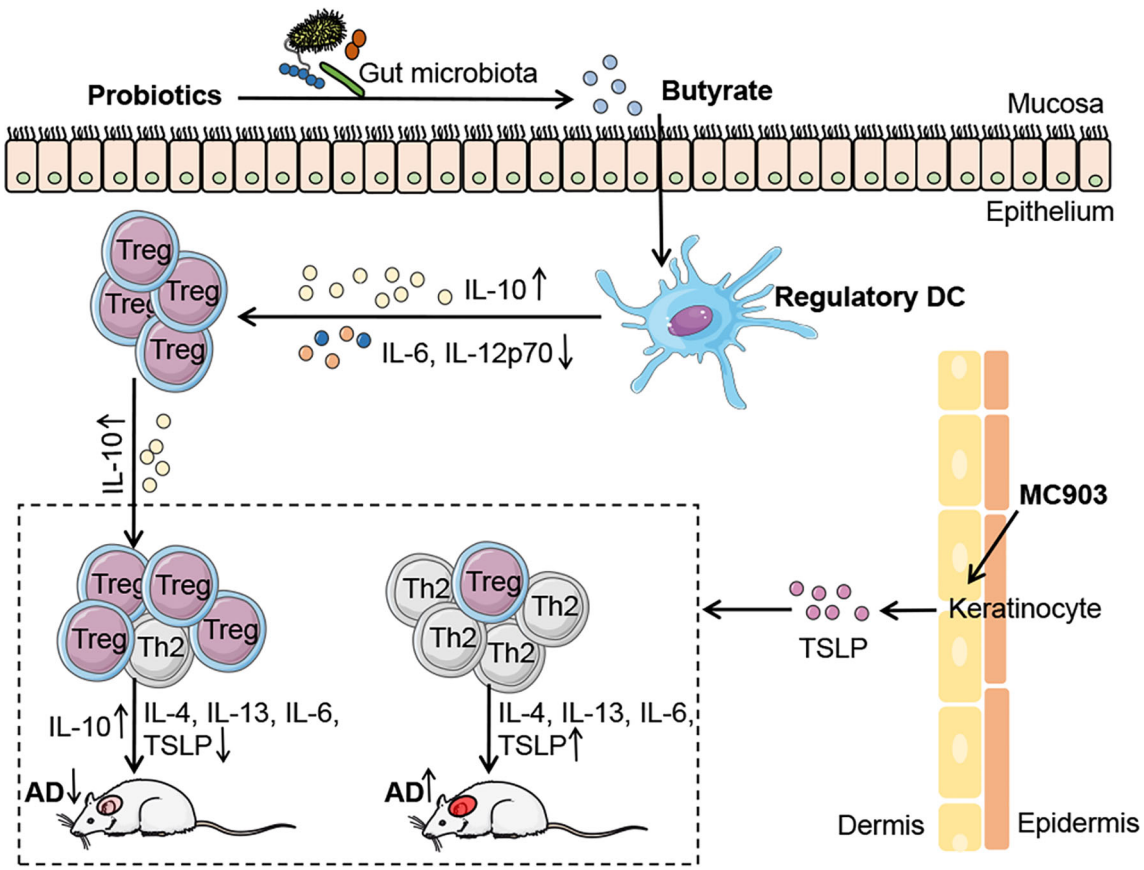

FIGURE 6 | | Schematic illustrating the underlying mechanism of probiotics in AD. IW5 administration restores the diversity of the gut microbiota in AD mouse models and increases the production of SCFAs (acetate, propionate, and butyrate). Butyrate induces DCregs production, which results in Tregs differentiation and amelioration of AD symptoms.

indicating that the effect of IW5 is dose-dependent. The most appropriate dose of probiotics still needs further exploration. A mixture of multiple strains of probiotics, instead of one probiotics strain, was used in our study, which might have advantages for the immuno-regulatory effects. Previous studies have demonstrated that multi-strain probiotics have optimal effects compared to single-strain probiotics (35). A mixture of selected strains of probiotics (IRT5) have shown more potent efficacy for disease control than single-strain probiotics (36). The enhanced benefits of multi-strain probiotics may be due to the complementary effects of constituent strains, additive and synergistic effects, and the cell-cell communication known as quorum sensing (37–40). The detailed mechanism of multiple strains of probiotics is still awaiting further exploration.

Probiotics have been reported to mitigate allergic diseases through the induction of Tregs, inhibition of Th2 immune responses, and promotion of intestinal DCregs expansion (2, 41, 42). Although innate immune responses play an important role in the MC903-induced AD-like dermatitis, in which TSLP and IL-33 produced by keratinocytes initiate the skin inflammation, adaptive immune cells are also required in the inflammation. Studies have demonstrated that the MC903-induced chronic inflammation is $CD4^+$ T cell-dependent (43), and Tregs are involved in the skin inflammation and play a regulatory role (44). Thus, Tregs might mediate the immuno-regulatory effects of DCregs in our study. DCregs, a type of semi-mature DCs, are the pivotal regulator of immune tolerance (45–47) and exhibit a tolerogenic phenotype that includes downregulation of co-stimulatory molecules (CD80, CD86) and upregulation of the immuno-modulatory molecule PD-L1 (48, 49). In recent years, $CD103^+$ DCs are considered the iconic mucosal DCregs, which have been shown to promote the differentiation of Tregs (50–52). We first found that IW5 administration promoted the production of DCregs *in vivo* and *in vitro* (**Figures 3A, B**, **S3B, C**), and *in vitro* co-culture experiment further showed that DCregs induced by IW5 promoted the induction of Tregs (**Figure 3C**). These results indicate that IW5 may alleviate AD symptoms *via* induction of DCregs and regulation of T cell immune responses, which resulted in an increased proportion of Tregs (**Figure 2B**) and decreased polarization of Th2 and Th1 cells (**Figure 2A**).

Previous studies have reported that the gut microbiota is closely related to allergic diseases (53). IW5 treatment modulated the structure of the gut microbiota, which might

account for the therapeutic effects of IW5 on the MC903-induced AD model (**Figures 4A, B**, **S4A**). The abundance of the genus *Bifidobacterium* was significantly decreased in the MC903-induced AD mouse model and was positively correlated with the Treg/Th2 ratio; while the genus *Bacteroides* was markedly increased in the AD model and was negatively correlated with the Treg/Th2 ratio. These changes were reversed by IW5 administration (**Figure 4B**). Our result is consistent with previous data highlighting the regulatory role of *Bifidobacterium* and *Bacteroides* in AD and (or) food allergy patients. For example, less colonized *Bifidobacteria* during the first year of life is associated with infants' allergic diseases (54); and the abundance of *Bifidobacterium* is an important determinant of Tregs maturation during early infancy (55). Conversely, some bacteria such as several strains of *Bacteroides* might increase the gut permeability and allergens exposure (56). The elevated relative abundance of *Bacteroides* species is also related to the non-IgE-mediated Cow's milk allergy, nut allergy, peanut allergy, or other atopic symptoms (57–60). Notably, IW5 administration did not increase all the components of IW5, but modified other bacteria of the gut microbiota, indicating an indirect effect of IW5 in the modulation of the gut microbiota.

SCFAs have strong immuno-regulatory effects in allergic diseases (2, 50, 61), and butyrate is one of the key immuno-regulatory metabolites for the differentiation of Tregs (31). We found that IW5 increased the production of SCFAs, including acetate, propionate, and butyrate (**Figure 4C**). *In vitro* co-culture experiment showed that butyrate increased the percentages of DCregs, whereas acetate and propionate did not have this effect (**Figures 5A, B**). These results suggest that IW5 might exert its effect *via* the induction of butyrate. Our *in vitro* study also showed that culture of IW5 with DCs resulted in increased number of DCregs, indicating that bacteria antigen might also induce the differentiation of DCregs (**Figure S3**), which is consistent with previous report that heat-killed probiotics induce $CD103^+$ DCs and attenuate inflammation (62, 63). As there is no difference in serum level of SCFAs between probiotics-treated mice and MC903 control mice (**Figure S4C**), it's probable that SCFAs might exert their effects in the gut, inducing the production of DCregs and Tregs, and the latter would migrate to other organs and tissue. Future work should pay more attention to the metabolites of the gut microbiota. Supplementing specific microbiota that produces beneficial metabolites and (or) developing drugs from metabolites would be a promising strategy for the regulation of local and (or) systemic inflammation.

DATA AVAILABILITY STATEMENT

The original contributions presented in the study are included in the article/**Supplementary Material**. The raw reads for 16S rRNA Sequencing were deposited in ENA under accession number PRJEB47618.

ETHICS STATEMENT

The animal study was reviewed and approved by the Animal Welfare Ethics Review Committee of the Institute of Dermatology, Chinese Academy of Medical Sciences.

AUTHOR CONTRIBUTIONS

BX and SL performed the experiments and analyzed the data. XX, XL, AW, YZ, and YL contributed to analysis the experimental work. BX, XY, and WL designed the experiments and wrote the manuscript. XY coordinated the research. All authors contributed to the article and approved the submitted version.

FUNDING

This work was supported by the Natural Science Foundation of China (82073446, 81972939, 81803144, 81703126), the Nanjing Incubation Program for National Clinical Research Centre (2019060001), the Key Project of Social Development in Jiangsu Province (BE2020632), the Medicine and Health Technology Innovation Project of Chinese Academy of Medical Sciences (2016-I2M-1-005), the Key Project of the Innovation Program of Shanghai Municipal Education Commission (2021-01-07-00-07-E00078), and the Milstein Medical Asian American Partnership Foundation (WL).

SUPPLEMENTARY MATERIAL

The Supplementary Material for this article can be found online at: https://www.frontiersin.org/articles/10.3389/fimmu.2021.775018/full#supplementary-material

REFERENCES

1. Weidinger S, Beck LA, Bieber T, Kabashima K, Irvine AD. Atopic Dermatitis. *Nat Rev Dis Primers* (2018) 4:1. doi: 10.1038/s41572-018-0001-z
2. Kang HJ, Kim GC, Lee CG, Park S, Sharma G, Verma R, et al. Probiotics-Derived Metabolite Ameliorates Skin Allergy by Promoting Differentiation of FOXP3(+) Regulatory T Cells. *J Allergy Clin Immunol* (2021) 147:1517–21. doi: 10.1016/j.jaci.2020.11.040
3. Schiavi E, Barletta B, Butteroni C, Corinti S, Boirivant M, Di Felice G. Oral Therapeutic Administration of a Probiotic Mixture Suppresses Established Th2 Responses and Systemic Anaphylaxis in a Murine Model of Food Allergy. *Allergy* (2011) 66:499–508. doi: 10.1111/j.1398-9995.2010.02501.x
4. Tan-Lim C, Esteban-Ipac N, Recto M, Castor M, Casis-Hao RJ, Nano A. Comparative Effectiveness of Probiotic Strains on the Prevention of Pediatric Atopic Dermatitis: A Systematic Review and Network Meta-Analysis. *Pediatr Allergy Immunol* (2021) 32:1255–70. doi: 10.1111/pai.13514
5. Jiang W, Ni B, Liu Z, Liu X, Xie W, Wu I, et al. The Role of Probiotics in the Prevention and Treatment of Atopic Dermatitis in Children: An Updated Systematic Review and Meta-Analysis of Randomized Controlled Trials. *Paediatr Drugs* (2020) 22:535–49. doi: 10.1007/s40272-020-00410-6

6. Li L, Han Z, Niu X, Zhang G, Jia Y, Zhang S, et al. Probiotic Supplementation for Prevention of Atopic Dermatitis in Infants and Children: A Systematic Review and Meta-Analysis. *Am J Clin Dermatol* (2019) 20:367–77. doi: 10.1007/s40257-018-0404-3
7. Chang YS, Trivedi MK, Jha A, Lin YF, Dimaano L, Garcia-Romero MT. Synbiotics for Prevention and Treatment of Atopic Dermatitis: A Meta-Analysis of Randomized Clinical Trials. *JAMA Pediatr* (2016) 170:236–42. doi: 10.1001/jamapediatrics.2015.3943
8. Kim SO, Ah YM, Yu YM, Choi KH, Shin WG, Lee JY. Effects of Probiotics for the Treatment of Atopic Dermatitis: A Meta-Analysis of Randomized Controlled Trials. *Ann Allergy Asthma Immunol* (2014) 113:217–26. doi: 10.1016/j.anai.2014.05.021
9. Panduru M, Panduru NM, Salavastru CM, Tiplica GS. Probiotics and Primary Prevention of Atopic Dermatitis: A Meta-Analysis of Randomized Controlled Studies. *J Eur Acad Dermatol Venereol* (2015) 29:232–42. doi: 10.1111/jdv.12496
10. Pelucchi C, Chatenoud L, Turati F, Galeone C, Moja L, Bach JF, et al. Probiotics Supplementation During Pregnancy or Infancy for the Prevention of Atopic Dermatitis: A Meta-Analysis. *Epidemiology* (2012) 23:402–14. doi: 10.1097/EDE.0b013e31824d5da2
11. Lee J, Seto D, Bielory L. Meta-Analysis of Clinical Trials of Probiotics for Prevention and Treatment of Pediatric Atopic Dermatitis. *J Allergy Clin Immunol* (2008) 121:116–21. doi: 10.1016/j.jaci.2007.10.043
12. Makrgeorgou A, Leonardi-Bee J, Bath-Hextall FJ, Murrell DF, Tang ML, Roberts A, et al. Probiotics for Treating Eczema. *Cochrane Database Syst Rev* (2018) 11:D6135. doi: 10.1002/14651858.CD006135.pub3
13. Boyle RJ, Bath-Hextall FJ, Leonardi-Bee J, Murrell DF, Tang ML. Probiotics for Treating Eczema. *Cochrane Database Syst Rev* (2008) 11:CD006135. doi: 10.1002/14651858.CD006135.pub2
14. Huang R, Ning H, Shen M, Li J, Zhang J, Chen X. Probiotics for the Treatment of Atopic Dermatitis in Children: A Systematic Review and Meta-Analysis of Randomized Controlled Trials. *Front Cell Infect Microbiol* (2017) 7:392. doi: 10.3389/fcimb.2017.00392
15. Verma R, Lee C, Jeun EJ, Yi J, Kim KS, Ghosh A, et al. Cell Surface Polysaccharides of Bifidobacterium Bifidum Induce the Generation of Foxp3(+) Regulatory T Cells. *Sci Immunol* (2018) 3:eaat6975. doi: 10.1126/sciimmunol.aat6975
16. Yang J, Ren F, Zhang H, Jiang L, Hao Y, Luo X. Induction of Regulatory Dendritic Cells by Lactobacillus Paracasei L9 Prevents Allergic Sensitization to Bovine Beta-Lactoglobulin in Mice. *J Microbiol Biotechnol* (2015) 25:1687–96. doi: 10.4014/jmb.1503.03022
17. Luu M, Visekruna A. Short-Chain Fatty Acids: Bacterial Messengers Modulating the Immunometabolism of T Cells. *Eur J Immunol* (2019) 49:842–8. doi: 10.1002/eji.201848009
18. Kim CH, Park J, Kim M. Gut Microbiota-Derived Short-Chain Fatty Acids, T Cells, and Inflammation. *Immune Netw* (2014) 14:277–88. doi: 10.4110/in.2014.14.6.277
19. Singh N, Gurav A, Sivaprakasam S, Brady E, Padia R, Shi H, et al. Activation of Gpr109a, Receptor for Niacin and the Commensal Metabolite Butyrate, Suppresses Colonic Inflammation and Carcinogenesis. *Immunity* (2014) 40:128–39. doi: 10.1016/j.immuni.2013.12.007
20. Song H, Yoo Y, Hwang J, Na YC, Kim HS. Faecalibacterium Prausnitzii Subspecies-Level Dysbiosis in the Human Gut Microbiome Underlying Atopic Dermatitis. *J Allergy Clin Immunol* (2016) 137:852–60. doi: 10.1016/j.jaci.2015.08.021
21. Gerasimov SV, Vasjuta VV, Myhovych OO, Bondarchuk LI. Probiotic Supplement Reduces Atopic Dermatitis in Preschool Children: A Randomized, Double-Blind, Placebo-Controlled, Clinical Trial. *Am J Clin Dermatol* (2010) 11:351–61. doi: 10.2165/11531420-000000000-00000
22. Cannarella L, Mari NL, Alcantara CC, Iryioda T, Costa NT, Oliveira SR, et al. Mixture of Probiotics Reduces Inflammatory Biomarkers and Improves the Oxidative/Nitrosative Profile in People With Rheumatoid Arthritis. *Nutrition* (2021) 89:111282. doi: 10.1016/j.nut.2021.111282
23. De Andres J, Manzano S, Garcia C, Rodriguez JM, Espinosa-Martos I, Jimenez E. Modulatory Effect of Three Probiotic Strains on Infants' Gut Microbial Composition and Immunological Parameters on a Placebo-Controlled, Double-Blind, Randomised Study. *Benef Microbes* (2018) 9:573–84. doi: 10.1186/cc10540
24. Chaves BD, Brashears MM, Nightingale KK. Applications and Safety Considerations of Lactobacillus Salivarius as a Probiotic in Animal and Human Health. *J Appl Microbiol* (2017) 123:18–28. doi: 10.1111/jam.13438
25. Holowacz S, Blondeau C, Guinobert I, Guilbot A, Hidalgo S, Bisson JF. Lactobacillus Salivarius LA307 and Lactobacillus Rhamnosus LA305 Attenuate Skin Inflammation in Mice. *Benef Microbes* (2018) 9:299–309. doi: 10.3920/BM2017.0084
26. Zhang Y, Wu T, Li W, Zhao Y, Long H, Liu R, et al. Lactobacillus Casei LC89 Exerts Antidiabetic Effects Through Regulating Hepatic Glucagon Response and Gut Microbiota in Type 2 Diabetic Mice. *Food Funct* (2021) 12:8288–99. doi: 10.1039/d1fo00882j
27. Yu J, Luo Y, Zhu Z, Zhou Y, Sun L, Gao J, et al. A Tryptophan Metabolite of the Skin Microbiota Attenuates Inflammation in Patients With Atopic Dermatitis Through the Aryl Hydrocarbon Receptor. *J Allergy Clin Immunol* (2019) 143:2108–19. doi: 10.1016/j.jaci.2018.11.036
28. Godon JJ, Zumstein E, Dabert P, Habouzit F, Moletta R. Molecular Microbial Diversity of an Anaerobic Digestor as Determined by Small-Subunit rDNA Sequence Analysis. *Appl Environ Microbiol* (1997) 63:2802–13. doi: 10.1128/AEM.63.7.2802-2813.1997
29. Coombes JL, Siddiqui KR, Arancibia-Carcamo CV, Hall J, Sun CM, Belkaid Y, et al. A Functionally Specialized Population of Mucosal CD103+ DCs Induces Foxp3+ Regulatory T Cells via a TGF-Beta and Retinoic Acid-Dependent Mechanism. *J Exp Med* (2007) 204:1757–64. doi: 10.1084/jem.20070590
30. Arpaia N, Campbell C, Fan X, Dikiy S, van der Veeken J, DeRoos P, et al. Metabolites Produced by Commensal Bacteria Promote Peripheral Regulatory T-Cell Generation. *Nature* (2013) 504:451–5. doi: 10.1038/nature12726
31. Furusawa Y, Obata Y, Fukuda S, Endo TA, Nakato G, Takahashi D, et al. Commensal Microbe-Derived Butyrate Induces the Differentiation of Colonic Regulatory T Cells. *Nature* (2013) 504:446–50. doi: 10.1038/nature12721
32. Smith PM, Howitt MR, Panikov N, Michaud M, Gallini CA, Bohlooly-Y M, et al. The Microbial Metabolites, Short-Chain Fatty Acids, Regulate Colonic Treg Cell Homeostasis. *Science* (2013) 341:569–73. doi: 10.1126/science.1241165
33. Koh A, De Vadder F, Kovatcheva-Datchary P, Backhed F. From Dietary Fiber to Host Physiology: Short-Chain Fatty Acids as Key Bacterial Metabolites. *Cell* (2016) 165:1332–45. doi: 10.1016/j.cell.2016.05.041
34. Sniffen JC, McFarland LV, Evans CT, Goldstein E. Choosing an Appropriate Probiotic Product for Your Patient: An Evidence-Based Practical Guide. *PloS One* (2018) 13:e209205. doi: 10.1371/journal.pone.0209205
35. Timmerman HM, Koning CJ, Mulder L, Rombouts FM, Beynen AC. Monostrain, Multistrain and Multispecies Probiotics–A Comparison of Functionality and Efficacy. *Int J Food Microbiol* (2004) 96:219–33. doi: 10.1016/j.ijfoodmicro.2004.05.012
36. Kwon HK, Lee CG, So JS, Chae CS, Hwang JS, Sahoo A, et al. Generation of Regulatory Dendritic Cells and CD4+Foxp3+ T Cells by Probiotics Administration Suppresses Immune Disorders. *Proc Natl Acad Sci USA* (2010) 107:2159–64. doi: 10.1073/pnas.0904055107
37. Chapman CM, Gibson GR, Todd S, Rowland I. Comparative *In Vitro* Inhibition of Urinary Tract Pathogens by Single- and Multi-Strain Probiotics. *Eur J Nutr* (2013) 52:1669–77. doi: 10.1007/s00394-013-0501-2
38. Adamberg S, Sumeri I, Uusna R, Ambalam P, Kondepudi KK, Adamberg K, et al. Survival and Synergistic Growth of Mixed Cultures of Bifidobacteria and Lactobacilli Combined With Prebiotic Oligosaccharides in a Gastrointestinal Tract Simulator. *Microb Ecol Health Dis* (2014) 25. doi: 10.3402/mehd.v25.23062
39. Di Cagno R, De Angelis M, Limitone A, Minervini F, Simonetti MC, Buchin S, et al. Cell-Cell Communication in Sourdough Lactic Acid Bacteria: A Proteomic Study in Lactobacillus Sanfranciscensis CB1. *Proteomics* (2007) 7:2430–46. doi: 10.1002/pmic.200700143
40. Di Cagno R, De Angelis M, Coda R, Minervini F, Gobbetti M. Molecular Adaptation of Sourdough Lactobacillus Plantarum DC400 Under Co-Cultivation With Other Lactobacilli. *Res Microbiol* (2009) 160:358–66. doi: 10.1016/j.resmic.2009.04.006
41. Kwon MS, Lim SK, Jang JY, Lee J, Park HK, Kim N, et al. Lactobacillus Sakei WIKIM30 Ameliorates Atopic Dermatitis-Like Skin Lesions by Inducing Regulatory T Cells and Altering Gut Microbiota Structure in Mice. *Front Immunol* (2018) 9:1905. doi: 10.3389/fimmu.2018.01905
42. Song J, Lim HX, Lee A, Kim S, Lee JH, Kim TS. Staphylococcus Succinus 14BME20 Prevents Allergic Airway Inflammation by Induction of Regulatory T Cells *via* Interleukin-10. *Front Immunol* (2019) 10:1269. doi: 10.3389/fimmu.2019.01269

43. Kitajima M, Kubo M, Ziegler SF, Suzuki H. Critical Role of TSLP Receptor on CD4 T Cells for Exacerbation of Skin Inflammation. *J Immunol* (2020) 205:27–35. doi: 10.4049/jimmunol.1900758
44. Xue Q, Li X, Li Y, Xu J, Wu Z, Wang J. Dialogue Between Gastrointestinal Tract and Skin: New Insights Into the Helicobacter Pylori and Atopic Dermatitis. *Helicobacter* (2021) 26:e12771. doi: 10.1111/hel.12771
45. Wu J, Liu M, Mang G, Yu S, Chen Q, Li T, et al. Protosappanin A Protects Against Experimental Autoimmune Myocarditis, and Induces Metabolically Reprogrammed Tolerogenic DCs. *Pharmacol Res* (2019) 146:104269. doi: 10.1016/j.phrs.2019.104269
46. Griffin GK, Lichtman AH. Two Sides to Every Proinflammatory Coin: New Insights Into the Role of Dendritic Cells in the Regulation of T-Cell Driven Autoimmune Myocarditis. *Circulation* (2013) 127:2257–60. doi: 10.1161/CIRCULATIONAHA.113.003261
47. Steinman RM. Decisions About Dendritic Cells: Past, Present, and Future. *Annu Rev Immunol* (2012) 30:1–22. doi: 10.1146/annurev-immunol-100311-102839
48. Torres-Aguilar H, Aguilar-Ruiz SR, Gonzalez-Perez G, Munguia R, Bajana S, Meraz-Rios MA, et al. Tolerogenic Dendritic Cells Generated With Different Immunosuppressive Cytokines Induce Antigen-Specific Anergy and Regulatory Properties in Memory CD4+ T Cells. *J Immunol* (2010) 184:1765–75. doi: 10.4049/jimmunol.0902133
49. Jansen M, Spiering R, Ludwig IS, van Eden W, Hilkens C, Broere F. Matured Tolerogenic Dendritic Cells Effectively Inhibit Autoantigen Specific CD4(+) T Cells in a Murine Arthritis Model. *Front Immunol* (2019) 10:2068. doi: 10.3389/fimmu.2019.02068
50. Hall JA, Grainger JR, Spencer SP, Belkaid Y. The Role of Retinoic Acid in Tolerance and Immunity. *Immunity* (2011) 35:13–22. doi: 10.1016/j.immuni.2011.07.002
51. Pabst O, Mowat AM. Oral Tolerance to Food Protein. *Mucosal Immunol* (2012) 5:232–9. doi: 10.1038/mi.2012.4
52. Tan J, McKenzie C, Vuillermin PJ, Goverse G, Vinuesa CG, Mebius RE, et al. Dietary Fiber and Bacterial SCFA Enhance Oral Tolerance and Protect Against Food Allergy Through Diverse Cellular Pathways. *Cell Rep* (2016) 15:2809–24. doi: 10.1016/j.celrep.2016.05.047
53. Kirjavainen PV, Apostolou E, Salminen SJ, Isolauri E. New Aspects of Probiotics–a Novel Approach in the Management of Food Allergy. *Allergy* (1999) 54:909–15. doi: 10.1034/j.1398-9995.1999.00103.x
54. Bjorksten B, Sepp E, Julge K, Voor T, Mikelsaar M. Allergy Development and the Intestinal Microflora During the First Year of Life. *J Allergy Clin Immunol* (2001) 108:516–20. doi: 10.1067/mai.2001.118130
55. Ruohtula T, de Goffau MC, Nieminen JK, Honkanen J, Siljander H, Hamalainen AM, et al. Maturation of Gut Microbiota and Circulating Regulatory T Cells and Development of IgE Sensitization in Early Life. *Front Immunol* (2019) 10:2494. doi: 10.3389/fimmu.2019.02494
56. Curtis MM, Hu Z, Klimko C, Narayanan S, Deberardinis R, Sperandio V. The Gut Commensal Bacteroides Thetaiotaomicron Exacerbates Enteric Infection Through Modification of the Metabolic Landscape. *Cell Host Microbe* (2014) 16:759–69. doi: 10.1016/j.chom.2014.11.005
57. Hua X, Goedert JJ, Pu A, Yu G, Shi J. Allergy Associations With the Adult Fecal Microbiota: Analysis of the American Gut Project. *EBiomedicine* (2016) 3:172–9. doi: 10.1016/j.ebiom.2015.11.038
58. Odamaki T, Xiao JZ, Sakamoto M, Kondo S, Yaeshima T, Iwatsuki K, et al. Distribution of Different Species of the Bacteroides Fragilis Group in Individuals With Japanese Cedar Pollinosis. *Appl Environ Microbiol* (2008) 74:6814–7. doi: 10.1128/AEM.01106-08
59. Kirjavainen PV, Arvola T, Salminen SJ, Isolauri E. Aberrant Composition of Gut Microbiota of Allergic Infants: A Target of Bifidobacterial Therapy at Weaning? *Gut* (2002) 51:51–5. doi: 10.1136/gut.51.1.51
60. Berni CR, De Filippis F, Nocerino R, Paparo L, Di Scala C, Cosenza L, et al. Gut Microbiota Composition and Butyrate Production in Children Affected by non-IgE-Mediated Cow's Milk Allergy. *Sci Rep* (2018) 8:12500. doi: 10.1038/s41598-018-30428-3
61. Roduit C, Frei R, Ferstl R, Loeliger S, Westermann P, Rhyner C, et al. High Levels of Butyrate and Propionate in Early Life are Associated With Protection Against Atopy. *Allergy* (2019) 74:799–809. doi: 10.1111/all.13660
62. Jia H, Ren S, Wang X. Heat-Killed Probiotic Regulates the Body's Regulatory Immunity to Attenuate Subsequent Experimental Autoimmune Arthritis. *Immunol Lett* (2019) 216:89–96. doi: 10.1016/j.imlet.2019.10.009
63. Zelaya H, Tada A, Vizoso-Pinto MG, Salva S, Kanmani P, Aguero G, et al. Nasal Priming With Immunobiotic Lactobacillus Rhamnosus Modulates Inflammation-Coagulation Interactions and Reduces Influenza Virus-Associated Pulmonary Damage. *Inflamm Res* (2015) 64:589–602. doi: 10.1007/s00011-015-0837-6

Conflict of Interest: Author XX is employed by 01life Institute.

The remaining authors declare that the research was conducted in the absence of any commercial or financial relationships that could be construed as a potential conflict of interest.

Publisher's Note: All claims expressed in this article are solely those of the authors and do not necessarily represent those of their affiliated organizations, or those of the publisher, the editors and the reviewers. Any product that may be evaluated in this article, or claim that may be made by its manufacturer, is not guaranteed or endorsed by the publisher.

Copyright © 2021 Xu, Ling, Xu, Liu, Wang, Zhou, Luo, Li and Yao. This is an open-access article distributed under the terms of the Creative Commons Attribution License (CC BY). The use, distribution or reproduction in other forums is permitted, provided the original author(s) and the copyright owner(s) are credited and that the original publication in this journal is cited, in accordance with accepted academic practice. No use, distribution or reproduction is permitted which does not comply with these terms.

frontiers in Immunology

ORIGINAL RESEARCH
published: 17 November 2021
doi: 10.3389/fimmu.2021.765528

Potential Association Between Dietary Fibre and Humoral Response to the Seasonal Influenza Vaccine

Alissa Cait[1], Anna Mooney[1,2‡], Hazel Poyntz[1,2‡], Nick Shortt[2,3‡], Angela Jones[1,2], Aurélie Gestin[1,2], Katie Gell[1], Alix Grooby[1], David O'Sullivan[1,2], Jeffry S. Tang[1,2], Wayne Young[2,4], Darmiga Thayabaran[2,3], Jenny Sparks[2,3], Tess Ostapowicz[2,3], Audrey Tay[2,5], Sally D. Poppitt[2,5], Sarah Elliott[2,6], Georgia Wakefield[2,6], Amber Parry-Strong[2,7], Jacqui Ralston[8], Richard Beasley[2,3], Mark Weatherall[9], Irene Braithwaite[2,3], Elizabeth Forbes-Blom[1,2†] and Olivier Gasser[1,2]**

[1] Malaghan Institute of Medical Research, Wellington, New Zealand, [2] High-Value Nutrition National Science Challenge, Auckland, New Zealand, [3] Medical Research Institute of New Zealand, Wellington, New Zealand, [4] AgResearch, Palmerston North, New Zealand, [5] Human Nutrition Unit, Department of Medicine, School of Biological Sciences, University of Auckland, Auckland, New Zealand, [6] Food Savvy, Wellington, New Zealand, [7] Center for Endocrine, Diabetes and Obesity Research Capital & Coast District Health Board (CCDHB), Wellington, New Zealand, [8] Institute of Environmental Science and Research Limited (ESR), National Centre for Biosecurity and Infectious Disease (NCBID), Upper Hutt, New Zealand, [9] Wellington School of Medicine, University of Otago, Wellington, New Zealand

Influenza vaccination is an effective public health measure to reduce the risk of influenza illness, particularly when the vaccine is well matched to circulating strains. Notwithstanding, the efficacy of influenza vaccination varies greatly among vaccinees due to largely unknown immunological determinants, thereby dampening population-wide protection. Here, we report that dietary fibre may play a significant role in humoral vaccine responses. We found dietary fibre intake and the abundance of fibre-fermenting intestinal bacteria to be positively correlated with humoral influenza vaccine-specific immune responses in human vaccinees, albeit without reaching statistical significance. Importantly, this correlation was largely driven by first-time vaccinees; prior influenza vaccination negatively correlated with vaccine immunogenicity. In support of these observations, dietary fibre consumption significantly enhanced humoral influenza vaccine responses in mice, where the effect was mechanistically linked to short-chain fatty acids, the bacterial fermentation product of dietary fibre. Overall, these findings may bear significant importance for emerging infectious agents, such as COVID-19, and associated *de novo* vaccinations.

Keywords: fibre, microbiome, influenza, vaccine, short chain fatty acids (SCFA)

OPEN ACCESS

Edited by:
Tobias R. Kollmann, University of Western Australia, Australia

Reviewed by:
David John Lynn, Flinders University, Australia
Bahaa Abu Raya, Children's & Women's Health Centre of British Columbia, Canada

****Correspondence:***
Olivier Gasser
ogasser@malaghan.org.nz
Alissa Cait
acait@malaghan.org.nz

†Present address:
Elizabeth Forbes-Blom, Department of Gastrointestinal Health, Nestlé Institute of Health Sciences, Nestle Research Lausanne, Lausanne, Switzerland

‡These authors have contributed equally to this work

Specialty section:
Received: *27 August 2021*
Accepted: *20 October 2021*
Published: *17 November 2021*

Citation:
Cait A, Mooney A, Poyntz H, Shortt N, Jones A, Gestin A, Gell K, Grooby A, O'Sullivan D, Tang JS, Young W, Thayabaran D, Sparks J, Ostapowicz T, Tay A, Poppitt SD, Elliott S, Wakefield G, Parry-Strong A, Ralston J, Beasley R, Weatherall M, Braithwaite I, Forbes-Blom E and Gasser O (2021) Potential Association Between Dietary Fibre and Humoral Response to the Seasonal Influenza Vaccine. Front. Immunol. 12:765528. doi: 10.3389/fimmu.2021.765528

INTRODUCTION

Vaccination is our best defence against severe illness and death caused by influenza viruses. However, immune responses to seasonal influenza vaccinations vary substantially in efficacy across the general population, leaving some individuals susceptible to infection each season, even after being vaccinated. The reason for this variation is mostly unknown.

The microbiota has been increasingly investigated in this context and found to contribute to the inter-individual variance in vaccine responses in mice and humans (1). There are now several lines of evidence that demonstrate a relationship between the gut microbiota and protective antibody responses during vaccination (2). Compelling animal studies have shown that a disrupted microbiome will impair vaccine-induced antibody responses (3–6). Despite this growing body of work, our understanding of whether the microbiome impacts these same immunological processes in humans is surprisingly under-studied. Only a limited number of clinical studies demonstrate correlations between microbiome features and impaired antibody responses (7–10), but mechanistic data is lacking.

Diet plays a substantial role in determining the composition of our microbiome and long-term dietary habits represent one of the most dominant environmental factors that influence gut microbiome composition (11). However, the potential links between dietary patterns of free-living, non-malnourished humans and vaccine responses have not yet been addressed or described. Of particular relevance in this context are dietary components that cannot be digested by the host, but are readily metabolized by resident microbes to support the symbiotic relationship between host and microbes (12, 13) – most importantly the microbial fibre fermentation products, short chain fatty acids (SCFAs) (14). The SCFAs with highest concentration in the healthy human gut are acetate (C2), propionate (C3), and butyrate (C4) (15). The relationship between dietary fibre, SCFAs, and antibody responses has been previously demonstrated to activate B cell metabolism and promote protective antibody responses during infection in a mouse model of *Citrobacter rodentium* infection (5). Whether dietary fibre similarly influences antibody responses in humans is currently unknown.

To understand the role of diet and the microbiome on antibody responses to the 2016 Trivalent Influenza Vaccine (TIV), Influvac® (Mylan, Illinois, USA) we previously performed and reported on a 6-month observational study on New Zealand adults who received TIV, collecting data on gut microbiota composition, diet, and humoral vaccine response (16) (Australia and New Zealand Clinical Trials Registry number ACTRN1261500 1365550). Here, after conducting *ad hoc* analyses to assess the impact of dietary fibre intake on TIV-specific humoral immune responses, we identify a correlation between fibre consumption and vaccine responses in individuals who are naïve to previous influenza vaccination. The observed correlation did however not reach statistical significance. Furthermore, in a corresponding animal model of TIV vaccination, we demonstrate that fibre consumption or supplementation with SCFAs can mediate a comparable immunological outcome, indicating that fibre consumption and subsequent production of microbially derived SCFAs can improve TIV-specific humoral immune responses. Taken together, these findings reveal an unappreciated role for a diet rich in fibre in inducing a robust antibody response to seasonal influenza vaccine.

METHODS

Clinical Study Design

122 healthy participants aged 18-64 received the 2016 trivalent influenza vaccine (TIV) as part of this study. Detailed study characteristics are described elsewhere (16). All participants who completed the study were included in our analysis, unless otherwise stated. Exclusion criteria included: *i.* a known severe reaction or allergy to any components of the influenza vaccine. *ii.* Any contraindications to vaccination per recommendations of the vaccine manufacturer. *iii.* A history of Guillain-Barre Syndrome within six weeks of receiving a previous influenza vaccine. *iv.* Any immune impairment that could confound immune testing. *v.* Already having received the 2016 seasonal influenza vaccine.

Fecal Samples

Stool samples were collected by participants using the OMNIgene GUT collection kit (DNA Genotek, Ontario, Canada). Samples were collected by participants in the three-day period prior to both Day Zero and Day 28. For microbiota profiling, DNA was extracted from faecal samples using the Nucleospin Soil kit (Macherey-Nagel (Duren, Germany) following the manufacturer's instructions. Briefly, 500 mg fecal sample was suspended in lysis buffer and mechanically disrupted using ceramic beads. Proteins and PCR inhibitors were then pelleted with the ceramic beads and the supernatant adjusted to DNA-binding conditions before being passed over Nucleospin soil column to bind the DNA. Residual substances were then removed by efficient washing. Finally, the DNA was eluted in 100 µl of RNAse-free water. DNA yield was assessed using the Quantus™ fluorometer (Promega, Madison, WA, USA) and DNA quality measured with the Nanodrop ND-1000 spectrophotometer (Thermofisher, Waltham, MA, USA). Amplification of the V1-V3 region of the 16S rRNA gene followed by 2 X 250 bp sequencing on the MiSeq platform was performed at NZ Genomics Ltd (NZGL) using the standard Illumina method (https://www.illumina.com/content/dam/illumina-support/documents/documentation/chemistry_documentation/16s/16s-metagenomic-library-prep-guide-15044223-b.pdf).

Microbiome Data Processing

Sequence data was trimmed, quality filtered, and clustered at 97% identity into Operational Taxonomic Units (OTUs) following the mothur SOP pipeline (17). Representative OTU sequences were assigned taxonomic classification using a Bayesian classifier against the Ribosomal database project (RDP) database (18). This generated an average of 50380.98 reads per sample, median 49514 reads (**Supplementary Figure 1**), clustered into 148038 OTUs. Before filtering, alpha diversity (Shannon measure) was calculated and plotted using Phyloseq. Data was transformed to a relative abundance [x/sum (x)] and filtered in Phyloseq to remove OTUs unclassified beyond the kingdom bacteria and OTUs that did not occur 2 or more times in 10% or more of samples, reducing the number of OTUs to 471. Data was further analysed in R using custom scripts and plotted using ggplot2 (19).

Microbiome qPCR

Bacterial DNA was extracted from faecal samples using QIAamp Fast DNA Stool Mini Kit according to the manufacturer's instructions. DNA concentration and purity was measured on a ND-1000 Nanodrop spectrophotometer (Thermofisher Scientific). Samples were stored at -20°C until required.

Proportions of dominant bacteria in the faeces were determined by quantitative PCR as previously described (20). A qPCR reaction mix was prepared by combining per reaction; 10 µL SYBR green PCR master mix, 1 µL each of forward and reverse primers (**Supplementary Table 1**) and 6 µL of DPEC-treated H2O. To each well of an optical 96-well reaction plate with barcode, 18 µL of prepared qPCR reaction mix and 2 µL of the DNA sample (standardised to 1 ng/µL) were added. The plate was covered with an optical adhesive film and centrifuged for approximately 30 seconds at 500 x g. All samples were run in duplicate and each plate included an H2O sample as a negative control. qPCR was run on a QuantStudio 7 Flex PCR system (Thermofisher Scientific) using the standard instrument settings for fast TaqMan 96-well plate assay.

Food Diaries

Self-reported dietary intake was assessed using a 7-day food diary. Participants recorded all meals and snacks consumed throughout 7 consecutive days, including beverages. Food diaries were analysed using the dietary software FoodWorks 7 (Xyris Software, Australia) at the Human Nutrition Unit of the University of Auckland, New Zealand. RCT design adherence was considered to be a reported daily energy intake of >1.2 x basal metabolic rate (BMR), using Schofield predicted BMR (21) based on gender, age, height and body weight of each participant at baseline.

Vaccine History

Vaccine history was collected in the form of a questionnaire. Participants self-reported if they had received the seasonal influenza in 2015, 2014, 2013, 2012, 2011 *or earlier.*

Hemagglutination Inhibition Assays

Influenza-specific antibody titres in serum were quantified using the HAI assay. Serum was separated from whole blood samples by centrifugation then stored at -70°C until use. HAI assays were performed for each influenza strain by the Institute of Environmental Science and Research Ltd, based at the National Centre for Biosecurity & Infectious Disease Upper Hutt, New Zealand. Briefly, serum samples were treated with receptor destroying enzyme and heat inactivated to remove nonspecific agglutinins. The samples were titrated out twofold, in duplicate, across a microtitre plate from 1:10 to 1:10240; then, four haemagglutinating units of the appropriate antigen were added. After a 30-min incubation step, 1% Guinea pig red blood cells (RBC) were added to all wells, including serum controls and test controls and were allowed to settle for an hour. Plates were read manually and titre endpoints determined as the last well where RBC agglutination was inhibited. Results were accepted if all controls (Serum and Antigen) gave expected results.

Participants were characterised into responder categories as follows: low responder if they had a <4 fold change for H1 and H3; medium responder if they had a ≥4 fold change for one strain and <4 fold change for the other strain; high responder if they had a ≥4 fold change for both H1 and H3.

Neuraminidase Inhibition Assays

Influenza-specific antibody NAI titres in serum were quantified using the Enzyme-Linked Lectin assay. Serum was separated from whole blood samples by centrifugation then stored at -70°C until use. Enzyme linked lectin assays were performed for each influenza strain by the Institute of Environmental Science and Research Ltd, based at the National Centre for Biosecurity & Infectious Disease Upper Hutt, New Zealand. Briefly, serum samples were heat inactivated at 56°C for one hour then titrated out twofold, in duplicate, across a microtitre dilution plate, from 1:10 to 1:5120. Titrated samples were transferred to a fetuin-coated test plate, including controls, and a standard amount of antigen added. After overnight incubation, peroxidase conjugated peptide nucleic acid was added to the washed plates followed by steps in which colour was developed. Plates were read on a BioTek plate reader. The reduction or absence of colour indicated inhibition of NAI activity due to the presence of NA-specific antibodies.

Mice

C57BL/6J mice were bred and maintained in the specific pathogen-free Biomedical Research Unit at the Malaghan Institute of Medical Research (Wellington, New Zealand). Mice were housed in autoclaved cages under specific pathogen free conditions. Mice were age and sex matched. Mice were used for experiments from 6-12 weeks of age. Both male and female mice were used. The Victoria University Animal Ethics Committee granted ethical approval for experimental animal procedures and all experiments were carried out in accordance with their guidelines. At experimental end points mice were humanely killed by CO_2 inhalation followed by cardiac puncture.

Mouse Diets

As indicated, breeding pairs and nursing dams were administered a zero-fibre diet (SF09-028, Specialty Feeds, Glen Forrest, Australia) or high fibre diet (7.5% Inulin, 7.5% Pectin SF15-086, Specialty Feeds). Pups born from respective breeding pairs were reared on this special diet for the duration of the experiment. All foods were autoclaved or irradiated prior to feeding for sterility.

Unless otherwise stated, mice were maintained on a meat-free rat and mouse standard diet. Other than the specified dietary alterations, paired diets in each experiment were designed to be otherwise nutritionally equivalent. Mice were administered foods *ad libitum* for the duration specified in each experiment.

Broad-Spectrum Antibiotic Cocktail Administration to Mice

The broad-spectrum antibiotic cocktail (ABX) consisted of vancomycin at 0.5 mg/mL, neomycin at 1 mg/mL, ampicillin

at 1 mg/mL and metronidazole at 1 mg/mL, dissolved in purified, acidified drinking water. This was administered to mice *ad libitum* for 14 days prior to TIV vaccination. Splenda artificial sweetener (4 mg/mL) and Hansell's strawberry essence (2 µL/mL) were added to improve palatability of the solution. Splenda and Hansell's strawberry essence were also added to the control water.

Short-Chain Fatty Acid Administration to Mice

Solutions of single SCFAs were prepared by adding 200 mM of sodium acetate, sodium butyrate or sodium propionate (Sigma-Aldrich, St Louis, MO) to autoclaved drinking water, at a concentration of 200mM and administered to mice *ad libitum* for 21 days prior to vaccination and throughout the remainder of the experiment. A mixed SCFA solution was prepared by adding sodium acetate (70 mM), sodium butyrate (20 mM) and sodium propionate (30 mM), to autoclaved acidified water and was administered to mice *ad libitum* for 14 days prior to initial vaccination and throughout the remainder of the experiment.

Trivalent Influenza Vaccine Administration to Mice

Influvac® 2016 inactivated TIV vaccine was diluted 1:4 in sterile PBS and 200 µL was administered subcutaneously (SC) at the tail base between the dorsal and right lateral vein, with mice receiving 1/10 of the full human dose of 500 µL. Mice received this dose on day 0, 7, and 14. Mice were sacrificed on D21 to evaluate antibody responses.

Serum TIV Enzyme Linked Immunosorbent Assays

Levels of TIV-specific IgG antibody in mouse serum were determined by ELISA. Briefly, each well of a 96 well Nunc Maxisorb plates was coated with 100 µL of Influvac® diluted to 25 µL/mL in Phosphate Buffered Saline (PBS) and incubated overnight at 4°C. Non-specific protein binding was blocked with the addition of 150 µL of 10% fetal bovine serum in PBS and incubated for 2 hours at room temperature. Serum samples were serially diluted in 10% FBS in PBS and 100 µL was added to each well. The plates were then incubated for 2 hours at RT. HRP-conjugated anti-mouse IgG secondary antibody were diluted in 10% FBS in PBS at 1:5000. 100 µL was added to each well and plates were incubated for 2 hours at RT. Finally, 100 µL of OptEIA 3,3',5,5'-Tetramethylbenzidine substrate was added. The reaction was stopped after 5-10 minutes with 50 µL of 1M sulphuric acid. The absorbance was read on Versa Max microplate reader at 450 nm. Before the initiation of each step, plates were washed five times with 0.05% TWEEN 20 in PBS, except following the blocking step.

Data Analysis and Statistics

All data analysis and statistics were performed using R-based computational tools. All figures were generated using ggplot2.

Seroconversions were logarithm transformed and analysis of these were on a transformed scale. Normality assumptions were well-met on the transformed scale. Logistic regression was used to explore the relationship between vaccination history and seroconversions and to explore the association between D0 antibody titers and vaccination history.

Beta-diversity was calculated using a Bray-Curtis dissimilarity index. Permutational multivariate analysis of variance (PERMANOVA) was used to explore the relationship between microbiome beta-diversity and categorical variables. Logistic regression was used to explore the relationship between beta-diversity and vaccination history. The relationship of alpha diversity with categorical variables was explored using ANOVA.

Rank correlation (Spearman) was used to explore the strength of association between logarithm-transformed seroconversion and average daily fibre intake.

Comparisons between vaccine responses in mouse groups were made using Student's t-test (two group comparison) or ANOVA (multiple group comparison).

RESULTS

Influenza Vaccination History Strongly Influences Vaccine Responses

122 healthy participants aged 18-64 received the 2016 trivalent influenza vaccine (TIV) as part of our study. Detailed study characteristics are described elsewhere (16). At the first visit, participants provided a food diary completed across the prior 7 days along with a stool sample collected between day 3 and 7 of diary completion (**Figure 1A**). In addition, an influenza vaccination history for 120 of the 122 participants was documented (**Figure 1B**). 21 of the participants (17.5%) had not received any previous influenza vaccination (naïve). Participants were stratified into low, medium, or high responders on the basis of their fold change in hemagglutinin (HAI)-specific antibodies to H1N1 and H3N2 pre-vaccination and 28 days post vaccination (seroconversion). These classifications broadly characterized the response to all three influenza strains in the vaccine (H1N1, H3N2, and B) for both HAI and neuraminidase (NAI) (**Figure 1C**).

We found that how recently participants received their last influenza vaccine had a significantly negative effect on the strength of the antibody response induced by vaccination (logistic regression; H1N1: t-ratio -9.538, P=2.49e-16; H3N2: t-ratio -6.988, P=1.78e-10; B: t-ratio -4.665, P=8.22e-06; **Figure 1D**). The frequency of vaccination (total number of vaccination events) also negatively impacted the strength of the antibody response to the 2016 TIV. The effect of vaccine history was consistent across the three influenza subtypes for both HAI and NAI seroconversion (logistic regression, **Figure 1E**). Vaccine history score was determined by combining both the frequency of previous vaccinations and the years since the most recent vaccination event (vaccination history score = frequency of previous vaccinations * years since most recent vaccine). There was no significant effect of vaccination history on the HAI or NAI baseline antibody titers (at Day 0) to the 2016 TIV-vaccine specific strains (**Supplementary Figure 2**; logistic regression, P>0.1). Because the B strain elicited a much weaker humoral response than the 2 influenza A strains, we focused on H1N1 and H3N2 for subsequent analysis.

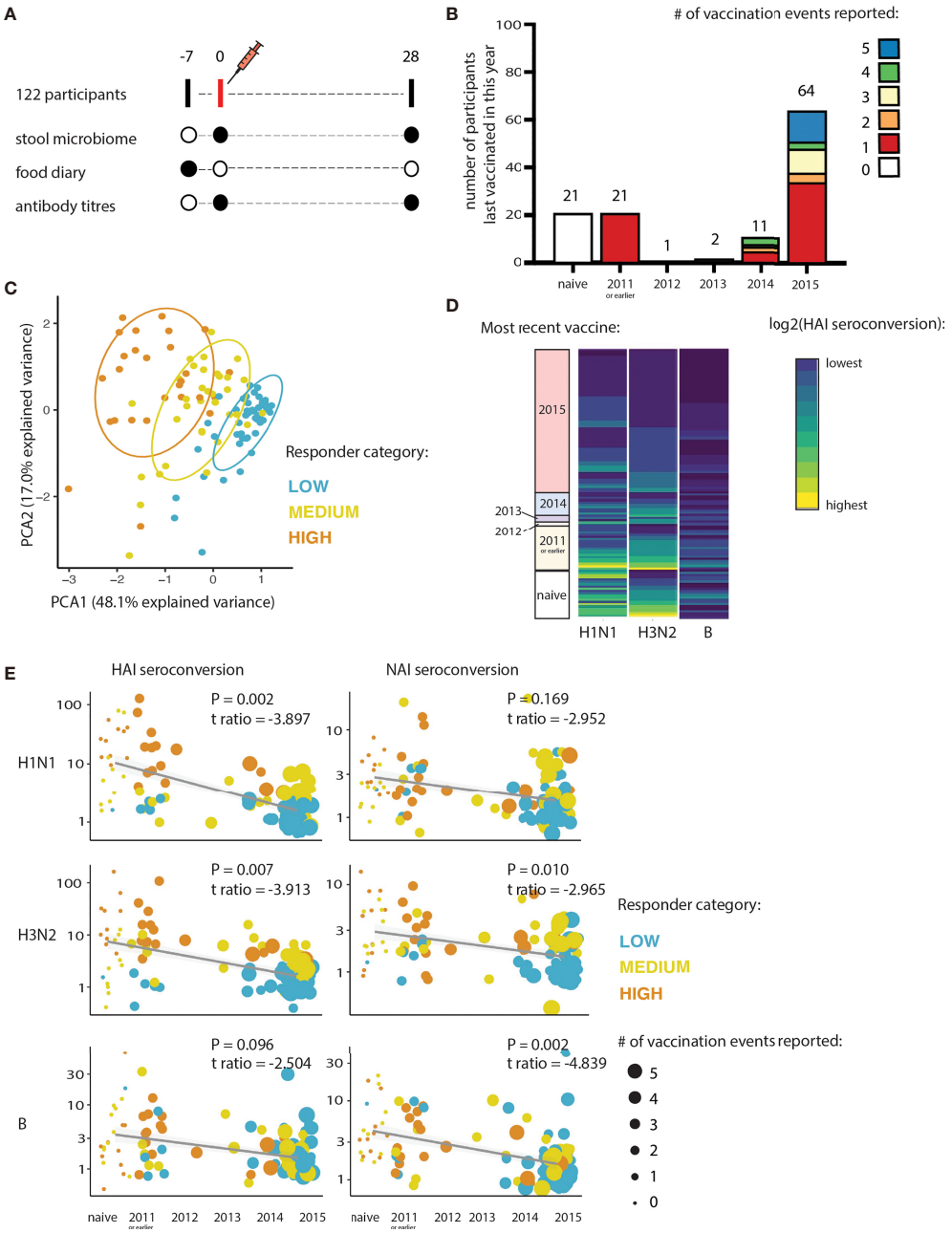

FIGURE 1 | Influenza vaccine responses are determined by vaccination history. **(A)** Schematic overview of sampling timepoints relative to the vaccination event. **(B)** Histogram summarizes the number of seasonal-influenza vaccines received self-reported by participants at least 4 years prior to the study (2012-2015 inclusive; or from 2011-2015 inclusive). **(C)** Principal component analysis of both HAI and NAI seroconversion of each participant. Participants are coloured according to their responder category. **(D)** Heatmap showing relationship between seroconversion and year of most recent seasonal-influenza vaccines received by participants in the 4 years prior to the study (2012-2015), and 2011 or earlier. Hemagglutinin (HAI) seroconversion to each of the influenza subtypes contained in the vaccine is shown. **(E)** Relationship between seroconversion and vaccine history. Hemagglutinin (HAI) and Neuraminidase (NAI) seroconversions are shown, as is the response to each of the influenza subtypes contained in the vaccine.

A Unique Microbiome Signature Is Correlated With the Vaccine Response to Each Influenza Strain

To investigate the role of the intestinal microbiome in shaping antibody responses to seasonal influenza vaccine, we collected faecal samples prior to vaccination (D0), and again at a particular day, between the day 25-28 timepoint, post vaccination (D28). An overview of the microbiome of each participant at each timepoint is shown in **Supplementary Figure 3**. We found that vaccine history did not significantly alter beta diversity (logistic regression,

P > 0.1, t-ratio 0.00553). Furthermore, there was no significant difference between the low, medium, or high vaccine responders in overall community composition (beta diversity, PERMANOVA, P >0.1) (**Figure 2A**). Our investigation did not identify any significant difference in Shannon-index (alpha diversity) between the low, medium, and high vaccine responders (ANOVA, P >0.1). This was true at D0 and at D28, and independent of vaccine history (**Figure 2B**). However, we did find a unique microbiome signature at the operational taxonomic unit (OTU) level associated with responsiveness to each of the influenza subtypes. Across all participants, we found 12 OTUs correlated with H1N1 seroconversion (Spearman correlation, $r > |0.15|$, $P_{adj} < 0.05$, **Supplementary Table 2.1** and **Supplementary Figure 4A)** and 13 OTUs correlated with H3N2 seroconversion (Spearman correlation, $r > |0.15|$, $P_{adj} < 0.05$, **Supplementary Table 2.2** and **Supplementary Figure 4B)**. We found stronger correlations between the microbiome and HAI seroconversion when we limited our analysis to individuals naïve to previous influenza vaccination. In naïve participants, we identified 10 OTUs that correlated with H1N1 seroconversion (Spearman correlation, $r > |0.15|$, $P_{adj} < 0.05$, **Figures 2C, D**, **Supplementary Table 3.1** and **Supplementary Figure 5A)** and 5 OTUs correlated with H3N2 seroconversion (Spearman correlation, $r > |0.15|$, $P_{adj} < 0.05$, **Figures 2C, D**, **Supplementary Table 3.2** and **Supplementary Figure 5B).** The OTU most strongly associated with a H1N1 seroconversion, Faecalibacterium prausnitzii **(Figure 2C)**, is well studied for its ability to immunomodulate, and for its ability to ferment dietary fibres to SCFAs (22).

Fibre Intake Positively Correlates With Vaccine Responses, Particularly in Individuals Previously Naïve to Influenza Vaccination

To assess if diet had any impact on microbiota and TIV specific response, we analysed participants' habitual dietary intake. Of particular interest to us was fibre intake, because of its known immunomodulatory properties (23). We first looked at microbial species that correlate with total dietary fibre intake and found 52 Operational Taxonomic Units (OTUs) that significantly increased with higher fibre intake (Spearman correlation, $P_{adj} < 0.05$, **Figure 3A**, **Supplementary Table 4** and **Supplementary Figure 6**). These OTUs were dominated by the class Clostridia, the class containing the majority of microbes with the ability to ferment indigestible fibre into SCFAs (**Figure 3A**) (24). As this class was disproportionately represented among the intestinal bacteria correlated with HAI seroconversion in vaccination naïve participants (14/15 = 93%), as compared to previously vaccinated participants (14/25 = 56%), we next looked at the inter-relationship between dietary fibre, antibody responses and vaccination history. Reflecting the marked preponderance of Clostridia within microbial classes associated with dietary fibre intake and *de novo* vaccine responses, we found the beneficial impact of dietary fibre on HAI seroconversion to be largely restricted to vaccination naïve individuals, albeit without reaching statistical significance in this under-powered subpopulation (Spearman correlation; H1N1 R =0.312, P=0.097; H3N2 R=0.181, P=0.059; **Figure 3B**).

In a more conservative analysis of the food diaries, of dietetic relevance, we excluded a) individual days in which participants reported an energy intake less than 1.2 X the Schofield predicted base metabolic rate and b) any participant that did not report at least 3 days with an energy intake higher than 1.2 X the Schofield predicted base metabolic rate. In both instances, similar trends were observed (**Supplementary Figure 7**).

Dietary Fibre and Fibre Fermentation Is Required for Optimal Antibody Response in a Mouse Model of Influenza Vaccination

Dietary fibre is fermented by the healthy human microbiome into SCFAs, which have been well studied for their immuno-modulatory properties (25). We therefore wanted to further investigate the role of fibre and fibre fermentation products in antibody production in mice with no previous exposure to influenza or influenza vaccine, similarly to previous observations documenting the influence of fibre on antibody production at steady-state and in the context of infection (5). We found that mice on a fibre-free diet had an impaired IgG_{total}, but not IgG1 antibody responses to TIV compared to those on a standard, high-fibre diet (**Figure 4A** and **Supplementary Figure 8A**). Next, we hypothesized that it was not the fibre itself, which was responsible for this phenotype, but rather the fibre fermentation products generated by the microbiota. To test this, we exposed mice to broad spectrum antibiotics to deplete their microbial fermentation capacity. Following three days of antibiotics, the frequencies of Firmicutes and Verrucomicrobia were diminished, while Actinobacteria and Bacteroidetes increased in frequency. After 10 days of antibiotics the faecal microbiota was further altered, with an expansion of Verrucomicrobia, Firmicutes and β-proteobacteria (**Supplementary Figure 9A**). Consistent with the concept that microbial fibre fermentation products contributed to the effect, we found that mice on antibiotics had impaired IgG_{total} antibody responses to TIV compared to their normo-biotic counterparts, as previously reported (3) (**Figure 4B**). The deficit in the TIV-specific antibody response could be seen as early as 14 days post vaccination in both TIV-specific total IgG, and TIV-specific IgG1 (**Supplementary Figure 9B**). The effect of antibiotic treatment was specific to the TIV-antibody response, and not a broad effect of the antibiotics on humoral immunity (**Supplementary Figure 9C**). Further supporting the concept that microbial fermentation of dietary fibre to SCFAs contributed to the TIV-specific antibody response, we found that supplementation of the SCFAs butyrate, acetate, and propionate to mice on a fibre-free diet phenocopied mice on a high fibre diet (**Figure 4C** and **Supplementary Figure 8B**). In the presence of adequate dietary fibre (control diet), the addition of acetate, butyrate, or propionate had no further benefit to antibody responses (**Figure 4D** and **Supplementary Figure 8B**).

DISCUSSION

The efficacy of the seasonal influenza vaccine varies significantly from person to person (26). A strong antibody response is crucial for effective protection against influenza. In this study, we found

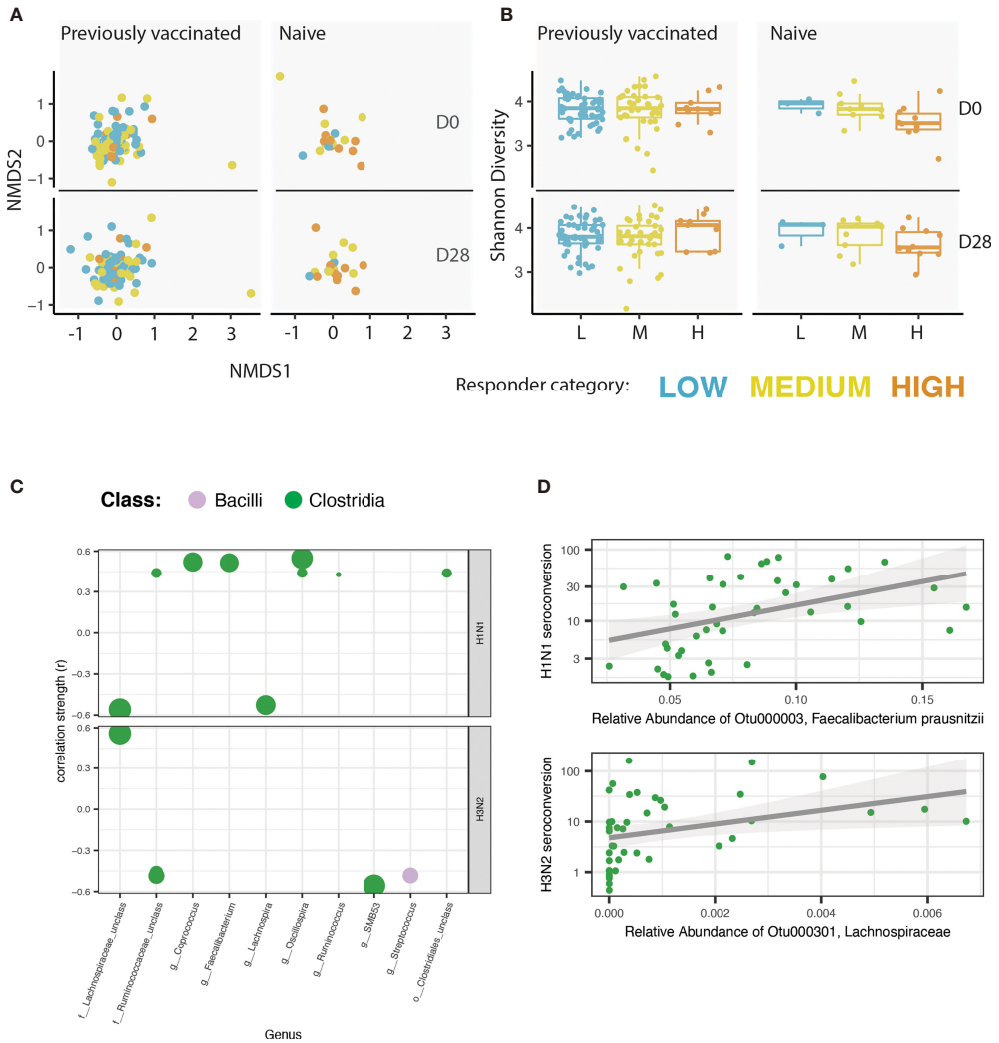

FIGURE 2 | A unique microbiome signature is correlated with the vaccine response to each of the influenza strains. **(A)** Non-metric multidimensional scaling (NMDS) of the microbiome for each participant. NMDS is faceted by vaccination history (naïve *vs*. previously vaccinated) and by timepoint [pre-vaccine (D0) or 25 - 28 days post vaccine (D28)]. Colour of each point reflects the responder category of the participant. **(B)** Shannon index of alpha diversity. Plot is faceted by vaccination history (naïve *vs*. previously vaccinated) and by timepoint (pre-vaccine or 28 days post vaccine). Colour of each point reflects the responder category of the participant. **(C)** Correlation analysis showing the strength of Spearman correlation of operational taxonomic units (OTUs) with HAI seroconversion in individuals previously naïve to influenza vaccination. Each point is one OTU. Colour of each point represents the class level taxonomic assignment of each OTU. OTUs are organized (x-axis) by genus, or by the lowest level of taxonomic hierarchy determined. Size of each point corresponds to -log (P value). Only OTUs with a correlation coefficient > |0.15| and an adjusted P value < 0.05 are shown. Plot is faceted by influenza strain: H1N1 (top), H3N2 (bottom). **(D)** Scatter-plot showing the correlation between the OTU with the strongest correlation with H1N1 seroconversion (Faecalibacterium prausnitzii; top) and H3N2 seroconversion (identified to the family level as Lachnospiraceae; bottom).

that dietary fibre intake in human participants appear to be contributory to mounting a robust vaccine response.

This study provides insight on the impact of prior vaccination events to influenza vaccine humoral immunity. We observed an inverse correlation between previous vaccination events and seroconversion across the three influenza subtypes, for both HAI and NAI. This phenomenon has been observed previously with other trivalent inactivated influenza vaccines (27–35). Noticeably, the impact of both diet and of the microbiome was greatest in those subjects who self-reportedly never received the seasonal influenza vaccine before participating in this study. Similarly, Hagan et al. found that the impact of antibiotic exposure to humoral immunity using the same vaccine in a human trial was greatest in subjects with low baseline titers (7). The authors hypothesized that mechanisms involved in recall responses could be more resilient to changes in the gut microbiota than those involved in a primary response (7), a hypothesis congruent with our observations.

A number of clinical studies have attempted to identify the microbial and molecular determinants of influenza vaccine

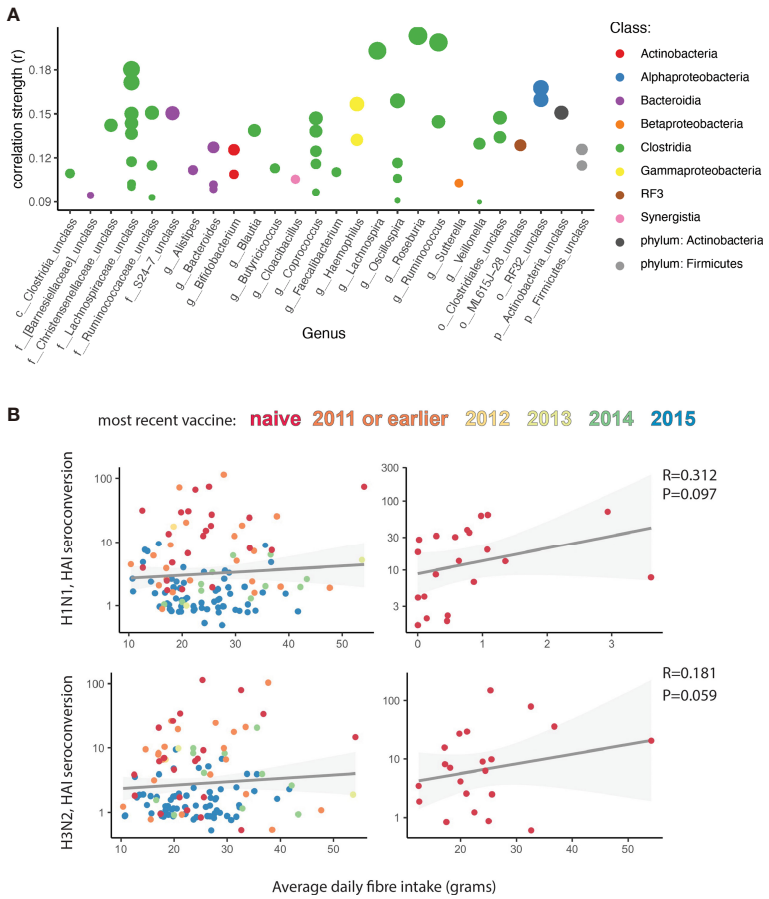

FIGURE 3 | Fiber intake correlates with influenza vaccine responses. **(A)** Correlation analysis showing strength of Spearman correlation of operational taxonomic units (OTUs) with average dietary fibre intake. Each point is one OTU. Colour of each point represents the class level taxonomic assignment of each OTU. OTUs are organized (x-axis) by genus, or lowest level of taxonomic hierarchy determined. Size of each point corresponds to -log (P value). Only OTUs with an adjusted P value < 0.05 are shown. **(B)** Correlation analysis of average dietary fibre intake with Hemagglutinin (HAI) seroconversion. Colour represents the number of self-reported seasonal influenza vaccinations each participant received in the last 5 years. On the left all participants are analysed. On the right only participants naïve to previous influenza vaccination are analysed. Grey shadow represents 95% confidence interval.

responsiveness, which is notoriously inconsistent throughout the general population (7–10). While these studies, alongside preclinical models (3–6), clearly demonstrate a microbiome-dependent effect, they have not provided actionable results. Importantly, our observations suggest that part of the microbial determinants of influenza vaccination responsiveness are secondary to dietary fibre intake -a finding which may generate new public health strategies to enhance population-based vaccination effectiveness.

Dietary fibre acts as the substrate for the microbial fermentation of SCFAs, which have been well studied as potent immune-modulatory metabolites capable of influencing cellular responses in locations beyond the gut. Systemic levels of SCFAs are most directly influenced by the amount of dietary fibre consumed (36). It has previously been observed in rats that dietary fibre intake potentiates IgA responses (37). SCFAs are the major dietary fibre metabolites responsible for augmenting antibody production in both mucosal tissues and systemically (5). Thus, our findings support the previously identified association of fibre consumption and antibody production.

Using a preclinical mouse model of TIV vaccination, we were able delineate the role of dietary fibre from SCFAs. We found that mice on a diet devoid of dietary fibre or mice lacking fermentation capacity (antibiotic treated) were inhibited in their antibody responses. Supplementing these mice with a mixture of SCFAs could restore antibody responses. Interestingly, SCFA administration together with high levels of dietary fibre did not further enhance antibody responses beyond a high fibre diet, indicating that SCFAs at supraphysiological concentrations have no added benefit in this context. Interestingly, while total vaccine-specific IgG levels were impaired in the absence of SCFAs, levels of vaccine-specific IgG1 were not. Future work should investigate how SCFA

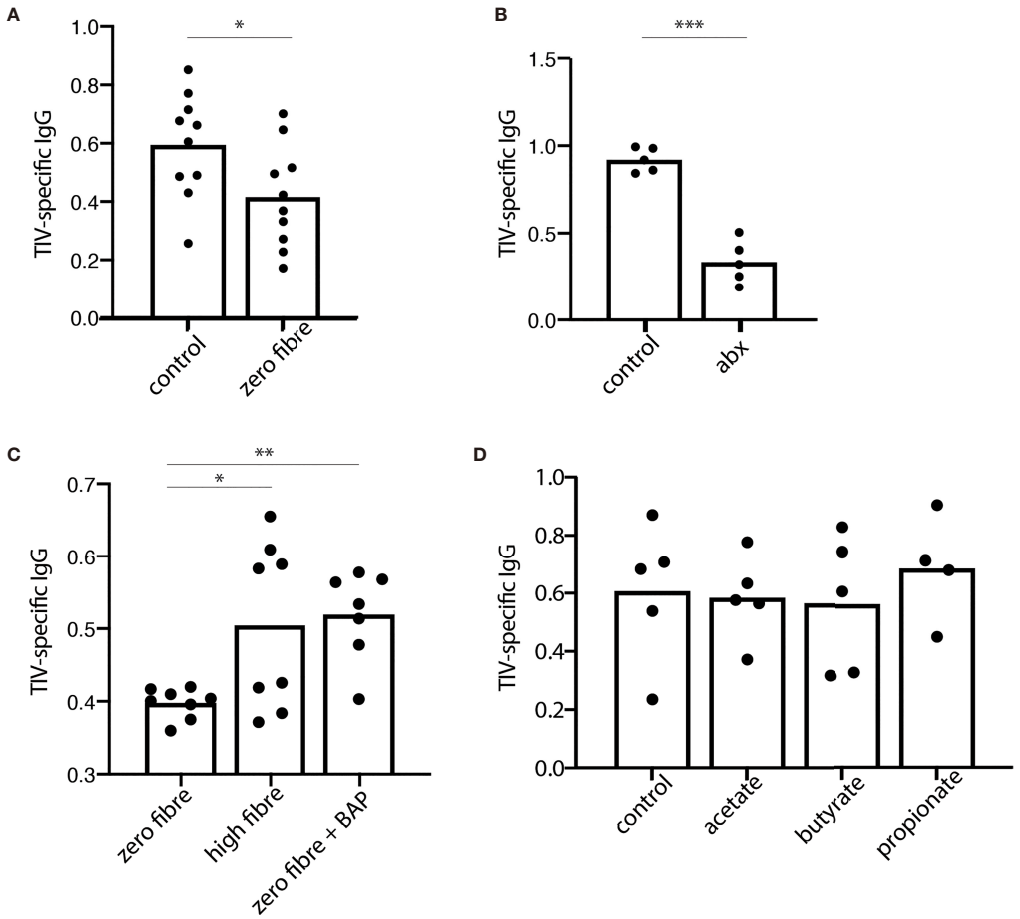

FIGURE 4 | Dietary fibre and fibre fermentation are required for optimal antibody response in a mouse model of influenza vaccination. 28 days after receiving the trivalent influenza vaccine (TIV), serum levels of TIV-specific IgG were assessed from mice allocated to various fibre interventions. **(A)** TIV-specific IgG in the serum from mice fed a control or zero fibre diet. **(B)** TIV-specific IgG from mice on a control diet, with (abx) or without (control) the addition of an antibiotic cocktail to the drinking water. **(C)** TIV-specific IgG from mice on a zero-fibre diet, a high fibre diet, or a zero fibre diet supplemented with a cocktail of short chain fatty acids containing butyrate, acetate, and propionate **(D)** TIV-specific IgG from mice on a control diet supplemented with acetate, butyrate, or propionate. Data from **(A, C)** are from two independent experiments; samples from replicate groups are combined for analysis [**(A)** n=5/treatment/experiment **(B)** n=3-4/treatment/experiment]. Data from **(B, D)** are representative from 2 independent experiments (n = 5/treatment/experiment). Error bars in all panels show standard error of the mean. *P < 0.05. **P < 0.01. ***P < 0.001. BAP, butyrate, acetate, and propionate.

levels impact vaccine specific IgG2 and IgG3, as presumably one or both subclasses are reduced.

In addition to dietary fibre, another major determinant of SCFA levels is the presence of microbial species capable of performing the fermentation (38). Understanding the microbial ecology of this process across individuals in relation to their vaccine-responses may provide important insight into how to optimize vaccine efficacy. Future work should look at SCFA production pathways using shot-gun metagenomics (39, 40). Integrating data around the microbiome, diet, and systemic levels of SCFAs will provide a clearer picture of how these metabolites influence vaccine responses.

Vaccines represent one of the most widely used and important public health interventions. Despite this, we do not fully understand why responses to vaccines vary widely between individuals and across populations, and perhaps more importantly, whether similar microbial, molecular or dietary determinants underlie the effectiveness to immunologically distinct vaccine formulations (e.g. adjuvanted *vs* non-adjuvanted, protein *vs* mRNA), as the impact of SCFA may very well be vaccine-specific (41). In this study we present data to suggest that public health messages to increase dietary fibre intake could assist in more successful vaccine protection.

DATA AVAILABILITY STATEMENT

The raw data supporting the conclusions of this article will be made available by the authors, without undue reservation. The microbiome data related to this study are available at European

Nucleotide Archive (http://www.ebi.ac.uk/ena) under study accession no PRJEB48578. Additional clinical data are available from the corresponding on request.

ETHICS STATEMENT

The studies involving human participants were reviewed and approved by New Zealand Central Health and Disability Ethics Committee. The patients/participants provided their written informed consent to participate in this study.

AUTHOR CONTRIBUTIONS

HP, NS, IB, and EF-B provided clinical study conceptualization. AC and OG formulated and coordinated the overarching investigation process. AC, AM, HP, NS, AJ, AGe, KG, AGr, WY, DT, JS, TO, AT, SP, SE, GW, AP-S, JR, RB, MW, IB, and EF-B acquired, curated and/or analysed data. AC, AM, KG, AGr, DO'S, JT, and OG provided critical review, commentary and/or revision of the data. The manuscript was written by AC, DO'S, and OG and commented on by all authors. All authors contributed to the article and approved the submitted version.

FUNDING

This work was supported by funding from the New Zealand Ministry for Business, Innovation and Employment (MBIE), as part of the High-Value Nutrition National Science Challenge, the independent research organization grant from the Health Research Council of New Zealand, and the Dines Family Charitable Trust, New Zealand.

ACKNOWLEDGMENTS

The authors thank the Biomedical Research Unit of the Malaghan Institute of Medical Research for animal husbandry, the staff of the Hugh Green Cytometry Core at the Malaghan Institute of Medical Research for expert support, and all colleagues at the Malaghan Institute for insightful discussion and advice.

SUPPLEMENTARY MATERIAL

The Supplementary Material for this article can be found online at: https://www.frontiersin.org/articles/10.3389/fimmu.2021.765528/full#supplementary-material

REFERENCES

1. Lynn DJ, Benson SC, Lynn MA, Pulendran B. Modulation of Immune Responses to Vaccination by the Microbiota: Implications and Potential Mechanisms. *Nat Rev Immunol* (2021) p:1–14. doi: 10.1038/s41577-021-00554-7
2. de Jong SE, Olin A, Pulendran B. The Impact of the Microbiome on Immunity to Vaccination in Humans. *Cell Host Microbe* (2020) 28(2):169–79. doi: 10.1016/j.chom.2020.06.014
3. Oh JZ, Ravindran R, Chassaing B, Carvalho FA, Maddur MS, Bower M, et al. TLR5-Mediated Sensing of Gut Microbiota is Necessary for Antibody Responses to Seasonal Influenza Vaccination. *Immunity* (2014) 41(3):478–92. doi: 10.1016/j.immuni.2014.08.009
4. Lynn MA, Tumes DJ, Choo JM, Sribnaia A, Blake SJ, Leong LEX, et al. Early-Life Antibiotic-Driven Dysbiosis Leads to Dysregulated Vaccine Immune Responses in Mice. *Cell Host Microbe* (2018) 23(5):653–60. e5. doi: 10.1016/j.chom.2018.04.009
5. Kim M, Qie Y, Park J, Kim CH. Gut Microbial Metabolites Fuel Host Antibody Responses. *Cell Host Microbe* (2016) 20(2):202–14. doi: 10.1016/j.chom.2016.07.001
6. Rocha CS, Hirao LA, Weber MG, Méndez-Lagares G, Chang WW, Jiang G, et al. Subclinical Cytomegalovirus Infection is Associated With Altered Host Immunity, Gut Microbiota, and Vaccine Responses. *J Virol* (2018) 92(13):e00167-18. doi: 10.1128/JVI.00167-18
7. Hagan T, Cortese M, Rouphael N, Boudreau C, Linde C, Maddur MS, et al. Antibiotics-Driven Gut Microbiome Perturbation Alters Immunity to Vaccines in Humans. *Cell* (2019) 178(6):1313–1328. e13. doi: 10.1016/j.cell.2019.08.010
8. Harris VC, Armah G, Fuentes S, Korpela KE, Parashar U, Victor JC, et al. Significant Correlation Between the Infant Gut Microbiome and Rotavirus Vaccine Response in Rural Ghana. *J Infect Dis* (2017) 215(1):34–41. doi: 10.1093/infdis/jiw518
9. Harris V, Ali A, Fuentes S, Korpela K, Kazi M, Tate J, et al. Rotavirus Vaccine Response Correlates With the Infant Gut Microbiota Composition in Pakistan. *Gut Microbes* (2018) 9(2):93–101. doi: 10.1080/19490976.2017.1376162
10. Cram JA, Fiore-Gartland AJ, Srinivasan S, Karuna S, Pantaleo G, Tomaras GD, et al. Human Gut Microbiota is Associated With HIV-Reactive Immunoglobulin at Baseline and Following HIV Vaccination. *PloS One* (2019) 14(12):e0225622. doi: 10.1371/journal.pone.0225622
11. Xu Z, Knight R. Dietary Effects on Human Gut Microbiome Diversity. *Br J Nutr* (2015) 113(S1):S1–5. doi: 10.1017/S0007114514004127
12. Makki K, Deehan EC, Walter J, Bäckhed F. The Impact of Dietary Fiber on Gut Microbiota in Host Health and Disease. *Cell Host Microbe* (2018) 23(6):705–15. doi: 10.1016/j.chom.2018.05.012
13. Belkaid Y, Hand TW. Role of the Microbiota in Immunity and Inflammation. *Cell* (2014) 157(1):121–41. doi: 10.1016/j.cell.2014.03.011
14. Macfarlane S, Macfarlane GT. Regulation of Short-Chain Fatty Acid Production. *Proc Nutr Soc* (2003) 62(1):67–72. doi: 10.1079/PNS2002207
15. Cummings J, Pomare E, Branch W, Naylor C, Macfarlane G. Short Chain Fatty Acids in Human Large Intestine, Portal, Hepatic and Venous Blood. *Gut* (1987) 28(10):1221–7. doi: 10.1136/gut.28.10.1221
16. Shortt N, Poyntz H, Young W, Jones A, Gestin A, Mooney A, et al. A Feasibility Study: Association Between Gut Microbiota Enterotype and Antibody Response to Seasonal Trivalent Influenza Vaccine in Adults. *Clin Trans Immunol* (2018) 7(3):e1013. doi: 10.1002/cti2.1013
17. Kozich JJ, Westcott SL, Baxter NT, Highlander SK, Schloss PD. Development of a Dual-Index Sequencing Strategy and Curation Pipeline for Analyzing Amplicon Sequence Data on the MiSeq Illumina Sequencing Platform. *Appl Environ Microbiol* (2013) 79(17):5112–20. doi: 10.1128/AEM.01043-13
18. Cole JR, Wang Q, Fish JA, Chai B, McGarrell DM, Sun Y, et al. Ribosomal Database Project: Data and Tools for High Throughput rRNA Analysis. *Nucleic Acids Res* (2014) 42(D1):D633–42. doi: 10.1093/nar/gkt1244
19. Wickham H. Elegant Graphics for Data Analysis. *Media* (2009) 35(211):10.1007. doi: 10.1007/978-0-387-98141-3
20. Matsuki T, Watanabe K, Fujimoto J, Takada T, Tanaka R. Use of 16S rRNA Gene-Targeted Group-Specific Primers for Real-Time PCR Analysis of Predominant Bacteria in Human Feces. *Appl Environ Microbiol* (2004) 70(12):7220–8. doi: 10.1128/AEM.70.12.7220-7228.2004
21. Schofield WN. Predicting Basal Metabolic Rate, New Standards and Review of Previous Work. *Hum Nutr Clin Nutr* (1985) 39:5–41.
22. Leylabadlo HE, Ghotaslou R, Feizabadi MM, Farajnia S, Moaddab SY, Ganbarov K, et al. The Critical Role of Faecalibacterium Prausnitzii in Human Health: An Overview. *Microbial Pathog* (2020) 149:104344. doi: 10.1016/j.micpath.2020.104344

23. Schley P, Field C. The Immune-Enhancing Effects of Dietary Fibres and Prebiotics. *Br J Nutr* (2002) 87(S2):S221–30. doi: 10.1079/BJNBJN/2002541
24. Flint HJ, Scott KP, Duncan SH, Louis P, Forano E. Microbial Degradation of Complex Carbohydrates in the Gut. *Gut Microbes* (2012) 3(4):289–306. doi: 10.4161/gmic.19897
25. Tan J, McKenzie C, Potamitis M, Thorburn AN, Mackay CR, Macia L. The Role of Short-Chain Fatty Acids in Health and Disease. *Adv Immunol* (2014) 121:91–119. doi: 10.1016/B978-0-12-800100-4.00003-9
26. Lewnard JA, Cobey S. Immune History and Influenza Vaccine Effectiveness. *Vaccines* (2018) 6(2):28. doi: 10.3390/vaccines6020028
27. Thompson MG, Naleway A, Fry AM, Ball S, Spencer SM, Reynolds S, et al. Effects of Repeated Annual Inactivated Influenza Vaccination Among Healthcare Personnel on Serum Hemagglutinin Inhibition Antibody Response to A/Perth/16/2009 (H3N2)-Like Virus During 2010-11. *Vaccine* (2016) 34 (7):981–8. doi: 10.1016/j.vaccine.2015.10.119
28. McLean HQ, Thompson MG, Sundaram ME, Meece JK, McClure DL, Friedrich TC, et al. Impact of Repeated Vaccination on Vaccine Effectiveness Against Influenza A (H3N2) and B During 8 Seasons. *Clin Infect Dis* (2014) 59(10):1375–85. doi: 10.1093/cid/ciu680
29. Beyer WE, de Bruijn IA, Palache AM, Westendorp RG, Osterhaus AD. Protection Against Influenza After Annually Repeated Vaccination: A Meta-Analysis of Serologic and Field Studies. *Arch Internal Med* (1999) 159 (2):182–8. doi: 10.1001/archinte.159.2.182
30. De Bruijn I, Remarque E, Jol-Van der Zijde C, Van Tol M, Westendorp R, Knook D. Quality and Quantity of the Humoral Immune Response in Healthy Elderly and Young Subjects After Annually Repeated Influenza Vaccination. *J Infect Dis* (1999) 179(1):31–6. doi: 10.1086/314540
31. Gardner EM, Bernstein ED, Dran S, Munk G, Gross P, Abrutyn E, et al. Characterization of Antibody Responses to Annual Influenza Vaccination Over Four Years in a Healthy Elderly Population. *Vaccine* (2001) 19 (32):4610–7. doi: 10.1016/S0264-410X(01)00246-8
32. Pyhälä R, Kumpulainen V, Alanko S, Forsten T. HI Antibody Kinetics in Adult Volunteers Immunized Repeatedly With Inactivated Trivalent Influenza Vaccine in 1990–1992. *Vaccine* (1994) 12(10):947–52. doi: 10.1016/0264-410X(94)90039-6
33. Keitel WA, Cate TR, Couch RB, Huggins LL, Hess KR. Efficacy of Repeated Annual Immunization With Inactivated Influenza Virus Vaccines Over a Five Year Period. *Vaccine* (1997) 15(10):1114–22. doi: 10.1016/S0264-410X(97)00003-0
34. Song JY, Cheong HJ, Hwang IS, Choi WS, Jo YM, Park DW, et al. Long-Term Immunogenicity of Influenza Vaccine Among the Elderly: Risk Factors for Poor Immune Response and Persistence. *Vaccine* (2010) 28(23):3929–35. doi: 10.1016/j.vaccine.2010.03.067
35. Huijskens E, Rossen J, Mulder P, van Beek R, van Vugt H, Verbakel J, et al. Immunogenicity, Boostability, and Sustainability of the Immune Response After Vaccination Against Influenza A Virus (H1N1) 2009 in a Healthy Population. *Clin Vaccine Immunol* (2011) 18(9):1401–5. doi: 10.1128/CVI.05046-11
36. McOrist AL, Miller RB, Bird AR, Keogh JB, Noakes M, Topping DL, et al. Fecal Butyrate Levels Vary Widely Among Individuals But are Usually Increased by a Diet High in Resistant Starch. *J Nutr* (2011) 141(5):883–9. doi: 10.3945/jn.110.128504
37. Kudoh K, Shimizu J, Wada M, Takita T, Kanke Y , InnamiS, et al. Effect of Indigestible Saccharides on B Lymphocyte Response of Intestinal Mucosa and Cecal Fermentation in Rats. *J Nutr Sci Vitaminol* (1998) 44(1):103–12. doi: 10.3177/jnsv.44.103
38. Yip W, Hughes MR, Li Y, Cait A, Hirst M, Mohn WW, et al. Butyrate Shapes Immune Cell Fate and Function in Allergic Asthma. *Front Immunol* (2021) 12:299. doi: 10.3389/fimmu.2021.628453
39. Vital M, Howe AC, Tiedje JM. Revealing the Bacterial Butyrate Synthesis Pathways by Analyzing (Meta) Genomic Data. *MBio* (2014) 5(2):mBio.00889-14. doi: 10.1128/mBio.00889-14
40. Cait A, Cardenas E, Dimitriu PA, Amenyogbe N, Dai D, Cait J, et al. Reduced Genetic Potential for Butyrate Fermentation in the Gut Microbiome of Infants Who Develop Allergic Sensitization. *J Allergy Clin Immunol* (2019) 144 (6):1638–47.e3. doi: 10.1016/j.jaci.2019.06.029
41. Sanchez HN, Moroney JB, Gan H, Shen T, Im JL, Li T, et al. B Cell-Intrinsic Epigenetic Modulation of Antibody Responses by Dietary Fiber-Derived Short-Chain Fatty Acids. *Nat Commun* (2020) 11(1):1–19. doi: 10.1038/s41467-019-13603-6

Conflict of Interest: SE and GW were employed by Food Savvy.

The remaining authors declare that the research was conducted in the absence of any commercial or financial relationship that could be construed as a potential conflict of interest.

Publisher's Note: All claims expressed in this article are solely those of the authors and do not necessarily represent those of their affiliated organizations, or those of the publisher, the editors and the reviewers. Any product that may be evaluated in this article, or claim that may be made by its manufacturer, is not guaranteed or endorsed by the publisher.

Copyright © 2021 Cait, Mooney, Poyntz, Shortt, Jones, Gestin, Gell, Grooby, O'Sullivan, Tang, Young, Thayabaran, Sparks, Ostapowicz, Tay, Poppitt, Elliott, Wakefield, Parry-Strong, Ralston, Beasley, Weatherall, Braithwaite, Forbes-Blom and Gasser. This is an open-access article distributed under the terms of the Creative Commons Attribution License (CC BY). The use, distribution or reproduction in other forums is permitted, provided the original author(s) and the copyright owner(s) are credited and that the original publication in this journal is cited, in accordance with accepted academic practice. No use, distribution or reproduction is permitted which does not comply with these terms.

frontiers in Microbiology

REVIEW
published: 25 January 2022
doi: 10.3389/fmicb.2021.812466

"Osteomicrobiology": The Nexus Between Bone and Bugs

*Asha Bhardwaj[1], Leena Sapra[1], Abhay Tiwari[2], Pradyumna K. Mishra[3], Satyawati Sharma[2] and Rupesh K. Srivastava[1]**

[1] Department of Biotechnology, All India Institute of Medical Sciences (AIIMS), New Delhi, India, [2] Centre for Rural Development & Technology, Indian Institute of Technology (IIT), New Delhi, India, [3] Department of Molecular Biology, ICMR-National Institute for Research in Environmental Health, Bhopal, India

A growing body of scientific evidence supports the notion that gut microbiota plays a key role in the regulation of various physiological and pathological processes related to human health. Recent findings have now established that gut microbiota also contributes to the regulation of bone homeostasis. Studies on animal models have unraveled various underlying mechanisms responsible for gut microbiota-mediated bone regulation. Normal gut microbiota is thus required for the maintenance of bone homeostasis. However, dysbiosis of gut microbiota communities is reported to be associated with several bone-related ailments such as osteoporosis, rheumatoid arthritis, osteoarthritis, and periodontitis. Dietary interventions in the form of probiotics, prebiotics, synbiotics, and postbiotics have been reported in restoring the dysbiotic gut microbiota composition and thus could provide various health benefits to the host including bone health. These dietary interventions prevent bone loss through several mechanisms and thus could act as potential therapies for the treatment of bone pathologies. In the present review, we summarize the current knowledge of how gut microbiota and its derived microbial compounds are associated with bone metabolism and their roles in ameliorating bone health. In addition to this, we also highlight the role of various dietary supplements like probiotics, prebiotics, synbiotics, and postbiotics as promising microbiota targeted interventions with the clinical application for leveraging treatment modalities in various inflammatory bone pathologies.

Keywords: osteomicrobiology, bone health, gut microbiota, probiotics, prebiotics

OPEN ACCESS

Edited by:
Tobias R. Kollmann, University of Western Australia, Australia

Reviewed by:
Huaxi Yi, Ocean University of China, China
Fintan Thomas Moriarty, AO Research Institute, Switzerland

****Correspondence:***
Rupesh K. Srivastava
rupesh_srivastava13@yahoo.co.in; rupeshk@aiims.edu

Specialty section:
This article was submitted to Microbial Immunology, a section of the journal Frontiers in Microbiology

Received: *10 November 2021*
Accepted: *31 December 2021*
Published: *25 January 2022*

Citation:
Bhardwaj A, Sapra L, Tiwari A, Mishra PK, Sharma S and Srivastava RK (2022) "Osteomicrobiology": The Nexus Between Bone and Bugs. Front. Microbiol. 12:812466. doi: 10.3389/fmicb.2021.812466

Abbreviations: GM, Gut Microbiota; IEC, Intestinal Epithelial Cells; SCFAs, Short Chain Fatty Acids; AhR, Aryl hydrocarbon Receptors; IBD, Inflammatory Bowel Disease; IBS, Inflammatory Bowel Syndrome, MSC; Mesenchymal Stem Cells; Runx2; Runt Related Transcription Factor 2; PTH, Parathyroid Hormone; IGF-1, Insulin like Growth Factor-1; MCSF, Macrophage Colony Stimulating Factor; RANKL, Receptor Activator of Nuclear Factor kappa-B Ligand; TRAP, Tartrate Resistant Acid Phosphatase; TNF, Tumor Necrosis Factor; IL, Interleukin; OPG, Osteoprotegerin; Ca, Calcium; RA, Rheumatoid Arthritis; CONV-R, Conventionally Raised; NOD, Nucleotide-binding Oligomerization Domain; BMMCs, Bone Marrow derived Macrophages; SPF, Specific Pathogen Free; GH, Growth Hormone; GAMs, Gut Associated Metabolites; M cells, Microfold cells; AMP, Anti-Microbial Peptides; MUC, Mucin; LPS, Lipopolysaccharide; sIgA, secretory IgA; TJ, Tight Junctions; TGF, Transforming Growth Factor; IFN, Interferon; PSA, Polysaccharide A; TLR, Toll Like Receptor; DC, Dendritic Cells; TPH, Tryptophan Hydroxylase; HDAC, Histone Deacetylase; GPCR, G Protein Coupled Receptor; BMD, Bone Mineral Density; FXR, Farnesoid X Receptor; Tgr5, G Protein Coupled Bile Acid Receptor 5; AMPK, AMP activated Protein Kinase; FOS, Fructooligosaccharides; XOS, Xylooligosaccharides; GOS, Galactooligosaccharides; AIP, Autoimmune Protocol; FMT, Fecal Microbiota Transplantation.

INTRODUCTION

Microbiota is the collection of microorganisms such as bacteria, viruses, archaea, fungi, protozoa, and eukaryotes that exist inside or outside the host. Although microbes are present on the entire host mucosal surface a majority of them reside in the gastrointestinal tract and are referred to as gut microbiota (GM) (Sommer and Bäckhed, 2013). The human GM consist of over 100 trillion microbes that encode more than 3.3 million genes (Qin et al., 2010; Rinninella et al., 2019). These microbes have coevolved with humans and provide numerous health benefits *via* the regulation of various biological processes (Eckburg, 2005). The human gut is primarily dominated by the *Firmicutes* and *Bacteroidetes* phyla which constitute over 90% of the intestinal microbiota (Eckburg, 2005; **Figure 1**). Other microbial phyla that are present in minor proportion are *Proteobacteria*, *Actinobacteria*, *Fusobacteria*, and *Verrucomicrobia* (Eckburg, 2005). Development of GM takes place after birth. At birth, neonates are devoid of any microbiota and acquire it only after birth when exposed to a vast array of microbes. The microbial composition of the infants depends on the mode of delivery (Dominguez-Bello et al., 2010). Infants born by vaginal delivery have a microbial composition similar to the mother's vagina consisting of mainly *Lactobacillus*, *Prevotella*, or *Sneathia* spp. However, babies born by C-section are depleted of bacterial species from the mother's vagina (Dominguez-Bello et al., 2010). They acquire most of the microbiota from the mother's skin and from the hospital which is dominated by *Staphylococcus*, *Corynebacterium,* and *Propionibacterium* spp. (Dominguez-Bello et al., 2010). Microbial composition is also affected by genetic and environmental factors (Schroeder and Bäckhed, 2016). Breastfeeding and antibiotic treatment also affect the microbiota composition during infancy. Later in life, the microbial composition is shaped by the type, quality, and quantity of diet. GM promotes human health and plays a very significant role in the regulation of immune and metabolic homeostasis (Thursby and Juge, 2017). Research from the past decade has revealed the effect of GM in the regulation of various physiological functions related to human health and its association with several diseases. GM enhances the extraction of energy from food, increases nutrient absorption, induces immune system development, and prevents the invasion of pathogens through the intestinal epithelial cells (IECs). GM produces various secondary metabolites such as short-chain fatty acids (SCFAs) and aryl hydrocarbon receptor (AhR) ligands which have a role in the regulation of several physiological functions related to human health. However, modifications in GM composition result in the progression of various gastrointestinal and metabolic disorders such as irritable bowel syndrome (IBS), inflammatory bowel disease (IBD), colorectal cancer, obesity, and type 2 diabetes (Guinane and Cotter, 2013; Wang et al., 2017). The role of GM in regulating human health is now emerging as one of the latest trends in integrative biology. Interestingly, recent studies have now revealed a nexus between GM and skeletal health. Accumulating evidence from these studies indicates that GM is associated with bone metabolism and a range of metabolic bone disorders. GM is a crucial regulator of bone homeostasis and maintains bone health *via* several mechanisms. Here we review all possible mechanisms through which GM regulates skeletal health starting with a brief discussion about bone.

BONE

The skeleton is among the largest organs of the human body and constitutes approximately 15% of the total human body weight (Su et al., 2019). Adult human bone is mainly composed of 80% cortical bone and 20% cancellous or trabecular bone (Clarke, 2008). Bone is a highly dynamic and metabolically active connective tissue that continuously undergoes remodeling throughout our life. Bone remodeling occurs with the help of three prime bone cells: bone-forming osteoblasts, bone-resorbing osteoclasts, and the embedded cells in a bone matrix called osteocytes. Osteoblasts are differentiated from mesenchymal stem cells (MSCs) that also give rise to various other types of cells such as adipocytes and chondrocytes (Schett and David, 2010). Differentiation of osteoblasts from MSCs is mainly induced by runt-related transcription factor 2 (Runx2) and its target gene, the Sp7 transcription factor (Srivastava et al., 2018). Osteoblasts produce various extracellular proteins such as type 1 collagen, alkaline phosphatase, osteocalcin, osteopontin, and osteonectin. These proteins deposit between the osteoblasts and the surface of the bone to form a matrix (Dar et al., 2018a).

Osteoclasts are specialized in bone resorption and are also known as bone eaters. Osteoclasts are multinucleated giant cells that are derived from myeloid precursors. Differentiation of osteoclasts depends on two important factors i.e., macrophage colony-stimulating factor (MCSF) and receptor activator of nuclear factor kappa-B ligand (RANKL) (Charles and Aliprantis, 2014). MCSF promotes the proliferation and survival of osteoclast progenitors whereas RANKL stimulates the differentiation of progenitors into osteoclasts (Schett and David, 2010). Osteoclasts attach to the surface of the bone to form a unique structure called a "sealing zone" which creates resorption space that is insulated from the extracellular space. Osteoclasts acidify the resorption space and degrade various organic and mineral contents of bone by releasing the lysosomal enzymes such as cathepsin K and tartrate-resistant acid phosphatase (TRAP) (Walsh et al., 2006). Osteoclasts also modulate their structure to form a ruffled border that increases the surface for transport of active hydrogen ions (H^+) through a proton pump in the sealing zone (Walsh et al., 2006). Recently, a new subset of bone cells named "Osteomorphs" has been reported. Osteomorphs are formed by the fission of RANKL stimulated multinucleated osteoclasts into daughter cells that *via* fusion can recycle back into osteoclasts. Single-cell RNA sequencing revealed that osteomorphs are different from osteoclasts and express several genes that are associated with bone structure and function (McDonald et al., 2021).

A subset of osteoblasts that are being entrapped in the calcified bone matrix is termed osteocytes. Osteocytes are derived from osteoblasts and are the most abundant and long-lived bone cells that constitute about 95% of the mature bone tissue. Osteocytes indirectly regulate the activity of osteoclasts and osteoblasts *via*

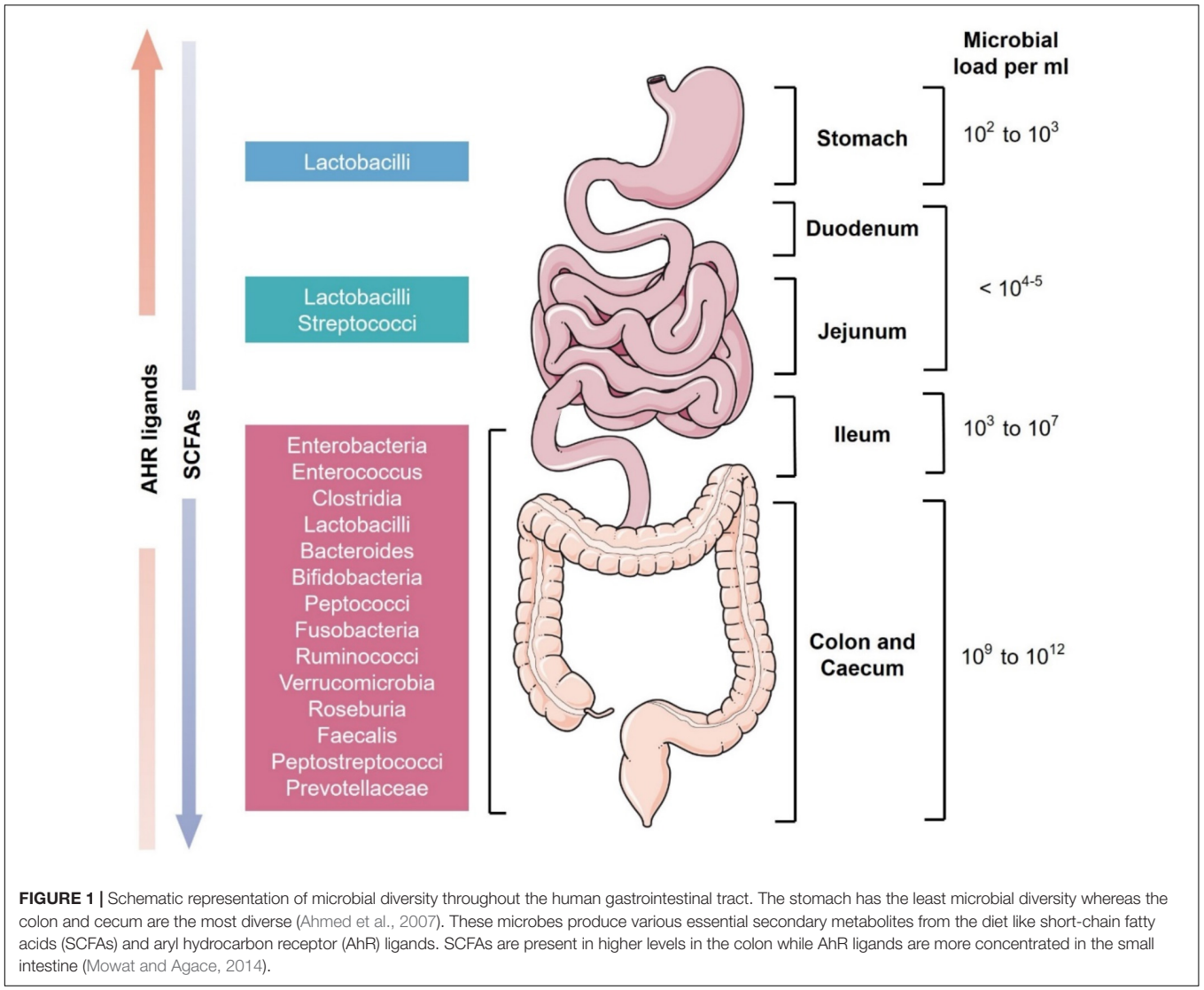

FIGURE 1 | Schematic representation of microbial diversity throughout the human gastrointestinal tract. The stomach has the least microbial diversity whereas the colon and cecum are the most diverse (Ahmed et al., 2007). These microbes produce various essential secondary metabolites from the diet like short-chain fatty acids (SCFAs) and aryl hydrocarbon receptor (AhR) ligands. SCFAs are present in higher levels in the colon while AhR ligands are more concentrated in the small intestine (Mowat and Agace, 2014).

the secretion of various regulatory factors. Osteocytes also have a role in calcium and phosphate metabolism. The most important function of osteocytes is that they act as bone mechanosensors (Qin et al., 2020). Osteocytes are believed to send signals to other osteocytes and osteoblasts on the surface of the bone in response to mechanical forces *via* their intricate cellular networks called canaliculi (Walsh et al., 2006).

Apart from these prime cells, there are osteomacs which also have a critical role in regulating bone metabolism. Osteomacs are stellate-shaped cells and account for approximately one-sixth of the total bone marrow cells (Srivastava et al., 2018). Osteomacs are present adjacent to osteoblasts and have a role in bone formation and osteogenic differentiation of MSCs (Chen et al., 2020).

Bone remodeling is a dynamic process and requires multiple interactions between osteoblasts and osteoclasts (**Figure 2**). Osteoblasts positively induce osteoclasts differentiation by secreting RANKL and MCSF and negatively by secreting RANKL decoy receptor osteoprotegerin (OPG) (Schett and David, 2010). Bone remodeling maintains the bone architecture and continuously replaces the old bone with the new one. Bone remodeling maintains bone integrity, restores bone microdamage, and regulates the release of calcium (Ca) and phosphorus (P) during normal host physiology (Dar et al., 2018a). Abnormalities in the bone remodeling process lead to several skeleton deformities. Bone remodeling is a complex process and is regulated by various biochemical and mechanical factors. Major factors that are involved in the regulation of bone remodeling are parathyroid hormone (PTH), estrogen, thyroid hormones, and glucocorticoids. Other factors that are pivotal players in bone remodeling are insulin-like growth factors (IGFs), bone morphogenetic proteins (BMPs), prostaglandins, vitamin D, tumor growth factor (TGF)-β, and cytokines (Hadjidakis and Androulakis, 2006; Dar et al., 2018a). Recent studies particularly on the germ-free (GF) mice have shown that GM is also a critical factor in the regulation of bone remodeling (Yan and Charles, 2017). GM influences the activity of bone cells and alteration in GM composition leads to skeleton

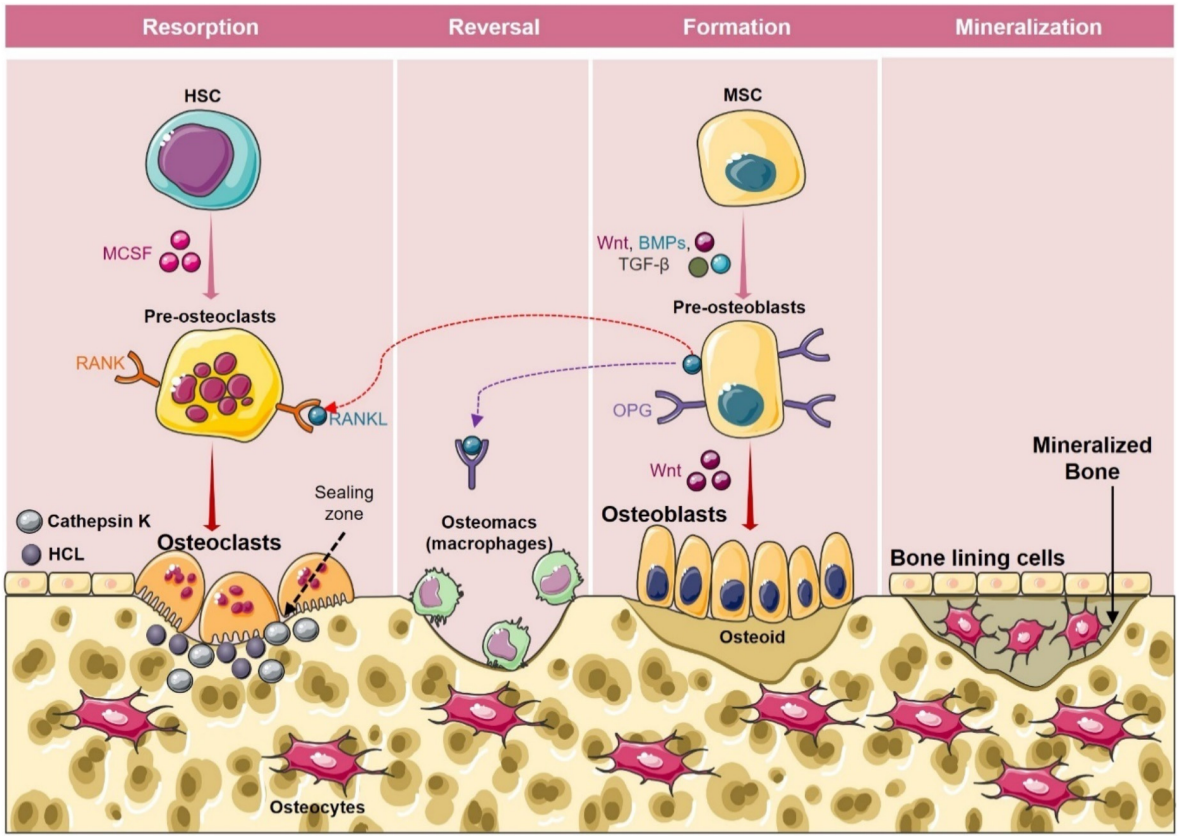

FIGURE 2 | Bone remodeling cycle. Bone remodeling occurs in four phases: (1) Activation phase: In this phase, M-CSF and RANKL promote the differentiation of osteoclast precursors into osteoclasts. (2) Resorption phase: During this phase mature osteoclasts with unique ruffled borders induce resorption of bone by secreting cathepsin K, and H^+ in the sealing zone. After resorption osteoclasts detach from the surface of the bone and undergo apoptosis. (3) Reversal phase: In the reversal phase osteoblasts' precursors get differentiated into mature osteoblasts and are recruited to the resorption site. (4) Formation phase: In this phase osteoblasts get occupied in the resorbed lacuna and start depositing the bone matrix. After the formation phase, osteoid gets mineralized and bone surface returns to resting phase with bone lining cells.

manifestations such as osteoporosis, rheumatoid arthritis (RA), and periodontitis (Ibáñez et al., 2019). Recent studies have established the important relationship between GM and bone health and is comprehensively reviewed here.

NEXUS BETWEEN GUT MICROBIOTA AND BONE HEALTH

GM influences the function of various organs and recently the effect of GM on bone health is catching significant attention. The association between GM and bone was first revealed in the study by Sjogren's group. They observed that female C57BL/6J GF mice had increased bone mass with decreased number of osteoclasts. GF mice also had a reduced number of $CD4^+$ T cells, osteoclast precursors, and inflammatory cytokines than the conventionally raised (CONV-R) mice (Sjögren et al., 2012). The same group in another study using female C57BL/6J GF mice from Pasteur Institute, France observed similar results i.e., female GF mice had increased bone mass than the CONV-R mice as they reported in the previous experiment with C57BL/6J GF mice raised in the gnotobiotic facility at the University of Gothenburg, Sweden (Ohlsson and Sjögren, 2018). Li et al. also observed related results on female C57BL/6J GF mice. They reported that a decrease in bone mass due to inflammatory conditions induced during sex steroid deficiency is mediated by GM. They observed that in GF mice, no bone loss occurred during sex steroid deficiency. In the presence of GM, sex steroid deficiency unregulated the production of osteoclastogenic and inflammatory cytokines such as tumor necrosis factor (TNF)-α, RANKL, and interleukin (IL)-17. However, in GF mice there was no such increase in the level of osteoclastogenic cytokines after sex steroid deficiency (Li et al., 2016). Therefore, GM might enhance bone resorption by increasing the level of inflammatory and osteoclastogenic cytokines as observed by Sjogren's group. Subsequently, several other studies using mice of the same genetic background i.e., C57BL/6J revealed the different mechanisms involved in GM-mediated bone resorption. Ohlsson et al. (2017) demonstrated that colonization of GM normalized the increased bone mass in GF mice. GM induced the expression of RANKL and TNF-α *via* activation of nucleotide-binding oligomerization domain-containing proteins

(NOD)1 and NOD2 signaling which induces osteoclastogenesis and thus bone resorption (Ohlsson et al., 2017). In another study, it was reported that bone marrow-derived mesenchymal stem cells (BMMCs) of GF mice showed high proliferation and osteogenesis. On the other hand, colonization of GF mice with specific pathogen-free (SPF) mice microbiota normalized the proliferation of BMMCs and decreased their osteogenesis (Xiao et al., 2017). Novince et al. (2017) showed that commensal microbiota promotes osteoclastogenesis along with simultaneously suppressing osteoblastogenesis which results in bone loss. Role of GM in inducing bone resorption is also supported by the studies including antibiotics. Low dose administration of antibiotics like penicillin, chlortetracycline and vancomycin at the early age increased the bone mineral density (BMD) of mice (Cho et al., 2012). Another study showed that low dose administration of penicillin enhanced the BMD and bone mineral content (BMC) of female C57BL/6J mice (Cox et al., 2014). However, in humans administration of broad spectrum antibiotics did not show any affect on bone health (Mikkelsen et al., 2018).

Above mentioned studies thus clearly indicate that GM regulates bone mass by promoting bone resorption but in reality, the effect of GM on bone is very complex as various factors are involved in GM-mediated regulation of bone health. These factors could be the strain and gender of mice used in the study. Some studies conducted on male mice of other strains evidenced that GM induces bone formation instead of bone resorption. It is reported that supplementation of *Lactobacillus plantarum* promoted juvenile growth and prevented stunted growth during chronic undernutrition in male BALB/c GF mice by stimulating growth hormone (GH) activity (Schwarzer et al., 2016). In male C57BL/6J mice antibiotic use decreased the BMC which in contrast to that observed in female C57BL/6J mice (Cox et al., 2014). Similarly, Yan et al. reported that long-term colonization of CB6F1 GF mice with microbiota from SPF mice enhances bone mass. Antibiotic treatment on the other hand inhibits bone formation. Yan et al. study showed that the net effect of GM on bone is not only dependent on the strain but partly on the duration of colonization also. They observed that colonization of GF mice for a short duration i.e., for one month severely decreases bone mass whereas for 8 months increases bone formation. Colonization of mice increases the level of IGF-1 in serum which at a shorter duration inhibits bone formation as it promotes osteoclast formation. On the contrary during long-term colonization, it induced bone formation. Also, short-term colonization enhanced the level of osteoclastogenic cytokines such as RANKL, TNF-α, and IL-1β. in both the colon and bone marrow (Yan et al., 2016). These studies thus reflect that GM can have both catabolic as well as anabolic effects depending on the strain, gender, and duration of colonization.

In contrast to the above-mentioned studies, Quach et al. reported that GM reconstitution does not affect the bone health of GF mice. They observed that colonization of GF mice (Swiss Webster and C57BL/6) with human and mice GM did not alter bone mass significantly. Also, there was no change in the number of osteoclasts precursors, T cells and in the expression of inflammatory cytokines after colonization (Quach et al., 2018). One reason that may be responsible for the differences observed in the study of Quach et al. from other studies is the mode of transplantation of microbiota. The method of colonization used by Sjögren et al. (2012) was coprophagy whereas Quach et al. (2018) used the intragastric gavage method. Thus, changes in the methods of colonization could be responsible for varied results. Other factors for the observed differences in results could be the vendors from where the GF mice were purchased and the animal facility where they were kept. Studies have shown that animals from different facilities harbor a different type of GM. Thus, unique microbiota composition at different animal facilities might also determine the effect of colonization on bone health in GF mice.

Various other studies have demonstrated the role of GM composition on bone health. It is observed that undernourished children have perturbed GM composition. Blanton et al. reported that transplantation of microbiota from undernourished children or infants to GF mice induced impaired growth phenotypes in GF mice. On the other hand cohousing of the GF mice that received the microbiota from the undernourished children with that receiving microbiota from healthy children prevented growth impairments in the recipient mice (Blanton et al., 2016). This supports the notion that microbial diversity determines the net effect of GM on bone health. Another study showed that alterations in the GM composition impairs bone mechanical properties and affect bone strength (Guss et al., 2017). Rios-Arce et al. (2020) reported that dysbiosis caused due to antibiotics treatment, induces bone loss in mice. On the other hand, *Lactobacillus reuteri* administration restored GM composition and alleviated bone loss. A recent study highlighted that transplantation of GM from young rats to aged rats having senile osteoporosis alleviated bone loss by restoring the GM composition of aged rats. This study thereby again supports that healthy GM-diversity promotes bone formation (Ma et al., 2021).

Taken together the effect of GM on bone is very complex and conflicting. Nevertheless, these studies point that GM has the potential to regulate bone homeostasis. To dissect and explore the nexus between GM and bone health a new field was proposed i.e., "Osteomicrobiology", a term coined by Ohlsson's group (Ohlsson and Sjögren, 2015). In the following sections, we will review various mechanisms involved in the reciprocal regulation between GM and skeletal health.

Role of Gut Microbiota in Maintaining Intestinal Integrity

The gut is populated by trillions of microorganisms. To prevent the invasion of microbes into intestinal lamina propria, IECs form the barrier between microbes and gut tissues. Barrier dysfunction allows the access of pathogens into the lamina propria resulting in uncontrolled immune response leading to various inflammatory disorders. The gut barrier is maintained by five different types of specialized epithelial cells. These cells are goblet cells, Paneth cells, microfold (M) cells, enteroendocrine cells, and absorptive enterocytes. Goblet cells secrete mucous which prevents direct contact between the microbiota and IECs.

Mucous is formed by different glycoproteins, the majority of which is Mucin 2 (MUC 2). Paneth cells and enterocytes secrete antimicrobial peptides (AMPs). AMPs are cationic peptides that can kill a wide range of gram-positive and gram-negative bacteria and their secretion is induced by lipopolysaccharide (LPS) and oligonucleotides. "M" cells are specialized epithelial cells of Peyer's patches that transcytose the gut luminal antigens. Enteroendocrine cells produce the hormone serotonin which regulates intestinal inflammation and maintains immune homeostasis (Muniz et al., 2012; Yu, 2012). Apart from specialized IECs, secretory IgA (sIgA) and tight junctions (TJs) also regulate the intestinal barrier. sIgA antibody is released onto the luminal surface where it coats the inflammatory commensals and leads to their neutralization. TJs are protein complexes present on the apical surface of enterocytes. TJs limit the passage of molecules through the IECs. Disruptions in the functioning of these specialized cells and TJs result in the leaky gut that is observed in various diseases such as IBD and IBS (Lee et al., 2018). Impaired gut integrity is also reported in various bone pathologies. Li et al. (2016) showed that the gut barrier is impaired during post-menopausal osteoporosis. They reported that sex steroid deficiency modifies the expression of TJ proteins causing enhanced intestinal permeability. Increased gut permeability further leads to expansion of Th17 cells and release of osteoclastogenic cytokines such as IL-17, RANKL, and TNF-α in the intestine and bone marrow resulting in bone resorption. Nakajima et al. observed impaired gut barrier function in periodontitis (Nakajima et al., 2015). Increased intestinal barrier dysfunction was reported to be associated with the pathology of RA (Matei et al., 2021). As gut integrity regulates bone health, proper maintenance of barrier function is required for inhibition of intestinal inflammation and thus inflammatory bone loss.

Gut microbiota maintains epithelial barrier and regulates gut integrity through various mechanisms (**Figure 3**). GM induces mucous secretion. GF animals have less mucous secretion because of fewer and smaller goblet cells in them than the CONV-R mice (Deplancke and Gaskins, 2001). GM promotes mucous secretion through the production of SCFAs. Butyrate which is one of the SCFAs produced by microbiota promotes the expression of MUC-2 in goblet cells and induces the production of AMPs from IECs (Liu et al., 2021). GM also stimulates the expression of junctional proteins. Administration of indole that is produced by commensal microbiota from tryptophan metabolism in GF mice upregulates the expression of TJ proteins in colonic epithelial cells by activating the pregnane X receptor (Shimada et al., 2013; Venkatesh et al., 2014). SCFAs such as butyrate also upregulates the expression of TJ proteins like claudin-1 and zonula occludens-1 (Liu et al., 2021). GM is required for IgA production. GF animals have a smaller number of IgA-producing B cells (Smith et al., 2007). GM induces the secretion of AMPs. IECs release AMPs by sensing bacteria which depends on the NOD2 and myeloid differentiation primary response 88 (MyD88) signaling. NOD2 recognizes the bacterial muramyl dipeptide and provides protective immunity. Sensing of bacteria by NOD2 results in the production of AMPs such as cryptdins. NOD2 deficient mice have decreased production of AMPs and are susceptible to infection from *Listeria monocytogenes* and *Mycobacterium paratuberculosis* (Ayabe et al., 2000; Kobayashi, 2005). MyD88 is a canonical downstream adapter protein of toll-like receptor (TLR) and IL-1 receptor families. MyD88 signaling maintains mucosal homeostasis and protects against bacterial pathogens like *Citrobacter rodentium* and *Salmonella enterica* (Bhinder et al., 2014). MyD88 signaling also induces the production of AMPs by IECs. Mice lacking MyD88 in IECs have reduced production of AMPs, e.g., RegIIIγ and Defa-rs1 and have decreased mucous secretion (Bhinder et al., 2014). GM also maintains barrier integrity by inducing immune cells to produce cytokines such as IL-22. Immune cells such as Th17 cells regulate the epithelial barrier functions by secreting IL-17 and IL-22. Differentiation of Th17 cells is mainly induced by single filamentous bacteria (SFB) which adhere to the epithelial cells of the small intestine and induce the expression of serum amyloids (SAA). SAA stimulates $CD11c^{+}$ myeloid cells to secrete IL-1β which along with other factors like IL-6 and TGF-β induce the differentiation of Th17 cells (Atarashi et al., 2011). Th17 cells then secrete the cytokines IL-22, IL-17A and IL-17F. These cytokines enhance the expression of AMPs such as β-defensin 2, S100A9, S100A7, and S100A8 (Liang et al., 2006). Parasitic helminths like *Nippostrongylus brasiliensis* stimulate IL-25 secretion from chemosensory tuft cells which are present in the gut epithelium. IL-25 activates the innate lymphoid cells (ILC)-2 to secrete IL-4 and IL-13 which further induces goblet cell hyperplasia and mucous secretion (Gerbe et al., 2016). Altogether these studies suggest that GM has a very significant role in the regulation and maintenance of gut epithelial cell integrity, which further has a role in the regulation of bone health.

The Gut-Immune-Bone Axis

From recent studies, it is observed that there is dynamic cross-communication between the skeleton and immune system. Both the systems share the common developmental niche i.e., bone marrow. Growing awareness of the close interrelationship between the bone and immune system has stimulated the development of a new field of immunology termed "Osteoimmunology" (Walsh et al., 2006). Osteoimmunology deals with the interaction between both these systems (Dar et al., 2018a). Immune cells by secreting various cytokines influence the development of bone. Immune cells such as Tregs, Bregs, and Th17 cells have the most important role in bone regulation. Th17 cells promote bone loss by stimulating osteoclastogenesis. Th17 cells induce bone resorption directly by secreting RANKL or indirectly *via* the production of IL-17. IL-17 is an osteoclastogenic cytokine that induces expression of RANKL on osteoclastogenesis supporting cells including stromal cells and osteoblasts. Moreover, IL-17 also promotes the production of inflammatory cytokines like TNF-α, IL-1, and IL-6 which further stimulate the expression and activity of RANKL (Wang et al., 2013). On the contrary, Tregs prevent bone loss by inhibiting osteoclastogenesis. It is reported that Tregs suppress MCSF and RANKL induced osteoclastogenesis in a dose-dependent manner. Zaiss et al. showed that Tregs suppressed osteoclasts differentiation partly *via* secretion of TGF-β, IL-4, and IL-10 but majorly through a cell-cell contact-dependent manner *via* cytotoxic T lymphocyte-associated

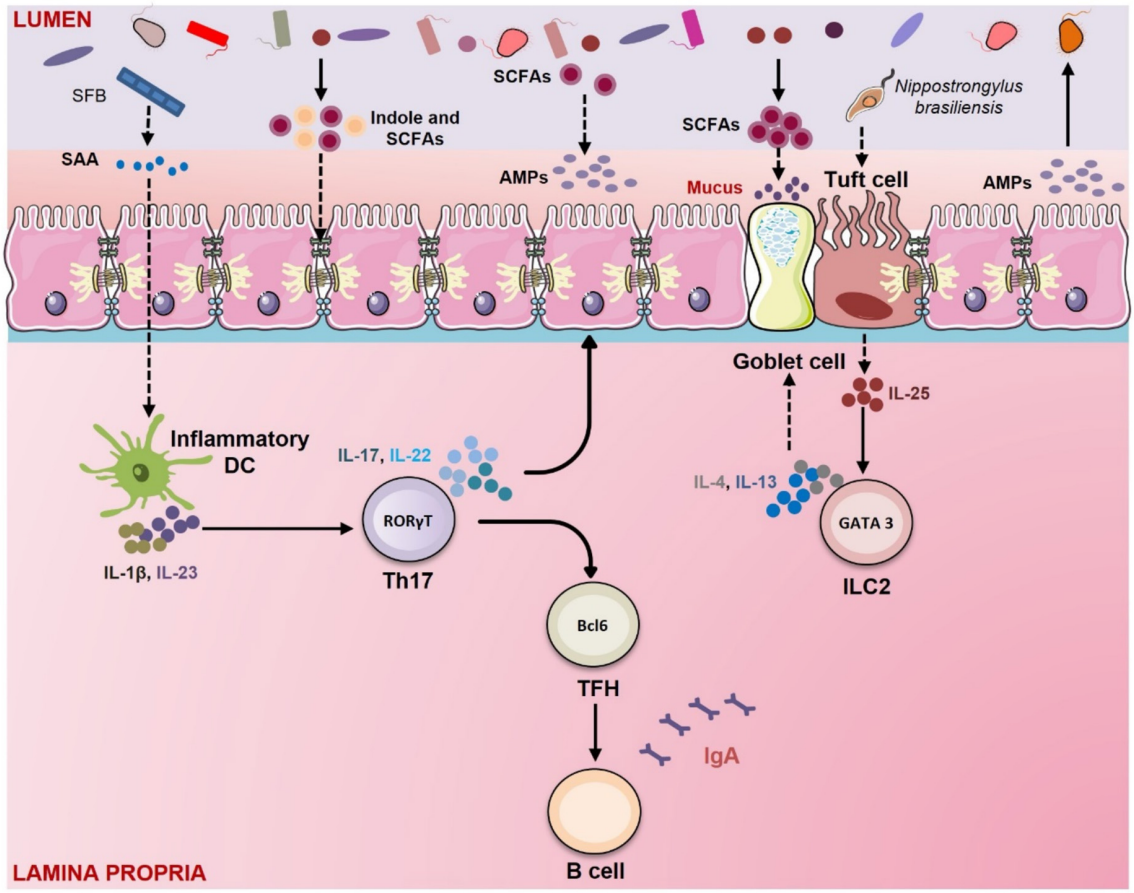

FIGURE 3 | Gut membrane integrity: Role of Gut Microbiota (GM) and immune system. GM has a crucial role in regulating gut permeability. GM maintains intestinal integrity *via* several mechanisms. In mice segmented filamentous bacteria (SFB) induce the secretion of serum amyloid A (SAA) from epithelial cells which further activates the dendritic cells to secrete IL-1β and IL-23. IL-1β and IL-23 promote the differentiation of Th17 cells which produce IL-17 and IL-22. These cytokines stimulate the epithelial cells to secrete antimicrobial peptides (AMPs). GM produces tryptophan metabolites like indole that enhance the expression of tight junction (TJ) proteins. Short-chain fatty acids (SCFAs) produced by GM promote the goblet cells to produce mucus. SCFAs such as butyrate also upregulate the expression of tight junction (TJ) proteins and induce the production of AMPs from epithelial cells. Parasites like *Nippostrongylus brasiliensis* promote the secretion of IL-25 from tuft cells. IL-25 stimulates the innate lymphoid cells (ILC)-2 to produce IL-4 and IL-13. These cytokines induce goblet cell hyperplasia and mucous secretion.

antigen 4 (CTLA-4) (Zaiss et al., 2007). On the other hand, Kim et al. showed that Tregs suppressed osteoclastogenesis in a cytokine-dependent manner and not in a cell-cell contact manner (Kim et al., 2007). Similarly, Luo et al. (2011) showed that human peripheral blood mononuclear cells (PBMCs) derived Tregs inhibited differentiation of osteoclasts *via* secretion of anti-osteoclastogenic cytokines like TGF-β and IL-10. Inflammation due to alteration in the Tregs-Th17 cell axis is one of the major factors involved in the pathogenesis of RA and periodontitis (Alunno et al., 2015; Gao et al., 2017). Studies from our lab have established the important role of the Treg-Th17 cell axis in ovariectomized (ovx) mice model (mice model for osteoporosis) (Dar et al., 2018b,c; Sapra et al., 2021c). Recently our group for the first time has established the significant role of regulatory B cells "Bregs" in inhibiting osteoclastogenesis in a contact-independent manner by secreting IL-10 thereby preventing bone loss in ovx mice model (Sapra et al., 2021b). Other immune cells such as Th1 and Th2 also regulate bone health in interferon (IFN)-γ and IL-4 dependent manner, respectively (Dar et al., 2018a). These studies point to the important role of the immune system in osteoporosis, a field with unexplored domains. To explore this interesting role of the immune system in osteoporosis, we proposed a novel field termed "Immunoporosis" which specifically deals with the role of various immune cells in the pathophysiology of osteoporosis (Srivastava et al., 2018; Sapra et al., 2021a).

It is reported that GM is required for the development of the immune system. Several implications in the immune system have been reported in the absence of GM in GF animals. GF animals have a reduced number of IgA secreting B cells and $CD4^+$ T cells in the lamina propria. They have smaller Peyer's patches with a reduced number of lymphoid follicles. GF animals have less developed B and T cell zones of the spleen and reduced secretion of IgG antibodies (Smith et al., 2007). On the contrary transfer of microbiota in GF animals restore the development of the immune system. It is observed that GM can maintain bone homeostasis

by regulating the immune system. Several studies have shown the role of GM in the development of immune cells. It is observed that colonization of GF mice with SFB and *Clostridia*-related species induces the development of T helper cells (Gaboriau-Routhiau et al., 2009). SFB induces the differentiation of Th17 cells (Talham et al., 1999; Wu et al., 2010). SFB is reported in mice but not in humans thus its role in inducing Th17 cells is reported in mice only. However, some studies have shown the presence of SFB in humans also but its role in the induction of Th17 cells is still not clear (Chen et al., 2018; Jonsson et al., 2020). But in humans another symbiont bacteria *Bifidobacterium adolescentis* is reported that just like SFB is sufficient to induce Th17 cells (Tan et al., 2016). *Clostridium* species particularly that from the cluster IV and XIVa stimulate the differentiation of Tregs (Atarashi et al., 2011). It is reported that in healthy individuals bacterial antigens are required for expansion and generation of Tregs (Strauch, 2005) along with maintaining the balance of Tregs and Th17 cells (Ivanov and Littman, 2010). Polysaccharide A (PSA) produced by *Bacteroides fragilis* induces the differentiation of Tregs and subsequently signals the differentiated Tregs *via* TLR 2 to suppress Th17 response (Wu and Wu, 2012). GM is also required for the development of Bregs. The LPS produced by gram-negative bacteria or microbiota induced production of IL-6 and IL-1β from the dendritic cells (DCs) and macrophages induce the differentiation of Bregs (Rosser et al., 2014; Rosser and Mauri, 2015). Altogether these studies decipher the important and convincing role of GM in modulating bone health *via* regulating the host immune system i.e., the Gut-Immune-Bone axis (**Figure 4**).

Gut Microbiota and Endocrine Regulation

Gut microbiota is now considered a novel endocrine organ and can maintain bone homeostasis by directing the activities of hormones which are crucial for bone regulation as discussed below:

Estrogen

Estrogen is the key hormone for bone development, as its deficiency results in the development of a disease condition termed post-menopausal osteoporosis. Estrogen regulates bone health either by its direct effect on the bone cells or by modulating the immune system. Estrogen suppresses bone loss by downregulating the expression of RANKL on mesenchymal cells. During estrogen deficiency, RANKL expression is enhanced on bone lining cells resulting in bone loss (Streicher et al., 2017). Luo et al. (2011) showed that estrogen prevents osteoclast differentiation by stimulating Tregs. Estrogen treatment enhances the suppressive capacity of Tregs by upregulating the expression of IL-10 and TGF-β. Estrogen also inhibits the development of Th17 cells and during estrogen deficiency differentiation of Th17 increases which promotes osteoclasts differentiation.

Gut microbiota regulates estrogen metabolism and increases the level of estrogen in the bloodstream. Estrobolome is the collection of microbial genes that are capable of metabolizing estrogen (Plottel and Blaser, 2011). Bacterial species containing the enzyme β-glucuronidases and β-glucuronides convert the conjugated form of estrogen into deconjugated form. Deconjugated estrogen enters into the circulation and binds to the estrogen receptors present on various organs such as the ovary, breast, testis, prostate, bone, and brain (Plottel and Blaser, 2011). Specific GM also processes phytoestrogens into estrogen metabolites. Phytoestrogens are polyphenols derived from the dietary compounds of plants such as soya, flaxseeds, fruits, and vegetables. Phytoestrogens have a structure similar to estrogens and thus can bind to estrogen receptors and induce estrogenic effects. Some intestinal bacteria transform phytoestrogens (e.g., isoflavones and lignans) to enterolignans which have more estrogenic activity (Bowey et al., 2003; Landete et al., 2016).

Parathyroid Hormone (PTH)

PTH is an 84 amino acids long polypeptide that is released from parathyroid glands. PTH regulates bone remodeling and promotes both bone formation and resorption depending on the duration of its treatment (Ma et al., 2001; Jilka et al., 2009; Silva and Bilezikian, 2015). GM has a role in the regulation of both PTH-mediated bone formation and resorption. Li et al. (2020) showed that PTH-induced bone formation is dependent on GM and PTH was unable to enhance bone mass in GF mice. Microbiota increases butyrate concentration which is required for PTH to enhance the level of Tregs in the bone marrow which then prevents bone loss. Another study by the same group reported that PTH promotes bone loss only in mice having SFB microbiota. SFB microbiota enables PTH to expand Th17 and TNF-α^+ T cells in the gut and promote their migration from gut to bone marrow where they lead to bone loss (Yu et al., 2020).

Insulin-Like Growth Factor (IGF)-1

IGF-1 belongs to the family of insulin-related proteins that stimulate skeleton development. IGF-1 promotes differentiation of osteoblasts and induces bone formation in an endocrine, paracrine and autocrine fashion (Giustina et al., 2008; Locatelli and Bianchi, 2014). GM regulates the activity of IGF-1. Yan et al. showed that long-term colonization of GF mice with microbiota from CONV-R mice stimulated bone formation by increasing production of IGF-1. In contrast, antibiotic treatment of CONV-R mice suppressed bone formation and decreased the level of IGF-1 in serum. Another study reported that *L. plantarum* supplementation along with prebiotic inulin increased the expression of IGF-1 in liver (Kareem et al., 2016). *L. plantarum* was also observed to regulate bone growth in infant mice during chronic undernutrition by enhancing the synthesis and activity of IGF-1 (Schwarzer et al., 2016). In support of the above studies, Avella et al. further reported that *L. rhamnosus* administration enhanced backbone calcification in zebrafish by inducing the IGF system (Avella et al., 2012).

Serotonin

Serotonin is a monoamine hormone and neurotransmitter required for the regulation of various brain functions and 95% of the serotonin is synthesized in the gastrointestinal tract by the enterochromaffin cells. Serotonin is also secreted by

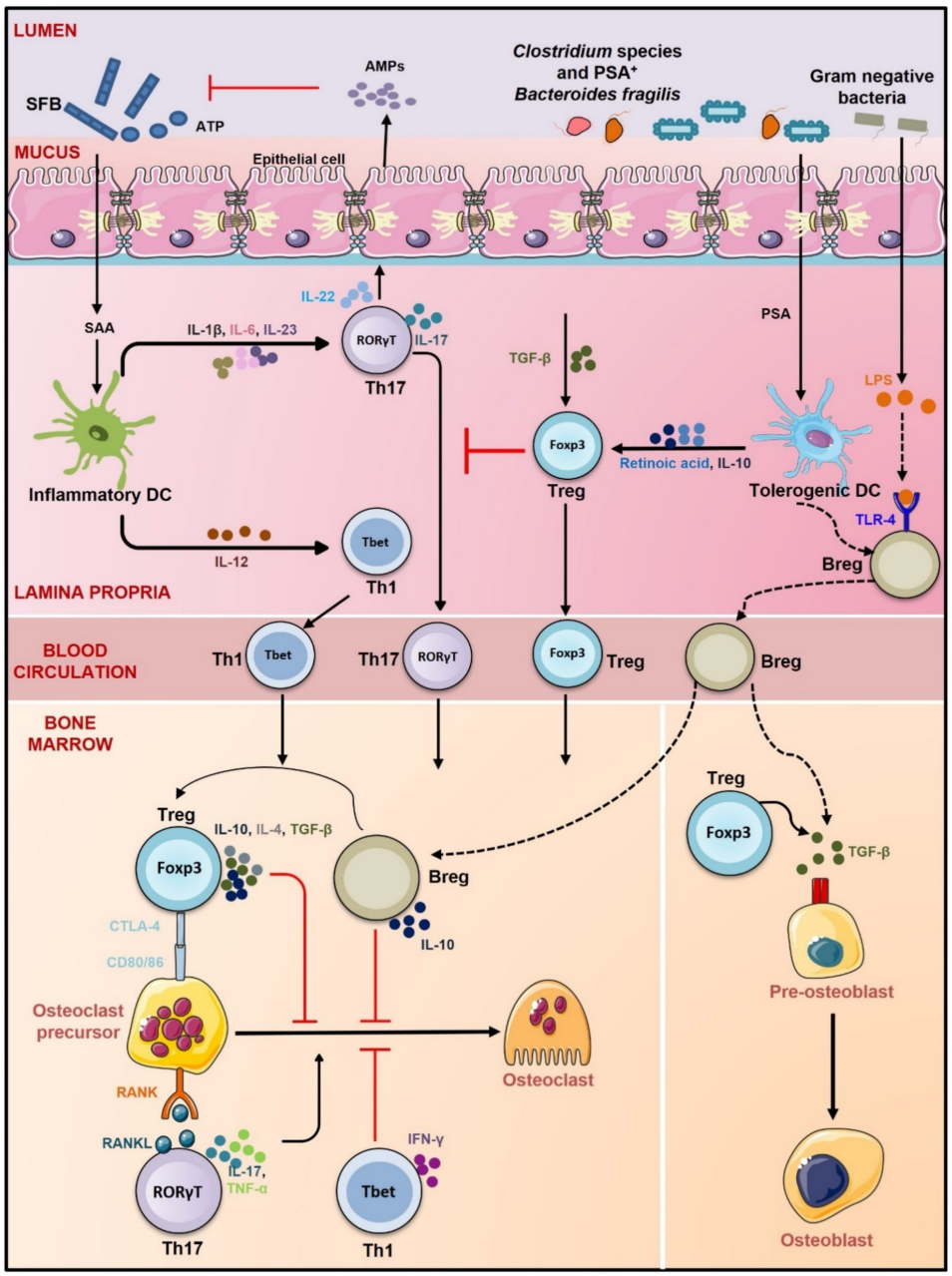

FIGURE 4 | Gut-Immune-Bone axis. GM promotes the development of Treg, Th1 cells, Breg, and Th17 cells. *Clostridium* species, *Bacteroidetes fragilis,* and gram-negative bacteria promote differentiation of Tregs and Bregs *via* inducing tolerogenic DCs whereas segmented filamentous bacteria (SFB) through induction of inflammatory DCs stimulate differentiation of Th17 cells (role of SFB in inducing Th17 cells is observed in mice only). Tregs, Bregs, and Th1 cells prevent osteoclastogenesis *via* CTLA-4, IL-10, IL-4, TGF-β, and IFN-γ, respectively. Th17 cells on the other hand promote osteoclastogenesis by secreting IL-17, RANKL, and TNF-α. Tregs also induce differentiation of osteoblasts *via* TGF-β. Bregs also secrete TGF-β and thus like Tregs might also regulate osteoblastogenesis. By promoting the development of both anti-osteoclastogenic and osteoclastogenic cells, GM regulates the balance between bone formation and resorption and thus maintains bone homeostasis lines represent proposed mechanism of action.

osteoclast precursors and raphe neurons and is called bone-derived and brain-derived serotonin, respectively. Serotonin has a very significant role in the regulation of bone metabolism. Serotonin can both stimulate and inhibit bone formation (Lavoie et al., 2017). Serotonin produced by osteoclast precursors stimulates bone formation by inducing osteoblastogenesis. Brain-derived serotonin also regulates bone remodeling positively and stimulates bone formation by inhibiting the suppressive effect of sympathetic neurons on osteoblasts. However, serotonin produced in the intestine inhibits bone formation by suppressing

the proliferation of osteoblasts *via* binding to the 5-HT1B receptors (Lavoie et al., 2017).

Gut microbiota upregulates serotonin synthesis in the intestine. In contrast, antibiotic treatment prevents serotonin secretion. Sjögren et al. (2012) showed that GF mice had reduced level of serum serotonin than SPF mice. Yano et al. (2015) demonstrated that colonization of GF mice with spore-forming bacteria restored the level of serum and colon serotonin to that of SPF mice. It is also reported that microbes like *Streptococcus*, *Corynebacterium,* and *E. coli* induced the synthesis of serotonin in cultures (Li L. et al., 2019). Reigstad et al. demonstrated that GM regulates serotonin synthesis by producing SCFAs. SCFAs enhance the expression of tryptophan hydroxylase (TPH1), the enzyme that produces serotonin in enterochromaffin cells (Reigstad et al., 2015).

Leptin

Gut microbiota regulates the gut-brain axis in part *via* the synthesis of leptin. Leptin is secreted by adipocytes and enterocytes and regulates various functions like neuroendocrine regulation, bone metabolism, and energy homeostasis (Upadhyay et al., 2015). GM enhances serum leptin levels. Queipo-Ortuño et al. (2013) observed that serum leptin level was positively correlated with the abundance of *Bifidobacterium* and *Lactobacillus* species. Another study reported that treatment of rats with antibiotic vancomycin reduced leptin in serum (Lam et al., 2012). Leptin inhibits the synthesis of brain-derived serotonin. Brain-derived serotonin binds to Ht2rC receptors present on ventromedial hypothalamic neurons and induces bone growth (Yadav et al., 2009). Leptin receptors (ObRb) are present on the raphe neurons or brainstem neurons that synthesize serotonin in the brain (Scott et al., 2009). Leptin binds to these receptors and inhibits the synthesis and release of serotonin from brainstem neurons (Yadav et al., 2011). Thus, GM-induced leptin can indirectly stimulate bone resorption by reversing the effect of brain-derived serotonin on bone growth.

Role of Gut Associated Metabolites (GAMs) in the Regulation of Bone Health

Metabolites produced by GM maintain bone homeostasis as discussed below (**Figure 5**).

Short-Chain Fatty Acids

SCFAs are secondary metabolites produced in the colon from bacterial fermentation of undigested complex carbohydrates (Rooks and Garrett, 2016). SCFAs are of many types e.g., acetate, propionate, butyrate, pentanoate, and hexanoate. SCFAs act as an energy source not only for the GM but also for the IECs. SCFAs regulate a diverse range of physiological functions related to human health. SCFAs are ligands for G protein-coupled receptors (GPCRs) and regulate the activity of various hematopoietic and non-hematopoietic cells through GPCRs. Regulatory activity of SCFAs requires signaling through GPCRs primarily *via* GPR43 (also named as FFAR2), GPR41 (also named as FFAR3), and GPR109A (also named as HCAR2) (Sivaprakasam et al., 2016). SCFAs are controllers of osteoclast metabolism. It is reported that supplementation of either a high fiber diet or SCFAs to mice prevented postmenopausal bone loss and RA by inhibiting osteoclasts differentiation. SCFAs (propionate and butyrate) treatment downregulate the expression of osteoclast genes such as tumor necrosis factor receptor-associated factor 6 (TRAF6) and nuclear factor of activated T-cells (NFATc1) resulting in decreased osteoclastogenesis (Lucas et al., 2018). SCFAs prevent bone loss by interacting with the FFAR2 receptor present on osteoclasts. Deterioration of maxillary bone was observed in FFAR2 deficient mice. Administration of a high fiber diet on the other hand partially restored the bone damage. *In vitro* increased osteoclastogenesis was observed in bone marrow cells derived from FFAR2 deficient mice whereas treatment with SCFAs and FFAR2 agonist phenylacetamide-1 prevented osteoclastogenesis (Montalvany-Antonucci et al., 2019). SCFAs regulate fibroblast activity and it is observed that propionate supplementation has a role in mitigating arthritis by preventing synovial fibroblasts mediated production of inflammatory mediators (Friščić et al., 2021). Apart from regulating the activity of osteoclasts, SCFAs also maintain immune homeostasis (**Figure 6**). SCFAs promote the induction of Tregs and inhibit the development of Th17 cells (Asarat et al., 2016). SCFAs induce differentiation of Tregs by interacting with the GPR43 receptor present on $CD4^+$ T cells (Smith et al., 2013; Rooks and Garrett, 2016). SCFAs are also inhibitors of histone deacetylases (HDACs). It is observed that treatment of naïve T cells with butyrate under Tregs polarizing conditions increased histone H3 acetylation in the promoter and conserved non-coding sequence of Foxp3 gene resulting in differentiation of Treg (Furusawa et al., 2013). Another SCFA acetate promoted acetylation of Foxp3 through inhibition of HDAC9 (Thorburn et al., 2015). SCFAs induced Tregs thereby alleviate bone loss by suppressing osteoclasts differentiation. These Tregs also inhibit bone loss by interacting with $CD8^+$ T cells. Tyagi et al. reported that butyrate-induced Tregs stimulate $CD8^+$ T cells in the bone marrow to secrete Wnt ligand Wnt10b. Wnt10b then further induces bone formation by activating the Wnt signaling in osteoblasts (Tyagi et al., 2018). Butyrate administration suppressed arthritis in mice by inducing Bregs. Butyrate supplementation enhances the production of 5-Hydroxyindole-3-acetic acid (HIAA), an AhR ligand that programs B cells to become Bregs which mitigate inflammatory arthritis (Rosser et al., 2020). Also, SCFAs can positively influence bone healing process by regulating the activity of bone cells and thus can be employed for fracture healing (Wallimann et al., 2021). Collectively, all these studies clearly establish that SCFAs supplementation can be exploited as a potential therapeutics for the management of various bone pathologies including osteoporosis, fractures and RA.

Bile Acids

Bile acids are surfactants or emulsifying agents that enhance the absorption and digestion of lipids. Primary bile acids such as cholic acid and chenodeoxycholic acid are produced in the liver by hepatocytes from cholesterol by several enzymatic reactions. Primary bile acids are then further processed by GM into secondary bile acids like deoxycholic and lithocholic acid in the colon where they regulate various metabolic pathways (Staels and Fonseca, 2009). Several studies have shown the role of bile acids in

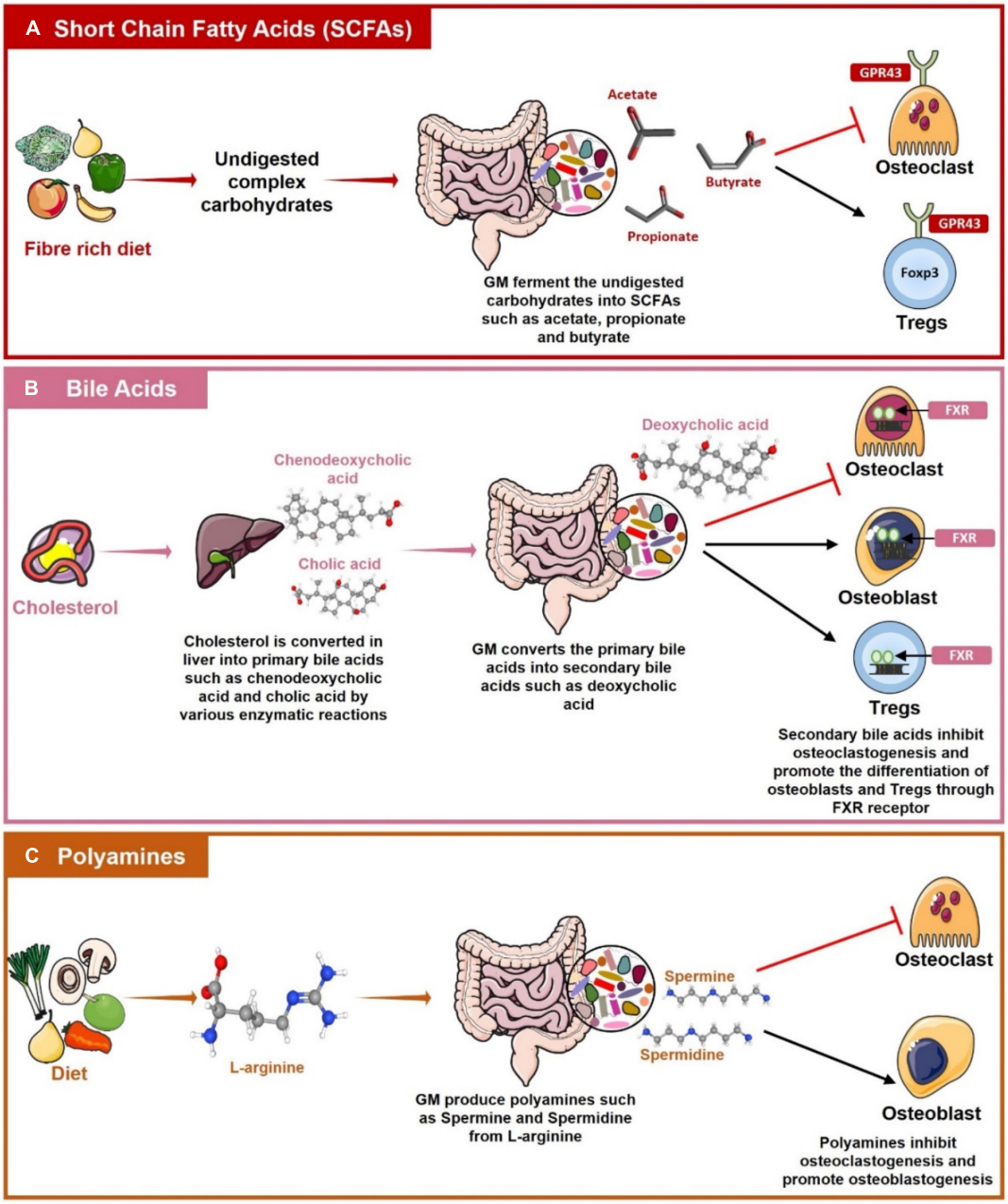

FIGURE 5 | Role of Gut Associated Metabolites (GAMs) in regulating Bone Health. **(A)** Gut microbiota (GM) produces short-chain fatty acids (SCFAs) such as acetate, propionate, and butyrate by the fermentation of dietary fibers. SCFAs then regulate bone health by inhibiting osteoclastogenesis and by promoting the differentiation of Tregs with the help of G-protein coupled receptor (GPR)-43. **(B)** Primary bile acids such as cholic acid and chenodeoxycholic acid are produced in the liver from cholesterol. These primary bile acids reach the intestine where GM converts them into secondary bile acids such as deoxycholic acids. Bile acids inhibit osteoclastogenesis whereas inducing osteoblasts and Tregs differentiation by interacting with Farnesoid X receptor (FXR). **(C)** L-arginine produced from the diet is metabolized by the GM into polyamines such as Spermine and Spermidine which have a role in suppressing osteoclastogenesis and promoting osteoblastogenesis.

the regulation of bone health. Decreased expression of G-protein coupled bile acid receptor 5 (Tgr5) is reported on PBMCs of RA patients as compared to healthy controls. Expression of Tgr5 was found to be negatively correlated with disease severity. On the other hand, treatment with lithocholic acid has been reported to decrease arthritis score in collagen II-induced arthritis mouse model along with suppressing inflammatory responses in RA patients (Li Z. et al., 2019). Zhao et al. reported that bile acids are positively correlated with BMD as osteoporotic and osteopenic post-menopausal women have significantly reduced levels of bile acids than healthy controls (Zhao et al., 2020). It is observed that bile acids induce differentiation of osteoblasts *via* stimulation of

farnesoid X receptor (FXR). Activation of FXR upregulates Runx2 and β catenin expression and thus promotes osteoblastogenesis (Cho et al., 2013). Bile acids also inhibit osteoclastogenesis by downregulating c-Fos and NFATc1 expression *via* FXR activation (Zheng et al., 2017). Li et al. showed that bile acids can inhibit osteoclastogenesis *via* induction of Tgr5. Tgr5 stimulation prevents osteoclast differentiation by increasing phosphorylation of AMP-activated kinase (AMPK) (Li S.-C. et al., 2019). They also reported that activation of both Tgr5 and FXR can prevent estrogen-induced bone loss (Li Z. et al., 2018). Bile acids are important modulators of the host immune system. It is observed that bile acids induce differentiation of Tregs by enhancing Foxp3 expression and suppressing differentiation of Th17 cells by directly binding to RORγt (Hang et al., 2019). Thus, bile acids also have the potential in regulating bone health *via* modulating the host immune system.

Polyamines

Polyamines are polycations that are required for various biological processes in the body such as cell growth, proliferation, and survival (Minois et al., 2011). The three main polyamines are spermine, spermidine and putrescine. Polyamines are required for the proper maintenance of bone health. It is reported that polyamine (spermidine and spermine) supplementation inhibits ovx induced bone loss *via* suppression of osteoclasts differentiation and proliferation (Yamamoto et al., 2012). Yamada et al. reported that daily supplementation of polyamines rich *Saccharomyces cerevisiae* S631 significantly prevented osteoclasts activation and bone loss in ovx mice (Yamada et al., 2019). Daily administration of spermine to rats ameliorated bone and cartilage destruction due to collagen-induced arthritis (Iezaki et al., 2012). Albert et al. (2015) reported that specific alterations in polyamines metabolism led to Snyder-Robinson Syndrome (SRS), a disease characterized by profound depletion of osteoclasts and osteoblasts. Recently, it has also been reported that warmth exposure prevents osteoporosis in mice by inducing the production of polyamines. Polyamines inhibit the differentiation of osteoclasts whereas promoting the differentiation of osteoblasts (Chevalier et al., 2020). Polyamines like spermidine modulate the immune system and have a role in the prevention of arthritis *via* inhibiting the polarization of inflammatory M1 macrophages (Yuan et al., 2021). Polyamines also have a very important role in maintaining gut integrity. They regulate the epithelial barrier of the gut by activating the transcription factor c-Myc which then upregulates the expression of TJ protein E-cadherin (Liu et al., 2009). Polyamines also regulate the gut barrier by stimulating the expression of TLR2 on IECs. It is reported that in the absence of polyamines expression of TLR2 decreases on IECs resulting in enhanced gut permeability (Chen et al., 2007).

Based on the above studies, it can be concluded that GM has a crucial role in the development of bone health and thus dysregulation of GM can lead to various inflammatory bone pathologies. Various drugs are currently being employed for the treatment of different bone disorders but restoring the dysregulated GM would be a path-breaking approach in managing various bone pathologies. GM can be modulated by diet, antibiotics, and drugs. Dietary interventions are the current favorite methods for the manipulation of GM. Dietary interventions include probiotics, prebiotics, synbiotics, and postbiotics. Biotics is the most favorable therapy for GM-associated disorders and can be easily adopted for preventing various bone pathologies. In the following sections, we will now review the possibility of employing dietary inventions as novel therapeutics for the treatment and management of various inflammatory bone pathologies.

DIETARY INTERVENTIONS AND MODULATION OF GUT MICROBIOTA

Dietary interventions that are most commonly in use for modulation of GM are discussed below:

Probiotics

Probiotics are live microorganisms which when administered in adequate amounts confer health benefits on the host. Probiotics are contained in various dietary supplements and fermented foods like yogurt, cheese, kefir, wine, bread, and kumis (Ozen and Dinleyici, 2015). The most widely used probiotics are *Lactobacillus* and *Bifidobacterium* species (Gupta and Garg, 2009). Probiotics are found effective against various clinical manifestations such as IBD, IBS, diabetes, obesity, and non-alcoholic fatty liver disease (Gupta and Garg, 2009; Verna and Lucak, 2010; Plaza-Diaz et al., 2019). Recently various studies have shown the role of probiotics in preventing bone disorders. One of the mechanisms *via* which probiotics attenuate bone loss is by preventing alterations in the GM composition. Dysbiosis is reported in various bone diseases. It is reported that the abundance of *Firmicutes* is significantly higher whereas that of *Bacteroidetes* is significantly lower in osteoporotic patients (Wang et al., 2017). Another study reported that osteoporotic patients have significantly higher proportions of *Faecalibacterium* and *Dialister* genera (Xu et al., 2020). Altered *Firmicutes*/*Bacteroidetes* ratio is also observed in RA, osteoarthritis, and periodontitis (Lourenço et al., 2018; Lee et al., 2019). Probiotics supplementation prevents the growth of various pathogenic bacteria thereby restoring the composition of gut flora and thus preventing dysbiosis-mediated bone loss. Studies have shown the role of probiotics like *Bifidobacterium* spp. and *Lactobacillus reuteri* in preventing dysbiosis-associated bone loss (Achi et al., 2019; Schepper et al., 2019). Probiotics also inhibit bone loss by preventing inflammation. Several studies including our own have shown the role of inflammation in bone loss. It is observed that the Tregs-Th17 cell axis alters during various bone diseases like osteoporosis, RA, osteoarthritis and periodontitis (Leipe et al., 2010; Kikodze et al., 2016; Gao et al., 2017; Li et al., 2017). Studies from our lab and other have shown that supplementation of probiotics such as *Lactobacillus acidophilus*, *Bacillus clausii,* and *Lactobacillus rhamnosus* prevent bone loss by restoring the pivotal "Treg-Th17 cell" balance, an important determinant of bone loss in osteoporosis (Dar et al., 2018b,c; Sapra et al., 2021c). Probiotics have also been reported in directly regulating

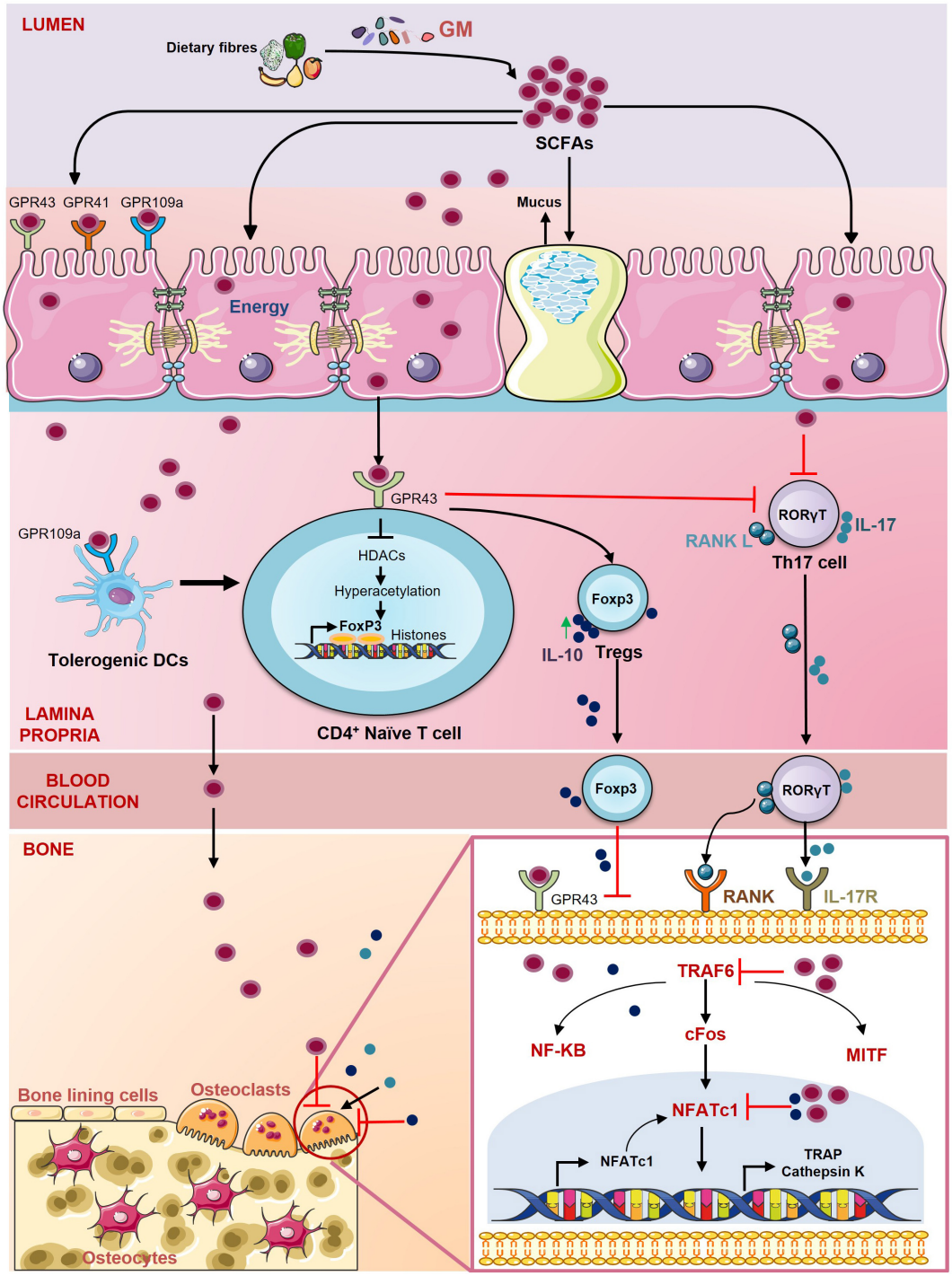

FIGURE 6 | Role of short-chain fatty acids (SCFAs) in regulating Bone Health. SCFAs are the energy source for the epithelial cells and regulate the activity of various hematopoietic and non-hematopoietic cells through the G protein-coupled receptors (GPCRs) such as GPR41, GPR43, GPR109a. SCFAs promote the differentiation of Tregs through inhibition of histone deacetylases (HDACs) and suppress the secretion of IL-17 from Th17 cells. SCFAs also stimulate the development of Tregs by inducing tolerogenic DCs. SCFAs inhibit the differentiation of osteoclasts by downregulating the expression of key osteoclastogenic markers TRAF6 and NFATc1.

bone cells e.g., *Lactobacillus reuteri* 6475 and *Lactobacillus rhamnosus* have a role in stimulating osteoblastogenesis along with inhibiting the development of osteoclasts (Quach et al., 2019; Sapra et al., 2021c). Probiotics such as *Bifidobacterium longum* and *Lactobacillus reuteri* 6475 enhance bone formation by decreasing gut permeability and increasing the absorption

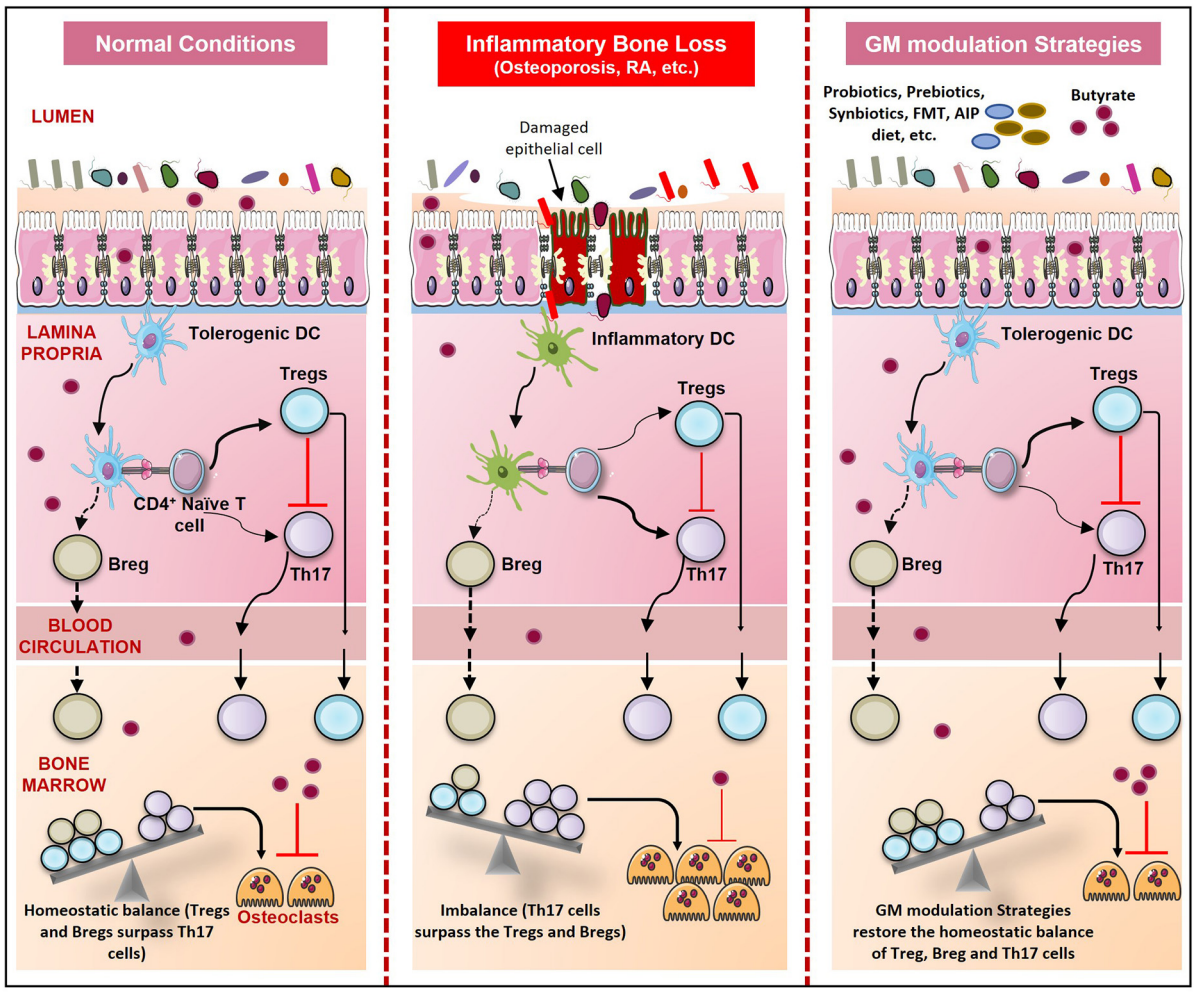

FIGURE 7 | GM modulation Strategies and Skeletal Health. During normal conditions, immune homeostasis is maintained. But in bone pathologies like osteoporosis, RA, and periodontitis due to dysbiosis, gut permeability increases resulting in an increase in the number of inflammatory Th17 cells. These Th17 cells outcompete the regulatory Tregs and Bregs which result in enhanced osteoclastogenesis and thus bone loss. Probiotics, prebiotics, synbiotics, postbiotics, FMT, Orthogonal niche engineering, autoimmune protocol diet (AIP), and Personalized GM modulation strategies prevent dysbiosis and restore the homeostatic balance of immune and bone cells.

of Ca and vitamin D (Rodrigues et al., 2012; Röth et al., 2019).

Prebiotics

Prebiotics are defined as "non-digestible food ingredient that beneficially affects the host by selectively stimulating the growth and activity of one or a limited number of bacteria in the colon, and thus improves host health" (Gibson et al., 2010). Common prebiotics is galactooligosaccharides (GOS), fructooligosaccharide (FOS), and trans-galactooligosaccharide (TOS). Prebiotics act as a nutrient source for GM and their degradation results in the formation of SCFAs (Davani-Davari et al., 2019). Prebiotics can selectively influence and modify GM composition by promoting the growth of certain microorganisms. Several recent studies have shown that prebiotics such as Konjoc oligosaccharides, GOS, FOS can significantly enhance bone mass by reversing dysbiosis (Ai et al., 2021; Zhang et al., 2021). Prebiotics also enhance bone mass by decreasing intestinal permeability and thus preventing systemic inflammation (Zhang et al., 2021). Xylo-oligosaccharides (XOS) treatment was observed to increase BMD by upregulating the expression of Ca transporters in the intestine (Gao and Zhou, 2020). It is reported that FOS also enhances osteogenesis and thus induces bone formation.

Synbiotics

Synbiotics are a mixture of probiotics and prebiotics. In May 2019, the International Scientific Association for Probiotics and Prebiotics defined synbiotics as "a mixture compromising live microorganisms and substrates selectively utilized by host microorganisms that confers a health benefit on the host". The concept of synbiotics has emerged nearly 25 years

TABLE 1 | Role of various Biotics in regulating bone health.

S. No.	Name	Animal species used	Findings	Disease	References
1.	*L. helveticus*	Sprague-Dawley rats	↑BMD ↑Bone strength	Osteoporosis	Narva et al., 2007
2.	*L. casei*	Wister rats	↓Arthritis score ↓Knee inflammation	Arthritis	Amdekar et al., 2012
3.	Yacon Flour and *Bifidobacterium longum*	Wister rats	↑Ca ↑P ↑Mg	-	Rodrigues et al., 2012
4.	*L. reuteri* ATCC PTA 6475	Balb/c mice	↑BV/TV ↑Tb. N ↑Tb. Th ↓Osteoclast activity	Osteoporosis	Britton et al., 2014
5.	*Bifidobacterium longum*	Sprague-Dawley rats	↑Serum osteocalcin ↑BV/TV ↑Tb. N ↑Tb. Th ↑BMD ↑Strength of femur	Osteoporosis	Parvaneh et al., 2015
6.	*L. rhamnosus* GG and VSL#3	C57BL6/J mice	↑BV/TV ↑Tb. N ↑TB. Th ↑Osteocalcin ↓Tb. Sp	Sex steroid deficiency	Li et al., 2016
7.	*L. casei* Shirota	Elderly patients	↓DASH score ↓Pain	Fracture	Lei et al., 2016
8.	Red clover extract rich in isoflavone aglycones and probiotics	Human females	↑BMD	Post-menopausal osteoporosis	Lambert et al., 2017
9.	*L. casei* Shirota	Human male and females	↓Serum hs-CRP	Knee osteoarthritis	Lei et al., 2017
10.	*Bacillus clausii*	BALB/c mice	↑BV/TV ↑Tb. Th ↑Tb. N ↓ Tb. S	Post-menopausal osteoporosis	Dar et al., 2018b
11.	*L. acidophilus*	BALB/c mice	↑BV/TV ↑Tb. Th ↑Tb. N ↓Tb. S	Post- menopausal osteoporosis	Dar et al., 2018c
12.	SCFAs	C57BL6/J mice	↑Osteoclastogenesis	Post-menopausal osteoporosis	Lucas et al., 2018
13.	*Bacillus subtilis* C-3102	Post-menopausal women	↑BMD	Post-menopausal osteoporosis	Takimoto et al., 2018
14.	*L. reuteri* 6475	Elderly women	↑BMD ↓TRACP-5b	Age-associated bone loss	Nilsson et al., 2018
15.	Fructooligosaccharides and mixture of *Enterococcus faecium*, *Pediococcus acidilactici*, *Bifidobacterium animalis*, and *L. reuteri*	Broilers	↑BMD ↑Bone area	Cyclic heat stress episodes	Yan et al., 2019
16.	*Lactobacillus paracasei* DSM 13434, *Lactobacillus plantarum* DSM 15312, and *Lactobacillus plantarum* DSM 15313	Post-menopausal women	↑BMD	Post-menopausal osteoporosis	Jansson et al., 2019
17.	XOS	ICR mice	↑BMD	-	Gao and Zhou, 2020
18.	*L. rhamnosus*	BALB/c mice	↑BV/TV ↑Tb. Th ↑Tb. N ↓Tb. S	Post- menopausal osteoporosis	Sapra et al., 2021c
19.	Lysates and supernatant of *B. coagulans*, *B. longum*, *L. acidophilus*, *L. rueteri*	Sprague-Dawley rats	↑BMD	Postmenopausal osteoporosis	Montazeri-Najafabady et al., 2019
20.	Culture supernatant of *L. salivarius* MG4265	-	↑Osteoclastogenesis	-	Jung et al., 2021

BMD, Bone mineral density; BV/TV, Bone volume over total volume; Tb. Th, Trabecular thickness; Tb. N, Trabecular number; Tb. S, Trabecular spacing; Ca, Calcium; P, Phosphorus; Mg, Magnesium; SCFAs, Short-chain fatty acids; GOS, Galactooligosaccharides; FOS, Fructooligosaccharide; XOS, Xylooligosaccharides.

ago where it is observed that probiotics and prebiotics can be combined. Synbiotics increase the survival and implantation of live microbial dietary supplements. Synbiotics are divided into complementary and synergistic synbiotics. In Complementary synbiotics both the probiotics and prebiotics work independently to provide health benefits to the host. However, in the synergistic approach, the substrate or the prebiotic enhances the functionality of the probiotics and both prebiotics and probiotics work synergistically to bring health benefits (Swanson et al., 2020). Common probiotics such as *Lactobacillus*, *Bifidobacterium,* and *Bacillus* species and prebiotics like FOS, XOS, and GOS are used for making symbiotic formulations (Pandey et al., 2015). Synbiotics enhance Ca absorption by increasing the expression of Ca-binding proteins. In postmenopausal women, it is observed that administration of fermented plasma milk enhanced oral bioavailability and concentration of isoflavones in plasma. Isoflavones are known to decrease the risk of osteoporosis (Ilesanmi-Oyelere and Kruger, 2020). Synbiotics treatment prevented bone loss in the high fat diet-fed rats by preventing osteoclastogenesis and increasing bone formation activities (Eaimworawuthikul et al., 2020). It is observed that synbiotics administration enhanced the level of bone mineral content, BMD, and bone area in broilers subjected to cyclic heat stress episodes (Yan et al., 2019). In rats, it is reported that administration of Yacon flour with *B. longum* increased the mineral contents of bone (Rodrigues et al., 2012).

Postbiotics

Postbiotics is a relatively new term introduced in the –'biotics' field. Postbiotics are functional bioactive compounds comprising of soluble factors such as metabolites and cell wall components released by the probiotics. Postbiotics constitute metabolic by-products such as SCFAs or factors released upon bacterial lysis such as teichoic acid, polysaccharides, peptidoglycan derived muropeptides, enzymes, peptides, cell surface proteins, and organic acids (Aguilar-Toalá et al., 2018). Jung et al. and Sapra et al. reported that culture supernatants of probiotics prevented RANKL induced osteoclastogenesis. Postbiotics also have a role in the prevention of bone loss. Recently, it is reported that supplementation of ovariectomized rats with lysates and supernatant of *L. casie*, *B. longum*, *B. cougulans*, *L. acidophilus,* and *L. reuteri* significantly increased BMD (Montazeri-Najafabady et al., 2019). Culture supernatants of probiotics prevented osteoclastogenesis of RAW 264.7 macrophages (Jung et al., 2021). We also reported that the culture supernatant of *L. rhamnosus* suppressed osteoclastogenesis *in vitro* (Sapra et al., 2021c). Collins et al. reported that secreted factors of *L. reuteri* prevented bone loss by modulating the immune system (Collins et al., 2019). As discussed earlier SCFAs which are secondary metabolites produced by GM prevent bone loss by modulating the immune system and inhibiting osteoclastogenesis (Lucas et al., 2018; Tyagi et al., 2018). Altogether, probiotics, prebiotics, synbiotics, and postbiotics are promising candidates for being employed as therapeutics in inhibiting inflammatory bone loss *via* various mechanisms (**Figure 7** and **Table 1**).

Orthogonal Niche Engineering

Apart from biotics, various other dietary approaches are used to modulate the GM composition. Recently a new technique called orthogonal niche engineering is harnessed to manipulate the GM. In orthogonal niche engineering microbes and substrate relationship is leveraged by using customized niche for an introduced bacterium. In prebiotics and synbiotics we generally use the common substrates that lead to a momentary increase in the organism's population but not the persistent engraftment of the organisms. However, in the case of orthogonal niche engineering, uncommon substrates are used. For example, Kearney et al. used a seaweed polysaccharide porphyrin to stably engraft the human commensal bacteria *B. plebeius* DSM 17135 to the mice's gut. The introduction of seaweed makes it exclusively accessible to the bacteria, enabling it to colonize and compete with the native commensals. Thus, orthogonal niche engineering provides a novel opportunity for the stable engraftment of microbes in the gut environment (Kearney et al., 2018; Wolter et al., 2021). As various probiotics are lost from the gut after a particular period, orthogonal niche engineering can be harnessed for stable engraftment of these probiotics (Wolter et al., 2021). But currently, studies on orthogonal niche engineering are limited and its role for the management of bone pathologies still needs to be explored.

Autoimmune Protocol (AIP) Diet

As dietary changes result in various autoimmune and inflammatory disorders, formulation of diet that prompts the restoration of immune homeostasis, termed as autoimmune protocol (AIP) diet is also proposed. AIP diet is a version of the paleo diet designed to avoid the inclusion of food that can trigger an unnecessary immune response. As a modern diet is not able to support the healthy microbiome, it results in compromised development of immune system (Singh et al., 2017). AIP diet controls the immune response and evidence supports its role in reducing inflammation and thus can be useful in the treatment of several inflammatory disorders (Wolter et al., 2021). As dysbiosis-associated immune responses promote bone resorption, AIP can also be a potential therapy for preventing inflammatory bone loss. But as there are not many studies in support of the AIP diet, well-designed investigations and clinical trials are required to study the effect of the AIP diet in the context of bone pathologies.

Fecal Microbiota Transplantation

Fecal microbiota transplantation (FMT) also holds the potential along with the dietary supplements in preventing GM-associated pathologies. In FMT, the fecal content of the healthy individual is transferred to the recipient having the perturbed GM resulting in the re-establishment of a healthy microbiome. FMT was first used for the treatment of *Clostridioides difficile* infection and was effective in treating 90% of the patients. After that FMT was explored for the management of several disorders like multiple sclerosis, RA, type 1 diabetes mellitus, IBD, Crohn's disease, ulcerative colitis, liver diseases, and various other metabolic disorders. Results from these studies gave mixed responses and

the effectiveness of FMT in these disorders is still controversial (Wargo, 2020; Wolter et al., 2021). Dysbiosis is associated with various bone pathologies and FMT can be exploited as a potential tool for restoration of perturbed GM in these pathologies (Xu et al., 2020). A recent study has shown the potential of FMT in preventing bone loss in a rat model of senile osteoporosis. It is reported that the transplantation of GM from healthy rats to aged rats having senile osteoporosis attenuated the bone loss by preventing dysbiosis in aged rats. After 24 weeks of FMT in aged rats, there was a significant increase in the bone parameters such as bone volume fraction, trabecular number, and thickness. FMT also increased the expression of TJ proteins like occludin and claudin in the recipient rats (Ma et al., 2021). This study shows the efficacy of FMT in preventing bone loss but still, there is controversy regarding the efficacy of FMT. Therefore, we proposed that a combination of FMT with dietary supplementations like probiotics and synbiotics can be another approach for the management of these inflammatory bone conditions. Giving a similar diet to the recipient as taken by the donor along with FMT can also be considered as a strategy to increase the efficacy of FMT.

Personalized Gut Microbiota Modulation Strategies

Modulation of GM by the above-used techniques is currently employed to prevent the pathogenesis of several disorders but mechanisms of their working are still not completely clear. Modulation of GM is giving varied results with less reproducibility. One reason could be the specific microbiome of every individual and thus one approach used for a person may not work for another person i.e., one size does not fit all. Therefore, a personalized approach could be encouraged *via* modulation of GM according to the need of the individual taking into consideration its health status and diet regime. As dysbiosis is observed in all types of bone pathologies such as RA, osteoporosis, and periodontitis sequencing of an individual's microbiome and then devising a GM modulation strategy according to the need of the individual with biotics would be a promising approach for management of GM associated bone pathologies.

CONCLUSION

Various studies are now supporting and establishing the role of GM in maintaining bone homeostasis. GM regulates bone metabolism by various mechanisms such as inducing the development of the immune system, maintaining gut permeability, and regulating the endocrine system. Microbial metabolites can also regulate bone health by directly affecting the process of bone remodeling or modulating the host immune system. Alteration in GM composition leads to various bone pathologies such as osteoporosis, RA, and periodontitis. These skeleton manifestations are affecting the lives of millions of people. Thus, interventions targeting the GM can be a promising approach both for the prevention and management of various bone pathologies. GM can be modulated by the use of antibiotics, diet, and drugs. Recent studies have shown that biotics (probiotics, prebiotics, synbiotics, and postbiotics) can prevent various bone disorders. They restore the normal GM composition and prevent bone resorption through several established mechanisms. They primarily regulate the immune system, intestinal barrier functions, and activity of bone cells along with enhancing Ca and vitamin D absorption. Therefore, probiotics, prebiotics, synbiotics, and postbiotics can be exploited as an effective and safer therapies for the management of various bone-related ailments. However, clinical trials at a large scale are needed to further delineate their efficacy in humans. Apart from biotics, orthogonal niche engineering, AIP diet, and FMT along with personalized GM modulation strategies could also be employed as promising therapeutic modalities in the management and treatment of various inflammatory bone disorders and therefore their role in skeleton health should be explored on priority.

AUTHOR CONTRIBUTIONS

RS contributed to the conceptualization and writing of the manuscript. AB participated in the writing and editing of the review. LS, AT, PM, and SS provided valuable inputs in the preparation of the manuscript. AB created the illustrations. All authors contributed to the article and approved the submitted version.

FUNDING

This work was financially supported by projects: DST-SERB (EMR/2016/007158), Govt. of India, Intramural project from All India Institute of Medical Sciences (AIIMS), New Delhi-India (AI-798), and AIIMS-IITD (AI-15) collaborative project sanctioned to RS.

ACKNOWLEDGMENTS

AB, LS, and RS acknowledge the Department of Biotechnology, AIIMS, New Delhi, India, for providing infrastructural facilities. AT and SS thank IIT New Delhi for infrastructural facilities. PM thanks ICMR-NIREH for the necessary facilities. Figures are created with the help of https://smart.servier.com.

REFERENCES

Achi, S. C., Talahalli, R. R., and Halami, P. M. (2019). Prophylactic effects of probiotic Bifidobacterium spp. in the resolution of inflammation in arthritic rats. *Appl. Microbiol. Biotechnol.* 103, 6287–6296. doi: 10.1007/s00253-019-09864-2

Aguilar-Toalá, J. E., Garcia-Varela, R., Garcia, H. S., Mata-Haro, V., González-Córdova, A. F., Vallejo-Cordoba, B., et al. (2018). Postbiotics: An evolving

term within the functional foods field. *Trends Food Sci. Technol.* 75, 105–114. doi: 10.1016/j.tifs.2018.03.009

Ahmed, S., Macfarlane, G. T., Fite, A., McBain, A. J., Gilbert, P., and Macfarlane, S. (2007). Mucosa-associated bacterial diversity in relation to human terminal ileum and colonic biopsy samples. *Appl. Environ. Microbiol.* 73, 7435–7442. doi: 10.1128/AEM.01143-07/ASSET/2C475B3D-6743-4017-9D4E-7EFB9023F2BB/ASSETS/GRAPHIC/ZAM0220783380003.JPEG

Ai, T., Hao, L., Shang, L., Wang, L., Li, B., and Li, J. (2021). Konjac Oligosaccharides Modulate the Gut Environment and Promote Bone Health in Calcium-Deficient Mice. *J. Agric. Food Chem.* 69, 4412–4422. doi: 10.1021/acs.jafc.0c07839

Albert, J. S., Bhattacharyya, N., Wolfe, L. A., Bone, W. P., Maduro, V., Accardi, J., et al. (2015). Impaired osteoblast and osteoclast function characterize the osteoporosis of Snyder - Robinson syndrome. *Orphanet J. Rare Dis.* 10:27. doi: 10.1186/s13023-015-0235-8

Alunno, A., Manetti, M., Caterbi, S., Ibba-Manneschi, L., Bistoni, O., Bartoloni, E., et al. (2015). Altered Immunoregulation in Rheumatoid Arthritis: The Role of Regulatory T Cells and Proinflammatory Th17 Cells and Therapeutic Implications. *Mediators Inflamm.* 2015, 1–12. doi: 10.1155/2015/751793

Amdekar, S., Roy, P., Singh, V., Kumar, A., Singh, R., and Sharma, P. (2012). Anti-Inflammatory Activity of *Lactobacillus* on Carrageenan-Induced Paw Edema in Male Wistar Rats. *Int. J. Inflam.* 2012:752015. doi: 10.1155/2012/752015

Asarat, M., Apostolopoulos, V., Vasiljevic, T., and Donkor, O. (2016). Short-Chain Fatty Acids Regulate Cytokines and Th17/Treg Cells in Human Peripheral Blood Mononuclear Cells in vitro. *Immunol. Invest.* 45, 205–222. doi: 10.3109/08820139.2015.1122613

Atarashi, K., Tanoue, T., Shima, T., Imaoka, A., Kuwahara, T., Momose, Y., et al. (2011). Induction of Colonic Regulatory T Cells by Indigenous Clostridium Species. *Science* 331, 337–341. doi: 10.1126/science.1198469

Avella, M. A., Place, A., Du, S.-J., Williams, E., Silvi, S., Zohar, Y., et al. (2012). Lactobacillus rhamnosus Accelerates Zebrafish Backbone Calcification and Gonadal Differentiation through Effects on the GnRH and IGF Systems. *PLoS One* 7:e45572. doi: 10.1371/journal.pone.0045572

Ayabe, T., Satchell, D. P., Wilson, C. L., Parks, W. C., Selsted, M. E., and Ouellette, A. J. (2000). Secretion of microbicidal α-defensins by intestinal Paneth cells in response to bacteria. *Nat. Immunol.* 1, 113–118. doi: 10.1038/77783

Bhinder, G., Stahl, M., Sham, H. P., Crowley, S. M., Morampudi, V., Dalwadi, U., et al. (2014). Intestinal Epithelium-Specific MyD88 Signaling Impacts Host Susceptibility to Infectious Colitis by Promoting Protective Goblet Cell and Antimicrobial Responses. *Infect. Immun.* 82, 3753–3763. doi: 10.1128/IAI.02045-14

Blanton, L. V., Charbonneau, M. R., Salih, T., Barratt, M. J., Venkatesh, S., Ilkaveya, O., et al. (2016). Gut bacteria that prevent growth impairments transmitted by microbiota from malnourished children. *Science* 351, aad3311–aad3311. doi: 10.1126/science.aad3311

Bowey, E., Adlercreutz, H., and Rowland, I. (2003). Metabolism of isoflavones and lignans by the gut microflora: a study in germ-free and human flora associated rats. *Food Chem. Toxicol.* 41, 631–636. doi: 10.1016/S0278-6915(02)00324-1

Britton, R. A., Irwin, R., Quach, D., Schaefer, L., Zhang, J., Lee, T., et al. (2014). Probiotic L. reuteri Treatment Prevents Bone Loss in a Menopausal Ovariectomized Mouse Model. *J. Cell. Physiol.* 229, 1822–1830. doi: 10.1002/jcp.24636

Charles, J. F., and Aliprantis, A. O. (2014). Osteoclasts: more than 'bone eaters.'. *Trends Mol. Med.* 20, 449–459. doi: 10.1016/j.molmed.2014.06.001

Chen, B., Chen, H., Shu, X., Yin, Y., Li, J., Qin, J., et al. (2018). Presence of Segmented Filamentous Bacteria in Human Children and Its Potential Role in the Modulation of Human Gut Immunity. *Front. Microbiol.* 9:1403. doi: 10.3389/fmicb.2018.01403

Chen, J., Rao, J. N., Zou, T., Liu, L., Marasa, B. S., Xiao, L., et al. (2007). Polyamines are required for expression of Toll-like receptor 2 modulating intestinal epithelial barrier integrity. *Am. J. Physiol. Liver Physiol.* 293, G568–G576. doi: 10.1152/ajpgi.00201.2007

Chen, K., Jiao, Y., Liu, L., Huang, M., He, C., He, W., et al. (2020). Communications Between Bone Marrow Macrophages and Bone Cells in Bone Remodeling. *Front. Cell Dev. Biol.* 8:598263. doi: 10.3389/FCELL.2020.598263

Chevalier, C., Kieser, S., Çolakoğlu, M., Hadadi, N., Brun, J., Rigo, D., et al. (2020). Warmth Prevents Bone Loss Through the Gut Microbiota. *Cell Metab.* 32, 575.e–590.e. doi: 10.1016/j.cmet.2020.08.012

Cho, I., Yamanishi, S., Cox, L., Methé, B. A., Zavadil, J., Li, K., et al. (2012). Antibiotics in early life alter the murine colonic microbiome and adiposity. *Nature* 488, 621–626. doi: 10.1038/nature11400

Cho, S. W., An, J. H., Park, H., Yang, J.-Y., Choi, H. J., Kim, S. W., et al. (2013). Positive regulation of osteogenesis by bile acid through FXR. *J. Bone Miner. Res.* 28, 2109–2121. doi: 10.1002/jbmr.1961

Clarke, B. (2008). Normal Bone Anatomy and Physiology. *Clin. J. Am. Soc. Nephrol.* 3, S131–S139. doi: 10.2215/CJN.04151206

Collins, F. L., Rios-Arce, N. D., Schepper, J. D., Jones, A. D., Schaefer, L., Britton, R. A., et al. (2019). Beneficial effects of Lactobacillus reuteri 6475 on bone density in male mice is dependent on lymphocytes. *Sci. Rep.* 9:8. doi: 10.1038/s41598-019-51293-8

Cox, L. M., Yamanishi, S., Sohn, J., Alekseyenko, A. V., Leung, J. M., Cho, I., et al. (2014). Altering the Intestinal Microbiota during a Critical Developmental Window Has Lasting Metabolic Consequences. *Cell* 158, 705–721. doi: 10.1016/j.cell.2014.05.052

Dar, H. Y., Azam, Z., Anupam, R., Mondal, R. K., and Srivastava, R. K. (2018a). Osteoimmunology: The Nexus between bone and immune system. *Front. Biosci.* 23:464–492. doi: 10.2741/4600

Dar, H. Y., Pal, S., Shukla, P., Mishra, P. K., Tomar, G. B., Chattopadhyay, N., et al. (2018b). Bacillus clausii inhibits bone loss by skewing Treg-Th17 cell equilibrium in postmenopausal osteoporotic mice model. *Nutrition* 54, 118–128. doi: 10.1016/j.nut.2018.02.013

Dar, H. Y., Shukla, P., Mishra, P. K., Anupam, R., Mondal, R. K., Tomar, G. B., et al. (2018c). Lactobacillus acidophilus inhibits bone loss and increases bone heterogeneity in osteoporotic mice *via* modulating Treg-Th17 cell balance. *Bone Rep.* 8, 46–56. doi: 10.1016/j.bonr.2018.02.001

Davani-Davari, D., Negahdaripour, M., Karimzadeh, I., Seifan, M., Mohkam, M., Masoumi, S. J., et al. (2019). Prebiotics: Definition, types, sources, mechanisms, and clinical applications. *Foods* 8:foods8030092. doi: 10.3390/foods8030092

Deplancke, B., and Gaskins, H. R. (2001). Microbial modulation of innate defense: goblet cells and the intestinal mucus layer. *Am. J. Clin. Nutr.* 73, 1131S–1141S. doi: 10.1093/ajcn/73.6.1131S

Dominguez-Bello, M. G., Costello, E. K., Contreras, M., Magris, M., Hidalgo, G., Fierer, N., et al. (2010). Delivery mode shapes the acquisition and structure of the initial microbiota across multiple body habitats in newborns. *Proc. Natl. Acad. Sci.* 107, 11971–11975. doi: 10.1073/pnas.1002601107

Eaimworawuthikul, S., Tunapong, W., Chunchai, T., Suntornsaratoon, P., Charoenphandhu, N., Thiennimitr, P., et al. (2020). Altered gut microbiota ameliorates bone pathology in the mandible of obese–insulin-resistant rats. *Eur. J. Nutr.* 59, 1453–1462. doi: 10.1007/s00394-019-02002-8

Eckburg, P. B. (2005). Diversity of the Human Intestinal Microbial Flora. *Science* 308, 1635–1638. doi: 10.1126/science.1110591

Friščić, J., Dürholz, K., Chen, X., Engdahl, C., Möller, L., Schett, G., et al. (2021). Dietary Derived Propionate Regulates Pathogenic Fibroblast Function and Ameliorates Experimental Arthritis and Inflammatory Tissue Priming. *Nutrients* 13:1643. doi: 10.3390/nu13051643

Furusawa, Y., Obata, Y., Fukuda, S., Endo, T. A., Nakato, G., Takahashi, D., et al. (2013). Commensal microbe-derived butyrate induces the differentiation of colonic regulatory T cells. *Nature* 504, 446–450. doi: 10.1038/nature12721

Gaboriau-Routhiau, V., Rakotobe, S., Lécuyer, E., Mulder, I., Lan, A., Bridonneau, C., et al. (2009). The Key Role of Segmented Filamentous Bacteria in the Coordinated Maturation of Gut Helper T Cell Responses. *Immunity* 31, 677–689. doi: 10.1016/j.immuni.2009.08.020

Gao, H., and Zhou, Z. (2020). Effect of Xylo-Oligosaccharides Supplementation by Drinking Water on the Bone Properties and Related Calcium Transporters in Growing Mice. *Nutrients* 12:3542. doi: 10.3390/nu12113542

Gao, L., Zhao, Y., Wang, P., Zhang, L., Zhang, C., Chen, Q., et al. (2017). Detection of Th17/Treg cells and related factors in gingival tissues and peripheral blood of rats with experimental periodontitis. *Iran. J. Basic Med. Sci.* 20, 294–300. doi: 10.22038/ijbms.2017.8359

Gerbe, F., Sidot, E., Smyth, D. J., Ohmoto, M., Matsumoto, I., Dardalhon, V., et al. (2016). Intestinal epithelial tuft cells initiate type 2 mucosal immunity to helminth parasites. *Nature* 529, 226–230. doi: 10.1038/nature16527

Gibson, G. R., Scott, K. P., Rastall, R. A., Tuohy, K. M., Hotchkiss, A., Dubert-Ferrandon, A., et al. (2010). Dietary prebiotics: current status and new definition. *Food Sci. Technol. Bull. Funct. Foods* 7, 1–19. doi: 10.1616/1476-2137.15880

Giustina, A., Mazziotti, G., and Canalis, E. (2008). Growth Hormone, Insulin-Like Growth Factors, and the Skeleton. *Endocr. Rev.* 29, 535–559. doi: 10.1210/er.2007-0036

Guinane, C. M., and Cotter, P. D. (2013). Role of the gut microbiota in health and chronic gastrointestinal disease: Understanding a hidden metabolic organ. *Therap. Adv. Gastroenterol.* 6, 295–308. doi: 10.1177/1756283X13482996

Gupta, V., and Garg, R. (2009). Probiotics. *Ind. J. Med. Microbiol.* 27:202. doi: 10.4103/0255-0857.53201

Guss, J. D., Horsfield, M. W., Fontenele, F. F., Sandoval, T. N., Luna, M., Apoorva, F., et al. (2017). Alterations to the Gut Microbiome Impair Bone Strength and Tissue Material Properties. *J. Bone Miner. Res.* 32, 1343–1353. doi: 10.1002/jbmr.3114

Hadjidakis, D. J., and Androulakis, I. I. (2006). Bone Remodeling. *Ann. N. Y. Acad. Sci.* 1092, 385–396. doi: 10.1196/annals.1365.035

Hang, S., Paik, D., Yao, L., Kim, E., Trinath, J., Lu, J., et al. (2019). Bile acid metabolites control TH17 and Treg cell differentiation. *Nature* 576, 143–148. doi: 10.1038/s41586-019-1785-z

Ibáñez, L., Rouleau, M., Wakkach, A., and Blin-Wakkach, C. (2019). Gut microbiome and bone. *Jt. Bone Spine* 86, 43–47. doi: 10.1016/j.jbspin.2018.02.008

Iezaki, T., Hinoi, E., Yamamoto, T., Ishiura, R., Ogawa, S., and Yoneda, Y. (2012). Amelioration by the Natural Polyamine Spermine of Cartilage and Bone Destruction in Rats With Collagen-Induced Arthritis. *J. Pharmacol. Sci.* 119, 107–111. doi: 10.1254/jphs.11241SC

Ilesanmi-Oyelere, B. L., and Kruger, M. C. (2020). The Role of Milk Components, Pro-, Pre-, and Synbiotic Foods in Calcium Absorption and Bone Health Maintenance. *Front. Nutr.* 7:578702. doi: 10.3389/fnut.2020.578702

Ivanov, I. I., and Littman, D. R. (2010). Segmented filamentous bacteria take the stage. *Mucosal Immunol.* 3, 209–212. doi: 10.1038/mi.2010.3

Jansson, P.-A., Curiac, D., Lazou Ahrén, I., Hansson, F., Martinsson Niskanen, T., Sjögren, K., et al. (2019). Probiotic treatment using a mix of three Lactobacillus strains for lumbar spine bone loss in postmenopausal women: a randomised, double-blind, placebo-controlled, multicentre trial. *Lancet Rheumatol.* 1, e154–e162. doi: 10.1016/S2665-9913(19)30068-2

Jilka, R. L., O'Brien, C. A., Ali, A. A., Roberson, P. K., Weinstein, R. S., and Manolagas, S. C. (2009). Intermittent PTH stimulates periosteal bone formation by actions on post-mitotic preosteoblasts. *Bone* 44, 275–286. doi: 10.1016/j.bone.2008.10.037

Jonsson, H., Hugerth, L. W., Sundh, J., Lundin, E., and Andersson, A. F. (2020). Genome sequence of segmented filamentous bacteria present in the human intestine. *Commun. Biol.* 3:485. doi: 10.1038/s42003-020-01214-7

Jung, J.-I., Baek, S.-M., Nguyen, T. H., Kim, J. W., Kang, C.-H., Kim, S., et al. (2021). Effects of Probiotic Culture Supernatant on Cariogenic Biofilm Formation and RANKL-Induced Osteoclastogenesis in RAW 264.7 Macrophages. *Molecules* 26:733. doi: 10.3390/molecules26030733

Kareem, K. Y., Loh, T. C., Foo, H. L., Akit, H., and Samsudin, A. A. (2016). Effects of dietary postbiotic and inulin on growth performance, IGF1 and GHR mRNA expression, faecal microbiota and volatile fatty acids in broilers. *BMC Vet. Res.* 12:163. doi: 10.1186/s12917-016-0790-9

Kearney, S. M., Gibbons, S. M., Erdman, S. E., and Alm, E. J. (2018). Orthogonal Dietary Niche Enables Reversible Engraftment of a Gut Bacterial Commensal. *Cell Rep.* 24, 1842–1851. doi: 10.1016/j.celrep.2018.07.032

Kikodze, N., Pantsulaia, I., and Chikovani, T. (2016). THE ROLE OF T REGULATORY AND TH17 CELLS IN THE PATHOGENESIS OF RHEUMATOID ARTHRITIS (REVIEW). *Georgian Med. News* 2016, 62–68.

Kim, Y. G., Lee, C.-K., Nah, S.-S., Mun, S. H., Yoo, B., and Moon, H.-B. (2007). Human CD4+CD25+ regulatory T cells inhibit the differentiation of osteoclasts from peripheral blood mononuclear cells. *Biochem. Biophys. Res. Commun.* 357, 1046–1052. doi: 10.1016/j.bbrc.2007.04.042

Kobayashi, K. S. (2005). Nod2-Dependent Regulation of Innate and Adaptive Immunity in the Intestinal Tract. *Science* 307, 731–734. doi: 10.1126/science.1104911

Lam, V., Su, J., Koprowski, S., Hsu, A., Tweddell, J. S., Rafiee, P., et al. (2012). Intestinal microbiota determine severity of myocardial infarction in rats. *FASEB J.* 26, 1727–1735. doi: 10.1096/fj.11-197921

Lambert, M. N. T., Thorup, A. C., Hansen, E. S. S., and Jeppesen, P. B. (2017). Combined Red Clover isoflavones and probiotics potently reduce menopausal vasomotor symptoms. *PLoS One* 12:e0176590. doi: 10.1371/journal.pone.0176590

Landete, J. M., Arqués, J., Medina, M., Gaya, P., de Las Rivas, B., and Muñoz, R. (2016). Bioactivation of Phytoestrogens: Intestinal Bacteria and Health. *Crit. Rev. Food Sci. Nutr.* 56, 1826–1843. doi: 10.1080/10408398.2013.789823

Lavoie, B., Lian, J. B., and Mawe, G. M. (2017). Regulation of Bone Metabolism by Serotonin. *Adv. Exp. Med. Biol.* 2017, 35–46. doi: 10.1007/978-3-319-66653-2_3

Lee, J. Y., Mannaa, M., Kim, Y., Kim, J., Kim, G. T., and Seo, Y. S. (2019). Comparative analysis of fecal microbiota composition between rheumatoid arthritis and osteoarthritis patients. *Genes* 10:10100748. doi: 10.3390/genes10100748

Lee, J., Wasinger, V., Yau, Y., Chuang, E., Yajnik, V., and Leong, R. (2018). Molecular Pathophysiology of Epithelial Barrier Dysfunction in Inflammatory Bowel Diseases. *Proteomes* 6, 17. doi: 10.3390/proteomes6020017

Lei, M., Guo, C., Wang, D., Zhang, C., and Hua, L. (2017). The effect of probiotic Lactobacillus casei Shirota on knee osteoarthritis: a randomised double-blind, placebo-controlled clinical trial. *Benef. Microbes* 8, 697–703. doi: 10.3920/BM2016.0207

Lei, M., Hua, L.-M., and Wang, D.-W. (2016). The effect of probiotic treatment on elderly patients with distal radius fracture: a prospective double-blind, placebo-controlled randomised clinical trial. *Benef. Microbes* 7, 631–637. doi: 10.3920/BM2016.0067

Leipe, J., Grunke, M., Dechant, C., Reindl, C., Kerzendorf, U., Schulze-Koops, H., et al. (2010). Role of Th17 cells in human autoimmune arthritis. *Arthritis Rheum.* 62, 2876–2885. doi: 10.1002/art.27622

Li, J.-Y., Chassaing, B., Tyagi, A. M., Vaccaro, C., Luo, T., Adams, J., et al. (2016). Sex steroid deficiency–associated bone loss is microbiota dependent and prevented by probiotics. *J. Clin. Invest.* 126, 2049–2063. doi: 10.1172/JCI86062

Li, J.-Y., Yu, M., Pal, S., Tyagi, A. M., Dar, H., Adams, J., et al. (2020). Parathyroid hormone–dependent bone formation requires butyrate production by intestinal microbiota. *J. Clin. Invest.* 130, 1767–1781. doi: 10.1172/JCI133473

Li, L., Rao, S., Cheng, Y., Zhuo, X., Deng, C., Xu, N., et al. (2019). Microbial osteoporosis: The interplay between the gut microbiota and bones *via* host metabolism and immunity. *Microbiologyopen* 8:810. doi: 10.1002/mbo3.810

Li, S.-C., Hsu, W.-F., Chang, J.-S., and Shih, C.-K. (2019). Combination of Lactobacillus acidophilus and Bifidobacterium animalis subsp. lactis Shows a Stronger Anti-Inflammatory Effect than Individual Strains in HT-29 Cells. *Nutrients* 11:11050969. doi: 10.3390/nu11050969

Li, Y., Luo, W., Zhu, S., and Lei, G. (2017). T Cells in Osteoarthritis: Alterations and Beyond. *Front. Immunol.* 8:356. doi: 10.3389/fimmu.2017.00356

Li, Z., Huang, J., Wang, F., Li, W., Wu, X., Zhao, C., et al. (2018). Dual Targeting of Bile Acid Receptor-1 (TGR5) and Farnesoid X Receptor (FXR) Prevents Estrogen-Dependent Bone Loss in Mice. *J. Bone Miner. Res.* 2018:3652. doi: 10.1002/jbmr.3652

Li, Z., Zhou, J., Luo, C., and Zhang, L. (2019). Activation of TGR5 alleviates inflammation in rheumatoid arthritis peripheral blood mononuclear cells and in mice with collagen II-induced arthritis. *Mol. Med. Rep.* 2019:10711. doi: 10.3892/mmr.2019.10711

Liang, S. C., Tan, X.-Y., Luxenberg, D. P., Karim, R., Dunussi-Joannopoulos, K., Collins, M., et al. (2006). Interleukin (IL)-22 and IL-17 are coexpressed by Th17 cells and cooperatively enhance expression of antimicrobial peptides. *J. Exp. Med.* 203, 2271–2279. doi: 10.1084/jem.20061308

Liu, L., Guo, X., Rao, J. N., Zou, T., Xiao, L., Yu, T., et al. (2009). Polyamines regulate E-cadherin transcription through c-Myc modulating intestinal epithelial barrier function. *Am. J. Physiol. Physiol.* 296, C801–C810. doi: 10.1152/ajpcell.00620.2008

Liu, P., Wang, Y., Yang, G., Zhang, Q., Meng, L., Xin, Y., et al. (2021). The role of short-chain fatty acids in intestinal barrier function, inflammation, oxidative stress, and colonic carcinogenesis. *Pharmacol. Res.* 165:105420. doi: 10.1016/j.phrs.2021.105420

Locatelli, V., and Bianchi, V. E. (2014). Effect of GH/IGF-1 on Bone Metabolism and Osteoporsosis. *Int. J. Endocrinol.* 2014, 1–25. doi: 10.1155/2014/235060

Lourenço, T. G. B., Spencer, S. J., Alm, E. J., and Colombo, A. P. V. (2018). Defining the gut microbiota in individuals with periodontal diseases: an exploratory study. *J. Oral Microbiol.* 10:1487741. doi: 10.1080/20002297.2018.1487741

Lucas, S., Omata, Y., Hofmann, J., Böttcher, M., Iljazovic, A., Sarter, K., et al. (2018). Short-chain fatty acids regulate systemic bone mass and protect from pathological bone loss. *Nat. Commun.* 9:55. doi: 10.1038/s41467-017-02490-4

Luo, C., Wang, L., Sun, C., and Li, D. (2011). Estrogen enhances the functions of CD4+CD25+Foxp3+ regulatory T cells that suppress osteoclast differentiation and bone resorption in vitro. *Cell. Mol. Immunol.* 8, 50–58. doi: 10.1038/cmi.2010.54

Ma, S., Wang, N., Zhang, P., Wu, W., and Fu, L. (2021). Fecal microbiota transplantation mitigates bone loss by improving gut microbiome composition and gut barrier function in aged rats. *PeerJ* 9:e12293. doi: 10.7717/peerj.12293

Ma, Y. L., Cain, R. L., Halladay, D. L., Yang, X., Zeng, Q., Miles, R. R., et al. (2001). Catabolic Effects of Continuous Human PTH (1–38) in Vivo Is Associated with Sustained Stimulation of RANKL and Inhibition of Osteoprotegerin and Gene-Associated Bone Formation. *Endocrinology* 142, 4047–4054. doi: 10.1210/endo.142.9.8356

Matei, D. E., Menon, M., Alber, D. G., Smith, A. M., Nedjat-Shokouhi, B., Fasano, A., et al. (2021). Intestinal barrier dysfunction plays an integral role in arthritis pathology and can be targeted to ameliorate disease. *Med* 2, 864.e–883.e. doi: 10.1016/j.medj.2021.04.013

McDonald, M. M., Khoo, W. H., Ng, P. Y., Xiao, Y., Zamerli, J., Thatcher, P., et al. (2021). Osteoclasts recycle *via* osteomorphs during RANKL-stimulated bone resorption. *Cell* 184, 1330.e–1347.e. doi: 10.1016/j.cell.2021.02.002

Mikkelsen, K. H., Vilsbøll, T., Holst, J. J., Hartmann, B., Knop, F. K., and Frost, M. (2018). No changes in levels of bone formation and resorption markers following a broad-spectrum antibiotic course. *BMC Endocr. Disord.* 18:60. doi: 10.1186/s12902-018-0291-x

Minois, N., Carmona-Gutierrez, D., and Madeo, F. (2011). Polyamines in aging and disease. *Aging* 3, 716–732. doi: 10.18632/aging.100361

Montalvany-Antonucci, C. C., Duffles, L. F., de Arruda, J. A. A., Zicker, M. C., de Oliveira, S., Macari, S., et al. (2019). Short-chain fatty acids and FFAR2 as suppressors of bone resorption. *Bone* 125, 112–121. doi: 10.1016/j.bone.2019.05.016

Montazeri-Najafabady, N., Ghasemi, Y., Dabbaghmanesh, M. H., Talezadeh, P., Koohpeyma, F., and Gholami, A. (2019). Supportive Role of Probiotic Strains in Protecting Rats from Ovariectomy-Induced Cortical Bone Loss. *Probiotics Antimicrob. Proteins* 11, 1145–1154. doi: 10.1007/s12602-018-9443-6

Mowat, A. M., and Agace, W. W. (2014). Regional specialization within the intestinal immune system. *Nat. Rev. Immunol.* 14, 667–685. doi: 10.1038/nri3738

Muniz, L. R., Knosp, C., and Yeretssian, G. (2012). Intestinal antimicrobial peptides during homeostasis, infection, and disease. *Front. Immunol.* 3:310. doi: 10.3389/fimmu.2012.00310

Nakajima, M., Arimatsu, K., Kato, T., Matsuda, Y., Minagawa, T., Takahashi, N., et al. (2015). Oral administration of P. gingivalis induces dysbiosis of gut microbiota and impaired barrier function leading to dissemination of enterobacteria to the liver. *PLoS One* 10:0134234. doi: 10.1371/journal.pone.0134234

Narva, M., Rissanen, J., Halleen, J., Vapaatalo, H., Väänänen, K., and Korpela, R. (2007). Effects of Bioactive Peptide, Valyl-Prolyl-Proline (VPP), and Lactobacillus helveticus Fermented Milk Containing VPP on Bone Loss in Ovariectomized Rats. *Ann. Nutr. Metab.* 51, 65–74. doi: 10.1159/000100823

Nilsson, A. G., Sundh, D., Bäckhed, F., and Lorentzon, M. (2018). Lactobacillus reuteri reduces bone loss in older women with low bone mineral density: a randomized, placebo-controlled, double-blind, clinical trial. *J. Intern. Med.* 284, 307–317. doi: 10.1111/joim.12805

Novince, C. M., Whittow, C. R., Aartun, J. D., Hathaway, J. D., Poulides, N., Chavez, M. B., et al. (2017). Commensal Gut Microbiota Immunomodulatory Actions in Bone Marrow and Liver have Catabolic Effects on Skeletal Homeostasis in Health. *Sci. Rep.* 7:5747. doi: 10.1038/s41598-017-06126-x

Ohlsson, C., and Sjögren, K. (2015). Effects of the gut microbiota on bone mass. *Trends Endocrinol. Metab.* 26, 69–74. doi: 10.1016/j.tem.2014.11.004

Ohlsson, C., and Sjögren, K. (2018). Osteomicrobiology: A New Cross-Disciplinary Research Field. *Calcif. Tissue Int.* 102, 426–432. doi: 10.1007/s00223-017-0336-6

Ohlsson, C., Nigro, G., Boneca, I. G., Bäckhed, F., Sansonetti, P., and Sjögren, K. (2017). Regulation of bone mass by the gut microbiota is dependent on NOD1 and NOD2 signaling. *Cell. Immunol.* 317, 55–58. doi: 10.1016/j.cellimm.2017.05.003

Ozen, M., and Dinleyici, E. C. (2015). The history of probiotics: the untold story. *Benef. Microbes* 6, 159–165. doi: 10.3920/BM2014.0103

Pandey, K. R., Naik, S. R., and Vakil, B. V. (2015). Probiotics, prebiotics and synbiotics- a review. *J. Food Sci. Technol.* 52, 7577–7587. doi: 10.1007/s13197-015-1921-1

Parvaneh, K., Ebrahimi, M., Sabran, M. R., Karimi, G., Hwei, A. N. M., Abdul-Majeed, S., et al. (2015). Probiotics (Bifidobacterium longum) Increase Bone Mass Density and Upregulate Sparc and Bmp-2 Genes in Rats with Bone Loss Resulting from Ovariectomy. *Biomed Res. Int.* 2015, 1–10. doi: 10.1155/2015/897639

Plaza-Diaz, J., Ruiz-Ojeda, F. J., Gil-Campos, M., and Gil, A. (2019). Mechanisms of Action of Probiotics. *Adv. Nutr.* 10, S49–S66. doi: 10.1093/advances/nmy063

Plottel, C. S., and Blaser, M. J. (2011). Microbiome and Malignancy. *Cell Host Microbe* 10, 324–335. doi: 10.1016/j.chom.2011.10.003

Qin, J., Li, R., Raes, J., Arumugam, M., Burgdorf, K. S., Manichanh, C., et al. (2010). A human gut microbial gene catalogue established by metagenomic sequencing. *Nature* 464, 59–65. doi: 10.1038/nature08821

Qin, L., Liu, W., Cao, H., and Xiao, G. (2020). Molecular mechanosensors in osteocytes. *Bone Res.* 81, 1–24. doi: 10.1038/s41413-020-0099-y

Quach, D., Collins, F., Parameswaran, N., McCabe, L., and Britton, R. A. (2018). Microbiota Reconstitution Does Not Cause Bone Loss in Germ-Free Mice. *mSphere* 3:17. doi: 10.1128/mSphereDirect.00545-17

Quach, D., Parameswaran, N., McCabe, L., and Britton, R. A. (2019). Characterizing how probiotic Lactobacillus reuteri 6475 and lactobacillic acid mediate suppression of osteoclast differentiation. *Bone Rep.* 11:100227. doi: 10.1016/j.bonr.2019.100227

Queipo-Ortuño, M. I., Seoane, L. M., Murri, M., Pardo, M., Gomez-Zumaquero, J. M., Cardona, F., et al. (2013). Gut Microbiota Composition in Male Rat Models under Different Nutritional Status and Physical Activity and Its Association with Serum Leptin and Ghrelin Levels. *PLoS One* 8:e65465. doi: 10.1371/journal.pone.0065465

Reigstad, C. S., Salmonson, C. E., Rainey, J. F. III, Szurszewski, J. H., Linden, D. R., Sonnenburg, J. L., et al. (2015). Gut microbes promote colonic serotonin production through an effect of short-chain fatty acids on enterochromaffin cells. *FASEB J.* 29, 1395–1403. doi: 10.1096/fj.14-259598

Rinninella, E., Raoul, P., Cintoni, M., Franceschi, F., Miggiano, G., Gasbarrini, A., et al. (2019). What is the Healthy Gut Microbiota Composition? A Changing Ecosystem across Age, Environment, Diet, and Diseases. *Microorganisms* 7:14. doi: 10.3390/microorganisms7010014

Rios-Arce, N. D., Schepper, J. D., Dagenais, A., Schaefer, L., Daly-Seiler, C. S., Gardinier, J. D., et al. (2020). Post-antibiotic gut dysbiosis-induced trabecular bone loss is dependent on lymphocytes. *Bone* 134:115269. doi: 10.1016/j.bone.2020.115269

Rodrigues, F. C., Castro, A. S. B., Rodrigues, V. C., Fernandes, S. A., Fontes, E. A. F., De Oliveira, T. T., et al. (2012). Yacon flour and bifidobacterium longum modulate bone health in rats. *J. Med. Food* 15, 664–670. doi: 10.1089/jmf.2011.0296

Rooks, M. G., and Garrett, W. S. (2016). Gut microbiota, metabolites and host immunity. *Nat. Rev. Immunol.* 16, 341–352. doi: 10.1038/nri.2016.42

Rosser, E. C., and Mauri, C. (2015). Regulatory B Cells: Origin, Phenotype, and Function. *Immunity* 42, 607–612. doi: 10.1016/j.immuni.2015.04.005

Rosser, E. C., Oleinika, K., Tonon, S., Doyle, R., Bosma, A., Carter, N. A., et al. (2014). Regulatory B cells are induced by gut microbiota–driven interleukin-1β and interleukin-6 production. *Nat. Med.* 20, 1334–1339. doi: 10.1038/nm.3680

Rosser, E. C., Piper, C. J. M., Matei, D. E., Blair, P. A., Rendeiro, A. F., Orford, M., et al. (2020). Microbiota-Derived Metabolites Suppress Arthritis by Amplifying Aryl-Hydrocarbon Receptor Activation in Regulatory B Cells. *Cell Metab.* 31, 837.e–851.e. doi: 10.1016/j.cmet.2020.03.003

Röth, D., Chiang, A. J., Hu, W., Gugiu, G. B., Morra, C. N., Versalovic, J., et al. (2019). Two-carbon folate cycle of commensal Lactobacillus reuteri 6475 gives rise to immunomodulatory ethionine, a source for histone ethylation. *FASEB J.* 33, 3536–3548. doi: 10.1096/fj.201801848R

Sapra, L., Dar, H. Y., Bhardwaj, A., Pandey, A., Kumari, S., Azam, Z., et al. (2021c). Lactobacillus rhamnosus attenuates bone loss and maintains bone health by skewing Treg-Th17 cell balance in Ovx mice. *Sci. Rep.* 11:1807. doi: 10.1038/s41598-020-80536-2

Sapra, L., Bhardwaj, A., Mishra, P. K., Garg, B., Verma, B., Mishra, G. C., et al. (2021b). Regulatory B Cells (Bregs) Inhibit Osteoclastogenesis and Play a Potential Role in Ameliorating Ovariectomy-Induced Bone Loss. *Front. Immunol.* 12:691081. doi: 10.3389/fimmu.2021.691081

Sapra, L., Azam, Z., Rani, L., Saini, C., Bhardwaj, A., Shokeen, N., et al. (2021a). "Immunoporosis": Immunology of Osteoporosis. *Proc. Natl. Acad. Sci. India Sect. B Biol. Sci.* [Preprint]. doi: 10.1007/s40011-021-01238-x

Schepper, J. D., Collins, F. L., Rios-Arce, N. D., Raehtz, S., Schaefer, L., Gardinier, J. D., et al. (2019). Probiotic Lactobacillus reuteri Prevents Postantibiotic Bone Loss by Reducing Intestinal Dysbiosis and Preventing Barrier Disruption. *J. Bone Miner. Res.* 34, 681–698. doi: 10.1002/jbmr.3635

Schett, G., and David, J.-P. (2010). The multiple faces of autoimmune-mediated bone loss. *Nat. Rev. Endocrinol.* 6, 698–706. doi: 10.1038/nrendo.2010.190

Schroeder, B. O., and Bäckhed, F. (2016). Signals from the gut microbiota to distant organs in physiology and disease. *Nat. Med.* 22, 1079–1089. doi: 10.1038/nm.4185

Schwarzer, M., Makki, K., Storelli, G., Machuca-Gayet, I., Srutkova, D., Hermanova, P., et al. (2016). Lactobacillus plantarum strain maintains growth of infant mice during chronic undernutrition. *Science* 351, 854–857. doi: 10.1126/science.aad8588

Scott, M. M., Lachey, J. L., Sternson, S. M., Lee, C. E., Elias, C. F., Friedman, J. M., et al. (2009). Leptin targets in the mouse brain. *J. Comp. Neurol.* 514, 518–532. doi: 10.1002/cne.22025

Shimada, Y., Kinoshita, M., Harada, K., Mizutani, M., Masahata, K., Kayama, H., et al. (2013). Commensal Bacteria-Dependent Indole Production Enhances Epithelial Barrier Function in the Colon. *PLoS One* 8:e80604. doi: 10.1371/journal.pone.0080604

Silva, B. C., and Bilezikian, J. P. (2015). Parathyroid hormone: anabolic and catabolic actions on the skeleton. *Curr. Opin. Pharmacol.* 22, 41–50. doi: 10.1016/j.coph.2015.03.005

Singh, R. K., Chang, H.-W., Yan, D., Lee, K. M., Ucmak, D., Wong, K., et al. (2017). Influence of diet on the gut microbiome and implications for human health. *J. Transl. Med.* 15:73. doi: 10.1186/s12967-017-1175-y

Sivaprakasam, S., Prasad, P. D., and Singh, N. (2016). Benefits of short-chain fatty acids and their receptors in inflammation and carcinogenesis. *Pharmacol. Ther.* 164, 144–151. doi: 10.1016/j.pharmthera.2016.04.007

Sjögren, K., Engdahl, C., Henning, P., Lerner, U. H., Tremaroli, V., Lagerquist, M. K., et al. (2012). The gut microbiota regulates bone mass in mice. *J. Bone Miner. Res.* 27, 1357–1367. doi: 10.1002/jbmr.1588

Smith, K., McCoy, K. D., and Macpherson, A. J. (2007). Use of axenic animals in studying the adaptation of mammals to their commensal intestinal microbiota. *Semin. Immunol.* 19, 59–69. doi: 10.1016/j.smim.2006.10.002

Smith, P. M., Howitt, M. R., Panikov, N., Michaud, M., Gallini, C. A., Bohlooly-Y, M., et al. (2013). The microbial metabolites, short-chain fatty acids, regulate colonic T reg cell homeostasis. *Science* 341, 569–573. doi: 10.1126/science.1241165

Sommer, F., and Bäckhed, F. (2013). The gut microbiota — masters of host development and physiology. *Nat. Rev. Microbiol.* 11, 227–238. doi: 10.1038/nrmicro2974

Srivastava, R. K., Dar, H. Y., and Mishra, P. K. (2018). Immunoporosis: Immunology of Osteoporosis—Role of T Cells. *Front. Immunol.* 9:657. doi: 10.3389/fimmu.2018.00657

Staels, B., and Fonseca, V. A. (2009). Bile Acids and Metabolic Regulation: Mechanisms and clinical responses to bile acid sequestration. *Diab. Care* 32, S237–S245. doi: 10.2337/dc09-S355

Strauch, U. G. (2005). Influence of intestinal bacteria on induction of regulatory T cells: lessons from a transfer model of colitis. *Gut* 54, 1546–1552. doi: 10.1136/gut.2004.059451

Streicher, C., Heyny, A., Andrukhova, O., Haigl, B., Slavic, S., Schüler, C., et al. (2017). Estrogen Regulates Bone Turnover by Targeting RANKL Expression in Bone Lining Cells. *Sci. Rep.* 7:6460. doi: 10.1038/s41598-017-06614-0

Su, N., Yang, J., Xie, Y., Du, X., Chen, H., Zhou, H., et al. (2019). Bone function, dysfunction and its role in diseases including critical illness. *Int. J. Biol. Sci.* 15, 776–787. doi: 10.7150/ijbs.27063

Swanson, K. S., Gibson, G. R., Hutkins, R., Reimer, R. A., Reid, G., Verbeke, K., et al. (2020). The International Scientific Association for Probiotics and Prebiotics (ISAPP) consensus statement on the definition and scope of synbiotics. *Nat. Rev. Gastroenterol. Hepatol.* 17, 687–701. doi: 10.1038/s41575-020-0344-2

Takimoto, T., Hatanaka, M., Hoshino, T., Takara, T., Tanaka, K., Shimizu, A., et al. (2018). Effect of Bacillus subtilis C-3102 on bone mineral density in healthy postmenopausal Japanese women: a randomized, placebo-controlled, double-blind clinical trial. *Biosci. Microbiota Food Heal.* 37, 87–96. doi: 10.12938/bmfh.18-006

Talham, G. L., Jiang, H.-Q., Bos, N. A., and Cebra, J. J. (1999). Segmented Filamentous Bacteria Are Potent Stimuli of a Physiologically Normal State of the Murine Gut Mucosal Immune System. *Infect. Immun.* 67, 1992–2000. doi: 10.1128/IAI.67.4.1992-2000.1999

Tan, T. G., Sefik, E., Geva-Zatorsky, N., Kua, L., Naskar, D., Teng, F., et al. (2016). Identifying species of symbiont bacteria from the human gut that, alone, can induce intestinal Th17 cells in mice. *Proc. Natl. Acad. Sci.* 113, E8141–E8150. doi: 10.1073/pnas.1617460113

Thorburn, A. N., McKenzie, C. I., Shen, S., Stanley, D., MacIa, L., Mason, L. J., et al. (2015). Evidence that asthma is a developmental origin disease influenced by maternal diet and bacterial metabolites. *Nat. Commun.* 6:8320. doi: 10.1038/ncomms8320

Thursby, E., and Juge, N. (2017). Introduction to the human gut microbiota. *Biochem. J.* 474, 1823–1836. doi: 10.1042/BCJ20160510

Tyagi, A. M., Yu, M., Darby, T. M., Vaccaro, C., Li, J.-Y., Owens, J. A., et al. (2018). The Microbial Metabolite Butyrate Stimulates Bone Formation *via* T Regulatory Cell-Mediated Regulation of WNT10B Expression. *Immunity* 49, 1116.e–1131.e. doi: 10.1016/j.immuni.2018.10.013

Upadhyay, J., Farr, O. M., and Mantzoros, C. S. (2015). The role of leptin in regulating bone metabolism. *Metabolism* 64, 105–113. doi: 10.1016/j.metabol.2014.10.021

Venkatesh, M., Mukherjee, S., Wang, H., Li, H., Sun, K., Benechet, A. P., et al. (2014). Symbiotic Bacterial Metabolites Regulate Gastrointestinal Barrier Function *via* the Xenobiotic Sensor PXR and Toll-like Receptor 4. *Immunity* 41, 296–310. doi: 10.1016/j.immuni.2014.06.014

Verna, E. C., and Lucak, S. (2010). Use of probiotics in gastrointestinal disorders: what to recommend? *Therap. Adv. Gastroenterol.* 3, 307–319. doi: 10.1177/1756283X10373814

Wallimann, A., Magrath, W., Thompson, K., Moriarty, T., Richards, R., Akdis, C., et al. (2021). Gut microbial-derived short-chain fatty acids and bone: a potential role in fracture healing. *Eur. Cells Mater.* 41, 454–470. doi: 10.22203/eCM.v041a29

Walsh, M. C., Kim, N., Kadono, Y., Rho, J., Lee, S. Y., Lorenzo, J., et al. (2006). Osteoimmunology: interplay between the immune system and bone metabolism. *Annu. Rev. Immunol.* 24, 33–63. doi: 10.1146/annurev.immunol.24.021605.090646

Wang, J., Wang, Y., Gao, W., Wang, B., Zhao, H., Zeng, Y., et al. (2017). Diversity analysis of gut microbiota in osteoporosis and osteopenia patients. *PeerJ* 5:e3450. doi: 10.7717/peerj.3450

Wang, M., Tian, T., Yu, S., He, N., and Ma, D. (2013). Th17 and Treg Cells in Bone Related Diseases. *Clin. Dev. Immunol.* 2013, 1–10. doi: 10.1155/2013/203705

Wargo, J. A. (2020). Modulating gut microbes. *Science* 369, 1302–1303. doi: 10.1126/science.abc3965

Wolter, M., Grant, E. T., Boudaud, M., Steimle, A., Pereira, G. V., Martens, E. C., et al. (2021). Leveraging diet to engineer the gut microbiome. *Nat. Rev. Gastroenterol. Hepatol.* [Preprint]. doi: 10.1038/s41575-021-00512-7

Wu, H.-J., and Wu, E. (2012). The role of gut microbiota in immune homeostasis and autoimmunity. *Gut Microbes* 3, 4–14. doi: 10.4161/gmic.19320

Wu, H.-J., Ivanov, I. I., Darce, J., Hattori, K., Shima, T., Umesaki, Y., et al. (2010). Gut-Residing Segmented Filamentous Bacteria Drive Autoimmune Arthritis *via* T Helper 17 Cells. *Immunity* 32, 815–827. doi: 10.1016/j.immuni.2010.06.001

Xiao, E., He, L., Wu, Q., Li, J., He, Y., Zhao, L., et al. (2017). Microbiota regulates bone marrow mesenchymal stem cell lineage differentiation and immunomodulation. *Stem Cell Res. Ther.* 8:213. doi: 10.1186/s13287-017-0670-7

Xu, Z., Xie, Z., Sun, J., Huang, S., Chen, Y., Li, C., et al. (2020). Gut Microbiome Reveals Specific Dysbiosis in Primary Osteoporosis. *Front. Cell. Infect. Microbiol.* 10:160. doi: 10.3389/fcimb.2020.00160

Yadav, V. K., Oury, F., Suda, N., Liu, Z.-W., Gao, X.-B., Confavreux, C., et al. (2009). A Serotonin-Dependent Mechanism Explains the Leptin Regulation of Bone

Mass, Appetite, and Energy Expenditure. *Cell* 138, 976–989. doi: 10.1016/j.cell.2009.06.051

Yadav, V. K., Oury, F., Tanaka, K. F., Thomas, T., Wang, Y., Cremers, S., et al. (2011). Leptin-dependent serotonin control of appetite: temporal specificity, transcriptional regulation, and therapeutic implications. *J. Exp. Med.* 208, 41–52. doi: 10.1084/jem.20101940

Yamada, T., Park, G., Node, J., Ozaki, K., Hiraiwa, M., Kitaguchi, Y., et al. (2019). Daily intake of polyamine-rich Saccharomyces cerevisiae S631 prevents osteoclastic activation and bone loss in ovariectomized mice. *Food Sci. Biotechnol.* 28, 1241–1245. doi: 10.1007/s10068-019-00561-4

Yamamoto, T., Hinoi, E., Fujita, H., Iezaki, T., Takahata, Y., Takamori, M., et al. (2012). The natural polyamines spermidine and spermine prevent bone loss through preferential disruption of osteoclastic activation in ovariectomized mice. *Br. J. Pharmacol.* 166, 1084–1096. doi: 10.1111/j.1476-5381.2012.01856.x

Yan, F. F., Mohammed, A. A., Murugesan, G. R., and Cheng, H. W. (2019). Effects of a dietary synbiotic inclusion on bone health in broilers subjected to cyclic heat stress episodes. *Poult. Sci.* 98, 1083–1089. doi: 10.3382/ps/pey508

Yan, J., and Charles, J. F. (2017). Gut Microbiome and Bone: to Build, Destroy, or Both? *Curr. Osteoporos. Rep.* 15, 376–384. doi: 10.1007/s11914-017-0382-z

Yan, J., Herzog, J. W., Tsang, K., Brennan, C. A., Bower, M. A., Garrett, W. S., et al. (2016). Gut microbiota induce IGF-1 and promote bone formation and growth. *Proc. Natl. Acad. Sci.* 113, E7554–E7563. doi: 10.1073/pnas.1607235113

Yano, J. M., Yu, K., Donaldson, G. P., Shastri, G. G., Ann, P., Ma, L., et al. (2015). Indigenous Bacteria from the Gut Microbiota Regulate Host Serotonin Biosynthesis. *Cell* 161, 264–276. doi: 10.1016/j.cell.2015.02.047

Yu, L. C.-H. (2012). Host-microbial interactions and regulation of intestinal epithelial barrier function: From physiology to pathology. *World J. Gastrointest. Pathophysiol.* 3:27. doi: 10.4291/wjgp.v3.i1.27

Yu, M., Malik Tyagi, A., Li, J.-Y., Adams, J., Denning, T. L., Weitzmann, M. N., et al. (2020). PTH induces bone loss *via* microbial-dependent expansion of intestinal TNF+ T cells and Th17 cells. *Nat. Commun.* 11:468. doi: 10.1038/s41467-019-14148-4

Yuan, H., Wu, S.-X., Zhou, Y.-F., and Peng, F. (2021). Spermidine Inhibits Joints Inflammation and Macrophage Activation in Mice with Collagen-Induced Arthritis. *J. Inflamm. Res.* 14, 2713–2721. doi: 10.2147/JIR.S313179

Zaiss, M. M., Axmann, R., Zwerina, J., Polzer, K., Gückel, E., Skapenko, A., et al. (2007). Treg cells suppress osteoclast formation: A new link between the immune system and bone. *Arthritis Rheum.* 56, 4104–4112. doi: 10.1002/art.23138

Zhang, Z., Lin, T., Meng, Y., Hu, M., Shu, L., Jiang, H., et al. (2021). FOS/GOS attenuates high-fat diet induced bone loss *via* reversing microbiota dysbiosis, high intestinal permeability and systemic inflammation in mice. *Metabolism* 119:154767. doi: 10.1016/j.metabol.2021.154767

Zhao, Y.-X., Song, Y.-W., Zhang, L., Zheng, F.-J., Wang, X.-M., Zhuang, X.-H., et al. (2020). Association between bile acid metabolism and bone mineral density in postmenopausal women. *Clinics* 75:e1486. doi: 10.6061/clinics/2020/e1486

Zheng, T., Kim, N.-Y., and Yim, M. (2017). Fexaramine Inhibits Receptor Activator of Nuclear Factor-κB Ligand-induced Osteoclast Formation *via* Nuclear Factor of Activated T Cells Signaling Pathways. *J. Bone Metab.* 24:207. doi: 10.11005/jbm.2017.24.4.207

Conflict of Interest: The authors declare that the research was conducted in the absence of any commercial or financial relationships that could be construed as a potential conflict of interest.

Publisher's Note: All claims expressed in this article are solely those of the authors and do not necessarily represent those of their affiliated organizations, or those of the publisher, the editors and the reviewers. Any product that may be evaluated in this article, or claim that may be made by its manufacturer, is not guaranteed or endorsed by the publisher.

Copyright © 2022 Bhardwaj, Sapra, Tiwari, Mishra, Sharma and Srivastava. This is an open-access article distributed under the terms of the Creative Commons Attribution License (CC BY). The use, distribution or reproduction in other forums is permitted, provided the original author(s) and the copyright owner(s) are credited and that the original publication in this journal is cited, in accordance with accepted academic practice. No use, distribution or reproduction is permitted which does not comply with these terms.

frontiers in Immunology

ORIGINAL RESEARCH
published: 23 February 2022
doi: 10.3389/fimmu.2022.815046

Altered Gut Microbiome and Fecal Immune Phenotype in Early Preterm Infants With Leaky Gut

Jose M. Lemme-Dumit[1,2], Yang Song[3], Hnin Wai Lwin[3], Claudia Hernandez-Chavez[3], Sripriya Sundararajan[1], Rose M. Viscardi[1], Jacques Ravel[3,4], Marcela F. Pasetti[1,2,4] and Bing Ma[3,4]**

[1] Department of Pediatrics, University of Maryland School of Medicine, Baltimore, MD, United States, [2] Center for Vaccine Development and Global Health, University of Maryland School of Medicine, Baltimore, MD, United States, [3] Institute for Genome Sciences, University of Maryland School of Medicine, Baltimore, MD, United States, [4] Department of Microbiology and Immunology, University of Maryland School of Medicine, Baltimore, MD, United States

Intestinal barrier immaturity, or "leaky gut", is the proximate cause of susceptibility to necrotizing enterocolitis in preterm neonates. Exacerbated intestinal immune responses, gut microbiota dysbiosis, and heightened barrier injury are considered primary triggers of aberrant intestinal maturation in early life. Inordinate host immunity contributes to this process, but the precise elements remain largely uncharacterized, leaving a significant knowledge gap in the biological underpinnings of gut maturation. In this study, we investigated the fecal cytokine profile and gut microbiota in a cohort of 40 early preterm infants <33-weeks-gestation to identify immune markers of intestinal barrier maturation. Three distinct microbiota types were demonstrated to be differentially associated with intestinal permeability (IP), maternal breast milk feeding, and immunological profiles. The *Staphylococcus epidermidis*- and Enterobacteriaceae-predominant microbiota types were associated with an elevated IP, reduced breast milk feeding, and less defined fecal cytokine profile. On the other hand, a lower IP was associated with increased levels of fecal IL-1α/β and a microbiota type that included a wide array of anaerobes with expanded fermentative capacity. Our study demonstrated the critical role of both immunological and microbiological factors in the early development of intestinal barrier that collectively shape the intestinal microenvironment influencing gut homeostasis and postnatal intestinal maturation in early preterm newborns.

Keywords: preterm infants, gut microbiome, fecal cytokines, local immune phenotype, intestinal barrier maturation

OPEN ACCESS

Edited by:
Magdalena Plebanski, RMIT University, Australia

Reviewed by:
Elisa L. Hill-Yardin, RMIT University, Australia
Jennifer Carla Boer, RMIT University, Australia

***Correspondence:**
Bing Ma
bma@som.umaryland.edu
Marcela F. Pasetti
Mpasetti@som.umaryland.edu

Specialty section:
This article was submitted to Microbial Immunology, a section of the journal Frontiers in Immunology

Received: *14 November 2021*
Accepted: *31 January 2022*
Published: *23 February 2022*

Citation:
Lemme-Dumit JM, Song Y, Lwin HW, Hernandez-Chavez C, Sundararajan S, Viscardi RM, Ravel J, Pasetti MF and Ma B (2022) Altered Gut Microbiome and Fecal Immune Phenotype in Early Preterm Infants With Leaky Gut. Front. Immunol. 13:815046. doi: 10.3389/fimmu.2022.815046

INTRODUCTION

A functional intestinal barrier is not just a static physical boundary but a dynamic, interactive tissue structure that combines a cellular barrier with chemical, immunological, and microbiological components (1, 2). The human intestinal epithelium harbors multiple specialized cell types and is supported by a diverse population of underlying immune cells; the tissue arrangement, interaction, and function are controlled by intricate cell contact-mediated signals and distinct cytokines and molecular mediators in the local microenvironment (2, 3).

A community of diverse microorganisms inhabiting the gastrointestinal tract, collectively referred as gut microbiota, contributes to intestinal homeostasis and overall health (4). It is well-accepted that the intestinal microbiota is established concurrently with the developing mucosal immunological barrier after birth (1, 5–8), although it has been argued that the human microbiota may develop even earlier in the prenatal intrauterine environment (9–12). The interactions of microorganisms with immune and non-immune cells that make up the human gut can evoke both an immediate and innate as well as a delayed, and more refined, immune response - a process known as "host-microbial crosstalk" that contains microbial penetration (13). The communications between epithelial cells, immune cells, and gut microbiota orchestrate immune responses to specific antigens and balance tolerance; these processes evolve through the different stages of life to accommodate host developmental needs (2, 7).

Microbial gut dysbiosis (e.g., low microbial diversity), or imbalanced gut microbial community (e.g., overabundance of Proteobacteria), is a common feature of premature intestine compared to term infants (14, 15). Multiple factors appear to be associated with microbial dysbiosis, such as aberrant peristalsis (16), lower gastric acid production (17), altered cell surface glycoconjugates (18), compromised mucin layer and reduced protective molecules (19), and deficient proteolytic enzyme activity (17). In a hyperpermeable infant gut, bacteria and bacterial products normally confined to the intestinal lumen are able to translocate into the inner host compartment, resulting in microbial invasion, mucosal inflammation, epithelial cell damage, necrosis, systemic infection, and ultimately multi-organ failure and death (20–22). The intestinal impairment-associated conditions have a high mortality (6.3%) and morbidity (34.1%) rate; infant survivors may suffer life-long health sequelae such as neurodevelopmental delay, liver failure, or short bowel syndrome (23, 24). In fact, intestinal prematurity is the greatest risk factor for developing necrotizing enterocolitis (NEC) (25, 26), a life-threatening, inflammatory bowel disease affecting approximately 7-10% preterm neonates with mortality as high as 30-50% (27–31). A thorough understanding of microbial and immunological factors that promote intestinal barrier function in early preterm newborns is, therefore, of paramount importance.

The repertoire and magnitude of cytokines and chemokines in preterm newborns remain largely uncharacterized, leaving a significant knowledge gap in understanding early intestinal barrier maturation. The analysis of immunological biomarkers traditionally involves blood or serum testing. Such sampling is invasive and is limited to circulating levels of immune markers, which is valuable for assessment for systemic immunity but not necessarily representative of the localized intestinal mucosa. Intestinal biopsies have been used to determine local microbiome cytokine signatures associated with neurodevelopmental disorder (32). Resected tissue better reflects host-microbe interactions. However, tissue scraping is overly invasive and impractical for studies involving infants. Alternatively, a relevant and non-invasive approach (with easier specimen collection) is fecal profiling of the localized intestinal cytokine microenvironment.

The intestinal immune system is regionally specialized in composition and function, and this distinctiveness has been attributed to anatomical and physiological elements, as well as the inhabiting microbiota (33, 34). Hence, the determination of immune mediators (e.g., cytokines and chemokines) evoked locally as a result of the host interaction with the intestinal microbial community is inherently advantageous to understand both immune quiescence during homeostasis and the inflammatory process that results from an epithelial barrier breach (6).

We previously reported an astonishing 42.5% prevalence of persistently elevated intestinal permeability (IP) in early preterm infants (<33 weeks) (35, 36), with IP being determined by the ratio of urine excretion of ingested sugar (lactulose and rhamnose) probes. Further, this aberrant intestinal maturation was found to be associated with the lack of breast milk feeding, prolonged antibiotics exposure, and perturbation in the development of the intestinal microbiota. In this study, we investigated cytokine and chemokine profiles in fecal extracts obtained from a cohort of 40 early preterm neonates (24-32 weeks of gestation) with both high and low IP at 7-10 days post-birth, to investigate their association with microbiological and neonatal factors implicated in intestinal barrier maturation. Three distinct gut microbiota types were revealed, which were differentially associated with IP and nutritional factors as well as distinct immunological profiles. Most outstandingly, infants with lower IP had increased levels of IL-1α/β and a type of gut microbiota with a more diversified array of anaerobic and facultative bacteria. Our study demonstrated distinct immunological and microbiological features during early stages of development of the intestinal barrier that collectively influence gut homeostasis and postnatal intestinal maturation in early preterm newborns.

RESULTS

Intestinal Permeability in Preterm Newborns

Through monitoring IP in previous studies, we and others have demonstrated that rapid intestinal barrier maturation occurs in most preterm infants during the first 7-10 days after birth, despite highly permeable gut at birth in most newborns (35–37). IP was determined as the ratio of two enterally administered sugar probes Lactulose (La) and Rhamnose (Rh), which are markers of intestinal paracellular and transcellular pathways, respectively (38, 39). High IP was defined as La/Rh ratio >0.05, as previously described and validated (35). Persistently elevated IP during the 7-10 days after birth indicated a delayed physiological maturity of the intestinal tract barrier in early preterm infants. In this study, we employed a cohort of 40 early preterm newborns 24 weeks ($24^{0/7}$)-32 weeks and 6 days ($32^{6/7}$) of gestation recruited at the Neonatal Intensive Care Unit (NICU) of University of Maryland Medical Center in Baltimore, Maryland. Twenty of these infants had high IP while the remaining had low IP 7-10 days after birth. Metagenomic sequencing was performed on fecal samples obtained from these 40 infants between 7 to 10 postnatal days. The IP values for the cohort ranged from 0.001 to 0.11 with an

average of 0.09 ± 0.09 (mean ± SD). Cohort subjects were 30.2 ± 2.43 weeks gestational age (GA) at birth. Their mean birth weight (BW) was 1,414 g (± 414.6 g); 21 (52.5%) neonates were classified as very low BW (VLBW, <1,500 g) and 8 (20.0%) were classified as extremely low BW (ELBW, <1,000 g). Sixteen of the infants (40.0%) were born with spontaneous vaginal delivery, the other 24 infants were delivered by cesarean section. The demographic, obstetric, and neonatal characteristics of the subjects are summarized in **Supplemental Table 1**.

Microbiome Type Correlates With Intestinal Permeability and Maternal Breast Milk Feed

The gut microbial community was determined by conducting whole community metagenomic sequencing of 61 fecal specimens collected from the 38 infants; 18 of them had more than one fecal sample collected during the 7-10 days after birth. A total of 1,721.8 million metagenomic sequence reads (average of ~28.2 million sequence reads per sample) were obtained after quality assessment (**Supplemental Table 2**). Taxonomic profiles were determined for all samples (**Supplemental Table 3**) and clustered into three distinct groups according to similarities in community composition and structure (**Figure 1A**). Two of these groups have a single species that is dominantly abundant (>95%): the *Staphylococcus epidermidis*-predominated community type (the "S" type), and Enterobacteriaceae (the "E" type) predominated by either *Klebsiella pneumoniae* or *Escherichia coli*. On the other hand, the "O" type of gut microbiota encompasses a wide array of anaerobic and facultative microorganisms and was not predominated by *S. epidermidis*, *K. pneumoniae* or *E. coli*. The O type demonstrated a significantly higher community bacterial diversity (p-value < 0.05) than the S type, which has the lowest level of bacterial diversity (**Figure 1A** and **Supplemental Figure 1**). The predominantly abundant taxa of the E and S types were shown to be Enterobacteriaceae (i.e., *K. pneumoniae* or *E. coli*) and *S. epidermidis*, respectively. The top abundant taxonomic groups of O type include *Bifidobacterium*, *Lactobacillales*, *Veillonellales*, *Clostridiales*. These data support our previous findings that intestinal barrier maturation correlates with the establishment and colonization of a diverse array of obligate and facultative anaerobes, particularly in the groups of *Actinobacteria*, *Lactobacillales*, *Veillonellales*, and *Clostridiales*, which are considered the 'successor' bacteria to the first colonizers *S. epidermidis* and Enterobacteria, during the establishment of commensal communities after birth (36, 44, 45).

We next examined the correlation of the three microbiota types (E, S and O) with IP and the known IP-associated factors that include GA, BW, mother's own breast milk (MOM) feed, and antibiotics (abx) duration (35, 36). Delivery mode was also associated with IP; infants delivered through cesarean section had significantly higher IP than those delivered through spontaneous vaginal birth (p value = 0.01, **Supplemental Figure 5**). The O microbiota type was associated with newborns that had low IP, later GA (≥ 28 weeks), higher BW (≥ 1,500g), and more cumulative amount of MOM (≥ 150-180 ml/kg of cumulative intake) by 7-10 postnatal days (**Figure 1B**). The S microbiota type, on the other hand, correlated with high IP, early GA (< 28 weeks), lower BW (< 1,500g), and less MOM (<150 ml/kg of cumulative intake). Preterm infants with E microbiota type had significantly higher IP than those with O type but not those with S type and high MOM intake. Further, GA and BW were similar in E and S type microbiota (**Figure 1B**).

Fecal IL-1α and IL-7 Correlated With Increased Microbial Biodiversity

We sought to investigate the profile of cytokines and chemokines in the fecal samples from preterm infants as markers of gut inflammation and mucosal adaptation to intestinal microbiota (**Figure 2** and **Supplemental Table 5**). Given the lack of information on local mucosal immune mediators in preterm infants, a broad panel of 16 cytokines and 14 chemokines produced and secreted by intestinal epithelial cells and immune cells was selected. The immune biomarkers were analyzed considering neonatal and nutritional factors including IP, GA and BW, MOM feed, and gut microbiota type. Out of a total of 30 cytokines and chemokines measured, 15 of them were detected, whereas the others were undetectable or below the limit of detection for the immunoassay. Strikingly, infants that exhibited higher IP and medium-to-low MOM intake presented reduced or undetectable levels for most of the cytokines independent of the gut microbiota type (**Figure 2**). This finding emphasizes the differences between the immature and mature intestine, and the distinctiveness of the preterm population as compared to term infants and adults.

Stool of infants with O type gut microbiota contained significantly higher levels of IL-1α and IL-7 as compared to S type samples (**Figure 2** and **Supplemental Figures 2A, B**). In a correlation analysis with individual species abundance using linear regression, IL-1α and IL-7 were shown to be both positively correlated with the relative abundance of *Enterococcus faecalis* and negatively correlated with *S. epidermidis* (**Supplemental Figure 3**).

Further, significantly increased levels of IL-12p70 were detected in O type microbiota as compared to E type (**Supplemental Figure 2C**). The presence of other cytokines including IL-12p40, IL-15, and IL-16 were also higher in O type specimens in comparison to S type group (**Figure 2**); whereas IL-6 was detected only in the stool of E type microbiota as compared to S and O type groups (**Figure 2** and **Supplemental Figure 2D**).

IL-1β and IL-1α Association With Low Intestinal Permeability

Comparative analysis of fecal cytokines in samples with high (La/Rh ≥0.05) or low IP (La/Rh <0.05) revealed a significant correlation between IL-1β and low IP (p-value < 0.01) (**Figure 3A**). IL-1β was also associated with less use of abx (≤ 3 days, p-value < 0.05) (**Figure 3B**). IL-1β levels showed a trend for correlation with MOM feed (p-value=0.067) (**Figure 3C**), while it did not associate with GA (**Figure 3D**). IL-1α levels showed a statistical trend for association with low IP (p-value=0.08) (**Figure 3E**) and was significantly increased in infants with less abx (p-value < 0.01) (**Figure 3F**), more MOM feed (p-value <0.05) (**Figure 3G**), and later GA (p-value < 0.01) (**Figure 3H**). These data suggest an important role for IL-1β and IL-1α in the multifactorial processes involved in enhanced intestinal barrier and immune

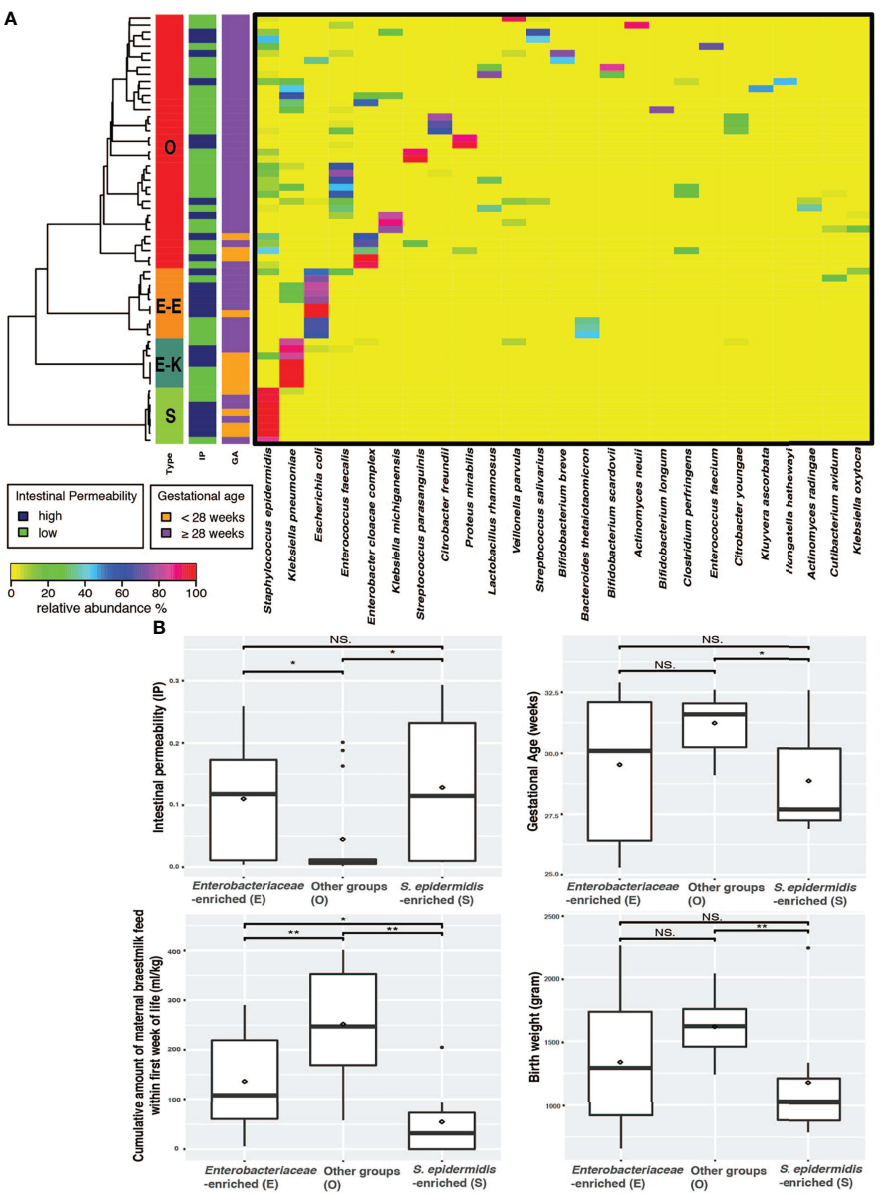

FIGURE 1 | Preterm infants exhibited three distinct microbiome types. **(A)** Heatmap of the 25 most abundant intestinal bacterial taxa and their relative abundance in samples collected from 38 preterm infants enrolled in the study. The taxonomic composition of the microbiomes used the data set of whole community metagenomic sequencing and the profile was generated by MetaPhlAn version 2 (40). Statistical significance was calculated using Wilcoxon rank sum test using *ggsignif* R package (41). Ward linkage clustering was used to cluster samples based on their Jensen-Shannon distance calculated in vegan package in R (42). The number of clusters was validated using gap statistics implemented in the *cluster* package in R (43) by calculating the goodness of clustering measure. **(B)** Boxplots of IP, GA, MOM, and BW depicting distribution of microbiota types in fecal samples of preterm newborns. Significance value was calculated using Wilcoxon rank sum test. *p < 0.05, **p < 0.01. Plotted are interquartile ranges (IQRs, boxes), medians (line in box), and mean (red diamond). IP, intestinal permeability; GA, gestational age; NS., not significant.

maturity. IL-1α was more closely linked with age and birth weight and may represent an immunological biomarker for age-appropriate intestinal maturation. On the other hand, IL-1β levels are most significantly correlated with IP that is irrespective of age, which suggests a potential influence in microbiota development. Still, postnatal intestinal maturation is a complex process that involves multiple factors that shape the infant gut environment, including the nervous system and mucosal lymphoid tissue development, and host-microbe interactions in addition to early microbial colonization (30, 48–50).

When compared with the abundance of individual species, IL-1β was found to be positively correlated with *Bacteroides* and *Clostridium perfringens* (**Supplemental Figure 3**). IL-16 and IL-12p70 levels showed a trend for correlation with less abx intake (p-value=0.2)

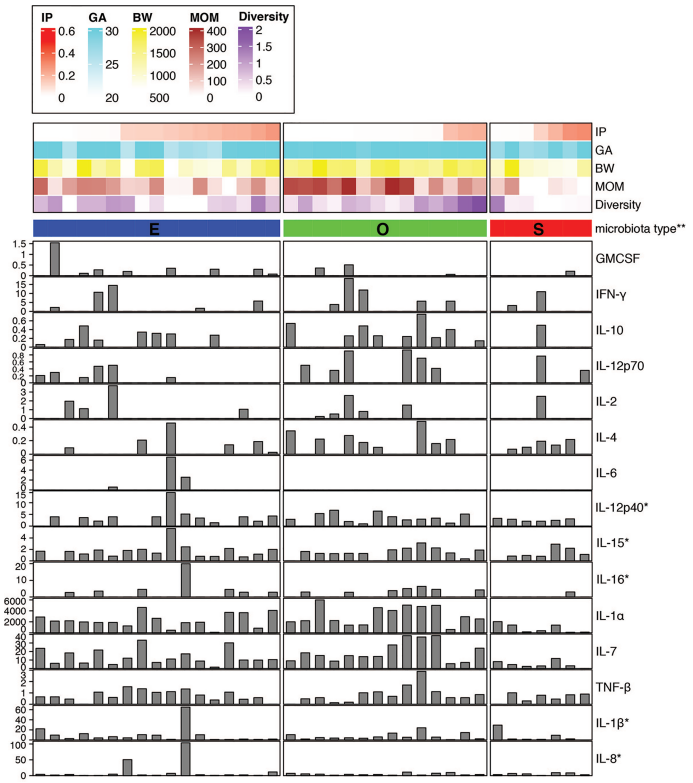

FIGURE 2 | Fecal cytokine profile associated with microbial diversity. Color map of microbial communities correlating with neonatal factors and barplot map of the 15 cytokines detected. Within-sample diversity was estimated using Shannon diversity index using Phyloseq R package (46). Plot was generated using R package 'complexheatmap' (47). *Value was scaled using square root. **Microbiota type was assigned according to the clustering pattern as shown in **Figure 1**. IP, intestinal permeability; GA, gestational age; BW, birth weight; MOM, mother's own breast milk cumulative volume use during the first week prior to IP measurement.

(**Figures 3J, N**). Strikingly, IL-10 was significantly increased in infants with less MOM feed (**Figure 3K**) and negatively correlated with the relative abundance of *Peptostreptococcus anaerobius* and *Veillonella parvula* (**Supplemental Figure 3**). Further, IL-12p40 was significantly associated with greater BW (**Figure 3L**) and found to be negatively correlated with *S. epidermidis* relative abundance (**Supplemental Figure 3**), which suggests that IL-12p40 may be involved in the reduction of *S. epidermidis* during microbial succession and the establishment of infant immunity, along with IL-1α and IL-7. Increased levels of IL-1β showed a statistical trend for association with spontaneous vaginal delivery (p-value=0.066) (**Figure 3I**), while granulocyte-macrophage colony-stimulating factor (GM-CSF) were significantly associated with this delivery mode (p-value=0.01) (**Figure 3M**). There was a trend of reduced IL-12p40 levels in infants with lower MOM feed (**Figure 3O**). IL-7 was significantly associated with later GA (p-value < 0.05) (**Figure 3P**).

High Inter-individual Variation of Cytokine Profile in S. epidermidis- and Enterobacteriaceae-Dominated Microbial Communities

Canonical Correspondence Analysis (CCA) on the taxonomic profiles further supported the presence of three distinct microbiota types, as described above (**Figure 4A**). Based on a scaled eigenvalue, the top taxonomic groups that contributed to the separation of the microbiota type in ordination analyses were identified (**Supplemental Table 4**). Both *S. epidermidis*- and Enterobacteriaceae-dominated microbial community shared a greater within-cluster similarity, or a "tight" clustering based on taxonomic (**Figure 4A**) and functional pathway profiles as determined by metagenomes (**Supplemental Figure 4**). CCA was also applied to visualize the patterns of gut microbial and fecal cytokine profiles in the preterm infants (**Figure 4B**). Both the S and the E microbiota types, particularly the *S. epidermidis*-dominated type, had a highly diversified immunological profile with much greater inter-individual variation that is, a "loose" cluster based on immune markers (**Figure 4B**). Conversely, the O type microbiota had a more diverse clustering of taxonomic groups and more diversified functional profiles and greater within-cluster similarity based on cytokine and chemokine profiles. These results indicate that host immunity to S or E microbiota types varies markedly among individuals. This inter-individual variation in immune profiles is indicative of an unstable and less defined immunological environment, which may relate to a lack of establishment of age-appropriate gut microbiota (**Figure 5**). These data suggest that as the intestinal microbiota becomes established with an age-appropriate bacterial

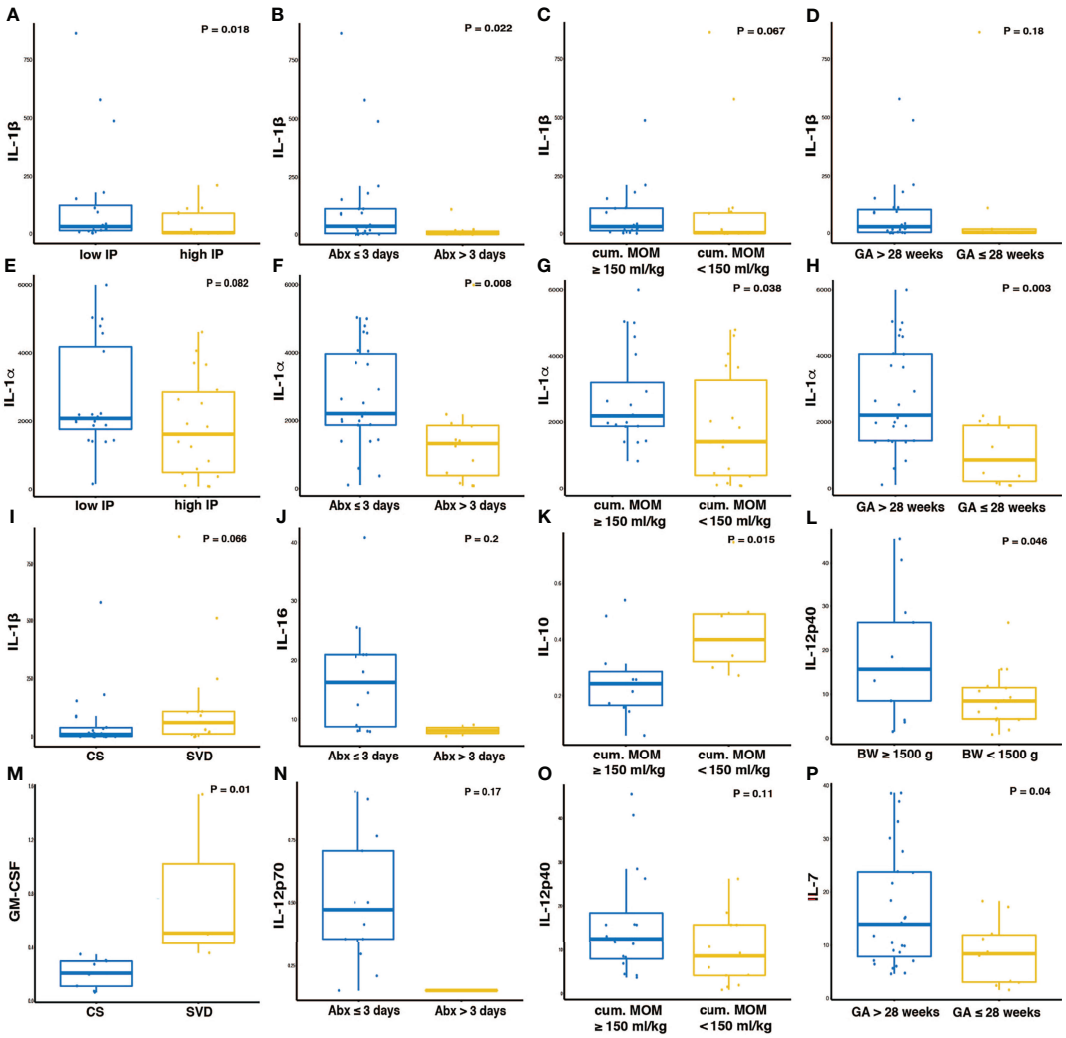

FIGURE 3 | IL-1α and IL-1β linked to lower IP and improved neonatal factors. Boxplots of the cytokine levels: **(A-D, I)** IL-1β, **(E–H)** IL-1α, **(J)** IL-16, **(K)** IL-10, **(L, O)** IL-12p40, **(M)** GM-CSF, **(N)** IL-12p70, **(P)** IL-7 between different categories. Plotted are interquartile ranges (IQRs, boxes), medians (line in box), and mean (red diamond). Significance value was calculated using Wilcoxon rank sum test using *ggsignif* R package (41). Asterisk denotes the level of significance. Threshold for early or late gestational age is 28 weeks, for low or high birth weight is 1,500 g, for longer or shorter abx exposure is 3 days during the first week after birth prior to IP measurement, for maternal breast milk feeding is 150-180 ml/kg of cumulative intake of MOM by 7-10 days of age, according to clinical convention and previously validation (35, 36). IP, intestinal permeability; GA, gestational age; BW, birth weight; MOM, mother's own breast milk (MOM) cumulative volume use during the first week prior to IP measurement; SVD, spontaneous vaginal delivery; CS, cesarean section.

colonization, the mucosal immunity in the preterm infants tend to be more stable and defined. Our findings highlight the importance of defining both immune profiles and microbiome to holistically understand postnatal intestinal maturation.

DISCUSSION

The pathophysiology of aberrant postnatal intestinal maturation is a multifactorial process that includes intestinal mucosa barrier immaturity, imbalance in microvascular tone, aberrant microbial colonization, and altered immune responses (30, 48, 49). We and others have previously shown that neonatal and clinical factors including GA or postmenstrual age, abx exposure, and exclusive breast milk feeding were associated with intestinal barrier function in early preterm infants (35, 52). Further, a delayed increase in intestinal bacterial biodiversity due to a lack of breast milk-derived or -promoted growth of *Bifidobacterium*, was shown to contribute to delayed growth and delayed intestinal maturation (35, 36, 53, 54). In this study, we sought to delineate the complex mechanisms governing intestinal barrier maturation by characterizing fecal cytokines and chemokines and interrogating correlates with IP-associated neonatal and microbiological factors. Integrative insights into the interplay between gut microbiota and the infant immune system are crucial to understanding the underpinning of intestinal

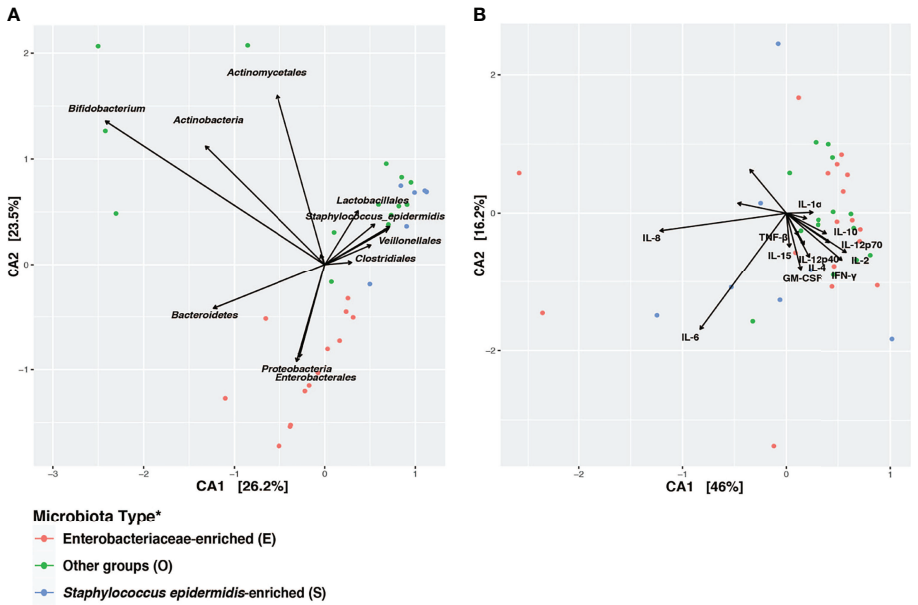

FIGURE 4 | Disparity in clustering patterns of taxonomic and immunological profiling among different microbiota types. Canonical Correspondence Analysis (CCA) of **(A)** microbial taxonomic groups; **(B)** cytokine profiles. CCA was based on Bray-Curtis distance. CA1 and CA2 selected as the major components based on the eigenvalue. A scaled eigenvalues was shown on the plot to represent the direction from the origin where a group has a larger than average value for the particular profile (42, 51). *Microbiota type was assigned according to the clustering pattern demonstrated in **Figure 1**.

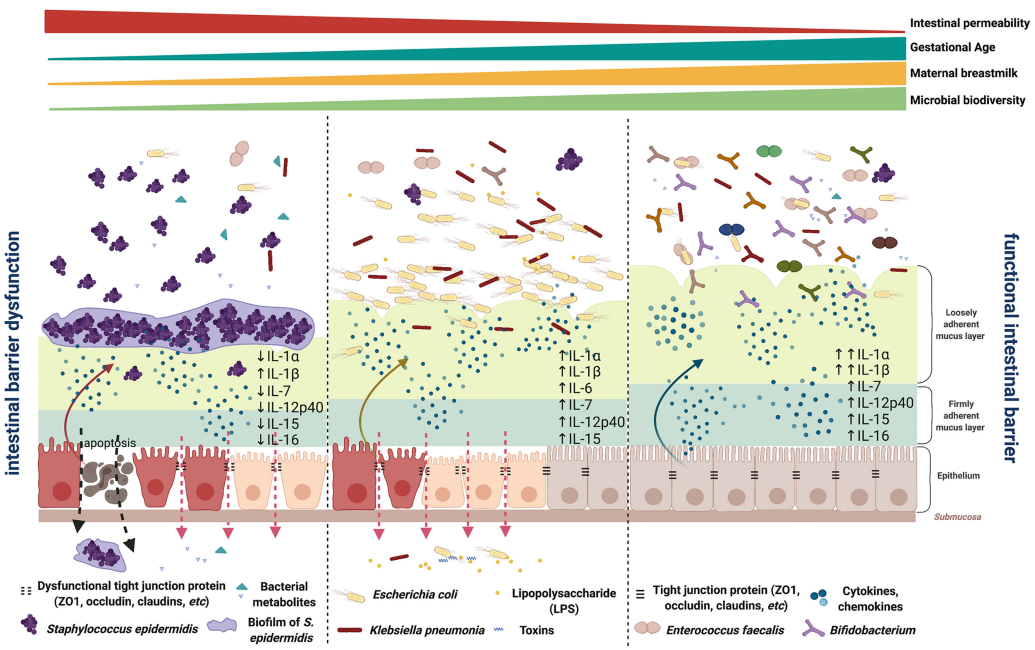

FIGURE 5 | Illustration of the intestinal barrier maturation in early preterm neonates with different microbiota types and cytokine profiles. An immature, compromised gut barrier may render the mucosa susceptible to invasion by opportunistic pathogens in the gut lumen. IP was linked with a microbial community dominated by a single species *S. epidermidis*, *K. pneumoniae*, or *E. coli*, with less defined cytokine profiles among individuals. A functional intestinal barrier was associated with neonates with later GA; higher BW; greater microbial community biodiversity that encompasses a wide array of anaerobic and facultative microorganisms not dominated by *S. epidermidis*, *K. pneumoniae*, or *E. coli*; and a trend of increased levels of IL-1α/β, IL-7, IL-12p40, IL-15, and IL-16. Schematic representation illustrates the distal intestine (not drawn to scale). Created with BioRender.com.

immaturity and to inform the development of novel therapeutics to prevent leaky gut in premature newborns.

Cytokines and growth factors are important mediators of intestinal epithelial cell development, differentiation, expansion, and immune activation (55). They are expressed endogenously by the midgestational intestine at higher levels as compared to the adult counterpart (56). After birth, the newborn and infant intestine continue to be influenced by cytokines and growth factors from colostrum and breast milk. Cytokine profiles are typically determined as circulating levels in serum samples. However, such measurements fail to reflect local cell-signaling and immune mediators. The profiling of cytokines in fecal extracts offers a snapshot of the mucosal intestinal environmental. While the approach may not fully recapitulate the host-microbe interactions that occur at the epithelial surface, it provides a reasonable and practical alternative to exceedingly invasive tissue sampling (e.g., biopsy, mucus biofilm sampling or tissue scrapping) which is neither practical nor feasible in routine pediatric studies. The differential abundance of specific gut bacteria has been associated with distinct cytokine responses, and this effect was exerted directly on the intrinsic cytokine production capacity of the immune cells rather than by influencing the number of cells in circulation (57). Profiling of stool cytokines represents a promising, non-invasive method to investigate the localized intestinal cytokine microenvironment, and when combined with microbiota data, it can be a powerful and practical tool to study neonatal intestinal disorders.

Numerous studies have documented an intestinal microbial succession that begins soon after birth (36, 58–60). The initial colonization right after birth includes facultative anaerobes, e.g., *S. epidermis* and Enterobacteriaceae, which are considered "first colonizers" of the infant gut. It is then rapidly followed by the accumulation of obligate anaerobes, including *Bifidobacterium*, *Bacteroides*, and *Clostridiales* with expanded fermentative metabolism capacity. Progressive succession of the early-life microbiota was shown to influence growth and maturation of the endocrine, mucosal immune, and central nervous systems (61). An imbalanced microbiome has been associated with increased risk of neonatal pathologies, including NEC and late-onset sepsis (LOS) (62). Infants with NEC are more likely to develop LOS mainly due to the translocation of intestinal bacteria across the epithelial barrier and the ensuing inflammation (63, 64). *S. epidermis* was shown to diminish rapidly after birth and is usually replenished by obligate anaerobes (36, 58–60). Persistent predominance of *S. epidermidis* and delayed or aberrant microbial succession was associated with growth impairment and predisposition to adverse health conditions (65, 66). *S. epidermidis* is actually the leading agent causing neonatal LOS and other inflammation-related neonatal conditions in preterm neonates including bronchopulmonary dysplasia, and the severity of these conditions is often underestimated (67–71). Though the mechanisms remain unclear, prematurity increased susceptibility of newborn pigs to *S. epidermidis*-associated sepsis, and mortality was related to an immature immune system (72). In the present study, the high IP-associated *S. epidermidis*-predominant community had the greatest inter-individual variation in cytokine responses among all three microbiota types, suggesting an unstable, inordinate mucosal immunity in the immature intestine microenvironment. Overall, our data demonstrate the three stages of microbial succession in early preterm infants, and most importantly, their associations with intestinal immunity during early intestinal maturation (**Figure 5**). The characterization of interactions between early microbial colonization and host immunity as well as their synergistic responses to IP-associated factors such as nutrition, age, and abx intake is pivotal to understand the mechanisms involved in postnatal epithelial barrier maturation.

The ability to derive energy from diet is important for microbial succession and shifting away from Bacilli or Enterobacteriaceae-predominant communities (65, 66, 73). In fact, the diversity of the microbiota remains low in early infancy and is dominated by species involved in human milk oligosaccharide (HMO) metabolism in breastfed infants. In the current study, we demonstrate that the O type microbiota, indicative of optimal microbial succession with a wide array of bacteria with increased fermentative capacity (i.e., *Bifidobacterium*, *Lactobacillus*, *Bacteroides*), is associated with improved intestinal barrier functions and distinct cytokine markers, primarily IL-1α/β.

Human milk is a rich source of nutrients and bioactive molecules including immunoglobulins, cytokines, and immune cells, which support tissue development and protect infants against infectious agents (74). We recently reported that human breast milk enhanced intestinal barrier function and ameliorated pro-inflammatory cytokines production in a human pediatric enteroid model (75). This beneficial effect appears to be mediated by HMO-utilizing *Bifidobacterium* species, whose abundance, we found, correlates with improved intestinal barrier integrity and which is genetically equipped to digest these nutrients. Further characterization of the interaction between HMOs' metabolism, intestinal microbiota, and immunological response will be important to obtain a detailed understanding of postnatal intestinal barrier maturation.

Clearly, the cytokine profile of a mature gut cannot be compared to the profile of the highly immature intestine in the early developmental stage. Increased levels of IL-1α/β in preterm infants were shown to be positively correlated with neonatal factors associated with improved intestinal barrier functions. While the IL-1 superfamily of cytokines has been linked with intestinal barrier dysfunction and gut inflammation in adults, these cytokines have pleiotropic functions, including support of gut homeostasis through various mechanisms (76). For instance, macrophage-derived IL-1β induces IL-2 secretion by ILC3 cells, and IL-2 is essential for maintaining Treg cells, immunological homeostasis, and oral tolerance to dietary antigens in the small intestine as shown in an *in vivo* mouse model (65). In addition, IL-1β, among other cytokines, stimulates the expression of polymeric immunoglobulin receptor and IgA transcytosis across a primary murine epithelial cell monolayer (77). Further, our results suggest that IL-1α and IL-1β relate to intestinal barrier function in a dichotomous way; IL-1β was most closely associated with IP, while IL-1α appeared to be correlated primarily with age-appropriate microbiota development. A previous study suggested that the production of IL-1β was regulated largely at a genetic level

and less influenced by microorganisms (78). Together, our results suggest a beneficial role for IL-1α/β in maintaining gut homeostasis during early development of immature gut. Follow-up studies with in-depth mechanistic interrogation are warranted.

Other cytokines detected in fecal samples and positively correlated with low IP and with other neonatal factors included IL-7, IL-16, and IL-12p40. IL-7 is recognized as an essential factor for lymphopoiesis (79). Intestinal epithelial cells supply local IL-7, as shown by mRNA expression and immunohistochemistry analyses of human intestinal biopsies, and exogenous addition of recombinant IL-7 to isolated lamina propria lymphocytes suggested that locally sourced IL-7 regulated intestinal lamina propria lymphocyte expansion (80). A mechanistic interrogation of IL-7 functions in transgenic mice showed that a dysregulation of colonic epithelial cell-derived IL-7 resulted in chronic inflammation associated with decreased frequencies of γδ T cells and $CD8\alpha\alpha^+$ cells in the inflamed area (81). In an infection model of *Citrobacter rodentium*, intestinal mucosa-derived IL-7 protected the host by controlling bacterial burden and intestinal damage (82). IL-7 stimulates extrathymic γδ T cell precursors and aggregation in cryptopatches in the intestinal mucosa (83). Intraepithelial lymphocytes (IELs), an heterogenous lymphocyte population comprised of γδ T cells among other subsets with anti-microbial and homeostatic functions, reside within the epithelial cell layer of the human gut and strengthen the mucosal barrier (84). IELs appear early in life and gradually accumulate with age after exposure to exogenous antigens (84). In our study, the presence of IL-7 in infants of late GA and less permeable intestine is consistent with expansion of gut γδ IELs during the perinatal period, which in turn promote epithelial cell proliferation and maturation (85). Once established in tissue, γδ IEL relies on the production of IL-15 by the intestinal epithelial cells (86). Our findings support IL-15 production in a microbiota-dependent manner which promotes IEL localization within the intestinal mucosa and function. In the absence of these barrier-enhancing factors, the infiltration of microbes could lead to local necrosis (i.e., NEC and LOS). Future mechanistic studies interrogating the role of IL-7 in the developing infant gut are warranted.

IL-16 is secreted by a variety of cells including lymphocytes and epithelial cells; it functions as chemoattractant of $CD4^+$ cells and triggers the production of pro-inflammatory cytokines by human monocytes (87, 88). Elevated levels of IL-16 have been reported in patients with inflammatory bowel disease and neonatal sepsis (89, 90). In the present study, a trend of increased levels of IL-16 was observed in infants with less abx exposure, reflecting local inflammation. We have also seen increased levels of IL-12p40 positively correlated with infant BW. IL-12p40 has a regulatory function; it competes with IL-12p70 for binding to the IL-12 receptor and is a chemoattractant of macrophages and dendritic cells (91). In an *in vivo* mouse model, IL-12p40 has been shown to limit progression of chronic inflammation by suppressing mucosal Th1 and Th17 responses *via* hypoxia-inducible factor-1α (92).

Unpredictably, IL-10 was inversely correlated with maternal milk feeding. IL-10 is a potent anti-inflammatory and immunosuppressive cytokine; an abundance of IL-10 may limit or downregulate host immune response to microbes (93). The presence/roles of IL-12p40 and IL-10 might be intertwined as compensatory. IL-12p40 production by LPS-stimulated human peripheral blood cells was found to increase following IL-10 blockade (94). In human neonatal cells, TCR/IL-12 stimulation downregulated the IL-10 pathway (95). Together, the local cytokines identified reflect intestinal barrier maturation as well as mucosal immune fitness and aptitude for immunosurveillance.

A study of cytokines in umbilical cord of healthy term newborns found no differences in the levels of inflammatory mediators when comparing normal spontaneous delivery vs. elective cesarean section, except for TGF-β1 (96). Others had reported increased circulating levels of IL-1β in neonates delivered vaginally as compared to those delivered by C-section (97). Similarly, we found that spontaneous vaginal delivery was associated with increased fecal IL-1β and GM-CSF of preterm infants, which suggests that gut maturation and mucosal immune cell seeding may require additional molecular drivers.

Given that cytokines were measured in the feces of breastfeeding infants, the presence of cytokines of maternal origin can be a confounder in the interpretation of infant responses (98). Future studies with larger sample size and longitudinal sampling of both infant and maternal specimens to capture the dynamics and evolution of microbes and immune features are warranted. Additionally, the immune modulatory effect of the microbiota may be exerted through the release of intermediary common mediators such as bacterial products or bioactive bacterial metabolites. The impact of metabolic activities of the microbial community in host-microbe interactions and immunological development remains to be elucidated. Likewise, the observed association between postnatal intestinal maturation and mode of delivery requires further validation. Comprehensive understanding of the role of gut cytokines, chemokines, and other molecular immune mediators in promoting intestinal homeostasis and in mitigating perturbation at early stages of intestinal development, will inform future targeted modulation to improve overall infant health.

CONCLUSION

Our study revealed a pattern of fecal cytokines associated with specific changes in gut microbiota and intestinal barrier maturation. Our findings revealed, for the first time, a potential beneficial role of IL-1α/β in age-appropriate microbiota development and low intestinal permeability in early preterm infants. A delayed microbiota maturation was associated with persistently elevated IP, less breast milk feeding, early GA and low BW, as well as inordinate cytokine profiles. These results support the promising, practical, and non-invasive analysis of cytokine and chemokine profiles in fecal samples to define immune phenotypes associated with gut maturation. A detailed definition of the factors affecting the early development of intestinal barrier functions and precise molecular mechanisms underlying gut homeostasis is necessary to prevent life threatening hyperpermeable gut-associated conditions, including NEC.

METHODS AND MATERIALS

Participants Description and Feeding Protocol

This study was approved and carried out in accordance with protocols approved by the institutional review boards of the University of Maryland School of Medicine and Mercy Medical Center. Written informed parental consent was obtained for all infants in accordance with approved protocol UMB HP-00049647. Forty preterm infants $24^{0/7}$-$32^{6/7}$ weeks GA were enrolled within 4 days after birth, and they represent combined cohorts enrolled during October 2018-June 2021. Prior to study procedures, a complete physical exam including infant's vital signs, weight, height, and head circumference was performed. Demographic, obstetric, and clinical data, as well as data on medication exposures, feeding practices, and adverse events were collected from the medical record. Threshold for early or late gestational age is 28 weeks, for low or high birth weight is 1,500 g, for longer or shorter antibiotics exposure is 3 days during the first week of life prior to IP measurement, as described previously (35, 36).

A standard feeding protocol was used for all preterm participants. Enteral feeds by the orogastric or nasogastric route were initiated between the first and fourth day of life depending on clinical stability. After initial feeds of 10 ml/kg expressed breast milk or 20 kcal/oz preterm formula or donor breast milk daily for 3-5 days, feedings were advanced by 20 ml/kg/d until 100 ml/kg/d was reached. The total volume of breast milk feeds was calculated as sum of the daily amount of milk intake per kilogram of the administered expressed mother's breast milk from initial feed day till postnatal day 7-10 when the IP was measured. Feedings were held or discontinued if there were signs of feeding intolerance such as abdominal distension, gastric residuals, or hematochezia, or for clinical deterioration. Maternal breast milk feeding threshold is 150-180 ml/kg of cumulative intake of MOM by 7-10 days of age, as described previously (35, 36).

In Vivo Intestinal Permeability (IP) Measurement

Among the 40 subjects used in this study, IP for 26 of them was measured in a previous study (35, 36); 14 eligible preterm infants received 1 ml/kg of the non-metabolized sugar probes on postnatal day 7-10, which included lactulose (La, Cumberland Pharmaceuticals, Nashville, TN), which is the marker of intestinal paracellular transport and rhamnose (Rh, Saccharides, Inc., Calgary, Alberta, Canada) the marker of intestinal transcellular transport. One milliliter of 8.6 g La and 140 mg Rh per 100 mL solution was administered enterally by nipple or by gavage *via* a clinically indicated orogastric tube (99). La/Rh was measured by high-pressure liquid chromatography (HPLC) in urine collected over a 4h period following administration of the sugar probes as previously described (35). High or low IP was defined by a La/Rh >0.05 or ≤0.05 respectively, as validated and applied previously (35). Urine samples were stored at -80°C until processed.

Fecal Sample Collection and Processing

Dry fecal samples (~1g) were collected during the same time period (postnatal day 7-10) as the dual sugar administration. Fecal specimens were placed immediately in sterile tube containers with attached screw cap and collection spoon (Globe Scientific Inc. Mahwah, NJ) and stored in -80°C freezer. Another aliquot of fecal samples were stored immediately in DNA/RNA shields (Zymo Research, Irvine, CA), which stabilizes and protects the integrity of nucleic acids to minimize the need to immediately process or freeze specimen for DNA extraction and metagenomic sequencing. Specimens were stored at -80°C until processed.

Cytokine and Chemokine Measurements

A 100 mg aliquot of each frozen dry fecal specimen was resuspended in 1 ml of extraction buffer [phosphate buffered saline (PBS, pH 7.4) containing 0.01% soybean trypsin inhibitor, 0.1% ethylenediaminetetraacetic acid, and 0.05% Tween 20, all from Sigma, St. Louis, MO] and ~1.5 g of 2.3 mm zirconium beads (Biospec, Bartlesville, OK) were incorporated. Fecal samples were subjected to 1-min beating cycle in a mini-beadbeater-8 tissue homogenizer (Biospec, Bartlesville, OK) and centrifuged at 14,000 rpm for 1h at 4°C. The supernatant was collected and stored at -80°C until use. IL-1β, IL-1α, IL-2, IL-4, IL-5, IL-6, IL-7, IL-8, IL-10, IL-12p40/IL-23, IL-12p70, IL-15, IL-16, IL-17, Eotaxin, Eotaxin-2, Eotaxin-3, IP-10, MCP-1, MCP-2, MCP-3, MCP-4, MDC, MIP-1α, MIP-1β, TARC, GM-CSF, TNF-β, VEGF-A, and IFN-γ were quantified in fecal supernatants using human multiplex immunoassays [Meso Scale Discovery (MSD), Rockville, MD] according to the manufacturer's protocol. Each fecal lysate was tested in duplicate. Plates were read using the QuickPlex SQ 120 (MSD, Rockville, MD). The concentration of each analyte was determined using standard calibrators and analyzed using the Meso Scale Discovery Workbench software v15.0 (MSD, Rockville, MD).

Fecal DNA Extraction, Metagenomic Library Construction and Sequencing

Genomic DNA was extracted from homogenized fecal samples stored in DNA/RNA shields using the fecal/soil microbe kits (Zymo, Irvine, CA) according to the manufacturer's instructions. Briefly, a 500 µl aliquot of fecal material mixture was homogenized using bead lysis and centrifuged down to remove lysate debris. Metagenomic sequencing libraries were constructed from the same DNA using Illumina Nextera XT flex kit according to the manufacturer recommendations. Libraries were then pooled together in equimolar proportions and sequenced on a single Illumina NovaSeq 6000 S2 flow cell at the Genomic Resource Center at the University of Maryland School of Medicine.

Intestinal Microbiome Analyses

Metagenomic sequence data were pre-processed using the following steps: 1) human sequence reads and rRNA LSU/SSU reads were removed using BMTagger v3.101 (100) using a standard human genome reference (GRCh37.p5) (101); 2) rRNA sequence reads were removed *in silico* by aligning all reads using Bowtie v1 (102) to the SILVA PARC ribosomal-subunit sequence database (103) (sequence read pairs were removed even if only one of the reads matched to the human genome reference or to rRNA); 3) the Illumina adapter was trimmed using Trimmomatic (104); 4) sequence reads with average quality greater than Q15 over a sliding window of 4 bp were trimmed before the window, assessed

for length, and removed if less than 75% of the original length; and 5) no ambiguous base pairs were allowed. The taxonomic composition of the microbiomes was established using MetaPhlAn version 2 (40). A heatmap was constructed from the 25 most abundant intestinal bacterial taxa measured by relative abundance in samples collected from 38 preterm infants enrolled in the study. Ward linkage clustering was used to cluster samples based on their Jensen-Shannon distance calculated in vegan package in R (42). The number of clusters was validated using gap statistics implemented in the *cluster* package in R (43) by calculating the goodness of clustering measure. Significance value for cytokine abundance in comparing categories was calculated using Wilcoxon rank sum test using *ggsignif* R package (41). Metagenomics dataset was mapped to the protein database UniRef90 (105) to ensure comprehensiveness in functional annotation, and was then summarized using HUMAnN2 (Human Microbiome Project Unified Metabolic Analysis Network) (v0.11.2) (106), which efficiently and accurately determines the presence, absence, and abundance of metabolic pathways in a microbial community. Further, HUMAnN2 employed a tiered search strategy that enables a species-resolved functional profiling of metagenomes to characterize the contribution to the functional pathways of a known species. Canonical Correspondence Analysis (CCA) was used in ordination analysis of the taxonomic profiles and cytokine profiles. Biplot was generated using vegan package (51, 107) based on the square root of bray-curtis distance. CA1 and CA2 are selected as the major components based on the eigenvalue. A species score was scaled proportional to the eigenvalues, representing the direction from the origin of a group having a larger than average value for the particular species (42, 51). The species scores greater than 1 are used to select the species that were considered the most significant contributors to each group. Only species/genera significantly (p value < 0.05) associated with at least one cytokine response were included. All species/genera were required to be detected in at least 1% of more than one sample. Plot was generated using R package 'complexheatmap' (47).

DATA AVAILABILITY STATEMENT

All metagenomic data were deposited in experiment ID SRX12885186 to SRX12885247 under BioProject PRJNA776332 (https://www.ncbi.nlm.nih.gov/bioproject/PRJNA776332) for open assessment. Other information, please refer to **Supplementary Material**.

ETHICS STATEMENT

This study was approved and carried out in accordance with protocols approved by the institutional review boards of the University of Maryland School of Medicine and Mercy Medical Center. Written informed parental consent was obtained for the participation of all infants in the study, in accordance with approved protocol UMB HP-00049647.

AUTHOR CONTRIBUTIONS

JML-D, MFP, and BM designed the research. SS, HL, CH-C, and RV conducted the clinical study and sample preparation. YS and BM performed the microbiome and statistical analyses. JML-D performed the cytokine and chemokine measurements. JML-D, JR, MFP, and BM wrote the paper. All authors contributed to the article and approved the submitted version.

FUNDING

This study was supported, in part, by The Gerber Foundation award (PID 6361), the National Institute of Diabetes and Digestive and Kidney Diseases (NIDDK) of the National Institutes of Health award number R21DK123674 (to BM), the National Institute of Allergy and Infectious Diseases (NIAID) of the National Institute of Health awards numbers U19AI145825 and P01AI125181 Immunology Core (to MFP), and the Institute for Clinical and Translational Research (ICTR) at University of Maryland Accelerated Translational Incubator Pilot (ATIP) award (PID 11).

ACKNOWLEDGMENTS

The authors thank Dr. Jonathan Meddings and Mr. Kim Le at the University of Calgary, Calgary, Alberta, Canada, for the HPLC analysis of urine samples. The authors thank Elise Janofsky for helping to conduct the clinical study.

SUPPLEMENTARY MATERIAL

The Supplementary Material for this article can be found online at: https://www.frontiersin.org/articles/10.3389/fimmu.2022.815046/full#supplementary-material

REFERENCES

1. Neish AS. Microbes in Gastrointestinal Health and Disease. *Gastroenterology* (2009) 136(1):65–80. doi: 10.1053/j.gastro.2008.10.080
2. Takiishi T, Fenero CIM, Camara NOS. Intestinal Barrier and Gut Microbiota: Shaping Our Immune Responses Throughout Life. *Tissue Barriers* (2017) 5(4):e1373208. doi: 10.1080/21688370.2017.1373208
3. Allaire JM, Crowley SM, Law HT, Chang SY, Ko HJ, Vallance BA. The Intestinal Epithelium: Central Coordinator of Mucosal Immunity. *Trends Immunol* (2018) 39(9):677–96. doi: 10.1016/j.it.2018.04.002
4. Drew L. Highlights From Studies on the Gut Microbiome. *Nature* (2020) 577(7792):S24–5. doi: 10.1038/d41586-020-00203-4
5. Palmer C, Bik EM, Digiulio DB, Relman DA, Brown PO. Development of the Human Infant Intestinal Microbiota. *PloS Biol* (2007) 5(7):e177. doi: 10.1371/journal.pbio.0050177
6. Maynard CL, Elson CO, Hatton RD, Weaver CT. Reciprocal Interactions of the Intestinal Microbiota and Immune System. *Nature* (2012) 489 (7415):231–41. doi: 10.1038/nature11551
7. Belkaid Y, Hand TW. Role of the Microbiota in Immunity and Inflammation. *Cell* (2014) 157(1):121–41. doi: 10.1016/j.cell.2014.03.011
8. Warner BB, Deych E, Zhou Y, Hall-Moore C, Weinstock GM, Sodergren E, et al. Gut Bacteria Dysbiosis and Necrotising Enterocolitis in Very Low Birthweight Infants: A Prospective Case-Control Study. *Lancet* (2016) 387 (10031):1928–36. doi: 10.1016/S0140-6736(16)00081-7

9. Theis KR, Romero R, Winters AD, Greenberg JM, Gomez-Lopez N, Alhousseini A, et al. Does the Human Placenta Delivered at Term Have a Microbiota? Results of Cultivation, Quantitative Real-Time PCR, 16s rRNA Gene Sequencing, and Metagenomics. *Am J Obstet Gynecol* (2019) 220267 (3):e261–7.e239. doi: 10.1016/j.ajog.2018.10.018
10. Younge N, McCann JR, Ballard J, Plunkett C, Akhtar S, Araujo-Perez F, et al. Fetal Exposure to the Maternal Microbiota in Humans and Mice. *JCI Insight* (2019) 4(19). doi: 10.1172/jci.insight.127806
11. Bi Y, Tu Y, Zhang N, Wang S, Zhang F, Suen G, et al. Multiomics Analysis Reveals the Presence of a Microbiome in the Gut of Fetal Lambs. *Gut* (2021) 70(5):853–64. doi: 10.1136/gutjnl-2020-320951
12. Walter J, Hornef MW. A Philosophical Perspective on the Prenatal In Utero Microbiome Debate. *Microbiome* (2021) 9(1):5. doi: 10.1186/s40168-020-00979-7
13. Bloom PD, Boedeker EC. Mucosal Immune Responses to Intestinal Bacterial Pathogens. *Semin Gastrointest Dis* (1996) 7(3):151–66.
14. van Elburg RM, Fetter WP, Bunkers CM, Heymans HS. Intestinal Permeability in Relation to Birth Weight and Gestational and Postnatal Age. *Arch Dis Child Fetal Neonatal Ed* (2003) 88(1):F52–5. doi: 10.1136/fn.88.1.F52
15. Claud EC. Neonatal Necrotizing Enterocolitis -Inflammation and Intestinal Immaturity. *Antiinflamm Antiallergy Agents Med Chem* (2009) 8(3):248–59. doi: 10.2174/187152309789152020
16. Berseth CL. Gut Motility and the Pathogenesis of Necrotizing Enterocolitis. *Clin Perinatol* (1994) 21(2):263–70. doi: 10.1016/S0095-5108(18)30345-2
17. Udall JNJr. Gastrointestinal Host Defense and Necrotizing Enterocolitis. *J Pediatr* (1990) 117(1 Pt 2):S33–43. doi: 10.1016/S0022-3476(05)81128-X
18. Dai D, Nanthkumar NN, Newburg DS, Walker WA. Role of Oligosaccharides and Glycoconjugates in Intestinal Host Defense. *J Pediatr Gastroenterol Nutr* (2000) 30 Suppl;2:S23–33. doi: 10.1097/00005176-200003002-00005
19. Lin J, Holzman IR, Jiang P, Babyatsky MW. Expression of Intestinal Trefoil Factor in Developing Rat Intestine. *Biol Neonate* (1999) 76(2):92–7. doi: 10.1159/000014146
20. Anand RJ, Leaphart CL, Mollen KP, Hackam DJ. The Role of the Intestinal Barrier in the Pathogenesis of Necrotizing Enterocolitis. *Shock* (2007) 27 (2):124–33. doi: 10.1097/01.shk.0000239774.02904.65
21. Fasano A. Physiological, Pathological, and Therapeutic Implications of Zonulin-Mediated Intestinal Barrier Modulation: Living Life on the Edge of the Wall. *Am J Pathol* (2008) 173(5):1243–52. doi: 10.2353/ajpath.2008.080192
22. Nanthakumar N, Meng D, Goldstein AM, Zhu W, Lu L, Uauy R, et al. The Mechanism of Excessive Intestinal Inflammation in Necrotizing Enterocolitis: An Immature Innate Immune Response. *PloS One* (2011) 6 (3):e17776. doi: 10.1371/journal.pone.0017776
23. Bedrick AD. Necrotizing Enterocolitis: Neurodevelopmental "Risky Business". *J Perinatol* (2004) 24(9):531–3. doi: 10.1038/sj.jp.7211158
24. Manuck TA, Rice MM, Bailit JL, Grobman WA, Reddy UM, Wapner RJ, et al. Preterm Neonatal Morbidity and Mortality by Gestational Age: A Contemporary Cohort. *Am J Obstet Gynecol* (2016) 215(1):103.e101–103 e114. doi: 10.1016/j.ajog.2016.01.004
25. Fitzgibbons SC, Ching Y, Yu D, Carpenter J, Kenny M, Weldon C, et al. Mortality of Necrotizing Enterocolitis Expressed by Birth Weight Categories. *J Pediatr Surg* (2009) 44(6):1072–1075; discussion 1075-1076. doi: 10.1016/j.jpedsurg.2009.02.013
26. Fox TP, Godavitarne C. What Really Causes Necrotising Enterocolitis? *ISRN Gastroenterol* (2012) 2012:628317. doi: 10.5402/2012/628317
27. Claud EC, Walker WA. Bacterial Colonization, Probiotics, and Necrotizing Enterocolitis. *J Clin Gastroenterol* (2008) 42 Suppl;2:S46–52. doi: 10.1097/MCG.0b013e31815a57a8
28. Guner YS, Friedlich P, Wee CP, Dorey F, Camerini V, Upperman JS. State-Based Analysis of Necrotizing Enterocolitis Outcomes. *J Surg Res* (2009) 157 (1):21–9. doi: 10.1016/j.jss.2008.11.008
29. Berman L, Moss RL. Necrotizing Enterocolitis: An Update. *Semin Fetal Neonatal Med* (2011) 16(3):145–50. doi: 10.1016/j.siny.2011.02.002
30. Neu J, Walker WA. Necrotizing Enterocolitis. *N Engl J Med* (2011) 364 (3):255–64. doi: 10.1056/NEJMra1005408
31. Ganapathy V, Hay JW, Kim JH. Costs of Necrotizing Enterocolitis and Cost-Effectiveness of Exclusively Human Milk-Based Products in Feeding Extremely Premature Infants. *Breastfeed Med* (2012) 7(1):29–37. doi: 10.1089/bfm.2011.0002
32. Luna RA, Oezguen N, Balderas M, Venkatachalam A, Runge JK, Versalovic J, et al. Distinct Microbiome-Neuroimmune Signatures Correlate With Functional Abdominal Pain in Children With Autism Spectrum Disorder. *Cell Mol Gastroenterol Hepatol* (2017) 3(2):218–30. doi: 10.1016/j.jcmgh.2016.11.008
33. Mowat AM, Agace WW. Regional Specialization Within the Intestinal Immune System. *Nat Rev Immunol* (2014) 14(10):667–85. doi: 10.1038/nri3738
34. Kim SH, Cho BH, Kiyono H, Jang YS. Microbiota-Derived Butyrate Suppresses Group 3 Innate Lymphoid Cells in Terminal Ileal Peyer's Patches. *Sci Rep* (2017) 7(1):3980. doi: 10.1038/s41598-017-02729-6
35. Saleem B, Okogbule-Wonodi AC, Fasano A, Magder LS, Ravel J, Kapoor S, et al. Intestinal Barrier Maturation in Very Low Birthweight Infants: Relationship to Feeding and Antibiotic Exposure. *J Pediatr* (2017) 183:31–36 e31. doi: 10.1016/j.jpeds.2017.01.013
36. Ma B, McComb E, Gajer P, Yang H, Humphrys M, Okogbule-Wonodi AC, et al. Microbial Biomarkers of Intestinal Barrier Maturation in Preterm Infants. *Front Microbiol* (2018) 9:2755. doi: 10.3389/fmicb.2018.02755
37. Weaver LT, Laker MF, Nelson R. Intestinal Permeability in the Newborn. *Arch Dis Child* (1984) 59(3):236–41. doi: 10.1136/adc.59.3.236
38. van Wijck K, Bessems BA, van Eijk HM, Buurman WA, Dejong CH, Lenaerts K. Polyethylene Glycol Versus Dual Sugar Assay for Gastrointestinal Permeability Analysis: Is It Time to Choose? *Clin Exp Gastroenterol* (2012) 5:139–50. doi: 10.2147/CEG.S31799
39. van Wijck K, Verlinden TJ, van Eijk HM, Dekker J, Buurman WA, Dejong CH, et al. Novel Multi-Sugar Assay for Site-Specific Gastrointestinal Permeability Analysis: A Randomized Controlled Crossover Trial. *Clin Nutr* (2013) 32(2):245–51. doi: 10.1016/j.clnu.2012.06.014
40. Segata N, Waldron L, Ballarini A, Narasimhan V, Jousson O, Huttenhower C. Metagenomic Microbial Community Profiling Using Unique Clade-Specific Marker Genes. *Nat Methods* (2012) 9(8):811–4. doi: 10.1038/nmeth.2066
41. Ahlmann-Eltze C. *Ggsignif* (2017). Available at: https://github.com/const-ae/ggsignif (Accessed June 16, 2018).
42. Oksanen J, Blanchet FG, Kindt R, Legendre P, Minchin PR, O'Hara RB, et al. *Vegan: Community Ecology Package. R Package Version 2.0-2*. CRAN (2011).
43. Maechler M. *Cluster: "Finding Groups in Data": Cluster Analysis Extended Rousseeuw Et Al* (2016) (Accessed Feb 7 2017).
44. Grier A, Qiu X, Bandyopadhyay S, Holden-Wiltse J, Kessler HA, Gill AL, et al. Impact of Prematurity and Nutrition on the Developing Gut Microbiome and Preterm Infant Growth. *Microbiome* (2017) 5(1):158. doi: 10.1186/s40168-017-0377-0
45. Korpela K, Blakstad EW, Moltu SJ, Strommen K, Nakstad B, Ronnestad AE, et al. Intestinal Microbiota Development and Gestational Age in Preterm Neonates. *Sci Rep* (2018) 8(1):2453. doi: 10.1038/s41598-018-20827-x
46. McMurdie PJ, Holmes S. Phyloseq: An R Package for Reproducible Interactive Analysis and Graphics of Microbiome Census Data. *PloS One* (2013) 8(4):e61217. doi: 10.1371/journal.pone.0061217
47. Gu Z, Eils R, Schlesner M. Complex Heatmaps Reveal Patterns and Correlations in Multidimensional Genomic Data. *Bioinformatics* (2016) 32 (18):2847–9. doi: 10.1093/bioinformatics/btw313
48. Mai V, Young CM, Ukhanova M, Wang X, Sun Y, Casella G, et al. Fecal Microbiota in Premature Infants Prior to Necrotizing Enterocolitis. *PloS One* (2011) 6(6):e20647. doi: 10.1371/journal.pone.0020647
49. Unger S, Stintzi A, Shah P, Mack D, O'Connor DL. Gut Microbiota of the Very-Low-Birth-Weight Infant. *Pediatr Res* (2015) 77(1-2):205–13. doi: 10.1038/pr.2014.162
50. Hao MM, Foong JP, Bornstein JC, Li ZL, Vanden Berghe P, Boesmans W. Enteric Nervous System Assembly: Functional Integration Within the Developing Gut. *Dev Biol* (2016) 417(2):168–81. doi: 10.1016/j.ydbio.2016.05.030
51. Jari Oksanen FGB, Friendly M, Kindt R, Legendre P, McGlinn D, Minchin PR, et al. *Vegan: Community Ecology Package. R Package*. CRAN (2016), version 2.4-1. ed.
52. Taylor SN, Basile LA, Ebeling M, Wagner CL. Intestinal Permeability in Preterm Infants by Feeding Type: Mother's Milk Versus Formula. *Breastfeed Med* (2009) 4(1):11–5. doi: 10.1089/bfm.2008.0114

53. Mackie RI, Sghir A, Gaskins HR. Developmental Microbial Ecology of the Neonatal Gastrointestinal Tract. *Am J Clin Nutr* (1999) 69(5):1035S–45S. doi: 10.1093/ajcn/69.5.1035s
54. Mshvildadze M, Neu J, Mai V. Intestinal Microbiota Development in the Premature Neonate: Establishment of a Lasting Commensal Relationship? *Nutr Rev* (2008) 66(11):658–63. doi: 10.1111/j.1753-4887.2008.00119.x
55. Renz H, Brandtzaeg P, Hornef M. The Impact of Perinatal Immune Development on Mucosal Homeostasis and Chronic Inflammation. *Nat Rev Immunol* (2011) 12(1):9–23. doi: 10.1038/nri3112
56. MohanKumar K, Namachivayam K, Ho TT, Torres BA, Ohls RK, Maheshwari A. Cytokines and Growth Factors in the Developing Intestine and During Necrotizing Enterocolitis. *Semin Perinatol* (2017) 41(1):52–60. doi: 10.1053/j.semperi.2016.09.018
57. Schirmer M, Smeekens SP, Vlamakis H, Jaeger M, Oosting M, Franzosa EA, et al. Linking the Human Gut Microbiome to Inflammatory Cytokine Production Capacity. *Cell* (2016) 167(4):1125–36.e1128. doi: 10.1016/j.cell.2016.10.020
58. La Rosa PS, Warner BB, Zhou Y, Weinstock GM, Sodergren E, Hall-Moore CM, et al. Patterned Progression of Bacterial Populations in the Premature Infant Gut. *Proc Natl Acad Sci USA* (2014) 111(34):12522–7. doi: 10.1073/pnas.1409497111
59. Backhed F, Roswall J, Peng Y, Feng Q, Jia H, Kovatcheva-Datchary P, et al. Dynamics and Stabilization of the Human Gut Microbiome During the First Year of Life. *Cell Host Microbe* (2015) 17(5):690–703. doi: 10.1016/j.chom.2015.04.004
60. Robertson RC, Manges AR, Finlay BB, Prendergast AJ. The Human Microbiome and Child Growth - First 1000 Days and Beyond. *Trends Microbiol* (2019) 27(2):131–47. doi: 10.1016/j.tim.2018.09.008
61. Macpherson AJ, de Aguero MG, Ganal-Vonarburg SC. How Nutrition and the Maternal Microbiota Shape the Neonatal Immune System. *Nat Rev Immunol* (2017) 17(8):508–17. doi: 10.1038/nri.2017.58
62. Stewart CJ, Embleton ND, Marrs EC, Smith DP, Nelson A, Abdulkadir B, et al. Temporal Bacterial and Metabolic Development of the Preterm Gut Reveals Specific Signatures in Health and Disease. *Microbiome* (2016) 4(1):67. doi: 10.1186/s40168-016-0216-8
63. Arboleya S, Binetti A, Salazar N, Fernandez N, Solis G, Hernandez-Barranco A, et al. Establishment and Development of Intestinal Microbiota in Preterm Neonates. *FEMS Microbiol Ecol* (2012) 79(3):763–72. doi: 10.1111/j.1574-6941.2011.01261.x
64. Collado MC, Cernada M, Neu J, Perez-Martinez G, Gormaz M, Vento M. Factors Influencing Gastrointestinal Tract and Microbiota Immune Interaction in Preterm Infants. *Pediatr Res* (2015) 77(6):726–31. doi: 10.1038/pr.2015.54
65. Subramanian S, Huq S, Yatsunenko T, Haque R, Mahfuz M, Alam MA, et al. Persistent Gut Microbiota Immaturity in Malnourished Bangladeshi Children. *Nature* (2014) 510(7505):417–21. doi: 10.1038/nature13421
66. Blanton LV, Charbonneau MR, Salih T, Barratt MJ, Venkatesh S, Ilkaveya O, et al. Gut Bacteria That Prevent Growth Impairments Transmitted by Microbiota From Malnourished Children. *Science* (2016) 351(6275):aad3311-1-7. doi: 10.1126/science.aad3311
67. Liljedahl M, Bodin L, Schollin J. Coagulase-Negative Staphylococcal Sepsis as a Predictor of Bronchopulmonary Dysplasia. *Acta Paediatr* (2004) 93(2):211–5. doi: 10.1080/08035250310008168
68. Alshaikh B, Yee W, Lodha A, Henderson E, Yusuf K, Sauve R. Coagulase-Negative Staphylococcus Sepsis in Preterm Infants and Long-Term Neurodevelopmental Outcome. *J Perinatol* (2014) 34(2):125–9. doi: 10.1038/jp.2013.155
69. Dong Y, Speer CP, Glaser K. Beyond Sepsis: Staphylococcus Epidermidis Is an Underestimated But Significant Contributor to Neonatal Morbidity. *Virulence* (2018) 9(1):621–33. doi: 10.1080/21505594.2017.1419117
70. Dong Y, Glaser K, Schlegel N, Claus H, Speer CP. An Underestimated Pathogen: Staphylococcus Epidermidis Induces Pro-Inflammatory Responses in Human Alveolar Epithelial Cells. *Cytokine* (2019) 123:154761. doi: 10.1016/j.cyto.2019.154761
71. Moles L, Gomez M, Moroder E, Bustos G, Melgar A, Del Campo R, et al. Staphylococcus Epidermidis in Feedings and Feces of Preterm Neonates. *PloS One* (2020) 15(2):e0227823. doi: 10.1371/journal.pone.0227823
72. Baek O, Brunse A, Nguyen DN, Moodley A, Thymann T, Sangild PT. Diet Modulates the High Sensitivity to Systemic Infection in Newborn Preterm Pigs. *Front Immunol* (2020) 11:1019. doi: 10.3389/fimmu.2020.01019
73. Schwarzer M, Makki K, Storelli G, Machuca-Gayet I, Srutkova D, Hermanova P, et al. Lactobacillus Plantarum Strain Maintains Growth of Infant Mice During Chronic Undernutrition. *Science* (2016) 351(6275):854–7. doi: 10.1126/science.aad8588
74. Turfkruyer M, Verhasselt V. Breast Milk and its Impact on Maturation of the Neonatal Immune System. *Curr Opin Infect Dis* (2015) 28(3):199–206. doi: 10.1097/QCO.0000000000000165
75. Noel G, In JG, Lemme-Dumit JM, DeVine LR, Cole RN, Guerrerio AL, et al. Human Breast Milk Enhances Intestinal Mucosal Barrier Function and Innate Immunity in a Healthy Pediatric Human Enteroid Model. *Front Cell Dev Biol* (2021) 9:685171. doi: 10.3389/fcell.2021.685171
76. McEntee CP, Finlay CM, Lavelle EC. Divergent Roles for the IL-1 Family in Gastrointestinal Homeostasis and Inflammation. *Front Immunol* (2019) 10:1266. doi: 10.3389/fimmu.2019.01266
77. Moon C, VanDussen KL, Miyoshi H, Stappenbeck TS. Development of a Primary Mouse Intestinal Epithelial Cell Monolayer Culture System to Evaluate Factors That Modulate IgA Transcytosis. *Mucosal Immunol* (2014) 7(4):818–28. doi: 10.1038/mi.2013.98
78. Li Y, Oosting M, Smeekens SP, Jaeger M, Aguirre-Gamboa R, Le KTT, et al. A Functional Genomics Approach to Understand Variation in Cytokine Production in Humans. *Cell* (2016) 167(4):1099–110.e1014. doi: 10.1016/j.cell.2016.10.017
79. Fry TJ, Mackall CL. The Many Faces of IL-7: From Lymphopoiesis to Peripheral T Cell Maintenance. *J Immunol* (2005) 174(11):6571–6. doi: 10.4049/jimmunol.174.11.6571
80. Watanabe M, Ueno Y, Yajima T, Iwao Y, Tsuchiya M, Ishikawa H, et al. Interleukin 7 Is Produced by Human Intestinal Epithelial Cells and Regulates the Proliferation of Intestinal Mucosal Lymphocytes. *J Clin Invest* (1995) 95(6):2945–53. doi: 10.1172/JCI118002
81. Watanabe M, Ueno Y, Yajima T, Okamoto S, Hayashi T, Yamazaki M, et al. Interleukin 7 Transgenic Mice Develop Chronic Colitis With Decreased Interleukin 7 Protein Accumulation in the Colonic Mucosa. *J Exp Med* (1998) 187(3):389–402. doi: 10.1084/jem.187.3.389
82. Zhang W, Du JY, Yu Q, Jin JO. Interleukin-7 Produced by Intestinal Epithelial Cells in Response to Citrobacter Rodentium Infection Plays a Major Role in Innate Immunity Against This Pathogen. *Infect Immun* (2015) 83(8):3213–23. doi: 10.1128/IAI.00320-15
83. Laky K, Lefrancois L, Lingenheld EG, Ishikawa H, Lewis JM, Olson S, et al. Enterocyte Expression of Interleukin 7 Induces Development of Gammadelta T Cells and Peyer's Patches. *J Exp Med* (2000) 191(9):1569–80. doi: 10.1084/jem.191.9.1569
84. Cheroutre H, Lambolez F, Mucida D. The Light and Dark Sides of Intestinal Intraepithelial Lymphocytes. *Nat Rev Immunol* (2011) 11(7):445–56. doi: 10.1038/nri3007
85. Khairallah C, Chu TH, Sheridan BS. Tissue Adaptations of Memory and Tissue-Resident Gamma Delta T Cells. *Front Immunol* (2018) 9:2636. doi: 10.3389/fimmu.2018.02636
86. Hu MD, Ethridge AD, Lipstein R, Kumar S, Wang Y, Jabri B, et al. Epithelial IL-15 Is a Critical Regulator of Gammadelta Intraepithelial Lymphocyte Motility Within the Intestinal Mucosa. *J Immunol* (2018) 201(2):747–56. doi: 10.4049/jimmunol.1701603
87. Cruikshank WW, Kornfeld H, Center DM. Interleukin-16. *J Leukoc Biol* (2000) 67(6):757–66. doi: 10.1002/jlb.67.6.757
88. Mathy NL, Scheuer W, Lanzendorfer M, Honold K, Ambrosius D, Norley S, et al. Interleukin-16 Stimulates the Expression and Production of Pro-Inflammatory Cytokines by Human Monocytes. *Immunology* (2000) 100(1):63–9. doi: 10.1046/j.1365-2567.2000.00997.x
89. Seegert D, Rosenstiel P, Pfahler H, Pfefferkorn P, Nikolaus S, Schreiber S. Increased Expression of IL-16 in Inflammatory Bowel Disease. *Gut* (2001) 48(3):326–32. doi: 10.1136/gut.48.3.326
90. Sugitharini V, Prema A, Berla Thangam E. Inflammatory Mediators of Systemic Inflammation in Neonatal Sepsis. *Inflamm Res* (2013) 62(12):1025–34. doi: 10.1007/s00011-013-0661-9
91. Cooper AM, Khader SA. IL-12p40: An Inherently Agonistic Cytokine. *Trends Immunol* (2007) 28(1):33–8. doi: 10.1016/j.it.2006.11.002
92. Marks E, Naudin C, Nolan G, Goggins BJ, Burns G, Mateer SW, et al. Regulation of IL-12p40 by HIF Controls Th1/Th17 Responses to Prevent Mucosal Inflammation. *Mucosal Immunol* (2017) 10(5):1224–36. doi: 10.1038/mi.2016.135

93. PrabhuDas M, Adkins B, Gans H, King C, Levy O, Ramilo O, et al. Challenges in Infant Immunity: Implications for Responses to Infection and Vaccines. *Nat Immunol* (2011) 12(3):189–94. doi: 10.1038/ni0311-189
94. Aschenbrenner D, Quaranta M, Banerjee S, Ilott N, Jansen J, Steere B, et al. Deconvolution of Monocyte Responses in Inflammatory Bowel Disease Reveals an IL-1 Cytokine Network That Regulates IL-23 in Genetic and Acquired IL-10 Resistance. *Gut* (2021) 70(6):1023–36. doi: 10.1136/gutjnl-2020-321731
95. Gutierrez-Reyna DY, Cedillo-Banos A, Kempis-Calanis LA, Ramirez-Pliego O, Bargier L, Puthier D, et al. IL-12 Signaling Contributes to the Reprogramming of Neonatal CD8(+) T Cells. *Front Immunol* (2020) 11:1089:1089. doi: 10.3389/fimmu.2020.01089
96. Tutdibi E, Hunecke A, Lindner U, Monz D, Gortner L. Levels of Cytokines in Umbilical Cord Blood in Relation to Spontaneous Term Labor. *J Perinat Med* (2012) 40(5):527–32. doi: 10.1515/jpm-2011-0204
97. Malamitsi-Puchner A, Protonotariou E, Boutsikou T, Makrakis E, Sarandakou A, Creatsas G. The Influence of the Mode of Delivery on Circulating Cytokine Concentrations in the Perinatal Period. *Early Hum Dev* (2005) 81(4):387–92. doi: 10.1016/j.earlhumdev.2004.10.017
98. Ballard O, Morrow AL. Human Milk Composition: Nutrients and Bioactive Factors. *Pediatr Clin North Am* (2013) 60(1):49–74. doi: 10.1016/j.pcl.2012.10.002
99. Rouwet EV, Heineman E, Buurman WA, ter Riet G, Ramsay G, Blanco CE. Intestinal Permeability and Carrier-Mediated Monosaccharide Absorption in Preterm Neonates During the Early Postnatal Period. *Pediatr Res* (2002) 51(1):64–70. doi: 10.1203/00006450-200201000-00012
100. Rotmistrovsky K, Agarwala R. *BMTagger: Best Match Tagger for Removing Human Reads From Metagenomics Datasets*. Bethesda, MD: NCBI/NLM, National Institutes of Health (2011).
101. Church DM, Schneider VA, Graves T, Auger K, Cunningham F, Bouk N, et al. Modernizing Reference Genome Assemblies. *PloS Biol* (2011) 9(7): e1001091. doi: 10.1371/journal.pbio.1001091
102. Langmead B, Trapnell C, Pop M, Salzberg SL. Ultrafast and Memory-Efficient Alignment of Short DNA Sequences to the Human Genome. *Genome Biol* (2009) 10(3):R25. doi: 10.1186/gb-2009-10-3-r25
103. Quast C, Pruesse E, Yilmaz P, Gerken J, Schweer T, Yarza P, et al. The SILVA Ribosomal RNA Gene Database Project: Improved Data Processing and Web-Based Tools. *Nucleic Acids Res* (2013) 41(Database issue):D590–6. doi: 10.1093/nar/gks1219
104. Bolger AM, Lohse M, Usadel B. Trimmomatic: A Flexible Trimmer for Illumina Sequence Data. *Bioinformatics* (2014) 30(15):2114–20. doi: 10.1093/bioinformatics/btu170
105. Kanehisa M, Goto S, Sato Y, Furumichi M, Tanabe M. KEGG for Integration and Interpretation of Large-Scale Molecular Data Sets. *Nucleic Acids Res* (2012) 40(Database issue):D109–14. doi: 10.1093/nar/gkr988
106. Franzosa EA, McIver LJ, Rahnavard G, Thompson LR, Schirmer M, Weingart G, et al. Species-Level Functional Profiling of Metagenomes and Metatranscriptomes. *Nat Methods* (2018) 15(11):962–8. doi: 10.1038/s41592-018-0176-y
107. Dixon P. VEGAN, a Package of R Functions for Community Ecology. *J Vegetation Sci* (2003) 14(6):927–30. doi: 10.1111/j.1654-1103.2003.tb02228.x

Conflict of Interest: The authors declare that the research was conducted in the absence of any commercial or financial relationships that could be construed as a potential conflict of interest.

Publisher's Note: All claims expressed in this article are solely those of the authors and do not necessarily represent those of their affiliated organizations, or those of the publisher, the editors and the reviewers. Any product that may be evaluated in this article, or claim that may be made by its manufacturer, is not guaranteed or endorsed by the publisher.

Copyright © 2022 Lemme-Dumit, Song, Lwin, Hernandez-Chavez, Sundararajan, Viscardi, Ravel, Pasetti and Ma. This is an open-access article distributed under the terms of the Creative Commons Attribution License (CC BY). The use, distribution or reproduction in other forums is permitted, provided the original author(s) and the copyright owner(s) are credited and that the original publication in this journal is cited, in accordance with accepted academic practice. No use, distribution or reproduction is permitted which does not comply with these terms.

frontiers in Immunology

ORIGINAL RESEARCH
published: 29 March 2022
doi: 10.3389/fimmu.2022.748284

Bruton's Tyrosine Kinase Supports Gut Mucosal Immunity and Commensal Microbiome Recognition in Autoimmune Arthritis

Rachel H. Bonami[1,2,3*], *Christina E. Thurman*[4], *Sonam Verma*[5], *Camille S. Westlake*[4], *Lindsay E. Nyhoff*[4], *Bridgette B. Barron*[4], *Andrea Reboldi*[6] and *Peggy L. Kendall*[2,3,4,5]

[1] Department of Medicine, Division of Rheumatology and Immunology, Vanderbilt University Medical Center, Nashville, TN, United States, [2] Department of Pathology, Microbiology and Immunology, Vanderbilt University Medical Center, Nashville, TN, United States, [3] Vanderbilt Institute for Infection, Immunology, and Inflammation (VI4), Nashville, TN, United States, [4] Department of Medicine, Division of Allergy, Pulmonary, and Critical Care, Vanderbilt University Medical Center, Nashville, TN, United States, [5] Department of Medicine, Division of Allergy and Immunology, Washington University School of Medicine, St. Louis, MO, United States, [6] Department of Pathology, University of Massachusetts Chan Medical School, Worcester, MA, United States

OPEN ACCESS

Edited by:
Oscar Gilberto Gomez-Duarte, University at Buffalo, United States

Reviewed by:
Mats Bemark, University of Gothenburg, Sweden
Trine N. Jorgensen, Case Western Reserve University, United States

***Correspondence:**
Rachel H. Bonami
rachel.h.bonami@vumc.org

Specialty section:
This article was submitted to Microbial Immunology, a section of the journal Frontiers in Immunology

Received: 27 July 2021
Accepted: 02 March 2022
Published: 29 March 2022

Citation:
Bonami RH, Thurman CE, Verma S, Westlake CS, Nyhoff LE, Barron BB, Reboldi A and Kendall PL (2022) Bruton's Tyrosine Kinase Supports Gut Mucosal Immunity and Commensal Microbiome Recognition in Autoimmune Arthritis. Front. Immunol. 13:748284. doi: 10.3389/fimmu.2022.748284

Bruton's tyrosine kinase (*Btk*) deficiency preferentially eliminates autoreactive B cells while sparing normal humoral responses, but has not been studied in mucosal immunity. Commensal microbes and intact BTK signaling have been independently shown to be essential for arthritis development in K/BxN mice. Here, we examine how BTK-mediated signaling interfaces with the gut microbiome. *Btk*-deficient K/BxN mice were found to have small Peyer's Patches with reduced germinal center and IgA class-switched B cells. IgA-switched plasma cells in small intestines were reduced, especially in villi of *Btk*-deficient mice. IgH CDR3 sequencing showed similar V gene diversity and somatic hypermutation frequency despite *Btk* deficiency but showed reduced CDR3 amino acid polarity, suggesting potential qualitative differences in the gut plasma cell repertoire. Small intestinal IgA was low and IgA coating of commensal bacteria was reduced. IgA-seq showed a shift in small intestinal microbes that are normally IgA-coated into the uncoated fraction in *Btk*-deficient mice. Overall, this study shows that BTK supports normal intestinal IgA development in response to commensals.

This manuscript was previously published as a preprint at: https://www.biorxiv.org/content/10.1101/2021.03.10.434762v2.

Keywords: B cells, IgA, Bruton's tyrosine kinase, microbiome, autoimmunity

INTRODUCTION

More IgA is produced daily than all other antibody isotypes combined, highlighting its importance to host health (1). IgA-deficient humans are relatively resistant to infection, presumably due to functional compensation by secreted IgM, but they do have a propensity for autoimmunity (2–4). B cell signaling contributions to IgA development require further study. B cells in mucosal lymphoid tissues undergo IgA class-switch and affinity maturation, giving rise to plasma cells that migrate to the small intestinal lamina propria. B2 B cells in Peyer's patches undergo T-dependent responses in germinal centers (GCs) while B1 cells that traffic from the peritoneal cavity are more likely driven by T-independent responses without requiring GCs (5–7). It is thought that commensal recognition by the immune system *via* IgA occurs primarily through T-independent responses, whereas pathogens more typically elicit T-dependent responses (6). This is a reciprocal process as microbes are required for adaptive immune structure formation in the gut; germ-free mice fail to develop normal Peyer's patch structures or IgA-secreting plasma cells (8). IgA coating of microorganisms can block their attachment to host epithelia, thereby helping to maintain barrier function, or alternatively promote their retention in the mucous layer (9, 10).

B cell functions depend upon signaling through the B cell receptor (BCR). The B cell signaling protein Bruton's tyrosine kinase (BTK) serves as a "rheostat" in mature B cells, acting to propagate and amplify signals. Anti-citrullinated protein antibody (ACPA)-positive, but not ACPA-negative rheumatoid arthritis patients show elevated BTK phosphorylation relative to healthy controls (11), highlighting a link between overzealous BTK signaling and ACPA production. Murine *Btk*-deficiency reduces GC formation and T-independent immune responses, as well as autoantibodies, but T-dependent responses can be elicited, and IgG levels are near normal (12–18). In humans, BTK is necessary for B cells to mature beyond the bone marrow, making study of *Btk*-deficiency in mature peripheral B cells difficult (19).

Btk-deficiency protects against autoimmune arthritis in K/BxN mice (12). This is consistent with a role for *Btk* in autoreactive B lymphocyte development and function, as autoantibodies provoke arthritis in this model (20). Commensal microorganisms are also central to autoimmune arthritis development, as germ-free or antibiotic-treated K/BxN mice are protected from spontaneous disease development (21). Conversely, segmented filamentous bacteria (SFB) (also known as *Candidata savagella*) mono-colonization drives autoimmune arthritis, confirming commensal bacteria can trigger disease (21).

Commensal bacteria exposure shapes the gut B cell repertoire (22). The impact of altered B cell receptor signaling on B lymphocyte responses is incompletely understood. Clinical applications for BTK inhibitors continue to increase and include autoimmune diseases such as rheumatoid arthritis (23). Serum IgA was found to be normal in *Btk*-deficient mice (14). Similarly, IgA^+ $B220^-$ cells in the large intestine (colon) were not changed by loss of BTK in a DSS-induced colitis model (24). B cell changes in the small intestine were not investigated in this model (24). Peyer's patches in the small intestine are a major site of gut B cell activation which support the development of gut IgA^+ plasma cells. The requirement for BTK in preserving normal small intestinal populations of B lymphocytes has been largely unexplored. We therefore investigated how *Btk*-deficiency impacts B lymphocyte populations and responses to commensal bacteria in the gut in the setting of autoimmune arthritis, with particular focus on small intestinal B cells and plasma cells. Peyer's patch GCs are dramatically reduced. B1a cells are absent as expected. IgA^+ plasma cells are present in *Btk*-deficient K/BxN mice but are significantly reduced in the villi where they normally predominate. IgA^+ plasma cells do not show diminished BCR diversity or somatic hypermutation, based on CDR3 analysis, although amino acid polarity is altered. However, IgA is reduced and IgA-coated bacterial composition is shifted in the small intestine of *Btk*-deficient mice. These data show impaired B cell receptor signaling shifts the dynamic interplay between host B lymphocytes and commensal bacteria in the gut.

Abbreviations: AID, activation-induced cytidine deaminase; ACPA, anti-citrullinated protein antibody; BCR, B cell receptor; BTK, Bruton's tyrosine kinase; GC, germinal center; MDS, multidimensional scaling; OTUs, operational taxonomic units.

MATERIALS AND METHODS

Animals and Disease Assessment

$Btk^{-/-}$/NOD mice were backcrossed to the NOD strain >20 generations and were generated as described previously (13). KRN C57BL/6 mice were a gift from Cristophe Benoist and Diane Mathis (Harvard Medical School, Boston MA). KRN male mice were bred to $Btk^{+/-}$/NOD female mice to generate $Btk^{+/y}$/K/BxN and $Btk^{-/y}$/K/BxN littermates. Mice were scored for arthritis beginning at weaning by the Chondrex mouse arthritis scoring system (https://www.chondrex.com/documents/Mouse%20CIA.pdf). Paw thickness of the hind footpad was measured using a dial gauge (13-159-9, Swiss Precision Instruments). Male mice were used in all studies. All mice were housed under specific pathogen-free conditions, or in the case of *P. distasonis* infection, in the ABSL-2 facility, and all studies were approved by the institutional animal care and use committee of Vanderbilt University, fully accredited by the AAALAC.

Mammalian Cell Isolation, Flow Cytometry, and Antibodies

The entire small intestine (duodenum, jejunum, and ileum) was dissected and intestinal contents were flushed by lavage with 5mL 1X PBS + EDTA-free Complete Mini Protease Inhibitor Cocktail Tabs (Roche). Peyer's patches were dissected from the small intestine and macerated in HBSS + 10% FBS. Lamina propria cells were isolated after Peyer's patches were removed from the entire small intestine as follows. Intestines were cut longitudinally and mucus was gently scraped off and discarded. Tissue was cut into ~0.5 cm pieces and incubated with HBSS +

5% bovine calf serum (BCS) + 2 mM EDTA at 37°C for 45 min while shaking. Recovered tissue was washed, minced, and incubated with 1.5 mg/ml collagenase VIII (from *Clostridium histolyticum*, Sigma-Aldrich) and 100 U DNase I (Sigma-Aldrich) at 37°C for 25 min while shaking. Cells were vortexed for 20 s and HBSS + 5% BCS was added, cells were pelleted, and resuspended in 40% Percoll (GE Healthcare). 70% Percoll was underlayed and the interface layer was recovered after centrifugation at 300 x g for 20 min at 4°C. Cells were pelleted, resuspended, and counted.

Cells were stained for flow cytometry in 1X PBS containing 0.1% sodium azide, 0.02% EDTA, and 0.05% BCS using the following reagents and reactive antibodies: B220 (6B2), CD19 (1D3), CD95/FAS (JO2), CD138 (281-2), GL7, Igκ (187.1), or Ghost Dye (BD Biosciences, eBioscience, or Tonbo Biosciences), and/or IgA (1040-09, 1040-02, or 1040-31, Southern Biotech). Lamina propria cells were stained intracellularly for CD138, as this protein was cleaved from the cell surface during the isolation protocol (not shown). In addition to surface Igκ and IgA staining, lamina propria cells were also stained intracellularly with Igκ and IgA-reactive antibodies to aid identification of surface BCR-negative plasma cells. The Cytofix/Cytoperm kit was used for intracellular permeabilization and staining (BD Biosciences). Samples were acquired using a BD Biosciences LSR II flow cytometer and FlowJo software (Tree Star, Inc) was used for data analysis.

Fecal and Small Intestinal Lavage Sample Preparation and ELISA

Freshly collected feces were initially weighed and resuspended at 0.1mg/mL in 1X PBS containing EDTA-free Complete Mini Protease Inhibitor Cocktail Tabs (Roche) per the manufacturer's instructions. Samples were subsequently spun at 4000 RPM for 10 min., supernatant was removed and spun for an additional 10min and resulting supernatant was sterile filtered through 0.22μm filters and stored at -20°C.

To collect small intestinal lavage for ELISA, the entire small intestine (duodenum, jejunum, and ileum) was collected from each mouse and immediately flushed with 5 mL 1X PBS containing EDTA-free Complete Mini Protease Inhibitor Cocktail Tabs (Roche) per the manufacturer's instructions to normalize sample collection across mice. Samples were subsequently spun at 400 x g for 5 min. and then passed through a 70 μm nylon cell strainer to remove large debris. Supernatant was then spun at 8000 x g for 10 min. to pellet bacteria and resulting supernatant was sterile filtered through 0.22μm filters and stored at -20°C prior to ELISA.

For detection of total IgA, plates were coated with goat anti-mouse IgM + IgG + IgA (H+L) (SouthernBiotech) diluted in 1X PBS, followed by blocking with 10% non-fat dry milk. Sera were diluted 1:50,000 in 1X PBS + 0.05% tween and incubated 2h at room temperature. Bound IgA or IgM antibody was detected by incubation with goat anti-mouse IgA-alkaline phosphatase (α chain-specific, SouthernBiotech) or goat anti-mouse IgM-alkaline phosphatase (μ chain-, SouthernBiotech), respectively diluted in veronal buffered saline (142 mM NaCL + 5 mM sodium barbital) + 15mM sodium azide + 0.5% FBS. Plates were washed 4X with 1X PBS + 0.05% tween after each incubation step. 10mg/mL *p*-nitrophenyl phosphate substrate (Sigma-Aldrich) was added and O.D. was read at 405 nm *using a* Microplate Autoreader (Bio-Tek Instruments). Intestinal IgA was quantified based on a standard curve that was generated using Purified Mouse IgA, κ Isotype Control (BD Biosciences).

Small Intestine Immunostaining

Small intestines were isolated from 8-11 wk-old *Btk*-sufficient and *Btk*-deficient K/BxN males, cleaned using chilled 1X PBS, and dissected longitudinally. Small intestines were divided into four parts and enumerated from proximal (duodenal) to distal (ileal) as SI1, SI2, SI3, and SI4. A swiss-roll was made from each section, fixed in 4% paraformaldehyde followed by a series of dehydration in 5-20% sucrose., and frozen in O.C.T. Compound (Tissue-Tek). 7μm sections were cut from the duodenum (SI1) and ileum (SI4) and used for immunostaining. Frozen sections were fixed using chilled 50:50 mixture of methanol and acetone for 10 min at room temperature, washed with distilled water followed by 1X PBS, then blocked using 1% bovine serum albumin for 1 h. Sections were then stained overnight at 4°C using primary antibodies for epithelial cell adhesion molecule (EpCAM) (1:400) Thermo Fisher Scientific, #21050-1-AP) and anti-IgA (1:200) (Southern Biotech, #1165-01). After washing with 1X PBS three times, anti-rabbit Alexa 488 (1:800) and anti-rat Alexa 633 (1:400), (Thermo Fisher Scientific, #A-11034 and #A-21094, respectively) were added for 1h at room temperature, followed by washing with 1X PBS. Counterstaining was performed using Hoechst dye and fixation in ProLong Diamond Antifade mounting medium. Images were captured from non-overlapping areas using a Zeiss LSM880 Confocal Laser Scanning Microscope with Airyscan. Overall, 136 images were scored in parallel by two blinded reviewers, with any differences of opinion resolved by a third blinded reviewer. IgA^+ cells were enumerated for villi and lamina propria separately, from 0 to 5 based on frequency of IgA^+ cells among $DAPI^+$ cells using a blind evaluation strategy (0 = 0% IgA; 1 = 1-20% IgA; 2 = 20-40% IgA; 3 = 40-60% IgA; 4 = 60-80% IgA; 5 = 80-100% IgA). Scores for villi and lamina propria were added for each image to yield total IgA for that image.

Plasma Cell IgH Sequencing

Lamina propria cells were prepared from freshly isolated small intestines as outlined above. Cells were stained for surface proteins, fixed with 0.5% paraformaldehyde for 5 minutes (to retain surface antibodies but limit potential DNA cross-linking), washed, and permeabilized with 0.1% saponin in 1X PBS containing 10% BCS, followed by staining for intracellular proteins using antibody clones outlined above. A BD FACSAria III was used to sort IgA^+ plasma cells that were resuspended in 1X PBS (live $B220^-$ $CD19^-$ intracellular IgA^+ surface IgA^- $CD138^+$ cells). Cell pellets were stored at -80°C prior to DNA extraction. DNA was isolated as a single batch using the QIAamp DNA Micro Kit (Qiagen) per the manufacturer's instructions. Mouse IgH CDR3 PCR amplification and sequencing was performed using the ImmunoSeq assay and sequence data were demultiplexed/

filtered/processed by Adaptive Biotechnologies (Seattle, WA) (25). This bulk sequencing approach uses a synthetic immune repertoire as an in-line template control and removes singlet sequences during data processing to enable normalization for both PCR efficiency and amplification bias to ensure processed data correspond to the absolute number of input molecules (26). IMGT/HighV-QUEST (https://www.imgt.org/HighV-QUEST/) was used to assign gene identities and identify mutations among sequences with productive rearrangements. VDJtools (https://vdjtools-doc.readthedocs.io/en/master/index.html) was used to compare repertoire diversity and CDR3 properties between the two groups.

Microbiome Sample Preparation and Sequence Analysis

Small intestines were dissected and intestinal contents were flushed by lavage as above and centrifuged at 400 x g for 5 min. Supernatant was then centrifuged at 8000 x g for 10 min to pellet bacteria. The bacterial pellet was resuspended in 1X PBS + 0.25% BSA + 5% normal goat serum (NGS), normalized for roughly similar numbers of bacteria based on O.D. 600 nm readings, and stained with Fc Block (BD Biosciences, clone 2.4G2), followed by SYTO BC (ThermoFisher) and goat anti-mouse IgA. Cells were sorted on a BD FACSAria III and cells were pelleted and stored at -80°C. DNA extraction, microbiome sequencing, and analysis was performed as a single batch by Microbiome Insights. Bacterial 16S rRNA v4 regions were PCR-amplified as in (27). Amplicons were sequenced with an Illumina MiSeq using the 250-bp paired-end kit (v.2). Sequences were denoised, taxonomically classified (Greengenes v. 13_8 reference database), and clustered into 97%-similarity operational taxonomic units (OTUs) using Mothur, v. 1.39.5 (28). Potential contamination was addressed by co-sequencing DNA amplified from specimens and from n=4 template-free controls and n=4 extraction kit reagents processed the same way as the specimens. Two positive controls, consisting of cloned SUP05 DNA, were also included (number of copies = 2*10^6). OTUs were considered putative contaminants (and were removed) if their mean abundance in controls reached or exceeded 25% of their mean abundance in specimens.

Statistical Analysis

GraphPad (Prism) was used for statistical comparisons of flow cytometry, ELISA, and disease study data. Immune repertoire and microbiome statistical analysis approaches are detailed in the relevant figure legends.

RESULTS

IgA-Switched and GC B Cells Are Reduced in Peyer's Patches of *Btk*-Deficient K/BxN Mice

Btk-deficiency protects against several spontaneous autoimmune diseases in mouse models (12, 13) and clinical trials investigating the efficacy of BTK inhibitors in human autoimmune disease are ongoing (reviewed in (29)). The small intestine is a major site of B cell activation in the gut, yet the impact of *Btk* deficiency on B lymphocyte development and function at this site has not been investigated. We previously reported that *Btk*-deficiency protects against autoimmune arthritis in K/BxN mice, a well-studied model of rheumatoid arthritis in which gut commensal bacteria are essential disease triggers (12, 21). We therefore investigated how *Btk* loss alters B cell numbers, isotype switch, and differentiation in the Peyer's patches and lamina propria of the small intestine in the setting of autoimmune arthritis. Total numbers of B cells, IgA^+ B cells, and GC B cells were significantly reduced in Peyer's patches of *Btk*-deficient K/BxN mice compared to *Btk*-sufficient K/BxN littermate controls (**Figure 1**). Significant reductions in these populations were still seen when numbers were normalized to the number of Peyer's patches collected, with the exception of GC B cells, which still trended lower with BTK loss ($p = 0.07$). In contrast to the observed numeric differences, the frequency of Peyer's patch B cells that differentiated into GC B cells or class-switched to IgA was not significantly different between $Btk^{+/y}$ and $Btk^{-/y}$ K/BxN mice; the average frequency of total B cells or IgA^+ B cells that acquired the GC phenotype was ~10% and 40%, respectively, regardless of BTK expression (**Figure 1**). Taken together, these data suggest *Btk*-deficiency reduces Peyer's patch B cell numbers overall, but does not block B cell class switching to IgA or participation in GC reactions for Peyer's patch B cells.

B1a B Cells Are Reduced in *Btk*-Deficient K/BxN Mice

IgA-secreting plasma cells in the small intestine derive from B2 cells in the Peyer's patches and lamina propria and B1 cells in the peritoneal cavity (5, 6, 30). B1a cells are dramatically reduced in *Btk*-deficient mice, while B1b cell numbers are normal (14). Consistent with observations in a non-autoimmune strain (14), B1a B cells were strongly reduced in the peritoneal cavity of *Btk*-deficient K/BxN mice (**Figure 2**). Thus, both peritoneal B1a and Peyer's patch B2 B cell plasma cell precursors are reduced in *Btk*-deficient K/BxN mice.

IgA^+ Plasma Cells Persist in *Btk*-Deficient K/BxN Mice but Are Reduced in Small Intestinal Villi

IgA^+ GC B cells in Peyer's patches and B1a cells, which serve as intestinal plasma cell precursors, were strikingly reduced (**Figures 1**, **2**). Lamina propria B cells can also serve as IgA plasma cell precursors (30). We therefore tested whether *Btk* loss also reduced IgA-switched B cells and plasma cells in the lamina propria using flow cytometry of cells extracted from the entire small intestinal luminal layer after removal of Peyer's patches. The number of total B cells and IgA-switched B cells present in the lamina propria was not altered by *Btk*-deficiency (**Figures 3A–C**). Downregulation of the classic B cell markers, B220 and CD19 complicates identification of plasma cells. Furthermore, CD138 expression was previously shown to fluctuate with disease on plasma cells in a mouse model of multiple sclerosis (31). We therefore used intracellular Igκ positivity to help identify potential antibody-secreting cells, as 95% of mouse B cells express Igκ (32). We observed two populations of $CD19^-$ $B220^-$ $CD138^+$ cells

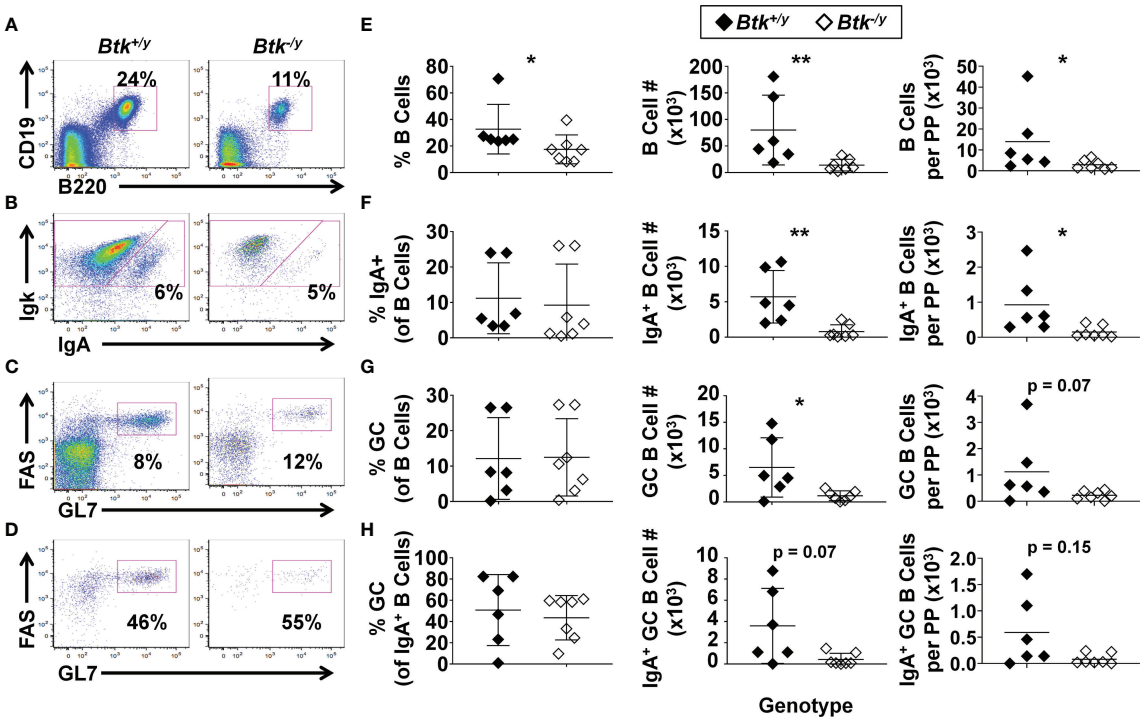

FIGURE 1 | *Btk* absence leads to reduced numbers of GC and IgA class-switched B cells in the Peyer's patches in K/BxN mice. Peyer's patches were harvested from 8-9 wk-old K/BxN (black) and *Btk*$^{-/y}$/K/BxN (white) littermates and cells isolated from all Peyer's patches dissected from each mouse were counted; n ≥ 6 mice per group, n = 5 independent experiments, as in Methods. Flow cytometry was used to identify the indicated subsets. **(A-D)** Representative plots for K/BxN (left) and *Btk*$^{-/y}$/K/BxN (right) mice depict **(A)** B cells (B220$^+$ CD19$^+$) among live singlet lymphocytes, **(B)** IgA$^+$ B cells among B220$^+$ CD19$^+$ live singlet lymphocytes, **(C)** GC B cells (GL7^{high} FAS^{high}) among B220$^+$ CD19$^+$ live singlet lymphocytes, and **(D)** GC B cells among IgA$^+$ B220$^+$ CD19$^+$ live lymphocytes. **(E-H)** Frequencies (left), numbers across all Peyer's patches harvested per mouse (middle), and numbers divided by the number of Peyer's patches harvested per mouse (right) are plotted for individual mice to show **(E)** total B cells, **(F)** IgA$^+$ B cells, **(G)** GC B cells, and **(H)** IgA$^+$ GC B cells. *p < 0.05, **p < 0.01, Mann-Whitney U test.

which were either surface BCR-positive or surface BCR-negative, which were analyzed separately. Prior studies showed this surface BCR-positive subset to lack cell proliferation markers such as Ki67, suggesting they were plasma cells, not plasmablasts (33). We will therefore designate both subsets as plasma cells but acknowledge the BCR-positive subsets may also contain plasmablasts, as our present study does not distinguish whether they are blasting. The majority of B220$^-$ CD19$^-$ CD138$^+$ plasma cell subsets in the lamina propria were IgA class-switched in both *Btk*-sufficient and deficient K/BxN mice (**Figures 3D, E**). CD138$^+$ IgA$^+$ plasma cell numbers were extremely low and not reduced by *Btk* loss. Among CD19$^-$ B220$^-$ intracellular Igκ$^+$ cells, we also observed a CD138$^-$ population, a subset of which expressed intracellular IgA (**Figure 3F**). This population may be an additional population of antibody-secreting cells in the lamina propria and was therefore analyzed separately. The numbers of CD19$^-$ B220$^-$ intracellular Igκ$^+$ CD138$^-$ cells trended lower but was not significantly reduced in *Btk*-deficient relative to *Btk*-sufficient K/BxN mice, both for total numbers (**Figure 3G**, p = 0.48) and in the IgA-switched population (**Figure 3H**, p = 0.31). Thus, IgA-switched antibody-secreting cells are present in the lamina propria despite marked reductions in Peyer's patch GC and B1a B cells in *Btk*-deficient mice. Preservation of lamina propria B cells, which presumably reside in isolated lymphoid follicles, could help explain the preservation of IgA-switched antibody-secreting cells observed in *Btk*-deficient mice.

Flow cytometry of total small intestinal lamina propria using this method has several limitations, including unrecognized inclusion of intraepithelial lymphocytes, small lymphoid follicles, and blood vessels. Furthermore, the majority of lamina propria cells that had an apparent plasma cell phenotype (CD19$^-$ B220$^-$ intracellular Igκ$^+$ intracellular IgA$^+$) stained negatively for the canonical plasma cell marker, CD138 (**Figure 3E** vs. **Figure 3H**). We therefore used immunofluorescent staining to better identify and locate IgA$^+$ plasma cells *in situ* (**Figure 4**). EpCAM (green) stains the epithelia, DAPI (blue) marks cell nuclei, and IgA (red) identifies plasma cells as typical large cells in villi and lamina propria ((34), **Figures 4A–D**). Plasma cells are normally found in greatest abundance in the duodenum, and gradually reduce distally, with the fewest found in the ileum. We therefore chose duodenal and ileal sections as representative for analysis. Sections were scored for proportion of IgA$^+$ cells among all DAPI$^+$ cells in villi or lamina propria areas of each section. IgA$^+$ plasma cells were found to be abundant in *Btk*-sufficient K/BxN duodenal sections and were particularly enriched in the intestinal villi, where they are well-positioned for IgA transepithelial transport (**Figures 4E, G**). Villi in the ileum of *Btk*-sufficient K/BxN similarly contained more IgA$^+$

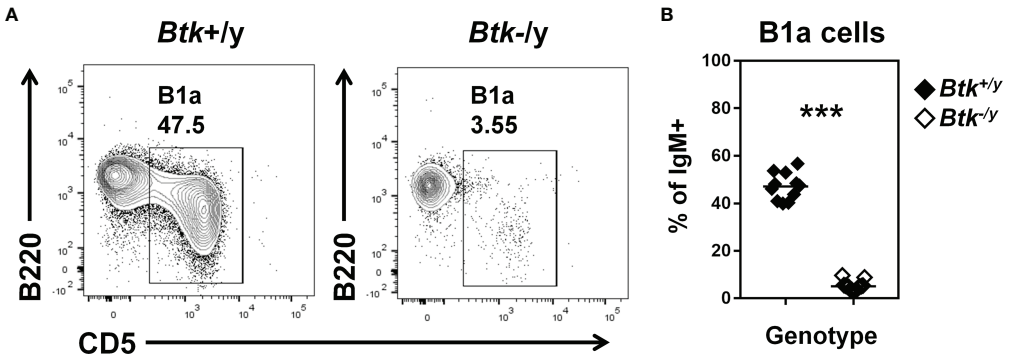

FIGURE 2 | B1a B cells are reduced in *Btk*-deficient K/BxN mice. Flow cytometry identifies B1a B cells in peritoneal lavage of K/BxN (black) and $Btk^{-/y}$/K/BxN (white) littermates, n ≥ 11 mice per group, n = 3 independent experiments. **(A)** Representative plots are gated on IgM^+ live singlet lymphocytes and indicate the frequency of B1a B cells ($B220^{low}$ $CD5^+$). **(B)** B1a B cell frequency is plotted for individual mice, ***p < 0.001, Mann-Whitney U test.

cells than the lamina propria (**Figures 4E, G**), although fewer IgA^+ cells were observed in the ileum overall than in the duodenum (**Figures 4F, H**). In contrast, the overall proportion of IgA^+ cells in *Btk*-deficient sections were significantly lower than in *Btk*-sufficient mice, which was most pronounced in duodenal villi (**Figures 4E–H**). The only area in which there was no difference in IgA^+ cells was the lamina propria of the ileal sections, where the lowest numbers of IgA^+ cells were also found in $Btk^{+/y}$ controls (**Figure 4G**). In addition, the overall condition of the intestinal epithelium and villi appeared subjectively less robust, with the epithelial layer staining more poorly, and villi often appearing shorter, although these features were not quantified in this study. Thus, IgA^+ plasma cells in *Btk*-deficient K/BxN mice are not appropriately localized to small intestinal villi.

Btk Loss Reduces Small Intestinal but Not Serum Levels of IgA in K/BxN Mice

Whereas intestinal production of IgA is severely compromised in germ-free mice, serum IgA levels are only reduced by half, suggesting the microbiota contributes to gut IgA production whereas a different process is driving circulating IgA production (6). Serum IgA levels in *Btk*-deficient mice are normal (14). As expected, serum concentrations of IgA were not significantly different between $Btk^{-/y}$ vs. $Btk^{+/y}$ K/BxN mice (**Figure 5A**). In contrast, levels of free (non-bacterial-bound) IgA were significantly reduced in small intestinal and fecal lavage harvested from $Btk^{-/y}$ vs. $Btk^{+/y}$ K/BxN mice (**Figures 5B, C**). Our data are consistent with separate routes of serum versus intestinal IgA production, and with suboptimal small intestinal villi localization of IgA^+ plasma cells and their precursors in *Btk*-deficient K/BxN mice.

Disrupted BTK Signaling Alters CDR3 Polarity, but Not Somatic Hypermutation or Clonal Diversity of Intestinal IgA^+ Plasma Cells

Intestinal IgA can derive from both T-independent and T-dependent GC responses (5, 6). Given the marked reduction in Peyer's patch GC B cell numbers (**Figure 1**) and reduction in free IgA present in the small intestinal lumen of $Btk^{-/y}$ K/BxN (**Figure 5**), we hypothesized the immunoglobulin repertoire of lamina propria IgA plasma cells would be altered. To test this hypothesis, lamina propria cells were isolated from the small intestines of $Btk^{+/y}$ K/BxN and $Btk^{-/y}$ K/BxN mice and IgA^+ plasma cells were flow cytometry-purified as identified in **Figure 3** ($B220^-$ $CD19^-$ $CD138^+$ intracellular IgA^+ surface IgA^-). Clear differences between *Btk*-sufficient and *Btk*-deficient IgA plasma cell heavy chain repertoires were not observed by multidimensional scaling (MDS) ordination plotting (**Figure 6A**). Repertoire diversity was unchanged (normalized Shannon-Wiener Index, p = 0.82, Mann-Whitney U test, **Figure 6B**) and there were no differences in the average rates of mutation in either framework region 3 (FW3) or the V or J regions of complementarity determining region 3 (CDR3) (**Figure 6C**) or in amino acid replacement mutations (not shown) between genotypes. A lower rate of mutation was observed in FW3 relative to CDR3, as expected in both groups (p < 0.01 in both genotypes, Mann-Whitney U test). A non-significant trend towards reduced CDR3 length in $Btk^{-/y}$ K/BxN mice was observed (p = 0.48, **Figure 6D**). No difference was observed in CDR3 amino acid charge, disorder, or pH (not shown), but a significant decrease in CDR3 amino acid polarity was observed in IgA^+ plasma cells isolated from $Btk^{-/y}$ K/BxN mice relative to $Btk^{+/y}$ mice (average: 6.80 vs. 7.28, p = 0.03, **Figure 6E**). These data indicate that *Btk*-deficient IgA^+ plasma cells undergo somatic hypermutation but show differences in CDR3 composition, suggesting the small intestinal plasma cell repertoire is qualitatively different when BCR signaling is altered.

Disruption of Normal B Cell Signaling Decreases IgA Coating of Small Intestinal Commensal Bacteria

The small intestine is the major site of interface between B lymphocytes and commensal microorganisms in the gut. To test whether BTK signaling loss altered IgA-coating of commensals, bacteria were collected from small intestinal lavage and the frequency of IgA-coated bacteria was assessed as in Methods.

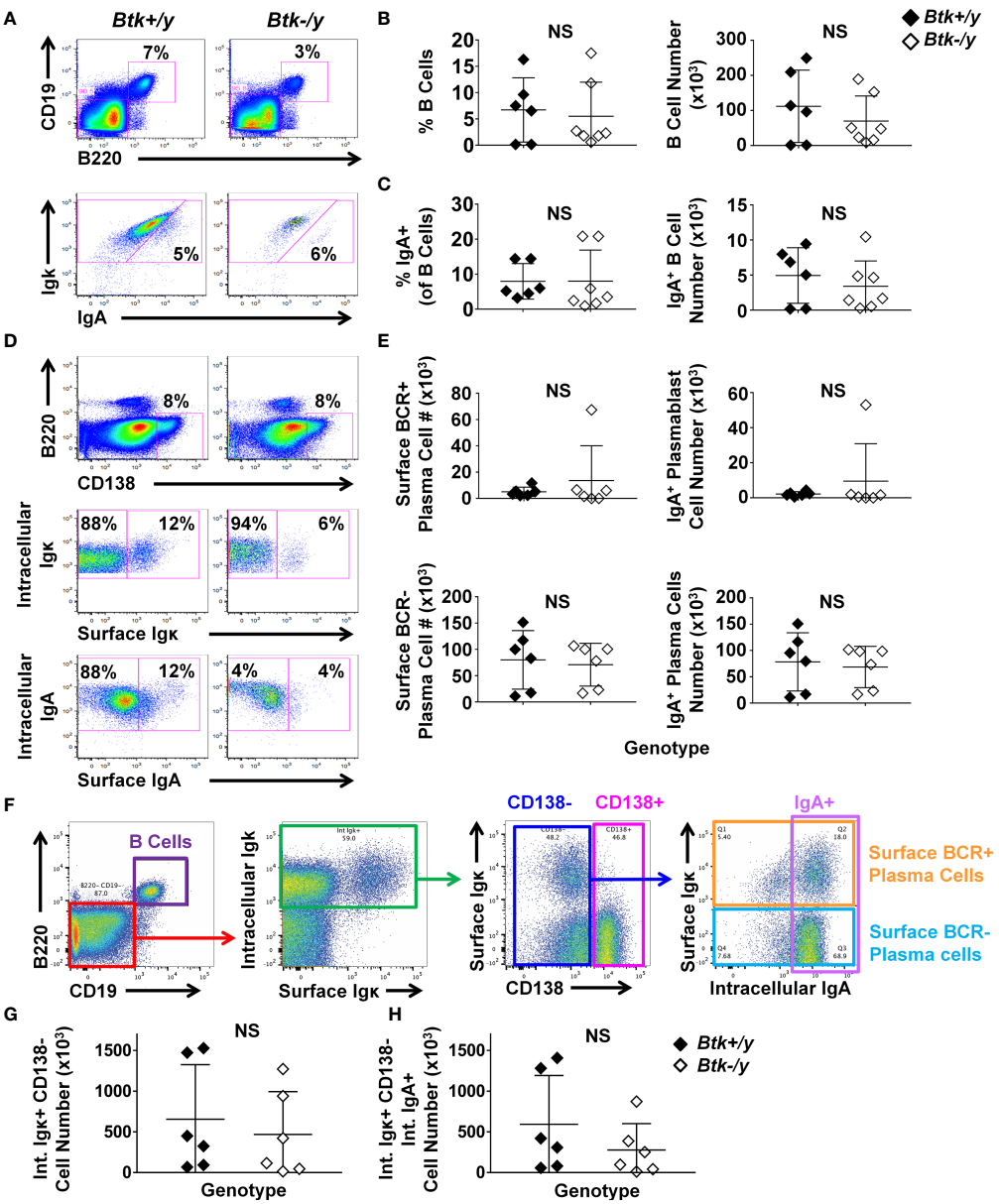

FIGURE 3 | IgA$^+$ plasma cells persist in the lamina propria of *Btk*-deficient K/BxN mice. Lamina propria cells were harvested from the entire small intestine of 8-9 wk-old K/BxN (black) and *Btk*$^{-/y}$/K/BxN (white) littermates as in Methods and cells were counted; n ≥ 6 mice per group, n = 5 independent experiments. Flow cytometry was used to identify the indicated subsets. **(A)** Representative plots depict total B cells (B220$^+$ CD19$^+$) among live singlet lymphocyte gated cells in K/BxN (left) and *Btk*$^{-/y}$/K/BxN (right) mice (top) and IgA$^+$ B cells among total B cells (bottom). **(B)** Total B cell frequencies (left) and numbers (right) and **(C)** IgA$^+$ B cell frequencies (left) and numbers (right) are shown. **(D, E)** Plasma cells were identified among B220$^-$ CD19$^-$ intracellular Igκ$^+$ CD138$^+$ live singlet cells as surface BCR-positive (surface Igκ$^+$), surface BCR-negative (surface Igκ$^-$), surface BCR-positive IgA (surface Igκ$^+$, surface IgA$^+$), and surface BCR-negative IgA (surface Igκ$^-$, intracellular IgA$^+$). **(D)** Representative plots depict the indicated subsets in K/BxN (left) and *Btk*$^{-/y}$/K/BxN (right). **(E)** Cell subset numbers are shown for surface BCR$^+$ plasma cells (top left), surface BCR$^+$ IgA$^+$ plasma cells (top right), surface BCR$^-$ plasma cells (bottom left), and surface BCR$^-$ IgA$^+$ plasma cells (bottom right). **(F–H)** CD138- cells with a plasma cell phenotype were further examined as follows. **(F)** Representative gating scheme shows B220$^+$ CD19$^+$ and B220$^-$ CD19$^-$ populations among live singlet lymphocytes (left). B220$^-$ CD19$^-$ cells (red) were further gated on intracellular Igκ$^+$ cells (green, middle, left), followed by identification of CD138$^-$ (blue) and CD138$^+$ (pink) cells (middle, right). Intracellular IgA expression was examined among CD138$^-$ cells (right, lavender), among which surface Igκ expression was used to delineate surface BCR-positive (orange) and surface BCR-negative (light blue) plasma cells. **(G, H)** Numbers of live singlet lymphocytes that were B220$^-$ CD19$^-$ intracellular Igκ$^+$ CD138$^-$ cells are shown for **(G)** total cells or **(H)** IgA-switched cells. No significant differences were observed between K/BxN and *Btk*$^{-/y}$/K/BxN groups, Mann-Whitney U test. NS, Not significant.

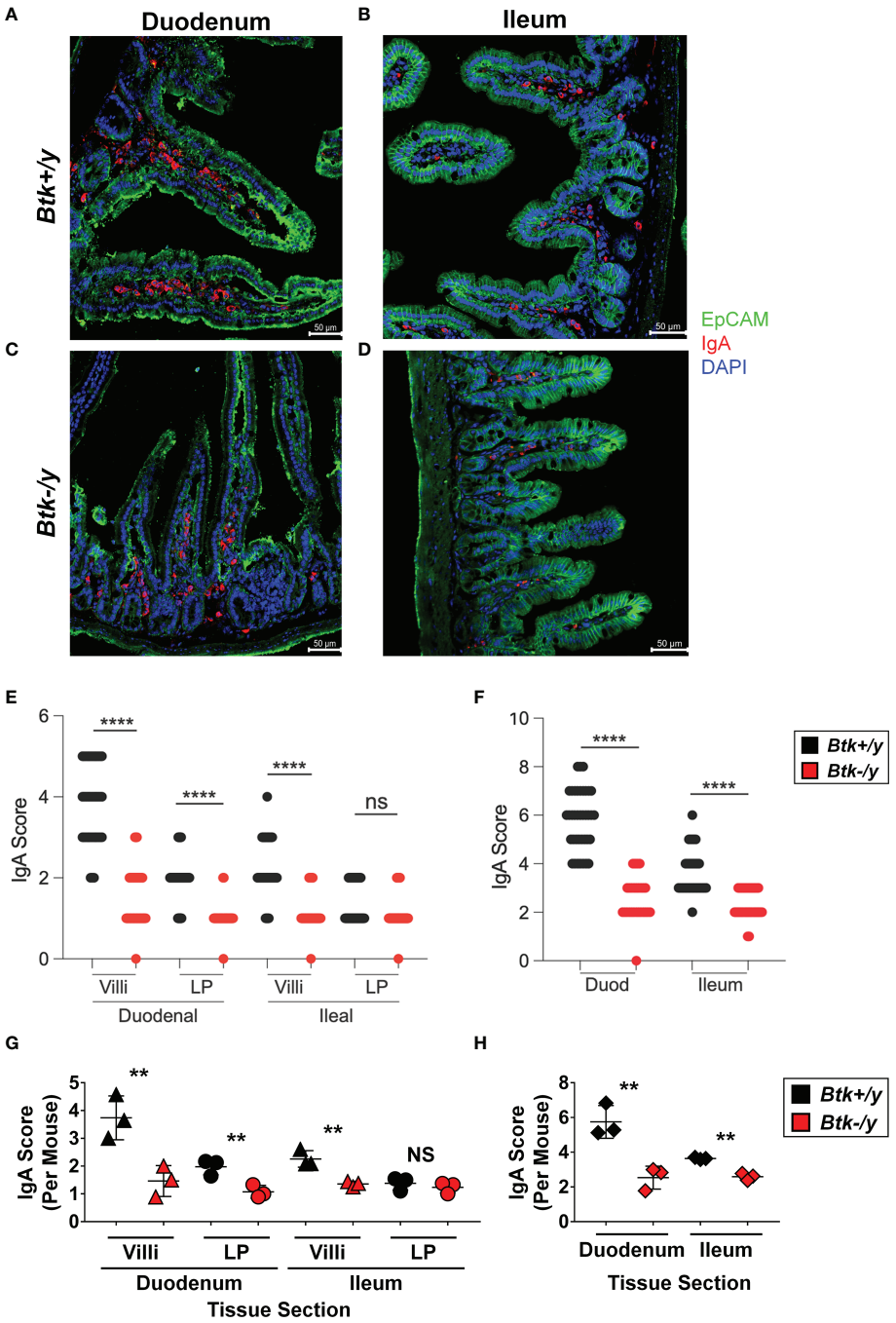

FIGURE 4 | *Btk*-deficiency alters IgA plasma cell localization in the small intestine of K/BxN mice. Small intestine was collected from 8-11wk-old $Btk^{+/y}$ (black) and $Btk^{-/y}$ (red) K/BxN mice (n = 3-4 mice per group) as described in Materials and Methods. Immunostaining for IgA (red), EpCAM (green), and DAPI (blue) was performed to identify IgA^+ cells in the small intestine villi and lamina propria. Representative images of non-overlapping areas of sections from each mouse are shown for **(A)** $Btk^{+/y}$/K/BxN and **(B)** $Btk^{-/y}$/K/BxN mouse S1 duodenal sections ($Btk^{+/y}$ S1 mean/min/max = 13/7/24 images per mouse; $Btk^{-/y}$ S1 mean/min/max = 9/6/12 images per mouse). Representative images for **(C)** $Btk^{+/y}$/K/BxN and **(D)** $Btk^{-/y}$/K/BxN mouse S4 ileal sections. ($Btk^{+/y}$ S4 mean/min/max = 17/10/23 images per mouse; $Btk^{-/y}$ S4 mean/min/max = 9/8/12 images per mouse). Scale bar represents 50 µm. **(E, F)** Analysis of IgA^+ plasma cell frequency in **(E)** duodenal and ileal villi and lamina propria (LP) and **(F)** duodenal and ileal overall tissues as measured by IgA score on immunofluorescent sections. Each dot represents a single image and data are compiled from n = 3-4 mice per genotype. ****$p < 0.0001$ ANOVA with Bonferroni correction. **(G, H)** Average IgA scores for each mouse are plotted for **(G)** villi and lamina propria (LP) or **(H)** total duodenal (S1) or ileal (S4) sections. **$p < 0.01$, NS, not significant, two-tailed t test with Welch's correction.

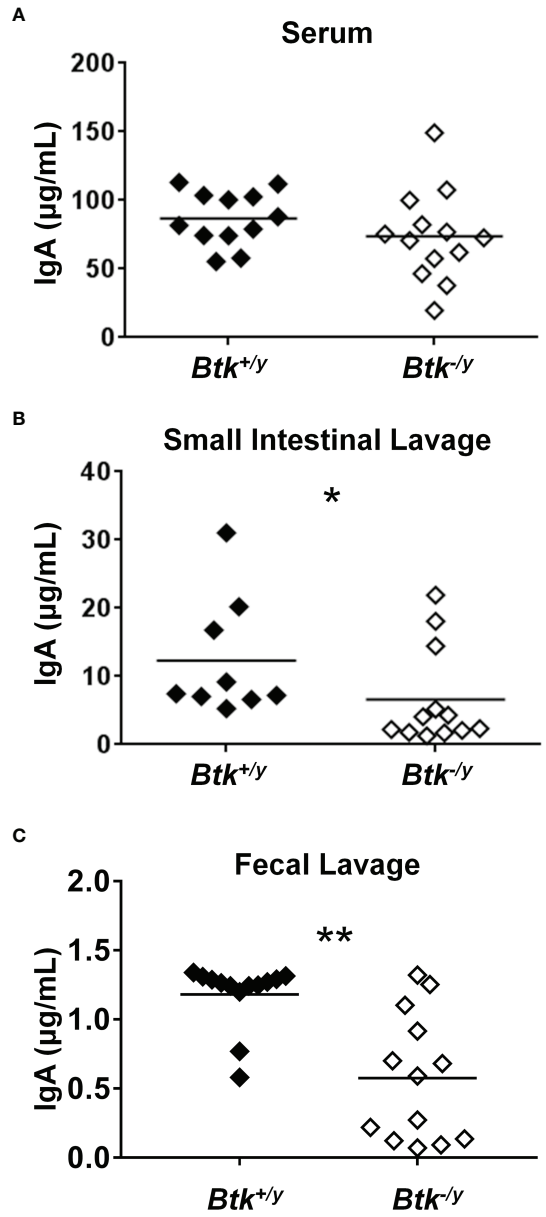

FIGURE 5 | IgA is reduced in the small intestine and feces, but not serum of *Btk*-deficient K/BxN mice. Serum, small intestinal lavage, and fecal lavage samples were collected from 8-9 week-old K/BxN and $Btk^{-/y}$/K/BxN mice as in *Methods*. Total IgA was measured by ELISA as in Methods for **(A)** serum, **(B)** small intestinal lavage, and **(C)** fecal lavage. n ≥ 9 mice per group, *p < 0.05, **p < 0.01, Mann-Whitney U test.

Consistent with previous studies (12), $Btk^{-/y}$ K/BxN mice showed less severe arthritis as compared to $Btk^{+/y}$ K/BxN mice (average arthritis scores were 4.7 vs. 12.1, respectively, p < 0.001, Mann-Whitney U test, **Figure 7A**). The average proportion of IgA-coated bacteria was reduced in $Btk^{-/y}$ vs. $Btk^{+/y}$ K/BxN mice (**Figures 7B, C**, 44% vs. 65%, respectively, p < 0.05). These data show that *Btk* loss impairs IgA-coating of commensal microbes, correlating with disease outcome in this autoimmune arthritis model.

Btk-Deficient Mice Can Produce IgA in Response to Commensal Microbes, but Some Bacteria Escape IgA Coating

IgA-seq (35, 36) was used to assess whether *Btk* loss altered community composition between IgA-coated and uncoated bacteria in the small intestine. No significant differences in Shannon (alpha) diversity were observed, although diversity trended higher in $Btk^{-/y}$ K/BxN (**Figure 7D**). OTU abundances were summarized into Bray-Curtis dissimilarities and PCoA ordination was performed to obtain graphical representation of microbiome composition similarity among the four groups: $IgA^{-}/Btk^{-/y}$ (green), $IgA^{-}/Btk^{+/y}$ (gold), $IgA^{+}/Btk^{-/y}$ (light blue), $IgA^{+}/Btk^{+/y}$ (dark blue) (**Figure 7E**). Permutational analysis of variance (PERMANOVA) determined significant differences in beta-diversity among IgA (p=0.014), and BTK (p=0.013) factors. IgA-coated and uncoated groups separated by PCoA analysis in *Btk*-sufficient mice and trended toward significance in pairwise analysis (p=0.08); this was expected, as IgA-uncoated bacteria are known to differ from IgA-coated bacteria (35, 36). This contrasts IgA coated and uncoated commensals from *Btk*-deficient mice, which overlap more in the PCoA (p=0.13). IgA-coated bacteria from *Btk*-deficient and -sufficient mice showed near-complete overlap (p=0.13), suggesting *Btk*-deficient B cells can respond to the same microbes that elicit IgA in normal B cells.

Figure 7F shows a per sample view of taxonomic composition visualizing the most abundant taxa at the family level. Statistical analysis testing the interaction between *Btk* genotype and IgA coating also identified fifteen differentially-abundant OTUs at the genus level, including *Muribaculaceae* and *Lachnospiraceae* family members, as well as *Bacteroidales* members that were unclassified at the family level (**Figure 7G**). Examples of these differentially abundant OTUs and adjusted p values are shown across all four groups in **Figure 7H**, with all remaining OTUs depicted in **Figure S1**. Twelve of these show a distinct pattern in which the OTU is highly abundant in IgA^{+} fractions from both genotypes, as well as the IgA-negative fraction in the *Btk*-deficient samples, but is not abundant in the IgA-negative fraction of the *Btk*-sufficient samples (**Figures 7G**, **S1**). *Muribaculaceae* are well-represented among these, as are *Bacteroidales*. Overall, these findings indicate that IgA from *Btk*-deficient B cells can bind the same commensal bacteria as IgA from normal B cells, but is deficient, either in abundance or affinity, resulting in inadequate coating, and escape of some microbes that are normally IgA coated into the IgA-uncoated fraction.

DISCUSSION

The microbiome, shaped by IgA, affects autoimmunity in complex ways (7, 21, 35, 37–40). However, until now the contributions of B lymphocyte signaling to these processes had not been studied. The work presented here uses the *Btk*-deficient

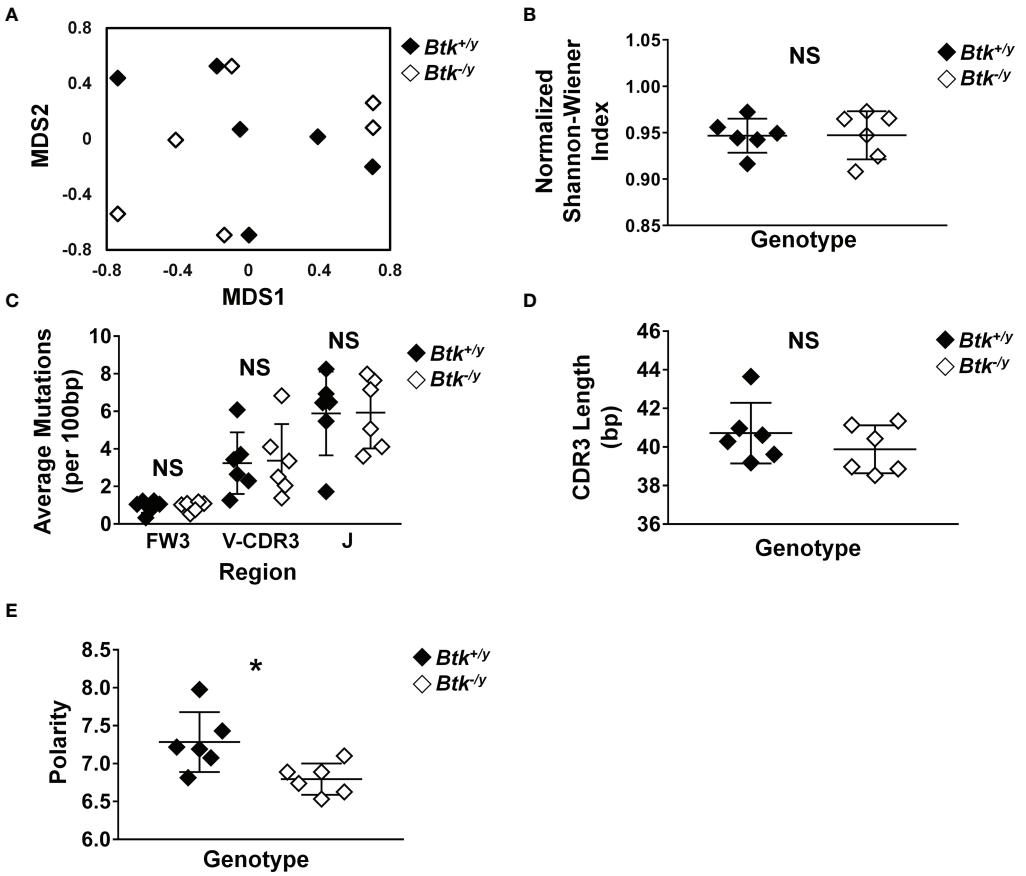

FIGURE 6 | Disrupted BTK signaling does not reduce somatic hypermutation but leads to altered CDR3 polarity in IgA$^+$ plasma cells in the small intestinal lamina propria. Lamina propria cells were harvested from the small intestines of K/BxN (black) and *Btk*$^{-/y}$/K/BxN (white) littermates from 3 litters as in Methods, n = 6 mice per group. IgA$^+$ plasma cells were identified as live singlet B220$^-$ CD19$^-$ CD138$^+$, surface IgA$^-$, intracellular IgA$^+$ cells and flow cytometry sorted. Cells were pelleted, DNA was isolated, and IgH sequencing was performed by Adaptive Technologies, as outlined in Methods. An average of 138 productively rearranged sequences were generated per mouse (range: 25-350). Sequence analysis was performed as detailed in Methods. IMGT/HighV-QUEST (http://www.imgt.org/IMGTindex/IMGTHighV-QUEST.php) was used to assign V(D)J genes and assess somatic mutations. VJDtools was used to analyze immunoglobulin gene attributes (https://vdjtools-doc.readthedocs.io/en/master/intro.html). Results were calculated for each individual mouse and are plotted. **(A)** MDS ordination was generated using the Jaccard Index. **(B)** Diversity was calculated using the normalized Shannon-Wiener index. **(C)** Somatic mutations in framework (FW) and complementarity determining regions (CDR) of productively rearranged IgH genes and the average number of mutations per 100 bp was calculated. **(D, E)** VDJtools was used to assess **(D)** CDR3 length and **(E)** amino acid polarity. *p < 0.05, NS, not significant, Mann-Whitney U test.

K/BxN mouse model to reveal that mucosal GC B cells and intestinal IgA rely in part on this B cell signaling protein. In the absence of *Btk*, appropriate IgA plasma cell localization to small intestinal villi, gut IgA, and IgA coating of commensal bacteria is reduced. Even in this suboptimal state, *Btk*-deficient B cells can still produce bacteria-reactive IgA and generate enough IgA$^+$ plasma cells to populate the lamina propria. However, this IgA is functionally incomplete, since some microbes that should be IgA-coated are found to be IgA-free, particularly those in the *Muribaculaceae* and *Bacteroidiales* families. Defective IgA responses may allow commensals which are normally cleared by IgA to flourish in *Btk*-deficient mice, or alternatively may limit the persistence of bacteria that rely on normal IgA for signaling activation or for mucous layer adherence (9, 10), which will require future study.

Commensal microbes are known to be required for autoimmune arthritis to occur in the K/BxN model (22). The findings reported here are therefore somewhat counterintuitive, since *Btk*-deficiency is protective, despite the fact that microbes escaping IgA could hypothetically be more available to trigger disease. Potential explanations for this paradox include the following. First, some commensal microbes use IgA for signaling as well as for their mucus layer retention (10), meaning their fitness may be reduced by ineffective IgA coating. Second, it is possible that there are disease-protective microbes among those that escape IgA coating to persist and compete for gut niches in this model. Third, commensal bacteria live as interdependent consortia, thus altered population coating by IgA may have downstream effects on the health, function, or survival of pathogenic microbes. Finally, it is possible that the

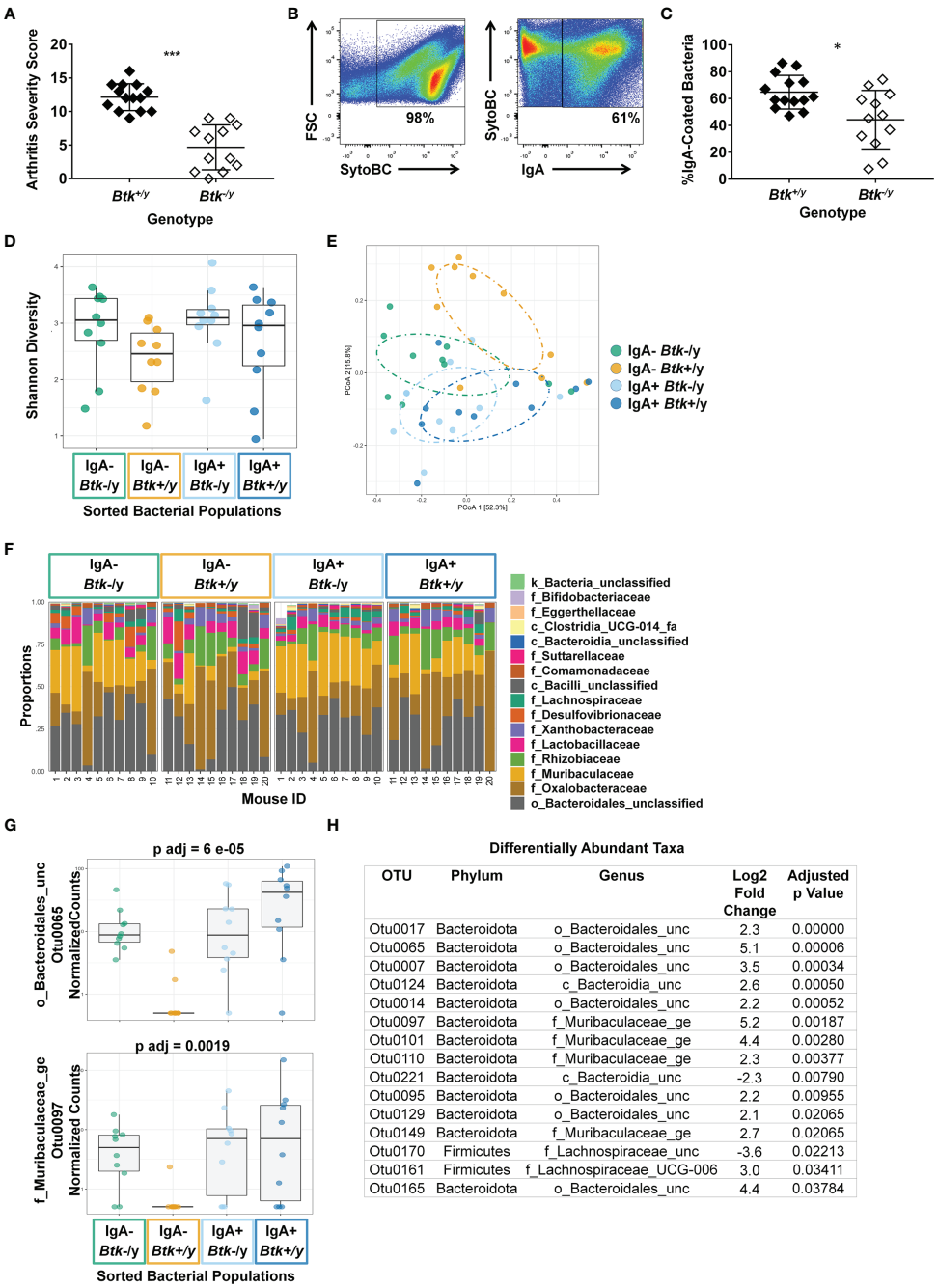

H

Differentially Abundant Taxa

OTU	Phylum	Genus	Log2 Fold Change	Adjusted p Value
Otu0017	Bacteroidota	o_Bacteroidales_unc	2.3	0.00000
Otu0065	Bacteroidota	o_Bacteroidales_unc	5.1	0.00006
Otu0007	Bacteroidota	o_Bacteroidales_unc	3.5	0.00034
Otu0124	Bacteroidota	c_Bacteroidia_unc	2.6	0.00050
Otu0014	Bacteroidota	o_Bacteroidales_unc	2.2	0.00052
Otu0097	Bacteroidota	f_Muribaculaceae_ge	5.2	0.00187
Otu0101	Bacteroidota	f_Muribaculaceae_ge	4.4	0.00280
Otu0110	Bacteroidota	f_Muribaculaceae_ge	2.3	0.00377
Otu0221	Bacteroidota	c_Bacteroidia_unc	-2.3	0.00790
Otu0095	Bacteroidota	o_Bacteroidales_unc	2.2	0.00955
Otu0129	Bacteroidota	o_Bacteroidales_unc	2.1	0.02065
Otu0149	Bacteroidota	f_Muribaculaceae_ge	2.7	0.02065
Otu0170	Firmicutes	f_Lachnospiraceae_unc	-3.6	0.02213
Otu0161	Firmicutes	f_Lachnospiraceae_UCG-006	3.0	0.03411
Otu0165	Bacteroidota	o_Bacteroidales_unc	4.4	0.03784

FIGURE 7 | IgA coating of microbes differs between *Btk*-deficient K/BxN mice and *Btk*-sufficient littermates. **(A)** An arthritis severity score was assigned to each paw (0-4) and the total arthritis severity score was calculated (0-16) for n ≥ 12 $Btk^{+/y}$ (black) or $Btk^{-/y}$ (white) K/BxN mice per group at the time of small intestinal harvest, ***p < 0.001, Mann-Whitney U test. **(B–H)** Bacteria were harvested from the small intestinal lavage of K/BxN and $Btk^{-/y}$/K/BxN littermates from 5 litters that were 8-9 wks old. Cells were stained with SytoBC and anti-IgA antibody and flow cytometry was used to identify and sort IgA-coated or uncoated bacteria. **(B)** Representative plots. **(C)** The frequency of IgA-coated bacteria is plotted for n ≥ 12 individual $Btk^{+/y}$ and $Btk^{-/y}$ K/BxN mice per group, *p < 0.05, Mann-Whitney U test. **(D–H)** DNA was isolated from bacteria sorted from $Btk^{+/y}$ and $Btk^{-/y}$ K/BxN mice based on being IgA coated or uncoated and microbiome sequencing and analysis was performed by Microbiome Insights using Mothur for the following four groups: $Btk^{-/y}$ IgA- (green), $Btk^{+/y}$ IgA- (gold), $Btk^{-/y}$ IgA+ (light blue), $Btk^{+/y}$ IgA+ (dark blue). The average number of quality filtered sequence reads per sample was 35446 (Range: 10,000-50,000). **(D)** Shannon diversity for each mouse is plotted; *Btk*: p = 0.06, IgA: p = 0.33, IgA : Btk interaction: p = 0.81, ANOVA. **(E)** Individual mice are plotted based on principle component analysis (PCoA). **(F)** Proportions of the indicated taxa at the family level are plotted for each of n = 10 mice per group. **(G, H)** The DESeq2 package was used to identify differentially abundant taxa among IgA variables using a linear model that included IgA, BTK, and BTK*IgA interactions. Normalized counts for two OTUs and corresponding adjusted p values are shown in **(G)**; other differentially abundant OTUs are shown in **(H)** and (**Figure S1**).

ability of *Btk*-deficiency to reduce autoreactive B cells simply overrides any microbiome contributions. These complex bacterial and immune interactions, and their disease effects, are the subject of ongoing studies.

IgA^+ plasma cells in mice normally arise from innate-like B1 cells from the peritoneal cavity as well as standard B2 B cells present in both Peyer's patches and isolated lymphoid follicles in the lamina propria (5, 6, 30). 25-50% of intestinal IgA produced in mice is B1 B cell-derived and the remaining 50-75% is produced by B cells from the B2 lineage (5, 6). As in non-autoimmune strains (14), we find a near absence of B1 cells in *Btk*-deficient K/BxN mice, severely limiting their contribution to IgA plasma cell generation. Given these innate-like B cells contribute to T-independent antibody production, the change in CDR3 polarity observed, and the reduction in frequency of commensals that are IgA coated, the IgA antibody repertoire is likely altered by *Btk*-deficiency. B2 cells normally form very large, active GCs in Peyer's patches. The reduced numbers of GC B cells in Peyer's patches are consistent with previous work demonstrating equally dramatic reduction of GC B cells in joint-draining popliteal lymph nodes of *Btk*-deficient K/BxN mice (12), and imply a general role for BTK in GC development or function. However, while numbers are reduced, frequencies of IgA^+ and GC B cells in the Peyer's patches do not differ, suggesting *Btk*-deficient B cells can still class switch to IgA despite impaired BCR signaling. This is also consistent with *Btk*-deficient T-dependent IgG responses that, while blunted at primary challenge, are adequate following subsequent T-dependent boost (14–16, 18, 41). Preserved T-dependent responses to commensals may similarly support the small reservoir of GC B cells in Peyer's patches of *Btk*-deficient K/BxN mice. These findings suggest that the remaining intestinal IgA in *Btk*-deficient K/BxN mice is driven by the same commensals that induce IgA under normal conditions. Isolated lymphoid follicles are found in the lamina propria which contain B cells that have a B2 phenotype and serve as IgA plasma cell precursors (30). Our lamina propria isolation protocol likely captures isolated lymphoid follicles. The extent of mutation observed in CDR3 (~5 mutations per 100bp) also suggests B2 origin of IgA^+ plasma cells, rather than B1, which tend to have lower levels of somatic hypermutation (42). Our findings are also in line with previous data showing that somatic hypermutation still occurs in Peyer's patch GC B cells even when surface BCR expression and signaling is ablated (43). Differences in clonal diversity were not observed, suggesting *Btk*-deficiency does not restrict immunoglobulin repertoire diversity. Of note, CDR3 analysis has limitations, including the absence of CDR1 and CDR2 analysis, which have historically been more commonly used in clonal and somatic hypermutation analyses, as well as lack of heavy and light chain BCR pairings. Repertoire analysis using single cell sequencing is planned to more fully define the characteristics of IgA that emerges when BTK is absent.

Expression of CD138 and downregulation of B220 and CD19 are classically used to define plasma cells. Plasma cells were additionally phenotypically defined in this study as being intracellular $Ig\kappa^+$, confirming they are B lineage cells. We however acknowledge the caveat that this phenotypically defined population was not confirmed to functionally secrete antibody. We detect an additional population of cells which lack the canonical B cell markers, B220 and CD19, yet express a BCR intracellularly based on Igκ positivity. Additional detection of intracellular IgA in the majority of these cells further supports a B lineage origin of these cells. This population of putative $CD138^-$ plasma cells shows a modest but not statistically-significant reduction in *Btk*-deficient K/BxN mice. Combined intracellular and extracellular staining for CD138, as well as cell viability dye exclusion suggests CD138-negativity is unlikely due to artifacts from the lamina propria processing protocol, but we cannot fully exclude this possibility. Further studies will be required to confirm whether these CD138-negative lamina propria cells are antibody-secreting cells.

Free IgA was reduced in small and large intestines of *Btk*-deficient K/BxN mice, as was the proportion of IgA-coated bacteria. This initially raised the possibility that commensal-driven IgA production was lacking, perhaps due to impaired GC processes, resulting in B cell failure to respond to bacteria that normally elicit IgA. It was therefore surprising that IgA from *Btk*-deficient mice targeted the same bacteria as normal B cells: there was no difference in IgA-coated community composition between *Btk*-deficient and *Btk*-sufficient K/BxN mice. This indicates BTK is not required to support specific commensal-driven production of IgA, at least in K/BxN mice. However, antigen epitope affinity may be lower or IgA levels may be insufficient to fully cover all of the targeted commensals, which, combined with suboptimal localization of plasma cells may allow some to escape IgA coating, as indicated by the shifting of uncoated IgA samples from *Btk*-deficient mice to more closely resemble IgA-coated fractions. This profile included many OTUs present exclusively in IgA^+ samples from *Btk*-sufficient animals: 12 individual, differentially-expressed OTUs were almost universally IgA coated in $Btk^{+/y}$ mice, contrasting their equal abundance in IgA^+ and IgA^- fractions from $Btk^{-/y}$ mice. Colitogenic bacteria were previously shown to be coated with higher levels of IgA, relative to non-pathogenic commensals (44). *Muribaculacea* and *Bacteroidales* members shift into the uncoated fraction in the small intestine of *Btk*-deficient K/BxN mice. Future studies are thus warranted to investigate their impact on arthritis development. Of note, Segmented Filamentous Bacteria (SFB), now known as *Candidata savagella*, drives arthritis in this model *via* T_H17 enhancement (21), but was not differentially expressed in any of our comparative data. It remains unclear whether *Btk* deficiency impacts IgA affinity for commensals or arthritogenic bacteria.

One additional consideration for this model is that BTK also plays a role in myeloid and mast cells. Although it was previously shown that BTK in myeloid cells was not necessary for arthritis in the K/BxN serum transfer model (12), this question has not been tested in the more robust spontaneous K/BxN model. BTK is important for TLR4 responses to LPS in addition to BCR responses, which is not independently analyzed here, but could be an important contributor (14). Finally, the T cell transgene that drives arthritis in K/BxN mice may also alter commensal immune responses, including, but not limited to, changes in T cell help to B cells.

Clinical use of BTK inhibitors is likely to continue to increase given the number of disease applications for which they are either approved or are being tested. Recent studies show BTK impacts autoreactive-prone B cell maturation, but not survival, and that BTK signaling is needed for normal T-independent type II responses in a timed *Btk* deletion model that mimics the scenario of clinical inhibition (45, 46). Our data suggest perturbation of B cell/IgA/commensal interactions is a likely outcome of BTK inhibition. This should be carefully considered with respect to individual patients, as changes that are beneficial in one setting (e.g. arthritis disease prevention by antibiotic treatment in autoimmune K/BxN mice) can be harmful in another (e.g. type 1 diabetes exacerbation by antibiotic treatment in non-obese diabetic mice) (21, 47). Overall, these data show for the first time that BTK-signaling contributes to IgA development and interaction with commensal bacteria and may alter host interactions with the microbiome.

DATA AVAILABILITY STATEMENT

The datasets presented in this study can be found in online repositories. The names of the repository/repositories and accession number(s) can be found below: https://www.ncbi.nlm.nih.gov/, BioProject PRJNA706065, https://clients.adaptivebiotech.com/pub/bonami-2021-biorxiv.

ETHICS STATEMENT

The animal study was reviewed and approved by Institutional Animal Care and Use Committee of Vanderbilt University, fully accredited by the AAALAC.

AUTHOR CONTRIBUTIONS

PK and RB designed the studies. RB, CT, SV, LN, and BB performed experiments. RB, CT, LN, CW, and AR performed data analysis. RB wrote the manuscript, which PK critically reviewed. All authors provided helpful experimental discussion. All authors approved the final version of this manuscript to be published and agree to be accountable for all aspects of the work in ensuring that questions related to the accuracy or integrity of any part of the work are appropriately investigated and resolved.

FUNDING

This work was supported by National Institutes of Health Grants R01-DK-084246 (PK), R01 AI155727 (AR), K12-HD-043483 (RB), and T32-AR-059039 (LN) and the Veteran's Affairs I01-BX-002882 (PK). This work was also supported through the Vanderbilt Medical Center Flow Cytometry Shared Resource (supported by the Vanderbilt Ingram Cancer Center [P30 CA68485] and the Vanderbilt Digestive Disease Research Center [DK058404]).

ACKNOWLEDGMENTS

Flow cytometry experiments were performed in the Vanderbilt Medical Center Flow Cytometry Shared Resource. Immunoglobulin heavy chain sequencing was performed by Adaptive Biotechnologies (Seattle, WA). We would like to thank Danyvid Olivares-Villagomez (Vanderbilt University Medical Center, Nashville, TN) for lamina propria isolation protocols and training and Wyatt McDonnell (Vanderbilt University, Nashville, TN) for immunoglobulin analysis advice. Microbiome sequencing and analysis was performed by Microbiome Insights (Vancouver, BC).

SUPPLEMENTARY MATERIAL

The Supplementary Material for this article can be found online at: https://www.frontiersin.org/articles/10.3389/fimmu.2022.748284/full#supplementary-material

REFERENCES

1. Woof JM, Kerr MA. The Function of Immunoglobulin A in Immunity. *J Pathol* (2006) 208:270–82. doi: 10.1002/path.1877
2. Odineal DD, Gershwin ME. The Epidemiology and Clinical Manifestations of Autoimmunity in Selective IgA Deficiency. *Clin Rev Allergy Immunol* (2020) 58:107–33. doi: 10.1007/s12016-019-08756-7
3. Aghamohammadi A, Cheraghi T, Gharagozlou M, Movahedi M, Rezaei N, Yeganeh M, et al. IgA Deficiency: Correlation Between Clinical and Immunological Phenotypes. *J Clin Immunol* (2009) 29:130–6. doi: 10.1007/s10875-008-9229-9
4. Mellander L, Bjorkander J, Carlsson B, Hanson LA. Secretory Antibodies in IgA-Deficient and Immunosuppressed Individuals. *J Clin Immunol* (1986) 6:284–91. doi: 10.1007/BF00917328
5. Kroese FG, Butcher EC, Stall AM, Lalor PA, Adams S, Herzenberg LA. Many of the IgA Producing Plasma Cells in Murine Gut Are Derived From Self-Replenishing Precursors in the Peritoneal Cavity. *Int Immunol* (1989) 1:75–84. doi: 10.1093/intimm/1.1.75
6. Macpherson AJ, Gatto D, Sainsbury E, Harriman GR, Hengartner H, Zinkernagel RM. A Primitive T Cell-Independent Mechanism of Intestinal Mucosal IgA Responses to Commensal Bacteria. *Science* (2000) 288:2222–6. doi: 10.1126/science.288.5474.2222
7. Fagarasan S, Kinoshita K, Muramatsu M, Ikuta K, Honjo T. *In Situ* Class Switching and Differentiation to IgA-Producing Cells in the Gut Lamina Propria. *Nature* (2001) 413:639–43. doi: 10.1038/35098100
8. Pollard M, Sharon N. Responses of the Peyer's Patches in Germ-Free Mice to Antigenic Stimulation. *Infect Immun* (1970) 2:96–100. doi: 10.1128/iai.2.1.96-100.1970
9. Mantis NJ, Forbes SJ. Secretory IgA: Arresting Microbial Pathogens at Epithelial Borders. *Immunol Invest* (2010) 39:383–406. doi: 10.3109/08820131003622635
10. Nakajima A, Vogelzang A, Maruya M, Miyajima M, Murata M, Son A, et al. IgA Regulates the Composition and Metabolic Function of Gut Microbiota by Promoting Symbiosis Between Bacteria. *J Exp Med* (2018) 215:2019–34. doi: 10.1084/jem.20180427
11. Corneth OBJ, Verstappen GMP, Paulissen SMJ, de Bruijn MJW, Rip J, Lukkes M, et al. Enhanced Bruton's Tyrosine Kinase Activity in Peripheral Blood B

Lymphocytes From Patients With Autoimmune Disease. *Arthritis Rheumatol* (2017) 69:1313–24. doi: 10.1002/art.40059
12. Nyhoff LE, Barron BL, Johnson EM, Bonami RH, Maseda D, Fensterheim BA, et al. Bruton's Tyrosine Kinase Deficiency Inhibits Autoimmune Arthritis in Mice But Fails to Block Immune Complex-Mediated Inflammatory Arthritis. *Arthritis Rheumatol* (2016) 68:1856–68. doi: 10.1002/art.39657
13. Kendall PL, Moore DJ, Hulbert C, Hoek KL, Khan WN, Thomas JW. Reduced Diabetes in Btk-Deficient Nonobese Diabetic Mice and Restoration of Diabetes With Provision of an Anti-Insulin IgH Chain Transgene. *J Immunol* (2009) 183:6403–12. doi: 10.4049/jimmunol.0900367
14. Khan WN, Alt FW, Gerstein RM, Malynn BA, Larsson I, Rathbun G, et al. Defective B Cell Development and Function in Btk-Deficient Mice. *Immunity* (1995) 3:283–99. doi: 10.1016/1074-7613(95)90114-0
15. Janeway CA, Barthold DR. An Analysis of the Defective Response of CBA/N Mice to T-Dependent Antigens. *J Immunol* (1975) 115:898–900.
16. Scher I, Berning AK, Asofsky R. X-Linked B Lymphocyte Defect in CBA/N Mice. IV. Cellular and Environmental Influences on the Thymus Dependent IgG Anti-Sheep Red Blood Cell Response. *J Immunol* (1979) 123:477–86.
17. Scher I, Steinberg AD, Berning AK. Paul WE. X-Linked B-Lymphocyte Immune Defect in CBA/N Mice. II. Studies of the Mechanisms Underlying the Immune Defect. *J Exp Med* (1975) 42:637–50. doi: 10.1084/jem.142.3.637
18. Boswell HS, Nerenberg MI, Scher I, Singer A. Role of Accessory Cells in B Cell Activation. III. Cellular Analysis of Primary Immune Response Deficits in CBA/N Mice: Presence of an Accessory Cell-B Cell Interaction Defect. *J Exp Med* (1980) 152:1194–309. doi: 10.1084/jem.152.5.1194
19. Conley ME, Parolini O, Rohrer J. Campana D. X-Linked Agammaglobulinemia: New Approaches to Old Questions Based on the Identification of the Defective Gene. *Immunol Rev* (1994) 138:5–21. doi: 10.1111/j.1600-065X.1994.tb00844.x
20. Korganow AS, Ji H, Mangialaio S, Duchatelle V, Pelanda R, Martin T, et al. From Systemic T Cell Self-Reactivity to Organ-Specific Autoimmune Disease *via* Immunoglobulins. *Immunity* (1999) 10:451–61. doi: 10.1016/S1074-7613(00)80045-X
21. Wu HJ, Ivanov II, Darce J, Hattori K, Shima T, Umesaki Y, et al. Gut-Residing Segmented Filamentous Bacteria Drive Autoimmune Arthritis *via* T Helper 17 Cells. *Immunity* (2010) 32:815–27. doi: 10.1016/j.immuni.2010.06.001
22. Li H, Limenitakis JP, Greiff V, Yilmaz B, Schären O, Urbaniak C, et al. Mucosal or Systemic Microbiota Exposures Shape the B Cell Repertoire. *Nature* (2020) 584:274–8. doi: 10.1038/s41586-020-2564-6
23. Crofford LJ, Nyhoff LE, Sheehan JH, Kendall PL. The Role of Bruton's Tyrosine Kinase in Autoimmunity and Implications for Therapy. *Expert Rev Clin Immunol* (2016) 12:763. doi: 10.1586/1744666X.2016.1152888
24. Guan D, Wang Z, Huo J, Xu S, Lam KP. Bruton's Tyrosine Kinase Regulates Gut Immune Homeostasis Through Attenuating Th1 Response. *Cell Death Dis* (2021) 12:1–15. doi: 10.1038/s41419-021-03702-y
25. Robins HS, Campregher PV, Srivastava SK, Wacher A, Turtle CJ, Kahsai O, et al. Comprehensive Assessment of T-Cell Receptor β-Chain Diversity in αβ T Cells. *Blood* (2009) 114:4099–107. doi: 10.1182/blood-2009-04-217604
26. Carlson CS, Emerson RO, Sherwood AM, Desmarais C, Chung M-W, Parsons JM, et al. Using Synthetic Templates to Design an Unbiased Multiplex PCR Assay. *Nat Commun* (2013) 4:1–9. doi: 10.1038/ncomms3680
27. Kozich JJ, Westcott SL, Baxter NT, Highlander SK, Schloss PD. Development of a Dual-Index Sequencing Strategy and Curation Pipeline for Analyzing Amplicon Sequence Data on the Miseq Illumina Sequencing Platform. *Appl Environ Microbiol* (2013) 79:5112–20. doi: 10.1128/AEM.01043-13
28. Schloss PD, Westcott SL, Ryabin T, Hall JR, Hartmann M, Hollister EB, et al. Introducing Mothur: Open-Source, Platform-Independent, Community-Supported Software for Describing and Comparing Microbial Communities. *Appl Environ Microbiol* (2009) 75:7537–41. doi: 10.1128/AEM.01541-09
29. Rip J, van der Ploeg EK, Hendriks RW, Corneth OBJ. The Role of Bruton's Tyrosine Kinase in Immune Cell Signaling and Systemic Autoimmunity. *Crit Rev Immunol* (2018) 38:17–62. doi: 10.1615/CRITREVIMMUNOL.2018025184
30. Wang C, McDonald KG, McDonough JS, Newberry RD. Murine Isolated Lymphoid Follicles Contain Follicular B Lymphocytes With a Mucosal Phenotype. *Am J Physiol Gastrointest Liver Physiol* (2006) 291:G595. doi: 10.1152/AJPGI.00525.2005
31. Rojas OL, Pröbstel A-K, Porfilio EA, Wang AA, Charabati M, Sun T, et al. Recirculating Intestinal IgA-Producing Cells Regulate Neuroinflammation *via* IL-10. *Cell* (2019) 176(3):610–24. doi: 10.1016/j.cell.2018.11.035
32. Takemori T, Rajewsky K. Lambda Chain Expression at Different Stages of Ontogeny in C57BL/6, BALB/c and SJL Mice. *Eur J Immunol* (1981) 11:618–25. doi: 10.1002/eji.1830110806
33. Di Niro R, Mesin L, Raki M, Zheng N-Y, Lund-Johansen F, Lundin KEA, et al. Rapid Generation of Rotavirus-Specific Human Monoclonal Antibodies From Small-Intestinal Mucosa. *J Immunol* (2010) 185:5377–83. doi: 10.4049/JIMMUNOL.1001587
34. Rios D, Wood MB, Li J, Chassaing B, Gewirtz AT, Williams IR. Antigen Sampling by Intestinal M Cells Is the Principal Pathway Initiating Mucosal IgA Production to Commensal Enteric Bacteria. *Mucosal Immunol* (2015) 9:907–16. doi: 10.1038/mi.2015.121
35. Bunker JJ, Flynn TM, Koval JC, Shaw DG, Meisel M, McDonald BD, et al. Innate and Adaptive Humoral Responses Coat Distinct Commensal Bacteria With Immunoglobulin A. *Immunity* (2015) 43:541–53. doi: 10.1016/j.immuni.2015.08.007
36. Kau AL, Planer JD, Liu J, Rao S, Yatsunenko T, Trehan I, et al. Functional Characterization of IgA-Targeted Bacterial Taxa From Undernourished Malawian Children That Produce Diet-Dependent Enteropathy. *Sci Transl Med* (2015) 7:276ra24. doi: 10.1126/scitranslmed.aaa4877
37. Fagarasan S, Muramatsu M, Suzuki K, Nagaoka H, Hiai H, Honjo T. Critical Roles of Activation-Induced Cytidine Deaminase in the Homeostasis of Gut Flora. *Science* (2002) 298:1424–7. doi: 10.1126/science.1077336
38. Liu X, Zeng B, Zhang J, Li W, Mou F, Wang H, et al. Role of the Gut Microbiome in Modulating Arthritis Progression in Mice. *Sci Rep* (2016) 6:30594. doi: 10.1038/srep30594
39. Cekanaviciute E, Yoo BB, Runia TF, Debelius JW, Singh S, Nelson CA, et al. Gut Bacteria From Multiple Sclerosis Patients Modulate Human T Cells and Exacerbate Symptoms in Mouse Models. *Proc Natl Acad Sci* (2017) 114:10713–8. doi: 10.1073/pnas.1711235114
40. Kverka M, Zakostelska Z, Klimesova K, Sokol D, Hudcovic T, Hrncir T, et al. Oral Administration of Parabacteroides Distasonis Antigens Attenuates Experimental Murine Colitis Through Modulation of Immunity and Microbiota Composition. *Clin Exp Immunol* (2011) 163:250–9. doi: 10.1111/j.1365-2249.2010.04286.x
41. Ridderstad A, GJ NOSSAL, Tarlinton DM. The Xid Mutation Diminishes Memory B Cell Generation But Does Not Affect Somatic Hypermutation and Selection. *J Immunol* (1996) 157:3357–65.
42. Hardy RR. B-1 B Cell Development. *J Immunol Ref* (2006) 177:2749–54. doi: 10.4049/jimmunol.177.5.2749
43. Casola S, Otipoby KL, Alimzhanov M, Humme S, Uyttersprot N, Kutok JL, et al. B Cell Receptor Signal Strength Determines B Cell Fate. *Nat Immunol* (2004) 5:317–27. doi: 10.1038/ni1036
44. Palm NW, de Zoete MR, Cullen TW, Barry NA, Stefanowski J, Hao L, et al. Immunoglobulin A Coating Identifies Colitogenic Bacteria in Inflammatory Bowel Disease. *Cell* (2014) 158:1000–10. doi: 10.1016/j.cell.2014.08.006
45. Nyhoff LE, Clark ES, Barron BL, Bonami RH, Khan WN, Kendall PL. Bruton's Tyrosine Kinase Is Not Essential for B Cell Survival Beyond Early Developmental Stages. *J Immunol* (2018) 200:2352–61. doi: 10.4049/jimmunol.1701489
46. Nyhoff LE, Griffith AS, Clark ES, Thomas JW, Khan WN, Kendall PL. Btk Supports Autoreactive B Cell Development and Protects Against Apoptosis But Is Expendable for Antigen Presentation. *J Immunol* (2021) 207:2922–32. doi: 10.4049/JIMMUNOL.2000558/-/DCSUPPLEMENTAL
47. Livanos AE, Greiner TU, Vangay P, Pathmasiri W, Stewart D, McRitchie S, et al. Antibiotic-Mediated Gut Microbiome Perturbation Accelerates Development of Type 1 Diabetes in Mice. *Nat Microbiol* (2016) 1:16140. doi: 10.1038/nmicrobiol.2016.140

Conflict of Interest: The authors declare that the research was conducted in the absence of any commercial or financial relationships that could be construed as a potential conflict of interest.

Publisher's Note: All claims expressed in this article are solely those of the authors and do not necessarily represent those of their affiliated organizations, or those of the publisher, the editors and the reviewers. Any product that may be evaluated in

this article, or claim that may be made by its manufacturer, is not guaranteed or endorsed by the publisher.

Copyright © 2022 Bonami, Thurman, Verma, Westlake, Nyhoff, Barron, Reboldi and Kendall. This is an open-access article distributed under the terms of the Creative Commons Attribution License (CC BY). The use, distribution or reproduction in other forums is permitted, provided the original author(s) and the copyright owner(s) are credited and that the original publication in this journal is cited, in accordance with accepted academic practice. No use, distribution or reproduction is permitted which does not comply with these terms.

frontiers | Frontiers in Immunology

ORIGINAL RESEARCH
published: 13 July 2022
doi: 10.3389/fimmu.2022.781148

Altered Intestinal Microbiomes and Lipid Metabolism in Patients With Prolonged Disorders of Consciousness

Jie Yu[1], Qisheng Cheng[1], Fangping He[1], Fanxia Meng[1], Yamei Yu[2], Chuan Xu[1], Xinrui Wen[1], Lirong Hong[3], Jian Gao[4], Jingqi Li[4], Gang Pan[5], Ming D. Li[6] and Benyan Luo[1]**

[1] Department of Neurology, First Affiliated Hospital, School of Medicine, Zhejiang University, Hangzhou, China, [2] Department of Neurology, Sir Run Run Shaw Hospital, Zhejiang University School of Medicine, Zhejiang, China, [3] Department of Rehabilitation, Hangzhou Hospital of Zhejiang Armed Police Corps, Hangzhou, China, [4] Department of Rehabilitation, Hangzhou Mingzhou Brain Rehabilitation Hospital, Hangzhou, China, [5] State Key Lab of Computer Aided Design & Computer Graphics, Hangzhou, China, [6] State Key Laboratory for Diagnosis and Treatment of Infectious Diseases, The First Affiliated Hospital, Collaborative Innovation Center for Diagnosis and Treatment of Infectious Diseases, Zhejiang University School of Medicine, Hangzhou, China

OPEN ACCESS

Edited by:
Oscar Gilberto Gomez-Duarte, University at Buffalo, United States

Reviewed by:
Wakiro Sato, National Center of Neurology and Psychiatry, Japan
Yu Liu, Sichuan University, China

***Correspondence:**
Benyan Luo
luobenyan@zju.edu.cn
Ming D. Li
ml2km@zju.edu.cn

Specialty section:
This article was submitted to Microbial Immunology, a section of the journal Frontiers in Immunology

Received: 22 September 2021
Accepted: 06 June 2022
Published: 13 July 2022

Citation:
Yu J, Cheng Q, He F, Meng F, Yu Y, Xu C, Wen X, Hong L, Gao J, Li J, Pan G, Li MD and Luo B (2022) Altered Intestinal Microbiomes and Lipid Metabolism in Patients With Prolonged Disorders of Consciousness. Front. Immunol. 13:781148. doi: 10.3389/fimmu.2022.781148

The intestinal microbiota regulate the brain function of the host through the production of a myriad of metabolites and are associated with various neurological diseases. Understanding the intestinal microbiome of patients with prolonged disorders of consciousness (DoC) is important for the evaluation and treatment of the disease. To investigate the differences in the intestinal microbiome and short-chain fatty acids (SCFAs) among patients in a vegetative state (VS), a minimally conscious state (MCS), and emerged from MCS (EMCS), as well as the influence of antibiotics on these patients, 16S ribosomal RNA (16S rRNA) sequencing and targeted lipidomics were performed on fecal samples from patients; in addition, analysis of the electroencephalogram (EEG) signals was performed to evaluate the brain function of these patients. The results showed that the intestinal microbiome of the three groups differed greatly, and some microbial communities showed a reduced production of SCFAs in VS patients compared to the other two groups. Moreover, reduced microbial communities and five major SCFAs, along with attenuated brain functional connectivity, were observed in MCS patients who were treated with antibiotics compared to those who did not receive antibiotic treatment, but not in the other pairwise comparisons. Finally, three genus-level microbiota—*Faecailbacterium, Enterococcus*, and *Methanobrevibacter*—were considered as potential biomarkers to distinguish MCS from VS patients, with high accuracy both in the discovery and validation cohorts. Together, our findings improved the understanding of patients with prolonged DoC from the intestinal microbiome perspective and provided a new reference for the exploration of therapeutic targets.

Keywords: prolonged disorders of consciousness, intestinal microbiome, short-chain fatty acid, brain functional connectivity, biomarkers

Abbreviations: EMCS, emerged from minimally conscious state; MCS, minimally conscious state; VS, vegetative state; GCS, Glasgow Coma Scale; CRS-R, Coma Recovery Scale—Revised scores; GOS-E, Glasgow Outcome Scale—Extended; GPT, glutamic–pyruvic transaminase; GOT, glutamic–oxaloacetic transaminase; LDH, lactate dehydrogenase; TBI, traumatic brain injury; Abx, antibiotic.

BACKGROUND

Patients who survived severe traumatic brain injury (TBI) usually fall into prolonged disorders of consciousness (DoC), which are of two major types: vegetative state (VS) and minimally conscious state (MCS) (1–3). VS patients retain the behavioral sleep–wake cycle, but present with unawareness of oneself or the environment, whereas MCS patients show reproducible signs of awareness and exhibit fluctuations in consciousness (4, 5). In addition, patients who recover functional object use or communication from the VS or the MCS state are referred to as emerged from minimally conscious state (EMCS) (5). Different from brain-dead patients, these three types of patients retain brain activity (6) and are not dependent on a ventilator for survival. They all receive enteral nutrition. Over the last few decades, numerous evaluations and treatments have been performed for the central nervous system of patients with prolonged DoC (7). However, little attention has been paid to the peripheral physiological environment, including the intestinal microecology, which can also influence brain function.

The intestinal microbiota can modify and regulate various chemical signals from the environment through the gut–microbiota–brain axis, which then circulate throughout the body (8). Recently, it has been demonstrated that the intestinal microbiota may directly influence human health and are associated with many neurological diseases (9). In addition, short-chain fatty acids (SCFAs) are lipids produced by some intestinal microbiota through the fermentation of dietary fiber that can act on the brain by regulating neuroplasticity and the immune system (10). For example, propionic acid in the serum and feces of patients with multiple sclerosis was significantly reduced compared with that of healthy subjects; however, disability stabilization and a reduction of the annual relapse rate and brain atrophy were observed after 3 years of propionic acid intake (11). Therefore, investigation of the differences in the intestinal microbiota and the levels of SCFAs in patients with different levels of consciousness can help in understanding their association with the restoration of brain function and consciousness and discovering potential therapeutic targets related to the intestinal microbiota.

Recently, the intestinal microbiome has been widely investigated to explore the differences in the intestinal microbiota during the occurrence and development of diseases, which has substantially contributed to our understanding of patient–microbiota interactions (12). In our previous studies, high-throughput sequencing of bacterial 16S ribosomal RNA (rRNA) was used to investigate the intestinal microbiome in patients with cognitive impairment, and it was found to be closely associated with brain functional connectivity (13, 14). However, the association between patients with prolonged DoC and their intestinal microbiota still remains unexplored. To address this knowledge gap, we examined both the intestinal microbiome using 16S rRNA sequencing and SCFAs using targeted lipidomics in fecal samples specific to different levels of consciousness. Moreover, intermittent use of antibiotics is usually observed in patients with TBI for the prevention of a wide variety of infections, especially ventilator-associated pneumonia (15). Therefore, we further compared the differences in the intestinal microbiome and the brain functional connectivity between patients with prolonged DoC receiving antibiotic treatment or not, with the ultimate goal of exploring the effects of antibiotics on the intestinal microbiota of patients with different levels of consciousness and whether these alterations can influence brain function restoration and the prognosis of these patients. Finally, we identified potential biomarkers that can distinguish MCS from VS patients and EMCS from MCS patients both in the discovery and validation cohorts.

MATERIALS AND METHODS

Ethics Statement

Written informed consent was obtained from the legal guardian of each patient. This study was approved by the Ethics Committee of the First Affiliated Hospital, School of Medicine (no. NCT04530968), Zhejiang University, Hangzhou Hospital of Zhejiang Armed Police Corps, China, and Hangzhou Mingzhou Brain Rehabilitation Hospital.

Subjects

The participants of this study are patients with severe TBI recruited from the rehabilitation units of Hangzhou Hospital of Zhejiang Armed Police Corps, China, and Hangzhou Mingzhou Brain Rehabilitation Hospital. These patients were randomly assigned into the discovery cohort (VS: $n = 13$, average age = 50.7 ± 13.2 years, 9 men and 4 women; MCS: $n = 15$, average age = 49.0 ± 9.8 years, 10 men and 5 women; and EMCS: $n = 15$, average age = 47.7 ± 12.1 years, 12 men and 3 women) and the validation cohort (VS: $n = 14$, average age = 57.5 ± 10.5 years, 10 men and 4 women; MCS: $n = 13$, average age = 56.3 ± 14.2 years, 10 men and 3 women; and EMCS: $n = 17$, average age, 53.0 ± 16.7 years; 11 men and 6 women). The Glasgow Coma Scale (GCS) was used to assess the severity of brain injury in the acute stage, and the Glasgow Outcome Scale—Expended (GOS-E) was used to assess the prognosis of patients at 6 months (16). Diagnosis of VS, MCS, or EMCS was based on the five assessments within 10 days by DoC experts using the Coma Recovery Scale—Revised (CRS-R) (5). In brief, VS patients can open their eyes and preserve sleep–wake cycles, but are unaware of themselves and their surroundings, MCS patients show reproducible signs of awareness and exhibit fluctuations in consciousness, while EMCS patients exhibit recovery of functional object uses or communication from prolonged DoC. All patients maintained this physiological state more than 1 month prior to enrollment and accepted the diet provided in the hospital for a long period; all patients received enteral nutrition from the hospital.

Patients with other causes of DoC and unstable consciousness state (there are signs of spontaneous recovery or deterioration within 1 week) were excluded from this study. We also excluded patients who had frequent and irregular seizures, as well as those who had been taking sedatives for a long time and continuously. We also excluded the following subjects: 1) had a history of using

antibiotics, probiotics, prebiotics, or synbiotics within 1 month before fecal sample collection; 2) those with severe malnutrition, infection, and drug or alcohol addiction, irritable bowel syndrome, and inflammatory bowel disease in the last year; and 3) those with schizophrenia, schizoaffective disorder, or primary affective disorder and combined severe heart, brain, liver, kidney, and hematopoietic system diseases or other serious primary diseases. Patients who received special treatments, such as transcranial magnetic stimulation (TMS) and transcranial direct current stimulation (tDCS), were also excluded. The demographic and clinical characteristics of the study participants are listed in **Table 1** and **Supplementary Table S5**.

Three other groups of patients who had a history of antibiotic use but conform to the other exclusion criteria were also recruited from these same hospitals: VS with antibiotics (VS-Abx) (n = 21, average age = 54.9 ± 11.8 years, 15 men and 6 women); MCS with antibiotics (MCS-Abx) (n = 17, average age = 62.8 ± 8.7 years, 12 men and 5 women); and EMCS with antibiotics (EMCS-Abx) (n = 9, average age = 61.0 ± 11.6 years, 5 men and 4 women). Some of the patients with DoC briefly received prophylactic antibiotic treatment to prevent aspiration pneumonia. Others continued treatment for a short period to prevent reinfection, even if the previous infection had been suppressed. The demographic and clinical characteristics of the patients are listed in **Table 1**.

All study participants were categorized based on their CRS-R scores, and centrally acting drugs, neuromuscular function blockers, and sedation were discontinued for at least 24 h when the samples were collected (17). Fasting plasma samples from all patients were collected on the day of fecal sample collection. Patients' intact skulls were also accepted for resting EEG recording.

Sample Collection and Extraction of Genome DNA

Fecal samples from EMCS, MCS, and VS patients were collected at admission and were processed in the laboratory within 4 h after collection. All fecal samples were dispensed in 2-ml Eppendorf tubes within half an hour, each tube packing 180 ± 20mg, and immediately stored at −80°C until analysis. Total genome DNA was extracted from the samples using the cetyltrimethylammonium bromide (CTAB) and sodium dodecyl sulfate (SDS) method (18). The DNA concentration and purity were monitored on 1% agarose gels. Based on the concentration, DNA was diluted to 1 ng/μl using sterile water.

Amplicon Generation, Polymerase Chain Reaction, and Sequencing

The isolated bacterial genomic DNA was used as a template for the PCR amplification of the V3–V4 regions of the bacterial 16S rRNA gene in a multiplex approach with forward primers. All PCR reactions were carried out with 15 μl of Phusion® High-Fidelity PCR Master Mix (New England Biolabs, Ipswich, MA, USA), 0.2 μM of forward and reverse primers, and about 10 ng of template DNA. Thermal cycling consisted of an initial denaturation at 98°C for 1 min, followed by 30 cycles of denaturation at 98°C for 10 s, annealing at 50°C for 30 s, and extension at 72°C for 30 s, and finally at 72°C for 5 min. The same volume of 1× loading buffer (containing SYB green) was mixed with the PCR products and electrophoresis performed on

TABLE 1 | Clinical characteristics of the patients in this study.

	Without antibiotic treatment				With antibiotic treatment			
	EMCS	**MCS**	**VS**	***p*-value**	**EMCS-Abx**	**MCS-Abx**	**VS-Abx**	***p*-value**
Patients (*n*)	15	15	13	–	9	17	21	–
Men, *n* (%)	12 (80.0)	10 (66.7)	9 (69.2)	0.691	5 (55.6)	12 (70.6)	15 (71.4)	0.668
Age (years)	52.7 ± 10.2	49.0 ± 9.8	58.3 ± 9.7	0.058	61.0 ± 11.6	53.4 ± 6.5	54.9 ± 11.8	0.058
GCS	7.1 ± 1.4	6.7 ± 1.2	7.0 ± 1.6	0.707	6.1 ± 1.2	6.9 ± 1.0	7.1 ± 1.5	0.114
CRS-R	22.4 ± 0.8	11.7 ± 3.1	6.0 ± 1.3	<0.001*	22.1 ± 1.4	11.9 ± 2.9	5.2 ± 1.3	<0.001*
GOS-E	3.3 ± 0.5	2.7 ± 0.8	2.1 ± 0.6	<0.001*	3.0 ± 0.0	2.1 ± 0.6	2.1 ± 0.4	<0.001*
Length of hospital stay (days)	172.5 ± 124.9	158.7 ± 92.5	101.0 ± 55.5	0.155	79.7 ± 49.6	120.3 ± 112.3	169.5 ± 142.7	0.248
Leukocytes (10^9/L)	5.4 ± 1.7	6.1 ± 2.0	6.5 ± 1.8	0.184	6.0 ± 1.4	6.5 ± 2.1	6.3 ± 2.1	0.817
Neutrophils (10^9/L)	3.7 ± 1.5	4.2 ± 1.8	4.3 ± 1.4	0.503	3.7 ± 1.2	4.7 ± 2.0	4.4 ± 1.8	0.415
Lymphocytes (10^9/L)	1.3 ± 0.4	1.3 ± 0.4	1.3 ± 0.4	0.931	1.4 ± 0.5	1.3 ± 0.5	1.2 ± 0.5	0.649
Monocytes (10^9/L)	0.4 ± 0.2	0.4 ± 0.2	0.5 ± 0.2	0.134	0.5 ± 0.1	0.5 ± 0.3	0.7 ± 1.2	0.805
Hemoglobin (g/L)	124.3 ± 14.9	124.9 ± 16.4	111.8 ± 10.3	0.045*	117.0 ± 10.9	105.5 ± 12.5	115.5 ± 13.3	0.030*
Platelets (10^9/L)	219.8 ± 45.9	199.1 ± 71.3	236.4 ± 58.3	0.263	209.2 ± 80.9	252.6 ± 89.0	221.5 ± 70.0	0.335
C-reactive protein (mg/L)	3.5 ± 3.7	3.2 ± 3.3	5.5 ± 4.3	0.142	4.0 ± 4.4	6.7 ± 4.0	4.6 ± 3.5	0.133
GPT (IU/L)	40.7 ± 31.5	39.3 ± 14.6	37.6 ± 25.4	0.601	24.3 ± 10.9	24.2 ± 14.2	27.3 ± 15.6	0.775
GOT (IU/L)	21.1 ± 10.6	21.3 ± 6.0	22.1 ± 10.0	0.677	18.9 ± 6.6	22.1 ± 14.9	21.3 ± 15.3	0.880
LDH (IU/L)	172.1 ± 34.5	201.4 ± 62.7	165.4 ± 49.0	0.135	159.3 ± 38.3	168.4 ± 59.8	153.5 ± 42.9	0.831
Creatinine (μmol/L)	50.7 ± 16.1	47.2 ± 12.9	36.7 ± 10.0	0.025*	43.4 ± 6.9	44.5 ± 19.1	38.2 ± 11.1	0.279
Homocysteine (μmol/L)	12.0 ± 2.2	9.9 ± 3.5	10.9 ± 1.6	0.101	9.6 ± 2.2	7.8 ± 2.9	8.7 ± 3.9	0.370
Cause	TBI	TBI	TBI	/	TBI	TBI	TBI	/

*Continuous variables are expressed as the mean ± SD. A * was considered statistically significant.*

GCS, Glasgow Coma Scale; CRS-R, Coma Recovery Scale—Revised scores; GOS-E, Glasgow Outcome Scale—Extended; GPT, glutamic–pyruvic transaminase; GOT, glutamic–oxaloacetic transaminase; LDH, lactate dehydrogenase; TBI, traumatic brain injury; VS, vegetative state; MCS, minimally conscious state; EMCS, emerged minimal conscious state; Abx, antibiotic.

2% agarose gel for detection. The PCR products were mixed in equidensity. Then, the mixture was purified with a Qiagen Gel Extraction Kit (Qiagen, Hilden, Germany). The sequencing libraries were generated using the TruSeq® DNA PCR-Free Sample Preparation Kit (Illumina, San Diego, CA, USA) following the manufacturer's recommendations, and index codes were added. The library quality was assessed on the Qubit@ 2.0 Fluorometer (Thermo Scientific, Waltham, MA, USA) and the Agilent Bioanalyzer 2100 system. Lastly, the library was sequenced on an Illumina NovaSeq platform and 250-bp paired-end reads were generated.

Short-Chain Fatty Acid Measurements

The samples were thawed on ice and diluted at 1:10 in sterile phosphate-buffered saline (PBS) solution, vortexed for 1 min, and centrifuged at 1,000 × *g* for 2 min at 4°C. As described in our previous study (19, 20), the supernatant was recovered and the pellet extracted with isopropyl ether. Aliquots (100 µl) were added into a 2-ml glass centrifuge tube and mixed with 50 µl of water with 15% phosphoric acid and 150 µl of 5 µg/ml 4-methyl valeric acid (internal standard, IS). The suspensions were homogenized with a vortex for about 1 min and centrifuged for 10 min at 12,000 × *g*. Of the supernatant, 1 µl was taken for GC-MS analysis using an Agilent Model 7890A/5975C GC-MS system. To quantify the SCFAs, a calibration curve for the concentration range 0.1–100 µg/ml was constructed. The IS was used to correct for injection variability between samples and for minor changes in the instrument response.

The samples were separated with an Agilent HP-INNOWAX capillary GC column (30 m × 0.25 mm ID × 0.25 µm). The initial temperature was 90°C, which was increased to 120°C at 10°C/min, after which it was increased to 150°C at 5°C/min and then to 250°C at 25°C/min, where it remained for 2 min. The carrier gas was helium (1.0 ml/min). The temperatures of the injection port and the transmission line were 250°C and 230°C, respectively. The electron bombardment ionization source, selected ion monitor (SIM) scanning mode, and the electron energy was 70 eV.

Data Processing

Sequence analysis was performed using Uparse software (21). All reads were deposited and grouped into operational taxonomic units (OTUs) at a sequence identity of 97%, and the taxonomic affiliation of the OTUs was determined with quantitative insights into microbial ecology (QIIME, version 1.8.0) against the Greengenes database, version 13.8 (22). The following downstream data analyses were conducted in R software. Alpha diversity was applied in analyzing the complexity of species diversity for a sample through four indices, namely, Chao1, Shannon, Simpson, and ACE (abundance-based coverage estimator). All these indices were calculated for the samples with QIIME (version 1.7.0) and displayed using R software (version 2.15.3). Principal coordinate analysis (PCoA) used unweighted and weighted UniFrac distance matrices and the Bray–Curtis distance matrix (23). The linear discriminant analysis (LDA) effect size (LEfSe) method was used to characterize the taxa with statistical significance and biological relevance. For LEfSe analysis, the Kruskal–Wallis test (alpha value of 0.05) and an LDA score >4 were used as thresholds. Pairwise comparisons were analyzed with the Mann–Whitney *U* test. Partial least squares latent structure discriminant analysis (PLS-DA) was performed using MetaboAnalyst 4.0 (www.metaboanalyst.ca) to observe the fecal microbiota structure in the different groups (13) based on the OTUs of the sequencing data from each sample. Variable importance in projection (VIP) reflects the importance of the variables that have the most significant contribution in the discrimination. Variables with VIP >1 are important contributors to the generation of the model. Based on Kyoto Encyclopedia of Genes and Genomes (KEGG) functional pathways, Phylogenetic Investigation of Communities by Reconstruction of Unobserved States (PICRUSt) (24) was used to predict the functional composition of the intestinal microbiome for each sample.

EEG Data Recording and Analysis

EEG signals were recorded using a 64-electrode BrainCap (Brain Products GmbH, Munich, Germany) in the International 10–20 system, and 1 of the 64 electrodes was placed under the right eye to record the electrooculogram (EOG). The electrode impedances were maintained below 10 kΩ. The signals were sampled at 1 kHz. EEG signals were referenced online to FCz (mid-frontal), but were referenced offline to a common average reference (25). Raw EEG data were digitally filtered between 0.1 and 46 Hz (bandpass filter). Baseline correction was also applied to all channels. EEG epochs with ocular, muscular, and other artifacts were visually identified and manually rejected (26). This was followed by an independent component analysis (ICA; InfoMax algorithm) to remove periodically recurring artifacts, including horizontal eye movements, blinks, and ECG artifacts. All preprocessing and analyses in this study were conducted in MATLAB software (The MathWorks, Natick, MA, USA).

A frequency spectrum was computed. An EEG power spectrum density (PSD) was generated using the Welch's method (one of the Fourier transforms) (26). The different frequency bands on the frequency spectrum were divided by 0.1–46 Hz to obtain the relative power values. The power values were then averaged across each frequency band—delta (1–4 Hz), theta (4–8 Hz), alpha (8–12 Hz), beta (12–30 Hz), and gamma (31–45 Hz)—and were averaged across all trials.

Functional connectivity assesses the functional communication between the brain regions by estimating the level of synchronization of the EEG signals (27). The phase lag index (PLI) aims to obtain a measure that provides reliable estimates of the phase synchronization between two signals and is insensitive to volume conduction (28). Here, the instantaneous phases were obtained by initially bandpass filtering the signals within the frequency bands defined above and subsequently using the Hilbert transform to obtain the phase of the corresponding analytic signal (28, 29). The phase difference distribution (1φ), as an index of asymmetry between a given pair of channels that were wrapped in the interval, can be obtained as follows:

$$PLI_{xy} = |\langle \mathrm{sgn}(\Delta\varphi(\tau)) \rangle|$$

Different from PLI, the weighted phase lag index (WPLI) is an improved measure of phase synchronization for electrophysiological signals in the presence of noise and volume conduction, and it calculates the weight of the contribution of the observed phase leads and lags by the magnitude of the imaginary component of the cross-spectrum (28).

$$\mathrm{WPLI} = \frac{|\langle \mathrm{Imag}(Sxy(f)) \rangle|}{\langle |\mathrm{Imag}(Sxy(f))| \rangle} = \frac{|<|\mathrm{Imag}(Sxy(f))| \cdot \mathrm{sgn}(\mathrm{Imag}(f))>|}{\langle |\mathrm{Imag}(Sxy(f))| \rangle}$$

The PLI and WPLI range between 0 and 1, with 0 indicating no correlation and 1 maximal correlation. The connectivity matrices were entered as repeated measures dependent variables into the network-based statistic (NBS) toolbox (30). All of the analyses were conducted in MATLAB software (The MathWorks, Natick, MA, USA).

Statistical Analysis

Continuous variables were reported as the mean ± SEM, and statistical comparisons were made using one-way analysis of variance (ANOVA) followed by *post-hoc* least significant difference (LSD) or an independent *t*-test. Non-normally distributed variables were expressed as interquartile ranges (IQRs), and comparisons were conducted using the Mann–Whitney *U* test, Kruskal–Wallis test, or the chi-square test. Receiver operating characteristic (ROC) analyses and least absolute shrinkage and selection operator (LASSO) regression were constructed to calculate the best cutoff points and areas under the curve (AUCs) for the candidate biomarkers. For correlation analysis, Spearman's rank test was performed. Statistical analysis was performed using SPSS version 23.0. *P*-values less than 0.05 after multiple comparison correction using the false discovery rate method were considered significant.

RESULTS

Clinical Characteristics of the Study Cohorts

In this study, 43 participants without antibiotic intervention and 47 participants with antibiotic intervention, including EMCS, MCS, and VS patients, were recruited for 16S rRNA sequencing of fecal samples. The demographic and clinical characteristics of the study cohorts are summarized in **Table 1**. As shown, there were no significant differences among the three groups with respect to age, sex, and length of hospital stay. We also recorded and compared the main biochemical indicators of patients on the day of fecal sample collection. No significant differences were found in these indicators, excluding the levels of hemoglobin and creatinine among the three groups with or without antibiotic intervention.

In order to exclude the influence of the severity of brain injury in the acute stage, we compared the GCS of the patients when they were admitted in the ICU and found no significant differences among the three groups with or without antibiotic use.

Alterations in the Microbiomes of VS, MCS, and EMCS Patients Without Antibiotic Treatment

To assess alterations in the intestinal microbiome of EMCS, MCS, and VS patients, 16S rDNA gene sequencing was performed on all samples. As shown in the Venn diagram, 971 OTUs were identified, of which 428 OTUs were shared among all samples. MCS and VS patients shared 515 of 919 OTUs, EMCS and VS patients shared 497 of 766 OTUs, and EMCS and MCS patients shared 464 of 877 OTUs (**Figure 1A**). The mean community richness values (ACE and Chao1 indices) were higher in the VS and MCS groups compared to the EMCS group (**Figures 1B, C**). However, there was no significant difference in the microbial diversity (Shannon and Simpson diversity indices) among the three groups (**Figures 1D, E**). Subsequently, we applied feature selection to identify the gut microbiota that maximized the identification of the EMCS, MCS, and VS groups *via* PLS-DA ($R^2 = 0.998$, $Q^2 = 0.842$) (**Figure 1G**). We also performed PCoA and cluster analysis (**Supplementary Figure S1A** and **Figure 1F**), the results of which were consistent with those of PLS-DA: the samples from the MCS group were located between the EMCS and VS groups, but were closer to those of the EMCS group. Furthermore, we identified the importance of fecal microbiota in the PLS-DA model based on the VIP score, which is the weighted sum of squares of the PLS loadings for that variable (19). Thirty-eight OTUs were identified based on a VIP score >2 (**Supplementary Figure S1B**). Of the fecal microbiota, *Lactococcus*, *Megamonas*, and *Enterococcus*, among others, were enriched in the VS group, while *Allisonella*, *Mogibacterium*, and *Campylobacter*, among others, were enriched in the EMCS group; however, most of the intestinal microbiota showed lower levels in the MCS group compared to the other two groups (**Supplementary Figure S1C**). Furthermore, we screened the top 10 OTUs with the highest relative abundance using a ternary plot. *Streptococcus* was enriched in EMCS patients, *Lactobacillus* was enriched in MCS patients, and *Megamonas* was enriched in VS patients (**Figure 1H**), suggesting that the interior structure of the intestinal microbiome was also altered in patients with different levels of consciousness.

Fecal Microbiota Taxonomic Differences Among EMCS, MCS, and VS Patients Without Antibiotic Treatment

To investigate specific alterations in the fecal microbiota of patients with different levels of consciousness, we assessed the relative abundances in the EMCS, MCS, and VS groups at the phylum, class, family, and genus levels (**Figures 2**, **3A**). In our study, none of the fecal microbiota at the phylum level showed significant differences among the three groups. At the class level, VS patients showed a marked decrease in the relative abundance

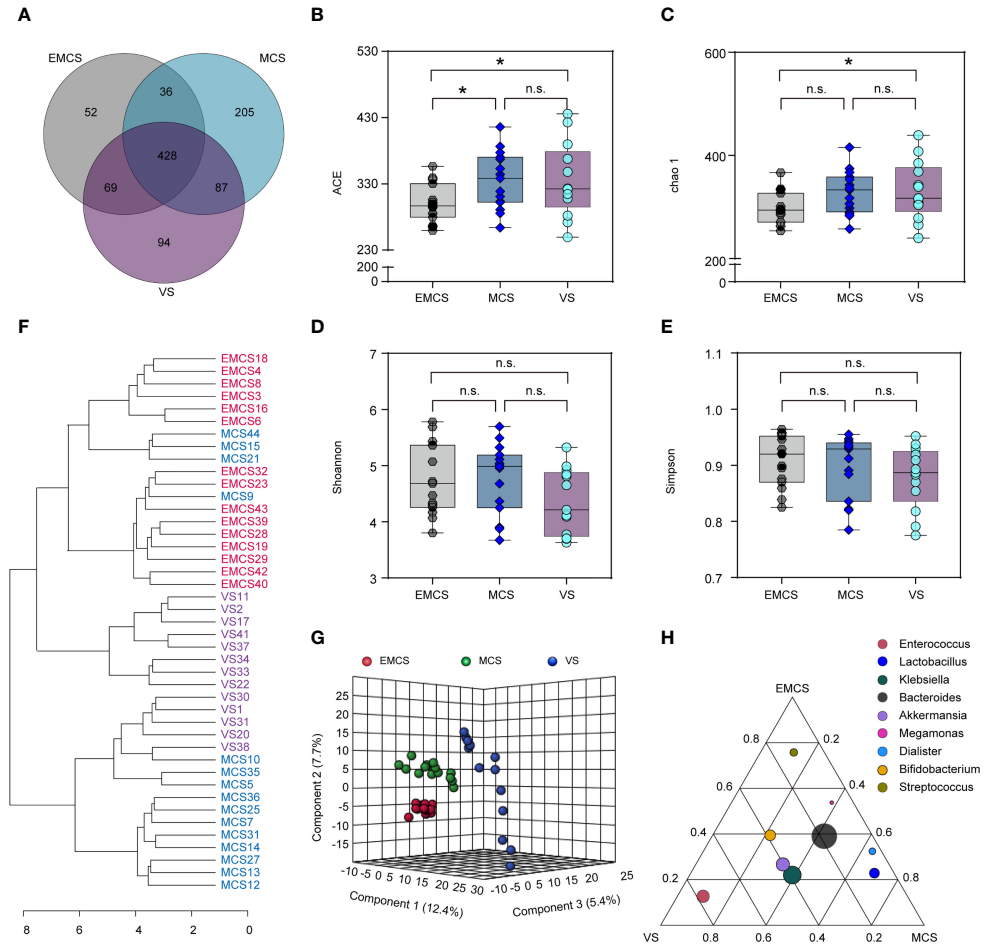

FIGURE 1 | Changes in the fecal microbial diversity and community structures of EMCS, MCS, and VS patients. **(A)** Venn diagram showing the overlap of the operational taxonomic units of the fecal microbiota across the three groups. **(B–E)** The α-diversity of the fecal microbiomes of three groups depicted according to ACE, Chao1, Shannon, and Simpson indices. Each box plot represents the median, interquartile range, minimum, and maximum values. **(F)** Dendrogram of the EMCS, MCS, and VS groups showing the clustering of all 43 samples. **(G)** PLS-DA score plots of the relative abundances of the microbiota in the EMCS, MCS, and VS groups. Three components explained 25.5% (12.4%, 5.4%, and 7.7%) of the variance among the three groups. Component scores are indicated as percent. Circles indicate individual samples from the EMCS, MCS, and VS groups.**(H)** Ternary plot depicting the number of genera (top 10 relative abundance) enriched in the EMCS, MCS, and VS groups. Each *circle* represents one genus, and the *size of the circle* reflects the relative abundance. *P*-values were determined using one-way ANOVA or the Kruskal–Wallis test. *$p < 0.05$; *n.s.*, no significant difference. *EMCS*, emerged from minimally conscious state; *MCS*, minimally conscious state; *VS*, vegetative state; *PLS-DA*, partial least squares discriminant analysis.

of Clostridia compared to the MCS and EMCS groups, while the relative abundance of Fusobacteriia showed alterations only between the MCS group and the EMCS group. Conversely, Deltaproteobacteria, the intestinal microbiota associated with inflammatory response (31), showed a higher relative abundance in the VS group than in the other two groups (**Figure 2A**), which indicated that the intestinal microenvironment of VS patients may be stimulated by chronic inflammation for a long period. Specifically, the subcategories Clostridiales and Lachnospiraceae and three genera—*Intestinibacter*, *Romboutsia*, and *Roseburia*—showed similar significant alterations in the microbiome of VS patients, which mostly explained the decreased abundance of Clostridia. Unexpectedly, *Eubacterium*, which is related to the production of intestinal butyric acid (32), showed a higher relative abundance in VS patients compared to EMCS patients. Similar significance was also found for Fusobacteriia, Deltaproteobacteria, and their corresponding order and family levels. In addition, Actinomycetaceae, Micrococcaceae, and Campylobacteraceae, which explained their order levels, showed higher relative abundance rates in the EMCS group than in the other two groups (**Figures 2B, C**). At the genus level, most of the intestinal microbiota that produced SCFAs or branched-chain fatty acids, such as *Bacteroides*, *Blautia*, *Lactobacillus*, *Roseburia*, and *Fusobacterium* (10, 33, 34), showed dramatically low abundance rates in patients in MCS or VS (**Figure 3A**).

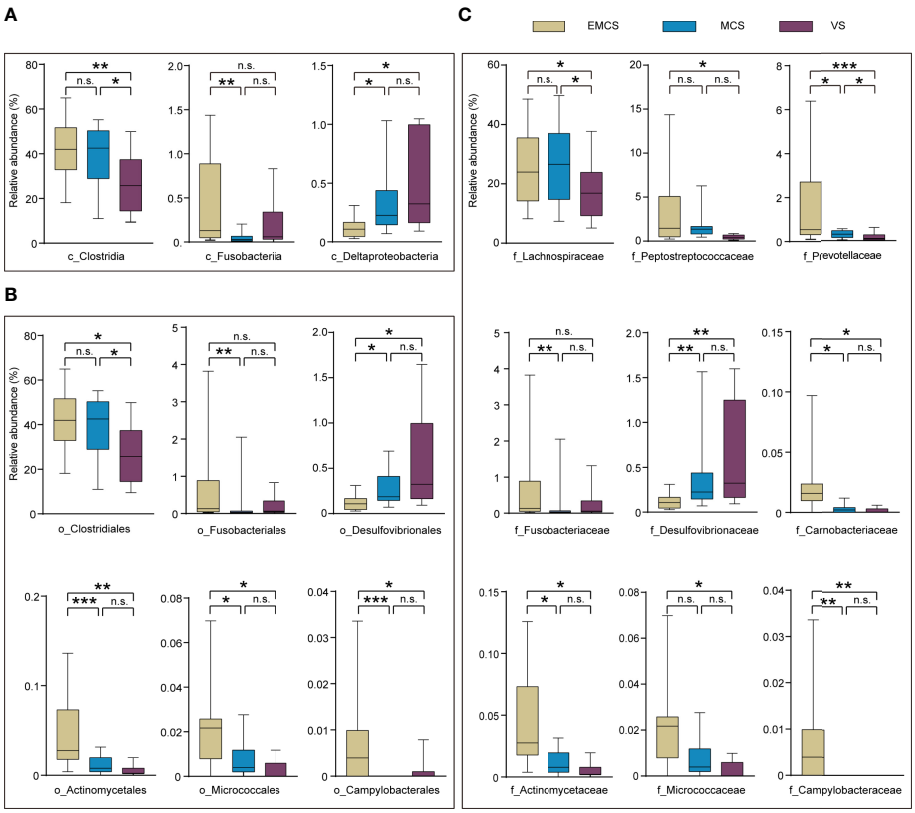

FIGURE 2 | Taxonomic differences of the class, family, and order levels in the fecal microbiota among EMCS, MCS, and VS patients. **(A–C)** Comparison of the relative abundance rates at the class level **(A)**, order level **(B)**, and family level **(C)** across the three groups. Each *box* represents an interquartile range (first and third quartiles) of taxon abundance, and the *middle line* corresponds to the median abundance. *No box* indicates that the fecal microbiota cannot be detected in the group. *P*-values were corrected using FDR. $^{*}p < 0.05$, $^{**}p < 0.01$, $^{***}p < 0.001$; *n.s.*, no significant difference. *c*, class; *f*, family; *o*, order; *EMCS*, emerged from minimally conscious state; *MCS*, minimally conscious state; *VS*, vegetative state; *FDR*, false discovery rate.

Fecal SCFA Differences Among EMCS, MCS, and VS Patients Without Antibiotic Treatment

SCFAs regulate the activity of neural cells and confer benefits for many neurological diseases through the gut–microbiota–brain axis (11, 35). To further explore the SCFAs in the intestinal tract of the patients in the three groups, they were also determined in the same fecal samples using targeted lipidomics. The results showed that the concentrations of acetic acid, propionic acid, and butyric acid were significantly decreased in the VS group (**Figures 3B–D**), which were consistent with the differences in plasma reported in our previous study (19). Other fatty acids such as isobutyric, isovaleric, valeric, and hexanoic acids were not significantly different among the three groups (**Figures 3E–H**). In the correlation analysis, *Bacteroides*, Clostridiales, and *Blautia* were significantly positively correlated with acetic acid or propionic acid. Moreover, some fecal microbiota including valeric acid-associated bacteria (Actinomycetaceae), *Roseburia*, and *Bacteroides* were significantly positively correlated with the CRS-R scores of patients, whereas the pathogenic microbial community (Desulfovibrionaceae) showed significant negative correlations with both the CRS-R and GOS-E scores (**Figure 3I**). This suggested the existence of a causal relationship between the disturbance of the microbial community and posttraumatic prolonged DoC, which may result from the reduction of the levels of SCFAs and the elevation of the pathogenicity.

Predicted Function Analysis of the Microbiome in EMCS, MCS, and VS Patients Without Antibiotic Treatment

To further predict the functional composition of the intestinal microbiome of prolonged DoC patients, PICRUSt2 was employed. **Table 2** shows the top 10 differential pathways between MCS and VS patients. Broad potential communication lines were identified between the gut microbiome and metabolism in EMCS, MCS, and VS patients, including folate transformation and L-threonine, L-arginine, L-tryptophan, and L-aspartate biosynthesis. Consistent with the trends in the PLS-DA and PCoA models, all of these pathways were significantly higher in the EMCS and MCS groups compared to the VS group. Some of these pathways, such as L-threonine biosynthesis, L-aspartate biosynthesis, and folate transformation, were also significantly higher in the EMCS group compared to the MCS group,

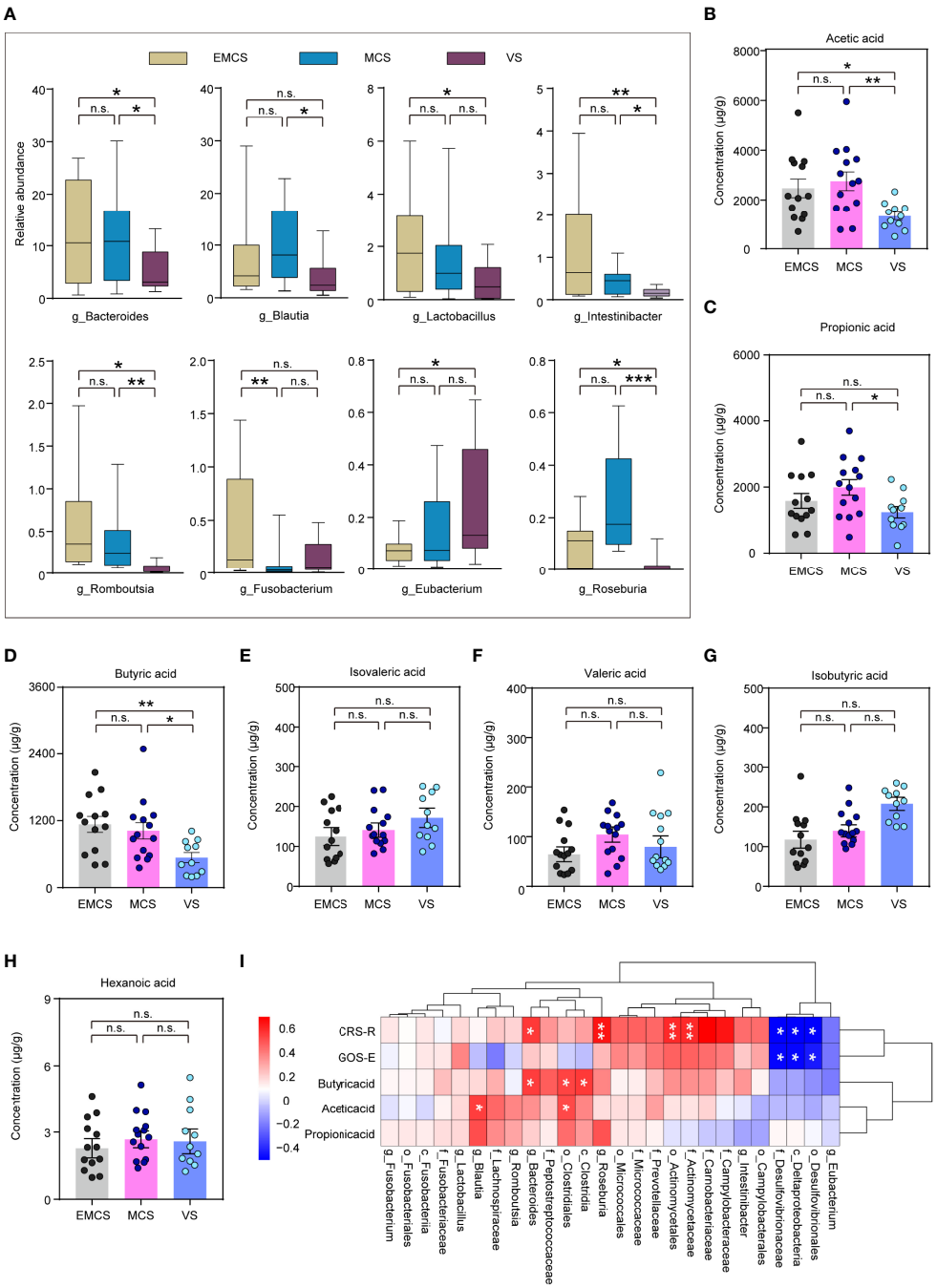

FIGURE 3 | Taxonomic differences at the genus level and differences in the short-chain fatty acids (SCFAs) in the fecal microbiota of EMCS, MCS, and VS patients. **(A)** Comparison of the relative abundance at the genus level across the three groups. Each *box* represents an interquartile range (first and third quartiles) of taxon abundance, and the *middle line* corresponds to the median abundance. *P*-values were corrected using FDR. **(B–H)** Comparison of the concentrations of the differential fecal SCFAs across the three groups. Data represent the mean ± SEM. **(I)** Heatmap of Spearman's rank correlation analysis between the altered fecal microbiota and SCFAs and the CRS-R scores. *Red* indicates positive correlation and *blue* denotes negative correlation. *P*-values were determined using one-way ANOVA or the Kruskal–Wallis test. $^{*}p < 0.05$, $^{**}p < 0.01$, $^{***}p < 0.001$; *n.s.*, no significant difference. *g*, genera; *CRS-R*, Coma Recovery Scale—Revised scores; *GOS-E*, Glasgow Outcome Scale—Extended; *EMCS*, emerged from minimally conscious state; *MCS*, minimally conscious state; *VS*, vegetative state; *FDR*, false discovery rate.

TABLE 2 | Pathway analysis of the EMCS, MCS, and VS groups using PICRUSt2.

Pathway	EMCS mean% (SD%)	MCS mean% (SD%)	VS mean% (SD%)	*p*-values		
				EMCS *vs.* MCS	EMCS *vs.* VS	MCS *vs.* VS
Gondoate biosynthesis	0.827 ± 0.088	0.836 ± 0.080	0.741 ± 0.059	0.782	0.005*	0.001*
cis-Vaccenate biosynthesis	0.768 ± 0.078	0.769 ± 0.068	0.701 ± 0.053	0.994	0.013*	0.007*
L-Threonine biosynthesis	0.681 ± 0.054	0.680 ± 0.061	0.609 ± 0.056	0.973	0.002*	0.004*
Folate transformations III	0.627 ± 0.046	0.625 ± 0.048	0.570 ± 0.047	0.901	0.003*	0.005*
L-Arginine biosynthesis II	0.537 ± 0.071	0.585 ± 0.061	0.510 ± 0.069	0.061	0.317	0.006*
L-Arginine biosynthesis I	0.540 ± 0.066	0.580 ± 0.053	0.503 ± 0.065	0.076	0.152	0.002*
L-Arginine biosynthesis IV	0.543 ± 0.000	0.579 ± 0.052	0.502 ± 0.064	0.079	0.138	0.002*
L-Tryptophan biosynthesis	0.528 ± 0.098	0.555 ± 0.067	0.481 ± 0.070	0.380	0.150	0.008*
L-Aspartate and L-asparagine biosynthesis	0.529 ± 0.071	0.520 ± 0.061	0.450 ± 0.066	0.724	0.005*	0.007*
Flavin biosynthesis	0.483 ± 0.091	0.529 ± 0.066	0.433 ± 0.051	0.128	0.080	<0.001*

*Data are given as mean% (SD%). A * was considered statistically significant.*
VS, vegetative state; MCS, minimally conscious state; EMCS, emerged minimal conscious state; PICRUSt, Phylogenetic Investigation of Communities by Reconstruction of Unobserved States.

suggesting that the synthesis of some essential amino acids in patients with low levels of consciousness may be weak, which is consistent with our previous metabolomics findings (19).

Fecal Microbiota Taxonomic and SCFA Differences Between Prolonged DoC Patients With and Without Antibiotic Treatment

Some prolonged DoC patients had been using antibiotics for a long time to prevent infection because of tracheotomy or hypostatic pneumonia (36). To explore the effects of antibiotics on the intestinal microbiome of patients with prolonged DoC, we compared the fecal microbiota taxonomic structure of the EMCS, MCS, and VS groups with that of the corresponding antibiotic treatment groups. The demographic and clinical characteristics of these cohorts are shown in **Supplementary Table S1**. The PLS-DA model showed a distinct separation of the MCS, VS, and their corresponding antibiotic treatment groups (R^2 = 0.978, Q^2 = 0.553) (**Figure 4A**). Interestingly, only the MCS group was significantly distinguished from its corresponding antibiotic treatment group (MCS-Abx) in the PCoA model (**Figure 4B**), but could not be observed in the EMCS and VS groups compared with their corresponding antibiotic treatment groups (EMCS-Abx and VS-Abx, respectively) (**Supplementary Figures S2A, B**). Specifically, we compared the taxonomic distributions of the fecal microbiota at the genus level in the MCS and MCS-Abx groups. The relative abundance of *Enterococcus*, *Dialister*, and *Blautia* showed significant differences between the MCS-Abx and MCS groups (**Figure 4C** and **Supplementary Table S2**), whereas no significant differences between EMCS and EMCS-Abx, as well as between VS and VS-Abx (**Supplementary Figures S2C, D**), were shown, suggesting that the intestinal microbiota of MCS patients were more sensitive to antibiotics than those of EMCS and VS patients. Additionally, both the mean community richness (ACE and Chao1) and microbial diversity (Shannon and Simpson diversity indices) were dramatically decreased in the MCS-Abx group compared to the MCS group (**Figure 4D**), but not in the other groups (**Supplementary Figures S2E, F**).

We found that most intestinal microbiota decreased and only a few (i.e., *Enterococcus* and *Halomonas*) were enriched in the MCS-Abx group, as shown in the heatmap (**Figure 4E**). We also performed MetaStat analysis to explore the most significantly different microbiota between these two groups (**Supplementary Table S3**). Of these, the three groups with the greatest differences included *Enterococcus*, which showed a higher relative abundance in the MCS-Abx group, with *Blautia* and *Dialister* showing the opposite (**Figure 4F**). Accordingly, most of the SCFAs in the fecal samples, including acetic, propionic, isobutyric, butyric, and isovaleric acids, dramatically decreased in the MCS-Abx group (**Figure 4G**) and were not significantly different in the other pairwise comparisons (**Supplementary Table S4**).

Behavioral Scale and EEG Reactivity Between MCS Patients Treated With and Without Antibiotics

Subsequently, we examined the differences of the brain function and prognosis of MCS patients treated with and without antibiotics. In this study, the CRS-R scores of all patients showed no significant differences between the prolonged DoC groups and their corresponding antibiotic treatment groups (**Supplementary Table S1**). To determine more objective evaluation indicators, we investigated the resting EEG spectral power and functional connectivity from a portion of the patients with intact skulls on the day of fecal collection. As expected, there were no significant differences in the CRS-R scores between the patients in the MCS group and those in the MCS-Abx group with intact skulls and who were selected for EEG recording (**Figure 5A**). Interestingly, patients in the MCS group showed higher power of the alpha band in the left hemisphere compared to those in the MCS-Abx group, especially in the frontal and parietal regions (**Figure 5B**). Furthermore, we screened out the relevant differential electrodes and found that their alpha power values were significantly lower in the MCS-Abx group (**Figure 5C**), suggesting that long-term antibiotic use may weaken the alpha band in the frontal parietal lobe of MCS patients. To better measure the differences between the two groups, we assessed functional connectivity including PLI and WPLI, which are

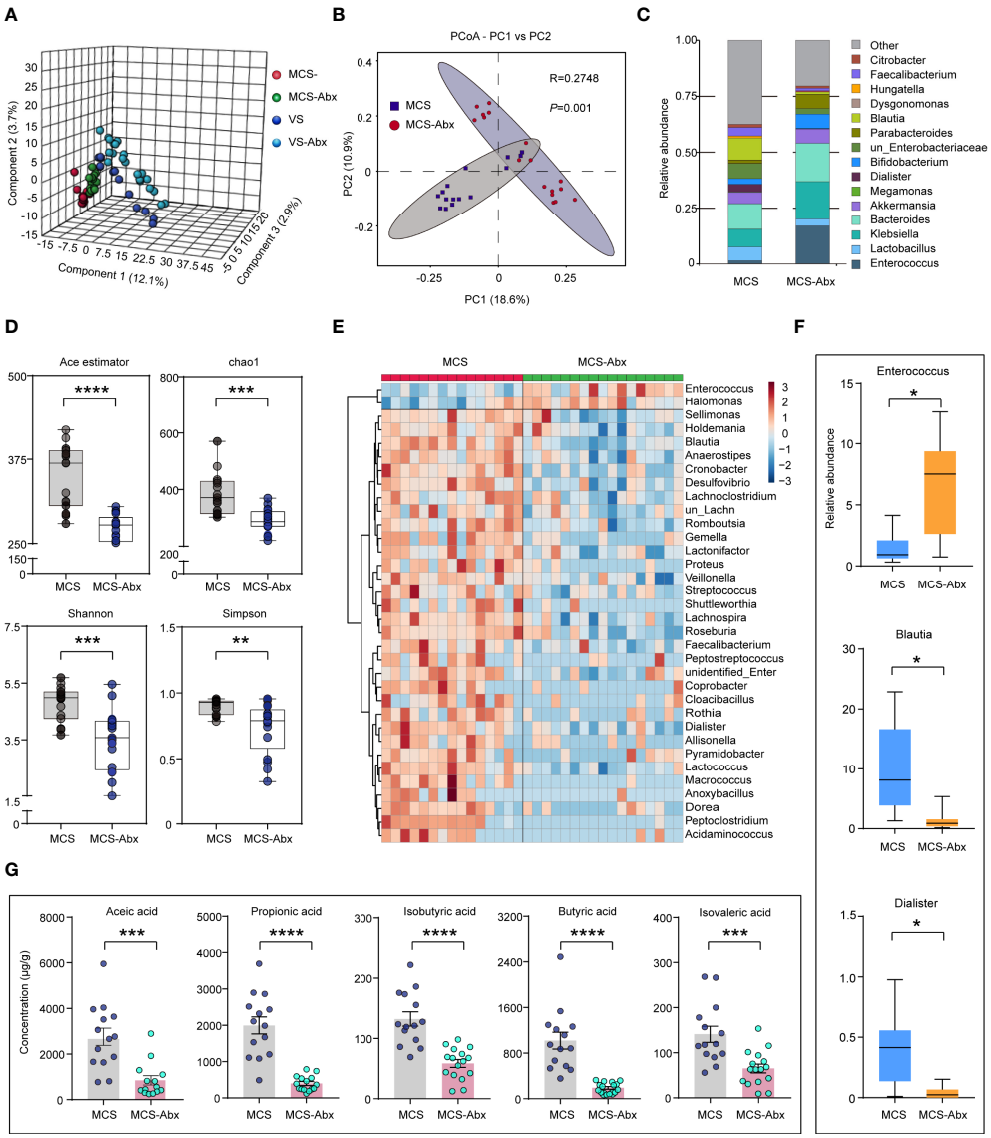

FIGURE 4 | Comparison of the fecal microbial diversity and community structures in MCS patients with or without antibiotic treatment. **(A)** PLS-DA score plots of the relative abundances of the microbiota in the MCS and MCS-Abx groups and in the VS and VS-Abx groups. Three components explained 18.7% (12.1%, 2.9%, and 3.7%) of the variance among the four groups. Component scores are indicated as percent. *Circles* indicate individual samples from the four groups. **(B)** Beta diversity results of the MCS and MCS-Abx groups assessed using principal coordinate analysis (PCoA). A total of 32 samples were used for PCoA. Two principal components (PCs) explained 29.5% (18.6% and 10.9%) of the variance between the groups (Bray–Curtis distance: MCS *vs*. MCS-Abx: $R = 0.2748$, $p = 0.001$). PC scores are indicated as percent. *Circles* indicate individual samples from the MCS and MCS-Abx groups. **(C)** Taxonomic distributions of the fecal microbiota at the genus level in the MCS and MCS-Abx groups. **(D)** The α-diversity of the fecal microbiomes between the MCS and MCS-Abx groups depicted according to ACE, Chao1, Shannon, and Simpson indices. Each *box plot* represents the median, interquartile range, minimum, and maximum values. **(E)** Heatmap of the most abundant metabolites in the MCS and MCS-Abx groups, as identified by the VIP scores in the PLS-DA. Each sample represents a single column. *Red* indicates the greater abundance of metabolites. **(F)** Top 3 differential fecal microbiota at the genus level by MetaStat analysis. Each *box* represents an interquartile range (first and third quartiles) of taxon abundance, and the *middle line* corresponds to the median abundance. *P*-values were corrected using FDR. **(G)** Comparison of the concentrations of the differential fecal short-chain fatty acids between the MCS and MCS-Abx groups. Data represent the mean ± SEM. *P*-values were determined using Student's *t*-test or the Kruskal–Wallis test and were corrected using FDR. $^{*}p < 0.05$, $^{**}p < 0.01$, $^{***}p < 0.001$, $^{****}p < 0.0001$; *n.s.*, no significant difference. *MCS*, minimally conscious state; *VS*, vegetative state; *Abx*, antibiotic; *PLS-DA*, partial least squares discriminant analysis; *VIP*, variable importance in projection; *FDR*, false discovery rate.

used to evaluate the connectivity between brain regions that share functional properties (37) and are decreased in many neurological diseases (38, 39). Using the NBS approach and a connected topoplot, we observed that the PLI and WPLI were significantly higher in the MCS group than in the MCS-Abx group in the alpha band. The significantly stronger connections were mainly located in the left frontal–occipital site. In addition, these two indicators in the MCS group were also prominently higher in the beta band, and the

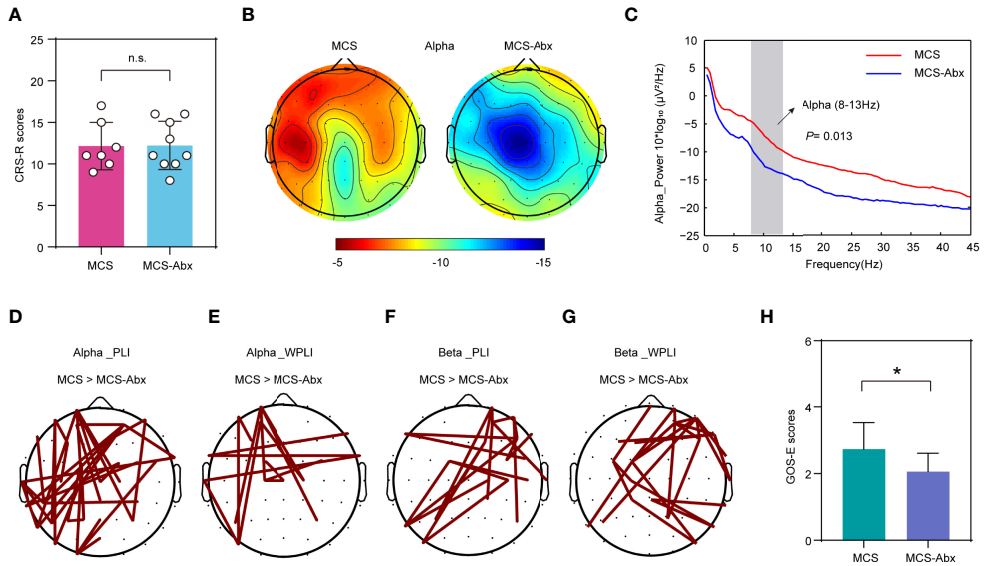

FIGURE 5 | Comparison of the behavioral scale and EEG signals of MCS patients with and without antibiotic treatment. **(A)** Comparison of the CRS-R scores of the patients with EEG recordings in the MCS and MCS-Abx groups. Data represent the mean ± SD. **(B)** Topography of the average degree of the alpha band power for the two groups. *Red* indicates greater alpha band power. **(C)** Spectral power in the MCS and MCS-Abx groups. Averaged alpha power for the differential electrodes (number of sites: 3, 5, 6, 11, 17, 18, 20, 21, 24, 28, 30, 31, 36, 38, 42, 44, and 48). The *vertical gray bar* highlights the portion of the graph corresponding to the alpha frequency ranges, both of which showed a significantly decreased power in the MCS-Abx group (p = 0.013). The *red line* denotes the MCS group and the *blue line* indicates the MCS-Abx group. **(D–G)** Connected topoplot of the PLI and WPLI between the MCS and MCS-Abx groups in the alpha and beta bands. NBS was used to identify the interregional connectivity that significantly differed between the groups for the alpha and beta bands. *Red lines* indicate higher connectivity in the MCS group than that in MCS-Abx group. **(D)** PLI in the alpha band (p = 0.010). **(E)** WPLI in the alpha band (p = 0.039). **(F)** PLI in the beta band (p = 0.002). **(G)** WPLI in the beta band (p = 0.006). **(H)** Comparison of the GOS-E scores followed for 6 months between the MCS and MCS-Abx groups. Data represent the mean ± SD. *P*-values were determined using Student's *t*-test or the Kruskal–Wallis test and were corrected using FDR. *p < 0.05; *n.s.*, no significant difference. *PLI*, phase lag index; *WPLI*, weighted phase lag index; *NBS*, network-based statistic; *CRS-R*, Coma Recovery Scale—Revised scores; *GOS-E*, Glasgow Outcome Scale—Extended; *MCS*, minimally conscious state; *Abx*, antibiotic; *FDR*, false discovery rate.

connection of the right frontal to the left occipital was the most significant (**Figures 5D–G**). To further investigate the effects of long-term antibiotic use on the prognosis of MCS patients, we compared their prognostic scores followed for 6 months and found that the GOS-E scores of the MCS group were higher than those of the MCS-Abx group (**Figure 5H**), suggesting that long-term antibiotic use may cause poor prognosis in these patients.

Identification of Gut Microbiome-Related Biomarkers to Distinguish EMCS, MCS, and VS Patients

To evaluate the diagnostic efficacy of the intestinal microbiome in patients with different levels of consciousness, LEfSe analysis was conducted to determine and distinguish the composition of the intestinal microbiota between the EMCS and MCS groups and between the MCS and VS groups. The intestinal microbiota of the patients in the MCS group was dominated by the genus *Faecalibacterium*, whereas the microbiome of the patients in the VS group was dominated by the genera *Enterococcus* and *Methanobrevibacter* (**Figure 6A**). We established a diagnostic panel of these three genera to distinguish MCS patients from VS patients, which were all included in the model using the LASSO algorithm. Thereafter, we assessed their diagnostic performance using ROC analysis with an AUC of 0.985 (cutoff = 0.548, p < 0.0001, 95%CI = 0.951–1.018) (**Figure 6B**). To validate the candidate biomarkers, they were tested in the validation cohorts (**Supplementary Table S5**), the results of which showed that they achieved high accuracy (AUC = 0.879, cutoff = 0.443, p < 0.0005, 95%CI = 0.772–1.019) (**Figure 6C**). When the EMCS group was compared with the MCS group, it was found that the intestinal microbiota of the former was dominated by *Streptococcus* and *Fusobacterium* at the genus level, whereas the microbiome of the latter was dominated by the genera *Lactococcus*, *Peptoclostridium*, *Phascolarctobacterium*, and *Megasphaera* (**Figure 6D**). The combination of *Streptococcus* and *Lactococcus* showed the highest LDA scores distinguishing patients in the EMCS group from those in the MCS group. Finally, the AUCs were 0.844 (cutoff = 0.609, p = 0.0018, 95%CI = 0.696–0.993) in the discovery cohort and 0.821 (cutoff = 0.434, p = 0.0002, 95%CI = 0.799–1.011) in the validation cohort using the LASSO algorithm and ROC analysis (**Figures 6E, F**). The discrimination validity was also examined using support vector machines. However, the AUCs were 0.654 for MCS to VS patients and 0.733 for EMCS to MCS patients (**Supplementary Figures S3A, B**), which were not better than those of the previous method.

To further investigate whether this panel can be extended to the antibiotic cohort, we performed the LASSO algorithm and ROC analysis in the antibiotic groups. The results revealed AUC

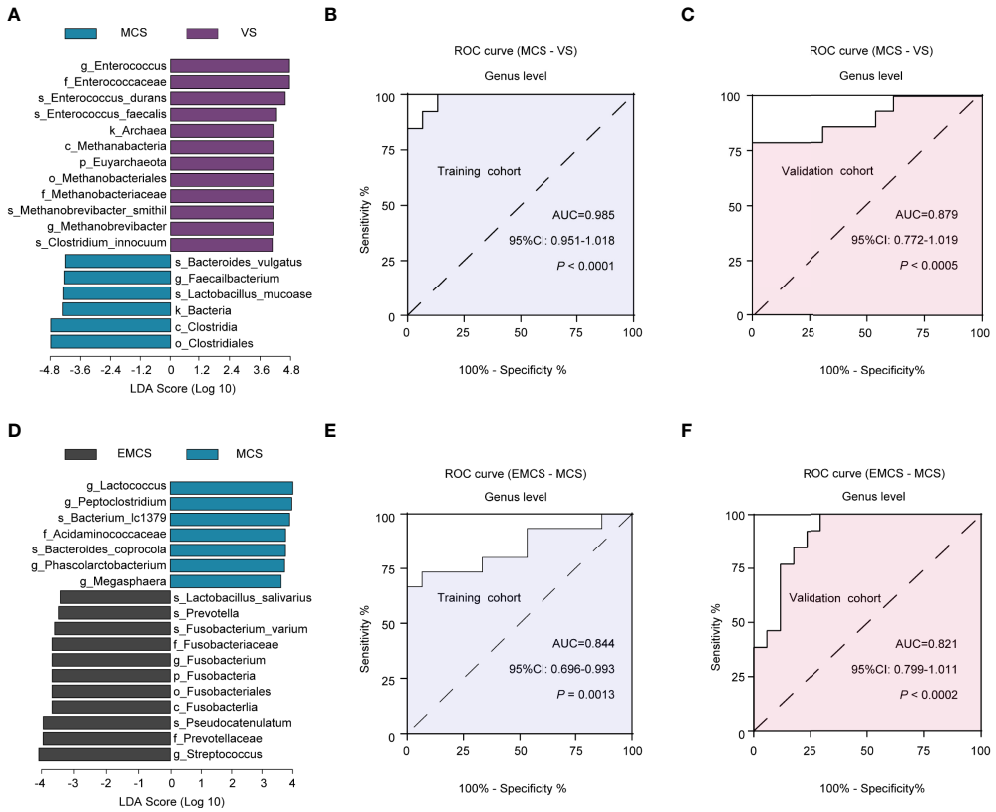

FIGURE 6 | Linear discriminant analysis (LDA) effect size (LEfSe) method used for the altered fecal microbiota and the identification of candidate biomarkers in the discovery and validation cohorts. **(A)** The LDA scores showed significant differences in the microbiota composition between the MCS and VS groups. Only those taxa with an LDA threshold >4 are shown. **(B, C)** ROC curves for *Enterococcus*, *Methanobrevibacter*, and *Faecalibacterium* used in distinguishing between MCS and VS patients in the discovery cohort **(B)** and in the validation cohort **(C)**. **(D)** The LDA scores showed significant differences in the microbiota composition between the EMCS and MCS groups. Only those taxa with an LDA threshold >3.5 are shown. **(E, F)** ROC curves for *Lactococcus* and *Streptococcus* used in distinguishing EMCS from MCS patients in the discovery cohort **(E)** and in the validation cohort **(F)**. *ROC*, receiver operating characteristic; *AUC*, area under the ROC curve; *EMCS*, emerged from minimally conscious state; *MCS*, minimally conscious state; *VS*, vegetative state.

values of 0.895 (cutoff = 0.017, $p = 0.0011$, 95%CI = 0.758–1.033) between the MCS-Abx and VS-Abx groups (**Supplementary Figure S3C**) and 0.647 (cutoff = 0.821, $p = 0.2235$, 95%CI = 0.420–0.875) between the EMCS-Abx and MCS-Abx groups (**Supplementary Figure S3D**).

DISCUSSION

In this study, we identified specific signatures of the fecal microbiota among patients with different levels of consciousness. We found that the altered intestinal microbiota was significantly correlated with the clinical behavioral scores (CRS-R scores) of the patients and the concentrations of SCFAs in their fecal samples. In the comparison of the groups with and without antibiotic treatment, only the MCS-Abx group showed dramatically different fecal microbiota and SCFAs relative to the MCS group, which is consistent with the EEG reactivity of the patients. Finally, we identified potential diagnostic biomarkers for distinguishing patients with different levels of consciousness both in the discovery and validation cohorts, which can also be extended to the antibiotic cohort. All of these findings indicate that alterations of the intestinal microbiota may play an important role in the identification of patients with different levels of consciousness and may influence the recovery of brain function in these patients, especially for MCS patients. To our knowledge, this is the first investigation of the intestinal microbiome in prolonged DoC patients and exploration of the effects of antibiotics on their intestinal microbiota and brain function. This study may provide a new perspective for the evaluation and treatment of patients with prolonged DoC.

Investigation of the intestinal microbiome can help explore its association with patients with different levels consciousness and provide a reference for nutrition-related interventions. All of the patients in our study received enteral nutrition from the hospital, which minimized the bias for gut microbiomes and lipid metabolism caused by different dietary habits. Different from that of TBI patients in the acute stage (40), the overall diversity and community richness of the intestinal microbiota were not altered among patients in the EMCS, MCS, and VS groups, and the same results have been shown in those who had experienced mild or

moderate/severe TBI several years ago, but who did not fall into prolonged DoC (41, 42). However, the structure of the intestinal microbiota of the three groups was shown to be dramatically different. A few beneficial microbial communities, such as *Bacteroides*, *Streptococcus*, and *Roseburia*, were enriched in EMCS patients, whereas some pathogenic microbial communities were enriched in VS patients, which indicated that the intestinal microecology might not return to its original state; however, a new dynamic balance was established when severe DoC patients entered into a chronic stage. Currently, only a few probiotics including *Lactobacillus* or *Bifidobacterium* are commonly used for a number of neurological diseases in the clinic (43, 44). More specific probiotics should be developed and available for prolonged DoC patients. Furthermore, the levels of acetic, propionic, and butyric acids, which comprise more than 95% of the total SCFA pool (10, 34) and are produced primarily from dietary fiber, were decreased in VS patients. A large number of studies have shown that SCFAs regulate a growing list of physiological and biochemical functions of the host, including the gut–brain axis (45) and immunological function (46). In our previous metabolomics study, we found that most of the metabolites containing SCFAs were also decreased in the plasma of VS patients (19). Therefore, it is essential to supplement sufficient SCFAs and dietary fiber for these patients. More importantly, most of the SCFAs are produced by the intestinal microbiota and can influence the brain (47). In our results, some of the differential SCFAs in the three groups also comprised the differential microbiota in these patients. For example, *Lactobacillus* can produce acetic acid (48), and *Roseburia* can influence the production of propionic and butyric acids (47). Additionally, some differential microbiota showed a high correlation with SCFAs, as well as with the CRS-R scores of the patients, which suggested that disturbance of the intestinal microbiota and reduction of the corresponding SCFAs may influence the recovery of consciousness after brain injury.

In our study, the patients in the antibiotic cohort had been administered piperacillin or cefoperazone for a long time. Interestingly, only the intestinal microbiome of the MCS patients was significantly altered relative to those who did not receive antibiotic treatment. Broad-spectrum antibiotics may decimate the intestinal microbiome (49). Although some pathogenic microbial communities, such as *Desulfovibrio* and *Macrococcus*, were significantly inhibited, a large number of beneficial bacteria accompanied by the production of SCFAs decreased sharply, which was not conducive to the recovery of the brain function of patients. A previous study demonstrated that antibiotics may influence the brain function through the gut–brain axis (50, 51), but they may also induce impaired consciousness in some patients with metabolic disorders (52, 53). In our study, the power of the alpha band in the antibiotic cohort was decreased in the frontal and parietal regions. The alpha band is considered to have an active role in network coordination and communication (54), and an increase of power and coherence of the frontal and parietal alpha frequency band has been observed when the brain of MCS patients was activated (55). These brain regions are critical areas of the default mode network (DMN), which has been shown to reflect the level of consciousness of DoC patients (56). Therefore, it is possible that the DMN is indirectly disrupted by antibiotics, thereby affecting the recovery of patients' consciousness. On the other hand, the brain network was damaged and the prognosis was poor in the antibiotic cohort, reflected in the weakened functional connectivity (PLI and WPLI) and GOS-E scores, suggesting that long-term antibiotic use may affect other consciousness-related networks and patient prognosis, even though this performance could not be observed in the CRS-R scale in time. Moreover, the alteration of the brain functional connectivity and the poor outcomes of MCS patients might explain the loss of abundant beneficial microbial communities caused by antibiotics. However, further work is needed to explain the causal relationship and identify the mechanisms underlying these alterations. In summary, when prolonged DoC patients are administered antibiotics for a long period in order to prevent infection, their intestinal microecology should also be protected.

Another important highlight of our study is that we identified biomarkers from the intestinal microbiome to distinguish between VS and MCS patients and between MCS and EMCS patients. Combining *Faecalibacterium*, *Enterococcus*, and *Methanobrevibacter*, we were able to distinguish MCS patients from VS patients with high accuracy in both the discovery and validation cohorts, and the diagnosis panel can be extended to the antibiotic cohort as well. We also used support vector machines to distinguish the three different levels of consciousness, which all showed higher accuracy, although weaker than that of the LASSO algorithm. In clinical practice, the CRS-R scale is commonly used for the diagnosis of VS or MCS patients, but lacks sufficient accuracy (57, 58). Although electrophysiology and imaging can also improve the accuracy (59–61), it is difficult to generalize their use due to the metal implants and incomplete skulls of a lot of patients. Our diagnostic indicators have some advantages, including being noninvasive and convenient to use. We also investigated potential biomarkers to distinguish EMCS patients from MCS and found two indicators with sufficient accuracy. However, this study also has some limitations. Firstly, it described the differences in the intestinal microbiome and brain function of patients with and without antibiotic treatment, but did not reveal the causal effect. We also cannot exclude some variations for the data from systemic inflammation, although there were no differences in the C-reactive protein levels in the different groups. Some variations from the diets may also influence the gut microbiomes of patients, although they were found to be similar. In addition, the sample size is limited, and the conclusion should be replicated in an independent study with a large sample size in the future.

CONCLUSION

In summary, we found that patients with different levels of consciousness have different intestinal microbiomes and SCFAs, which may influence brain function, especially in MCS patients. Moreover, *Faecalibacterium*, *Enterococcus*, and *Methanobrevibacter* were considered as potential biomarkers distinguishing MCS from VS patients with high accuracy both in the discovery and validation cohorts.

DATA AVAILABILITY STATEMENT

The datasets presented in this study can be found in online repositories. The names of the repository/repositories and accession number can be found below: NCBI, PRJNA813677.

ETHICS STATEMENT

The studies involving human participants were reviewed and approved by the Ethics Committee of the First Affiliated Hospital, School of Medicine, Zhejiang University. The patients/participants provided written informed consent to participate in this study.

AUTHOR CONTRIBUTIONS

BL and JY conceived the project. JY, ML, and BL designed the experiments. JG, JL and LH screened the patients. JY, YY, XW, and QC collected and repackaged the stool samples. FH extracted the genome DNA. JY and FM completed the microbiome analysis. JY, CX, and GP completed the EEG analysis. JY, ML, and BL wrote the manuscript. All authors discussed, reviewed, and edited the manuscript. All authors contributed to the article and approved the submitted version.

FUNDING

This work was supported by grants from the Natural Science Foundation of China (nos. 82071173 and 81901068). This work was also supported by the Key Realm R&D Program of Guangzhou (202007030005).

ACKNOWLEDGMENTS

The authors thank the patients and volunteers for their participation in this study.

SUPPLEMENTARY MATERIAL

The Supplementary Material for this article can be found online at: https://www.frontiersin.org/articles/10.3389/fimmu.2022.781148/full#supplementary-material

Supplementary Figure 1 | Beta diversity and clustering analysis of the fecal microbiota among patients with EMCS, MCS and VS. Related to . **(A)** Beta diversity results of the three groups were assessed by principal coordinate analysis (PCoA); A total of 43 samples and used for PCoA. Two PCs explain 22.1% (18.4% and 13.7%) of variance among the groups (Bray-Curtis distances: EMCS vs. VS: R= 0.1938, P=0.004; EMCS vs. MCS: R= 0.0540, P= 0.064; MCS vs. VS: R= 0.1869, P= 0.003). PC scores are indicated as %; circles indicate individual samples from EMCS, MCS and VS groups. **(B)** Heatmap of the most abundant metabolites among the three groups, as identified by VIP scores in PLS-DA. Each sample represents a single column. Red color indicates the greater abundance of metabolite. PLS-DA, Partial least-squares discriminant analysis; VIP, variable importance in projection; EMCS, Emerged from Minimally Conscious State; MCS, minimally conscious state; VS, vegetative state.

Supplementary Figure 2 | Comparison of the fecal microbial diversity and community structures in VS and EMCS patients treated with or without antibiotics. Related to. **(A)** Beta diversity results of the VS and VS-Abx groups were assessed by principal coordinate analysis (PCoA); A total of 33 samples and used for PCoA. Two PCs explain 35.1% (24.1% and 11.0%) of variance between the groups (Bray-Curtis distances: VS vs. VS-Abx: R= 0.0059, *P*=0.453). PC scores are indicated as %; circles indicate individual samples from VS and VS-Abx groups. **(B)** Beta diversity results of the EMCS and EMCS-Abx groups were assessed by PCoA; A total of 24 samples and used for PCoA. Two PCs explain 28.5% (17.2% and 11.3%) of variance between the groups (Bray-Curtis distances: EMCS vs. EMCS-Abx: R= 0.1336, P=0.063). PC scores are indicated as %; circles indicate individual samples from EMCS and EMCS-Abx groups. **(C, E)**: Taxonomic distributions of fecal microbiota of genus level in VS and VS-Abx groups, EMCS and EMCS-Abx groups. **(D, F)** The α-diversity of the fecal microbiome between VS and VS-Abx groups, EMCS and EMCS-Abx groups depict according to ACE, Chao 1, Shannon index and Simpson index. Each box plot represents the median, interquartile range, minimum, and maximum values. n.s., no significant difference; EMCS, Emerged from Minimally Conscious State; VS, vegetative state; Abx, treated with antibiotics.

Supplementary Figure 3 | ROC analysis of the candidate biomarkers in the antibiotic cohorts. **(A)** Matrix Diagram and AUC calculated by support vector machine between MCS and VS groups. **(B)** Matrix Diagram and AUC calculated by support vector machine between EMCS and MCS groups. **(C)** ROC curves for *Enterococcus*, *Methanobrevibacter* and *Faecailbacterium* for use in distinguishing MCS patients and VS patients in discovery cohort; **(D)** ROC curves for *Lactococcus* and *Streptococcus* for use in distinguishing MCS patients and VS patients in antibiotics cohort. AUC, area under the receiver-operating characteristic curve. EMCS, Emerged from Minimally Conscious State; MCS, minimally conscious state; VS, vegetative state; Abx, treated with antibiotics.

REFERENCES

1. Cruse D, Chennu S, Chatelle C, Bekinschtein TA, Fernandez-Espejo D, Pickard JD, et al. Bedside Detection of Awareness in the Vegetative State: A Cohort Study. *Lancet* (2011) 378:2088–94. doi: 10.1016/S0140-6736(11)61224-5
2. Monti MM, Laureys S, Owen AM. The Vegetative State. *BMJ* (2010) 341: c3765. doi: 10.1136/bmj.c3765
3. Bernat JL. Chronic Disorders of Consciousness. *Lancet* (2006) 367:1181–92. doi: 10.1016/S0140-6736(06)68508-5
4. Jennett B, Plum F. Persistent Vegetative State After Brain Damage. A Syndrome in Search of a Name. *Lancet* (1972) 1:734–7. doi: 10.1016/s0140-6736(72)90242-5
5. Machado C. The Minimally Conscious State: Definition and Diagnostic Criteria. *Neurology* (2002) 59:1473; author reply 1473–4. doi: 10.1212/wnl.59.9.1473
6. Chennu S, Annen J, Wannez S, Thibaut A, Chatelle C, Cassol H, et al. Brain Networks Predict Metabolism, Diagnosis and Prognosis at the Bedside in Disorders of Consciousness. *Brain* (2017) 140:2120–32. doi: 10.1093/brain/awx163
7. Bourdillon P, Hermann B, Sitt JD, Naccache L. Electromagnetic Brain Stimulation in Patients With Disorders of Consciousness. *Front Neurosci* (2019) 13:223. doi: 10.3389/fnins.2019.00223
8. Cryan JF, O'Riordan KJ, Cowan CSM, Sandhu KV, Bastiaanssen TFS, Boehme M, et al. The Microbiota-Gut-Brain Axis. *Physiol Rev* (2019) 99:1877–2013. doi: 10.1152/physrev.00018.2018
9. Morais LH, Schreiber H, Mazmanian SK. The Gut Microbiota-Brain Axis in Behaviour and Brain Disorders. *Nat Rev Microbiol* (2020) 19:241–255. doi: 10.1038/s41579-020-00460-0
10. den Besten G, van Eunen K, Groen AK, Venema K, Reijngoud DJ, Bakker BM. The Role of Short-Chain Fatty Acids in the Interplay Between Diet, Gut Microbiota, and Host Energy Metabolism. *J Lipid Res* (2013) 54:2325–40. doi: 10.1194/jlr.R036012

11. Duscha A, Gisevius B, Hirschberg S, Yissachar N, Stangl GI, Eilers E, et al. Propionic Acid Shapes the Multiple Sclerosis Disease Course by an Immunomodulatory Mechanism. *Cell* (2020) 180:1067–1080 e16. doi: 10.1016/j.cell.2020.02.035
12. Krautkramer KA, Fan J, Backhed F. Gut Microbial Metabolites as Multi-Kingdom Intermediates. *Nat Rev Microbiol* (2020) 19::77–94. doi: 10.1038/s41579-020-0438-4
13. Liu P, Wu L, Peng G, Han Y, Tang R, Ge J, et al. Altered Microbiomes Distinguish Alzheimer's Disease From Amnestic Mild Cognitive Impairment and Health in a Chinese Cohort. *Brain Behav Immun* (2019) 80:633–43. doi: 10.1016/j.bbi.2019.05.008
14. Liu P, Jia XZ, Chen Y, Yu Y, Zhang K, Lin YJ, et al. Gut Microbiota Interacts With Intrinsic Brain Activity of Patients With Amnestic Mild Cognitive Impairment. *CNS Neurosci Ther* (2020) 27:163–173. doi: 10.1111/cns.13451
15. Robba C, Rebora P, Banzato E, Wiegers EJA, Stocchetti N, Menon DK, et al. Incidence, Risk Factors, and Effects on Outcome of Ventilator-Associated Pneumonia in Patients With Traumatic Brain Injury: Analysis of a Large, Multicenter, Prospective, Observational Longitudinal Study. *Chest* (2020) 158:2292–303. doi: 10.1016/j.chest.2020.06.064
16. Yeatts SD, Martin RH, Meurer W, Silbergleit R, Rockswold G, Barsan WG, et al. Sliding Scoring of the Glasgow Outcome Scale - Extended (GOS-E) as Primary Outcome in Traumatic Brain Injury Trials. *J Neurotrauma* (2020) 37:2674–2679. doi: 10.1089/neu.2019.6969
17. Giacino JT, Kalmar K, Whyte J. The JFK Coma Recovery Scale-Revised: Measurement Characteristics and Diagnostic Utility. *Arch Phys Med Rehabil* (2004) 85:2020–9. doi: 10.1016/j.apmr.2004.02.033
18. Ishtikhar M, Siddiqui Z, Husain FM, Khan RA, Hassan I. Comparative Refolding of Guanidinium Hydrochloride Denatured Bovine Serum Albumin Assisted by Cationic and Anionic Surfactants *via* Artificial Chaperone Protocol: Biophysical Insight. *Spectrochim Acta A Mol Biomol Spectrosc* (2020) 225:117510. doi: 10.1016/j.saa.2019.117510
19. Yu J, Meng F, He F, Chen F, Bao W, Yu Y, et al. Metabolic Abnormalities in Patients With Chronic Disorders of Consciousness. *Aging Dis* (2020) 12, 386–403. doi: 10.14336/AD.2020.0812
20. Xiong N, Gao X, Zhao H, Cai F, Zhang FC, Yuan Y, et al. Using Arterial-Venous Analysis to Characterize Cancer Metabolic Consumption in Patients. *Nat Commun* (2020) 11:3169. doi: 10.1038/s41467-020-16810-8
21. Edgar RC. UPARSE: Highly Accurate OTU Sequences From Microbial Amplicon Reads. *Nat Methods* (2013) 10:996–8. doi: 10.1038/nmeth.2604
22. Caporaso JG, Kuczynski J, Stombaugh J, Bittinger K, Bushman FD, Costello EK, et al. QIIME Allows Analysis of High-Throughput Community Sequencing Data. *Nat Methods* (2010) 7:335–6. doi: 10.1038/nmeth.f.303
23. Vogt NM, Kerby RL, Dill-McFarland KA, Harding SJ, Merluzzi AP, Johnson SC, et al. Gut Microbiome Alterations in Alzheimer's Disease. *Sci Rep* (2017) 7:13537. doi: 10.1038/s41598-017-13601-y
24. Langille MG, Zaneveld J, Caporaso JG, McDonald D, Knights D, Reyes JA, et al. Predictive Functional Profiling of Microbial Communities Using 16S rRNA Marker Gene Sequences. *Nat Biotechnol* (2013) 31:814–21. doi: 10.1038/nbt.2676
25. Poulsen C, Picton TW, Paus T. Age-Related Changes in Transient and Oscillatory Brain Responses to Auditory Stimulation in Healthy Adults 19-45 Years Old. *Cereb Cortex* (2007) 17:1454–67. doi: 10.1093/cercor/bhl056
26. He F, Wu M, Meng F, Hu Y, Gao J, Chen Z, et al. Effects of 20 Hz Repetitive Transcranial Magnetic Stimulation on Disorders of Consciousness: A Resting-State Electroencephalography Study. *Neural Plast* (2018) 2018:5036184. doi: 10.1155/2018/5036184
27. Nentwich M, Ai L, Madsen J, Telesford QK, Haufe S, Milham MP, et al. Functional Connectivity of EEG Is Subject-Specific, Associated With Phenotype, and Different From fMRI. *Neuroimage* (2020) 218:117001. doi: 10.1016/j.neuroimage.2020.117001
28. Stam CJ, Nolte G, Daffertshofer A. Phase Lag Index: Assessment of Functional Connectivity From Multi Channel EEG and MEG With Diminished Bias From Common Sources. *Hum Brain Mapp* (2007) 28:1178–93. doi: 10.1002/hbm.20346
29. Anastasiadou MN, Christodoulakis M, Papathanasiou ES, Papacostas SS, Hadjipapas A, Mitsis GD. Graph Theoretical Characteristics of EEG-Based Functional Brain Networks in Patients With Epilepsy: The Effect of Reference Choice and Volume Conduction. *Front Neurosci* (2019) 13:221. doi: 10.3389/fnins.2019.00221
30. Zalesky A, Fornito A, Bullmore ET. Network-Based Statistic: Identifying Differences in Brain Networks. *Neuroimage* (2010) 53:1197–207. doi: 10.1016/j.neuroimage.2010.06.041
31. Nagata N, Xu L, Kohno S, Ushida Y, Aoki Y, Umeda R, et al. Glucoraphanin Ameliorates Obesity and Insulin Resistance Through Adipose Tissue Browning and Reduction of Metabolic Endotoxemia in Mice. *Diabetes* (2017) 66:1222–36. doi: 10.2337/db16-0662
32. Zaiss MM, Jones RM, Schett G, Pacifici R. The Gut-Bone Axis: How Bacterial Metabolites Bridge the Distance. *J Clin Invest* (2019) 129:3018–28. doi: 10.1172/JCI128521
33. Macfarlane S, Macfarlane GT. Regulation of Short-Chain Fatty Acid Production. *Proc Nutr Soc* (2003) 62:67–72. doi: 10.1079/PNS2002207
34. Cummings JH, Pomare EW, Branch WJ, Naylor CP, Macfarlane GT. Short Chain Fatty Acids in Human Large Intestine, Portal, Hepatic and Venous Blood. *Gut* (1987) 28:1221–7. doi: 10.1136/gut.28.10.1221
35. Li JM, Yu R, Zhang LP, Wen SY, Wang SJ, Zhang XY, et al. Dietary Fructose-Induced Gut Dysbiosis Promotes Mouse Hippocampal Neuroinflammation: A Benefit of Short-Chain Fatty Acids. *Microbiome* (2019) 7:98. doi: 10.1186/s40168-019-0713-7
36. Robba C, Rebora P, Banzato E, Wiegers EJA, Stocchetti N, Menon DK, et al. Incidence, Risk Factors, and Effects on Outcome of Ventilator-Associated Pneumonia in Patients With Traumatic Brain Injury: Analysis of a Large, Multicenter, Prospective, Observational Longitudinal Study. *Chest* (2020) 158:2292–2303. doi: 10.1016/j.chest.2020.06.064
37. Biswal BB, Van Kylen J, Hyde JS. Simultaneous Assessment of Flow and BOLD Signals in Resting-State Functional Connectivity Maps. *NMR BioMed* (1997) 10:165–70. doi: 10.1002/(sici)1099-1492(199706/08)10:4/5<165::aid-nbm454>3.0.co;2-7
38. Kiiski H, Rueda-Delgado LM, Bennett M, Knight R, Rai L, Roddy D, et al. Functional EEG Connectivity is a Neuromarker for Adult Attention Deficit Hyperactivity Disorder Symptoms. *Clin Neurophysiol* (2020) 131:330–42. doi: 10.1016/j.clinph.2019.08.010
39. Briels CT, Schoonhoven DN, Stam CJ, de Waal H, Scheltens P, Gouw AA. Reproducibility of EEG Functional Connectivity in Alzheimer's Disease. *Alzheimers Res Ther* (2020) 12:68. doi: 10.1186/s13195-020-00632-3
40. Treangen TJ, Wagner J, Burns MP, Villapol S. Traumatic Brain Injury in Mice Induces Acute Bacterial Dysbiosis Within the Fecal Microbiome. *Front Immunol* (2018) 9:2757. doi: 10.3389/fimmu.2018.02757
41. Brenner LA, Stamper CE, Hoisington AJ, Stearns-Yoder KA, Stanislawksi MA, Brostow DP, et al. Microbial Diversity and Community Structures Among Those With Moderate to Severe TBI: A United States-Veteran Microbiome Project Study. *J Head Trauma Rehabil* (2020) 35:332–41. doi: 10.1097/HTR.0000000000000615
42. Urban RJ, Pyles RB, Stewart CJ, Ajami N, Randolph KM, Durham WJ, et al. Altered Fecal Microbiome Years After Traumatic Brain Injury. *J Neurotrauma* (2020) 37:1037–51. doi: 10.1089/neu.2019.6688
43. Mazzini L, Mogna L, De Marchi F, Amoruso A, Pane M, Aloisio I, et al. Potential Role of Gut Microbiota in ALS Pathogenesis and Possible Novel Therapeutic Strategies. *J Clin Gastroenterol* (2018) 52 Suppl 1:S68–70. doi: 10.1097/MCG.0000000000001042. Proceedings from the 9th Probiotics, Prebiotics and New Foods, Nutraceuticals and Botanicals for Nutrition & Human and Microbiota Health Meeting, held in Rome, Italy from September 10 to 12, 2017.
44. Akkasheh G, Kashani-Poor Z, Tajabadi-Ebrahimi M, Jafari P, Akbari H, Taghizadeh M, et al. Clinical and Metabolic Response to Probiotic Administration in Patients With Major Depressive Disorder: A Randomized, Double-Blind, Placebo-Controlled Trial. *Nutrition* (2016) 32:315–20. doi: 10.1016/j.nut.2015.09.003
45. Dalile B, Van Oudenhove L, Vervliet B, Verbeke K. The Role of Short-Chain Fatty Acids in Microbiota-Gut-Brain Communication. *Nat Rev Gastroenterol Hepatol* (2019) 16:461–78. doi: 10.1038/s41575-019-0157-3
46. Bachem A, Makhlouf C, Binger KJ, de Souza DP, Tull D, Hochheiser K, et al. Microbiota-Derived Short-Chain Fatty Acids Promote the Memory Potential of Antigen-Activated CD8(+) T Cells. *Immunity* (2019) 51:285–297 e5. doi: 10.1016/j.immuni.2019.06.002
47. Zietek M, Celewicz Z, Szczuko M. Short-Chain Fatty Acids, Maternal Microbiota and Metabolism in Pregnancy. *Nutrients* (2021) 13:285–297 e5. doi: 10.3390/nu13041244

48. Shen J, Zhang J, Zhao Y, Lin Z, Ji L, Ma X. Tibetan Pig-Derived Probiotic Lactobacillus Amylovorus SLZX20-1 Improved Intestinal Function *via* Producing Enzymes and Regulating Intestinal Microflora. *Front Nutr* (2022) 9:846991. doi: 10.3389/fnut.2022.846991
49. Ferrer M, Mendez-Garcia C, Rojo D, Barbas C, Moya A. Antibiotic Use and Microbiome Function. *Biochem Pharmacol* (2017) 134:114–26. doi: 10.1016/j.bcp.2016.09.007
50. Karakan T, Ozkul C, Kupeli Akkol E, Bilici S, Sobarzo-Sanchez E, Capasso R. Gut-Brain-Microbiota Axis: Antibiotics and Functional Gastrointestinal Disorders. *Nutrients* (2021) 13:389. doi: 10.3390/nu13020389
51. Angelucci F, Cechova K, Amlerova J, Hort J. Antibiotics, Gut Microbiota, and Alzheimer's Disease. *J Neuroinflamm* (2019) 16:108. doi: 10.1186/s12974-019-1494-4
52. Ozturk S, Kocabay G, Topcular B, Yazici H, Cagatay AA, Bahat G, et al. Non-Convulsive Status Epilepticus Following Antibiotic Therapy as a Cause of Unexplained Loss of Consciousness in Patients With Renal Failure. *Clin Exp Nephrol* (2009) 13:138–44. doi: 10.1007/s10157-008-0115-9
53. Lee JY, Kang KP, Kim W, Park SK, Lee S. An Overlooked Cause of Impaired Consciousness in a Hemodialysis Patient. *Korean J Intern Med* (2012) 27:367. doi: 10.3904/kjim.2012.27.3.367
54. Palva S, Palva JM. New Vistas for Alpha-Frequency Band Oscillations. *Trends Neurosci* (2007) 30:150–8. doi: 10.1016/j.tins.2007.02.001
55. Cavinato M, Genna C, Formaggio E, Gregorio C, Storti SF, Manganotti P, et al. Behavioural and Electrophysiological Effects of tDCS to Prefrontal Cortex in Patients With Disorders of Consciousness. *Clin Neurophysiol* (2019) 130:231–8. doi: 10.1016/j.clinph.2018.10.018
56. Vanhaudenhuyse A, Noirhomme Q, Tshibanda LJ, Bruno MA, Boveroux P, Schnakers C, et al. Default Network Connectivity Reflects the Level of Consciousness in Non-Communicative Brain-Damaged Patients. *Brain* (2010) 133:161–71. doi: 10.1093/brain/awp313
57. Childs NL, Mercer WN, Childs HW. Accuracy of Diagnosis of Persistent Vegetative State. *Neurology* (1993) 43:1465–7. doi: 10.1212/wnl.43.8.1465
58. Andrews K, Murphy L, Munday R, Littlewood C. Misdiagnosis of the Vegetative State: Retrospective Study in a Rehabilitation Unit. *BMJ* (1996) 313:13–6. doi: 10.1136/bmj.313.7048.13
59. Fernandez-Espejo D, Bekinschtein T, Monti MM, Pickard JD, Junque C, Coleman MR, et al. Diffusion Weighted Imaging Distinguishes the Vegetative State From the Minimally Conscious State. *Neuroimage* (2011) 54:103–12. doi: 10.1016/j.neuroimage.2010.08.035
60. Yu Y, Meng F, Zhang L, Liu X, Wu Y, Chen S, et al. A Multi-Domain Prognostic Model of Disorder of Consciousness Using Resting-State fMRI and Laboratory Parameters. *Brain Imaging Behav* (2020) 15:1966–1976. doi: 10.1007/s11682-020-00390-8
61. Erlbeck H, Real RG, Kotchoubey B, Mattia D, Bargak J, Kubler A. Basic Discriminative and Semantic Processing in Patients in the Vegetative and Minimally Conscious State. *Int J Psychophys* (2017) 113:8–16. doi: 10.1016/j.ijpsycho.2016.12.012

Conflict of Interest: The authors declare that the research was conducted in the absence of any commercial or financial relationships that could be construed as a potential conflict of interest.

Publisher's Note: All claims expressed in this article are solely those of the authors and do not necessarily represent those of their affiliated organizations, or those of the publisher, the editors and the reviewers. Any product that may be evaluated in this article, or claim that may be made by its manufacturer, is not guaranteed or endorsed by the publisher.

Copyright © 2022 Yu, Cheng, He, Meng, Yu, Xu, Wen, Hong, Gao, Li, Pan, Li and Luo. This is an open-access article distributed under the terms of the Creative Commons Attribution License (CC BY). The use, distribution or reproduction in other forums is permitted, provided the original author(s) and the copyright owner(s) are credited and that the original publication in this journal is cited, in accordance with accepted academic practice. No use, distribution or reproduction is permitted which does not comply with these terms.

frontiers | Frontiers in Microbiology

ORIGINAL RESEARCH
published: 08 September 2022
doi: 10.3389/fmicb.2022.813576

The Gut Bacteria Dysbiosis Contributes to Chronic Graft-Versus-Host Disease Associated With a Treg/Th1 Ratio Imbalance

Yulian Wang, Lisi Huang, Tian Huang, Suxia Geng, Xiaomei Chen, Xin Huang, Peilong Lai, Xin Du* and Jianyu Weng**

Department of Hematology, Guangdong Provincial People's Hospital, Guangdong Academy of Medical Sciences, Guangzhou, China

OPEN ACCESS

Edited by:
Tobias R. Kollmann, University of Western Australia, Australia

Reviewed by:
David Gondek, Ithaca College, United States
Jun-chang Guan, Bengbu Medical College, China

***Correspondence:**
Peilong Lai
13570931198@163.com
Xin Du
miyadu@hotmail.com
Jianyu Weng
wengjianyu1969@163.com

Specialty section:
This article was submitted to Microbial Immunology, a section of the journal Frontiers in Microbiology

Received: *12 November 2021*
Accepted: *21 June 2022*
Published: *08 September 2022*

Citation:
Wang Y, Huang L, Huang T, Geng S, Chen X, Huang X, Lai P, Du X and Weng J (2022) The Gut Bacteria Dysbiosis Contributes to Chronic Graft-Versus-Host Disease Associated With a Treg/Th1 Ratio Imbalance. Front. Microbiol. 13:813576. doi: 10.3389/fmicb.2022.813576

Introduction: Dysbiosis of gut bacteria has been discovered in a large number of autoimmune diseases. However, the influence of the gut bacteria in the mice model of chronic sclerodermatous graft-versus-host disease (Scl-GVHD), a disease that resembles an autoimmune disease characterized by chronic inflammation of multiple organs, such as skin, remains elusive. Here, we explore the role of gut bacteria in an Scl-cGVHD mice model.

Methods: We established a mouse model of Scl-cGVHD, collected fecal flora, analyzed the composition, and diversity of intestinal flora using 16S rDNA amplicon sequencing, and detected the proportion of Treg and Th1 cells in splenocytes of Scl-cGVHD mice. To verify the immunoregulatory effect of Scl-cGVHD intestinal flora, we prepared bacterial extracts, co-cultured with splenocytes *in vitro*, and used flow cytometry to detect T cell differentiation and cytokine secretion.

Results: By examining T-cell differentiation in splenocytes of cGVHD mice, we found that Treg cells were significantly reduced (15.27 ± 0.23 vs. 12.23 ± 0.47, $p = 0.0045$) and Th1 cells were increased (1.54 ± 0.18 vs. 6.68 ± 0.80, $p = 0.0034$) in cGVHD mice. Significant differences were observed in the composition and diversity of the gut bacteria in mice with Scl-cGVHD versus without GVHD. Analysis of mice fecal bacteria samples ($n = 10$, 5 Scl-cGVHD and 5 Non-GVHD) showed significant separation [$R = 0.732$, $p = 0.015$, non-parametric analysis (ANOSIM)] in Scl-cGVHD and non-GVHD mice. The abundance of the family and genus *Ruminococcaceae* bacteria decreased and the family *Lachnospiraceae* and limited to the species *Lachnospiraceae_bacterium_DW17* increased in Scl-cGVHD mice. *In vitro* results of the cellular level study suggest that the bacteria extracts of gut microbiota from Scl-cGVHD mice modulated the splenic T cells toward differentiation into $CD4^+IFN\text{-}\gamma^+$ Th1 cells (14.37 ± 0.32 vs. 10.40 ± 2.19, $p = 0.036$), and the percentage of $CD4^+CD25^+Foxp3^+$ Tregs decreased (6.36 ± 0.39 vs. 8.66 ± 0.07, $p = 0.001$) compared with the non-GVHD mice. In addition, the secretion of proinflammatory interferon- γ (IFN-γ) cytokine in the supplement of cellular culture was increased (4,898.58 ± 235.82 vs. 4,347.87 ± 220.02 pg/ml, $p = 0.042$)

in the mice model of the Scl-cGVHD group, but anti-inflammatory interleukin (IL)-10 decreased (7,636.57 ± 608.05 vs. 9,563.56 ± 603.34 pg/ml, $p = 0.018$).

Conclusion: Our data showed the different composition and diversity of gut bacteria in the Scl-cGVHD mice. The dysbiosis of gut bacteria may regulate the differentiation ratio of Treg and Th1 cells, which was associated with Scl-cGVHD.

Keywords: chronic graft-versus-host disease, gut bacteria, dysbiosis, Treg, Th1

INTRODUCTION

Graft-versus-host disease (GVHD) is a life-threatening complication characterized by multi-organ dysfunction due to immune dysregulation after allogeneic hematopoietic stem cell transplantation (allo-HSCT) (Im et al., 2016; Annalisa et al., 2018; Zeiser et al., 2021), which is a potentially curative treatment for hematologic malignancies. According to the clinic manifestations and the time of occurrence, GVHD was classified as acute GVHD (aGVHD) and chronic GVHD (cGVHD), which the former inducing acute inflammatory reaction and the latter mediates the fibrotic pathological damage of various tissues and organs throughout the whole body (Ferrara et al., 2009; Min, 2011). Although the pathogenesis of cGVHD remained to be somewhat ill-defined, there were several T-helper lineages associated with the targeted tissue damage in chronic GVHD (Sarantopoulos et al., 2015; Jin et al., 2016). Th1 cells were reported to be the predominant cytotoxic effectors in sclerodermatous cGVHD (Im et al., 2016; Lai et al., 2018). Treg cells have been demonstrated to maintain the balance between autoimmunity and tolerance by suppressing the proliferation and effector functions of T, B, NK cells, and antigen presenting cells (APCs) (Sakaguchi et al., 2008; Kumar et al., 2019). A reduced percentage of Treg cells was shown to induce the development of cGVHD (Koreth et al., 2011; Du et al., 2017). Furthermore, in our previous studies, we also found that the therapy targeted to increase the ratio of the number of Treg cells and decrease the differentiation of T-helper lineages cells was shown to be effective in alleviating sclerodermatous cGVHD (Wang et al., 2017; Chen et al., 2018). Some factors have been reported to induce the pathophysiology of cGVHD, such as HLA-type, conditioning regimen, and the prolongation of aGVHD (Ringdén et al., 2017; Santoro et al., 2018; Saraceni et al., 2019). Recently, the dysbiosis of gut microbiota was demonstrated to play an important role in the development of acute gastrointestinal graft-versus-host disease (Mathewson et al., 2016; Peled et al., 2016) and a variety of autoimmune diseases, such as multiple sclerosis (MS) (Jangi et al., 2016), inflammatory bowel disease (IBD) (Chu et al., 2016), type 1 diabetes (Forbes et al., 2018), rheumatoid arthritis (RA) (Vatanen et al., 2018), systemic lupus erythematosus (SLE) (Luo et al., 2018) *via* modulating the differentiation of T-helper lineages in human and mice.

In multiple sclerosis, *Akkermansia muciniphila* and *Acinetobacter calcoaceticus* increased in patients with MS, which induced proinflammatory responses that revealed a pronounced effect on stimulating Th1 differentiation, but *Parabacteroides distasonis* stimulated anti-inflammatory Treg cells was reduced in patients with MS (Cekanaviciute et al., 2017). In the mice model of SLE, a decrease in *Lactobacillaceae* and an increase in *Lachnospiraceae* were observed. In patients with SLE, the relative abundance of *Lachnospiraceae* was significantly greater. In the aGVHD mice model, dysbiosis including decreased *Clostridiales* and increased *Enterobacteriales* was observed (Jenq et al., 2012; Simms-Waldrip et al., 2017). In human aGVHD, a previous retrospective study has indicated that the relative abundance of *Lachnospiraceae* and *Ruminococcaceae* was positively correlated to the percentage of Treg cells, influencing the development of acute gut GVHD (Han et al., 2018). Accordingly, a large number of gut bacteria species have been demonstrated to have immunomodulatory effects on the differentiation of T-helper lineages, which are devoted to the pathogenesis of cGVHD. The gut microbiota played a vital role in the development of aGVHD, but whether gut bacteria differ in chronic sclerodermatous GVHD versus non-GVHD individuals has not been reported. Taken together, we analyzed the relative abundance of gut microbiota in the mice model of chronic sclerodermatous GVHD and the immunoregulation of microbiota on the differentiation of Treg and Th1 cells.

MATERIALS AND METHODS

Chronic Sclerodermatous Graft-Versus-Host Disease Mice Model

The male B10.D2 mice (10–12 weeks old, Jackson Laboratory) and female BALB/cJ mice (10–12 weeks old, Beijing Vital River Laboratory Animal Technology Co., Ltd.) were used to establish the mice model of sclerodermatous cGVHD that could simulate Scl-GVHD and systemic sclerosis in humans as described previously (Wang et al., 2017; Lai et al., 2018). Briefly, recipient female BALB/cJ mice received total body irradiation with 700 cGy Cs137 ray and were transplanted by tail vein injection with 8×10^6 bone marrow cells and 8×10^6 spleen cells from B10.D2 mice (1:1, Scl-cGVHD mice model; 1:0, non-GVHD). The clinical score, body weight loss, and activities of the recipient mice were monitored every 3 days beginning at Day 14 after bone marrow transplantation (BMT). Chronic sclerodermatous GVHD was assessed using an established system as reported previously (Lai et al., 2018). All experiments used on mice in this study were approved by the animal experimental ethics committee of Guangdong Provincial People's Hospital.

Hematoxylin-Eosin Staining of Skin Tissues

Skin tissues from mice were collected and fixed in 10% formaldehyde and then embedded in paraffin. Hematoxylin-Eosin (HE) staining was conducted to examine histopathological changes in the skin. The results of the HE staining were observed by light microscopy.

Microbiota Sampling, DNA Extraction and Sequencing, and Metagenome Analysis

Fecal pellets were collected from chronic sclerodermatous GVHD or non-GVHD mice 35 days after bone marrow transplantation. All fecal pellets were stored at –80°C until they were processed for DNA extraction and sequencing. The fecal bacterial genomic DNA was extracted by cetyltrimethylammonium bromide (CTAB) or sodium dodecyl sulfate (SDS) method, and the purity and concentration of the DNA were detected by agarose gel electrophoresis. The appropriate amount of fecal bacterial genomic DNA was diluted to 1 ng/μl with sterile water (n = 5 per group). PCR amplification was performed using the diluted genomic DNA as a template and 16S V4 region primers, the forward primer: GTGCCAGCMGCCGCGGTAA, and the reverse primer: GGACTACHVGGGTWTCTAAT. Phusion® High-Fidelity PCR Master Mix with GC Buffer and high-efficiency high-fidelity enzyme. The intestinal flora DNA library was constructed by using the Thermofisher's Ion Plus Fragment Library Kit 48 rxns library kit. The constructed library was sequenced using the Thermo Fisher's Ion S5TMXL by Novogene bioinformatics Technology Co., Ltd. Uparse software was used to cluster all clean reads of all samples. By default, the sequence is clustered into Operational Taxonomic Units (OTUs) with 97% identity. At the same time, the representative sequence of OTUs is selected according to the algorithm principle. The most frequently occurring sequences in OTUs were screened as representative sequences of OTUs. The UniFrac distance was calculated with Qiime software (Version 1.9.1). Diluted curves, beta diversity index analysis, principal component analysis (PCA), and principal coordinates analysis (PCoA) diagram drawing were performed by R software (Version 2.15.3). Analysis of similarities (Anosim) analysis was used by the R vegan package. The LEfSe analysis was analyzed with LEfSe software.

Bacterial Extracts Preparation

We prepared bacterial extracts using an experimental approach based on a report by Cekanaviciute E. (Cekanaviciute et al., 2017). Briefly, total microbiota were isolated from cGVHD and non-GVHD mice stool samples by suspending 1–2 mg stool sample in 3 ml of PBS, removing the precipitate at low-speed centrifugation (40 g, 3 min), passing the supernatant through a 40 μm cell strainer and washing with 1.5 ml of PBS for two times by centrifuging at 8,000 rpm. Isolated bacteria were heat-inactivated at 65°C for 1 h, lysed with protease inhibitor and phosphatase inhibitor, and sonicated at 4°C for 2–3 min. Extracted bacteria protein concentrations were measured with the BCA protein assay kit.

Mice Splenocytes Isolation, Cultures, and Activation

The splenocytes were isolated from female BALB/cJ mice and cultured in RPMI-1640 (Gibco) supplemented with 10% fetal bovine serum (FBS, Gibco), 1% penicillin/streptomycin (Sigma) at 37°C with 5% CO_2. The splenocytes were counted and planked at 1 × 10^6 cells/ml concentration and activated with IL-2 (40 ng/ml), anti-CD3 (5μg/ml), and anti-CD28 (2μg/ml) for 5 days, in the presence of bacterial extracts (1μg/ml) from Scl-cGVHD mice or non-GVHD mice.

Flow Cytometry for Splenocytes

The Th1 and Treg cells were determined by $CD4^+IFN\gamma^+$, $CD4^+CD25^+Foxp3^+$. The following antibodies were used to stain mice splenocytes: anti-CD4-FITC (eBioscience), anti-IFN-γ-APC (eBioscience), anti-CD25-APC (eBioscience), and anti-Foxp3-PE (eBioscience). Transcription factors Foxp3 were stained with antibodies after being formulated by the Foxp3/transcription factor staining buffer set. For interferon- γ (IFN-γ) detection, cells were cultured with a 1 × cell stimulation cocktail (plus protein transport inhibitors) for 4–6 h, fixed and permeabilized with a fixation and permeabilization buffer before staining with antibodies. Flow cytometry was performed on a BD CantoII cell analyzer and analyzed by FlowJo software (TreeStar). The percentage of Th1 and Treg cells was defined as Th1 and Treg cells within the $CD4^+$ T cells.

Cytokines Analysis

The proinflammatory cytokine IFN-γ and the immunoregulatory mediators IL-10 levels were detected using the BD™ Cytometry Bead Array kit.

Statistical Analysis of *in vitro* Data

Statistical significance of expression of $CD4^+$ T lymphocyte differentiation was determined using a two-tailed Student's t-test. If the data were non-normally distributed, a two-tailed non-parametric Mann–Whitney test was applied instead. The percentage of Th1 and Treg cells was analyzed with FlowJo. SPSS 20.0 was used to analyze and GraphPad Prism 6 software was applied to plot the data. A p-value of < 0.05 was determined to be statistically significant.

RESULTS

Successful Establishment of Sclerodermatous Chronic Graft-Versus-Host Disease Mice Model

To analyze the role of gut microbiota and the relationship with the differentiation of Treg and Th1 cells on the sclerodermatous cGVHD, we established the mice model of sclerodermatous cGVHD ($B10D2^{H2d}♂ \rightarrow BALB/cJ^{H2d}♀$). The clinical manifestation of the sclerodermatous cGVHD mice is characterized by ulceration, escharotic, depilation, and sclerosis. Skin histopathological analysis with HE staining showed that the epidermal layer thickened, subsclerodermatous fat decreased,

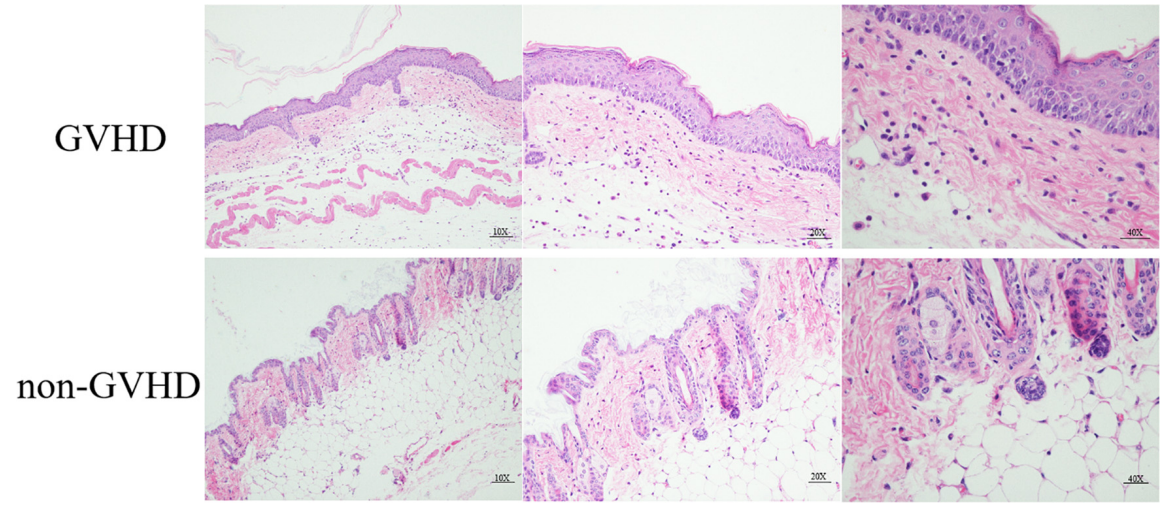

FIGURE 1 | Histopathological HE staining analysis of skin from sclerodermatous chronic graft-versus-host disease (cGVHD) mice. Compared with the control group, the pathological damage to the skin in cGVHD mice was mainly manifested by obvious hyperplasia of the epidermis, massive collagen deposition in the dermis, extensive lymphocyte infiltration, severe subsclerodermatous fat atrophy, and a significant decrease in the number of hair follicles.

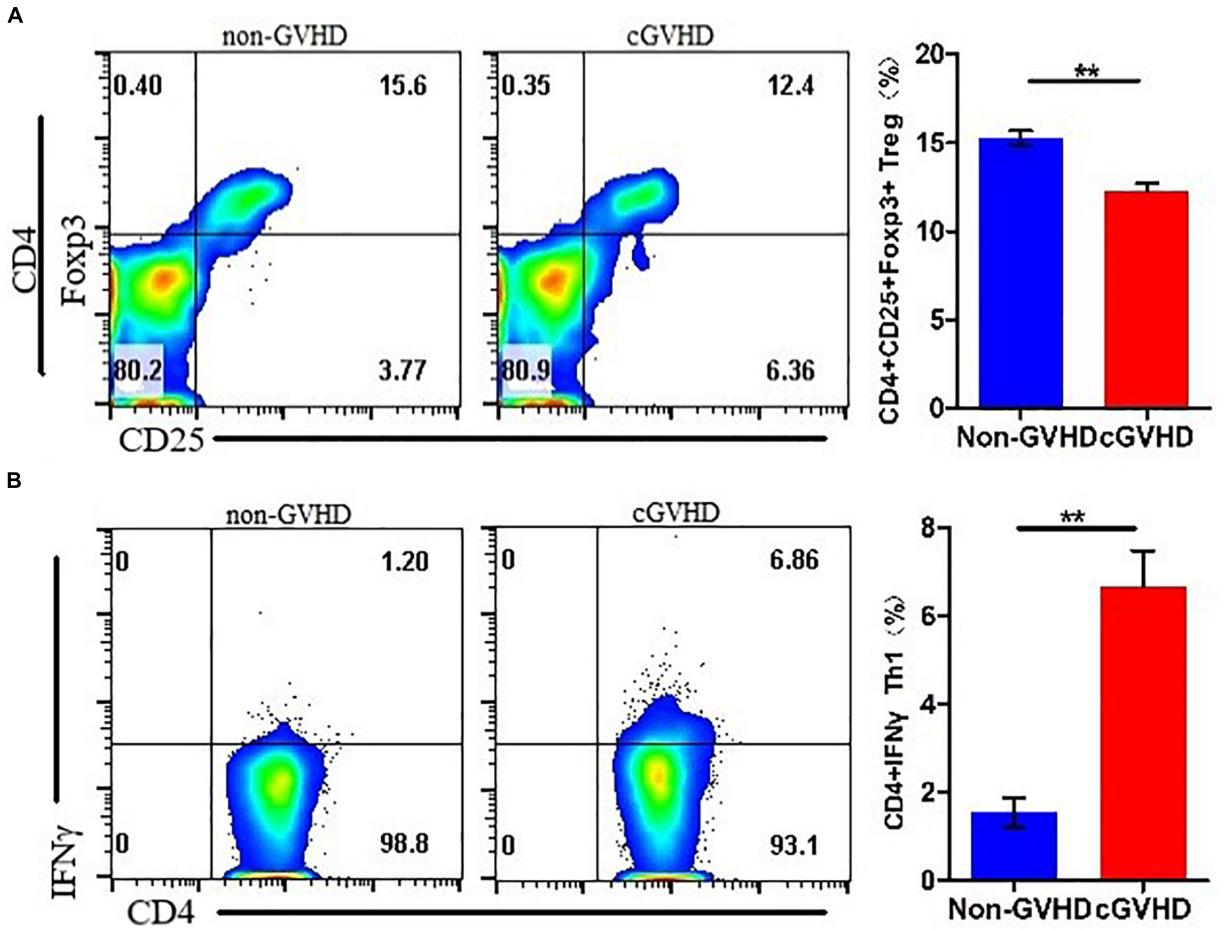

FIGURE 2 | Decreased proportion of Treg cells and increased Th1 cells in splenocytes of sclerodermatous cGVHD mice. **(A)** The proportion of Treg cells in the spleen cells of cGVHD mice was significantly reduced ($n = 3$, $^{**}p < 0.01$). **(B)** Increased Th1 cells in splenocytes of sclerodermatous cGVHD ($n = 3$, $^{**}p < 0.01$).

collagen deposited, a large number of inflammatory cells infiltrated the dermis, and hair follicles decreased (**Figure 1**).

The Differentiation Proportion of Treg and Th1 Cells in the Splenocytes of Sclerodermatous Chronic Graft-Versus-Host Disease Mice

To understand the differentiation of Treg and Th1 cells in splenocytes of sclerodermatous cGVHD mice, we detected the proportion of CD4 + CD 25^{+}Foxp3^{+} Tregs (**Figure 2A**) and $CD4^{+}$IFN-γ^{+} Th1 cells (**Figure 2B**) by flow cytometry and found a decreased proportion of Treg cells and increased Th1 cells in splenocytes of sclerodermatous cGVHD mice.

Composition and Diversity of Gut Bacteria in Mice Model of Sclerodermatous Chronic Graft-Versus-Host Disease

To determine the composition and diversity of gut bacteria on the sclerodermatous cGVHD mice, we analyzed fecal pellets collected at a diseased time point (35 days) after transplantation. The gut bacteria communities in the mice model of sclerodermatous cGVHD changed compared with non-GVHD mice by 16S rDNA sequencing (**Figure 3**). The rarefaction analysis curves in the Scl-cGVHD and non-GVHD groups were smooth and approached to saturation (**Figure 3A**). It indicated that the sequencing data had high quality and adding more data

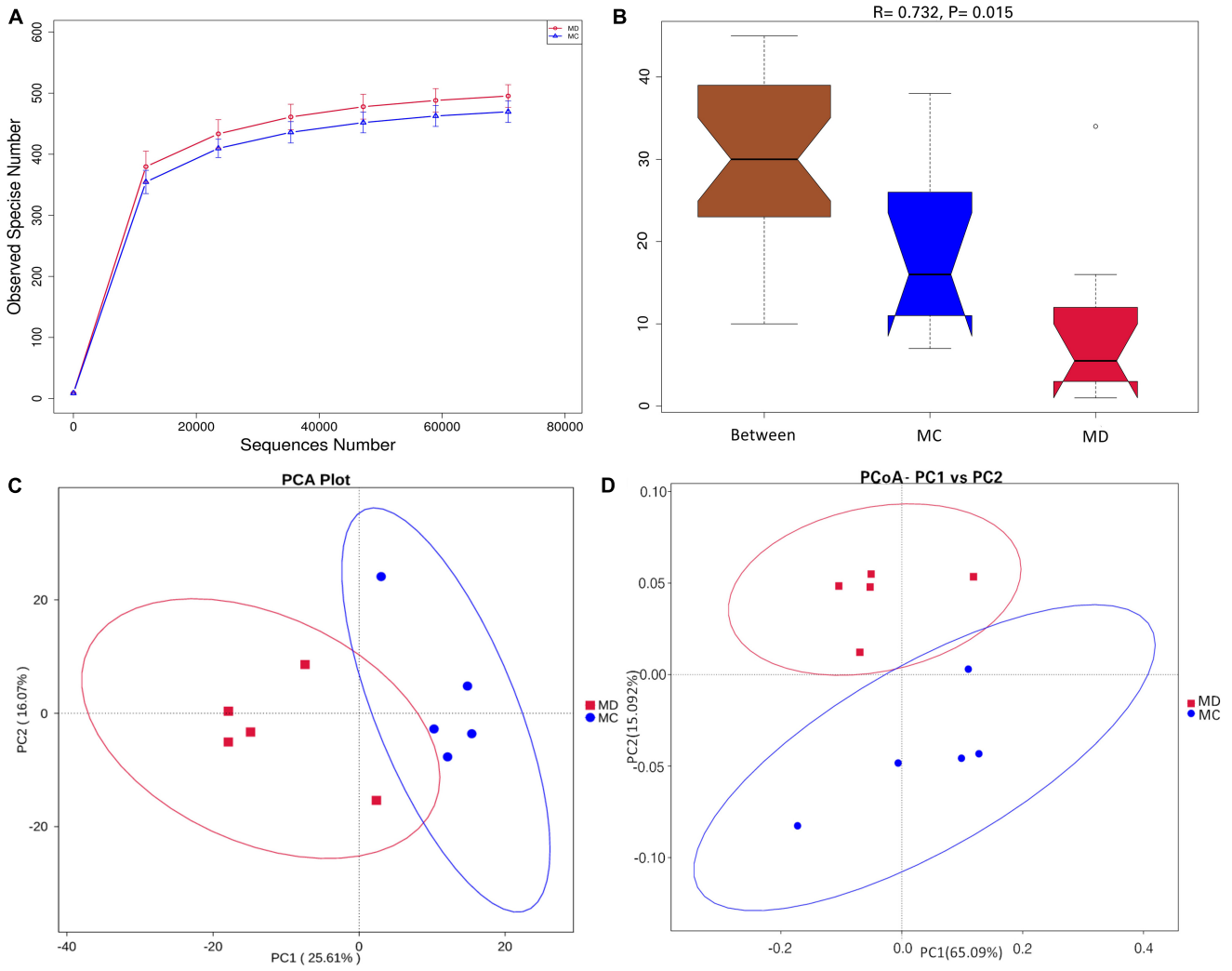

FIGURE 3 | The composition and diversity of gut bacteria in mice model of sclerodermatous cGVHD. Fecal pellets were collected 35 days after transplantation [n = 10, 5 sclerodermatous cGVHD (MD group) and 5 non-GVHD mice (MC group)] and were subjected to 16S rDNA sequencing analysis. **(A)** Rarefaction curves of the species number in the sclerodermatous cGVHD (MD group) and non-GVHD mice (MC group). **(B)** ANOISM analysis of the beta diversity of the samples significantly separated the groups when $R > 0$ and $p < 0.05$. **(C,D)** Principal component analysis (PCA) and principal coordinates analysis (PCoA) plot (weighted_UniFrac distances) of beta diversity showed the difference in overall community structures between sclerodermatous cGVHD and non-GVHD mice.

would only produce a very small number of new species. Analysis of community structure between the groups showed a significant separation [R = 0.732, p = 0.015, non-parametric analysis (ANOSIM)] (**Figure 3B**), suggesting a clear difference in the gut bacteria composition in the Scl-cGVHD and non-GVHD mice. PCA and PCoA (weighted_UniFrac distances) of beta diversity showed a clear distinction of gut bacteria between the sclerodermatous cGVHD and non-GVHD mice (**Figures 3C,D**).

To determine whether the absence or presence of specific bacterial taxa was associated with sclerodermatous cGVHD, we compared the gut bacteria composition of the sclerodermatous cGVHD and non-GVHD mice (**Figure 4**). The top10 microbes at the phylum (**Figure 4A**), family (**Figure 4B**), and genus (**Figure 4C**) levels and the specific bacterial taxa by LEfSe analysis were shown in **Figures 4D,E**, indicating the variations in the composition of the gut bacteria. Analyses of microbes at the phylum level revealed the dominance of *Bacteroidetes*, *Firmicutes,* and *Proteobacteria* in both GVHD and non-GVHD mice. The relative abundance of the phylum *Bacteroidetes*, *Firmicutes,* and *Proteobacteria* was not different between the non-GVHD and sclerodermatous cGVHD mice. The Phylum *Melainabacteria* was lower in the sclerodermatous cGVHD mice. At the family level, the gut microbiota *Lachnospiraceae* was enriched in the fecal of sclerodermatous cGVHD mice compared with the non-GVHD mice, and the dominant specific species in *Lachnospiraceae,* such as *Lachnospiraceae_bacterium_DW17*, *Lachnospiraceae_bacterium_615*, *Lachnospiraceae_bacterium_COE1,* and *Lachnospiraceae_bacterium_DW59* were increased in Scl-cGVHD mice. Whereas, the gut bacteria community in the sclerodermatous cGVHD mice was decreased in the family *Ruminococcaceae*, *Rikenellaceae, Tannerellaceae, and Bifidobacteriaceae.* At the genus level, the genus *unidentified_Ruminococcaceae*, *Alistipes*, *Parabacteriodes*, *and Bifidobacterium* were lower and *Blautia*, *Ralstonia,* and *Parasutterella* were higher in sclerodermatous

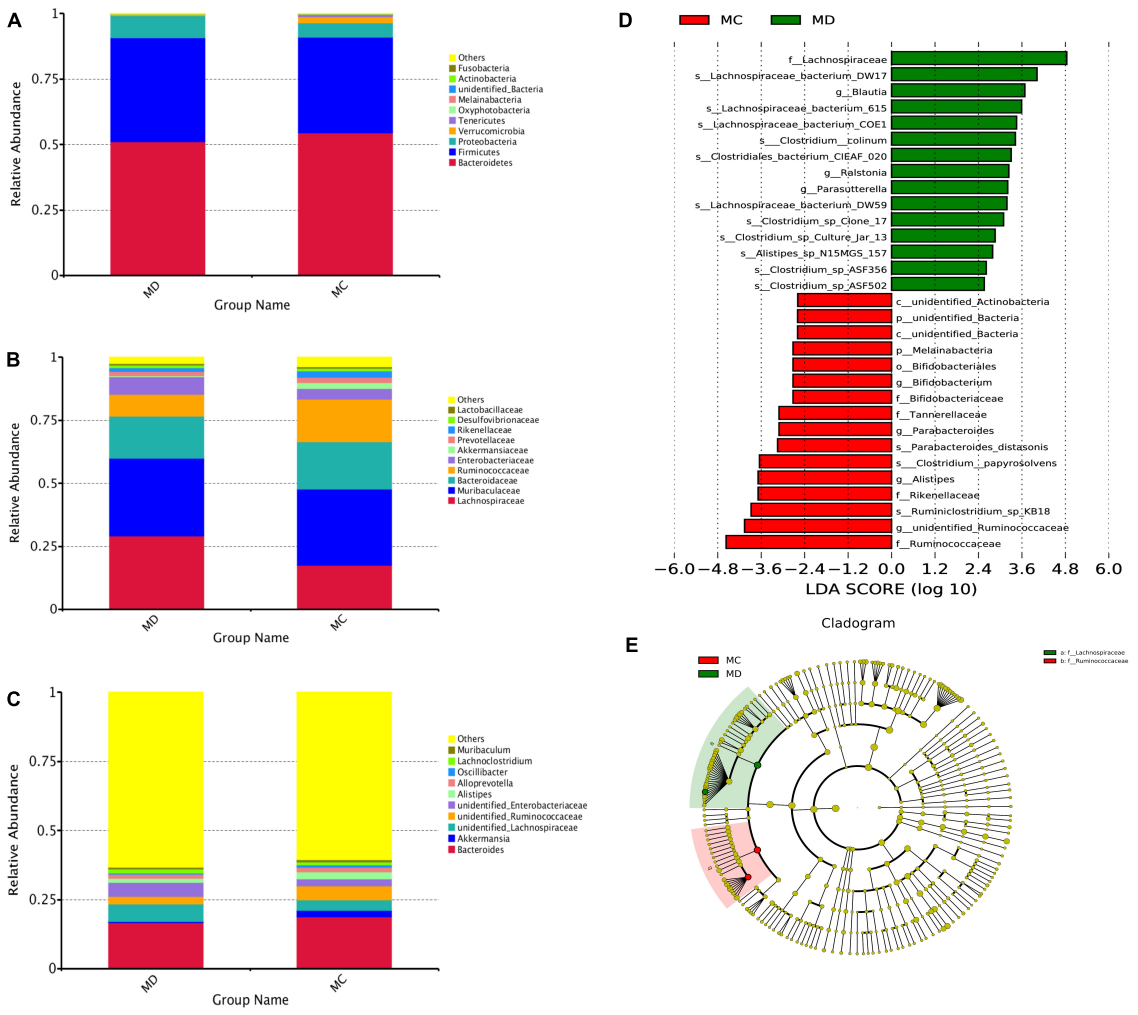

FIGURE 4 | The specific bacterial taxa associated with sclerodermatous cGVHD. **(A–C)** The top 10 relative abundances of bacteria at phylum **(A)**, family **(B)**, and genus **(C)** levels in fecal samples from the mice with or without sclerodermatous cGVHD. **(D,E)** LEfSe analysis indicated that the listed microbiomes were significantly different ($p < 0.05$).

cGVHD mice. Specifically, we also observed other gut bacteria species, such as *Ruminiclostridium_sp_KB18*, *Clostridium_papyrosolvens*, and *Parabacteroids_distasonis* were decreased in sclerodermatous cGVHD mice (**Supplementary Material**).

Sclerodermatous Chronic Graft-Versus-Host Disease-Associated Gut Bacteria Inhibit Tregs and Promote Th1 Cells Differentiation *in vitro*

To validate the hypothesis that gut bacteria taxa altered in sclerodermatous cGVHD mice play functional roles in regulating immune responses. To validate the hypothesis, we established an *in vitro* model system by exposing splenocytes from healthy female BALB/cJ mice to a suspension of bacterial extracts that were heat-killed and sonicated gut microbes of Scl-cGVHD and non-GVHD mice and used the flow cytometry to test T-cells differentiation. We found that the bacterial extracts from the sclerodermatous cGVHD mice reduced the proportions of CD $25^{+}Foxp3^{+}$ Tregs within $CD4^{+}$ T cells (**Figures 5A,B**) and promoted the differentiation of Th1 ($CD4^{+}IFN\text{-}\gamma^{+}$) cells (**Figures 5C,D**). These results indicated that gut bacteria from sclerodermatous cGVHD mice restrains immunoregulatory T-cell development and potentially exacerbates inflammation. Furthermore, we examined the proinflammatory (IFN-γ) and anti-inflammatory (IL-10) cytokines in three sclerodermatous cGVHD and three non-GVHD plates after incubating SPC

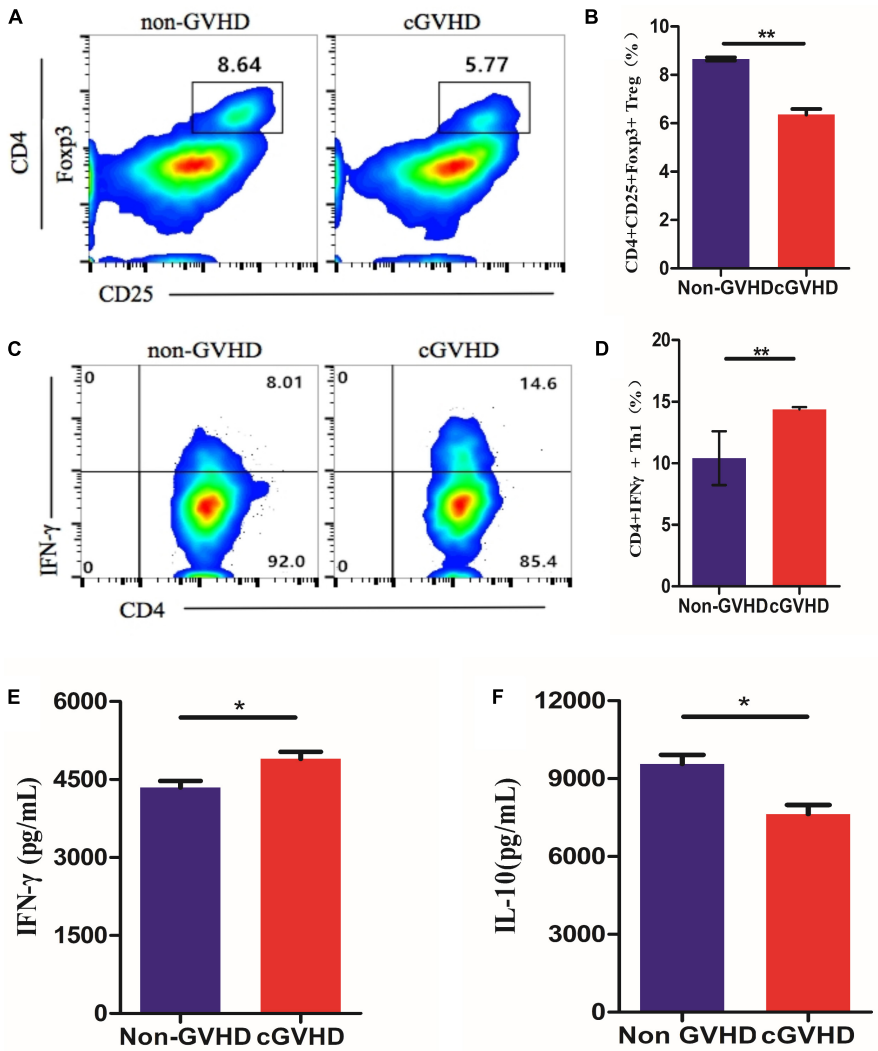

FIGURE 5 | Sclerodermatous cGVHD-associated gut bacteria inhibit Tregs and promote Th1 lymphocytes Differentiation *in vitro*. **(A,B)** Representative flow cytometry plots and quantification of $CD25^{+}Foxp3^{+}$ Tregs within $CD4^{+}$ T cells differentiated in response to bacterial extracts from sclerodermatous cGVHD and non-GVHD mice ($n = 3$, $^{**}p < 0.01$). **(C,D)** The percentage of interferon- γ (IFN-γ^{+}) in $CD4^{+}$ T cells significantly increased by stimulating bacterial extracts from sclerodermatous cGVHD compared with the non-GVHD group ($n = 3$, $^{**}p < 0.01$). **(E,F)** The concentration of anti-inflammatory interleukin-10 (IL-10) and IFN-γ was detected by the CBA kit. The secretion of IL-10 decreased but IFN-γ increased markedly in the supernatant stimulated by bacterial extract from sclerodermatous cGVHD mice ($n = 3$, $^{*}p < 0.01$).

for 5 days with bacteria extracts. The bacterial extracts from sclerodermatous cGVHD mice tended to induce an increased concentration of IFN-γ production from T cells but decreased anti-inflammatory IL-10 levels in comparison with non-GVHD mice (**Figures 5E,F**).

DISCUSSION

Numerous studies on microbes have demonstrated that the gut bacteria community was involved in the etiopathogenesis of several inflammatory autoimmune diseases (Forbes et al., 2018; van der Meulen et al., 2019). However, the diversity and composition of the gut bacteria on sclerodermatous cGVHD were not reported. In our study, we analyzed the gut bacteria from sclerodermatous cGVHD mice by using 16S rDNA sequencing. In sclerodermatous cGVHD mice, significant difference in the gut bacteria community was observed versus non-GVHD mice. The microbiota from sclerodermatous cGVHD mice tended to be less diverse. Fewer relative abundance of *Ruminococcaceae* and more *Lachnospiraceae* were found in the sclerodermatous cGVHD mice. The studies of *Ruminococcaceae* were consistent with other studies (Han et al., 2018), which reported that *Ruminococcaceae* was negatively corrected with severe aGVHD by regulating the differentiation ratio of Treg cells in human aGVHD. A significantly lower relative abundance of the *Lachnospiraceae* was shown in gut aGVHD. However, we observed a higher relative abundance of the *Lachnospiraceae* in Scl-cGVHD mice. This is possibly due to differences in the study, such as (1) there may be similarities in the gut bacteria of patients with sclerodermatous cGVHD versus non-GVHD; (2) our mouse model is mainly characterized by scleroderma, which is different from gut aGVHD and may be more likely to the SLE, which was also characterized with autoimmune antibodies and it was reported that *Lachnospiraceae* was increased in patients with SLE and mice.

A study by Im A showed that Th1 was the predominant cytotoxic effector on the skin in cGVHD (Im et al., 2016), and we found that the percentage of Treg cells was decreased in the sclerodermatous cGVHD mice in our previous study (Wang et al., 2017). In addition, we found a decreased percentage of Treg cells and an increased percentage of Th1 cells in splenocytes of Scl-cGVHD mice. While it was always consistent with the studies previously reported. Interactions between the differentiation of $CD4^+$ T cells and commensal gut bacteria were not well understood. Recently, it was shown that the *Bacteroidales* regulated the differentiation of Treg cells and *A. calcoaceticus* and *A. muciniphila* induced the differentiation of Th1 cells. *Rumminococcaceae* was found to be positively associated with the differentiation of Treg cells and *Enterobacteriaceae* was negatively associated with it. In this study, we prepared the bacterial extracts of the microbiota from sclerodermatous cGVHD mice to validate the regulatory function *in vitro*. We first examined the ratio of Th1 cells and Treg cells and proinflammatory IFN-γ and immunoregulatory IL-10 cytokines in three sclerodermatous cGVHD and three non-GVHD mice after incubating spleen cells with bacterial extracts. We found that the bacterial extracts from sclerodermatous cGVHD mice demonstrated the regulatory effect on the differentiation of Th1 and Treg cells by inducing the secretion of immunosuppressive cytokine IFN-γ and inhibiting immunoregulatory IL-10. It will be important in further studies that we try to enroll a population of sclerodermatous cGVHD patients and analyze the gut microbiotas. *In vitro*, we will prepare the bacterial extracts of gut bacteria from patients with sclerodermatous cGVHD and non-GVHD and culture the specific microbiome to verify the function of the differentiation of $CD4^+$ T cells. Furthermore, in the sclerodermatous cGVHD mice model, we will evaluate the curative effect on fecal microbiota transplantation by gavaging the bacteria extracts from non-GVHD mice to the sclerodermatous cGVHD mice. In this way, the influence of gut bacteria on patients with sclerodermatous cGVHD patients and mice models may be achieved, enabling us to understand whether fecal microbiota transplantation may be used as a new target treatment for sclerodermatous cGVHD.

CONCLUSION

In conclusion, our results demonstrate an altered gut bacteria community in our established sclerodermatous cGVHD mice. Further, the abnormal gut bacteria extracts from the sclerodermatous cGVHD mice would inhibit the differentiation ratio of Tregs and promote the differentiation of the Th1 cells by regulating the secretion of proinflammatory cytokine IFN-γand the anti-inflammatory cytokine IL-10. Our data provide evidence that dysbiosis of the gut bacteria community may be a potential risk factor for the development of cGVHD. Regulation of the gut bacteria community would be a novel therapy for cGVHD treatment.

DATA AVAILABILITY STATEMENT

The datasets presented in this study can be found in online repositories. The names of the repository/repositories and accession number(s) can be found below: Dryad, https://doi.org/10.5061/dryad.zs7h44jd1.

ETHICS STATEMENT

The animal study was reviewed and approved by the Animal Experimental Ethics Committee of Guangdong Provincial People's Hospital.

AUTHOR CONTRIBUTIONS

YW, PL, XD, and JW conceived and designed the experiments and wrote the manuscript. YW, LH, TH, XC, SG, and XH

performed the experiments. YW and PL analyzed the data. All authors contributed to the article and approved the submitted version.

FUNDING

This study was supported by the National Natural Science Foundation of China (grant no. 81870121) and the Guangdong Basic and Applied Basic Research Foundation, China (grant nos. 2019A1515012049 and 2019A1515010094).

SUPPLEMENTARY MATERIAL

The Supplementary Material for this article can be found online at: https://www.frontiersin.org/articles/10.3389/fmicb.2022.813576/full#supplementary-material

REFERENCES

Annalisa, R., Myriam, L., Andrea, B., Boris, A., Jan, J., Cornelissen, A. E., et al. (2018). Post-transplant cyclophosphamide for graft-versus-host disease prophylaxis in HLA matched sibling or matched unrelated donor transplant for patients with acute leukemia, on behalf of ALWP-EBMT. *J. Hematol. Oncol.* 11:40. doi: 10.1186/s13045-018-0586-4

Cekanaviciute, E., Yoo, B. B., Runia, T. F., Debelius, J. W., Singh, S., Nelson, C. A., et al. (2017). Gut bacteria from multiple sclerosis patients modulate human T cells and exacerbate symptoms in mouse models. *Proc. NatI. Acad. Sci. U.S.A.* 114, 10713–10718. doi: 10.1073/pnas.1711235114

Chen, X., Lai, P., Wang, Y., Luo, C., Ling, W., Zeng, L., et al. (2018). Emerging role of C5a/C5aR IL-17A axis in cGVHD. *Am. J. Transl. Res.* 10, 2148–2157.

Chu, H., Khosravi, A., Kusumawardhani, I. P., Kwon, A. H. K., Vasconcelos, A. C., Cunha, L. D., et al. (2016). Gene-microbiota interactions contribute to the pathogenesis of inflammatory bowel disease. *Science* 352, 1116–1120. doi: 10.1126/science.aad9948

Du, J., Paz, K., Thangavelu, G., Schneidawind, D., Baker, J., Flynn, R., et al. (2017). Invariant natural killer T cells ameliorate murine chronic GVHD by expanding donor regulatory T cells. *Blood* 129, 3121–3125. doi: 10.1182/blood-2016-11-752444

Ferrara, J. L., Levine, J. E., Reddy, P., and Holler, E. (2009). Graft-versus-host disease. *Lancet* 373, 1550–1561. doi: 10.1016/S0140-6736(09)60237-3

Forbes, J. D., Chen, C., Knox, N. C., Marrie, R. A., El-Gabalawy, H., de Kievit, T., et al. (2018). A comparative study of the gut microbiota in immune-mediated inflammatory diseases-does a common dysbiosis exist? *Microbiome* 6, 221–235. doi: 10.1186/s40168-018-0603-4

Han, L., Jin, H., Zhou, L., Zhang, X., Fan, Z., Dai, M., et al. (2018). Intestinal microbiota at engraftment In?uence acute graft-versus-host disease via the Treg/Th17 Balance in Allo-HSCT recipients. *Front. Immunol.* 9:669. doi: 10.3389/fimmu.2018.00669

Im, A., Hakim, F. T., and Pavletic, S. Z. (2016). Novel targets in the treatment of chronic graft-versus-host disease. *Leukemia* 31, 543–554. doi: 10.1038/leu.2016.367

Jangi, S., Gandhi, R., Cox, L. M., Li, N., von Glehn, F., Yan, R., et al. (2016). Alterations of the human gut microbiome in multiple sclerosis. *Nat. Commun.* 7:12015. doi: 10.1038/ncomms12015

Jenq, R. R., Ubeda, C., Taur, Y., Menezes, C. C., Khanin, R., and Dudakov, J. A. (2012). Regulation of intestinal inflammation by microbiota following allogeneic bone marrow transplantation. *J. Exp. Med.* 209, 903–911. doi: 10.1084/jem.20112408

Jin, H., Ni, X., Deng, R., Song, Q., Young, J., and Cassady, K. (2016). Antibodies from donor B cells perpetuate sclerodermatous chronic graft-versus-host disease in mice. *Blood* 127, 2249–2260. doi: 10.1182/blood-2015-09-668145

Koreth, J., Matsuoka, K., Kim, H. T., McDonough, S. M., Bindra, B., Alyea, E. P., et al. (2011). Interleukin-2 and regulatory t cells in graft-versus-host disease. *N. Engl. J. Med.* 365, 2055–2066. doi: 10.1056/NEJMoa1108188

Kumar, P., Saini, S., Khan, S., Lele, S. S., and Prabhakar, B. S. (2019). Restoring self-tolerance in autoimmune diseases by enhancing regulatory T-cells. *Cell. Immunol.* 339, 41–49. doi: 10.1016/j.cellimm.2018.09.008

Lai, P., Chen, X., Guo, L., Wang, Y., Liu, X., Liu, Y., et al. (2018). A potent immunomodulatory role of exosomes derived from mesenchymal stromal cells in preventing cGVHD. *J. Hematol. Oncol.* 11:135. doi: 10.1186/s13045-018-0680-7

Luo, X. M., Edwards, M. R., Mu, Q., Yu, Y., Vieson, M. D., Reilly, C. M., et al. (2018). Gut microbiota in human systemic lupus erythematosus and a mouse model of lupus. *Appl. Environ. Microbiol.* 844:e02288–17. doi: 10.1128/AEM.02288-17

Mathewson, N. D., Jenq, R., Mathew, A. V., Koenigsknecht, M., Hanash, A., Toubai, T., et al. (2016). Gut microbiome-derived metabolites modulate intestinal epithelial cell damage and mitigate graft-versus-host disease. *Nat. Immunol.* 17, 505–513. doi: 10.1038/ni.3400

Min, C. K. (2011). The pathophysiology of chronic graft-versus-host disease: the unveiling of an enigma. *Korean J. Hematol.* 46, 80–87. doi: 10.5045/kjh.2011.46.2.80

Peled, J. U., Hanash, A. M., and Jenq, R. R. (2016). Role of the intestinal mucosa in acute gastrointestinal GVHD. *Blood* 128, 2395–2402. doi: 10.1182/blood-2016-06-716738

Ringdén, O., Labopin, M., Sadeghi, B., Mailhol, A., Beelen, D., Fløisand, Y., et al. (2017). What is the outcome in patients with acute leukaemia who survive severe acute graft-versus-host disease? *J. Intern. Med.* 283, 166–177. doi: 10.1111/joim.12695

Sakaguchi, S., Yamaguchi, T., Nomura, T., and Ono, M. (2008). Regulatory T Cells and immune tolerance. *Cell* 133, 775–787. doi: 10.1016/j.cell.2008.05.009

Santoro, N., Labopin, M., Giannotti, F., Ehninger, G., Niederwieser, D., Brecht, A., et al. (2018). Unmanipulated haploidentical in comparison with matched unrelated donor stem cell transplantation in patients 60 years and older with acute myeloid leukemia: a comparative study on behalf of the ALWP of the EBMT. *J. Hematol. Oncol.* 11:55. doi: 10.1186/s13045-018-0598-0

Saraceni, F., Labopin, M., Brecht, A., Kröger, A., Eder, M., Tischer, J., et al. (2019). Fludarabine-treosulfan compared to thiotepa-busulfan-fludarabine or FLAMSA as conditioning regimen for patients with primary refractory or relapsed acute myeloid leukemia: a study from the acute leukemia working party of the European society for blood and marrow transplantation (EBMT). *J. Hematol. Oncol.* 12:44.

Sarantopoulos, S., Blazar, B. R., Cutler, C., and Ritz, J. (2015). B Cells in chronic graft-versus-host disease. *Biol. Blood Marrow Transplantat.* 21, 16–23.

Simms-Waldrip, T. R., Sunkersett, G., Coughlin, L. A., Savani, M. R., Arana, C., Kim, J., et al. (2017). Antibiotic-induced depletion of anti-inflammatory clostridia is associated with the development of graft-versus-host disease in pediatric stem cell transplantation patients. *Biol. Blood Marrow Transplantat.* 23, 820–829. doi: 10.1016/j.bbmt.2017.02.004

van der Meulen, T. A., Harmsen, H. J. M., Vilac, A. V., Kurilshikovd, A., Lieferse, S. C., Zhernakovad, A., et al. (2019). Shared gut, but distinct oral microbiota composition in primary Sjögren's syndrome and systemic lupus erythematosus. *J. Autoimmun.* 97, 77–87. doi: 10.1016/j.jaut.2018.10.009

Vatanen, T., Franzosa, E. A., Schwager, R., Tripathi, S., Arthur, T. D., Vehik, K., et al. (2018). The human gut microbiome in early-onset type 1 diabetes from the TEDDY study. *Nature* 562, 589–594. doi: 10.1038/s41586-018-0620-2

Wang, Y., Lai, P., Chen, X., He, C., Huang, X., Geng, S., et al. (2017). Attenuation of cGVHD by C5a/C5aR blockade is associated with increased frequency of Treg. *Sci. Rep.* 7:3603. doi: 10.1038/s41598-017-03700-1

Zeiser, R., Polverelli, N., Ram, R., Hashmi, S. K., Chakraverty, R., Middeke, J. M., et al. (2021). Ruxolitinib for glucocorticoid-refractory chronic graft-versus-host disease. *N. Engl. J. Med.* 385, 228–238. doi: 10.1056/NEJMoa2033122

Conflict of Interest: The authors declare that the research was conducted in the absence of any commercial or financial relationships that could be construed as a potential conflict of interest.

Publisher's Note: All claims expressed in this article are solely those of the authors and do not necessarily represent those of their affiliated organizations, or those of the publisher, the editors and the reviewers. Any product that may be evaluated in this article, or claim that may be made by its manufacturer, is not guaranteed or endorsed by the publisher.

Copyright © 2022 Wang, Huang, Huang, Geng, Chen, Huang, Lai, Du and Weng. This is an open-access article distributed under the terms of the Creative Commons Attribution License (CC BY). The use, distribution or reproduction in other forums is permitted, provided the original author(s) and the copyright owner(s) are credited and that the original publication in this journal is cited, in accordance with accepted academic practice. No use, distribution or reproduction is permitted which does not comply with these terms.

Advantages of publishing in Frontiers

OPEN ACCESS
Articles are free to read for greatest visibility and readership

FAST PUBLICATION
Around 90 days from submission to decision

HIGH QUALITY PEER-REVIEW
Rigorous, collaborative, and constructive peer-review

TRANSPARENT PEER-REVIEW
Editors and reviewers acknowledged by name on published articles

Frontiers
Avenue du Tribunal-Fédéral 34
1005 Lausanne | Switzerland

Visit us: www.frontiersin.org
Contact us: frontiersin.org/about/contact

REPRODUCIBILITY OF RESEARCH
Support open data and methods to enhance research reproducibility

DIGITAL PUBLISHING
Articles designed for optimal readership across devices

FOLLOW US
@frontiersin

IMPACT METRICS
Advanced article metrics track visibility across digital media

EXTENSIVE PROMOTION
Marketing and promotion of impactful research

LOOP RESEARCH NETWORK
Our network increases your article's readership